FACULTY OF BIOLOGY

DEPARTMENT OF MICROBIOLOGY AND GENETICS

AREA: GENETICS

INSTITUTE FOR AGRIBIOTECHNOLOGY RESEARCH

Analysis of development and virulence factors and the effect of NO on germination and the cell cycle in *Botrytis cinerea*.

PhD. THESIS

-Francisco Anta Fernández-

Supervised by:

Dr. Ernesto Pérez Benito and José María Díaz Mínguez

Salamanca, 2021

FACULTAD DE BIOLOGÍA

DEPARTMENTO DE MICROBIOLOGÍA Y GENÉTICA

AREA: GENÉTICA

INSTITUTO DE INVESTIGACIÓN EN AGROBIOTECNOLOGÍA

Análisis del desarrollo y de factores de virulencia y el efecto del NO en la germinación y el ciclo celular en *Botrytis cinerea*.

Tesis Doctoral

-Francisco Anta Fernández-

Directores:

Dr. Ernesto Pérez Benito y José María Díaz Mínguez

Salamanca, 2021

Dr. D. Ernesto Pérez Benito, Profesor Titular de Universidad, y **Dr. D. José María Díaz Mínguez**, Catedrático de Universidad, del Área de Genética del Departamento de Microbiología y Genética de la Facultad de Biología de la Universidad de Salamanca,

CERTIFICAN:

Que la presente Memoria titulada "**Análisis del desarrollo y de factores de virulencia y el efecto del NO en la germinación y el ciclo celular en *Botrytis cinerea***", ha sido realizada en el Departamento de Microbiología y Genética de la Facultad de Biología y en el Instituto Hispano-Luso de Investigaciones Agrarias de la Universidad de Salamanca, bajo nuestra dirección, por **D. Francisco Anta Fernández**, y cumple las condiciones exigidas para optar al grado de Doctor por la Universidad de Salamanca.

Dr. D. Carlos Nicolás Rodríguez, Coordinador del Programa de Doctorado en Agrobiotecnología (RD 99/2011) de la Universidad de Salamanca,

CERTIFICO:

Que la presente Memoria titulada "**Análisis del desarrollo y de factores de virulencia y el efecto del NO en la germinación y el ciclo celular en *Botrytis cinerea***", ha sido realizada en el Departamento de Microbiología y Genética de la Facultad de Biología y en el Instituto Hispano-Luso de Investigaciones Agrarias de la Universidad de Salamanca, bajo la dirección del **Dr. D. Ernesto Pérez Benito** y del **Dr. D. José María Díaz Mínguez**, por **D. Francisco Anta Fernández**, y cumple las condiciones exigidas para optar al grado de Doctor por la Universidad de Salamanca.

Este trabajo se ha llevado a cabo en el Laboratorio 1 del Instituto Hispano-Luso de Investigaciones Agrarias (CIALE), Departamento de Microbiología y Genética, de la Universidad de Salamanca bajo la dirección del Profesor Dr. Ernesto Pérez Benito y del Profesor Dr. José María Díaz Mínguez y al amparo de los proyectos de investigación MINECO: AGL2015-66131-C2- 1-R del actual Ministerio de Asuntos Económicos y Transformación Digital y MICINN: PID2019-1106005RB-100 del Ministerio de Ciencia e Innovación. Durante el desarrollo de la Tesis he disfrutado de una ayuda de la Junta de Castilla y León destinada a financiar la contratación predoctoralde personal investigador, cofinanciada por el Fondo Social Europeo (Orden de 26 de junio, de la Consejería de Educación según resolución EDU/529/2017). También realicé una Estancia Virtual Breve que complementó el trabajo presentado en esta Tesis en el laboratorio del Profesor Dr. Jan van Kan de la Universidad de Wageningen (Países Bajos).

Publicaciones científicas relacionadas con los resultados obtenidos en esta Tesis Doctoral y otros trabajos publicados durante el período de formación predoctoral:

- Acosta Morel, W., Marques-Costa, T.M., Santander-Gordón, D., **Anta Fernández, F.**, Zabalgogeazcoa, I., Vázquez de Aldana, B.R., Sukno, S.A., Díaz-Mínguez, J.M. and Benito, E.P. (2019) Physiological and population genetic analysis of *Botrytis* field isolates from vineyards in Castilla y León, Spain. Plant Pathol. 68: 523-536.
- Acosta Morel, W., **Anta Fernández, F.,** Baroncelli, R., Becerra, S., Thon, M.R., van Kan, J.A.L., Díaz-Mínguez, J.M. and Benito, E.P.. (2021). A major effect gene controlling development and pathogenicity in *Botrytis cinerea* identified through genetic analysis of natural mycelial non-pathogenic isolates. Frontiers in Plant Science. 12:663870.
- **Anta-Fernández, F.** *et al*. Nitric oxide regulates germination and development in *Botrytis cinerea*. (In preparation).

Agradecimientos

A mis padres y a mi hermana.

A Ernesto Pérez Benito por haber estado siempre disponible para ayudarme en la realización de este trabajo.

A mis compañeros del laboratorio, Borja, Sioly, Mariana, Virginia, Wilson y muchos otros. Esta tesis también es, de alguna manera, fruto de su trabajo.

INDICES

General index

Index of figures

Index of tables

Abbreviations and terms of common use

ATP	Adenosine triphosphate
Bc	*Botrytis cinerea*
BLASTN	Nucleotide- nucleotide Basic Local Alignment Search Tool
BLASTP	Protein-protein Basic Local Alignment Search Tool
BME	Bacto Malt Extract
bp	Base pairs
°C	Celsius grade
***cdc*2**	Cell division cycle 2
***cdc*25**	Cell division cycle 25
cDNA	Complementary DNA
CDP-Star	Disodium 2-chloro-5-(4-methoxyspiro[1,2-dioxetane-3,2'-(5-chlorotricyclo[3.3.1.1^{3,7}]decan])-4-yl]-1-phenyl phosphate
CFW	Calcofluor white stain
cm	Centimeter
cPTIO	2 - (4-carboxyphenyl) - 4, 4, 5, 5 - tetramethylimidazoline - 1 - oxyl - 3 - oxide
Ct	Threshold cycle
C-terminal	Carboxyterminal
Cys	Cysteine
Da	Dalton
DAPI	4',6-diamidino-2-phenylindole
DEG	Differentially expressed gene
DEPC	Diethylpyrocarbonate
DETA	Diethylenetriamine
DIG	Digoxigenin-11-dUTP
DNA	*Deoxyribonucleic acid*
DNase	Deoxyribonuclease
dNTP	Deoxynucleotide 5´-triphosphate
dpi	Days post inoculation
dsRNA	Double-stranded ribonucleic acid
DTT	Dithiothreitol
dUTP	2'-Deoxyuridine-5'-triphosphate
EDTA	Ethylenediaminetetraacetic acid
***et al*.**	*Et alii* / *Et aliae* / *Et alia* (and others)
f. sp.	*Forma specialis* / *Formae speciales* (Special form/s)
FAD	Flavin adenine dinucleotide

FC	Fold change
GFP	Green fluorescent protein
GO	Gene Ontology
***fhg*1**	Flavohemoglobin 1
GPS-SNO	Group-based Prediction System for prediction of kinase-specific phosphorylation sites
GPS-YNO2	Group-based Prediction System for prediction of tyrosine nitration sites
h	hours
H_2O_2	Hydrogen peroxide
HOG	High-Osmolarity Glycerol
hpi	Hours post inoculation
Hyg	Hygromycin
ID	Identifier
IPTG	Isopropyl β-D-1-thiogalactopyranoside
Kan	Kanamycin
kb	Kilobases
kDa	Kilodalton
KH_2PO_4	Potassium dihydrogen phosphate
L	Liter
L-NNA	Nω-nitro-L-arginine
M	Molar
M	Mass
MAPK	Mitogen-activated protein kinase
***mbp*1**	Mlu1-box-binding protein 1
***mcm*1**	MiniChromosome Maintenance 1
MEA	Malt Extract Agar
med	medusa
mg	Milligram
niaD	Nitrate reductase
min	Minute(s)
mL	Millilitre
mM	Millimolar
mm	Millimeter
MOPS	3-(*N*-morpholino) propanesulfonic acid
mRNA	messenger RNA
N	Normal
N-terminal	Aminoterminal
NADH	Nicotinamide-adenine-dinucleotide
NADPH	Nicotinamide adenine dinucleotide phosphate

Indices

NCR	Nitrogen Catabolite Repression
ng	Nanogram
nM	Nanomolar
nm	Nanometer
NO	Nitric oxide
$\mathbf{NO_2^-}$	Nitrite
$\mathbf{NO_3^-}$	Nitrate
NOS	Nitric oxide synthase
nt	Nucleotide
O_2	Molecular oxygen
ORF	Open reading frame
***orp*1**	Orphan gene required for pathogenicity 1
padj	Adjusted p value
PCR	Polymerase chain reaction
PDA	Potato Dextrose Agar
PDB	Potato Dextrose Broth
PEG	Polyethyleneglycol
pH	Potential of hydrogen
pM	Picomolar
qRT-PCR	Quantitative real-time PCR
RNA	Ribonucleic acid
RNAseq	RNA sequencing
RNS	Reactive Nitrogen Species
ROS	Reactive oxygen species
rpm	Rounds per minute
RQ	Relative quantity of transcript
RT-PCR	Reverse transcription polymerase chain reaction
S	Sulfur
SDS	Sodium dodecyl sulfate
SD	Standard deviation
SH	Schaedler
sp.	Species
SSC	Saline-sodium citrate
***swi*4**	Switching gene 4
swi6	Switching gene 6
TAE	Tris-Acetate + Na_2-EDTA
TCA	Tricarboxylic acid
TE	Tris-Cl + Na_2-EDTA
Tm	Melting temperature

Tris	Trishydroxymethyl aminomethane
U	Unit (Enzyme activity)
UTR	Untranslated region
V	Volts
V	Volume
VCGs	Vegetative compatibility groups
vs.	Versus
WT	Wild-type
x g	Gravitational acceleration
X-gal	5-bromo-4-chloro-3-indolyl β-D-galactopyranoside
Δ	Deletion/Delta
λ	Wavelength
µg	Microgram
µL	Microliter
µm	Micrometer
µM	Micromolar

SUMMARY

Summary

Nitric oxide (NO) is a small free radical with important and varied functions in different biological systems. In the fungal kingdom, the molecule performs a vast signalling function ranging from modulation of sexual and asexual development and secondary metabolism to colonization and infection of the host plant. Due to these multiple functions and its short lifetime, of a few seconds, a balance that maintains an adequate concentration of NO in each stage of the fungus life cycle through both the biosynthesis reactions of the molecule and its detoxification mechanisms is essential (Cánovas *et al*., 2016).

Fungi can produce NO in two ways. The oxidative pathway is similar to the oxidative pathway present in mammals in that the enzyme nitric oxide synthase (NOS) catalyzes the conversion of L-arginine to L-citrulline producing nitric oxide. However, it is a poorly characterized pathway due to the absence of NOS-like proteins in fungal genomes (Li *et al*., 2010; Samalova *et al*., 2013). The other pathway is the reducing pathway, which requires the synergistic action of the enzyme nitrate reductase to convert nitrate to nitrite and of the enzyme nitrite reductase, which mediates the conversion of nitrite to NO and is considered to be the most important enzymatic source of NO in fungi (Horchani *et al*., 2011; Zhao *et al*., 2020).

The catabolic mechanisms of NO are intended to combat the toxicity of the molecule when it reaches high concentrations in cells, which can trigger nitrosative stress (Brown and Borutaite, 2006; Fitzpatrick and Kim, 2015; Marroquin-Guzman *et al*., 2017). These mechanisms are mainly based on oxidoreduction reactions of NO or its derived forms, and among them the flavohemoglobins that constitute the inducible NO detoxification mechanism best described in fungal models stand out (Forrester and Foster, 2012). These enzymes are chimeric globins formed by an N-terminal globin domain and an adjacent, C-terminal redox-active protein domain and their function is described as NO dioxygenase that requires NADPH, FAD and O_2 to turn NO into NO^- (Hausladen *et al*., 1998; Gardner *et al*., 1998).

Botrytis cinerea is a necrotrophic plant pathogenic fungus that infect more than 200 crop species, causing gray mould disease with great losses of agronomic production worldwide. The fungus has a single gene, *Bcfhg*1, that encodes a functional flavohemoglobin of which it has been suggested that it could be more related to the modulation of endogenous NO levels produc ed by the fungus during specific developmental stages than to the protection of the fungus against toxic levels of the molecule (Turrion - Gomez *et al*., 2010; Turrion-Gomez *et al*., 2011).

In this regard, with the intention of characterizing the physiological processes in which NO metabolism is relevant in the fungus, our research group carried out an analysis of a microarray experiment of gene expression profiling in response to modulating drugs of NO levels in spores of wild type B05.10 and *ΔBcfhg*1 strains, a mutant strain defective in the *Bcfhg*1 gene (Daniela Santander, Doctoral Thesis. University of Salamanca). This analysis made it possible to identify, in the case of the

mutant strain, that the functional categories 'cell cycle', 'DNA synthesis' and 'nucleolus activity' were repressed by the action of the molecule. More specifically, the genes with a higher level of repression were the orthologs of the *mcm* (2-7) genes of *S. cerevisiae*, genes whose gene products make up a protein complex essential for the formation of the origins of replication and for the initiation of DNA synthesis (Lei and Tye, 2001) and that are expressed between the M phase and the G1 phase of the cell cycle (Enserink and Kolodner, 2010). The expression of this group of genes is controlled by the transcription factor *mcm*1. A strong repression of genes that are specifically expressed in the G1 phase was also found.In this yeast, the expression of G1-specific genes is controlled by the complexes MBF, a transcription factor made up of *mbp*1 and *swi*6, and SBF, a transcription factor made up of *swi*4 and *swi*6. MBF preferentially controls the expression of genes related to DNA replication and repair, while SBF regulates the expression of genes involved in cell cycle progress, cell morphogenesis, and spindle polar body duplication (Enserink and Kolodner, 2010). The ortholog of the gene encoding the CDC25 phosphatase enzyme from *S. pombe* was also repressed. *cdc*25 participates in the activation of *cdk*1 (*cdc*2 in *S. pombe*) by dephosphorylation. The latter is a key enzyme in the regulation of the cell cycle since it controls the entry of the cell to the mitosis phase from the G2 phase. Other genes that were differentially expressed in this analysis, but in B05.10, were *Bcmed* and *Bcorp*1. The first is a transcriptional regulator factor that was upregulated when the spores were cultured in the presence of the NO scavenger, c-PTIO. The second encodes a hypothetical protein and was induced when the fungus was exposed to NO.

In this context, in the present work we set out to analyse the function of several of the aforementioned genes as encoders for cell cycle regulatory proteins and potential nitric oxide targets. In addition, we considered the functional characterization of the *Bcmed* and *Bcorp*1 genes.

Chapter I first describes the modulating effect that NO has on the asexual development of *B. cinerea*. Germination tests were carried out in which spores of the B05.10 and *ΔBcfhg*1 strains of the fungus were incubated in the presence of the drugs DETA, a NO donor, c-PTIO, a NO scavenger, and L-NNA, an inhibitor of mammalian nitric oxide synthase activity, at different sampling times. The counts, estimates and staining with the DAPI dye made on the cultures determined that NO has an immediate but transitory negative regulatory effect on germination, elongation of the germ tube and the nuclear division rate of the fungus. Flavohemoglobin BcFHG1 appears as a protein with a powerful protective function against these effects.

The immediacy and transience observed in the action of NO suggest a rapid signalling action by the molecule and led us to hypothesize that, under the evaluated conditions, NO would be affecting the activity of components essential for cell cycle progress through the covalent modification of cysteine (S- nitrosylation) and tyrosine (tyrosine nitration) residues. Specifically, we proposed that the molecule would affect the proteins encoded by the genes *mbp*1, *swi*4, *swi*6, *cdc*2, *cdc*25 and *mcm*1. This list was completed with the inclusion of the gene encoding the enzyme nitrate reductase, *niaD*. This protein plays a relevant role in NO homeostasis since it participates in the reductive synthesis of the molecule and in its regulation

during fungal development (Cánovas *et al*., 2016). Furthermore, a possible S-nitrosylation of the Cys residues on the surface of this protein in plants has been described *in silico* (Fu *et al*., 2018).

These proteins were then subjected to an analysis that aimed to determine the possible alteration of their activity due to post-translational modifications caused by the action of the molecule. Once the homologous genes selected in *S. cerevisiae* and *S. pombe* were identified in the *B. cinerea* genome, the construction of a translational fusion in which the gene sequence encoding the GFP protein was fused to the C-terminus of each of the genes of interest using Gateway technology (Invitrogen) was carried out. Several transforming strains were obtained for each fusion protein, but the assessment of S- nitrosylation and/or nitration levels of these was not possible due to the inability to purify them from total protein extracts.

On the other hand, to gain information about the physiological factors and processes that mediate the response to NO previously observed in germinating spores and that can be affected by the NO detoxifying function of a flavohemoglobin, it was decided to perform an analysis of compared transcriptomics in response to exogenous NO by RNAseq (Wang *et al*., 2009). In the experimental conditions considered in the pharmacological studies, the expression pattern of the germinating spores of the fungus in NO exposed with non-exposed conditions was compared for strains B05.10 and *ΔBcfhg*1, respectively. The germinating spore expression pattern of both strains was also compared in non-exposed conditions to eliminate genes that could have changed their expression because of the mutation. The analysis of the results of the three comparisons shows an influence of NO on numerous and diverse mechanisms and systems that include nitrogen metabolism, asexual and sexual development and secondary metabolism.

In wild type spores, exogenous NO represented an alternative nitrogen source for the fungus, the nitrate produced from the oxidation of NO by the action of flavohemoglobin. Nitrate must have acted as a transcriptional inducer, favouring the activation of the genes of its assimilation pathway, including nitrate reductase (*BcniaD*) and nitrite reductase (*BcniiA*). Next, by the action of *BcniaD* and *BcniiA*, the nitrate was reduced to ammonium, which was incorporated into the cellular amino acid pool via glutamate and glutamine biosynthesis (Schinko *et al*., 2010). Finally, the cell would have detected the repressing nitrogen source (ammonium/glutamine/glut amate) triggering the Nitrogen Catabolite Repression (NCR). This is a transcriptional regulation program that allows fungi to use alternative or non- preferential nitrogen sources (nitrate, nitrite, purines, amides, most amino acids, and proteins) when there are no preferential sources (ammonia, glutamine, and glutamate) (Milhomem Cruz-Leite *et al*., 2020). On the other hand, there is a certain alteration mediated by the regulation by calcium and MAP (Mitogen-Activated Protein) kinase cascades, of the balance between fermentative and respiratory metabolism, of the tricarboxylic acid (TCA) cycle and the γ-aminobutyric acid (GABA) shunt (an alternative energy production pathway activated during cellular stress, when the function of TCA cycle is compromised) and the High-Osmolarity Glycerol (HOG)-MAPK pathway, a two-component osmosensor

system that responds to different types of stress, reporting intact capacity of the B05.10 strain to deal with the effects of nitrosative stress and regain its normal homeostatic state (Baltussen *et al*., 2019).

In mutant spores, changes in the expression of numerous genes related to the generation and detoxification of reactive nitrogen and oxygen species and the activation of the mitochondrial retrograde response (a retro-communicating of the mitochondria with the nucleus as a consequence of the adaptation to stress and which results in the promotion of cytoprotective mechanisms) (Schumacher *et al*., 2014) show the greater susceptibility of this unprotected system to nitrosative stress imposed by exogenous NO. Likewise, the absence of flavohemoglobin determined a more intense NCR than in B05.10 whose activation would be attributed to the production of NO_2^- from the spontaneous oxidation of NO (Yamasaki, 2000; Schinko *et al*., 2010). The nitrite thus formed would have activated *BcniiA* in the mutant cells, ultimately producing the repressing nitrogen source. On the other hand, now the alteration of the balance between fermentative and respiratory metabolism and of the HOG-MAPK pathway suggests a possible entry into a state of dormancy or quiescence of fungal cells as a consequence of the stress situation derived from exposure to NO. In addition, a strong influence of the molecule on the secretome and secondary metabolism of the fungus was observed, especially in the latter, where a negative regulatory effect dependent on *Bcfhg*1 on the structural genes of the melanin biosynthesis pathway stands out (Schumacher, 2015; Baltussen *et al*., 2019).

The comparison of the pattern of the germinating spores of both strains in non-exposed conditions, allowed to detect the presence of regulatory sequences of the genes neighbouring *Bcfhg*1 within the DNA fragment deleted in the strain *ΔBcfhg*1 during its generation (Turrion-Gomez *et al*., 2010). Furthermore, a certain regulatory role was attributed, in a NO-dependent manner, to *Bcfhg*1 on the expression of a gene related to the GO term of integral component of membrane.

Chapter II focuses on the characterization of the *Bcmed* gene in *B. cinerea*.

MedA was first described by Clutterbuck (1969) in a mutational analysis of individual morphological mutants in *A. nidulans*. In this species, *ΔmedA* mutants show a delay in the production of phialides, a reduced number of conidia, the emergence of secondary conidiophores and overproduction of primary sterigmata (metulae) in a branching pattern that produces medusoid-like conidiophores. This incorrect morphology has been attributed, in part, to modified *brlA* and *abaA* expression since it has been established that *medA* modulates the conidiation core regulatory pathway (*brlA*> *abaA*> *wetA*) at several levels. Since then, *medA* has also been studied in other filamentous fungi where conserved homologues are found.

In *B. cinerea*, *Bcmed* gene is annotated with the code Bcin12g00460 (GenBank) and is located in chromosome 12. Two splice variants are annotated for this gene. Bcin12g00460.1 encompasses 5 exons and its predicted ORF generates a 719 amino acids protein. The second splice variant, Bcin12g00460.2, also codes for the same protein. However, the 5' UTR of this variant is longer and more complex, deriving from alternative splicing of one additional intron within 5' UTR. This causes the appearance of a sixth exon

in that area compared to the first transcript. A phylogenetic analysis determined that *Bcmed* amino acid sequence shows high homology along the entire sequence with those of representatives of the *Ascomycota*, *Basidiomycota* and *Mucoromycota* divisions and the highest conservation was found around the region where *MedA* minimal nuclear localization domain have been described in *A. fumigatus* (Abdallah *et al*., 2012).

A RT-qPCR analysis of the expression pattern of *Bcmed* determined that its transcripts are present throughout the different developmental stages during the first 20 hours of the development of the fungus in liquid medium with agitation. The gene is expressed in a stable and constitutive way during the early stages of development, and its level of expression increases 25 -fold during the growth of mature mycelium.

To determine the function of *Bcmed* we followed a strategy consisting of the deletion of the gene and analysis of the resulting phenotypes. Two mutant strains, *ΔBcmed*34 and *ΔBcmed*84, were obtained by transformation of B05.10 strain protoplasts with a plasmid carrying a hygromycin resistance expression cassette flanked by the 5' and 3' regions of the *Bcmed* gene, which allows its integration into the homologous *locus* of the genome of the fungus through homologous recombination.

The two strains deficient in the *Bcmed* gene are affected in their ability to grow saprophytically on synthetic media, with a considerable delay in their growth compared to B05.10. Their growth pattern is altered, leading to dense and compact colonies. The mycelium arising presents beige hyphae that never acquire the characteristic dark brown coloration of the strain and that have a lower septa frequency than the wild type. It is incapable of producing macroconidia, although it does produce microconidia, but in lower density. Likewise, their capacity to infect the host plant is impaired showing a reduced aggressiveness, probably due to alterations in its capacity for saprophytic growth and development.

In order to demonstrate that the observed mutant phenotype was specifically due to the deletion of the gene, attempts to obtain a complemented mutant strain were carried out. For this, a vector with a nourseothricin selection marker, different from that of hygromycin used to generate the mutant, and where the *Bcmed* wild-type allele was cloned using the Gateway methodology (Invitrogen) was used. Through protoplasts transformation of the strain *ΔBcmed*84 the wild-type allele, together with the nourseothricin selection marker, was introduced in an unknown place in the mutant genetic background. However, this strain failed to show full complementation as complete recovery of normal behaviour in terms of development was not achieved, always presenting intermediate phenotypes between the mutant and the wild type. A possible cause that would explain this result is that the ectopic integration of *Bcmed* may have resulted in an inadequate level or temporal pattern of transcription, either because of the wrong chromatin context or because of the occurrence of meiotic silencing by unpaired DNA in an ectopic location (Shiu *et al*., 2001; Rodenburg *et al*., 2018).

The mutant phenotype of *B. cinerea* shows differences with the mutants for orthologs in *A. nidulans* and *A. fumigatus* where the deletion of the gene did not result in a mycelium defective in the

growth of its hyphae or sterile, lacking conidiophores, but it affected the morphology of these causing the appearance of aberrant-looking conidiophores (Clutterbuck, 1969; Busby, *et al*., 1996; Ichinomiya *et al*., 2005; Etxebeste *et al*., 2010; Gravelat *et al*., 2010; Al Abdallah *et al*., 2012). In *F. oxysporum*, the conidiophores are replaced by rod-shaped cells in a single chain in the mutant in the *ren*1 gene, ortholog of *Bcmed*, but its growth capacity on synthetic media was not affected (Ohara *et al*., 2004). A similar phenotype was detected in the mutants of the *M. grisea* orthologous gene where hyphal growth was not affected by the mutation, but the formation of conidiophores was affected, which were replaced by an acropetal pattern of conidiation (Lau and Hamer, 1998; Nishimura *et al*., 2000). These differences among the mutants for the *Bcmed* orthologs could be due to the different architecture of the conidiophore among species, which would have caused the activity of the *Bcmed* protein to have specialized to a certain degree, regulating the expression of different target genes than do its orthologs (Yu *et al*., 2006, Mah *et al*., 2006; Gravelat *et al*., 2010; Canessa *et al*., 2013; Schumacher *et al*., 2014; Cohrs *et al*., 2016; Schumacher, 2017; Schumacher and Tudzynski, 2012; Chen *et al*., 2010).

Finally, in chapter III, the results of the first analyses carried out for the characterization of the *Bcorp*1 gene are collected, which is in a preliminary stage.

Transposon tagging is a technique based on the use of transposons, which due to their ability to be excised from their initial location and integrated into another new region of the genome, allow the identification of genes of interest as insertion of a transposon both disrupts and tags a gene (Becker *et al*., 2001; Dufresne and Daboussi, 2010). Villalba *et al*. (2001) used this technique, introducing impala, a Tc1- mariner transposable element from *F. oxysporum*, in a *M. grisea* nitrate reductase-deficient mutant by transformation. A copy of impala inserted in the promoter of *niaD* encoding *A. nidulans* nitrate reductase was used in the transformation, so the impala excision was monitored by restoration of prototrophy for nitrate. One non-pathogenic mutant (rev77) was obtained. The flanking areas of the impala insertion site in rev77 were analysed and the mutant was successfully complemented with a 3 -kb genomic fragment from a wild-type *locus*. This gene, called 'orphan gene required for pathogenicity 1' (*ORP1*), was found to be essential for penetration of rice leaves and barley tissue.

Homology comparisons made by BLASTP identified the B. cinerea Bcin09g01160 (GenBank) gene product as sharing significant homology with *M. grisea orp*1. The gene is located on chromosome 9 and gives rise to two transcripts. Bcin09g01160.1 is 6088 nt in length and consists of five exons of which only the last two are coding exons. Its translation initiates within the fourth exon giving rise to an 859 amino acids protein. Bcin09g01160.2 is 6022 nt in length and shares with the first one the first, second, fourth and fifth exons, but an intron is recognized within the third exon and alternatively spliced giving rise to a transcript derived from six exons. It is also codes for the same 859 amino acids. The *Bcorp*1 sequence presented a highly conserved region in the central region of its sequence of approximately 130 amino acids in a phylogenetic analysis performed with orthologs present in several species representing only Pezizomycotina, since a BLASTP-type analysis reported its absence in other subdivisions.

Summary / Resumen

The analysis of the function of *Bcorp*1 is based on the same approach used for the characterization of *Bcmed*, the evaluation of the phenotypes of mutant strains lacking the gene. These strains were obtained using a vector harbouring the 5' and 3' regions of the *Bcorp*1 in a position such that they flank a hygromycin resistance expression cassette. Through protoplasts transformation of strain B05.10, the antibiotic resistance cassette was integrated in the *locus* of the Bcin09g01160 gene, producing a substitution between the two through a homologous recombination event between the corresponding sequences of the flanking regions of the mutant and the wild-type allele copies. Three mutant strains, *ΔBcorp*1-3, *ΔBcorp*1-19 and *ΔBcorp*1-45 were obtained.

These mutant strains do not show obvious developmental alterations compared to B05.10. They develop at the same rate as the control strain giving rise to the characteristic dark brown mycelium of this strain that contains spore-laden conidiophores that are capable of germination. On the other hand, preliminary virulence tests carried out on bean and grapevine leaves show that *Bcorp*1, like its ortholog in *Magnaporthe*, is involved in pathogenicity. Both observations indicate that the gene is a pathogenicity factor considering as such those genes necessary for disease development, but not essential for the pathogen to complete its lifecycle *in vitro* (Idnurm and Howlett, 2001). More specifically, although the *Bcorp*1 gene mutation does not seem to have affected the ability of the fungus to infect bean plants, it does seem to be involved during grapevine infection, where the mycelium of the mutant strains was unable to expand from the inoculum and to form lesions. These results together with the consulting of online available RNAseq data during *B. cinerea* infection in different hosts (Reboledo *et al*., 2020; De Cremer *et al*., 2013; Coolen *et al*., 2016; Srivastava *et al*., 2020; Haile *et al*., 2020) suggest that *Bcorp*1 role could be dependent on the host, the gene being specifically activated during grapevine infection.

In addition to the virulence assays, a differential expression analysis using RNAseq has been carried out between mycelium samples of B05.10 strain and one of the three deletion mutant strains obtained, *ΔBcorp*1-19, grown in solid medium. Currently the results of this analysis are being evaluated and it is expected that they will inform about the cellular processes that are affected in fungal cells due to the deletion of *Bcorp*1 during saprophytic growth.

Resumen

El óxido nítrico es una molécula señalizadora con funciones importantes y variadas en los distintos grupos taxonómicos, incluyendo a los hongos. En este reino, la molécula ha sido pobremente estudiada, pero se sabe que desempeña una vasta función señalizadora que abarca desde la modulación del desarrollo sexual y asexual y del metabolismo secundario hasta la colonización e infección de la planta hospedadora. Debido a estas múltiples funciones y su tiempo de vida corto, de unos pocos segundos, se hace fundamental la presencia de un balance que mantenga una concentración adecuada de NO en cada estado del ciclo de vida del hongo a través tanto de las reacciones de biosíntesis de la molécula como de sus mecanismos de detoxificación (Cánovas et al., 2016).

Hasta el momento, dos vías de síntesis de NO han sido identificadas en hongos. La ruta oxidativa implicaría la presencia de una vía similar a la ruta oxidativa presente en mamíferos en la que la enzima óxido nítrico sintasa (NOS) cataliza la conversión de L-arginina a L-citrulina produciendo óxido nítrico. Sin embargo, se trata de una ruta poco caracterizada debido a la ausencia de proteínas similares a la NOS (NOSLs) en los genomas fúngicos (Li et al., 2010; Samalova et al., 2013). La otra ruta es la ruta reductora, que requiere la acción sinérgica de la enzima nitrato reductasa para convertir el nitrato a nitrito y de la enzima nitrito reductasa que media la conversión de nitrito a NO y se considera que es la fuente enzimática de NO más importante en hongos (Horchani et al., 2011; Zhao et al., 2020).

Los mecanismos catabólicos del NO están destinados a combatir la toxicidad de la molécula cuando alcanza altas concentraciones en las células, lo que puede desencadenar estrés nitrosativo (Brown and Borutaite, 2006; Fitzpatrick and Kim, 2015; Marroquin-Guzman *et al*., 2017).

Estos mecanismos se basan principalmente en reacciones de oxidorreducción del NO o de sus formas derivadas, y entre ellos destacan las flavohemoglobinas que constituyen el mecanismo de desintoxicación inducible del NO mejor descrito en modelos fúngicos (Forrester and Foster, 2012). Estas enzimas son globinas quiméricas formadas por un dominio globina N-terminal y un dominio adyacente con actividad redox y de posición C-terminal. Su función se describe como NO dioxigenasas que requieren NADPH, FAD y O_2 para convertir NO en NO_3^- (Hausladen *et al*., 1998; Gardner *et al*., 1998).

Botrytis cinerea es un hongo patógeno necrotrófico vegetal que infecta a más de 200 especies de cultivos, causando la enfermedad del moho gris con grandes pérdidas de producción agronómica en todo el mundo. El hongo tiene un solo gen, *Bcfhg*1, que codifica una flavohemoglobina funcional de la cual se ha sugerido que podría estar más relacionada con la modulación de los niveles de NO endógeno producidos por el hongo durante etapas específicas del desarrollo que con la protección del hongo contra niveles tóxicos de la molécula (Turrion-Gomez *et al*., 2010; Turrion-Gomez *et al*., 2011).

En este sentido, con la intención de caracterizar los procesos fisiológicos en los que el metabolismo del NO es relevante en el hongo, nuestro grupo de investigación realizó un análisis de un experimento de microarray de perfiles de expresión génica en respuesta a fármacos moduladores de los

niveles de NO en esporas de la cepa silvestre B05.10 y de *ΔBcfhg*1, cepa mutante defectuosa en el gen *Bcfhg*1 (Daniela Santander, Tesis Doctoral. Universidad de Salamanca). Este análisis permitió identificar, en el caso de la cepa mutante, que las categorías funcionales "ciclo celular", "síntesis de ADN" y "actividad nucleolo" fueron reprimidas por la acción de la molécula. Más específicamente, los genes con mayor nivel de represión fueron los ortólogos de los genes *mcm* (2-7) de *S. cerevisiae*, genes cuyos productos génicos conforman un complejo proteico esencial para la formación de los orígenes de la replicación y para la iniciación. de síntesis de ADN (Lei y Tye, 2001) y que se expresan entre la fase M y la fase G1 del ciclo celular (Enserink y Kolodner, 2010). La expresión de este grupo de genes está controlada por el factor de transcripción *mcm*1. También se encontró una fuerte represión de genes que se expresan específicamente en la fase G1. En esta levadura, la expresión de genes específicos de G1 está controlada por los complejos MBF, un factor de transcripción compuesto por *mbp*1 y *swi*6, y SBF, un factor de transcripción compuesto por *swi*4 y *swi*6. MBF controla preferentemente la expresión de genes relacionados con la replicación y reparación del ADN, mientras que SBF regula la expresión de genes implicados en el progreso del ciclo celular, la morfogénesis celular y la duplicación del cuerpo polar del huso (Enserink y Kolodner, 2010). También se reprimió el ortólogo del gen que codifica la enzima fosfatasa CDC25 de *S. pombe*. *cdc*25 participa en la activación de *cdk*1 (*cdc*2 en *S. pombe*) por desfosforilación. Esta última es una enzima clave en la regulación del ciclo celular ya que controla la entrada de la célula a la fase de mitosis desde la fase G2. Otros genes que se expresaron diferencialmente en este análisis, pero en B05.10 fueron *Bcmed* y *Bcorp*1. El primero es un factor regulador transcripcional que fue diferencialmente inducido cuando las esporas se cultivaron en presencia del secuestrador de NO, c -PTIO. El segundo codifica para una proteína hipotética y se indujo cuando el hongo se expuso al NO.

En este contexto, en el presente trabajo nos propusimos analizar la función de varios de los genes antes mencionados como codificadores de proteínas reguladoras del ciclo celular y posibles dianas de óxido nítrico. Además, se consideró la caracterización funcional de los genes *Bcmed* y *Bcorp*1.

El capítulo I describe en primer lugar el efecto modulador que tiene el NO sobre el desarrollo asexual de *B. cinerea*. Se realizaron ensayos de germinación en las que se incubaron esporas de las cepas B05.10 y *ΔBcfhg*1 del hongo en presencia de los fármacos DETA, un donador de NO, c -PTIO, un secuestrador de NO, y L-NNA, un inhibidor de la actividad óxido nítrico sintasa de mamíferos, en diferentes tiempos de muestreo. Los recuentos, estimaciones y tinciones con el colorante DAPI realizados en los cultivos determinaron que el NO tiene un efecto regulador negativo inmediato pero transitorio sobre la germinación, la elongación del tubo germinativo y la tasa de división nuclear del hongo. La flavohemoglobina BcFHG1 se presenta como una proteína con una potente función protectora frente a estos efectos.

La inmediatez y transitoriedad observada en la acción del NO sugiere una rápida acción de señalización por parte de la molécula y nos condujo a plantear la hipótesis de que, e n las condiciones evaluadas, el NO estaría afectando a la actividad de componentes esenciales para el progreso del ciclo celular a través de la modificación covalente de residuos de cisteína (S-nitrosilación) y de tirosina

(nitración de tirosina). En concreto, propusimos que la molécula afectaría a las proteínas codificadas por los genes *mbp*1, *swi*4, *swi*6, *cdc*2, *cdc*25 y *mcm*1. Esta lista se completó con la inclusión del gen que codifica para la enzima nitrato reductasa, *niaD*. Esta proteína juega un papel relevante en la homeostasis del NO ya que participa en la síntesis reductora de la molécula y en su regulación durante el desarrollo fúngico (Cánovas *et al*., 2016). Además, se ha descrito *in silico* una posible S-nitrosilación de los residuos de cisteína en la superficie de esta proteína en plantas (Fu *et al*., 2018).

Posteriormente, estas proteínas fueron sometidas a un análisis que tuvo como objetivo determinar la posible alteración de su actividad debido a modificaciones postraduccionales provocadas por la acción de la molécula. Una vez que los genes homólogos seleccionados en *S. cerevisiae* y *S. pombe* se identificaron en el genoma de *B. cinerea*, se llevó a cabo la construcción de una fusión traduccional en la que la secuencia del gen que codifica la proteína GFP fue fusionada al extremo C-terminal de la proteína codificada por cada uno de los genes de interés utilizando la tecnología Gateway (Invitrogen). Se obtuvieron varias cepas transformantes para cada proteína fusión, pero la evaluación de los niveles de S-nitrosilación y/o nitración de estas no fue posible debido a la incapacidad para purificarlas a partir de extractos de proteínas totales.

Por otro lado, para obtener información sobre los factores y procesos fisiológicos que median la respuesta al NO previamente observada en las esporas en germinación y que pueden verse afectados por la función desintoxicante del NO de una flavohemoglobina, se decidió realizar un análisis de transcriptómica comparada en respuesta a NO exógeno mediante RNAseq (Wang *et al*., 2009). En las condiciones experimentales consideradas en los estudios farmacológicos, se comparó el patrón de expresión de las esporas en germinación del hongo en condiciones de exposición a NO con condiciones de no exposición para las cepas B05.10 y *ΔBcfhg*1, respectivamente. El patrón de expresión de esporas en germinación de ambas cepas también se comparó en condiciones de no exposición para eliminar genes que podrían haber cambiado su expresión debido a la mutación. El análisis de los resultados de las tr es comparaciones muestra una influencia del NO en numerosos y diversos mecanismos y sistemas que incluyen el metabolismo del nitrógeno, el desarrollo asexual y sexual y el metabolismo secundario.

En las esporas de tipo silvestre, el NO exógeno representó una fuente de nitrógeno alternativa para el hongo, el nitrato producido a partir de la oxidación del NO por la acción de la flavohemoglobina. El nitrato debe haber actuado como inductor transcripcional, favoreciendo la activación de los genes de su vía de asimilación, entre los que se encuentran la nitrato reductasa (*BcniaD*) y la nitrito reductasa (*BcniiA*). A continuación, mediante la acción de *BcniaD* y *BcniiA*, el nitrato fue reducido a amonio, que se incorporó al pool celular de aminoácidos mediante la biosíntesis de glutamato y glutamina (Schinko *et al*., 2010). Finalmente, la célula habría detectado la fuente de nitrógeno represor (amonio / glutamina / glutamato) desencadenando la represión catabólica por nitrógeno (RCN). La RCN se trata de un programa de regulación transcripcional que permite a los hongos utilizar fuentes de nitrógeno alternativas o no preferenciales (nitrato, nitrito, purinas, amidas, la mayoría de los aminoácidos y proteínas) cuando no existen fuentes preferenciales (amoniaco, glutamina y glutamato) (Milhomem Cruz-Leite *et al*., 2020). Por

otro lado, existe una cierta alteración mediada por la regulación por calcio y cascadas de MAPKs (proteínas quinasas activadas por mitógenos), del balance entre el metabolismo fermentativo y respiratorio, del balance entre el ciclo del ácido tricarboxílico (TCA) y del GABA (ácido γ-aminobutírico) shunt (una vía alternativa de producción de energía activada durante el estrés celular, cuando la función del ciclo de TCA está comprometida) y de la vía

"del glicerol de alta osmolaridad" (HOG, por sus siglas en inglés)-MAPK, un sistema osmosensor de dos componentes que responde a diferentes tipos de estrés. Estos resultados informan de la capacidad intacta de la cepa B05.10 para hacer frente a los efectos del estrés nitrosativo y recuperar su estado homeostático normal (Baltussen *et al*., 2019).

En las esporas mutantes, cambios en la expresión de numerosos genes relacionados con la generación y desintoxicación de especies reactivas de nitrógeno y oxígeno y de la activación de la respuesta retrógrada mitocondrial (una retrocomunicación de la mitocondria con el núcleo como consecuencia de la adaptación al estrés y que se traduce en la promoción de mecanismos citoprotectores) (Schumacher *et al*., 2014) muestran la mayor susceptibilidad de este sistema desprotegido al estrés nitrosativo impuesto por el NO exógeno.

Asimismo, la ausencia de la flavohemoglobina determinó una RCN más intensa que en B05.10 cuya activación se atribuiría a la producción de NO_2^- procedente de la oxidación espontánea de NO (Yamasaki, 2000; Schinko *et al*., 2010). El nitrito así formado habría activado *BcniiA* en las células mutantes, produciendo en último término la fuente de nitrógeno represor. Por otro lado, ahora la alteración del equilibrio entre el metabolismo fermentativo y respiratorio y la de la vía HOG-MAPK sugiere una posible entrada en un estado de latencia o quiescencia de las células fúngicas como consecuencia de la situación de estrés derivada de la exposición al NO. Además, se observó una fuerte influencia de la molécula sobre el secretoma y el metabolismo secundario del hongo, especialmente en este último, donde destaca un efecto regulador negativo dependiente de *Bcfhg*1 sobre los genes estructurales de la vía de biosíntesis de la melanina (Schumacher, 2015; Baltussen *et al*., 2019).

La comparación del patrón de las esporas en germinación de ambas cepas en condiciones de no exposición permitió detectar la presencia de secuencias reguladoras de los genes vecinos a *Bcfhg*1 dentro del fragmento de ADN delecionado en la cepa *ΔBcfhg*1 durante su generación (Turrion-Gomez *et al*., 2010). Además, se atribuyó a *Bcfhg*1 un cierto papel regulador, dependiente del NO, sobre la expresión de un gen relacionado con el término GO de componente integral de membrana.

El capítulo II se centra en la caracterización del gen *Bcmed* en *B. cinerea*.

MedA fue descrito por primera vez por Clutterbuck (1969) en un análisis mutacional de mutantes morfológicos individuales en *A. nidulans*. En esta especie, los mutantes *ΔmedA* muestran un retraso en la producción de fiálides, un número reducido de conidios, la aparición de conidióforos secundarios y la sobreproducción de esterigmas primarios (métulas) en un patrón de ramificación que produce conidióforos de tipo medusoide. Esta morfología incorrecta se ha atribuido, en parte, a la expresión

modificada de *brlA* y *abaA*, ya que se ha establecido que *medA* modula los genes que componen la vía reguladora nuclear de conidiación (*brlA*> *abaA*> *wetA*) a varios niveles. Desde entonces, *medA* también se ha estudiado en otros hongos filamentosos donde se encuentran homólogos conservados.

En *B. cinerea*, el gen *Bcmed* está anotado con el código Bcin12g00460 (GenBank) y está ubicado en el cromosoma 12. Dos variantes de splicing están anotadas para este gen. Bcin12g00460.1 abarca 5 exones y su ORF predicha genera una proteína de 719 aminoácidos. La segunda variante, Bcin12g00460.2, también codifica la misma proteína. Sin embargo, la 5' UTR de esta variante es más larga y compleja, y procede del splicing alternativo de un intrón adicional dentro de la 5' UTR. Esto provoca la aparición de un sexto exón en esa zona en comparación con el primer transcrito. Un análisis filogenético determinó que la secuencia de aminoácidos de *Bcmed* muestra una alta homología a lo largo de toda la secuencia con las de representantes de las divisiones *Ascomycota*, *Basidiomycota* y *Mucoromycota* y el mayor grado de conservación se encontró alrededor de la región donde se ha descrito el dominio mínimo de localización nuclear de *MedA* en *A. fumigatus*. (Abdallah *et al*., 2012).

Un análisis por RT-qPCR del patrón de expresión de *Bcmed* determinó que sus transcritos están presentes a lo largo de las diferentes etapas de desarrollo durante las primeras 20 horas del desarrollo del hongo en medio líquido con agitación. El gen se expresa de forma estable y constitutiva durante las primeras etapas del desarrollo, y su nivel de expresión aumenta 25 veces durante el crecimiento del micelio maduro.

Para determinar la función de *Bcmed* seguimos una estrategia consistente en la deleción del gen y el posterior análisis de los fenotipos resultantes. Se obtuvieron dos cepas mutantes, *ΔBcmed*34 y *ΔBcmed*84, mediante la transformación de protoplastos de la cepa B05.10 con un plásmido que lleva un casete de expresión de resistencia a higromicina flanqueado por las regiones 5' y 3' del gen *Bcmed*, lo que permite su integración en el *locus* homólogo del genoma del hongo mediante recombinación homóloga.

Las dos cepas deficientes en el gen *Bcmed* se ven afectadas en su capacidad para crecer saprofíticamente en medios sintéticos, con un retraso considerable en su crecimiento en comparación con B05.10. Su patrón de crecimiento está alterado, dando lugar a colonias densas y compactas. El micelio resultante presenta hifas beige que nunca adquieren la coloración marrón oscura característica de la cepa y que tienen una septación más espaciada que la silvestre. Es incapaz de producir macroconidios, aunque sí microconidios, pero en menor densidad. Asimismo, su capacidad de infectar a la planta hospedadora se ve afectada mostrando una agresividad reducida, probablemente debido a las alteraciones en su capacidad de crecimiento saprofítico y desarrollo.

Para demostrar que el fenotipo mutante observado se debía específicamente a la deleción del gen, se llevaron a cabo intentos de obtener una cepa mutante complementada. Para ello, se utilizó un vector con un marcador de selección para nourseotricina, diferente al de la higromicina utilizado para generar el mutante, y donde se clonó el alelo silvestre de *Bcmed* mediante la metodología Gateway (Invitrogen). Mediante la transformación de protoplastos de la cepa *ΔBcmed*84, el alelo de tipo silvestre,

junto con el marcador de selección para nourseotricina, se introdujo en un lugar desconocido en el fondo genético mutante. Sin embargo, esta cepa no mostró una complementación completa ya que no se logró la recuperación completa del comportamiento normal en términos de desarrollo, pre sentando siempre fenotipos intermedios entre el mutante y el silvestre. Una posible causa que explicaría este resultado es que la integración ectópica de *Bcmed* puede haber resultado en un nivel o patrón temporal de transcripción inadecuados, ya sea por un contexto de cromatina incorrecto o por la ocurrencia de silenciamiento meiótico por ADN desapareado en una ubicación ectópica (Shiu *et al*., 2001; Rodenburg *et al*., 2018).

El fenotipo mutante de *B. cinerea* muestra diferencias con los mutantes para los ortólogos en *A. nidulans* y *A. fumigatus* donde la deleción del gen no resultó en un micelio defectuoso en el crecimiento de sus hifas o estéril, carente de conidióforos, pero sí afectó a la morfología de estos provocando la aparición de conidióforos de aspecto aberrante (Clutterbuck, 1969; Busby, *et al*., 1996; Ichinomiya *et al*., 2005; Etxebeste *et al*., 2010; Gravelat *et al*., 2010; Al Abdallah *et al*., 2012). En *F. oxysporum*, los conidióforos son reemplazados por células en forma de bastón unidas formando una sola cadena en el mutante en el gen *ren*1, ortólogo de *Bcmed*, pero su capacidad de crecimiento en medios sintéticos no se vio afectada (Ohara *et al*., 2004). Se detectó un fenotipo similar en los mutantes del gen ortólogo de *M. grisea* donde el crecimiento de las hifas no se vio afectado por la mutación, pero sí la formación de conidióforos, los cuales fueron reemplazados por un patrón acropétalo de conidiación (Lau y Hamer, 1998; Nishimura *et al*., 2000). Estas diferencias entre los mutantes para los ortólogos de *Bcmed* podrían deberse a la diferente arquitectura del conidióforo entre las especies, lo que habría provocado que la actividad de la proteína *Bcmed* se especializara hasta cierto punto, regulando la expresión de genes diana diferentes a los de sus ortólogos (Yu *et al*., 2006, Mah *et al*., 2006; Gravelat *et al*., 2010; Canessa *et al*., 2013; Schumacher *et al*., 2014; Cohrs *et al*., 2016; Schumacher, 2017; Schumacher and Tudzynski, 2012; Chen *et al*., 2010).

Finalmente, en el capítulo III se recogen los resultados de los primeros análisis realizados para la caracterización del gen *Bcorp*1, la cual se encuentra en una etapa preliminar.

El transposon tagging es una técnica basada en el uso de transposones, que debido a su capacidad para ser escindidos de su ubicación inicial e integrados en otra nueva región del genoma, permiten la identificación de genes de interés ya que la inserción de un transposón interr umpe y marcaun gen al mismo tiempo (Becker *et al*., 2001; Dufresne and Daboussi, 2010). Villalba *et al*. (2001) utilizaron esta técnica, introduciendo impala, un elemento transponible Tc1 -mariner de *F. oxysporum*, en un mutante de *M. grisea* deficiente en la nitrato reductasa por transformación. En la transformación se usó una copia del impala insertada en el promotor de *niaD* que codifica para la nitrato reductasa de *A. nidulans*, por lo que la escisión del impala se controló mediante la restauración de la prototrofía al nitrato. Se obtuvo un mutante no patógeno (rev77). Se analizaron las áreas flanqueantes del sitio de inserción del impala en rev77 y el mutante se complementó con éxito con un fragmento genómico de 3 kb de un *locus*

de tipo silvestre. Se descubrió que este gen, llamado "gen huérfano necesario para la patogenicidad 1" (ORP1, por sus siglas en inglés), es esencial para la penetración en hojas de arroz y cebada.

Las comparaciones de homología realizadas por BLASTP detectaron que el producto del gen Bcin09g01160 (GenBank) de *B. cinerea* comparte una homología significativa con *orp*1 de *M. grisea*. El gen se encuentra en el cromosoma 9 y da lugar a dos transcritos. Bcin09g01160.1 tiene una longitud de 6088 nucleótidos y consta de cinco exones de los cuales solo los dos últimos son exones codificantes. Su traducción se inicia dentro del cuarto exón dando lugar a una proteína de 859 aminoácidos.

Bcin09g01160.2 tiene 6022 nucleótidos de longitud y comparte con el primero los exones primero, segundo, cuarto y quinto, pero existe un intrón dentro del tercer exón y el splicing alternativo da lugar a un transcrito procedente de los seis exones resultantes. También codifica para los mismos 859 aminoácidos. La secuencia de *Bcorp*1 presentó una región altamente conservada en su región central de aproximadamente 130 aminoácidos en un análisis filogenético realizado con ortólogos presentes en varias especies representantes tan solo de Pezizomycotina, ya que un análisis tipo BLASTP reportó su ausencia en otras subdivisiones.

El análisis de la función de *Bcorp*1 se basa en el mismo enfoque utilizado para la caracterización de *Bcmed*, la evaluación de los fenotipos de cepas mutantes que carecen del gen. Estas cepas se obtuvieron usando un vector que alberga las regiones 5' y 3' de *Bcorp*1 en una posición tal que flanquean un casete de expresión de resistencia a higromicina. Por medio de la transformación de protoplastos dela cepa B05.10, el casete de resistencia al antibiótico se integró en el *locus* del gen Bcin09g01160, produciendo una sustitución entre los dos mediante un evento de recombinación homóloga entre las secuencias correspondientes de las regiones flanqueantes de las copias alélicas mutante y silvestre. Se obtuvieron tres cepas mutantes, *ΔBcorp*1-3, *ΔBcorp*1-19 y *ΔBcorp*1-45.

Estas cepas mutantes no muestran alteraciones obvias del desarrollo en comparación con B05.10. Se desarrollan al mismo ritmo que la cepa control dando lugar al micelio marrón oscuro característico de esta cepa que contiene conidióforos cargados de esporas que son capaces de germinar. Por otro lado, los ensayos preliminares de virulencia realizados en hojas de judía y vid muestran que *Bcorp*1, al igual que su ortólogo en *Magnaporthe*, está involucrado en la patogenicidad. Ambas observaciones indican que el gen es un factor de patogenicidad considerando como tal a aquellos genes necesarios para el desarrollo de la enfermedad, pero no esenciales para que el patógeno complete su ciclo de vida *in vitro* (Idnurm y Howlett, 2001). Más específicamente, aunque la mutación del gen *Bcorp*1 no parece haber afectado la capacidad del hongo para infectar plantas de judía, su proteína parece estar involucrada en la infección de la vid, donde el micelio de las cepas mutantes no pudo expandirse desde el inóculo y formar lesiones. Estos resultados, junto con la consulta de datos de RNAseq disponibles online y obtenidos durante la infección por *B. cinerea* de diferentes hospedadores (Reboledo *et al*., 2020; De Cremer *et al*., 2013; Coolen *et al*., 2016; Srivastava *et al*., 2020; Haile *et al*., 2020), sugieren que la función de *Bcorp*1 podría depender del hospedador, ya que el gen se induce específicamente durante la infección de la vid.

Además de los ensayos de virulencia, se ha realizado un análisis de expresión diferencial utilizando la tecnología de RNAseq entre muestras de micelio de la cepa B05.10 y de una de las tres cepas mutantes obtenidas por deleción, *ΔBcorp*1-19, cultivadas en medio sólido. Actualmente se están evaluando los resultados de este análisis y se espera que informen sobre los procesos celulares que se ven afectados en las células fúngicas debido a la deleción de *Bcorp*1 durante el crecimiento saprofítico.

Introduction

1. General aspects

Botrytis cinerea is a necrotrophic plant pathogenic fungus that infect more than 200 crop species, causing great losses of production worldwide. Its disease is called gray mould, name derived from the greyish colour and velvety texture characteristic of infected tissues.

The pathogen owns several features that make it difficult to control. It is a ubiquitous microorganism with presence in almost all climates and shows a wide variety of pathogenicity factors and mechanisms that allow it to attack the host plant in many different ways. This is strengthened by its numerous sources of inoculum, some of which allow it to survive for a long time in crop debris (Williamson *et al*., 2007).

The fungus exhibits a necrotrophic lifestyle, killing the host plant cells before colonization and feeding on the dead tissues. Although, it is mainly a pathogen of aerial parts of the plant such as leaves, flowers, fruits, buds, and stems, it can also infect seeds, both during their development and the post-harvest period (Elad *et al.*, 2004).

Besides, it is known that it can penetrate the host in an early stage of crop development and remains in a quiescent mode for long time until the environmental conditions and physiological state of the plant are favourable for the disease to begin. At this time, it can infect healthy tissues even modulating their defensive response for its own benefit (Van Kan, 2006; Williamson *et al*., 2007).

B. cinerea causes considerable economic losses in a wide range of crops which it attacks, including mainly dicotyledonous hosts, but also some monocotyledonous plant species. This, along with its scientific importance due to its biology and ecology features, have caused *B. cinerea* to be considered as the second phytopathogenic fungus in order of importance, and as a model for necrotrophic pathogens in molecular plant pathology (Elad *et al.*, 2015; Dean *et al*., 2012; van Kan, 2006).

2. Systematics

Botrytis genus is one of the oldest phytopathogenic genus and was described for the first time in 1729 by Michaeli and was related to the gray mould disease by Smith in 1900 (Smith, 1900). Later, Persoon described five species, among which he included one of the species described by Michaeli, *B. cinerea*. The relationship with its teleomorph *Botryotinia* spp. was established in the middle of the 20th century (Groves y Loveland, 1953) and the genus *Botrytis* was redefined by Hennebert (Hennebert, 1973), comprising today 30 recognized species and one hybrid. The genus *Botrytis* Persoon is composed by two clades. *B. cinerea* forms the first one along with *B. pelargonii*, *B. fabae*, *B. pseudocinerea* and *B. calthae*, all of them infecting uniquely dicots. The second clade is significantly more diverse and contains most species of the genus (Staats *et al*., 2005; Hyde *et al*., 2014).

B. cinerea is the name of the asexual state, its anamorph, while its sexual state is called *Botryotinia fuckeliana* (Williamson *et al*., 2007). It belongs to the fungi kingdom, division Ascomycota,

class Leotiomycetes, order Helotiales and family Sclerotiniaceae. Unlike for most fungal species, the name of the asexual state is the one accepted at all levels to identify the pathogen and not the sexual one (XVI International Botrytis Symposium, 2013, Bary, Italy).

3. Life cycle

In the life cycle of *B. cinerea* can be delimited a sexual phase and an asexual one (Figure 1).

The anamorph state is more frequent in nature. Under this state, *B. cinerea*, as typical ascomycete, shows a mycelium that changes its appearance according to the medium where it grows. If it grows inside the host plant, its mycelium will be septate and colourless while if it does on the plant tissue or artificial media, it will form cottony masses of branched and intertwined olive -brown hyphae whose diameter ranges between 11 µm and 23 µm.

This mycelium also generates specialized aerial hyphae at the ends of which structures 1 to 3 mm in length are differentiated and which constitute the conidiophores. These branch out abundantly ending in an elongated apical cell, the place where the conidia are produced, and that provides the representative appearance of the species as a thickened and arborescent raceme packed with macroconidia (Figure 2). These conidia are ovoid or globular, grayish, with a smooth texture and a size of 10 -12 × 8-10 µm, unicellular and their interior normally houses between 5 and 10 nuclei. It is common to expose mycelium, in synthetic media, to light in the near ultraviolet wavelengths because this radiation stimulates the formation of conidia (Epton and Richmond, 1980).

These macroconidia constitute the vegetative or asexual spores of the fungus and are its main mechanism of dispersion because they spread easily with the help of air, water or insects, and under high relative humidity and warm temperatures they germinate producing mycelium that starts again the asexual cycle. On the other hand, from old mycelium, the fungus can produce microconidia, smaller spherical conidia (2 to 3 µm in diameter), which, like macroconidia, are unicellular structures.

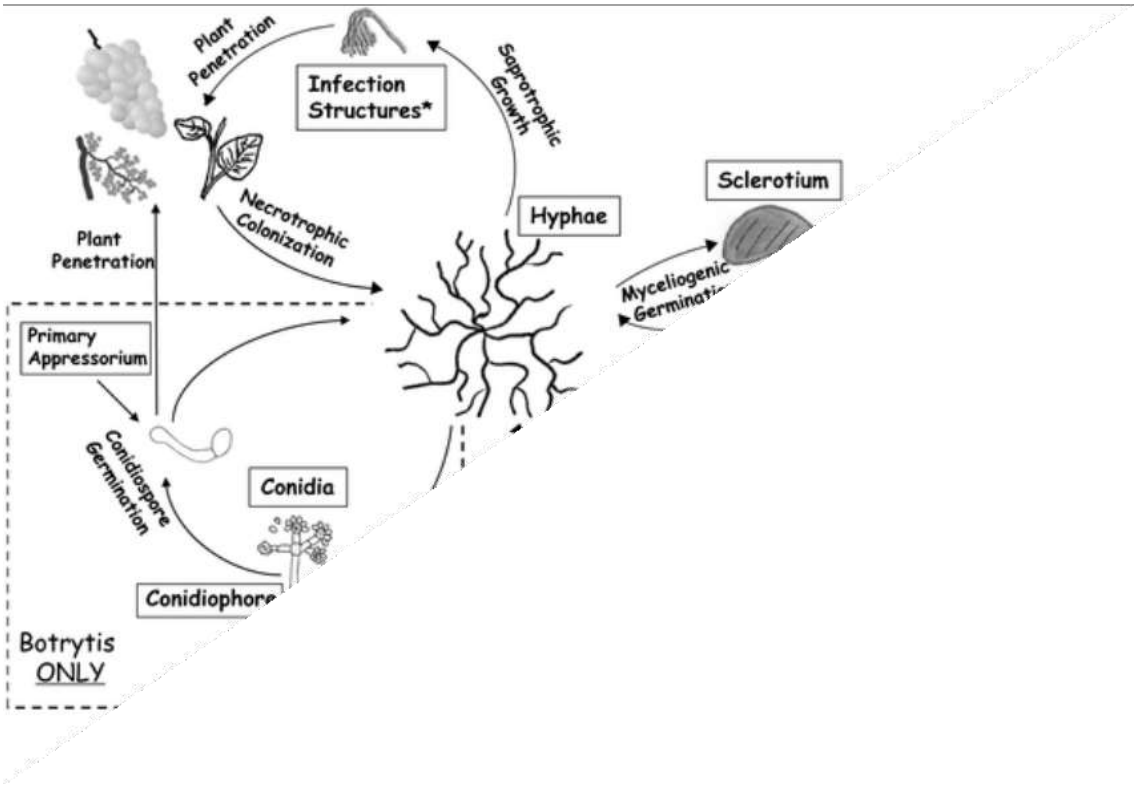

Figure 1. Life cycle of *B. cinerea* (and *S. sclerotiorum*) with the different development stages (sexual and asexual) (taken from Amselem *et al*., 2011).

A significant survival mechanism that mycelium shows in the presence of unfavourable environmental conditions are the sclerotia, discoidal or spherical resistance structures, with a size of 2 -4 × 1-3 mm and strongly adhered to the substrate. A mass of aggregated mycelium filaments constitutes the sclerotium marrow, which is covered by melanized cortical cells, initially whitish, but later acquire a dark colour, that prevent internal mycelium from desiccation and preserve it from ultraviolet radiation and the attack of microorganisms for long periods of time (Backhouse and Willetts, 1984). The sclerotium germinates once adverse conditions have been overcome and new mycelium develops. This last developmental stage takes place in a short period of time if the fungus is grown *in vitro*, on synthetic media.

Most field isolates of *B. cinerea* are heterothallic because they belong to one of two alternative sexual forms, each determined by the presence of a particular allelic form of the gene responsible for the sexual type, the MAT1-1 allele or the MAT1-2 allele (Faretra *et al*., 1988). The presence of the sexual form of the fungus in most crops has been scarcely referenced. However, the sexual cycle is liable to start when isolates of different sexual types coincide and the environmental conditions are appropriate. On the other hand, isolates capable of reacting sexually with the two sexual types described have also been described with very little frequency (Faretra and Pollastro, 1996; van der Vlugt-Bergmans *et al*., 1993). In any case, microconidia act as male parent in the cross because they carry out the spermatization of the sclerotia of the opposite sex strains (which act as female parent). This process of "fertilization" constitutes the beginning of the sexual cycle and continues with the production of apothecia (Figure 2) that present asci

with eight binucleated ascospores resulting from a meiosis process. Finally, the sexual or asexual cycle will be restarted by the mycelium produced after the germination of these ascospores. Alternatively, this mycelium can infect the host plant.

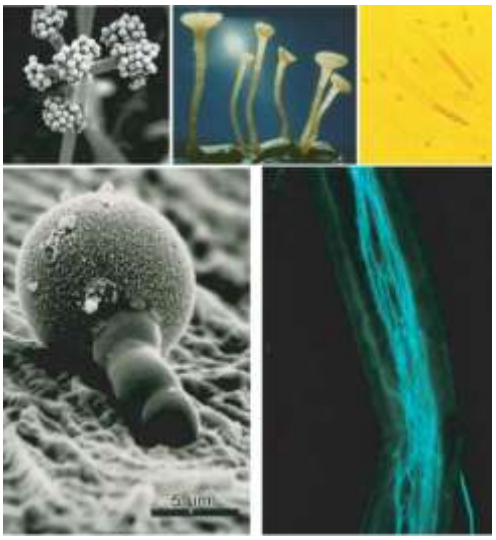

Figure 2. *B. cinerea* in different phases of its life cycle. Clockwise from top left: conidiophore with spores, apothecia, two asci with 8 ascospores, mycelium infecting a plant and germinating spore (taken from Williamson *et al.*, 2007).

4. Cycle of infection and epidemiology

Figure 3 shows a general and simplified diagram of the infection cycle of *B. cinerea*. Although the host can be infected by both asexual and sexual spores, conidia are the most important form of propagation of the pathogen during the vegetative period of the host plant. For its part, its survival and reproduction in successive years is based on the sclerotia and the mycelium itself. The cycle that conidia follow is divided into well-defined phases of germination in primary spots of infection, production, and dissemination, influenced by fluctuations in temperature and humidity in the early hours of the morning (Jarvis, 1962).

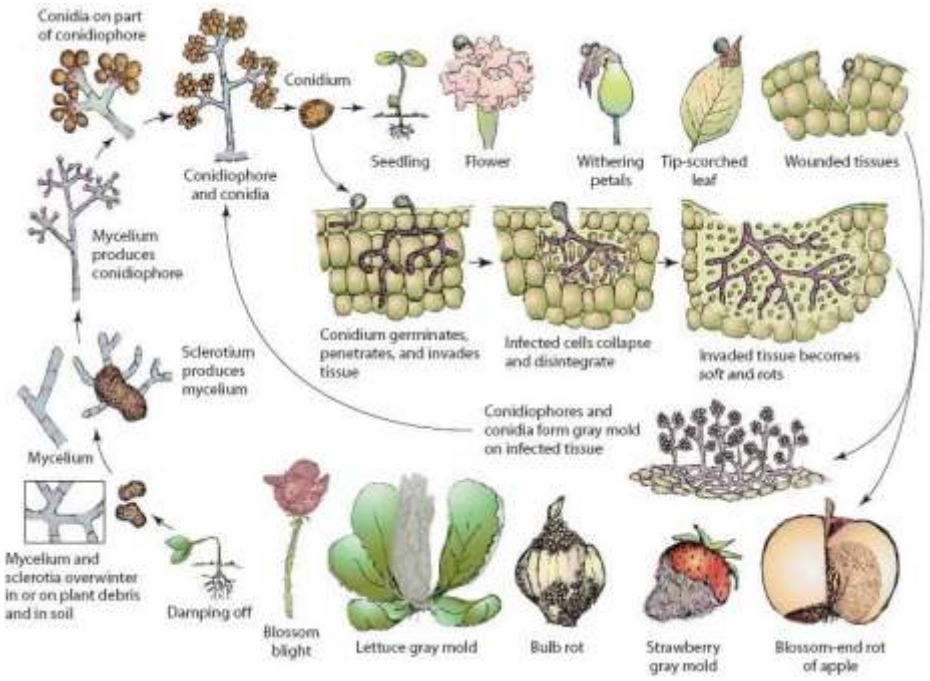

Figure 3. Infection cycle of *B. cinerea* (taken from Agrios, 2005).

Airborne or insect-mediated transport of *B. cinerea* conidia to the host plant is the beginning of the general infection cycle. Once on the host surface, the conidium germinates and begins the germinative development if the environment conditions allow it, while strongly adheres to the surface of plant cells. During this phase, in many species, the conidium develops penetration structures similar to the appressoria described in other species of phytopathogenic fungi, consisting of swelling of the germ tubes tips. The appressoria formed by *B. cinerea* resemble those developed by species of the genera *Colletotrichum* or *Magnaporthe*, because of the melanin present in the cell matrix associated with the fungal cell wall (Doss *et al*., 2003), but they differ from these in the lack of septum that isolates the appressorium from the germ tube, necessary to reach high osmotic pressures. This is the reason why *B. cinerea* appressoria are insufficient on their own, although they are necessary (Gourgues *et al*., 2004), for penetration into the host tissue to be successful. In other cases, penetration appears to occur directly through the cuticle and the cell wall, involving different enzymes that break down components of the wall.

Floral organs are important sites for the initiation of infection in small-fruited plants for several reasons (Figure 3): the stigmatic fluid is used by the conidium as a nutritive medium in some types of flowers. In addition, the germ tube can reach the ovary by following the path created by the pollen tubes. The infected petals are vehicles of the inoculum that, under conditions of high relative humidity and after being spread by the wind, infect other flowers whose petals will in turn become a new source of inoculum, which would trigger a series of infection cycles and successive sporulation that would result in a complete loss of the culture. Insects also play an important role in the infection cycle of *B. cinerea* because they cause lesions in plant tissues through which the pathogen can enter, in addition to acting as dispersal agents for their conidia.

The establishment phase of the fungus takes place after its penetration into the plant tissue and causes the death of cells adjacent to the point of penetration. At the same time, the defensive response of the plant causes the formation of a primary lesion. From this moment on, the pathogen remains localized in the necrotic areas of the primary lesion because the host's defence mechanisms seem to control the pathogen. This situation constitutes the latency phase. If after a while, the fungus is able to overcome the defensive barriers of the plant, it will begin to spread through the adjacent plant tissue in a short period of time with the consequent colonization and maceration of the affected tissue. The fungus produces a new generation of spores in this infected tissue that can start the cycle of infection.

In winter, the fungus is preserved as mycelium on senescent tissue or seeds or as sclerotia in plant remains of the host. In spring the environmental conditions begin to be favourable, which causes the growth of the pathogen and the production of conidiophores and multinucleated conidia. Later, these conidia will be dispersed by insects, rain, and the wind. These macroconidia will be deposited on new hosts on which they will germinate, initiating the infection and spreading the disease again. Finally, the vegetative propagation cycle will be completed by generating new mycelium with the capacity to sporulate.

However, disease is often not triggered, and no symptoms appear when *B. cinerea* comes into contact with host tissues. This phenomenon is enhanced if the environmental conditions are unfavourable for the development of the fungus. If this happens, the pathogen remains in a dormant state that usually begins in flowering and lasts for long periods of time, remaining in this state during the development and ripening phase of the fruits and even after harvesting them. If conditions are favourable in the post- harvest phase, the fungus feeds on the nutrient-rich tissues of the fruits after restarting its activity and wreaks havoc on the harvest.

B. cinerea is problematic from an epidemiological point of view because it is a ubiquitous fungus that has a host range comprising more than 200 different species, is also easily spread and can infect virtually all types of tissues and organs of the plant (van Kan, 2006). This causes that the control of the pathogen is undoubtedly difficult even if the most appropriate measures are applied to eliminate sources of inoculum and to control the fungus on a particular crop and under specific conditions.

5. Disease control methods

There are five categories in which the most frequently used strategies for the control of the disease caused by *B. cinerea* can be grouped: chemical control, biological control, cultural practices and methods, methods of stimulating plant defence responses and genetic improvement of the resistance to the disease.

Chemical control is based on the use of chemical pesticides in a prophylactic way and is the simplest method to control an epidemic of the fungus in many crops. Botryticides are varied in their mode of action including toxicants and molecules affecting specifically respiration, cytoskeleton,

osmoregulation, sterol and amino-acid biosynthesis. However, despite its efficacy, its effects on the environment, human health and the appearance of resistance cases (target-site modifications and multiple drug resistance), relegate its use to a combination with appropriate cultural practices (Kretschmer *et al*., 2009; Leroch *et al*., 2013; Fillinger *et al*., 2016).

Biological control is an alternative to chemical control and its harmful effects and relies on the inhibitory activity against *B. cinerea* of three main groups of biopesticides: live microorganisms, plant extracts and mineral oils and organic acids (Nicot *et al*., 2011). The group of live microorganisms is the one that contains the largest number of commercial botryticides products that include bacteria (*Bacillus*, *Pseudomonas*), actinomycetes (*Streptomyces*), yeasts (*Aureobasidium*, *Candida*) and fungi (*Trichoderma* , *Gliocladium*, *Chlonostachys*, *Ulocladium*). There are also products on the market based on extracts of the tea tree (*Melaleuca alternifolia*) and the giant knotweed (*Reynoutria sachalinensis*) with antifungal activity. Within the third group, paraffinic oil and neem oil stand out as the two most common products with control over the fungus. The modes of action of these products are very disparate (reduction in the concentration of nutrients available to the fungus, modification of the plant surface properties, production of microbial compounds, parasitism, interference with pathogenicity processes, reduction of inoculum production or stimulation of the induced resistance) and its main disadvantage is its inconsistency in field conditions (Fillinger *et al*., 2016).

Cultural practices differentiate between hosts that are found outdoors, such as open field crops and orchards, and those that are grown in the greenhouse. In the former, the management and sanitation of the crop canopy is the most important measure. Generally, the limiting factors for the development of the disease are the presence of liquid water and high humidity, so reducing the density of the plantation, removing the senescent tissues or the leaves near the fruits favours aeration by decreasing the relative humidity and the time of presence of the water. These measures are also applicable inside a greenhouse, but here the number of variables that can be controlled is greater. Active heating and ventilation systems can prevent environmental conditions that promote disease from occurring (Dik and Wubben, 2004). Also, passive heating, that is, the high temperatures reached under plastic roofs during the day, has a negative effect on the incidence of the disease, while it can increase production yield (Elad *et al*., 2014b). In addition, the use of polyethylene films that modifies the spectrum of light, absorbing near ultraviolet light, to cover the crops reduces the incidence of infection by negatively affecting the fungus sporulation (Reuveni *et al*., 1989). Covering the soil with polyethylene reduces relative humidity and dew in addition to supplying a physical barrier between the fungus found in the soil and the plant and the buried irrigation systems avoid humidity at the base of the stems compared to those found above the ground (Shpialter *et al*., 2009).

Other factors to consider for both indoor and outdoor crops are plant nutrition and the use of resistant cultivars. Regarding the first, calcium, nitrogen and potassium stand out as important elements because they affect the susceptibility of the host to pathogens (Engelhard 1989). On the other hand,

certain physical rather than genetic characteristics of the host can facilitate or hinder the development of gray mold disease.

Most of the above measures require intensive labour and some can have deleterious effects on fruiting (Fillinger *et al*., 2016).

The methods that control diseases induced by *B. cinerea* by stimulating the induced resistance in the plant are related to two categories already mentioned, biological control and cultural practices. Biotic compounds with a suppressive effect on the fungus are known, such as the plant hormones salicylic acid and β-amino butyric acid (Reglinski *et al*., 1997). Likewise, there are non-pathogenic or pathogenic microorganisms and plant extracts capable of activating induced systemic resistance (ISR) or systemic acquired resistance (SAR) of the host. Emodin and physcion, active compounds from *Reynoutria sachalinensis*, have been shown to induce ISR (Schmitt *et al*., 1996, 2005) and *Bacillus subtilis* strain QST 713 appears to activate a pathway (related to induction of the pathogenesis related PR1 gene) and induce ISR as well (Ongena *et al*., 2010). Among the abiotic agents are those fertilizers with key elements to activate the plant's defenses: nitrogen (Mundy, 2008), soluble forms of silicon that provide strength to cell walls and improve resistance to *B. cinerea* (Miceli *et al*., 1999; Jacometti *et al*., 2007), copper that can suppress the attack of the pathogen by eliciting the accumulation of peroxidases, phenols, resveratrol and anthocyanins (Coulomb *et al*., 1998) and Ca^{2+} whose resistance-creating effect against *B. cinerea* was correlated with increased levels of cellulose and pectins soluble in oxalate and alkali (Miceli *et al*., 1999).

Genetic improvement for resistance against *B. cinerea* is difficult because different resistance mechanisms are involved in different stages of the disease development. Therefore, each state must be analysed individually to identify its resistance traits. To make matters worse, the resistance response and the stability of its expression are influenced by genotypes and environmental conditions. It is therefore essential to identify traits that are highly related to the resistance response (Bond *et al*., 1994). Despite these drawbacks, there are studies that describe potential targets to improve the resistance of a crop to the fungus through breeding programs or genetic engineering. For example, a rice chitinase gene exhibit enhanced resistance to gray mold in transgenic cucumber plants (Tabei *et al*., 1998) or a heat shock protein HSP24 is involved in the BABA-induced resistance to *B. cinerea* in postharvest grapes (Li *et al*., 2021). In wild species of the genus *Solanum* related to cultivated tomato (*Solanum lycopersicum*), a certain level of resistance has been described in leaves and stems to *B. cinerea* (Guimarães *et al*., 2004; ten Have *et al*., 2007). Thus, it has been possible to identify several quantitative trait *loci* (QTLs) that allow *Solanum habrochaites* to resist attack by *B. cinerea* (Finkers *et al*., 2007), which increases the prospects for control of this pathogen in tomato species.

Special mention should be made of postharvest treatment where it is essential to adopt a holistic approach in integrated management to minimize the losses caused by the fungus at this stage of production.

All the control methods mentioned in this section help to control and suppress the damage caused by the fungus. However, they do not control the disease at all and that is why it is necessary to develop strategies that are really effective. Although its infection cycle can be defined with greater or lesser success, aspects such as the host, environmental conditions, agricultural practices or the geographical region introduce a certain variation when establishing the most adequate control method. A greater understanding of their epidemiology, aerobiology and the genetic variability and diversity of their natural populations is necessary.

6. Genetic diversity

B. cinerea shows an extraordinary variability in phenotypic traits that make it a model for the study of sources of variation in filamentous fungi, in particular plant pathogens. The cause of this wide variation and its ability to adapt lies in its genetic characteristics, among which the mutation within long-lived somatic lineages stands out. However, in our system there are other processes and mechanisms that can be considered as additional sources of diversity in the evolution of its genome (Fillinger *et al*., 2016): its predominantly heterokaryotic nature, a complex ploidy, the presence and activity of a large variety of extrachromosomal gene elements (mitochondrial DNA (De Miccolis Angelini *et al*., 2012; Yin *et al*., 2012), plasmids (Hiratsuka *et al*., 1987) and mycoviruses), the existence of somatic compatibility and the occurrence of sexual recombination in its lifecycle.

The number of nuclei in *B. cinerea* depends on the stage of development in which it is found. Thus, hyphae and conidia are multinucleated structures. Specifically, macroconidia contain between 3 and 6 nuclei (Grindle, 1979; Lorenz and Eichorn, 1983; Shirane *et al*., 1988, 1989) while microconidia havea single nucleus. On the other hand, during the sexual cycle, young asci contain a single diploid nucleus that, after undergoing meiosis followed by mitosis, gives rise to eight ascospores with one nucleus each and these, once mature, will contain four nuclei (Lorenz and Eichorn, 1983; Faretra and Antonacci, 1987).

The karyotype of *B. cinerea* has been researched using pulsed-field gel electrophoresis (PFGE) showing great variability among different isolates (Van Kan *et al*., 1993; Pollastro, 1996; Vallejo *et al*., 1996, 2002). Its genome size is estimated to vary from 13.2 –22.6 Mbp (Vallejo *et al*., 2002) to 33.9–39.7 Mbp (Van Kan *et al*., 1993), according to different assumptions taken into account in this technique. At present, the almost complete assembly of the strain B05.10 genome (Van Kan *et al*., 2017) is available, which is composed of a total of 18 chromosomes of which 10 are full length from telomere to telomere and it is believed that meiotic crossover between homologous chromosomes containing heterologous regions generates variation in the length thereof. Furthermore, the existence of hete roploidy in the fungus is known. All these aspects suggest that the sexual crossing process is restricted to haploid nuclei, while heteroploidy is allowed in somatic cells (Beever and Weeds, 2004).

Somatic compatibility is the ability of certain isolates of numerous species of fungi to fuse their hyphae during vegetative development, giving rise to heterokaryotes, biological entities in which nuclei

of different types coexist. On the basis of somatic compatibility, fungal species have been characterized and subdivided into vegetative compatibility groups (VCGs). In our system, the genetic basis for vegetative compatibility / incompatibility is unknown, but it is believed to be similar to the system of other ascomycetes where it is determined by a number of *het loci*, which vary by species and exist in two or three allelic states (Glass *et al*., 2000). Using auxotrophic mutants, multiple different VCGs have been identified in this species, which is consistent with the presence of at least six *het* genes. *B. cinerea* has a high level of vegetative incompatibility that has important biological implications, especially preventing the transfer of deleterious genetic elements between colonies such as mycovirus and senescence plasmids.

The wide variety among field isolates and the high number of individual haplotypes (Van der Vlugt-Bergmans *et al*., 1993) and of VCGs (Pollastro *et al*., Unpublished; Beever and Weeds, 2004) indicate that sexual reproduction occurs in nature, although it has not been observed frequently. As stated above, our system is mainly heterothalic because the sexual reproduction process is controlled by a single *locus* (MAT1) with two idiomorphs, MAT1-1 and MAT1-2. However, it also exhibits homothalism. A few self- fertile isolates have been observed to possess the two idiomorphs simultaneously (Faretra and Grindle , 1992) while heterokaryosis is considered to be the main cause of homothalism because a single multinucleated conidium could contain nuclei carrying opposite idiomorphs (Faretra *et al*., 1988).

Mycoviruses are known to infect *B. cinerea* (Howitt *et al*., 1995; Pearson and Bailey, 2013; De Guido *et al*., 2005; Wu *et al*., 2007, 2010). They mostly consist of dsRNA viruses that appear to be in a cryptic state (Howitt *et al*., 1995; Santomauro *et al*., Unpublished), but a few cases have been associated with hypovirulence (Wu *et al*., 2007, 2010; Zhang *et al*., 2010; Potgieter *et al*., 2013). Studies on the electrophoretic migration patterns indicates a broad variation in number, molecular size and abundance of viral genomic dsRNA segments, thus suggesting a frequent occurrence of mixed infections of multiple viruses in single isolates of the fungus (Fillinger *et al*., 2016).

The genome of *B. cinerea* presents transposable elements (TEs) that belong to both class I retroelements (LTRs) and class II DNA transposons (MITEs, TIRs) (Amselem *et al*., 2011) and together represent about 1.3% of the fungus genome (Staats and Van Kan, 2012). Giraud *et al*. (1999) distinguished between two types of *B. cinerea* strains, transposa and vacuma, based on two transposons, Boty and Flipper, which later showed differences in relation to aspects of pathogenicity and biology (Martinez *et al*., 2005; Pollastro *et al*., 2007 ; Samuel *et al*., 2012) and the occurrence of RIP (Repeat-Induced Point mutation) activity has been observed in its genome, a fungal-specific defense mechanism that counteracts the deleterious effects of transposable elements (Galagan and Selker , 2004; Martinez *et al*., 2008). Therefore, the presence of these elements in the genome is considered as one more source of their plasticity and genetic variability.

Inteins represent potential critical points for meiotic recombination in our fungus because it has been shown that they can participate in "homing" processes (Bokor *et al*., 2010). These processes consist

of gene conversion events occurring during meiosis and they are mediated by site-specific endonuclease (HEG), normally encoded within self-splicing genetic elements, such as group I introns and inteins.

OBJECTIVES

Objectives

The specific objectives of this work are:

- To study the regulatory effect of NO on the germination and development of *B. cinerea* and the physiological processes affected in a wild-type genetic background in comparison with a mutant genetic background, lacking the *Bcfhg*1 gene, encoding a flavohemoglobin enzyme.
- To evaluate the regulatory effect of NO on the cell cycle in *B. cinerea* through post-translational modifications of regulatory proteins.
- The functional characterization of the *Bcmed* gene of *B. cinerea*.
- The functional characterization of the *Bcorp*1 gene of *B. cinerea*.

MATERIALS AND METHODS

1. Organisms

1.1 Bacteria

Escherichia coli strain DH5α [F^-, Φ80d*lac*Z△M15, △ (lacZYA-argF)U169, *deoR*, *recA1*, *endA1*, *hsdR*17 (r_k-,m_k+), *phoA*, *supE*44, λ^- , *thi*-1, *gyrA*96, *relA*1] was used in bacterial transformation experiments and for routine plasmid multiplication. The One Shot® *ccd*B Survival™ 2 $T1^R$ strain [Competent Cells F-*mcr*A Δ(*mrr-hsd*RMS-*mcr*BC) Φ80*lac*ZΔM15 Δ*lac*X74 *rec*A1 *ara*Δ139 Δ(*araleu*)7697 *gal*U *gal*K *rps*L (Str^R) *end*A1 *nup*G *fhu*A::*IS2*] was used for the cloning and amplification of pDONR™221 and pFPL -Gh for the use of Gateway technology (Invitrogen, Carlsbad, CA, USA).

1.2 Fungi

B05.10 is a haploid strain obtained in the laboratory of Professor Paul Tudzynski (Wilhelms Universität Münster, Germany) by treatment with benomyl (Büttner *et al*., 1994; Quidde *et al*., 1999) from the reference field isolate SAS56 (Faretra *et al*., 1988) obtained from grapevine. Isolate B05.10 is highly virulent in most of the hosts it infects and is genetically stable. Its genome has recently been sequenced and annotated using various precision technologies (Amselem *et al*., 2011; van Kan *et al*., 2017). Due to its great efficiency in transformation, this isolate is also used in most laboratories as a standard receptor strain (Tudzynski and Kokkelink, 2009).

*ΔBcfhg*1 is a mutant strain defective in the *Bcfhg*1 gene (Bcin04g06230), encoding the BCFHG1 enzyme. This strain was obtained by Juan Luis Turrión-Gómez in the Genetics laboratory of the CIALE (Turrion-Gomez *et al*., 2010).

*ΔBcmed*34 and *ΔBcmed*84 are two mutant strains lacking the *Bcmed* gene (Bcin12g00460) and obtained by Alejandro Alonso Díaz in the Genetics laboratory of the Institute for Agribiotechnology Research (CIALE) by transforming the B05.10 strain of *B. cinerea*. For this, the plasmid pAAD4 was used as transforming DNA, a vector of origin equivalent to pAAD8 and carrier of an expression cassette that allows to express the bacterial gene for resistance to hygromycin under the control of the *OliC* gene promoter of *A. nidulans* and the *trpC* gene terminator of *A. nidulans* flanked by the 5 'and 3' regions of the *Bcmed* gene, 487bp and 926bp, respectively.

*ΔBcmed*16 is a mutant strain obtained in the same protoplast transformation assay that gave rise to *ΔBmed*34 and *ΔBcmed*84. However, it carries a copy of the mutant type allele (the hygromycin resistance expression cassette flanked by the 5' and 3' regions of the *Bcmed* gene) arranged in tandem with the wild-type allele due to a single recombination event on the 3' flank of the gene . It was obtained by Alejandro Alonso Díaz in the Genetics laboratory of the CIALE.

1.3 Plants and fruits

The bean plants (*Phaseolus vulgaris*) used in this work are plants of the Blanca Riñón variety grown in the El Barco de Ávila-Piedrahíta region (Ávila, Spain). The vine plants (*Vitis vinifera*) are of Juan

García (red grape) and Verdejo (white grape) varieties. Fruits for inoculations are from the seedless Sweet Globe Green variety (South Africa) (purchased at the supermarket).

2. Culture media and conditions

2.1 Bacteria

E. coli was cultured in LB medium (Luria-Bertani), liquid or solid, for transformation experiments and for obtaining plasmid DNA. This medium is composed of 0.5% yeast extract (Difco); 1% bactotryptone (Difco); 1% NaCl. When the required medium was solid, 1.5% bacteriological agar (Conda) was added. The incubation temperature was 37°C and in the case of culture in liquid medium, the flasks were incubated in the dark, with 250 rpm shaking in a Künher 1SF-1-W orbital incubator.

For the selection of colonies resistant to antibiotics, these were added to the already sterilized medium: kanamycin at a concentration of 50 µg/µL; ampicillin at a concentration of 100 µg/µL.

All bacterial strains were stored in cryovials at -80 °C in sterile 25% glycerol (V/V).

2.2 Fungi

Liquid medium culture of *B. cinerea*

The culture of mycelium in a poor and synthetic liquid medium is the appropriate method when large amounts of biological material without impurities are required and therefore it was the method used for the extraction of nucleic acids and proteins from the fungus and for microscopy tests. The medium chosen for this was Gamborg B5 medium supplemented with sucrose and KH_2PO_4 (detailed in the Table 1). 125 mL baffled bottom flasks containing 30 mL of this medium were inoculated, depending on the strain, with a spore suspension at a final concentration of $5 \cdot 10^5$ spores/mL or with a group of 10 - 12 agar plugs with mycelium from the periphery of the colony and were kept in incubation at 22°C, in the dark and at a shaking speed of 180 rpm in a Künher 1SF-1-W orbital incubator. The incubation time depended on the subsequent use of the mycelium, being 96 hours for DNA extraction.

For the culture of mycelium to obtain protoplasts, the malt extract medium (detailed in the Table 1) was used. 500 mL baffled bottom flasks containing 100 mL of this medium were inoculated, depending on the strain, with a spore suspension at a final concentration of $5 \cdot 10^5$ spores/mL or with a group of 10 - 12 agar plugs with peripheral mycelium of the colony, and they were kept in incubation at 22°C, in the dark and at a shaking speed of 180 rpm in the orbital incubator for 16 -18 hours or 96 hours depending on the growth rate of the strain used.

For microscopy analyses, 125 mL baffled bottom flasks containing 50 mL of malt extract medium (detailed in the Table 1) were inoculated with 5 - 7 mycelium agar plugs from the periphery of the colony and kept in incubation at 22°C, in the dark and at 180 rpm shaking in a Künher 1SF -1-W orbital incubator for 96 hours.

In the analyses of the effect of nitric oxide (NO) on the *B. cinerea* development, Petri dishes were used because the liquid culture in shake flasks favours the aggregation of the spores as they germinate, which greatly hinders their subsequent observation under the microscope and their differe ntiation into individual units during counting. Static culture avoids aggregation and thus facilitates subsequent counts by allowing biological units to be distinguished from one another.

For the NO analysis tests on the fungus germination, the PDB medium was used at half the concentration established by the manufacturer, PDB ½ (detailed in the Table 1). This medium was used to obtain a conidia suspension at a final concentration of $5{\cdot}10^5$ spores/mL of the corresponding strain. Subsequently, the necessary volume (60 µL) of the conidia suspension was deposited in 55 mm diameter Petri dishes and they were kept at 22°C in the dark and without shaking in a FRIOCELL 222 germination chamber until the moment of imaging.

To determine the influence of NO on the nuclear spore division of the fungus, spore suspensionsof the strains of interest were prepared at a concentration of $5{\cdot}10^5$ spores/mL in ½ PDB medium (detailed in the Table 1). Subsequently, 15 mL of the suspensions were deposited in 55 mm Petri dishes, and these were incubated at 22°C in the dark and without shaking in the germination chamber until the moment of image acquisition (0 hpi and 4 hpi).

To obtain samples for the transcriptional analysis performed by RNAseq on the strains B05.10 and *ΔBcfhg*1 in response to NO exposure, spores of both strains were inoculated at a final concentration of $5 \cdot 10^5$ spores/mL in square plates of 120 mm side size containing 25 mL of PDB ½ medium. The plates were kept at 22°C in the dark and without shaking in a FRIOCELL 222 germination chamber for the necessary times (see section 20 of Materials and Methods).

Solid medium culture of *B. cinerea*

The routine cultivation of the different strains of *B. cinerea* for their maintenance was carried out in solid medium on Petri dishes of 55 mm or 90 mm in diameter with MEA medium (detailed in the Table 1), with or without the corresponding selection antibiotic in the case of the mutant and complemented strains. The inoculum consisted of a drop of a suspension of spores or mycelium, depending on the strain, from the biological material stored in glycerol at -80°C, or, more usually, a piece of agar with mycelium from a previous plate. The plates thus inoculated were cultured at 22°C and in the dark in the germination chamber for the time necessary for the strain to cover its surface.

To obtain macroconidia of the different strains, 55 mm or 90 mm diameter Petri dishes were used with PDA medium supplemented with an extract of tomato leaves (detailed in the Table 1) in order to stimulate sporulation (Benito *et al*., 1998). 10 µL of a suspension of biological material of the corresponding strain were deposited on the plates, either of a stock conserved in glycerol at -80°C or of a fresh stock prepared in sterile distilled water and conserved at 4°C and incubated at 22°C in the dark in the germination chamber for the time necessary for the mycelium to cover the entire surface of the plate. After this time, the plates were exposed to long wave ultraviolet light (280 - 420 nm) for seven hours to

promote sporulation. Finally, the plates were kept again at 22°C and in the dark for a further week to optimize spore production.

For microconidia production analysis assays and for the production of mycelium to be used in the aggressiveness evaluation assays, the different strains were grown in 90 mm diameter Petri dishes with MEA, PDA or Gamborg B5 media, the latter supplemented with sucrose and KH_2PO_4 (detailed in the Table 1), depending on the experiment. For the saprophytic growth analysis tests, the same media were used, but on square plates of 120 mm side. In all these tests, with the exceptions indicated, the incubation was carried out at 22°C and in the dark in the germination chamber for a time that varied depending on the trait to be studied.

For the microscopy analysis on solid medium, 90 mm Petri dishes with MEA medium (detailed in the Table 1) were used, the surface of which was covered or not, depending on the aspect to be studied, with cellophane discs (Novocel flexibles®). Once inoculated, the plates were kept at 22°C and in the dark in the germination chamber for 3-7 days depending on the growth capacity of the strain. In those cases in which it was necessary to use cellophane, 90 mm diameter discs of this material, previously sterilized, were placed in the centre of the plates and spread with a glass spreader before carrying out the inoculation.

In the protoplast transformation assays, these were seeded in 90 mm diameter Petri dishes with SH-Agar medium supplemented with the corresponding selection antibiotic (detailed in the Table 1). Subsequently, the selection of the candidates for transformants through several rounds of culture to achieve homokaryosis was carried out in Petri dishes of 55 mm diameter with MEA medium with the appropriate selective agent (detailed in the Table 1) and the obtaining of monosporic cultures was carried out on 90 mm diameter Petri dishes with MEA medium (detailed in Table 1). The incubation of the fungus in these three stages was carried out at 22°C and in the dark in the germination chamber for the time required for each stage in particular.

For obtaining samples for the transcriptional analysis performed by RNAseq on the strains B05.10 and *ΔBcorp*1-19, 90 mm Petri dishes with MEA medium covered with a cellophane sheet were inoculated with plugs of vegetative mycelia from the edge of fungal colonies of the indicated strains actively growing. The inoculated plates were incubated in a germination chamber at 22°C with a photoperiod of 16 hours of light and 8 hours of darkness for 96 hours (see section 20 of Materials and Methods).

Table 1. Composition of the culture media used in the growth of *B. cinerea*.

Medium	Composition / quantity per litre of distilled water
Gamborg's B-5 – Plant salts (AppliChem)[1]	3.26 g
BME (Bacto Malt Extract, Difco)	10 g
MEA (Malt Extract Agar, Difco)[2]	33.6 g
PDA (Potato Dextrose Agar, Difco)[3]	39 g
SH-Agar[4]	Sucrose 0.6M; Tris-HCl pH 6.5 5mM; $(NH_4)H_2PO_4$ 1mM; bacteriological agar 0.8%
PDB (Potato Dextrose Broth, Difco)[5]	24 g

[1] Supplemented with 10 mM Sucrose and 10 mM KH_2PO_4 pH 6.5. When it was used as a solid medium, it was supplemented with 2% bacteriological agar.

[2] For the selection of transformants, it was supplemented with hygromycin B (Thermofisher) at 50 µg / mL or nourseothricin (Jena Bioscience) at 50 µg / mL.

[3] When it was used to stimulate the sporulation of the fungus, it was supplemented with 25% (w/v) of crushed tomato leaf extract.

[4] It was supplemented with hygromycin B (Thermofisher) at 70 µg / mL or nourseothricin (Jena Bioscience) at 50 µg / mL.

[5] It was used at half the concentration stipulated by the manufacturer (1.2 g of PDB per 100 mL of water).

2.3 Plants and fruits

Vine plants (*Vitis vinifera*)

Maintenance in greenhouse

The grapevine plants from which the leaves were obtained for the aggressiveness evaluation experiments were grown in individual 20 L pots with soil, in the greenhouse of the Institute for Agribiotechnology Research of the University of Salamanca. The plants were pruned annually in winter and watered regularly with running water.

Maintenance in germination chamber

The vine leaves cut, processed, and infected as described in section 7.1 of Materials and Methods, were placed inside plastic trays with the bottom moistened and of sufficient height to avoid contact of the leaves with the sealing plastic. Then the trays were sealed with plastic film to achieve the most favourable conditions for the infection of the pathogen (relative humidity > 95%) and obtain reproducible results in the infection tests. Subsequently, the trays were incubated inside an IBERCEX phytotron at 22°C with a photoperiod of 16 hours of light and 8 hours of darkness until the time of measurement of the lesions.

Grapes (*V. vinifera*)

The grapes used in the virulence tests of this work were commercially acquired in the days prior to their use. Once inoculated they were kept in incubation under the same conditions established for the leaves.

Bean plants (*P. vulgaris*)

Seed germination

The bean plants of the Blanca Riñón variety were also grown in the greenhouse. First, the seeds were disinfected with a 2% (V/V) sodium hypochlorite solution for 5 minutes; this was completely removed by successive washings with sterile distilled water. Next, they were sown in alveoli containing sterile vermiculite (Projar, SA), in groups of two or three seeds. These were incubated at 25°C with a photoperiod of 16 hours of light and 8 hours of darkness for 7 -10 days, after which the seedlings were individually transferred to pots with plant substrate. These were kept for a further 7 days in the greenhouse before being used in the infection experiments. At all times, the plants were watered regularly with running water.

Growth in germination chamber

In the infection tests (see section 7.2 of Materials and Methods), the plants with the inoculated leaves were placed inside plastic boxes (placing a maximum of four plants per box) measuring 32 cm x 36 cm x 42 cm. A small amount of tap water was deposited at the bottom of the boxes, and these were sealed with adhesive tape to maintain conditions of high relative humidity (> 95%) inside. The boxes were arranged stacked in the phytotron at 22°C with a photoperiod of 16 hours of light and 8 hours of darkness until the moment of data collection.

3. Handling of *B. cinerea*

3.1 Harvesting and counting of *B. cinerea* spores

The spores were collected with a maximum time of 10 days before their use in the corresponding test. 5 mL of sterile Milli-Q water was added to the PDA + Tomato plate containing the sporulated mycelium and with the help of a glass spreader, under aseptic conditions, the surface was rubbed to release the conidia. Subsequently, the spore suspension was poured into a 50 mL tube through a funnel with glass wool to remove mycelium debris. Spores were washed by centrifugation: a first centrifugation at 800 rpm for three minutes followed by two centrifugations at 3000 rpm for eight minutes. At the end of each centrifugation, the supernatant was discarded, the pellet was resuspended with 3 mL of distilled water, and the tube was vortexed. After the last centrifugation, the spore counting was carried out.

From the tube with the previously shaken spore stock, a 1:100 dilution was prepared. After shaking the resulting suspension, the spores were counted using a Thoma counting chamber (Zuzi) and 9 µL of the 1:100 dilution for each net ruling.

To obtain the spore concentration of the stock suspension, the following formula was used:

$$\text{nº spores/mL} = \bar{X} \cdot 25 \cdot 10000 \cdot \text{DF}$$

where $\bar{X}$ is the mean of the number of spores counted in the central large square of each net ruling, previously divided by the number of medium squares into which the central square of a net ruling is divided (16); 25 is the number of small squares into which each median square of the central large square of a net ruling is divided; 10000 is the chamber factor and refer s to the sample volume that occupies the space between the coverslip and the central large square of the net ruling: 1 mm in length × 1 mm width × 0.1 mm height = 0.1 mm^3 = 10^{-4} mL) and DF is the dilution factor used (1:100).

3.2 Strains conservation

The spore stocks were kept at 4°C for a maximum of one week for their short-term use, while, for their long-term conservation, biological material of the strain was mixed with 15 -25% glycerol (V/V) and stored in cryovials at -80°C. The biological material used to store the strain depended on whether it sporulated or not. In the case of the sporulating strains, the macroconidia were the material used to preserve them, while the mycelium was the material chosen to preserve the strains that were not capable of producing spores. In the latter case, the mycelium was obtained following the procedure described in section 8.1 of Materials and Methods for obtaining mycelium grown in liquid medium for staining with Lactophenol cotton blue.

3.3 Obtaining monosporic cultures

Once the primary transformants, obtained in the different transformation events and that were not affected in their sporulation capacity, had passed the selection stage consisting of culturing through successive passages in the presence of the selective agent to achieve homokaryosis, we proceeded to obtain monosporic cultures of each of them. The mycelium derived from the germination of an individual spore shows a greater uniformity in its behaviour compared to the mycelium derived from multiple spores and typical of a primary transformant. This is due to the stability of the transformed nuclei, which is greater in monosporic culture because all their nuclei come from the three to six transformed nuclei present in the original spore.

To obtain the monosporic cultures, the spores were collected from the plate with the sporulating mycelium of the primary transformant (see section 3.1 of Materials and Methods) and an aliquot of 100 µL of them was seeded in a 90 mm diameter Petri dish with MEA or PDA medium (with or without the corresponding selection agent) by spreading it with a glass spreader. After incubating the plate overnight under the growth conditions established for the pathogen (see section 2.2 of Materials and Methods), single spores germinated and separated from each other can be observed by means of a dissecting microscope. Then, with the help of a sterile dissecting needle or scalpel, six of these germlings were transferred to a 90 mm Petri dish, with the same medium, where they were placed uniformly distributed.

Finally, once their growth was verified, the incipient mycelia were individualized in 45 mm plates containing the same medium as in previous steps.

The spores produced by these monosporic cultures were collected and used for the elaboration of stocks for their long-term conservation in glycerol (see sections 3.1 and 3.2 of Materials and Methods).

4. Saprophytic growth assays

To evaluate the growth capacity of the different strains in solid synthetic media, the wide part of a 10-100 µL micropipette tip (5 mm in diameter) was used and agar cylinders were made with mycelium from the inner edge of a growing colony. With the help of a toothpick, these cylinders were placed in the center of square 120 mm plates with the different culture media. The plates were kept in incubation while measurements of two perpendicular diameters of the colonies were taken at the times of interest (24h , 48h, 72h, 96h, 120h and 144h after inoculation). The diameter finally considered for each colony, at each sampling time, was the mean of the two diameters recorded in each case.

5. Sporulation assays

The sporulation evaluation was a qualitative and non-quantitative analysis whose objective was to determine whether the ability to sporulate of a particular strain had been affected by the mutation it harboured. In this sense, the evaluation was carried out in 90 mm Petri dishes with the established culture media and the same inoculum source described for the saprophytic growth tests was used (see section 4 of Materials and Methods). The plates inoculated were kept in incubation under the growth conditions established for the fungus (see section 2.2 of Materials and Methods) until the colony almost reached the edge of the plate (the edge of the colony should ideally be 0.5 - 1.0 cm from the edge of the plate). At this time, the plates were exposed to long wave ultraviolet light (280 -420 nm) for seven hours to promote sporulation and were again kept under normal growth conditions for a further week to optimize spore production. After this time, a photographic record of the plates was carried out.

6. Microconidia production assays

To study the production of microconidia, 90 mm Petri dishes containing the different media were inoculated with agar discs with mycelium in a manner equivalent to that described for the saprophytic growth tests (see section 4 of Materials and Methods). The plates were kept in incubation under the growth conditions established for the pathogen (see section 2.2 of Materials and Methods) for 48 hours to stimulate their initial growth from the inoculum. The plates were then placed inside an opaque container and incubated at low temperature (13°C - 14°C) for approximately one month. After this acclimatization period, the plates, still inside the opaque container, were incubated at 0°C for another month. The plates were kept in dark at all times. Finally, a photographic record of the plates and the

extracts of the biological material collected by means of the procedure established in section 3.1 of Materials and Methods was carried out.

7. Infection assays on leaves

7.1 Infection assays on *V. vinifera* leaves

The leaves of vine plants of the Juan García and Verdejo varieties were cut and inserted by the petiole in blocks of inert and absorbent florist material (floral foam or sponge) previously saturated in running water and the blocks were placed on 90 mm Petri dishes with the same type of water.

This structure was placed in plastic trays in whose bottom sheets of absorbent paper moistened with water were placed. A plastic grid was placed on top of the paper sheets to avoid contact of the inoculated leaves with the moistened bottom. The inoculations were carried out by placing mycelium discs from 90 mm Petri dishes with MEA medium (see section 2.2 of Materials and Methods) on the leaves so that the face of the disc with mycelium was in contact with the surface of the leaf and, at the same time, it was not placed on top of any main conductive vessel. The inoculated leaves were kept in the germination chamber under the conditions detailed in section 2.3 of Materials and Methods and the aggressiveness of the strains was evaluated by estimating the mean diameter of the necrotic lesion produced at 120 hours after inoculation.

7.2 Infection assays on *P. vulgaris* leaves

The primary leaves of bean plants of the Blanca Riñón variety approximately two weeks old were inoculated with agar discs with mycelium of the different strains, grown in 90 mm Petri dishes with MEA medium, following the steps described in section 2.2 of Materials and Methods. For this, four mycelium discs of the strain in question were placed in each of the two cotyledon leaves of each plant, in the manner described for the vine infection tests (see section 7.1 of Materials and Methods). Subsequently, the plants were grown in the phytotron under the conditions detailed in section 2.3 of Materials and Methods. At 72 hours after inoculation, the aggressiveness of the strains was evaluated by the mean of the measurements of the two perpendicular diameters of the lesions present on the leaves.

7.3 Infection assays on *V. vinifera* table grapes

Prior to the infection test, the grapes were disinfected by incubation in 0.5% sodium hypochlorite for 2 minutes. They were then washed with sterile water three times and allowed to air dry in a laminar flow hood. For the infection test, the fruits were placed in 120 mm square Petri dishes without a lid and adhered to the bottom surface by means of double-sided tape. The grapes were placed perpendicular to the tape and were wounded in its widest part, the equator, with a sterile needle (2 mm deep). Subsequently, 5 mm agar plugs containing fresh mycelium from the edge of fungal colonies actively growing on MEA plates (see section 2.2 of Materials and Methods) were placed on top of the wound with the mycelium in contact with the fruit surface. The materials thus inoculated were incubated in closed

plastic boxes, to maintain high humidity conditions, in the germination chamber under the conditions detailed in section 2.3 of Materials and Methods. The aggressiveness of the strains was evaluated at 120 and 192 hours after inoculation by taking photographs that allowed a visual estimation of their degree of virulence.

8. Microscopy analysis

8.1 Lactophenol cotton blue staining

When the mycelium was grown on solid medium, a small sample was taken with sterile forceps and resuspended in a 1.5 mL tube containing 50 µL of Milli-Q water, where it was disaggregated by vortexing. Next, 10 µL of the mycelium suspended in water was placed on a slide. When the mycelium was obtained by culture in liquid medium, it was collected, in a 50 mL tube, by successive centrifugations at 3000 rpm for 5 minutes and the pellet was resuspended in 20 mL of Milli-Q water. After disaggregating the mycelium by vortexing, 30 µL of the suspended mycelium was placed on a slide.

To carry out the staining of the samples of both origins, 10 µL of Lactophenol cotton blue dye (Fluka® analytical) was added, and a coverslip was placed on them after a 5 -minute incubation at room temperature. This dye contains the aniline blue dye that has the property of adhering to chitin, which is why it is used to colour fungal structures.

8.2 Calcofluor white staining

In this case, the fungus was grown in plates covered with cellophane discs (see section 2.2 of Materials and Methods). Using a sterile forceps, the cellophane sheet was lifted until completely detached from the medium and transferred to an empty 90 mm Petri dish. Warm Milli-Q water was added to the cellophane until it was submerged, and the plate was gently shaken until the mycelium was detached from the cellophane, renewing the water as it cooled. Subsequently, with the forceps, sections of the periphery of the mycelium sheet were cut, placed on a slide and Calcofluor white stain (CFW, Fluka® analytical) and potassium hydroxide (KOH) 10% (m/V) were added, in equal proportion and in sufficient volume to cover the sample. It was thus incubated for 10 minutes in the dark. CFW is a fluorochrome that binds nonspecifically to cellulose and chitin in fungal cell walls and fluoresces from bright green to blue when excited with ultraviolet wavelength light. For its part, KOH is a strong base that is added to the stain to clarify the organic material, leaving the fungal structures intact. After the incubation time, excess dye and KOH were removed by washing with small volumes of Milli-Q water added to the sample with a micropipette. After drying the remaining water, a volume of 30 µL of Milli-Q water was placed on the sample and then a coverslip, the edges of which were sealed with clear nail polish to avoid the long-term drying of the preparation.

8.3 DAPI staining

In the study of the effect of NO on the nuclear division process of the fungus, stainings were carried out with the colouring agent DAPI (4', 6-diamino-2-phenylindole) (NucBlue® Fixed Cell Stain ReadyProbes™ reagent), (Life Technologies™ USA). DAPI is a fluorescent marker that is used to stain nuclei in both living and fixed cells because it can pass through the cell membrane.

The 15 mL suspensions of spores cultured as detailed in section 2.2 of Materials and Methods were collected in 10 mL tubes with successive centrifugations of 3000 rpm 5 minutes each. The pellets were then washed twice with 1 mL of Milli-Q water and after removing the supernatant from the last washing centrifugation, 1 mL of the fixing solution (100% ethanol (V/V) and acetic acid in a 3:1 ratio) was added to each tube. The samples were thus preserved at 4°C overnight. After this time, the tubes were centrifuged at 3000 rpm for 5 minutes and washed twice with 1 mL of Milli-Q water with the same centrifugation parameters. Finally, the spores were resuspended in 1 mL of Milli-Q water and staining was carried out. For this, two drops of the commercial preparation of DAPI dye were added to each tube and incubated at room temperature for 10 minutes. After this time, the samples were washed with 1 mL of Milli-Q water and the cells were pelleted by means of a centrifugation at 3000 rpm for 5 minutes. The washing was repeated and after removing the supernatant, the spores were resuspended in 1 mL of 25% glycerol (V/V).

For observation under the fluorescence microscope, 10 µL of the glycerol-fixed spores suspension was placed on each extreme of a slide, covered with a coverslip, and its edges sealed with transparent nail polish with the intention of long-term preservation. Finally, pictures of the preparations were taken under the fluorescence microscope after the edges sealed had completely dried (15-20 minutes).

The study of the effect of the mutation of the *Bcmed* gene on nuclear morphology was carried out in mycelium samples grown on Petri dishes covered with cellophane (see section 2.2 of Materials and Methods) that were obtained in the same way in which it was done for Calcofluor white staining (see section 8.2 of Materials and Methods).

Once the samples were on the slide, 1 mL of the fixation solution (2% formaldehyde in 100% methanol (V/V)) was added, and they were incubated for 2 minutes at room temperature. After this time, the fixation solution was removed by two successive washes consisting of immersing the samples in 1 mL of Milli-Q water and subsequent incubation of 2 minutes.

After removing the water from the last wash, 2 drops of the DAPI dye were added to each sample and incubated for 10 minutes in the dark and at room temperature. Subsequently, the excess dye was removed by two washes under the same conditions as the previous ones. After drying the traces of water, the samples were covered with 60 µL of glycerol at 25% (V/V) and covered with a coverslip, the edges of which were sealed with transparent nail polish.

For the visualization of the fungal structures in each of the microscopy tests described above, an optical microscope (LEICA DM LB optical microscope, Leica Microsystems) was used, using a red suppression filter (BG38, blue filter) under illumination of an EBQ 100 isolated-L/131-26B light source (Leistungselektronik JENA GmbH) with a mercury vapor bulb (Osram) when the excitation of a fluorescent dye and the consequent visualization of the emitted fluorescence were necessary. The images were captured, with the lenses of ×10, ×20, ×40 and ×100 magnification according to the experiment, with a LEICA DC300F digital camera (Leica Microsystems) with the help of the Leica IM 1000 Image Manager software (Leica Microsystems). ImageJ 1.47V software (National Institutes of Health, USA) was used to process the images and make the different counts and measurements of the fungal structures.

9. Germination assays with NO

Germination tests can be divided into two groups depending on when the corresponding chemical agent was added to the spore suspension with the working concentration. Thus, a part of the tests is made up of those experiments in which the chemical agents were added immediately before depositing the droplets of the spore suspensions on the plates and another part is made up of those experiments in which the chemical agents were added to the cultures after they were kept in incubation for the time necessary so that the germination program of the spores could be triggered. Specifically, the awaited incubation time in this group of tests was 4 hours.

Each one of the 55mm Petri dishes, containing the spore suspension, represented an individual culture and was kept in incubation as detailed in section 2.2 of Materials and Methods until the moment of taking images. At the times indicated according to the experiment (2h, 3h, 4h, 6h, 8h and 10h) the percentage of germination and the length of the germ tube were quantified, and the effect of the different chemical agents was evaluated:

- Diethylenetriamine (DETA, Sigma Aldrich): is an amine used as a nitric oxide donor. It was added to the culture medium to a final concentration of 250 μM.
- Nω-nitro-L-arginine (L-NNA, Sigma Aldrich): it was used as an inhibitor of nitric oxide synthase (NOS) activity in the fungus at a final concentration of 1 mM.
- 2 - (4-carboxyphenyl) - 4, 4, 5, 5 - tetramethylimidazoline - 1 - oxyl - 3 - oxide (cPTIO, Sigma Aldrich): was used as nitric oxide scavenger at a final concentration of 500 μM.

To evaluate the percentage of germination with the different treatments, the spores were classified into three groups according to the length of their germination tube: spores that had not started the germination process (state 0), spores whose germination tube had an equal length or less than the diameter of the ungerminated spore (state 1) and spores whose germ tube had a length greater than the diameter of the ungerminated spore (state 2).

10. Nucleic acid extraction

10.1 Genomic DNA of *B. cinerea*

As indicated in section 2.2 on Materials and Methods, shaking liquid culture was the most frequently used procedure to obtain fungal material from which to obtain DNA. Prior to the extraction protocol, the mycelium produced was collected in a 50 mL tube by means of successive centrifugations at 3000 rpm for 5 minutes and, subsequently, it was washed with 25 mL of sterile distilled water with the same centrifugation parameters. The pellet obtained was placed on filter paper where the agar dice were discarded because their permanence in the sample could hinder the subsequent extraction of the DNA. Next, the mycelium was wrapped in the filter paper and pressure was applied to favour the exit of the water, repeating this step with new paper until the sample was completely dry. Once the mycelium acquired a rubbery and dry texture, it was stored in an aluminium foil envelope, frozen in liquid nitrogen and stored in the deep freezer (-80°C) while waiting for its homogenization. This consisted of grinding the tissue in mortar and in the presence of liquid nitrogen until a homogeneous powder was obtained, which was preserved in fractions of approximately 250 mg of powder in 1.5 mL tubes, in the deep freezer until the moment of extraction of the genetic material.

In addition to the above, when it was wanted to avoid the incubation time involved in the culture in liquid medium, DNA was also extracted from mycelium samples obtained from the fungus cultivated in plates with solid medium. In this case, the aerial mycelium was collected from the entire surface of the plate by scraping it with a sterile blade of a scalpel, avoiding collecting the culture medium. The mycelium thus obtained was deposited in a 1.5 mL tube, frozen in liquid nitrogen and lyophilized before carrying out the extraction. This dehydration technique was used instead of filter paper due to the small amount of sample obtained from the plate.

For lyophilization, the cap of the 1.5 mL tube containing the sample was pierced with a pricker to allow the creation of a vacuum inside and was placed in a lyophilizer (Virtis advantage) connected to a vacuum pump (Savant ValuPump VLP120) for 6 –8 hours. Once the sample was dehydrated, it was pulverized with the help of a sterile glass rod and the DNA was extracted immediately.

The protocol used to extract DNA from homogenated tissue samples from both sources was the same. First, 400 µL extraction/lysis buffer (200 mM Tris; 25 mM EDTA; 250 mM NaCl and 0.5% SDS), 200 µL phenol and 200 µL isoamyl chloroform (24:1 chloroform and isoamyl alcohol) were added with vigorous vortexing after adding each volume. The resulting homogeneous suspension was centrifuged for 30 minutes at 4°C and 7500 rpm and the upper aqueous phase was transferred to a 1.5 mL tube. 3 µL of RNAse (Roche) (10 mg/mL) was added to the extract and it was incubated at 37°C for 15 minutes. Subsequently, 1 volume of phenol-isoamyl chloroform was added, it was gently agitated by inversion and centrifuged for 15 minutes at 4°C and 7500 rpm. The aqueous phase was collected again in a new 1.5 mL tube, 1 volume of isoamyl chloroform (24:1) was added, the tube was mixed by gentle inversion and centrifuged at 8000 rpm for 10 minutes at 4°C. The upper aqueous phase was transferred to a new 1.5 mL

tube and 2.5 volumes of cold absolute ethanol and 0.3 M of AcNa (sodium acetate) pH 5.2 were added and the mixture was incubated at -20°C for a minimum time of 30 minutes to precipitate the DNA. After this time, the mixture was centrifuged for 20 minutes at 4°C at a speed of 13500 rpm The supernatant was removed, a wash was made with 70% ethanol (V/V) with vortexing, and the tube was centrifuged at 12000 rpm for 5 minutes at room temperature. The supernatant was discarded, the pellet was allowed to dry completely, either using a Savant DNA 120 SpeedVac Concentrator vacuum kit (ThermoFisher Scientific) or by leaving the 1.5 mL tube open at room temperature for a few minutes, and the pellet was resuspended in 100 µL of sterile Milli-Q water or TE buffer (10 mM Tris pH 8 - 8.5; 1 mM EDTA pH 8).

Finally, the concentration and quality of the genetic material obtained were determined in a Nanodrop ND-1000 (Thermo Scientific) and its integrity was verified by agarose gel 0.6% (m/V) electrophoresis using the molecular weight marker High DNA Mass Ladder (Invitrogen) (see sections 10.4 and 14.1 of Materials and Methods), as a reference. DNA was stored at -20°C.

10.2 Plasmid DNA of *E. coli*

Alkaline denaturation with SDS

It is a modified and adapted protocol of the Plasmid Mini-Preps Using Wizard Kit (Promega) with which bacterial DNA of sufficient quality was obtained to be used in the routine analysis of transformed colonies by means of PCR reactions or enzymatic digestions.

A 10 mL tube with a 5 mL culture of LB medium supplemented with the appropriate selection antibiotic and inoculated with the colony under study was incubated for 16 hours under the conditions described in section 2.1 of Materials and Methods. After this time, the culture was centrifuged at 4000 rpm for 5-10 minutes and, after discarding the supernatant, the pellet was resuspended in 250 µL of resuspension solution (50 mM Tris-HCl pH 7.5; 10 mM EDTA; RNase A 100 µg/mL). The mixture was transferred to a 1.5 mL tube and 250 µL of the lysis solution (0.2 M NaOH; 1% SDS (m/V)) was added. After mixing by inversion 10 times, it was incubated at room temperature for a maximum of 5 minutes and 250 µL of the neutralization solution (1.32 M potassium acetate; pH 4 .8) was added. After shaking again by inversion 10 times, the mixture was centrifuged at 13000 rpm for 15 minutes and the supernatant was transferred, by decantation, to a new 1.5 mL tube containing 800 µL of cold isopropanol. The contents were mixed immediately by inversion and centrifuged at 10000 rpm for 15 minutes. The isopropanol accumulated in the supernatant was discarded by decantation and the pellet was completely dried using the vacuum equipment or by leaving the tube open at room temperature for a few minutes. Finally, 50 µL of sterile Milli-Q water was added and the pellet resuspended, allowing its incubation at room temperature for 15 minutes. Once the pellet was resuspended, its concentration and quality were determined using a Nanodrop ND-1000 and its integrity was verified on a 0.6% (m/V) agarose gel using the molecular weight marker High DNA Mass Ladder as a reference (Invitrogen) (see sections 10.4 and 14.1 of Materials and Methods). DNA was stored at -20°C.

Commercial kit for plasmid purification

To obtain plasmid DNA with a high degree of purity, the NucleoSpin® Plasmid kit (Macherey-Nagel) was used following the protocol recommended by the trading house. In this case, we also started from 5 mL bacterial cultures and the quality and integrity of the DNA obtained were checked in the same way as in the previous section, keeping it at -20°C until its use for the construction of plasmids or sequencing reactions.

10.3 Total RNA

Extraction with TRIzol® method

A protocol with minor modifications derived from the original version recommended by the manufacturer was used, keeping the samples on ice throughout the process to avoid RNA degradation.

1 mL of TRIzol® (Invitrogen) was added to the 1.5 mL tube with the mycelium so that the sample volume never exceeded 10% of the volume of TRIzol® used for lysis. Next, a sterile glass rod was used to grind the sample until a cloudy mixture was obtained and its homogenization was promoted by pipetting or vortexing. The tube was then centrifuged at 12000 x g for 10 minutes at 4°C and the supernatant was transferred to a new 1.5 mL tube. This was incubated for 5 minutes at room temperature to allow the complete dissociation of the nucleoprotein complexes, 200 µL of chloroform was added and it was incubated at room temperature for 3 minutes after mixing by pipetting. The tube was then centrifuged at 12000 x g for 15 minutes at 4°C and the upper aqueous phase was transferred to a new 1.5 mL tube, avoiding transferring the remains of the interface or of the organic phase to the new tube. Then, RNA precipitation took place, for which 500 µL of isopropanol was added and mixed with the rest of the components by pipetting and the mixture was incubated at room temperature for 10 minutes. The tube was then centrifuged at 12000 x g for 10 minutes at 4°C, after which the formation of a white precipitate, the RNA, was verified and the supernatant was discarded. The pellet was washed twice by resuspending it in 1 mL of 75% ethanol (V/V) (diluted in sterile Milli-Q water treated with DEPC 1% (V/V)), homogenization by pipetting and centrifugation at 7500 x g for 5 minutes at 4°C, discarding the supernatant at the end of each one. To remove traces of ethanol, the tubes were allowed to dry for 10 minutes at room temperature or, alternatively, using a Savant vacuum kit for 1 minute. Finally, 50 µL of sterile Milli-Q water treated with DEPC 1% (V/V) was added to the pellet and it was incubated at 60°C for 10 minutes to favour its resuspension.

Commercial RNA extraction kit

The commercial SV Total RNA Isolation System Z3105 kit (Promega) was used according to the manufacturer's recommended instructions for RNA extraction routinely and preferentially over the previous method. We always started from samples of 30 mg of lyophilized mycelium and crushed with a sterile glass rod before starting the extraction.

The RNA samples obtained by either of the two previous extraction methods were treated with DNase from the commercial Turbo DNA-free™ kit (Ambion, Invitrogen) for the elimination of contaminating DNA. For this, the manufacturer's recommendations were followed. Likewise, the RNA

samples were quantified in a Nanodrop ND-1000 and their integrity was verified by electrophoresis in a 1% (m/V) agarose gel (see sections 10.4 and 14.2 of Materials and Methods).

10.4 Nucleic acid quantification

The concentration and quality of the nucleic acids was determined by performing a spectral measurement of a 2 µL aliquot of the sample on a NanoDrop® ND-1000 spectrophotometer. Specifically, there were two reference parameters:

The ratio of sample absorbance at 260 and 280 nm (A_{260}/A_{280}) reports the purity of the sample in relation to protein contamination so that ratios close to 1.8 and 2 are indicative of pure DNA and RNA, respectively.

The ratio of sample absorbance at 260 and 230 nm (A_{260}/A_{230}) is a secondary measure of nucleic acid purity and reports the presence of organic compounds or chaotropic agents that absor b at 230 nm. The values of this ratio indicative of a pure nucleic acid range between 1.8 - 2.2.

The values estimated by the spectrophotometer were corroborated by electrophoresis of aliquots of the samples (3 - 5% of the DNA stock or 1 µg of the RNA stock) in agarose gels at 0.6% (m/V) for DNA and 1% (m/V) for RNA, using appropriate molecular weight markers (see section 14 of Materials and Methods).

11. Protein manipulation

11.1 Protein extraction

The mycelium samples obtained by culture in liquid medium for 6 hours and 20 hours as detailed in section 2.2 of Materials and Methods were collected by centrifugation at 3000 rpm for 5 minutes at 4°C in 50 mL tubes, combining the contents of several flasks of the same strain in a single tube. After washing the pellet with 45 mL of sterile Milli-Q water cooled to 4°C, it was centrifuged at 3000 rpm for 5 minutes at 4°C and the supernatant was discarded. The pellet obtained was resuspended in 5 mL of cold sterile Milli-Q water and the mixture was transferred to a 2 mL tube with a screw cap previously weighed by multiple transfer steps of 1.5 mL volumes followed by sedimentation at 15000 x g for 5 minutes and 4°C and discarding the supernatant. Once the pellet was in the 2 mL tube, it was centrifuged at 13200 rpm for1 minute at 4°C and the remaining supernatant was removed with a pipette. At this time, the tube was weighed again, kept on ice, and stored at -80°C until extraction.

The extraction of the protein fraction was carried out using the standardized method in the laboratory of Dr. Pedro San Segundo, which includes the use of trichloroacetic acid (TCA) for the precipitation of proteins. First, the mycelium was resuspended in 100 µL of 20% TCA (V/V) and 0. 5 mL of 425-600 µm diameter glass beads (Sigma Aldrich) were added. The sample was homogenized by two short bursts of 15 seconds at 400 rpm in a BeadBug™ Mini Homogenizer Model D1030 (E) (Benchmark),

followed by incubation of the tube on ice for 1 minute and a third burst of 30 seconds at the same speed. The base of the tube was then pierced with a hot needle and placed in a 1.5 mL tube. The tubes thus assembled were centrifuged at 2000 rpm for 1 minute at 4°C and the beads were washed by adding 200 µL of 5% TCA (V/V) with the same centrifugation parameters. The purpose of this washing is to recover the maximum of cell lysate that could remain between the beads. At this point, the flow-through in the 1.5 mL tube was divided into two fractions transferring 25% of the volume to a new 1.5 mL tube destined for the quantification of the protein concentration. The remaining 75% was used for downstream applications. The two fractions were centrifuged at 3000 rpm for 3 minutes at 4°C to pellet the proteins and the supernatant was discarded with a pipette. The protein pellet obtained in the larger fraction was resuspended in the corresponding volumes of Sample Buffer 2X (SB2X) (100 mM Tris-HCl pH 6.8; 4% SDS (m/V); 200 mM DTT; 20% Glycerol (V/V); 0.2% Bromophenol blue (m/V); 1mM Phenylmethanesulfonyl fluoride; 1X complete™ EDTA-free Protease Inhibitor Cocktail (Roche)) and Tris-HCl 2M pH = 8.8, calculated from the difference in weight obtained between the empty tube and the tube containing the sample. The volume of SB2X required was obtained by multiplying by 5000 the difference in weight between the tubes and the volume of Tris-HCl 2M pH = 8.8 used was always half the volume of SB2X. For its part, the fraction destined to determine the protein concentration was resuspe nded in one volume of Tris-HCl 2M pH = 8.8 calculated with the same procedure used for the larger fraction. Once both pellets were completely resuspended, the minor fraction was stored at -80°C until the moment of measuring the concentration, while the other fraction was heated in a Thermomixer comfort thermoblock (Eppendorf) at 99°C for 5 minutes. Then, it was centrifuged at 13200 rpm for 5 minutes, the supernatant was collected and transferred to a new 1.5 mL tube and stored at -80°C until use in subsequent applications.

11.2 Protein purification

The attempts to purify the translational fusions with the green fluorescent protein generated in this work were carried out using the immunoprecipitation technique, with the GFP -Trap® technology (Chromotek) and the recommendations established by this trading house. This technology consists of a high quality GFP-binding protein based on a single domain antibody coupled to agarose beads.

The collection of the mycelium samples, their homogenization, and the subsequent obtaining of the two fractions of cell lysate in 5% TCA (V/V) were carried out following the procedures described in the previous section. However, to achieve protein purification, the proteins of the larger fraction were pelleted by centrifugation at 3000 rpm for 3 minutes at 4°C and after discarding the supernatant, the pellet was resuspended in 500 µL of Dilution buffer (10 mM Tris-HCl pH 7.5; 150 mM NaCl; 0.5 mM EDTA; in distilled water). A 50 µL aliquot of the resuspended pellet was taken and mixed with 50 µL of SB2X and stored at -80°C until resolution by SDS-PAGE. This fraction constituted the 'input'.

On the other hand, the required volume of resin, containing the agarose beads with the GFP - binding proteins, was estimated according to the binding capacity established by the manufacturer, and was equilibrated by two successive washes with Dilution buffer . In each wash, the resin was resuspended in 250 µL of the previously cooled buffer and subsequently sedimented at 2700 x g for 2 minutes at 4°C.

At the end of the centrifugation, as much of the supernatant as possible was removed and the volume of cell lysate was added to the volume of resin with gentle mixing. The mixture obtained was incubated with moderate shaking and at 4°C for 16 hours, after which it was centrifuged at 2000 x g at 4°C for 2 minutes. After centrifugation, the supernatant was discarded, reserving a 50 µL fraction that corresponded to the 'non-bound' fraction (all those proteins that have not been retained by the antibodies on the agarose beads). This aliquot was mixed with 50 µL of SB2X and stored at -80°C until visualization on the polyacrylamide gel.

Then, the pellet was subjected to two washes. In the first one, the pellet was resuspended in 2,1 mL of ice-cold dilution buffer and then centrifuged at 2000 x g at 4°C for 2 minutes. After removing the supernatant, the second wash was performed with 2.1 mL of Wash buffer (10 mM Tris-HCl pH 7.5; 500 mM NaCl; 0.5 mM EDTA; in distilled water) and the same centrifugation parameters. The pellet was then resuspended in 100 µL of SB2X and boiled at 95°C in a Thermomixer comfort thermoblock (Eppen dorf) for 10 minutes to dissociate the immune complexes from the beads. The beads were collected by centrifugation at 2700 x g for 2 minutes at 4°C and the supernatant was transferred to a new 1.5 mL tube and stored at -80°C to perform SDS-PAGE with it. This volume was called bound because it contained the proteins specifically 'bound' to the anti-GFP antibodies of the beads present in the resin.

The three fractions obtained during the procedure, 'input', 'non-bound' and 'bound', were resolved by SDS-PAGE and stained with Coomassie blue (see sections 14.3 of Materials and Methods). Comparison of the resulting band patterns made it possible to estimate the efficiency of the purification process. Alternatively, they were analysed by Western blot.

11.3 Protein quantification

The protein concentration of the extracts obtained in the previous section was estimated using the Bradford method (Bradford MM, 1976), measuring the absorbance of the sample at 595 nm in a BioPhotometer® v1.32 spectrophotometer (Eppendorf) and interpolating the value in a standard curve made from 10 dilutions of bovine serum albumin (Bio-Rad Protein Assay Kit II) with concentrations from 0.1 µg/µL to 1 µg/µL. To prepare the standard curve, the instructions indicated by the manufactur er were followed and to measure the sample, 10 µL of the minor fraction of the extract were used (see section 11.1 of Materials and Methods), which represented 25% of the total volume, undiluted and mixed with 200 µL of Dye reagent diluted 1:4 in sterile Milli-Q water and filtered on Whatman 3MM paper.

12. Cloning Vectors

12.1 pGEM®-T-Easy

It is a high copy number plasmid (origin of replication of the filamentous bacteriophage f1), of 3015 bp used for the cloning of PCR fragments and that is acquired in a linearized way in a kit from the commercial company Promega. It has an additional deoxythymidine at each of its 3' ends, which improves

the cloning efficiency of PCR products, since the usual thermostable polymerases frequently add a deoxyadenosine at the 3' ends of the amplified fragments.

In addition to the gene for resistance to the antibiotic ampicillin, the plasmid has the coding region of the α-peptide of the enzyme β-galactosidase (lacZ) as a selection marker. The insertion of the fragment of interest within the coding region of the peptide causes its inactivation, allowing the recombinant clones to be identified based on their colour, in the presence of X-gal and IPTG in the culture medium.

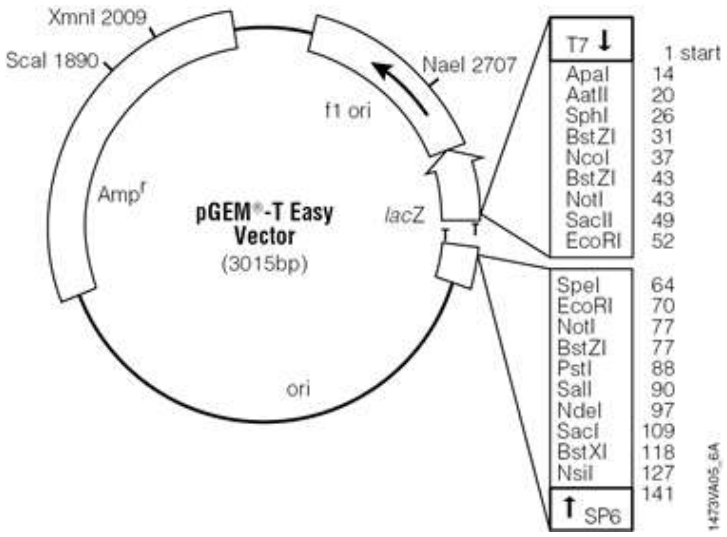

Figure 4. Circular map of the cloning vector pGEM®-T-Easy.

12.2 pBluescript II SK (+)

It is a 2961 bp high copy number plasmid (ColE1 and f1 origins of replication) derived from plasmid pUC19. Like pGEM®-T-Easy, this vector also carries the ampicillin antibiotic resistance gene and the coding region of the α-peptide of the β-galactosidase enzyme (lacZ) as phenotype selection markers. MCS refers to the multiple cloning site or polylinker that comprises up to 21 unique recognition sites for restriction enzymes and its orientation determines the SK or KS designation of the plasmid, depending on whether restriction site for the *Kpn*I enzyme is the closest to the lacZ promoter and that of the *Sac*I enzyme the furthest from the promoter (KS) or vice versa (SK).

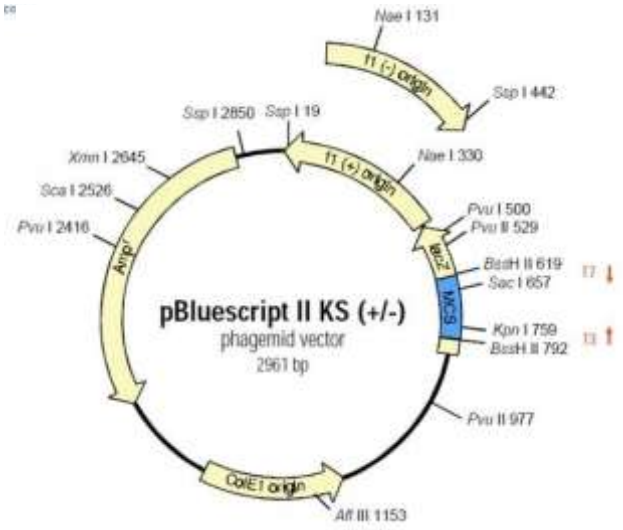

Figure 5. Circular map of plasmid pBluescript II SK (+/-).

12.3 pDONR™221

It is a high copy number plasmid (pUC origin of replication), of 4762 bp and that has been adapted to the Gateway® technology, a cloning method based on the properties of the site -specific recombination of bacteriophage lambda (Landy, 1989). The plasmid is designed to react, by means of a BP recombination reaction, with a PCR product flanked by the *attB* ends, giving rise to a new vector called Entry clone that contains the PCR product flanked by the *attL* sites. This constitutes the first stage of the two-step system of this technology for the expression of a gene of interest.

In addition to the attP1 and attP2 sites (bacteriophage λ-derived DNA recombination sequences that allow recombinational cloning of the gene of interest from an *attB* PCR product), the vector contains the lethal gene for *E. coli ccdB* for negative selection of the plasmid, the chloramphenicol resistance gene for counterselection of the plasmid and the kanamycin resistance gene for plasmid selection in *E. coli*.

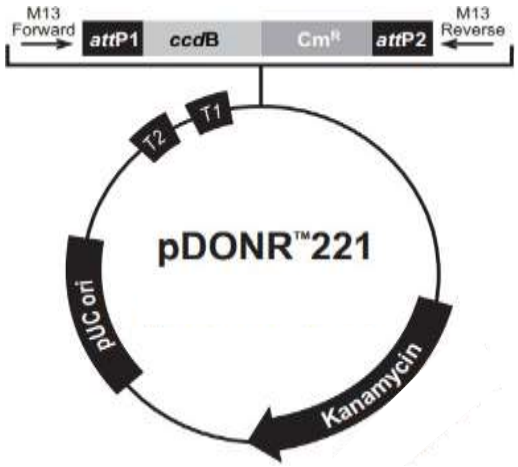

Figure 6. Circular map of plasmid pDONR™ 221.

12.4 pFPL-Gh (Gong *et al*., 2015).

This 11720 bp, high copy number vector (pUC origin of replication) is derived from vector pCAMBIA1300 (Cambia, Canberra, Australia) and has been adapted to Gateway® technology making it a Destination vector. It carries the *attR*1 and *attR*2 sites to perform an LR recombination with the Entry clone, described in the previous plasmid. This reaction constitutes the second stage of the two-step system of this technology and makes it possible to obtain a new vector called Expression clone that is subsequently introduced into the biological system of interest.

The plasmid also contains a hygromycin resistance cassette as a selection marker, the green fluorescent protein (GFP) gene to generate molecular fusions, and fungal terminator sequences. The vector was designed and provided by the laboratory of Dr. Mark Farman from the University of Kentucky (Lexington, USA).

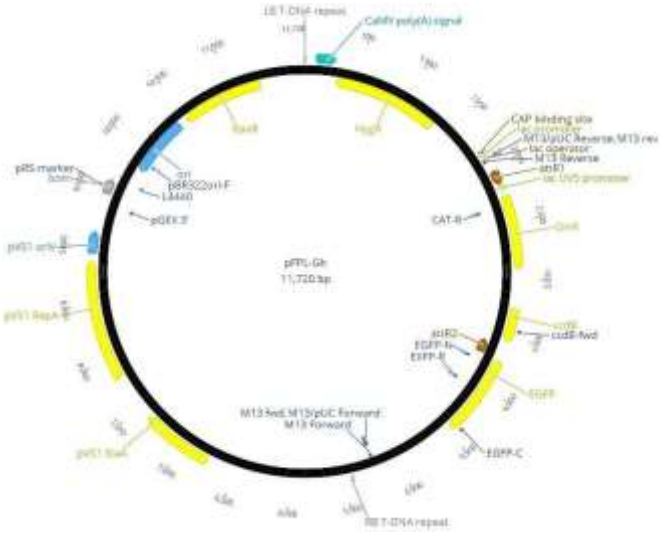

Figure 7. Circular map of plasmid pFPL-Gh.

12.5 pNR4

The 7379 bp long, high copy number plasmid (pUC origin of replication) was provided by Dr. Jan A.L. van Kan (Wageningen University, the Netherlands). It contains the AttP1 and AttP2 sites for use by Gateway® technology, the nourseothricin resistance cassette as a selectable marker for fungi, and the *ccdB* gene and the chloramphenicol resistance gene for negative selection and counterselection of the plasmid in *E. coli*, respectively.

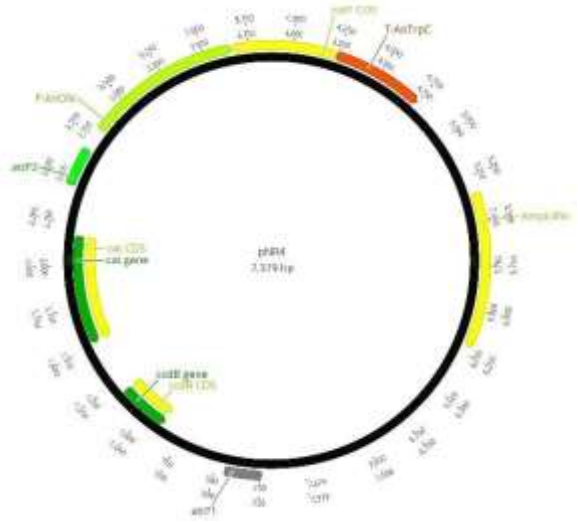

Figure 8. Circular map of plasmid pNR4.

12.6 p47-13

It is a vector of 6890 bp and of high copy number (origin of replication pUC) that was generated in the course of the work carried out by David Pescador in his Doctoral Thesis. It carries the hygromycin resistance cassette made up of the bacterial *hph* gene flanked by the promoter of the *OliC* gene from *Aspergillus nidulans* and the terminator of the *trpC* gene from the same fungus. This cassette is flanked in turn by a 617 base pair fragment derived from the 5' flanking region of the *Bcmimp1* gene and by a 737 base pair fragment derived from the final part of the coding region of this gene and its 3' non-coding region (Benito Pescador *et al*., 2016).

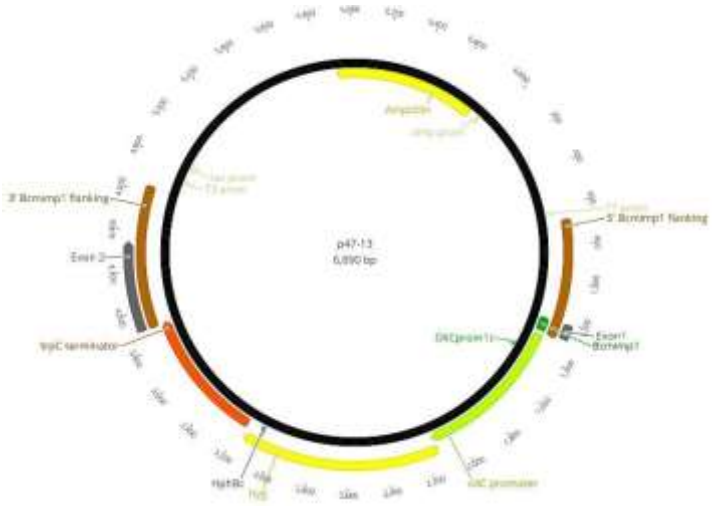

Figure 9. Circular map of plasmid p47-13.

12.7 pAAD4

It is a vector of 6893 bp that was generated in the course of the work carried out by Alejandro Alonso Díaz in his Master thesis. It carries the hygromycin resistance cassette made up of the bacterial *hph* gene flanked by the promoter of the *OliC* gene from *A. nidulans* and the terminator of the *trpC* gene from the same fungus. This cassette is flanked by the 5' and 3' regions of the *Bcmed* gene, of 487 bp and 926 bp, respectively, which allows their integration into the homologous *locus* of the fungal genome through homologous recombination. It was used to obtain the *ΔBcmed* strains (Alejandro Alonso Díaz, Master thesis. University of Salamanca).

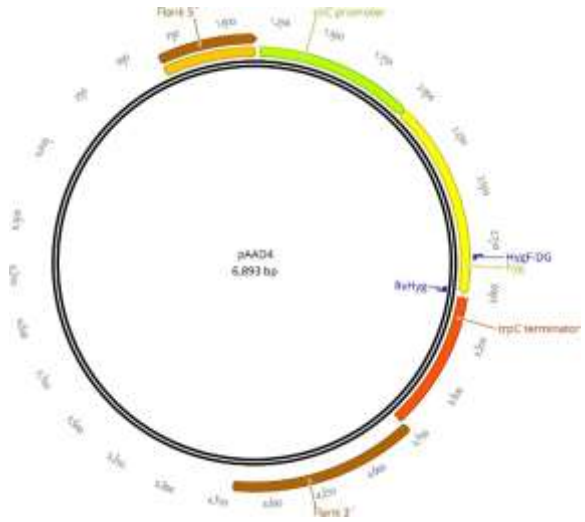

Figure 10. Circular map of plasmid pAAD4.

12.8 pAAD8

It is a vector of 7102 bp that was generated in the course of the work carried out by Alejandro Alonso Díaz in his Master thesis. It carries the hygromycin resistance cassette made up of the bacterial *hph* gene flanked by the promoter of the *OliC* gene from *A. nidulans* and the terminator of the *trpC* gene from the same fungus. This cassette is flanked by the 5' and 3' regions of the *Bcorp*1 gene, of 696 bp and 929 bp, respectively, which allows their integration into the homologous *locus* of the fungal genome through homologous recombination. It was used to obtain the *ΔBcorp*1 strains.

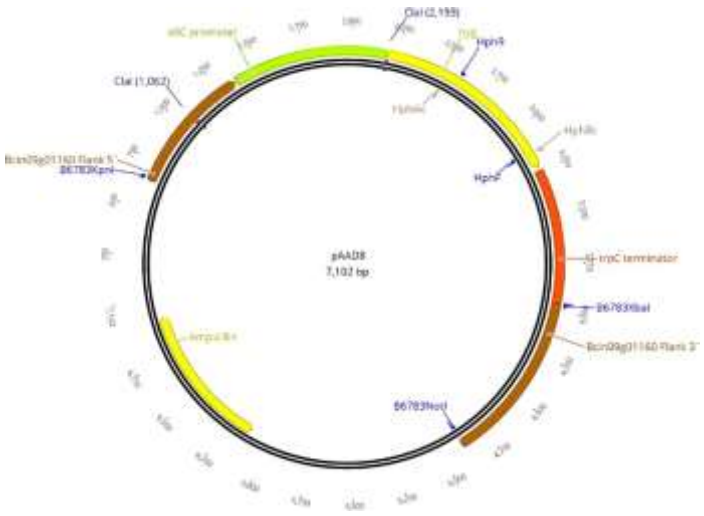

Figure 11. Circular map of plasmid pAAD8.

13. Nucleic acid manipulation

13.1 Restriction enzyme treatment

Enzymes distributed by different commercial companies (Takara, Roche, New England Biolabs) were used to carry out the restriction endonuclease DNA digestions. The recommendations of the corresponding manufacturer were always followed for their handling. However, c ertain parameters were kept constant, such as the final concentration of the saline buffer, which was always 1X and the incubation temperature of the reaction, which was always 37°C. The incubation time was generally 16 hours, with possible extra enzyme additions as a reinforcement to achieve better digestion performance.

Treatment of DNA with restriction enzymes was used for the physical characterization of plasmids and DNA fragments, for the cloning of the latter and for Southern blot analysis.

13.2 Ligations with T4 DNA Ligase

T4 DNA Ligase catalyzes the joining of two double-stranded DNA or RNA strands between the 5'-phosphate and 3'-hydroxyl groups of adjacent nucleotides in a cohesive ends or blunt-ended configuration and requires ATP as a cofactor. For the ligation reactions necessary to carry out this work, T4 DNA Ligase from Roche was used, which is supplied with the corresponding 10X ligation buffer containing ATP (660 mM Tris HCl, 50 mM $MgCl_2$, 50 mM DTT, 10 mM ATP, pH 7.5).

The ligations were made according to the manufacturer's recommendations. For this, the DNA (vector and/or insert) was heated to 65°C prior to ligation, which was carried out in volumes of 10 or 15 µL with the appropriate dilutions of the ligation buffer and 1 µL of the enzyme at a concentration of 1 U/µL. Subsequently, the incubation was carried out at 16°C overnight.

A second T4 DNA Ligase was used when the plasmid added to the ligation was the vector pGEM®-Teasy (Promega). This is supplied with its own 2X Rapid Ligation Buffer (60 mM Tris-HCl (pH 7.8), 20 mM $MgCl_2$, 20 mM DTT, 2 mM ATP and 10% polyethylene glycol) and with its own T4 DNA Ligase enzyme. For its use, the manufacturer's instructions were followed.

13.3 Gateway® Cloning

The Gateway® cloning method (Invitrogen) was used following the protocol recommended by the supplier. It uses the properties of the site-specific recombination of bacteriophage lambda (Landy, 1989) to facilitate the transfer of heterologous DNA sequences, flanked by modified att sites, between vectors (Hartley *et al*., 2000). Two reactions conform the basis of the system:

- BP reaction: The enzyme clonase BP catalyses the recombination reaction of a substrate with *attB* sites (can be a PCR product or a linearized vector) with a substrate with *attP* sites (donor vector) to create an Entry vector containing *attL* sites.
- LR reaction: The LR enzyme catalyses the recombination reaction of a substrate with *attL* sites (Entry vector) with a substrate with *attR* sites (target vector) to create an Expression vector containing *attB* sites.

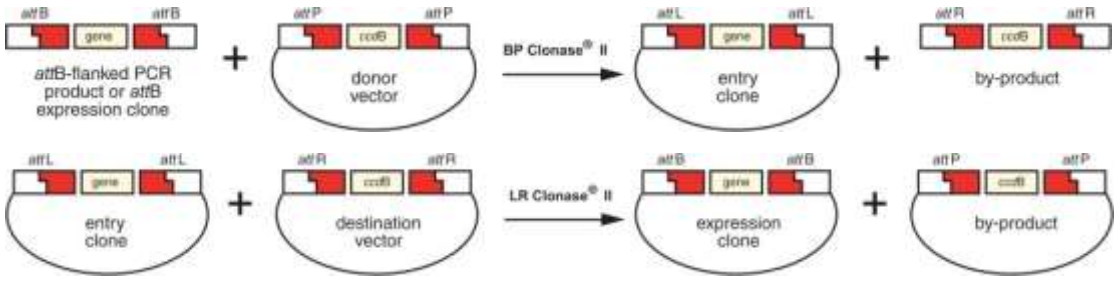

Figure 12. Scheme of the Gateway® Cloning System.

14. Electrophoresis

14.1 DNA electrophoresis

DNA electrophoresis were performed in agarose gels dissolved in 1X TAE buffer (40 mM Tris Base; 40 mM acetic acid; 1 mM EDTA; pH 8) in percentages between 0.6 and 3% (m/V) according to the size of the fragment to be analysed.

The gels were placed inside horizontal cuvettes where they were immersed in the same 1X TAE buffer. Before loading the samples into the wells, they were mixed with electrophoresis loading buffer (0.1% bromophenol blue (m/V); 0.1% xylene cyanol FF (m/V); 30% glycerol (V/V)) in a 5:1 ratio to facilitate the entry of the DNA into the well and the monitoring of the separation of the sample in the gels while they are running. One of the wells was always reserved for a sample of a molecular weight marker (1 kb

Plus DNA Ladder, Invitrogen) whose pattern of bands covered the size range of the DNA fragments of interest, also allowing their concentration and size to be estimated. For the separation of the DNA fragments, a variable voltage between 6 and 10 V/cm was applied depending on the range of sizes to be resolved and the amount of DNA.

Once the fragments had been separated, they were visualized with the intercalating agent ethidium bromide. To do this, the gels were incubated for 15 minutes in a solution of this agent (0.5 µg/mL) in 1X TAE buffer, followed by washing with distilled water for 10 minutes to remove excess dye. Finally, the DNA was visualized in a transilluminator with ultraviolet light (λ = 260 nm) and images were taken using an AlphaImager MINI (Simple Protein) visualization equipment.

14.2 RNA electrophoresis

RNA electrophoresis was performed under denaturing conditions according to the indications of Sambrook *et al*. (1989) and the recommendations from Roche (manual for the labelling of probes with digoxigenin (DIG)) and Promega (manual for RNA analysis), with the precaution of using DEPC-treated water for the preparation of all buffers and solutions, thus avoiding RNA degradation.

The gels were prepared by dissolving agarose in 1X MOPS electrophoresis buffer (40 mM MOPS; 10 mM sodium acetate; 1 mM EDTA; pH 7) at a percentage of 1% (m/V). To this mixture, 2% (V/V) formaldehyde was added after the agarose melted and allowed to cool to 55°C. After the gel had solidified, it was placed inside a 15 or 30 cm horizontal electrophoresis cell and immersed in 1X MOPS electrophoresis buffer. A sample volume equivalent to 1 µg of RNA was always used, which was mixed with 2 volumes of buffer for RNA samples (1 mL deionized formamide; 350 µL 37% formaldehyde; 200 µL 5X MOPS buffer), incubated at 65°C for 5 minutes to achieve denaturation and chilled on ice for 2 minutes. Subsequently, 2 µL of loading buffer (50% glycerol (V/V); 1 mM EDTA; 0.4% bromophenol blue (m/V)) was added and the mixture was loaded onto the gel. Electrophoresis took place for approximately 2 hours at a voltage of 4-5 V/cm inside a fume hood.

After 2 hours, RNA visualization was performed with ethidium bromide in a similar manne r as described for DNA. However, in this case, the dyeing solution was prepared by dissolving the dye (0.5 µg/mL) in DEPC-treated distilled water and the incubation time in it was 5 minutes. Furthermore, the subsequent washing was carried out by incubating the gel, for a minimum of 3 hours, in distilled water treated with DEPC. Finally, the quantity and quality of the RNA separated on the gel was checked by exposing it to ultraviolet light (λ = 260 nm) in a transilluminator and the corresponding images were taken with the AlphaImager MINI (Simple Protein) visualization equipment.

14.3 Polyacrylamide gel electrophoresis (SDS - PAGE)

The preparation of the polyacrylamide gels was carried out following the recommendations of the Mini-PROTEAN® Tetra Cell kit (Bio-Rad) and the subsequent electrophoresis was carried out according to the manual "A guide to polyacrylamide gel electrophoresis and detection" (Bio-Rad) under denaturing

conditions to ensure that the protein loses its three-dimensional structure and thus its migration is proportional to the charge and size of the protein, but not to its shape.

The protein extract samples were already in the loading buffer (SB2X), in which they had been resuspended at the end of the extraction protocol (see section 11.1 of Materials and Methods). A variable volume of the extract containing between 5 µg and 10 µg of protein was resolved in duplicate, using two gels run simultaneously (one intended for the visualization of the samples by means of Coomassie blue staining and the other intended for the detection of protein(s) of interest by Western blot). The gels were of the single-percentage type, formed by a resolving gel at 7% or 10% of 37.5:1 acrylamide:bisacrylamide depending on the size of the protein to be analysed (7% or 10% Acrylamide / bisacrylamide 37.5:1, 0.375M Tris-HCl, pH 8.8, 0.1% SDS, 0.05% TEMED, 0.05% APS) and a stacking gel (4% Acrylamide / bisacrylamide 37.5:1, 0.126 M Tris-HCl, pH 6.8, 0.1% SDS, 0.1% TEMED, 0.05% APS). Wells not occupied by samples were filled with 5 µL of SB2X to avoid lateral dispersion of the samples during electrophoresis, always reserving one well for a sample of a molecular weight marker (Precision Plus Protein ™ Dual Color Standards, Bio- Rad). Electrophoresis was carried out in the 1X electrophoresis buffer recommended by the manufacturer (25 mM Tris base; 250 mM glycine; 0.1% SDS (m/V)) at a constant voltage of 80V for a time of 2 hours and 30 minutes. After this time, the gels were washed by immersion in distilled water to eliminate the traces of SDS and then they were subjected to subsequent applications of Coomassie blue staining or Western blot.

The visualization of the protein extracts and the approximate estimation of their concentration was carried out by immersing the gel in 25 mL of staining solution (45% methanol, 10% glacial acetic acid, 25% distilled water, 3 g/L Coomassie Brilliant Blue G250), previously filtered with Whatman 3MM paper, where it remained in incubation, with moderate shaking and at room temperature for a minimum time of 30 minutes. When this incubation time was over, the gel was washed four times, using 25 mL of fresh destaining solution in each of them (45% methanol, 10% glacial acetic acid, 25% distilled water). The washes were carried out with moderate agitation, at room temperature and with a duration of 15 minutes in the first three and 16 hours in the last one. After the last wash, the gel was covered with a plastic film sheet and a photographic record of it was made using a scanner.

15. Recovery of DNA fragments from gel.

The gels where the samples were loaded with the fragments to be recovered were made with a low percentage of agarose (0.6 - 0.7% (m/V)) that varied according to the size of the fragment and were subjected to electrophoresis with a low voltage thus favouring the resolution of the pattern. After completion of the electrophoresis, the gel was stained with ethidium bromide and washed as indicated in section 14.1 of Materials and Methods. Next, the piece of gel containing the DNA of interest was cut with the help of a scalpel and a VWR Geneview transilluminator and placed inside a 1.5 mL tube previously weighted. Finally, for the recovery of the DNA fragment, the commercial NucleoSpin® Gel and PCR Clean-

Up kit (Macherey-Nagel) was used, following the recommendations indicated in the manual of the commercial company.

16. Transformations

16.1 Transformation of *E. coli* by heat shock

Preparation of competent cells

The protocol used to obtain competent cells is based on that described by Hanahan *et al*. (1995).

First, a 20 mL culture of LB medium was inoculated with a single colony of the *E. coli* DH5α and incubated for 16 hours at 37°C and 300 rpm. After this incubation time, 5 mL of the culture was used to inoculate 500 mL of LB medium without antibiotics, and this was kept in incubation at 37°C and 300 rpm until the optical density at λ = 550 nm was 0.48. The culture was then pelleted by centrifugation at 960 x g and 4°C for 10 minutes, the supernatant was discarded, and the pellet was resuspended in 150 mL of cold TFB1 (for 1 L of distilled water: 12.092 g $RbCl_2$; 6.28 g $MnCl_2$; 2.94 g potassium acetate; 1.09 g $CaCl_2$; 15% glycerol (V/V); pH 5.8 adjusted with 0.2 M acetic acid. Sterilized by filtration) by gentle manual shaking and keeping the cells cold. When the pellet was completely resuspended, the cells were incubated on ice for five minutes and pelleted by centrifugation at 1000 x g and 4°C for 15 minutes. After discarding the supernatant, the cell pellet was resuspended in 20 mL of cold TBF2 solution (for 1 L of distilled water:
2.093 g MOPS; 1.209 g $RbCl_2$; 8.32 g $CaCl_2$; 15% glycerol (V/V); pH 7 adjusted with 10N NaOH. Sterilized by filtration) by gentle manual shaking and incubated on ice for 15 minutes. Finally, this volume was distributed in aliquots of 100 µL that were stored at -80°C until the moment of use.

Transformation procedure

Transformations of *E. coli* with plasmids were carried out using the heat shock method. For this, 100 µL of competent cells, previously thawed on ice, was mixed with a volume of plasmid DNA that varied depending on its concentration, never exceeding 10% of the volume of the cells. The mixture was incubated on ice for 20 minutes and subsequently at 37°C for 2 minutes (or alternatively for 1 minute anda half at 42°C) to cause heat shock. The mixture was then incubated on ice for 2 minutes, 500 µL - 1000 µL of LB medium was added and the tube was incubated for 50 minutes at 37°C and 300 rpm. This step gives the bacteria enough time to generate the antibiotic resistance proteins enc oded in the plasmid and for which they will be selected later. After the incubation time had elapsed, the cells were seeded in 90 mm Petri dishes with LB medium in the presence of the selective agent and incubated for 16 hours at 37°C to favour the growth of individual colonies of transformed bacteria.

16.2 Transformation of *B. cinerea*

Obtaining protoplasts

Both the process of obtaining protoplasts of *B. cinerea* and their transformation were carried out following the procedures described by Hamada *et al*. (1997).

The mycelium cultivated for 16-18 hours, or 96 hours as indicated in section 2.2 of Materials and Methods, was collected in a 50 mL tube by successive centrifugations at 4000 rpm for 3 minutes. The pellet was then washed with 45 mL of sterile MQ water with vortexing and pelleted by centrifugation at 4000 rpm for 3 minutes. After discarding the supernatant, the pellet was washed twice with 50 mL of KC solution (0.6M KCl; 50 mM $CaCl_2$ dihydrate) with vortexing and subsequent centrifugation at 4000 rpm for 6 minutes. The pellet obtained after discarding the supernatant was resuspended in 30 mL of a solution of *Trichoderma harzianum* lysis enzymes (Sigma Aldrich) at 0.5% (m/V) in KC and sterilized by filtration. The mixture was transferred to a 50 mL glass flask and incubated at 22°C and 170 rpm in an orbital incubator for 2 hours or 4 hours depending on the strain used, regularly checking the density and quality of the protoplasts with a microscope.

The obtained protoplasts were transferred to a 50 mL tube, filter ed through a nylon mesh of 25 µm pore diameter when the protoplasts came from spores or 10 µm pore diameter when the protoplasts came from plugs of agar with mycelium. Once the entire volume had been filte red, the protoplasts were pelleted by centrifugation at 1500 rpm for 5 minutes and after discarding the supernatant, the y were resuspended in 30 mL of previously cooled KC solution. Next, the protoplasts were centrifuged at 1000 rpm and 4°C for 8 minutes, the supernatant was discarded, and the pellet obtained was washed two more times with cold KC solution and the same centrifugation parameters. After the last sedimentation, the supernatant was discarded, the protoplasts were resuspended in the remaining volume of KC solution and kept on ice until their use for transformation.

Transformation procedure

To carry out the transformation, the transforming DNA (2 µg - 5 µg of PCR product or 5 µg - 10 µg of plasmid DNA) was diluted in a 1.5 mL tube containing 95 µL of KC solution and 5 µL of 5mM spermidine and the mixture was incubated on ice for 5 minutes. 100 µL of the protoplasts sample was added to the suspension with the DNA and the mixture was incubated on ice for another 5 minutes. Then 100 µL of polyethylene glycol solution (25% PEG 3350 (V/V); 50 mM $CaCl_2$; 10 mM Tris-HCl pH 7.4) was added and the mixture was incubated for 20 minutes at room temperature. Another 500 µL of polyethylene glycol solution was added, the suspension was mixed gently, and the incubation was prolonged for a further 10 minutes. Then, 200 µL of KC solution was added and the suspension was gently mixed by inversion. Subsequently, aliquots of 500 µL of the protoplasts suspension with the DNA were transferred to 50 mL tubes where they were mixed with 50 mL of liquid SH-Agar medium (see section 2.2 of Materials and Methods) by gentle shaking and then the resulting mixture was deposited in 10 mm Petri dishes adding 10 mL per plate. The protoplasts were allowed to regenerate by incubating them at 22°C for 16-20 hours in the dark and then the plates were overlaid with liquid SH-Agar at 50°C containing 70 µg/mL of hygromycin B (Thermofisher) or 50 µg/mL of nourseothricin (Jena Bioscience) for selection. The first colonies from transformed protoplasts began to emerge after 72-96 hours of incubation at 22°C in the dark. These colonies were individually transferred to 55 mm Petri dishes with MEA medium

supplemented with the corresponding selection antibiotic (50 µg/mL hygromycin B or 50 µg/mL nourseothricin) to promote homokaryosis of the transformed nuclei.

17. Polymerase chain reactions

17.1 Conventional polymerase chain reaction (PCR)

The conventional PCR reactions used to amplify DNA fragments were differentiated into two types based on the size and expected quality of the amplified fragment. In both cases, the reactions were carried out by mixing the following components:

- Template DNA: its amount varied depending on the type and purity of the DNA used, being between 10 - 50 ng when it was fungal genomic DNA and 0.01 - 10 ng when it was plasmid DNA. On the other hand, during the analysis of the bacterial colonies obtained in the different transformations of *E. coli*, a preliminary analysis was carried out by PCR with non-purified bacterial DNA. For this, 2 µL of a cell suspension obtained by dissolving in 50 µL of sterile Milli-Q water a portion of the colony taken with a toothpick were used as a template.

- Primers: Oligonucleotides, of variable length, flanking the DNA fragment to be amplified, were used, and added to the reaction at a final concentration of 0.2 µM. The primers were designed based on the sequence of the annotated genomes of our system and available in the databases (section 22 of Materials and Methods) and for whose use the Geneious software (Biomatters) was employed. Subsequently, the Vector NTI Advance ™ 9 (Invitrogen) program allowed us to analyse the thermodynamic characteristics of the primers and their ability to form duplexes, mainly attending to two aspects, their length and GC content, so that they presented an annealing temperature close to 60°C. IDT (Integrated DNA Technologies Inc., USA) was the company in charge of synthesizing the oligonucleotides used in this work and which are listed in Table 8 (Appendix).

- DNA polymerase: different DNA polymerase enzymes were used depending on the purpose o f the amplification.

  DNA polymerase (Biotools): it derives from the thermophilic organism *Thermus thermophilus* and was used for routine checks such as the verification of cloned fragments in recombinant plasmids or the identification of positive transformants. It was added to the PCR reaction at the rate of one unit for every 20 µL of reaction.

  KAPA HiFi HotStart DNA Polymerase (Kapa Biosystems): due to its low error rate and high affinity for DNA, this enzyme was used when amplification of a fragment larger than 3 kb with high fidelity was necessary. 0.5 units were added in every 25 µL of reaction.

- Reaction Buffer: it was always used the buffer supplied with the enzyme employed for each application. Following the recommendations of the commercial company, they were added to the reaction at a final concentration of 1X.

- dNTPs: As with the reaction buffer, each enzyme was used with its own stock of dNTPs. In both cases, the stock consisted of a mixture of the four deoxyribonucleotides at equimolar concentrations that was added to the reaction at a final concentration of 0.2 mM in the case of the DNA polymerase enzyme (Biotools) and 0.3 mM in the case of the enzyme KAPA HiFi HotStar t DNA Polymerase (Kapa Biosystems).

Conventional PCR reactions, containing the above components, were performed in a final reaction volume of between 20 and 25 µL depending on the purpose of the amplification, in sterile 0.2 mL tubes and using a GeneAmp PCR System 9700 thermal cycler (Applied Biosystems).

The profile of the PCR program began with a denaturation step at 94°C for 5 minutes, followed by 30 to 40 amplification cycles, each consisting of a first denaturation phase at 94°C for 1 minute, a second phase of 30 seconds for the annealing of the primers at the optimum temperature and dependent on the design of their sequences (48°C - 68°C) and a third extension phase at 72°C and whose duration depended on the fragment size to amplify and the elongation rate estimated for the polymerase used (it was always 1000 bp per 1 minute). The program profile concluded with a final extension cycle at 72°C for 7 minutes.

A variant of conventional PCR is the semiquantitative PCR. This type of PCR was used to determine the expression level of the *cdc*25 and *swi*6 genes, both encoding cell cycle regulatory proteins, in transformants carrying a translational fusion between the gene encoding the GFP protein and one of the selected genes. This PCR modality, carried with this objective, involved the preparation of two reactions for each gene analysed in which the same amount of cDNA of the transformant was used as a template. The primer pair added to the first reaction was designed to amplify a fragment of the junction area between the two genes that made up each fusion. In this way, the amplified fragment would derive from a fusion between the 3' end and the 5' end of the structural region of the gene of interest and of the *gfp* gene, respectively. The primer pair added to the second reaction was designed to amplify a fragment consisting of only part of the structural region sequence of the endogenous ubiquitin-encoding *Bcubq*1 gene. As it is a single copy gene in the genome of the fungus and has a constitutive expression profile, *Bcubq*1 can be used as a reference to characterize the expression levels of the genes of interest by comparing the fluorescence intensities of the bands corresponding to one and the other amplification products in the gels stained with ethidium bromide.

For each transformant analysed, the pair of reactions was carried out in parallel and exposed to equivalent programs with the minimum possible differences. Furthermore, the number of amplification cycles remained within the exponential region of the amplification curve (25 - 30 cycles) because it is the optimal stretch where intensity differences attributable to variations in expression levels can be

appreciated. All these considerations allowed a visual estimation of the expression level of both translational fusions.

17.2 Reverse transcription (RT-PCR). cDNA synthesis

The synthesis of cDNA by reverse transcription was carried out using the commercial PrimeScript™ RT Reagent kit (Takara Biosystems) following the manufacturer's recommendations, so that, for a reaction, the following components were added:

- Total RNA: 500 ng of RNA, previously treated with DNase to eliminate genomic DNA remains (section 10.3 of Materials and Methods), were used.
- Reaction Buffer: This buffer already contains a mixture of dNTPs and the Mg^{2+} ion and was added to the reaction at a final 1X concentration.
- Oligo-dT primer: the use of this type of primer restricts cDNA synthesis to that copied strictly from the messenger RNA fraction of the sample because this primer contains a sequence of thymines that anneals to the poly-A chain that mRNA present at their 3' end. It was added to a final concentration of 2.5 µM.
- Prime Script RT reverse transcriptase: 0.25 µL was used.

The reactions, containing the above components, were carried out in RNase-free 0.2 µL tubes, in a final reaction volume of 10 µL completed with sterile Milli-Q water treated with DEPC and using a GeneAmp PCR System 9700 thermal cycler (Applied Biosystems).

The profile of the RT-PCR program consisted of a step at 37°C for 15 minutes during which the cDNA is synthesized, followed by a step at 85°C for 5 seconds that causes inactivation of the enzyme. The cDNA thus obtained was stored at -80°C until later use.

Prior to their use in real-time quantitative PCR (RT-qPCR) reactions, cDNA samples were analysed by conventional PCR to determine their quality and the possible presence of contaminating genomic DNA. For this, the same pair of primers that would later be used in the RT-qPCR reactions were used as they flanked an intron in the sequence of the gene of interest, allowing the distinction of the possible genomic origin of the amplified fragment by difference of size.

17.3 Real-time quantitative PCR (qPCR)

The expression analysis of the *Bcmed* gene was performed using RT-qPCR based on the use of the SYBR® Green dye that binds to double-stranded DNA molecules by emitting a fluorescent signal during binding.

Each quantitative PCR reaction was done in a 10 µL volume containing the following components:

- KAPA™ SYBR® FAST qPCR Kit Master Mix (2X) ABI Prism™ (KAPA Biosystems): This cocktail contains a DNA polymerase enzyme, SYBR Green I fluorescent dye, $MgCl_2$, dNTPs and stabilizers. It was added to a final concentration of 1X.

- Primers: They were designed to amplify cDNA fragments of between 100 and 200 base pairs with an amplification efficiency of between 92% and 98%. This aspect was analysed prior to use and was calculated with StepOne™ Software V2.3 (Applied Biosystems) from the slope of the regression line that best adjusted to the threshold cycle values (Ct, threshold cycle) of six serial dilutions of genomic DNA used as template. The primers used were added to the reaction at a concentration of 600 nM and are listed in Table 8 (Appendix).
- cDNA: 1 µL of the product obtained from the reverse transcription reaction carried out as described in the previous section, was added.

The reactions, containing the previous components, were deposited in 0.1 mL multiwell plates in triplicate for each combination of gene and condition, from samples of at least three biological replicates and two technical replicas of cDNA synthesis.

The RT-qPCR profile used was programmed in a StepOnePlus™ Real-Time PCR System (Applied Biosystems) thermal cycler, in accordance with the equipment manufacturer's instructions for the use of SYBR® Green as a quantifier and had an initial phase at 95°C for 2 minutes and 40 amplification cycles of 95°C for 3 seconds and 60°C for 30 seconds. A third step was added to collect the data related to the dissociation temperature (Tm) of all the PCR products and thus obtain the dissociation curve (Melting curve) whose analysis allows to identify nonspecific amplifications.

The relative quantification of gene expression was performed with StepOne ™ Software V2.3 (Applied Biosystems) and Microsoft Excel 365 (Microsoft Corporation, USA), using the C_T comparison method (Bustin, 2000; Pfaffl, 2001). This method makes it possible to compare the amplification of the gene of interest, normalized to the amplification of an endogenous control gene of constitutive expression, under the different conditions with the amplification of the same gene of interest, also normalized, in the reference condition. In this work, the genes of *B. cinerea BcactA* and *Bcubq*, coding for actin and ubiquitin, respectively, were used as endogenous control genes.

The C_T value is equivalent to the number of PCR cycles at which the sample's fluorescence signal reaches the detection threshold, which is the level of fluorescence, automatically or manually set, above the baseline (baseline fluorescence) and within the exponential growth region of the PCR product amplification curve. It is therefore a value inversely proportional to the amount of cDNA in the sample, since the greater the amount of the molecule in a sample, the lower the number of cycles (C_T) required to reach this threshold.

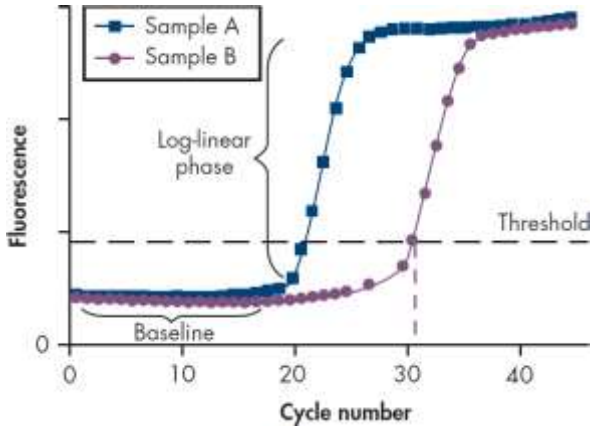

Figure 13. Typical amplification plot. Amplification plots showing increases in fluorescence from 2 samples (A and B). Sample A contains a higher amount of starting template than sample B. The Y-axis is on a linear scale (QIAGEN®).

In order to know the relative amount of transcript or RQ (Relative Quantity of transcript) using this method, the difference between the C_T value of the gene of interest and that of the control gene (ΔC_T) is calculated, for the problem conditions and the one used as reference. Next, the difference between the ΔC_T value of the different problem conditions and that of the control condition, taken as a reference, is calculated. This gives $\Delta\Delta C_T$. Finally, the value of RQ is calculated according to the following formula:

$$RQ = 2^{-\Delta\Delta CT}$$

The value of 2 on the power base refers to a 100% PCR reaction efficiency, that is, the amount of PCR product doubles with each cycle. The control or reference condition is the one on which all the problem conditions are normalized and to which a value RQ = 1 is arbitrarily assigned.

On the other hand, the qPCR technique was also used for the analysis of the number of copies of the fusion allele, which carries a translational fusion of the *cdc25*, *swi6*, *mbp1*, *cdc2* or *niaD* genes with the *gfp* gene, in the transformants analysed in the context of the analysis of the effect of NO on the cell cycle.

The process for preparing the reactions was the same as that described above for the analysis of the *Bcmed* gene. However, genomic DNA from wild-type strain B05.10 and from the different transformants was used instead of cDNA as template substrate and the endogenous control gene was the single copy *BcactA* gene. Furthermore, the primer pairs used amplified a fragment of between 100 and 200 base pairs from the native region of the corresponding fusion allele.

The data obtained were processed with StepOne ™ Software V2.3 (Applied Biosystems) and Microsoft Excel 365 (Microsoft Corporation, USA) and the method used to estimate the number of copies of the fusion allele in the mutants was adapted from that of Hoebeeck *et al.* (2007).

First, the difference between the mean C_T value of the native gene in each fusion, obtained in the reaction in which genomic DNA from the wild-type strain was used, and that obtained in the reaction

in which genomic DNA of the transformant in question was used, was calculated (ΔC_T). The value resulting from this difference was used to calculate Q (relative amount of the native gene in the transformant with respect to the calibrator, the wild-type strain) using the following formula:

$$Q = 2^{\Delta CT}$$

Next, the same calculation was performed with the mean C_T values for the endogenous control gene, thus obtaining its corresponding Q value that was used as a normalization factor, NF. Finally, the estimated number of copies of the fusion allele was determined by the following formula applied to each transformant:

$$\text{Estimated number of copies} = \frac{Q}{NF}$$

18. Hybridizations

18.1 Probe labelling

To carry out the labelling of the probes, the non-radioactive PCR DIG Labeling Mix (Roche) was used, based on the biochemical properties of digoxigenin, a steroid derived from the plants *Digitalis purpurea* and *Digitalis lanata* that is easy to bind to anti-digoxigenin antibodies. These antibodies are conjugated to the alkaline phosphatase enzyme that acts on the chemiluminescent substrate CDP -Star whose signal is collected by a suitable detection equipment.

First, it was necessary to optimize the conditions for the synthesis of the fragment by PCR. Once a single band corresponding to the DNA fragment of the expected size was obtained, its labelling was carried out. Two PCR reactions were carried out in parallel, the composition of which was identical, except for the dNTPs. In one of them, the mixture of normal dNTPs was replaced by the commercial Polymerase Chain Reaction Digoxigenin Labeling Mix (Roche) containing dUTPs bound to digoxigenin that were incorporated into the amplicon during its amplification. In the other reaction, used as a positive control, standard unlabelled dNTPs were used. Subsequently, by means of agarose gel electrophoresis, it was possible to verify the correct labelling of the probe due to the difference in size between the fragment carrying the dUTPs with digoxigenin and the positive control, the size of the latter being smaller due to the absence of the steroid in its composition.

The probes obtained were stored at -20°C until their use in Southern blot analysis, where they were reused until a decrease in their hybridization efficiency was detected.

18.2 Southern blot

DNA hybridizations using the Southern blot technique were performed following the guidelines of Sambrook *et al*. (1989), the "DIG Application Manual for Filter Hybridization" (Roche) and the manual "Hybond-N; nylon membrane" (Amershan).

Between 10 and 15 µg of the genomic DNA under analysis were digested as described in section 13.1 of Materials and Methods, in 200 µL reactions and using enzymes that would yield an informative pattern of bands. After the incubation time, DNA digestion was verified by electrophoresis in agarose gels of an aliquot that represented one tenth of each reaction.

Once the complete digestion of the DNA had been verified, the rest of the volume of the digestions was concentrated in a vacuum equipment (Savant DNA 120 SpeedVac Concentrator (ThermoFisher Scientific)) to a volume of 20 µL. Alternatively to this step, the digestion volume was precipitated by incubation at -80°C for 2 hours after the addition of 2.5 volumes of 100% ethanol (V/V) and 0.1 volumes of 3M sodium acetate pH 5.2. Then, the DNA was pelleted by centrifugation at 13200 xg at 4°C for 30 minutes and, after discarding the supernatant, it was washed twice by r esuspension in 1 mLof 70% ethanol (V/V) and subsequent centrifugation at 7500 xg for 5 minutes. The ethanol residues were dried in the vacuum equipment and the DNA was resuspended in 20 µL of sterile Milli-Q water.

The digested DNA samples were loaded in agarose gels at 0.8% (m/V) and subjected to electrophoresis applying a voltage of 4 V/cm for 7 -8 hours for a correct separation of the digested fragments. The gels were visualized with ethidium bromide as indicated in section 14.1 of Materials and Methods and were conveniently marked to identify the different lanes and their orientation.

Subsequently, a conditioning of the DNA was carried out to favour its transfer from the gel to the membrane. This conditioning was composed of four stages carried out at room temperature (22 -25°C) and with moderate agitation: depurination, denaturation, neutralization, and equilibration. To perform the depurination step, the gel was exposed to ultraviolet light (λ = 260 nm) for 5 minutes. During this exposure, the ultraviolet light creates nicks in the DNA that facilitate the transfer of DNA fragments larger

than 10 kb. Denaturation consists of an alkaline treatment of the DNA that causes its denaturation and breakage through the depurinated sites in the previous stage, resulting in smaller fragments that are easier to transfer. For this, the gel was immersed in the denaturing solution (0.5 M NaOH; 1.5 M NaCl) by two 15-minute incubations each, and then washed with distilled water for 5 minutes. The gel was then immersed in the neutralization solution (0.5 M Tris-HCl pH 7.5; 1.5 M NaCl), in two incubations of 15 minutes each, to neutralize the pH of the gel. The equilibration step was carried out by incubating the gel in 10X SSC (1.5 M NaCl and 0.15 M sodium citrate, pH 7) for 10 minutes.

After the incubation time in the 10X SSC solution, the DNA was transferred from the gel to a nylon membrane (Nylon Hybond-N, GE Healthcare Life Sciences) by means of a transfer unit.

For this, on a glass tray containing the 10X SSC transfer buffer, a rectangular plastic plate, of little thickness, but resistant, was placed perpendicular to it. The plate was covered with two overlapping sheets of Whatman 3MM paper of sufficient dimensions so that their ends were immersed in the buffer contained in the tray. Next, three sheets of Whatman 3MM paper, of the same dimensions as the gel and previously moistened in 10X SSC, were placed in a superimposed manner on the centre of the two previous sheets and the gel was placed on them with the face of the wells facing the sheets. The marked and properly oriented nylon membrane and three more sheets of dried Whatman 3 MM paper were placed on the gel, all with the same dimensions as the gel. To avoid evaporation of the transfer buffer and to guarantee its ascent only through the gel, the glass tray, the plastic support and the perimeter of the gel, sandwiched by the membrane and the sheets of Whatman 3MM paper, were sealed with sheets of plastic film. In this unit of transfer thus described, the transfer of the DNA takes place by capillarity due to the pressure that is applied over the entire area of the gel equally and that is caused by a pile of absorbent paper and a weight of approximately 1 Kg, both placed on the gel and membrane. In this way, the buffer moves from the region with a high water potential (the glass tray) to the region with a low water potential (the absorbent paper stack). This flow moves DNA from the gel to the membrane, where it is bound by ion exchange interactions.

After a minimum transfer time of 16 hours, the unit was disassembled, and the efficiency of the process was estimated by checking the presence of remains of the digested DNA in the gel stained with an ethidium bromide solution (see section 14.1 of Materials and Methods). On the other hand, the

membrane was washed by immersion in 2X SSC (0.3 M NaCl and 0.03 M sodium citrate, pH 7), for 10 min with stirring and after allowing it to dry, it was placed between two sheets of dried Whatman 3MM pape r. It was then exposed to two pulses of ultraviolet light (Stratalinker ®, Stratagene) lasting a few seconds to fix the DNA to the membrane. The membrane was then subjected to the prehybridization process or, alternatively, it was stored at 4°C and in the dark between two blotting papers until later use.

To perform prehybridization, the membrane was placed inside a hermetically sealed glass tube where the prehybridization solution (5X SSC; N-laurylsarcosine 0.1% (m/V); 0.02% SDS (m/V); blocking reagent (Roche) 1% (m/V)) was added in sufficient volume to always keep it moist and it was incubated at 65°C with moderate circular shaking for at least 1 hour. After this time, the hybridization of the membrane was carried out, a process that varied slightly depending on the number of uses of the probe. For the probes that were used for the first time, these were denatured by incubation at 100°C for 10 minutes and added to the prehybridization solution. On the other hand, the reused probes were already diluted in the prehybridization solution. Therefore, to carry out the hybridization, the prehybridization solution was replaced by the solution containing the previously denatured probe. The hybridization step lasted 16 hours at the same temperature and agitation as those used during the prehybridization.

At the end of the hybridization period, the probe solution was removed and stored at -20°C. The membrane was then washed by two incubations with shaking in 100 mL of 2X wash solution (2X SSC; 0.1% SDS (m/V), in sterile Milli-Q water) for 5 minutes each and at room temperature. After these two washes, two more washes were made with 100 mL of 0.1X wash solution (0.1X SSC; 0.1% SDS (m/V), prepared in sterile Milli-Q water). Each wash lasted 15 minutes and was done at 65°C with circular agitation.

Detection of the probe was carried out at room temperature using solutions diluted in buffer 1 (100 mM maleic acid; 150 mM NaCl; pH 7.5; in distilled water). First, the membrane was equilibrated for 5 minutes and shaking in 30 mL wash buffer (buffer 1 with 0.3% Tween 20 (V/V)) and then blocked in 30 mL of buffer 2 (buffer 1 with blocking reagent 1% (m/V) (Blocking Reagent, Roche)), shaking for 45 minutes. After this incubation period, the anti-DIG-alkaline phosphatase antibody (Roche) was added in a ratio of 1:20000 to the 30 mL of buffer 2 so that it was not deposited directly on the membrane and the incubation was prolonged for an additional 45 minutes. The membrane was then washed twice with wash

buffer, with shaking, to remove traces of antibody that did not bind to the probe. Each wash lasted 20 minutes, each using 30 mL of buffer.

The membrane was then immersed in 30 mL of detection buffer (100 mM Tris-HCl; 10 mM NaCl; pH 9.5; in distilled water) where it was incubated for 5 minutes with shaking. After this time, the membrane was placed, correctly oriented, on an acetate-type plastic sheet and 500 µL of the CDP-Star chemiluminescent substrate (Roche) diluted in detection buffer at a concentration of 0.25 mM was added. This step was carried out by depositing small volumes of the diluted substrate over the entire surface of the membrane, then wrapping it in the acetate sheet and spreading the substrate by rubbing the outer face of the wrapper. The membrane wrapped in this way was incubated for 5 minutes in the dark and then placed between two new acetate sheets where chemiluminescence was detected using the ChemiDoc MP detection equipment (Bio-Rad) and following the recommendations of the commercial house.

Once the detection process was finished, it was subjected to three washes with 0.1X washing solution to remove the probe adhered to it, making it possible to use it in new hybridizations. In each wash, carried out every 24 hours, 100 mL of new solution heated to boiling was poured onto the membrane, to later allow its incubation at room temperature and with moderate agitation. After the washes, the dry membrane was stored at 4°C between two dry sheets of Whatman 3MM paper to be used in subsequent hybridizations.

19. Western Blot

All protein detection assays by Western Blot were carried out following the general instructions contained in the "Protein Blotting Guide" manual (Bio-Rad), performing all incubations in the different buffers, unless otherwise indicated, in moderate stirring and at room temperature.

The polyacrylamide gel containing the protein samples obtained and separated according to their molecular weight as described in sections 11 and 14.3 of Materials and Methods, was incubated in the 1X transfer buffer (25 mM Tris-HCl pH 8.3; 192 mM Glycine; 20% Methanol; in distilled water) for 15 minutes to remove any remaining electrophoresis buffer salts. At the same time, the polyvinylidene fluoride membrane (Immobilon-P, Millipore), with the dimensions of the gel, is soaked in 100% methanol for 1 minute and then equilibrated in 200 mL of 1X transfer buffer for 5 minutes.

Once the gel and the membrane had been prepared as indicated, the transfer was carried out using the wet-type electrophoretic transfer modality. For this, the Mini Trans-Blot® Electrophoretic Transfer Cell (Bio-Rad) system was used, in which the gel and the membrane were placed properly oriented and in contact, in the centre of a folding support. Flanking the gel and the membrane, a sheet of 3MM Whatman paper, measuring 10 cm x 7.5 cm, and a pad were placed on each side, all of them previously moistened in the 1X transfer buffer. The folding support was closed ensuring the immobility of the multilayer system inside and was inserted into the transfer module. This, in turn, was placed inside the transfer tank containing 1X transfer buffer, where it was submerged. The assembly was completed by adding a refrigeration unit (previously cooled to -20°C), a magnetic stirrer rod and the closing cap with the power cables. The transfer took place at a constant voltage of 30V / 90mA for 16 hours. Throughout the process, the tank was kept on a magnetic stirrer, inside a chamber refrigerated at 4°C to, together with the refrigeration unit, avoid temperature rise, which could lead to low transfe r efficiencies.

Once the transfer process was finished, the transfer unit was disassembled, the membrane was duly labelled, and the detection step was carried out by means of immunodetection. On the other hand, the gel was stained with Coomassie blue (see section 14.3 of Materials and Methods) to check the efficiency of the transfer.

To begin immunodetection, the membrane was washed in 50 mL of Tris-buffered saline (20 mM Tris-HCl pH 7.5; 500 mM NaCl; in sterile Milli-Q water) for 10 minutes and blocked by incubation in 20 mL of blocking solution (1X TBS with 5% (m/V) milk powder (Nestlé)) for 1 hour. After this time, the traces of blocking solution were eliminated by two consecutive washes of 10 minutes each in 25 mL of T-TBS washing solution (1X TBS with 0.1% Tween 20 (V/V)) and then the membrane was incubated with the primary antibody Anti-GFP-HRP (Anti-Green Fluorescent Protein-Horseradish Peroxidase, MACS antibodies) overnight at 4°C and with constant shaking. This was used in a 1:1000 ratio in blocking solution and its conjugation with horseradish peroxidase simplified the process, making incubation with a secondary antibody unnecessary. The membrane was then washed six times with T-TBS wash solution, each using 20 mL of fresh solution and an incubation time of 10 minutes. These washes were aimed at reducing the background during the subsequent detection. After the sixth wash, the excess T-TBS solution was dried by placing the membrane between two sheets of Whatman 3MM paper for a few moments and then placed properly oriented on a sheet of plastic film where the chemiluminescent substrate SuperSignal West Femto Maximum Sensitivity (Thermo scientific) was added. The reagent was prepared by mixing its two components (Stable Peroxide Solution and Luminol / Enhancer Solution) in equal parts and was added in small volumes that were distributed over the entire surface of the membrane. This was then wrapped in the plastic film sheet and the uniform distribution of the reagent was promoted by gently rubbing the outer face of the wrapper. The membrane wrapped in this way was incubated for 5 minutesin the dark and then placed between two acetate sheets where it was developed using the ChemiDoc MP detection equipment (Bio-Rad) in accordance with the recommendations of the commercial company.

20. Differential expression analysis

To analyse the effect that exposure to NO determines on the transcriptome of the germinating fungus spores, batches of spores of the wild-type strain B05.10 and of the mutant strain lacking the geneencoding flavohemoglobin *ΔBcfhg*1 were obtained according to the procedure described in section 3.1 of Materials and Methods and inoculated at a final concentration of $5 \cdot 10^5$ spores/mL in square plates of 120 mm size containing 25 mL of PDB ½ medium. The cultures were kept in incubation under the standard conditions (see section 2.2 of Materials and Methods) for 4 hours to allow the activation of their germination program. After this time, the cultures were divided into three fractions, for both strains. The first consisted of those cultures whose spores were collected and processed at the end of this 4 -hour incubation period. The spores of the cultures of the second fraction were also collected, after incubation of 4 hours, using a glass spreader and transferred to a 50 mL tube where the exogenous NO donor DETA was added to a final concentration of 250 µM. However, after vigorously shaking the mixture, the spores were returned to the corresponding square plate and kept in incubation for two more hours, after which they were collected. The spores of the third and last fraction of cultures were not collected at 4 hours but were kept in continuous incubation during the total 6-hour period that the test lasted.

To collect the spores at 4 hours or 6 hours, depending on the culture fraction to which they belonged, the bottom of the square Petri dish was scraped with a glass spreader and the content was transferred to a 50 mL tube. After pelleting the spores by centrifugation at 3000 rpm for 5 minutes, the supernatant was discarded, and the pellet was washed with 25 mL of Milli-Q water and the same centrifugation parameters. The supernatant was removed, the pellet was resuspended in 1 mL of Milli -Q water and transferred to a 1.5 mL tube. Once in the 1.5 mL tube, the mixture was vortexed vigorously and centrifuged at 5000 rpm for 2 minutes. At the end of this centrifugation period, the supernatant was removed and the pellet was resuspended, by vortexing, in 500 µL of RNAlater® Sol ution buffer (Invitrogen) where it was incubated for 1 hour at 4°C. The objective of this incubation was to allow the solution to enter the cells of the mycelium to contact with the RNA and thus stabilize it. Finally, the mixture was centrifuged at 10000 rpm for 3 minutes and after removing the supernatant, it was frozen in liquid nitrogen and stored at -80°C.

Three independent biological experiments were carried out, obtaining three repetitions for each of the six samples resulting from the combination of condition and strain:

- Sample 1: Spores of the wild-type strain B05.10 grown for 4 hours without exposure to NO.
- Sample 2: Spores of the wild-type strain B05.10 grown for 6 hours without exposure to NO.
- Sample 3: Spores of the wild-type strain B05.10 grown for 4 hours and then exposed to NO for 2 hours.
- Sample 4: Spores of the mutant strain *ΔBcfhg*1 grown for 4 hours without exposure to NO.
- Sample 5: Spores of the mutant strain *ΔBcfhg*1 grown for 6 hours without exposure to NO.

- Sample 6: Spores of the mutant strain *ΔBcfhg*1 grown for 4 hours and then exposed to NO for 2 hours.

From these samples, the Genomic Sciences Laboratory, of the North Carolina State University, carried out their complete processing applying the massive RNA sequencing strategy (RNAseq) developed by Wang *et al*. (2009). Mycelium samples from a fourth biological replica of each condition were preserved to carry out the validation of the results obtained in the RNAseq analysis, if necessary, later. The US entity carried out the extraction of RNA from the mycelium samples and analysed their integrity with a Q/C analysis using a Bioanalyzer. This population of RNA was then converted into a directional cDNA library for subsequent sequencing using 1 lane of HiSeq 2500 (125 bp SE).

Fastq read quality was assessed using FastQC High Throughput Sequence QC Report (v.0.11.7). The reads were then mapped to the *B. cinerea* genome (B05.10 ASM14353v4) using Hisat2 (v.2.1.0). For each library, the number of reads mapped to each gene was counted using StringTie -eB (v.1.3.5). Differential expression analysis between the pairwise comparisons of interest was performed with the DESeq2 (v.1.28.1) R package considering the genes as differentially expressed (DEG) when $|\log_2 \text{foldchange}| > 2$ and $p_{adjusted} \leq 0.05$.

Gene ontology (GO) enrichment analysis was performed on the sets of differentially expressed genes of two of the three comparatives analysed (sample 2 versus sample 3 and sample 5 versus sample 6). The matrix containing the total set of genes from *B. cinerea* was annotated with InterProScan Version 5.52-86.0 (Jones *et al*., 2014). Fisher's exact tests were performed on the GO terms associated with the significantly up- and downregulated genes (adjusted P value of < 0.05, any fold change) and REVIGO (Supek *et al*., 2011) was used to trim the resulting lists of significantly overrepresented GO terms.

On the other hand, to analyse the functions of the *Bcorp*1 gene product participates in, a differential gene expression analysis was also performed by RNAseq between the B05.10 and *ΔBcorp*1-19 strains. To obtain the biological material, 90 mm Petri dishes with MEA medium covered with a cellophane sheet were inoculated with plugs of vegetative mycelia from the edge of fungal colonies of the indicated strains actively growing under the same conditions. The inoculated plates were incubated in a germination chamber at 22°C with a photoperiod of 16 hours of light and 8 hours of darkness for 96 hours. After this time, the mycelium grown on the cellophane sheets of an area equivalent to the outer circular crown of the colony, about 10 mm thick, was collected. To do this, the surface of the plastic was scraped with the help of sterile tweezer, the mycelium obtained was immersed in 1.5 mL tubes containing 500 µl of RNAlater® Solution buffer (Invitrogen) and these were frozen in liquid nitrogen and stored at - 80°C.

Three independent biological tests were carried out, obtaining three repetitions for the samples of both strains. The subsequent steps of RNA extraction from the mycelium samples, the construction of the cDNA library, its sequencing and the quality and differential expression analyses were carried out in a manner equivalent to the transcriptional analysis performed on the strains B05.10 and *ΔBcfhg*1 in response to NO exposure.

21. DNA sequencing

The constructions and other DNA fragments of interest generated in this work were sequenced to detect the presence of point mutations in their sequences. For this, the DNA fragment derived from a PCR and the plasmid DNA (see section 10.2 of Materials and Methods) were purified with the NucleoSpin® PCR and Gel Clean-up and NucleoSpin® Plasmid (Macherey-Nagel) purification kits, respectively, according to the recommendations of the commercial house. Next, a NanoDrop ND-1000 spectrophotometer (Thermo Scientific) was used, which allowed the concentration of the samples to be determined in order to estimate the volume required for their sequencing.

Sanger-type sequencing (Sanger *et al*., 1977) was the sequencing method used and was performed at the Genomic and Proteomic Se quencing Service of the University of Salamanca using a 3100 Genetic Analyzer capillary automatic sequencer (Applied Biosystems). This service requires 100 ng of DNA for 1 kb fragments from PCR or an amount between 400 and 600 ng for plasmid DNA sequencing in reactions of 8 µL of total volume to which the primer corresponding to a final concentration of 3.2 pM was added.

22. Bioinformatics methods

Identification of genes, obtaining gene and protein sequences in FASTA format, performing searches with the BLAST algorithm (Basic Local Alignment Search Tool) (Altschul *et al*., 1990) and sequence analysis (identification of promoter regions, domains, and other features) were made with the following browsers of (fungal) genomes:

- NCBI (Nacional Center for Biotechnology Information, https://www.ncbi.nlm.nih.gov/).
- EnsemblFungi (http://fungi.ensembl.org/index.html and https://doi.org/10.1093/nar/gkz890)
- *Botrytis cinerea* Portal (https://bionfo.bioger.inrae.fr/botportalpublic and http://dx.doi.org/10.15454/IHYJCX)
- Joint Genome Institute (https://genome.jgi.doe.gov/portal/. PMID 24225321 and DOI 10.1093/nar/gkr947)

Geneious 10.2.6 software (Biomatters, https://www.geneious.com/) was used for routine DNA and amino acid sequence analysis by performing alignments, restriction analysis, oligonucleotide design and searches for BLAST type in the public databases to which it is linked.

The automatic search of the functional categories of the annotations of the genes that appearedas differentially expressed in the differential expression analysis using RNAseq was carried out with InterProScan Version 5.52-86.0 (Jones *et al*., 2014; https://www.ebi.ac.uk/interpro/search/sequence/) to obtain the PFAM, IPR and GO terms and with the automatic annotation server BlastKOALA (Kanehisa *et al*., 2016; https://www.kegg.jp/blastkoala/) to obtain the KEGG terms and their description:

- KEGG (Kyoto Encyclopedia of Genes and Genomes) is a compendium of databases on genomes, biological pathways, diseases, drugs, and chemical substances (Kanehisa and Goto, 2000; Kanehisa, 2019; Kanehisa *et al*., 2021).
- InterPro (The Integrated Resource of Protein Domains and Functional Sites) contains information of protein families, domains, and functional sites. Provides the IPR terms (Blum *et al*., 2020).
- Pfam (Protein Families) is a database of protein families that includes protein domains (Mistry *et al*., 2021).
- Gene Ontology provides an ontology of defined terms that report properties of a given gene product. This ontology comprises three domains: cellular component, molecular function, and biological process (Ashburner *et al*., 2000; The Gene Ontology Consortium, 2021).

Blast2go software (Götz *et al*., 2008) was used to complete the functional annotation of those genes that appeared as differentially expressed in the aforementioned analysis, but for which the automatic search process for functional annotations using InterProScan and BlastKOALA did not give results. The software is linked to Gene Ontology Annotation database and InterPro collection of databases.

Manual inspection of the differentially expressed genes in this analysis, which led to the classification of a fraction of them into nine functional categories, was carried out using the aforementioned databases together with the Uniprot database (Universal protein. The UniProt Consortium, 2021), which collects information on protein sequences and functional information.

GPS-SNO 1.0 (Xue *et al*., 2008) and GPS-YNO2 1.0 (Liu *et al*., 2011) are two computational software implemented in JAVA that use a group-based S-nitrosylation and nitration predicting and scoring method to the prediction of S-nitrosylation sites and nitration sites in proteins, respectively. Both were used in the analysis of the sequences of the products encoded by the *cdc*25, *cdc*2, *mbp*1, *swi*6, *mcm*1 and *niaD* genes.

23. Computer programs

The images obtained during the tests of characterization of the *Bcmed* and *Bcorp1* genes and the modulating effect of NO on the development of the fungus were processed and analysed with ImageJ 1.49 and Fiji programs (National Institutes of Health, USA Rasband, 1997-2018; Schindelin *et al*., 2012) and the resulting numerical data were statistically analysed with Statgraphics Centurion XVI software (Statgraphics Technologies, Inc.).

Microsoft Office 365 (Microsoft Corporation) was the suite used for creating and editing text documents, figures, and tables and for bibliographic editing.

CHAPTER I.

Effect of nitric oxide on development in *B. cinerea*.

Introduction

Nitric oxide is a signalling molecule with important and varied functions in different taxonomic groups, including fungi (Cánovas *et al*., 2016). In this kingdom, the molecule has been poorly studied, but it is known to play a vast signalling role ranging from modulation of sexual and asexual development and secondary metabolism to host plant colonization and infection. Due to these multiple functions and its short lifetime, of a few seconds, the presence of a balance that maintains an adequate concentration of NO in each stage of the fungus life cycle is essential through both the biosynthesis reactions of the molecule and its detoxification mechanisms (Cánovas *et al*., 2016).

So far, two NO synthesis pathways have been identified in fungi, the oxidative pathway, and the reductive pathway. The first would imply the presence of a pathway similar to the oxidative pathway present in mammals in which the enzyme nitric oxide synthase (NOS) catalyses the conversion of L - arginine to L-citrulline producing nitric oxide. However, it is a poorly characterized pathway due to the absence of NOS-like proteins (NOSLs) in fungal genomes or, in the case of fungi with genes annotated as such in their genomes, due to the lack of a confirmed relationship between these hypothetical NOSLs and NO synthesis (Li *et al*., 2010; Samalova *et al*., 2013). The reducing pathway, on the other hand, requires the synergistic action of the enzyme nitrate reductase to convert nitrate to nitrite and of the enzyme nitrite reductase, which mediates the conversion of nitrite to NO and is considered to be the most important enzymatic source of NO in fungi (Horchani *et al*., 2011; Zhao *et al*., 2020).

On the other side of the coin are the catabolic mechanisms of NO that aim to combat the toxicity of the molecule. At high concentrations, such as those reached in fungal cells during infection of the host plant, NO can lead to nitrosative stress through the generation of the nitrosonium cation (NO^+) and the nitrosyl anion (NO^-) and to oxidative stress when it reacts with oxygen producing dinitrogen trioxide (N_2O_3), nitrite anion (NO^{-2}), peroxynitrite ($ONOO^-$) and ultimately nitrogen dioxide (NO_2). All these species are highly reactive and capable of causing the inactivation of proteins necessary for physiological processes or the damage of cellular lipids through their oxidation or nitration (Brown and Borutaite, 2006; Fitzpatrick and Kim, 2015; Marroquin-Guzman *et al*., 2017). Faced with this situation, fungi have multiple mechanisms based mainly on oxidoreduction reactions of NO or its derived forms. S-nitrosoglutathione reductase (GSNOR), which reacts with GSNO, a natural reservoir of NO, giving rise to ammonia and glutathione disulfide (GSSG) (Zhao *et al*., 2016), thioredoxin reductase that eliminates the NO of the S- nitrosylated motifs of the affected proteins (Zhao *et al*., 2016; Zheng *et al*., 2011) and the cytochrome P450 NO reductase (P450nor), which catalyzes the reduction of NO to N_2O (Hendriks *et al*., 2000), are examples of reductase enzymes involved in this detoxification process. Among the oxidases, there are nitronate monooxygenase that causes oxidative denitrification of nitroalkanes at the same time that it generates nitrate and nitrite (Marroquin-Guzman *et al*., 2017) and flavohemoglobins (FHbs), which constitute the inducible mechanism of detoxification of NO best described in fungal models (Forrester and Foster, 2012).

FHbs are chimeric globins formed by an N-terminal globin domain and an adjacent, C-terminal redox-active protein domain and their function is described as NO dioxygenase that requires NADPH, FAD and O_2 to turn NO into NO^- (Hausladen *et al*., 1998; Gardner *et al*., 1998). The heme group, which reacts with O_2, is in the globin domain while the C-terminal redox active domain contains potential binding sites for FADH and for NAD(P)H that participate in the recycling of the oxidized heme (Hausladen *et al*., 2001). Instead, under anaerobic conditions FHbs consume NO to produce N_2O with the involvement of NADH (Durner *et al*., 1999; Kim *et al*., 1999).

Other proteins different from oxidoreductases and that contribute to resistance to nitrosative stress are porphobilinogen deaminase hemC, which promotes the activity of FHbs through unknown mechanisms, and nitrosothionein, which reacts with NO and GSNO to generate an S-nitrosylated peptide (Zhou *et al*., 2013; Zhao *et al*., 2020).

Regarding its signalling mechanisms, the molecule has been characterized in different taxonomic groups and two classes of mechanisms have been differentiated depending on the partic ipation or not of the soluble enzyme guanylyl cyclase (sGC), a heme-containing, heterodimeric receptor that selectively binds to NO even in the presence of oxygen (Boon and Marletta, 2005). In the NO-cGMP dependent signalling, NO binds to the heme iron of the enzyme activating its catalytic domain through a conformational change. Once activated, this protein promotes the conversion of GTP to cyclic GMP (cGMP) (Friebe and Koesling, 2003). The cGMP produced, in turn, acts directly with downstream effectors such as the family of cyclic nucleotide-gated channels, and cGMP-regulated phosphodiesterases and cGMP-dependent protein kinases (Lucas *et al*., 2000; Boolell *et al*., 1996; Biel *et al*., 1999). The latter constitute the central downstream mediators of this pathway and mediate pathway-specific cellular responses through the phosphorylation of phosphorylation-dependent transcriptional factors. Finally, these transcriptional factors regulate the expression of several genes involved in many physiological processes (Zhao *et al*., 2020). The NO-cGMP independent signaling is constituted by the regulation of protein activity by NO either through binding to transition metals of metalloproteins (metal nitrosylation) or covalent modification of cysteine (S-nitrosylation) and tyrosine (tyrosine nitration) residues (Amal *et al*., 2019; Heinrich *et al*., 2013; Nathan *et al*., 2009).

The signalling function of nitric oxide has beneficial consequences when the gas is at low concentrations, controlling essential biological processes, such as signal transduction from the cell surface into the cell, responses to abiotic and biotic stresses, as well as development or secondary metabolism. However, an excess of its production can generate a nitrosative stress in the cells with possible microbiostatic or microbicidal effects, as in the case of its influence on the cell cycle.

1. Nitric oxide and development

In *Aspergillus*, as in *Botrytis*, conidia form on conidiophores after a period of mycelial growth. The development of the conidiophores as well as the posterior conidiation are regulated in a conserved

manner by the core conidiation genes *BrlA*, *AbaA*, and *WetA*. The sequential expression of these three transcription factors establishes a linear regulatory pathway (*brlA*> *abaA*> *wetA*) that controls the expression of other conidiation genes responsible for the growth, differentiation, and secondary metabolism processes that take place during this stage (Krijgsheld *et al*., 2013). The fully developed conidia remain in a dormant state until the proper environmental conditions for germination are met. Until that time, there is an active transcriptional activity within the conidia that maintains and regulates this latency period (Novodvorska *et al*., 2013). This activity is controlled by the following groups of proteins characterized to some extent (Baltussen *et al*., 2019):

- The velvet family of proteins. This family includes VELA, VELB, VELC, and VOSA proteins, regulated by *AbaA*. These proteins are key regulators of conidiation, maturation and viability of spores, trehalose biogenesis and resistance to thermal, oxidative, and UV stresses. Some negatively regulate the germination (Sarikaya Bayram *et al*., 2010; Park *et al*., 2012; Park *et al*., 2012b; Eom *et al*., 2018; Ni and Yu, 2007).

- *MybA* and *AtfA*. *Myba* is a transcription factor that is not controlled by the central regulators *BrlA* and *AbaA* and, at the same time, it controls the expression of *wetA* and velvet regulators *vosA* and *velB*. It regulates cell wall constitution through repeat-rich glycosylphosphatidylinositol (GPI) -anchored cell wall protein *CspA* and is also involved in trehalose biosynthesis and in response to oxidative stress (Tao and Yu, 2011; Park *et al*., 2012; Park *et al*., 2012b; Valsecchi *et al*., 2017). *AtfA* is a bZip (basic-region leucine zipper)-type transcription factor that positively regulates genes related to stress tolerance (oxidative and thermal) and negatively regulates genes related to germination (Hagiwara *et al*., 2016; Hagiwara *et al*., 2014).

- Compatible Solutes. The accumulation of compatible solutes such as sugars, sugar alcohols, amino acids, and betaine serve as protection against drought, heat, and other stressors. The sugars trehalose and mannitol stand out. The first is essential against thermal and oxidative stress, dehydration and for long-term viability. The second accumulates in dormant conidia and is degraded during germination and also has a role in resistance against high temperature and oxidative stress (Ni and Yu, 2007; Wyatt *et al*., 2013; Fillinger *et al*., 2001; van Leeuwen *et al*., 2013; Al-Bader *et al*., 2010; Wyatt *et al*., 2014).

- Heat Shock Proteins (HSPs). They are a family of intracellular proteins with a variety of different functions, but the majority act as molecular chaperones or as proteases that are upregulated by a variety of different stressors. HSPs play a major role in the recovery from cell stress by acting as catalytic enzymes assisting in the refolding of mismatched or aggregated proteins (Cagas *et al*., 2011; Suh *et al*., 2012; Jolly and Morimoto, 2000; Priya *et al*., 2013; Lamoth *et al*., 2014).

- The conidial cell wall and surface proteins. The polysaccharide cell wall is essential for fungal cell growth and protection against environmental stresses. Its fibrillar nucleus is composed of branched ß-(1,3)-glucan to which other polysaccharides such as chitin are covalently attached.

Dormant conidia have a melanin-pigmented layer above the cell wall that is important for maintaining the structure and rigidity of the cell wall. In fungi, two types of melanin are found, 1,8-dihydroxynaphthalene (DHN) melanin and L-3,4-dihyroxyphenylalanine (L-DOPA) melanin. This layer of melanin is covered by an outer layer, a rodlet layer. In *A. fumigatus*, this layer is exclusively composed of hydrophobic RodA proteins that maintain the integrity of the cell wall (Fontaine *et al*., 2010; Valsecchi *et al*., 2017; Eisenman and Casadevall, 2012; Bayry *et al*., 2014; Pihet *et al*., 2009).

- Dehydrin-like proteins. This group of proteins initially described in plants, has been detected in *Aspergillus* conidia and has been attributed a protective role in a chaperone-like manner against different types of stress. Thus, the dehydrin-like proteins DprA and DprB are involved in protection against oxidative, osmotic, and pH stress, while DprC is involved in the protection against freeze stress (Wong *et al*., 2011; Close, 1996; Wong *et al*., 2012; Wartenberg *et al*., 2012).

- The High-Osmolarity Glycerol–Mitogen-Activated Protein Kinase Pathway. (HOG)-MAPK pathway (HOG pathway) is a two-component osmosensor system that responds to extracellular signals (osmotic, oxidative, and temperature stress) by transmitting this information through a cascade of mitogen-activated protein kinases (MAPKs). In *Aspergillus*, the MAPKs MpkC and SakA are the main effectors of the pathway. SakA interacts with MpkC to activate the cell wall integrity (CWI) path. In addition, SakA activates the transcription factor AtfA and the hypothetical osmotic stress regulator OsrA, which, in turn, regulates the expression of the genes encoding dehydrin- like proteins DprA, DprB and DprC (Hagiwara *et al*., 2014; Wong Sak Hoi *et al*., 2011; Wong Sak Hoi *et al*., 2012; Atay and Skotheim, 2017; Kawasaki *et al*., 2002; Furukawa *et al*., 2005; Lara- Rojas *et al*., 2011; Jaimes-Arroyo *et al*., 2015).

Dormant spores begin to germinate as soon as they detect the appropriate environmental conditions, being able to differentiate four stages: breaking of spore dormancy; isotropic swelling; establishment of cell polarity and formation of a germ tube and maintenance of polar growth (Lamarre, 2008). According to Baltussen *et al*. (2019), most filamentous fungi require the presence of low molecular mass nutrients, such as inorganic salts, sugars, and amino acids for conidial germination (Carlile and Watkinson, 1994). The presence of carbon sources is detected by a heterotrimeric G protein pathway and by the Ras signalling pathway, thus controlling germination. The latter also controls the change from isotropic growth to polarized growth (Osherov and May, 2000; Som and Kolaparthi, 1994). The alpha subunit of the heterotrimeric G protein may in turn activate the cAMP-PKA signalling pathway, ultimately regulating germ tube growth, trehalose mobilization, and response to cell wall damage during early germination (Fillinger *et al*., 2002; Shwab *et al*., 2017). For its part, calcium signalling appears to be non- essential for the early stages of conidial germination, but the Ca^{2+} cation and calmodulin, a calcium- binding protein, can activate the heterodimeric protein calcineurin and the pathway that bears its name. A downstream effector of calcineurin is the transcription factor CrzA that influences germination, polarized growth, and cell wall structure (Juvvadi *et al*., 2014).

Although these pathways maintain their regulatory action throughout the entire germination process, there are other more dynamic cellular mechanisms and processes whose activity is more specific to a particular germination stage of development.

Latent conidia contain stored mRNAs that could be prepared for rapid activation and translation during dormancy break when environmental conditions are conducive (d'Enfert, 1997). This break is associated with a change from a fermentative metabolism to a respiratory metabolism (Lamarre *et al*., 2008). At the same time, the outer layer of the conidial cell is shed and the rodlets are degraded by aspartic proteases, melanin being able to remain (Langfelder *et al*., 2001). Possible external stressors that can come into contact with the conidial cell wall, altering it, cause the activation of the CWI pathway through the MAPK pathway (van de Veerdonk *et al*., 2017).

After dormancy break, the first morphological change of the germinating conidium is isotropic growth. In this phase, the spore grows isotropically adding new material to the cell wall equally in all directions, doubling its diameter or more at the end of this stage (Baltussen *et al*., 2018; Thakur and Shankar, 2017). During this process, the cell wall extends, which translates into an increase in transcripts involved in its remodelling, such as chitin synthases and GPI-anchored glucanosyltransferases (van Leeuwen, 2013; Jiang *et al*., 2008). This expansion process coincides with metabolic activities required for cellular growth, such as protein synthesis and carbohydrate metabolism (Krebs/ Tricarboxylic acid cycle (TCA) cycle) (Cagas *et al*., 2011).

Isotropic growth is followed by polarized growth. During this phase, the germ tube is formed and for this, an axis of polarity and the deposition of cortical markers are establishe d. Subsequently, polarity components such as the Cdc42 module and the polarisome are recruited as cortical markers. Henceforth, polar growth is maintained by the morphogenetic machinery, composed of actin, septins, cell wall biosynthetic enzymes (chitin synthases, 1,3-ß-glucanosyltransferases, enzymes related to sphingolipid biosynthesis), the vesicle trafficking system, signaling pathways (cell cycle and DNA processing), landmark proteins, Arp2/3 (actin-related proteins 2/3) complexes, polarisome, and Rho GTPase modules, that is directed to the site of polarization to add new cell material (Harris and Momany, 2004; Momany, 2002; Harris, 2006; Riquelme, 2013; Lin *et al*., 2014; Riquelme *et al*., 2018; Baltussen *et al*., 2019).

NO is known to participate in the regulation of asexual development, such as in the formation of sporangiophores and pycnidia, conidiation, spore germination and appressorial formation (Gong *et al*., 2007; Wang and Higgins, 2005; Prats *et al*., 2008; Maier *et al*., 2001; Ninnemann and Maier, 1996) and in that of sexual development, as in the formation of cleistothecia (Baidya *et al*., 2011, Zhao *et al*., 2020). Furthermore, its presence has been detected in fungal cells from during the transition from vegetative growth to conidia with a mature appressorium (Maier *et al*., 2001; Wang and Higgins, 2005; Gong *et al*., 2007; Turrion-Gomez and Benito, 2011; Samalova *et al*., 2013; Zhang *et al*., 2015; Marcos *et al*., 2016).

The molecule appears to have a versatile role in asexual development depending on the species. Thus, it can cause an inhibition or delay of conidia and germination, as in *Colletotrichum coccodes* (Wang

and Higgins, 2005). Or it may have the opposite effect, as in *Magnaporthe oryzae*, *Puccinia striiformis* f. sp. *Tritici*, *P. blakesleeanus*, *Cryphonectria parasitica* and in *C. minitans* (Maier *et al*., 2001; Gong *et al*., 2007; Li *et al*., 2010; Samalova *et al*., 2013; Yin *et al*., 2016). It has also been seen to affect the expression of the *brlA* conidiation regulator gene in *Aspergillus* (Marcos *et al*., 2016; Zhao *et al*., 2020).

In the case of sexual development, the influence of NO seems to be more uniform promoting its activation to the detriment of asexual processes. This is the case of *Aspergillus* where the concentration of the molecule influences the expression of the sexual development regulatory transcription factor *nsdD* (Baidya *et al*., 2011; Marcos *et al*., 2016; Zhao *et al*., 2020).

2. Nitric oxide and secondary metabolism

Botrytis spp. it is capable of producing a wide variety of secondary metabolites of different nature and function. These compounds can be grouped into families according to their chemical nature: terpenes, polyketides, non-ribosomal peptides, prenylated tryptophan derivatives, or hybrids between these four main classes (Wiemann and Keller, 2014; Collado and Viaud, 2016).

Among the terpenes are Botrydial and its derivatives, with phytotoxic function (Deighton *et al*., 2001), abscisic acid with a possible function in manipulating the host (Collado and Viaud, 2016) and carotenoid pigments and retinal with protective function against oxidative stress and light, respectively (Schumacher *et al*., 2014).

The botcinic acid, botcinins and botrylactone are phytotoxic and antifungal polyketides (Cutler *et al*., 1993, 1996; Tani *et al*., 2005, 2006). Melanin and bikaverin are also in this family, which are pigments with a protective function against UV radiation and other types of stress (Scharf *et al*., 2014) or antimicrobial function (Limon *et al*., 2010).

Orphan secondary metabolites constitute a group of compounds whose presence has been detected in the fungus, but the genes that participate in their biosynthetic pathways have not yet been identified (Collado and Viaud, 2016). This is the case with several trihydroxamate siderophores produced by *Botrytis* under iron limiting conditions (Konetschny-Rapp *et al*., 1988), the polyketides botrallin (Overeem and Van Dijkman, 1968; Kameda *et al*., 1974) and ramulosin (Stierle *et al*., 1998), the hybrids 4-acetoxytetrahydrobotryslactone (Colmenares *et al*., 2002), botryslactone (Kimura *et al*., 1995), BSF-A (Kimura *et al*., 1993) and cinereain (Cutler *et al*., 1988) and mycosporine 2, a metabolite photoprotector capable of absorbing UV radiation (Fabre-Bonvin *et al*., 1976; Arpin *et al*., 1977).

NO participates in fungal secondary metabolism in two ways. On the one hand, as a signaling molecule and on the other, as one of the fractions that will be integrated into the structure of the metabolites or as one of the intermediates during their synthesis (Zhao *et al*., 2020).

In the first case, a positive regulatory function of the molecule on secondary metabolism mediated by Gram-negative bacterial cell wall constituent lipopolysaccharide has been described.

Lipopolysaccharides, which are stimulators of inducible NOS activity in mammalian cells, increase NO production followed by an increase or activation of secondary metabolite production in fungi such as *Penicillium* sp., *Aspergillus* sp., *Rhizopus oryzae* and *Thanatephorus cucumeris* (Khalil *et al*., 2014). Similar results have been observed by varying NO levels in co-culture systems or using modulating drugs in the basidiomycetes *Inonotus obliquus* (Zhao *et al*., 2015) and *Russula griseocarnosa* (Dong *et al*., 2012) and in the ascomycete *A. nidulans* (Baidya *et al*., 2011). Likewise, a negative regulatory function of secondary metabolism has been observed by NO burst in *I. obliquus* where the molecule compromised by S-nitrosylation the activity of key enzymes involved in styrylpyrone biosynthesis (Zhao *et al*., 2016a; b). In both modes of regulation, the detailed mechanisms by which the molecule performs its regulatory action are still unknown.

In the second case, NO would be involved in secondary metabolism as a substrate for actinobacterial P450nor (Barry *et al*., 2012). This enzyme is believed to contribute significantly to NO denitrification and environmental N_2O emission in fungi (Kizawa *et al*., 1991, Zhao *et al*., 2020). However, through a phylogenetic analysis it has been affiliated with nondenitrifying actinobacterial sequences involved in secondary metabolism and included in candidate biosynthetic gene clusters in numerous fungal species (Higgins *et al*., 2018). The presence of a functional nitro group in the structure of a metabolite is a way to increase its toxicity or functional specificity (Kovacic and Somanathan, 2014) and although a variety of this type of compounds has already been isolated from fungi (Parry *et al*., 2011), the underlying synthesis reactions have yet to be ascertained (Kovacic and Somanathan 2014).

3. Nitric oxide and cell cycle

The cell cycle, by which a cell grows and divides into two daughter cells, is made up of four stages: G1 (the cell grows and, if conditions are right, engages in the division process), S (the DNA is synthesized and chromosomes replicated), G2 (shorter stage than G1 in which products necessary for the next stage are synthesized) and M (chromosomes are separated and the cell is divided into two). After the end of the M phase, the cells complete the cycle by entering the G1 phase again (Li *et al*., 2004). It is a vital biological process whose regulation is highly conserved among eukaryotic organisms. Among them, yeasts (the budding yeast *Saccharomyces cerevisiae* and the fission yeast *Schizosaccharomyces pombe*) have long been a group used for their study because of their convenience for both classical and molecular genetic analysis (Nurse, 1985).

Cell cycle regulation is a highly complex process, but it is widely known that, in eukaryotic cells, the cell cycle is regulated in a refined way by cascades of phosphorylations and dephosphorylations of key proteins where cyclins constitute one of the most important regulatory elements. It is a family of transient proteins that are synthesized cyclically, hence its name, during the advancement of the cell cycle. Each cyclin is associated with a stage, transition or set of stages of the process during which its levels increase intensely helping to drive the events of that phase or period. Specifically, they perform their function through the formation of complexes with cyclin-dependent kinase enzymes (CDKs) activating their kinase

function in the latter. The CDKs thus activated carry out the phosphorylation of their tar get proteins. The interaction with cyclins not only allows the activation of their kinase activity but is also important for the recruitment and selection of substrates existing an overlap between substrates that are phosphorylated by the various cyclin-CDK complexes. However, the expression of the cyclins takes place in an orderly manner, allowing the different cyclin-CDK complexes to phosphorylate the correct proteins at the correct time, guaranteeing cell cycle progression.

In addition to the activating action of cyclins, CDKs also undergo regulation by cyclin dependent kinase inhibitors (CKIs) that inhibit CDKs, by other kinases that activate them through phosphorylations (cyclin dependent kinase activating kinases (CAKs)) or deactivate (tyrosine kinases), by phosphatase enzymes that reverse the phosphorylations of other regulatory elements and by acetyl transferases that regulate CDKs through acetylation (Enserink and Kolodner, 2010). This regulatory network would be completed with transcription factors, proteins that bind to specific DNA sequences to control their transcription and control points, molecular mechanisms that evaluate if the cellular conditions are adequate to allow the passage from one phase of the cycle to the next. These mechanisms preve nt certain events such as DNA damage from being maintained throughout the successive phases.

According to Enserink and Kolodner (2010), in the *S. cerevisiae* cell cycle, the proteins related to its regulation are synthesized as part of different transcriptional programs that are activated in the different phases. It is common for the proteins synthesized in each transcriptional program to perform functions and control important processes for the next stage of the cycle. This form of regulation guarantees the unidirectional advancement of the cell cycle, an aspect that is reinforced by the presence of positive and negative feedback loops.

Within this regulatory configuration, *cdk*1, also called *cdc*28 (*cdc*2 in *S. pombe*) is the most important of the six CDKs that yeast has since it alone is necessary and sufficient to drive the cell cycle. This kinase interacts with nine different cyclins throughout the successive stages: three G1 cyclins (*cln*1, *cln*2 and *cln*3) and six B-type cyclins (*clb*1-6).

Initially, *cdk*1 is inactive during the G1 phase due to low concentrations of cyclins and the presence of the CKIs SIC1 and FAR1. Its activity increases at the end of this phase when cyclin concentrations increase and CKIs are degraded. This is when the CLN3-CDK1 complex activates the transcription of a set of around 200 genes that make up the G1 cluster. CLN3-CDK1 regulates the expression of this cluster by means of two transcription factors, MBF and SBF. MBF (MLU1-box binding factor) is formed by *mbp*1 and *swi*6 and binds to promoters that contain the MCB (MLU1 cell cycle box) promoter element, inducing the transcription of genes involved in DNA replication and repair. For its part, SBF (SCB binding factor), a complex between *swi*4 and *swi*6, binds promoters with the SCB element (Swi4/6 cell cycle box) and regulates the transcription of genes related to cell cycle progression, morphogenesis cellular and spindle pole body duplication (*cln*1 and *cln*2 among others). Both the three G1 cyclins CLN1-3 and CLB5,6 are involved in proper entry into S phase.

As the cell moves from G1 to S phase, Cyclin-CDK1 (CLB6-CDK1) complexes can regulate SBF and MBF processing to turn off the first phase transcriptional program. However, the transcriptional repressor NRM1 seems to be the main one in charge of turning off the program by inhibiting MBF.

During the G1-S transition, a second regulatory transcriptional program takes place by the forkhead transcription factor HCM1, resulting in the expression of genes that make up the two gene clusters of the S phase (among them, the transcription factors *fkh*1, *fkh*2 and *ndd*1). The expression of *hcm*1 is believed to be controlled by MBF and SBF since its promoter region has binding sites for both complexes.

In this transition period, the CKIs *far*1 and *sic*1 are also expressed. FAR1 inhibits CLN-CDK1 complexes while SIC1 is thought to inhibit CLB-CDK1 complexes.

From S phase to M phase, a group of approximately 35 genes is expressed (*cdc*5, *swi*5 and *ace*2, among them). This group constitutes the CLB2 cluster, so named because its kinetics is similar to that of the cyclin CLB2, and it seems to be regulated by forkhead transcription factors FKH1 and FKH2. The rate- limiting transcriptional transactivator NDD1, the polo kinase CDC5 and the MCM1 transcription factor take part in this. CDK1 also controls transcription of the CLB2 cluster in multiple ways through CLB-CDK1 complexes.

During the S phase, DNA replication takes place where CLB5,6 participate preventing firing of origins of replication that have already fired. Also, CLB5 is necessary for efficient DNA replication. CLB3,4 are also involved in this task. Both are expressed from S phase until anaphase and take part in spindle assembly and the G2/M-phase transition.

*Clb*1,2 are expressed during the G2-M phase and destroyed at the end of M phase and are involved in regulation of mitotic events such as spindle elongation.

Between the M phase and the beginning of the G1 phase, four gene clusters are expressed: the MCM cluster, the MAT cluster, the PHO regulon and the SC1 cluster.

- The expression of MCM cluster genes (including MCM2 -7, SWI4, and CLN3) is controlled by the MCM1 transcription factor. The MCM2-7 complex is especially important in the replication of chromosomes, during the S phase, where it acts as an ATP-dependent helicase that unwinds DNA and which is involved in both initiation of DNA replication and replication fork progression.
- The MAT cluster (where the CKIs FAR1 is included) is normally induced by mating pheromones but is also expressed to some degree during the M-G1 interface. Its expression depends on MCM1 and the transcription factor STE12.
- The PHO regulon includes genes involved in scavenging and transporting phosphate. CDK1 indirectly participates in the regulation of the expression of this cluster through PHO2, PHO4, PHO5 AND BAS1.

- Expression of the SIC1 cluster is controlled by the transcription factors SWI5 and ACE2, both being negatively regulated by CDK1. CDK1 activity stays high until anaphase, when it drops because cyclins are destroyed and CKIs are re-expressed. The CKIs FAR1 and SIC1 are thought to bind cyclin-CDK complexes and prevent the kinase from interacting with its substrates. This inactivation of the kinase at the end of the M phase would allow the dephosphorylation of SWI5 and ACE2 and the consequent induction of the SIC1 cluster. Furthermore, together with CDC14 phosphatase (released at this time in the cycle to dephosphorylate Cdk1 targets), it contributes to the exit from mitosis and the resetting of the cell cycle towards a basic G1 state characterized by low CDK1 activity and status hypophosphorylated of CDK1 targets.

The upstream regulation of CDK1 described in the previous paragraphs would be complemented by the following regulatory elements:

- CAK1, the *S. cerevisiae* CAK, is required to activate CDK1, in addition to cyclins. CAK1 phosphorylates CDK1 which exposes the substrate binding region of its structure and increases the number of contacts between CDK1 and cyclins promoting the affinity of CDK1 for them. The phosphorylation can be reversed by phosphatases PTC2 and PTC3.

- CDK1 undergoes regulation by acetylation within its kinase domain. However, the acetyl transferase that acetylates it remains unknown.

- SWE1 (WEE1 in *S. cerevisiae*) is a tyrosine kinase that phosphorylates CDK1 in response to cellular stresses. This phenomenon constitutes a checkpoint that has been referred to as the morphogenesis checkpoint. In presence of a perturbation of the actin or septin cytoskeleton, this checkpoint is activated preventing Swe1 degradation, thereby inhibiting CDK1 and delaying the cell cycle in G2. However, this inhibitory effect of SWE1 on CDK1 is reversed by the tyrosine phosphatase MIH1 (CDC25 in *S. pombe*) to promote entry into mitosis.

It is precisely this MIH1 phosphatase that appears to represent an important target for nitric oxide in an environment of nitrosative stress. Majumdar *et al*. (2012) investigated the molecular mechanisms of cell cycle control and stress response in *S. pombe* under nitrosative stress. They proposed, among other aspects, that the microbiostatic effect observed in the cells treated with the NO donor detaNONOate was a consequence of the direct action of the molecule on the regulation of the cell cycle. Specifically, they suggested that exogenous NO directly inhibited CDC25 activity by S-nitrosylation, which in turn prevented the activation of *cdc*2 (*cdk*1) by phosphatase (an essential activation in yeast cells to obtain functional CDC2). This caused a mitotic delay in cells through G2/M checkpoint activation and the occurrence of DNA rereplication without entering into mitosis. Likewise, they indicated that nitrosative stress did not influence regulation by *wee*1.

In the case of *S. cerevisiae*, treatment with the same NO donor caused the alteration of the expression of 209 genes related to DNA structure, replication, transcription, and translation and of 10

genes related to the category of kinase, phosphorylase and signal transduction, among others. Of these, two genes upregulated and involved in recovery from DNA damage, *hug*1 and *ddr*48, stood out. HUG1 is involved in the *mec1*-mediated checkpoint pathway that responds to DNA damage or replication arrest, and its transcription is induced by DNA damage. DDR48 is a DNA damage-responsive protein, and its expression has been shown to be increased in response to heat-shock stress or treatments that produce DNA lesions (Horan *et al*., 2006).

In this context, this chapter addresses the study of the influence of NO on development in *B. cinerea*, fungus that produces NO, in a regulated way, both during saprophytic growth and *in planta*. It has a single gene, *Bcfhg*1, that encodes a functional flavohemoglobin involved in NO detoxification and of which it has been suggested that it could be more related to the modulation of endogenous NO levels produced by the fungus during specific developmental stages than to the protection of the fungus during the host plant infection (Turrion-Gomez *et al*., 2010; Turrion-Gomez and Benito, 2011). Furthermore, previous studies carried out in our research group already reported defects in the development of the fungus grown in the presence of exogenous NO and attributed to a possible effect of the molecule on the cell cycle (Daniela Santander, Doctoral Thesis. University of Salamanca). Through an approach that combines the use of microscopy techniques, the use of modulatory drugs of NO levels and the development of a global expression analysis, the aim is to identify the physiological processes in which this gas participates in the fungus and at the same time characterize the underlying genetic factors.

Results

1. Pharmacological analysis on the strains B05.10 and *ΔBcfhg1*.

1.1 Germination kinetics of *B. cinerea* strain B05.10 *in vitro*

As a starting point to analyse the modulating effect of NO on development in our system, the germination kinetics of the reference strain, B05.10, was characterized under the culture conditions considered for the analysis (see section 2.2 of Materials and Methods), in the absence of any modifying treatment of NO levels. This analysis establishes the reference situation for later comparisons.

The working spore suspensions were obtained from batches of fresh spores collected as indicatedin section 3.1 of Materials and Methods. The drops of the spore suspensions prepared in PDB ½ medium were deposited on Petri dishes that were kept in the dark and at 22 °C for the selected times (0, 2, 4, 6, 8 and 10 h). Then, representative images were taken under the microscope that were used to estimate the germination percentages and germ tube lengths. In these experiments, the fraction of germinated spores was estimated with respect to the total number spores analysed, considering that a spore had germinated when wall rupture and emission of the primordium of the germ tube was observed ([spores in stage 1 + spores in stage 2]/total number of spores) (see epigraph 9 of the Materials and Methods section). The data obtained are presented in Figure 14.

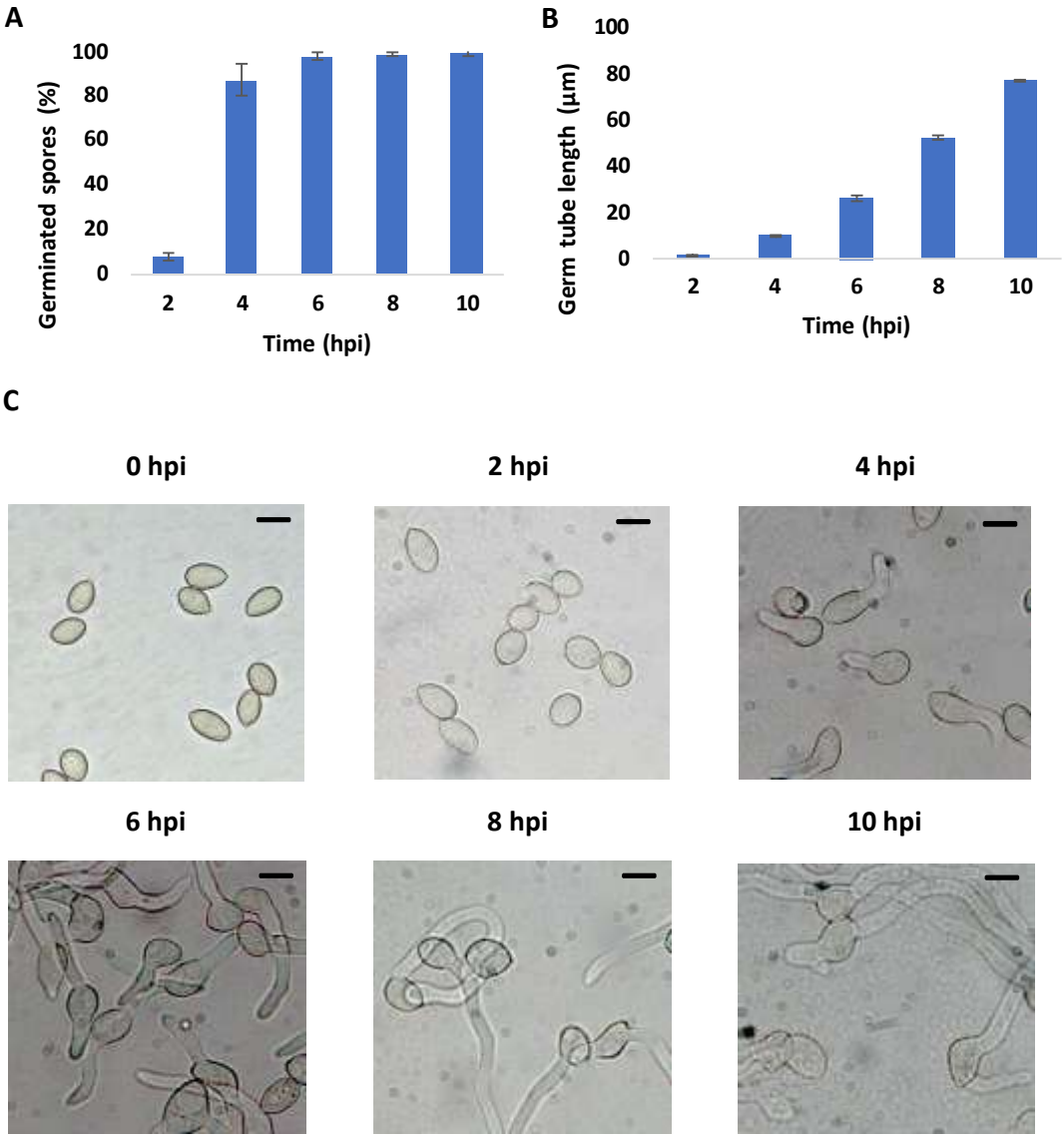

Figure 14. (A) Germination kinetics and (B) germ tube growth of spores of the *B. cinerea* wild type strain B05.10 grown in PDB ½ medium under static culture conditions. The germination of the spores and the length of the germ tube were determined after 2h, 4h, 6h, 8h and 10h of incubation. The graphs show the means of three replicates ± SD. (C) Representative images of the germination process of the strain B05.10 at the moments considered in (A) and (B). Scale bars, 10 µm.

The *B. cinerea* macroconidia germination was a non-synchronous process in our experimental conditions that showed kinetics similar to sigmoidal and where the growth rate of the germ tubes had an evolution reminiscent of linear kinetics. The germination of the spores was 8% after 2 h of incubation and this percentage increased drastically to 87% at 4 h. Almost all the spores had germinated at 6 h reaching the total in later samplings (Figure 14A). Moreover, the germ tubes length for 4, 6, 8 and 10 h was of 10 µm, 27 µm, 53 µm and 78 µm, respectively (Figure 14B).

1.2 Effect of DETA, cPTIO and L-NNA on *B. cinerea* strains B05.10 and *ΔBcfhg*1 germination.

The influence of NO on the germination of the fungus was analysed in the flavohaemoglobin knockout mutant strain *ΔBcfhg*1 and compared with its effect on the strain B05.10. To this end, both

strains were cultivated in the presence of a series of chemical modulators of NO levels: DETA, a NO producer; cPTIO, a NO scavenger, and L-NNA, an inhibitor of mammalian NOS enzyme.

Following the procedures indicated in sections 2.2 and 9 of Materials and Methods, the working spore suspensions were prepared, the chemicals were added at the desired concentrations and the droplets of the suspensions were dispensed on Petri dishes that were incubated for the relevant times in the dark and at 22 °C. Finally, the counts and estimates of the corresponding germination percentages were carried out on representative images taken with the microscope at 3 hpi (Figure 1 5), a moment initially selected to evaluate the effect on germination at which the percentage of germinated spores in the strain B05.10 is between 50% and 60%, and at 10 hpi (Figure 16), a time point at which all the spores have already germinated.

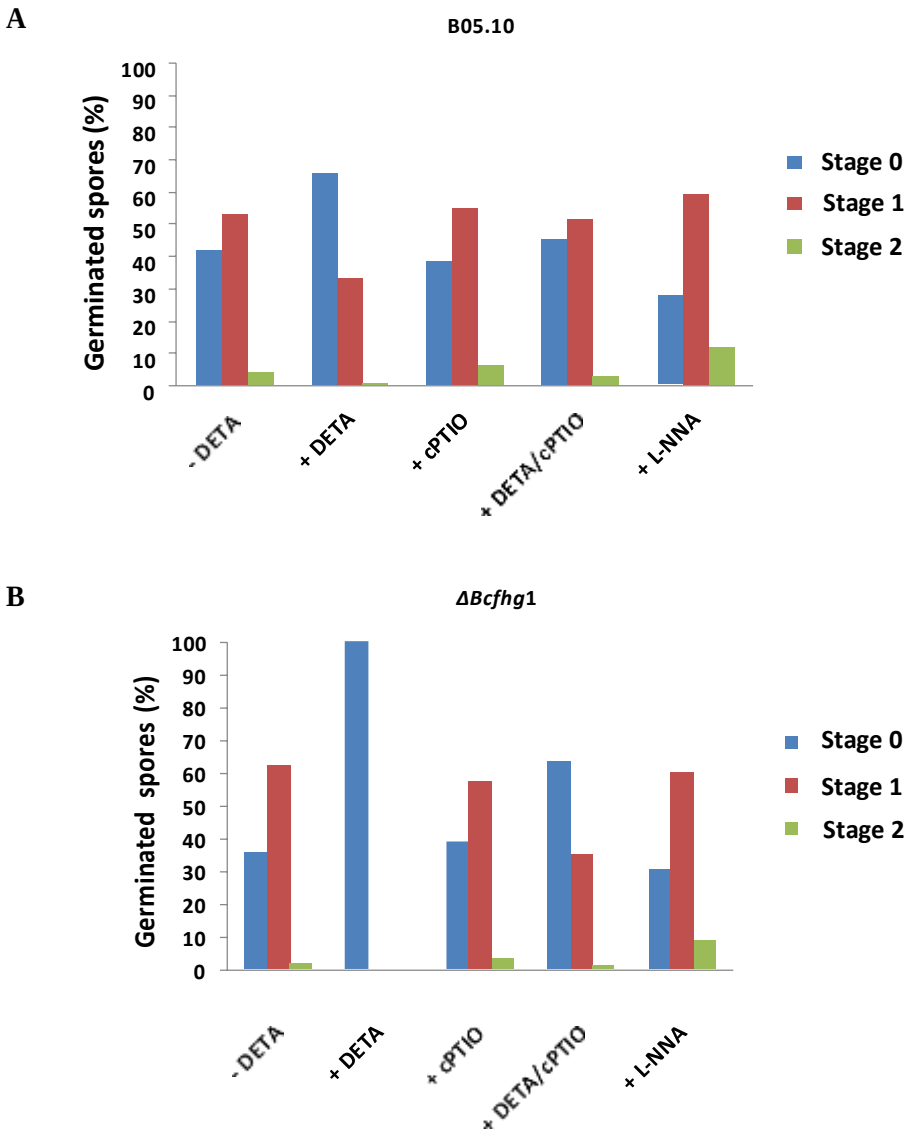

Figure 15. Effect of addition of the NO donor DETA, the NO scavenger cPTIO and the NOS inhibitor L-NNA in the germination of spores of the *B. cinerea* strains B05.10 (A) and Δ*Bcfhg*1 (B), after 3 hours of incubation. The reagents concentration was 250 µM DETA, 500 µM cPTIO, and 1mM L-NNA. The experiment was repeated at least twice obtaining similar results; The data shows the results of a typical experiment.

The results presented in Figure 15A show that the germination rate of the wild-type strain was reduced by exposure to DETA. The percentage of spores in stage 0 at 3 hpi and in the absence of NO was 42%, while it was 53.62% and 4.35% in stage 1 and 2, respectively. These constitute the reference values in our system. In the presence of 250 µM DETA, the percentage of ungerminated spores (state 0) increased to 66% while the percentages of spores decreased in states in which the germ tube has not exceed the diameter of the spore (33.34%) or it has (0.71%). Wild type behaviour was restored by adding simultaneously 250 µM DETA and 500 µM of cPTIO (stage 0: 45.24%; stage 1: 51.59% and stage 2: 3.17%).

On the other hand, when B05.10 spores were incubated in the presence of 500 µM of cPTIO or 1mM of L-NNA, a small increase in germination was observed compared to the control situation without DETA. This increase is the consequence of a decrease in the percentage of non-germinated spores and an increase in the percentages of spores in states 1 and 2 for both conditions (38.46% in state 0; 55% in state 1 and 6.51 % in state 2 in the presence of 500 µM of cPTIO and 27.87% in state 0; 59.84% in state 1 and 12.30% in state 2 in the presence of 1mM of L-NNA). The effect is more evident in the case of the NOS enzyme inhibitor.

No obvious differences are observed between the *ΔBcfhg*1 strain and the wild-type strain in their behaviour in the absence of DETA, although the percentage of spores in stage 0 is slightly lower in the mutant strain (35,6% vs. 42%). However, net differences are observed between both strains in the presence of NO, as addition of 250 µM of DETA caused a total blockage of the germination process of the mutant strain at 3 hpi (Figure 15B). When the mutant was incubated in the presence of the donor and the NO scavenger together, 63.31% of the spores did not germinate, while 35.25% were found in state 1 and 1.44% in state 2. These last two percentages are slightly lower when compared to B05.10 for the same conditions. In any case, this suggests that the germination blockage in the mutant strain in the presence of the NO donor was broken as a consequence of the simultaneous addition of the NO scavenger and shows that the germination blockage observed is a consequence only of exposure to exogenous NO. In the presence of cPTIO alone or of L-NNA, the *ΔBcfhg*1 strain behaved essentially as the wild-type strain.

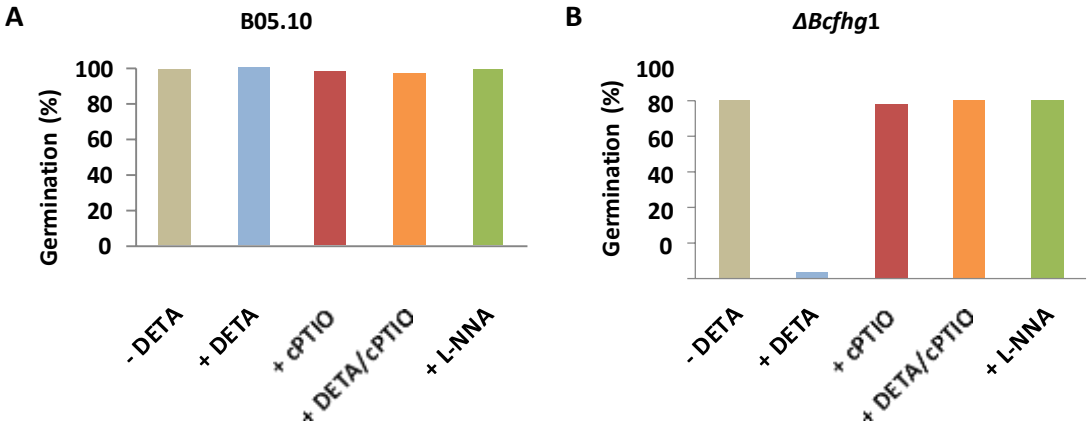

Figure 16. Effect of the NO donor DETA, the NO scavenger cPTIO and the NOS inhibitor L-NNA in the *B. cinerea* strains B05.10 (A) and Δ*Bcfhg*1 (B), after 10 hours of incubation. The reagent concentrations were 250 µM DETA, 500 µM cPTIO, and 1mM L-NNA. The experiment was repeated at least twice obtaining similar results; the data reflects a typical experiment.

The germination percentages obtained for the strain B05.10 after ten hours of incubation (Figure 16A) indicate, in principle, that the effect of NO on germination is a 'delay' effect, not a loss of viability of a fraction of spores, since practically 100% of them have germinated at this time in all the treatments considered. Depending on the treatment, the spores germinate later (more slowly) or earlier and, consequently, the mean lengths of the germ tubes are different in some conditions and others depending on the delay or advance that germination experienced (results not shown), but after 10 hours all the spores have germinated. The same behaviour is observed in the case of the spores of the mutant strain, with the exception of those that were incubated in the presence of the exogenous NO donor. In this treatment, only 3-4% of the spores managed to germinate after 10 hours of incubation. This observation demonstrates that the added donor maintains an effective concentration of NO in the culture medium for at least these first 10 hours of incubation and, therefore, supports the initial proposition regarding the delaying effect that gas has on germination of the fungus.

1.3 Quantification of the effect of DETA on *B. cinerea* strain B05.10 germination along time.

Once it was verified that the inhibition of germination and development experienced by *B. cinerea* spores in the presence of DETA was a consequence of the NO released, the next step was to precisely quantify the effect that the molecule causes on the germination of both strains as a function of time.

In the case of the B05.10 strain, its spores were exposed to 250 µM DETA during different incubation times: 2h, 4h, 6h, 8h and 10h, after which the percentages of spores in each stage of development (0, 1 and 2) were quantified. The experiments were repeated three times, obtaining the results shown in Figure 17.

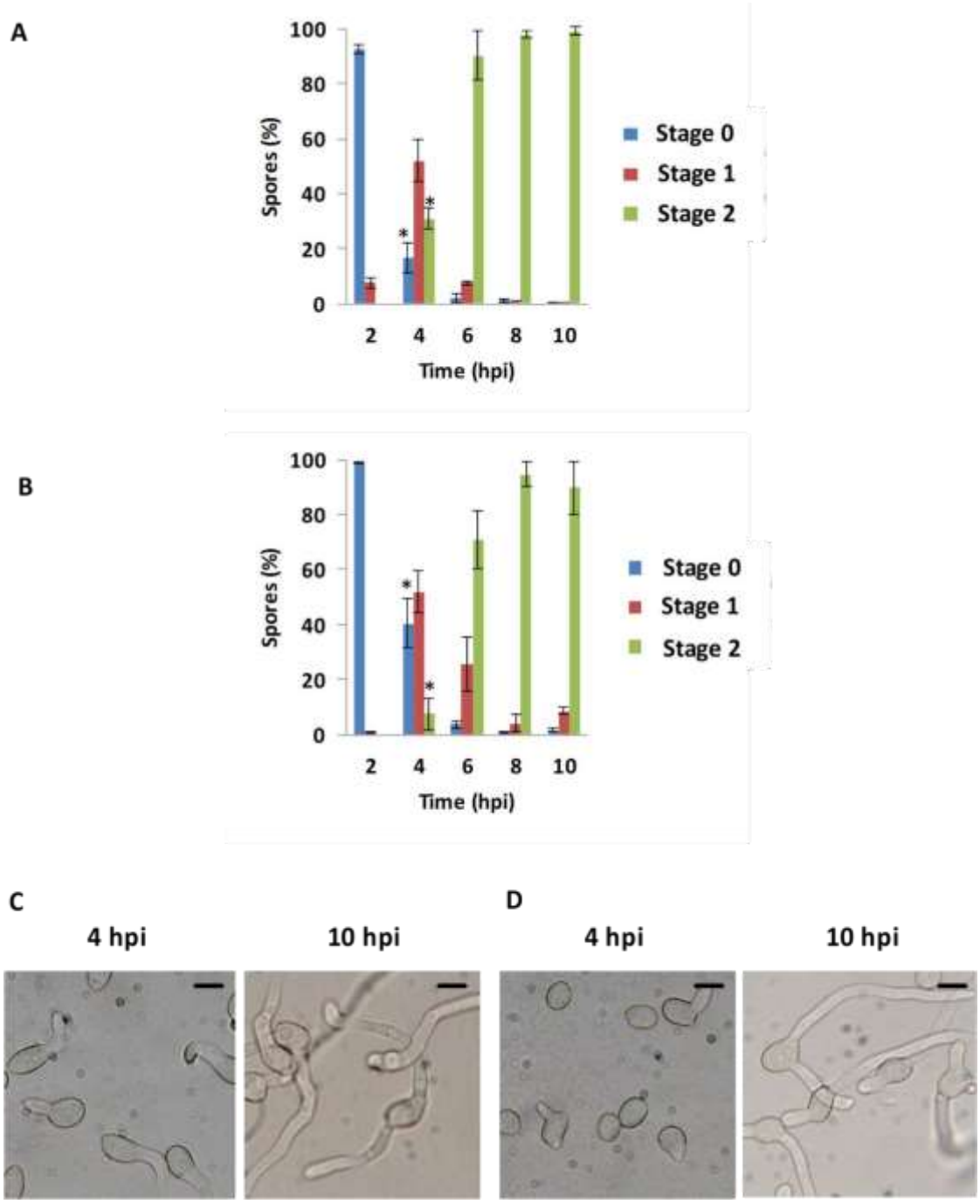

Figure 17. Percentages of spores in the different stages of development (0, 1 and 2) for the *B. cinerea* strain B05.10 in the absence (A) and in the presence (B) of 250 µM DETA. The data were taken at different sampling times: 2h, 4h, 6h, 8h and 10h. Values are the means of three replicates (± SD). (* indicates significant differences at P <0.05 - Student's t - between the condition analysed in the presence of 250 µM DETA, panel B, and its reference situation, panel A, in the absence of DETA). Representative images of the germination process of the strain B05.10 at 4 hpi and 10 hpi in the absence (C) and in the presence (D) of 250 µM DETA. Scale bars, 10 µm.

If the germination percentages of the B05.10 strain spores are observed according to their development stage at the different sampling times, a global vision of the influence of the exogenous NO addition is obtained (Figure 17).

In the absence of the NO donor, 92.45% of the spores were found in stage 0 at 2h, 17% at 4h, 2.15% at 6h, 1.24% at 8h and the 0.83% at 10h. The percentage of spores in stage 1 predominates at 4h (52%) and decreases in subsequent samplings. Spores in the third stage of development are the most frequent from 6h onwards (90.28% at 6 h, 97.86% at 8 h and 98.98% at 10 h) (Figures 17A and 17C). Therefore, germination in the wild type strain takes place between 2 h and 4 h of incubation, and the time point 4 h can be considered as the most informative in order to quantify possible ef fects on germination rates given the observed distribution of the spores in the three stages considered.

If this profile is compared with that of spores subjected to an exogenous supply of NO, a profile is observed, as might be expected, in general lines similar to that observed in the absence of DETA, but with important differences. Thus, non-germinated spores predominate at 2h (98.86%), but even to a greater extent than in the absence of DETA (92.4%). The percentage of non-germinated spores subsequently decreases gradually, although this is always higher than in the samples not treated with DETA considered at the same time points (particularly evident in the times in which these percentages are still notable, at 4h and 6h). On the other hand, the spores in stage 1 are the most frequent at 4 h (51.81%). At this time point the spores in stage 2 constitute a very low percentage (7.7%) compared to the situation of no exposure to DETA (31%). In the later times, 6, 8 and 10h, the spores in stage 2 predominate, but the percentages of spores in stage 0 and stage 1 are always greater than in equivalent times of the samples not treated with DETA (Figures 17B and 17D).

These results once again reveal the delay in germination that the spores of the B05.10 strain experience in the presence of the NO donor compared to the control situation, which was already observed in the previous section. In addition, they point to 4 hpi as the most appropriate moment, of the time interval considered, to appreciate the effects of NO on the germination of the wild-type strain. At this timepoint, the change in spore distribution in the three stages of development that we are considering becomes more evident. In the absence of DETA, the spores in stage 1 predominate and the class corresponding to stage 0 is a minority. In the presence of NO, the class corresponding to stage 2 is a minority, while the fraction of spores in stage 0 increases its percentage more than double.

Being the 4 hpi the moment in which the differences between the considered treatments, absence vs. presence of DETA, are best appreciated, we decided to carry out a statistical analysis on the data corresponding to this time. The Student's t test was then applied, which allowed to conclude that there are no significant differences between the number of spores in stage 1 in the medium with the donor and the number of spores in the same stage in the medium without the donor, but that they do exist for spores in stages 0 and 2 between the two conditions (Figure 17A). It can be concluded that the germination of the strain B05.10 spores is influenced by the addition of DETA, which delays germination.

1.4 Quantification of the effect of DETA on *B. cinerea* strain *ΔBcfhg*1 germination along time.

In order to quantify the effect of NO on the germination of the *ΔBcfhg*1 strain as a function of time, and in parallel with the tests carried out with the B05.10 strain, spores of the mutant strain were exposed to 250 µM DETA for 2h, 4h, 6h, 8h and 10h. The measurement of the effect that NO causes on the germination of this strain as a function of time was based on the quantification of the percentages of spores in each stage of development (0, 1 and 2) for each sampling time. In Figure 18, the results obtained after carrying out three repetitions of the experiment are presented.

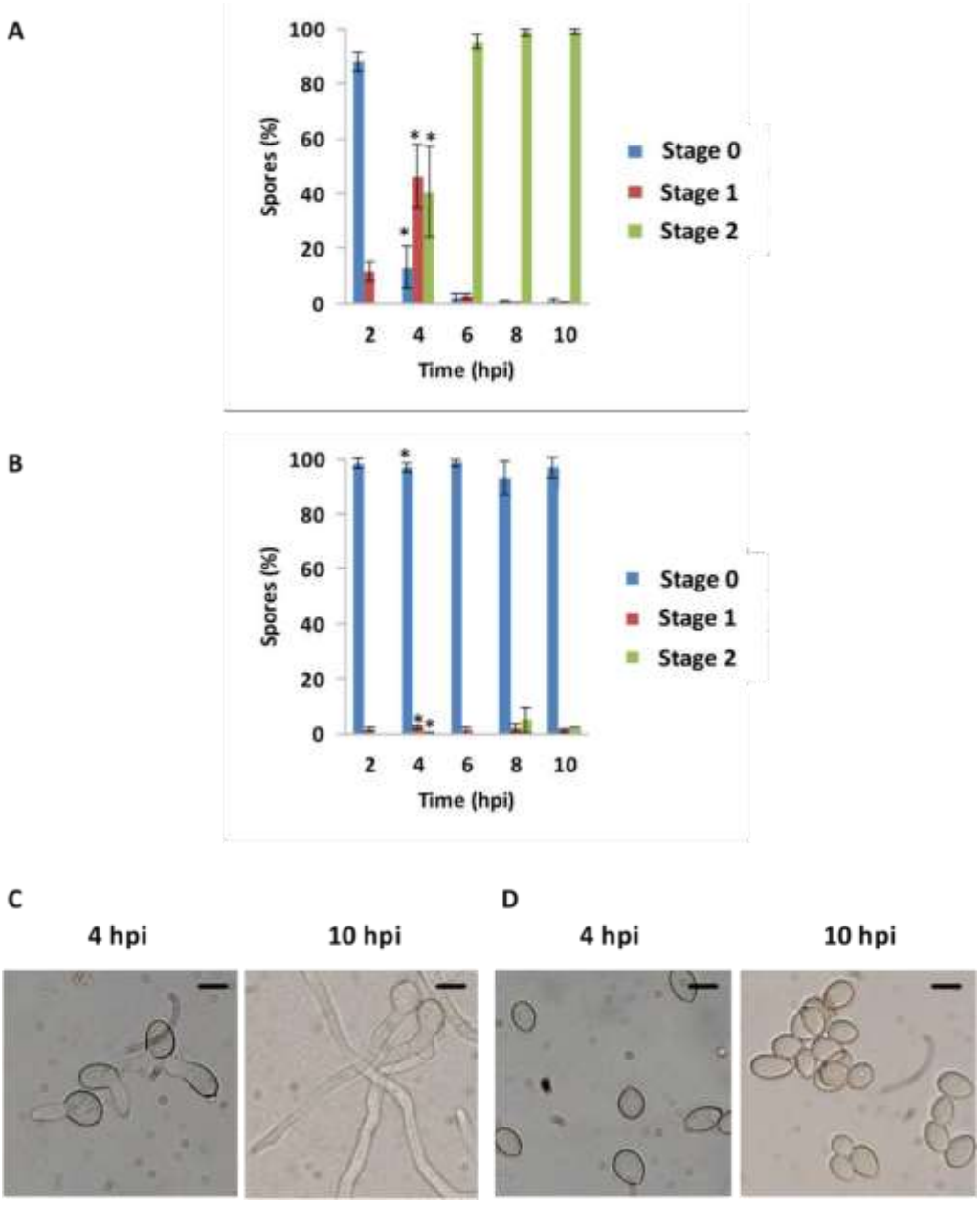

Figure 18. Percentages of spores in the different stages of development (0, 1 and 2) for the *B. cinerea* strain *ΔBcfhg*1 in the absence (A) and in the presence (B) of 250 µM DETA. The data were taken at different sampling times: 2h, 4h, 6h, 8h and 10h. Values are the means of three replicates (± SD). (* indicates the presence of significant differences at P <0.05 - Student's t - between the condition analysed in the presence of 250 µM DETA, panel B, and its reference situation, panel A, in the absence of DETA). Representative images of the germination process of the strain *ΔBcfhg*1 at 4 hpi and 10 hpi in the absence (C) and in the presence (D) of 250 µM DETA. Scale bars, 10 µm.

In the absence of DETA (Figure 18A and 18C), the behaviour of the spores of the *ΔBcfhg*1 strainis essentially the same as that of the spores of the B05.10 strain at all times considered (Figure 17A). In particular, at 4 hpi the percentage of germinated spores in both cases is very similar, 87% in the mutant strain and 83% in the B05.10 strain. On the other hand, there are no significant differences when the percentages of spores in the same stage are statistically compared between both strains, for this timepoint (data not shown). This means that in the absence of exogenous NO the mutant strain does not show any obvious alteration in its germination pattern in comparison with the wild-type strain.

When the NO donor was present in the medium, the non-germinated mutant spores reached percentages much higher than those of the germinated spores (stages 1 and 2) at all sampling times. Specifically, between 93% and 98% of the spores had their germination blocked for all the times studied, while an average of 3% of spores managed to germinate (Figures 18B and 18D). In order to maintain the parallelism between the analyses carried out on each strain, the focus was once again on the results found at 4 hpi, to carry out the statistical analysis on the behaviour of the mutant strain. The application of the Student t analysis to the germination data of the *ΔBcfhg*1 strain for the same conditions as for the B05.10 strain, that is, presence and absence of DETA (using the latter as a control), demonstrated the existenceof differences significant ($p < 0.05$), in this case, for the three stages of development of the spores analysed (Figure 18A), with the percentage of spores in state 0 being much higher in the presence of NO and the percentages of spores in state 1 and state 2 being much lower also in the presence of NO.

Therefore, the intense influence that exogenous NO has on the germination of the *ΔBcfhg*1 strain due to its mutation in the *Bcfhg*1 gene, encoding the enzyme responsible for detoxifying nitric oxide, is once again revealed. It cannot be said that, in the presence of NO, germination in the mutant strain experiences a delay, but rather that it is almost completely blocked. These results are consistent with those previously obtained during the evaluation of the effects of the different modulating chemicals on NO levels. In both cases, the percentage of germinated spores after 10 hours of cultivation is minimal (i t does not exceed 5%).

1.5 Sensitivity threshold of the *B. cinerea* strain *ΔBcfhg*1 to DETA in relation to the strain B05.10.

As the two strains, the wild type and the *ΔBcfhg*1 mutant, respond differently to the NO donor at the concentration used in the previous analysis, we next attempted to determine the sensitivity threshold to the NO donor of both strains. To this end, spores of the two strains were incubated in the presence of increasing concentrations of NO (0 µM, 7.5 µM, 15 µM, 30 µM, 62.5 µM, 125 µM, 250 µM and 500 µM DETA). After 4 hours of incubation the germination percentage (spores in stage 1 + spores in stage 2) was quantified and after 10 hours of inoculation the length of the germ tube was estimated, both determinations done on representative images taken at the indicated time points. The results obtained are shown in Figure 19.

Figure 19. 1Effects of DETA on germination (A) and germ tube growth (B) in *B. cinerea* strains B05.10 and *ΔBcfhg*1. Percentage of germinated spores and the germ tube length were determined after 4 h and 10 h of incubation, respectively, under the different concentrations of the NO donor indicated. Values are the means of three replicates (± SD).

The results related to the germination of the spores (state 1 + state 2) of the strain B05.10 are indicative that the fungus responds differently to different concentrations of NO, there being a threshold concentration that separates and allows differentiating two answers. At very low concentrations of the NO donor (7.5 µM), the wild-type strain responds by reducing its germination efficiency to a value of 70.11%, a reduction of 21% with respect to the efficiency shown in the absence of exogenous NO (89.19%). If the concentration of DETA continues to increase, then the fungus moderately increases its germination efficiency to values of 77.23% and 78% at 15 and 30 µM of donor, respectively. It is in this concentration range, between 15 and 30 µM, where we can consider that there is a threshold concentration, exceeding which, the germination efficiency decreases as the donor concentration

continues to increase, observing a reduction in the germination rate in a dose-dependent manner (73.64%, 67.57%, 56.16% and 39.72% for 62.5 µM, 125 µM, 250 µM and 500 µM DETA, respectively).

For its part, the mutant strain was drastically affected in its germination even at low concentrations of DETA (91.72%, 4.21%, and 1.28% for 0 µM, 7.5 µM, and 15 µM DETA, respectively), being unable to germinate when the donor concentration was greater than 15 µM (Figure 19A).

In the case of the effect of the NO donor on the length of the germ tube it is also possible to distinguish two different responses as a function of the donor concentration in the wild-type strain. At very low concentrations of DETA (7.5 µM), the length of the germ tubes is 55 µm on average, a length 28% shorter than that observed in the absence of DETA (76 µm). However, this difference is less in the case of concentrations of 15 and 30 µM, which mark the concentration that we have considered threshold in the effect of DETA and where the spores presented germ tubes of 60 µm and 61 µm of average length, respectively. Once again, once this concentration is exceeded, the length of the germ tube is reduced in a dose-dependent manner by increasing the donor concentration (50 µm, 47 µm, 38 µm and 27 µm for 62.5 µM, 125 µM, 250 µM and 500 µM. DETA, respectively) (Figure 19B).

Spores of the *ΔBcfhg*1 strain showed a mean germ tube length of 84 µm when incubated in the absence of the NO donor, similar to that of the spores of the wild-type strain in the same condition. However, the mutant spores underwent a more drastic response to exposure to NO than that shown by wild-type spores, with the length of their germ tubes being significantly reduced at very low donor concentrations (39 µm and 16 µm for 7, 5 µM and 15 µM donor, respectively). At higher concentrations the germination of this strain was null (Figure 19A) and, consequently, the length of the germ tube could not be estimated (Figure 19B).

1.6 Effect of NO on nuclear division during germination of *B. cinerea* strains B05.10 and *ΔBcfhg*1.

The alterations in the germination program observed in both strains when exposed to DETA suggests that NO was affecting nuclear division processes in the fungus. To address this question, we decided to determine the number of nuclei in spores of the two strains during early stages of germination when exposed to the NO donor in comparison with the number of nuclei in non-exposed spores.

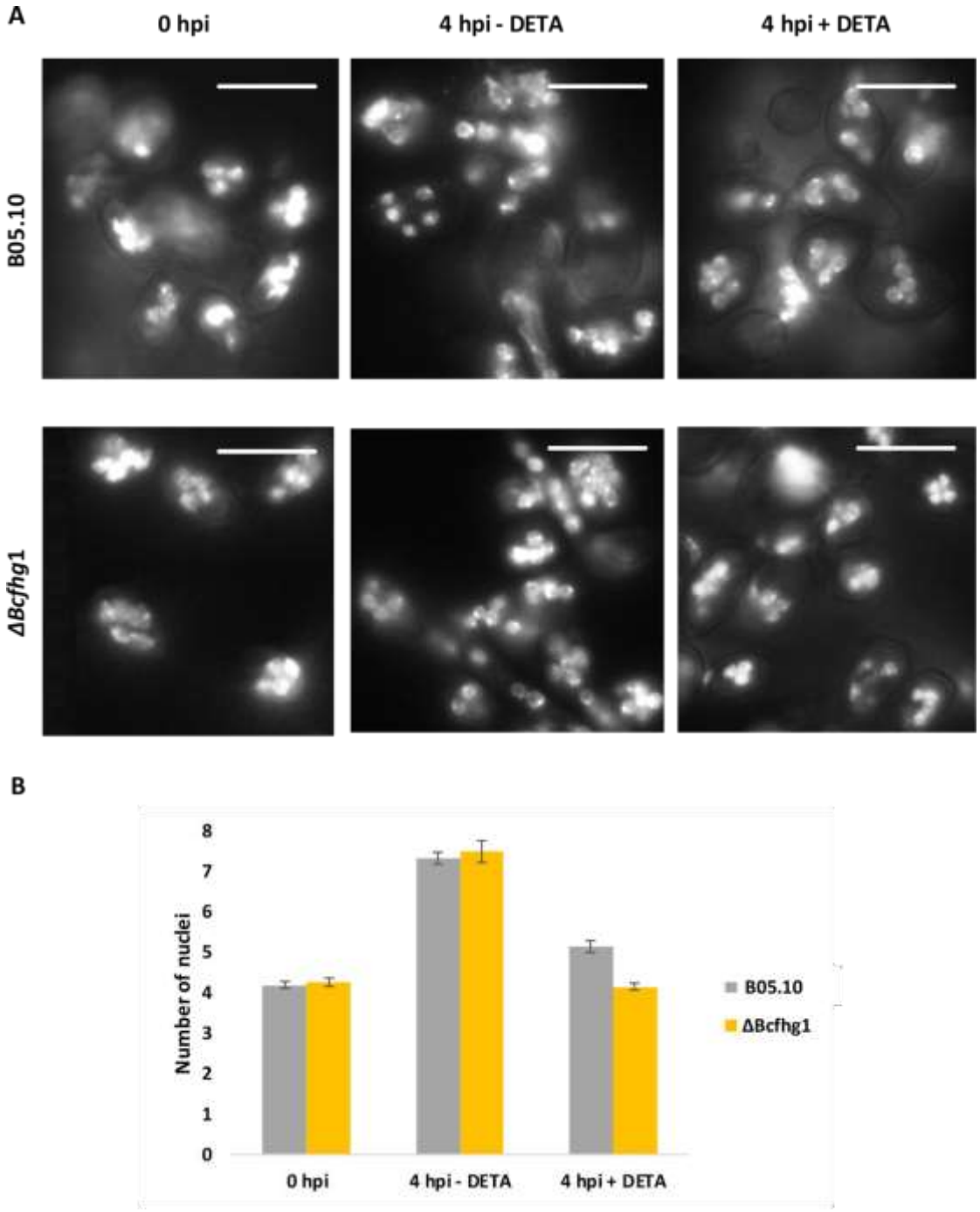

Figure 20. (A) Representative images of DAPI staining preparations of spores of the wild-type strain B05.10 and of the mutant strain *ΔBcfhg*1 of *B. cinerea* in static culture at 0 hours and after 4 hours of incubation in the absence and in the presence of DETA. Scale bars, 10 µm. (B) Average number of nuclei of the B05.10 and *ΔBcfhg*1 strains spores at the times and conditions considered in A. The nuclei count was carried out on spores kept in static culture in 15 ml of PDB½ medium. The NO exposure treatment was performed with a final concentration of 250 µM DETA. Values are the means of three replicates (± SD).

As on previous occasions, the reference behaviour is represented by the strain B05.10 incubated in the absence of the NO donor. The spores of this wild-type strain at 0 hours have an average of 4 nuclei. After 4 hours of incubation, most of the spores have already germinated and the germ tube is in active growth. In these spores the average number of nuclei per spore is 7, that is to say, it almost doubles in

relation to the situation of spores at rest. In the presence of DETA, a clear decrease in the number of nuclei is evidenced, with 5 being the mean number of nuclei per germinated spore in this situation.

Nuclear division in the spores of the mutant strain *ΔBcfhg*1 incubated in the absence of exogenous NO follows a path parallel to that followed by this process in the reference strain, because at 0 hours and 4 hours of incubation, the mean number of nuclei was around 4 and 7, respectively. The behaviour of both strains in the absence of DETA is essentially the same. However, the behaviour of the *ΔBcfhg*1 strain is very different from that of B05.10 in the presence of exogenous NO: after 4 hours of culture in the presence of DETA, the mean number of nuclei of the mutant spores is close to 4.

Therefore, it is observed that the delay in germination and in the development of the germ tubein the wild-type strain previously observed in the presence of DETA is accompanied by a reduction in the rate of nuclear division. In the case of the flavohemoglobin enzyme-deficient strain, the exogenous NO not only prevents its spores from germinating, but also appears to paralyze nuclear division in them.

1.7 Effect of the DETA once the germination program has been launched.

So far, we have analysed the effect of NO on development in *B. cinerea* derived from its permanent exposure to the molecule. We then set out to find out the degree of immediacy with which NO exerts its effect on germination, germ tube development and the rate of nuclear division of the pathogen. For this purpose, in the following series of tests, the fungus was exposed to the donor after 4 hours of incubation, during which the activation of the proteome in charge of controlling cell division and elongation of the germinative primordium takes place, analysing its impact in subsequent samplings.

1.7.1. Immediacy of the NO effect on the *B. cinerea* strain B05.10 germination.

Spores of strain B05.10 were incubated for 4 hours in PDB ½ medium under the same static culture conditions used in the experiments described throughout this chapter. At the end of this incubation period, the necessary volume of the exogenous NO donor DETA was added to half of the Petri dishes with the corresponding cultures to reach a concentration of 250 µM. After properly mixing the donor with the spore suspension, these were returned to the incubation conditions indicated above until 6 and 8 hours after the start of the culture, at which time representative images of the corresponding samples were taken and served to carry out counts and estimates of germination and germ tube growth rates. These estimates were also carried out (at the same times considered in the previous case) on the other half of the prepared plates, those in which the spore suspensions were not exposed to NO after 4 hours of culture, to its use as a reference situation. The corresponding data were also taken from samples taken at 0 hours and at 4 hours in the absence of NO. The graphical representations of the results of this section after doing the experiments in triplicate are shown in figure 21.

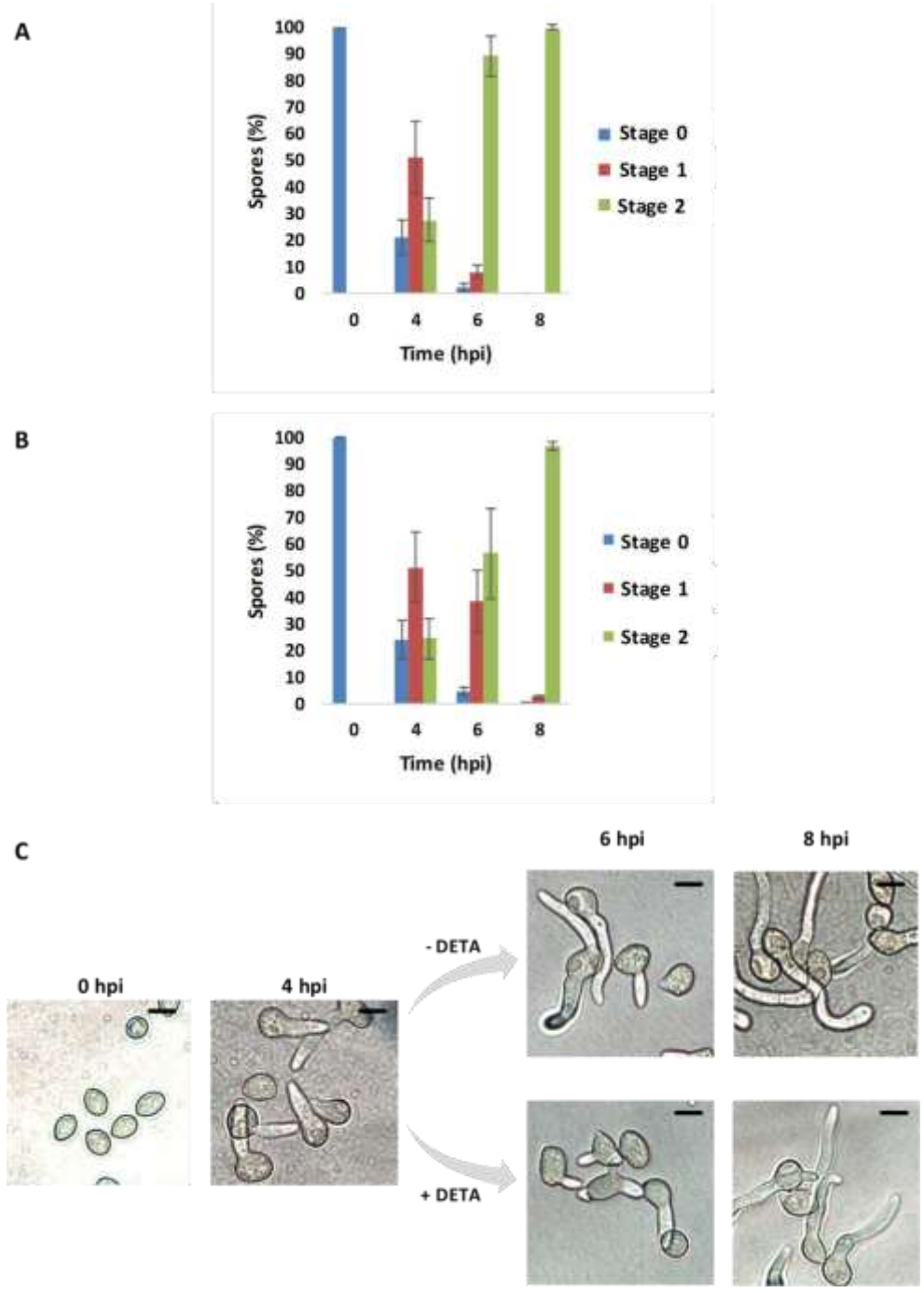

Figure 21. 2Percentages of spores in the different stages of development (0, 1 and 2) for the *B. cinerea* strain B05.10 without addition (A) and with addition (B) of 250 µM of DETA at 4 hours of incubation. The data were taken at the different sampling times: 0h, 4h, 6h and 8h. Values are the means of three replicates (± SD). Representative images of the germination process of the strain B05.10 at the moments considered without addition and with addition of 250 µM of DETA at 4 hours of incubation (C). Scale bars, 10 µm.

The behaviour of the strain B05.10 at 0 hours and 4 hours of incubation, before the exogenous supply of NO, is similar to that observed for this strain under these same conditions on previous evaluations: at 0 hours, the spores have not started the germination process while at 4 hours the spores in stage 1 represented the highest percentage of the set of spores, around 51%, compared to the values of spores in stages 0 and 2: 21 - 24 % and 25-28%, respectively (Figure 21). The similarity is maintained at

6 hpi and at 8 hpi if there is no exogenous NO addition to the culture medium at 4 hpi: practically all the spores, 89.2%, were found in developmental stage 2 at 6 hpi, a very high percentage compared to the values of the spores in stages 0 and 1 (2.5% and 8.3%, respectively). At 8 hpi, germination was complete, all spores having reached stage 2 of development (Figure 21A).

However, when this addition takes place, the behaviour of the B05.10 strain temporarily deviates from the reference behaviour. 2 hours after the addition of DETA to the culture, that is, 6 hours from the start of incubation, the percentage of spores in stage 2 continues to be the highest of the three but reaching a lower value (56.5%) than the one presented in the reference situation at this same time. Simultaneously, the non-germinated spores have doubled (4.7%) compared to the reference value and the spores in stage 1 have increased considerably (38.8%) (Figure 21B). But as mentioned, these differences are temporary since, after 4 hours from the donor's addition, which translates into 8 hours from the beginning of the culture, the percentages of spores in each of the stages of development again resemble those obtained in the reference condition without DETA for the same sampling time: practically 100% of the spores have reached their stage 2 of development.

These results allow us to conclude that the exogenous NO provided by DETA to the spores of the B05.10 strain, once its germination program has been launched, has an immediate effect delaying germination, a delay that it is possible to detect after only two hours from the addition and that translates, on the one hand, in a decrease in the number of spores in stage 2, and on the other, in an increase in the percentages of spores in stages 0 and 1, especially the latter. However, this delay is not long-lasting since the spores return to their normal behaviour four hours after the addition of DETA.

1.7.2. Immediacy of the NO effect on the *B. cinerea* strain *ΔBcfhg*1 germination.

The *ΔBcfhg*1 strain was analysed in parallel under the same experimental conditions (Figure 22).

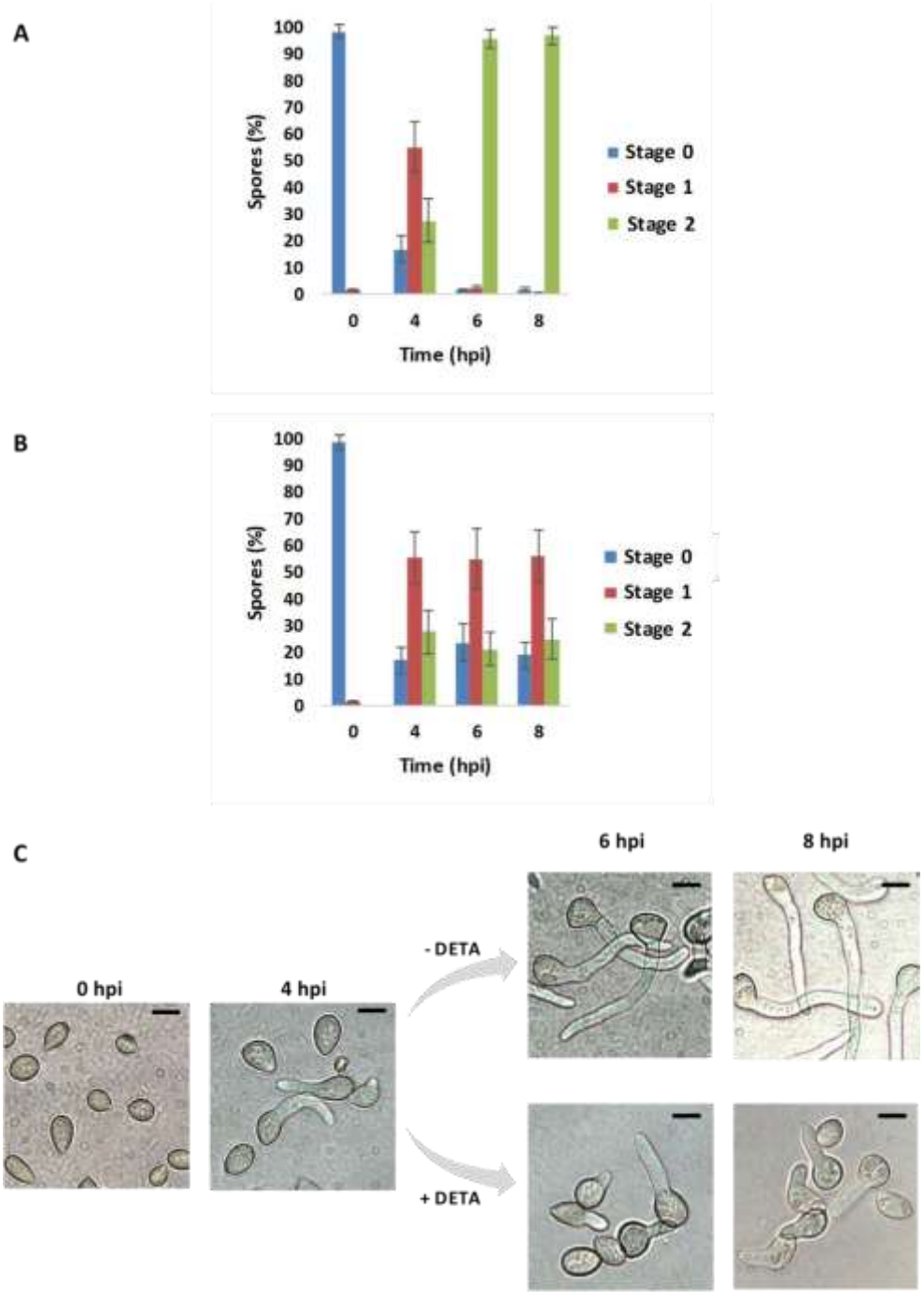

Figure 22. Percentages of spores in the different stages of development (0, 1 and 2) for the *B. cinerea* mutant strain *ΔBcfhg*1 without addition (A) and with addition (B) of 250 µM of DETA at 4 hours of incubation. The data were taken at the different sampling times: 0h, 4h, 6h and 8h. Values are the means of three replicates (± SD). Representative images of the germination process of the strain *ΔBcfhg*1 at the moments considered without addition and with addition of 250 µM of DETA at 4 hours of incubation (C). Scale bars, 10 µm.

The data obtained show that the *ΔBcfhg*1 strain exhibits a behaviour similar to that shown on previous occasions for the same experimental conditions and for all sampling times if the contribution of exogenous NO does not take place (Figure 22A). Furthermore, its behaviour is essentially the same as that of the wild-type strain (Figure 21A).

Thus, practically no spores had started germination at 0 hpi. At 4 hpi, 83% of them had already germinated; Specifically, 55.3% of the spores were in stage 1 of development and 27.7% were in stage 2 (Figure 22). At 6 hpi, practically all the spores had already germinated (Figure 22A).

However, when NO donor is added after 4 hours of incubation, important differences are observed on samples taken at later times: both at 6 hpi and at 8 hpi the percentage of spores that have germinated and are found in stage 1 predominates (55% and 56%, respectively), while non-germinated spores constitute 23.8% at 6 hpi and 19% at 8 hpi and germinated spores in stage 2 of development represent a 21.2% at 6 hpi and 25% at 8 hpi (Figure 22B). This distribution of spores in the three developmental stages at these two time points is essentially the same already observed at the moment of DETA addition. Therefore, we can say that addition of DETA 'freezes' the germination process of the *ΔBcfhg*1 spores and that this effect lasts at least 4 hours since it is added.

1.7.3. Immediacy of the NO effect on the *B. cinerea* germ tube elongation.

The data obtained in the tests carried out in the last two sections were also analysed in order to evaluate the behaviour of the germ tube of the spores of the B05.10 and *ΔBcfhg*1 strains when the exogenous NO donor, at 250 µM concentration, was added to the cultures after four hours of incubation. This new analysis of the same data constitutes a complement to the germination results obtained in the mentioned sections. In addition, an estimate is made of the average growth rate of these hyphal primordia in the two-hour intervals between the sampling times considered (4 hours, 6 hours, and 8 hours).

Previously, a first approach was made to the study of the effect of exogenous NO on the elongation of the germ tube of both strains. However, the data obtained there are not comparable with those obtained in this section since then the spores were cultured in the presence of NO from the beginning of the experiment and in this last series of experiments the spores have already triggered the germination program before the moment in which they are exposed to the NO donor. We must remember again that in this case we are interested in evaluating the degree of immediacy with which the effect of exposure to NO is manifested once the germination program has been launched.

Figures 23 and 24 show the results obtained in the evaluation of the germ tube length in strains B05.10 and *ΔBcfhg*1, respectively, when DETA is added (or not) 4 hours after the start of incubation.

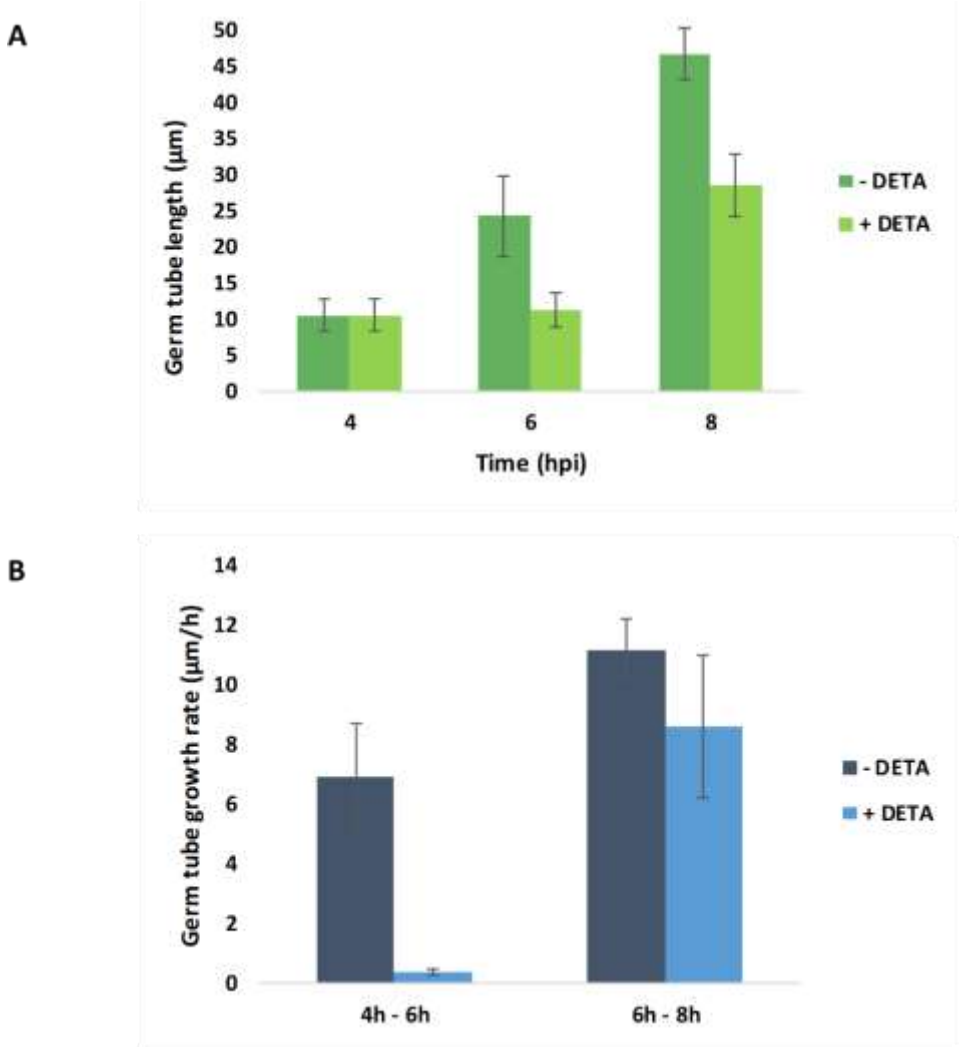

Figure 23. 3Germ tube length (A) and germ tube growth rate (B) of *B. cinerea* wild type strain B05.10 grown in PDB ½ medium under static culture conditions without addition and with addition of 250 µM of DETA at 4 hours of incubation. Values are the means of three replicates (± SD).

The germ tubes of the spores of the strain B05.10 grow as shown in previous analysis in our experimental conditions when the DETA addition does not take place after 4 hours of incubation : the average germ tube length is 10.5 µm mean at 4 hours, 24.4 µm at 6 hours and 46.8 µm at 8 hours of incubation (Figure 23A). For its part, the average growth speed reached in the first time interval, that is, between 4 hours and 6 hours, is 6.9 µm/h, while in the second interval, between 6 hours and 8 hours, this parameter increases to 11.2 µm/h (Figure 23B). However, if exogenous NO is added to the cultures after 4 hours of incubation, a decrease is observed in the length of the tubes and consequently in the speed with which they grow for all the times and intervals considered. Thus, the tubes presented an average elongation speed of 0.36 µm/h between 4 hours and 6 hours of incubation, the latter instant in which the spores showed tubes of 11.3 µm of average length. After this moment, the tube s grew at a rate of 8.62 µm per hour reaching 28.5 µm in mean length at 8 hours of incubation, four hours after the addition of the donor.

The results obtained in this section for this strain are congruent with those obtained for its germination under the same conditions: The NO released to the culture by DETA after spending 4 hours of incubation causes a delay effect of the extension of the germ tubes due to a stagnation of their growth in the first two hours of influence of exogenous NO. This effect can be considered immediate and temporary because, after 2 more hours, the spores seem to have resumed the process of elongation of their tubes, which still testifies to the delay suffered.

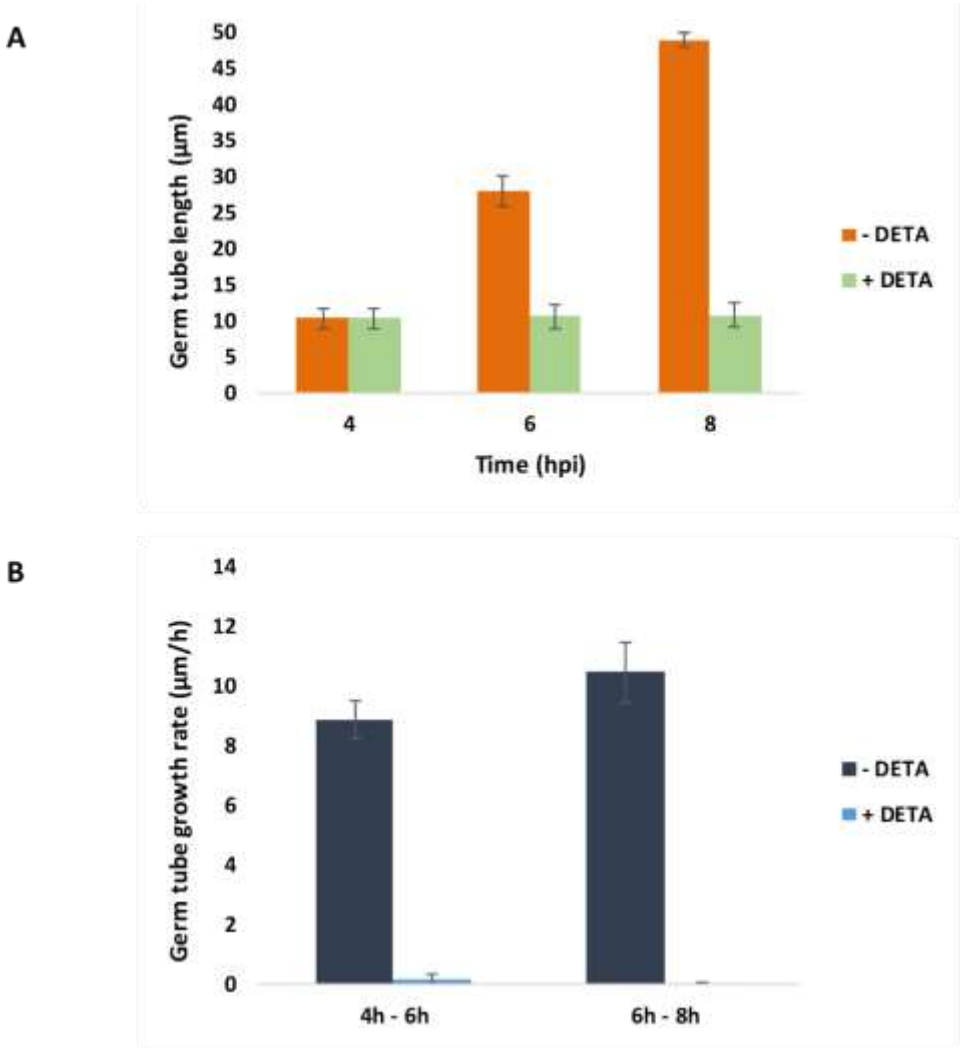

Figure 24. Germ tube length (A) and germ tube growth rate (B) of *B. cinerea* mutant strain *ΔBcfhg*1 grown in PDB ½ medium under static culture conditions without addition and with addition of 250 µM of DETA at 4 hours of incubation. Values are the means of three replicates (± SD).

Figure 24 shows the results obtained in the course of the analysis of the strain *ΔBcfhg*1. When the spores of this mutant strain are not exposed to the NO donor after 4 hours of incubation, the growth of their germ tubes resembles that of the spore tubes of the reference strain B05.10 for the same conditions. Thus, 10.3 µm is the mean length of the germ tubes of the mutant spores at 4 hours, 28.1 µm at 6 hours and 49 µm at 8 hours from the start of incubation of the mutant cultures (Figure 2 4A). On the other hand, the values of the mean germ tubes elongation speed are similar to those presented by the

spores of the reference strain for the intervals considered: 8.9 µm/h between 4 hours and 6 hours of incubation and 10.5 µm/h between 6 hours and 8 hours of incubation (Figure 2 4B).

For their part, the spores that were exposed to exogenous NO experienced a 'paralysis' of the growth of their germ tubes, a paralysis that we can propose taking into account that the average length of their tubes remained practically constant both at 6 hours and at 8 hours in relation to the length observed at 4 hours, before the addition of the NO donor (Figure 24A) and that the average growth rate of these in the two time intervals evaluated was practically zero (Figure 24B).

1.7.4. Immediacy of the NO effect on the *B. cinerea* nuclear division rate.

Analogously to the characterization of the effect of NO on the elongation of the germ tube carried out in the previous section, the content of nuclei and the rate of nuclear division of the germinating spores of the B05.10 and *ΔBcfhg*1 strains were evaluated. These were incubated in ½ PDB medium for 4 hours and then exposed, or not, to the NO donor following the same dynamics as in previous sections. The results obtained on the wild-type strain are presented in figure 25 and those of the tests carried out on the mutant strain in Figure 26.

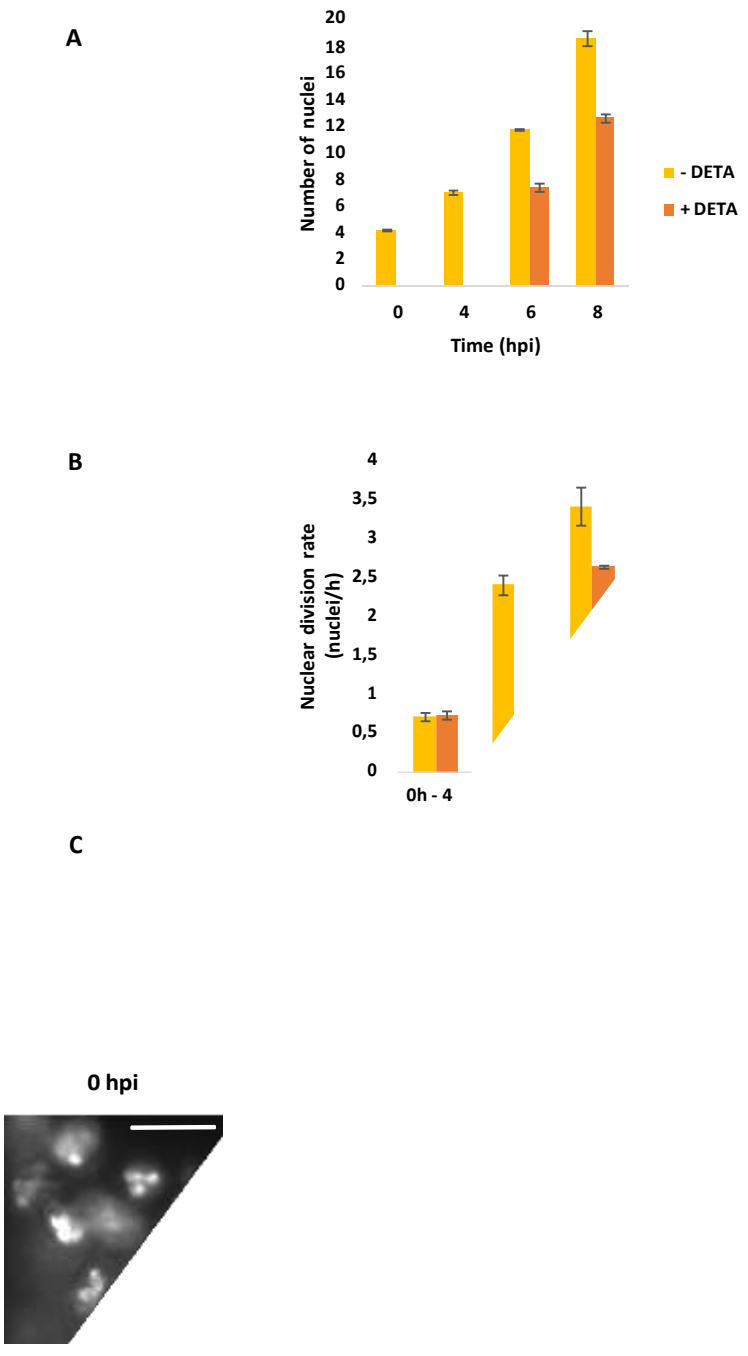

Figure 25. Average number of nuclei (A) and nuclear division rate (B) of the *B. cinerea* B05.10 strain spores without addition and with addition of 250 µM of DETA at 4 hours of incubation. The data were taken at the following sampling times: 0h, 4h, 6h and 8h. Values are the means of three replicates (± SD). Representative images of a DAPI staining of B05.10 strain spores through their germination process at the moments considered without addition and with addition of 250 µM of DETA at 4 hours of incubation (C). Scale bars, 10 µm.

The spores of the wild-type strain showed an increase in their number of nuclei during the first 8 hours of their germination process in the absence of exogenous NO. At 0 hpi, the spores have an average number of nuclei of 4.20, a value that agrees with previous results where an equivalent average number of nuclei was obtained for the spores of this strain under the same conditions. During the first 4-hour interval, the nuclei

divided at a rate of 0.72 nuclei/hour, the spores of the 4 hpi showing a mean value of

7.10 nuclei. This value also agrees with that obtained previously for the spores of this strain grown under the same conditions. During the following two hours, the nuclei experience an increase in their division rate to 2.4 nuclei/hour, which causes the spores at 6 hpi to have 11.91 nuclei on average, most of them already distributed along length of the germ tube. In the last 2 -hour stretch evaluated, the nuclear division rate increased again, reaching a value of 3.4 nuclei/hour. Finally, at 8 hpi, the last timepoint considered, the spores already present long germ tubes loaded with nuclei, containing on average 18.75 of these units (Figure 25).

The addition of the exogenous NO donor at 4 hpi caused a temporary reduction in the rate of nuclear division. The spores exposed to DETA presented a mean number of nuclei at 6 hpi of 7.47, which represents a very small increment in relation to the number at time point 4 hours. Then, nuclear division rate is very low (0.18 nuclei/hour) during the first two hours after the addition of DETA. This observation fits with the one described in previous sections for the germination rate and the elongation of the germ tube. Again, this delay effect, which is immediate, is also temporary, with the division rate recovering to 2.64 nuclei/hour in the next 2-hour stretch (Figure 25). The germlings of the 8 hpi have 12.75 nuclei on average, a value that indicates a resumption of the rate of nuclear division, as already observed with the rate of elongation of the germ tube.

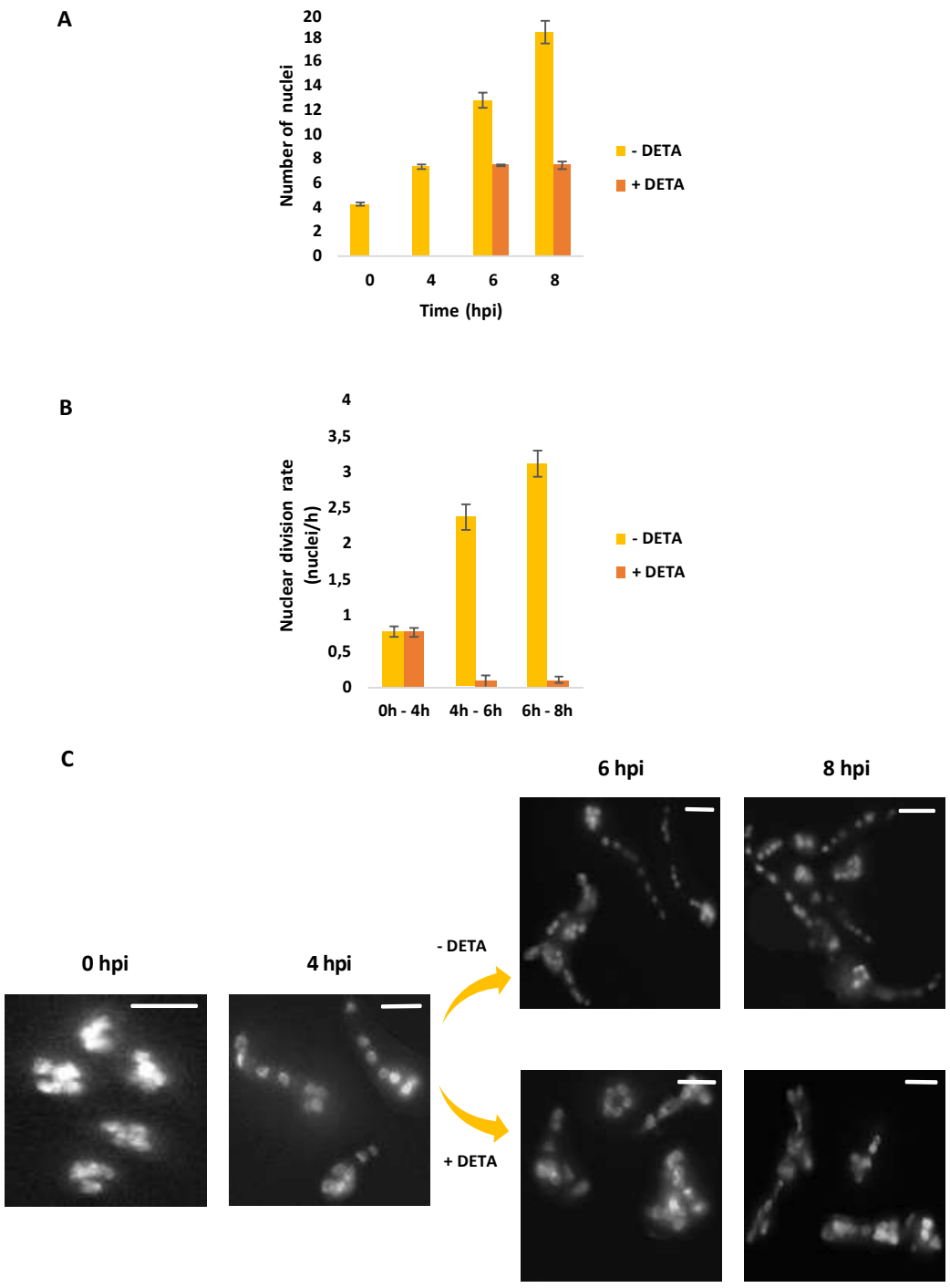

Figure 26. Average number of nuclei (A) and nuclear division rate (B) of the *B. cinerea ΔBcfhg1* strain spores without addition and with addition of 250 µM of DETA at 4 hours of incubation. The data were taken at the following sampling times: 0h, 4h, 6h and 8h. Values are the means of three replicates (± SD). Representative images of a DAPI staining of *ΔBcfhg1* strain spores through their germination process at the moments considered without addition and with addition of 250 µM of DETA at 4 hours of incubation (C). Scale bars, 10 µm.

The strain deficient in the flavohemoglobin coding gene showed a behaviour indistinguishable from that of the wild strain when DETA was not present in the culture medium. In contrast, the presence of 250 µM of the drug caused a lasting block of the two parameters evaluated.

The resting mutant spores, at 0 hpi, have 4.27 nuclei on average. This value increases to 7.35

nuclei on average after the first 4 hours of culture with a nuclear division rate of 0.77 nuclei/hour. During

the next 2-hour period, from 4 hpi to 6 hpi, the spores see their nuclear division rate increases to 2.37 nuclei/hour, as the average nuclear number is 12.77 at time point 6 hours if the NO donor has not been added at 4 hpi. On the contrary, this parameter falls sharply during the same interval if the addition of the drug took place (0.08 nuclei/hour). This causes that the exposed fraction contains 7.52 nuclei on average. In the last 2-hour stretch, the nuclear division rate remained practically zero (0.09 nuclei/hour) in the exposed fraction. On the other hand, the unexposed fraction maintained the normal rhythm of development with a division speed of 3.12 nuclei/hour during the last interval and 18 nuclei on average at 8 hpi (Figure 26).

2. Differential gene expression analysis in response to NO exposure.

The assays carried out in the previous section on the B05.10 and *ΔBcfhg*1 strains indicate that the germination process of *B. cinerea* spores is influenced by the action of nitric oxide once the spores come into contact with this molecule. Specifically, the results show the effect of temporary delay or long- term freezing that the germination process experiences due to the addiction of the molecule and that the occurrence of one or the other result ultimately depends on the presence of a functional flavohemoglobin in the pathogen. These observations confirms that NO affects developmental processes in *B. cinerea* and provides support to previous propositions of a key role of the flavohemoglobin BCFHG1 modulating NO metabolism during growth from a more global point of view than that initially proposed as a regulator of the concentration of the molecule during the host-pathogen interaction (Turrion-Gomez *et al*., 2010). Therefore, at this point, the determination of the fungal physiological processes, and genetic factors involved in them, that can be affected by NO and the role of the flavohemoglobin modulating the NO levels was shown to be relevant. With this intention, it was decided to perform a comparative transcriptomic analysis in response to exogenous NO both in the wild-type strain and in the *ΔBcfhg*1 mutant using RNAseq (Wang *et al*., 2009). This approach was devised assuming that the fungus, when incubated under conditions of exposure to exogenous NO, must give rise to induced transcriptomic profiles where changes in gene expression patterns will inform about the nature of the proce sses and the physiological functions in which NO participates in this organism. Comparison of the expression patterns of the wild type and of the flavohemoglobin deficient mutant will facilitate information about the protective role against nitrosative stress of the enzyme.

Figure 27 depicts a diagram of the experimental setup considered. As shown, to make the analysis coherent and more informative, the conditions for the expression analysis were the same considered to evaluate germination efficiencies, germ tube elongation rates and nuclear division rates.

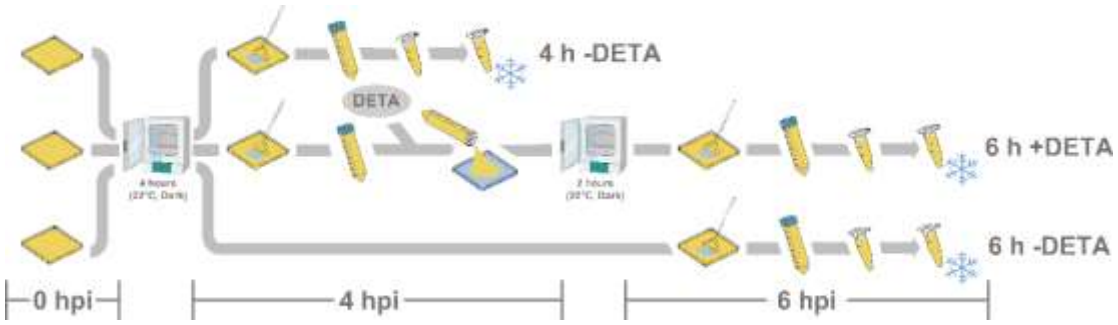

Figure 27. Scheme of the experimental procedure designed for the differential gene expression analysis in response to NO exposure.

Fungal material from three biological of each of the following samples were collected:

- Sample 1: Spores of the wild-type strain B05.10 grown for 4 hours without exposure to NO.
- Sample 2: Spores of the wild-type strain B05.10 grown for 6 hours without exposure to NO.
- Sample 3: Spores of the wild-type strain B05.10 grown for 4 hours and then exposed to NO for 2 hours.
- Sample 4: Spores of the mutant strain *ΔBcfhg*1 grown for 4 hours without exposure to NO.
- Sample 5: Spores of the mutant strain *ΔBcfhg*1 grown for 6 hours without exposure to NO.
- Sample 6: Spores of the mutant strain *ΔBcfhg*1 grown for 4 hours and then exposed to NO for 2 hours.

These 18 samples were submitted to the NCSU sequencing lab for RNAseq analysis. Upon reception of the samples data, an initial quality control analysis performed with the FastQC program indicated that the data generated from 17 libraries were appropriate for expression analysis. One of the replicas of sample 6 did not pass the quality test and was discarded. Therefore, subsequent analysis that included sample 6 were done using the data of the two remaining replicates.

Of all the comparisons that can be established among the six samples, it was decided to start with the one that faces sample 2 with sample 3. This comparison will allow knowing which genes are affected by the presence of exogenous NO released to the environment by the donor in the biological reference system, the strain B05.10. Genes whose expression is induced or repressed will reveal the fungal cell dynamics of an intact wild-type genetic background under conditions of nitrosative stress. This analysis necessarily constitutes a starting point prior to the analysis of the role played by the detoxifying function of flavohemoglobin in this situation and which will be studied later.

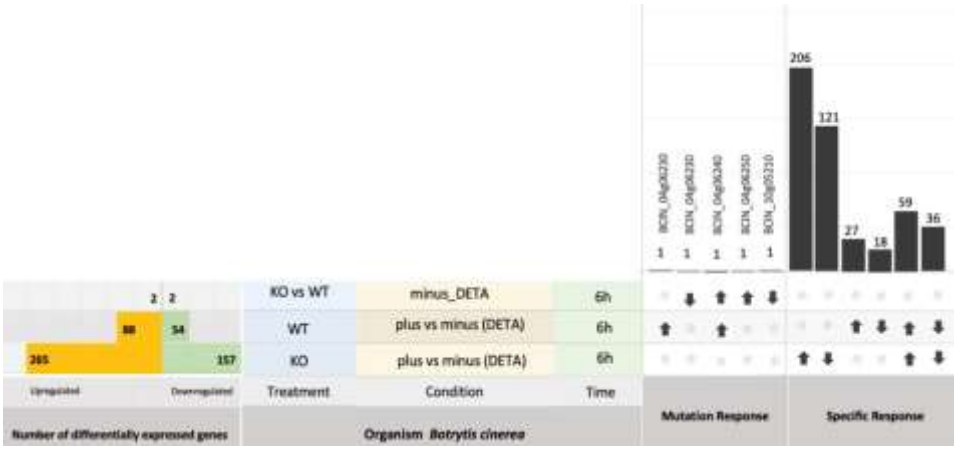

Figure 28. Summary of the differential gene expression analysis in response to NO in the B05.10 and *ΔBcfhg*1 strains.

The changes in gene expression of the comparison 2 versus 3 were analysed, obtaining 142 differentially expressed genes (adjusted P value of < 0.05 and $\log_2$(fold change [FC]) of > 2 or < -2). Of these, 88 were upregulated and 54 downregulated genes (Figure 28) (the complete list of DEGs is presented in the Table 9, Appendix). GO term enrichment analysis on the upregulated genes showed an overrepresentation of 19 terms as oxidation-reduction process, nitrate metabolic process, reactive nitrogen species metabolic process, nitric oxide biosynthetic process, nitric oxide metabolic process, reactive oxygen species biosynthetic process, siroheme biosynthetic process, sulfate assimilation and DNA catabolic process, among others (Table 2). On the other hand, GO term enrichment analysis on the downregulated genes showed an overrepresentation of 12 terms, among which were metal ion homeostasis, cation homeostasis, inorganic ion homeostasis, oxidation-reduction process, glutamate metabolic process, chemical homeostasis, and isoprenoid biosynthetic process (Table 2).

Table 2. GO terms enriched among genes whose expression increases and decreases in response to NO in the B05.10 strain (sample 2 vs sample 3).

Comparison 2 versus 3 (upregulated genes)				
GO.ID	Term	Annotated genes	Annotated DEGs	P value
GO:0055114	oxidation-reduction process	767	19	1.80E-05
GO:0042126	nitrate metabolic process	3	2	0.00027
GO:0042128	nitrate assimilation	3	2	0.00027
GO:2001057	reactive nitrogen species metabolic process	3	2	0.00027
GO:0071941	nitrogen cycle metabolic process	4	2	0.00053
GO:0006809	nitric oxide biosynthetic process	1	1	0.00956
GO:0019058	viral life cycle	1	1	0.00956
GO:0019079	viral genome replication	1	1	0.00956

GO:0046209	nitric oxide metabolic process	1	1	0.00956
GO:1903409	reactive oxygen species biosynthetic process	1	1	0.00956
GO:0016032	viral process	2	1	0.01903
GO:0019354	siroheme biosynthetic process	2	1	0.01903
GO:0042136	neurotransmitter biosynthetic process	2	1	0.01903
GO:0046156	siroheme metabolic process	2	1	0.01903
GO:0044403	symbiotic process	3	1	0.02841
GO:0044419	interspecies interaction between organism	3	1	0.02841
GO:0000103	sulfate assimilation	4	1	0.03771
GO:0006308	DNA catabolic process	4	1	0.03771
GO:0006783	heme biosynthetic process	5	1	0.04692

Comparison 2 versus 3 (downregulated genes)

GO.ID	Term	Annotated genes	Annotated DEGs	P value
GO:0055070	copper ion homeostasis	1	1	0.0038
GO:0055076	transition metal ion homeostasis	1	1	0.0038
GO:0055065	metal ion homeostasis	2	1	0.0075
GO:0042592	homeostatic process	39	2	0.0091
GO:0050801	ion homeostasis	3	1	0.0113
GO:0055080	cation homeostasis	3	1	0.0113
GO:0098771	inorganic ion homeostasis	3	1	0.0113
GO:0055114	oxidation-reduction process	767	7	0.0147
GO:0006536	glutamate metabolic process	5	1	0.0187
GO:0065008	regulation of biological quality	63	2	0.0227
GO:0048878	chemical homeostasis	8	1	0.0298
GO:0008299	isoprenoid biosynthetic process	13	1	0.048

Enrichment analysis is indicative of the state of nitrosative and oxidative stress experienced by the germinating spores when exposed to the donor and the nature of the reactions and cellular machinery set in motion in response. However, this information is insufficient if what is desired, as in this case, is to find out what are the specific processes influenced by NO metabolism in a situation of nitrosative stress. Therefore, it became necessary to approach these results in a different way, characterizing the genes more individually by means of databases and prediction servers of annotated sequences (see section 22 of Materials and Methods).

This manual inspection of the identified differentially expressed genes (DEGs) led to the characterization of 78 genes (56 upregulated and 22 downregulated) according to the terms and names associated with their identification codes in the different databases. The largest group among the upregulated genes that could be characterized consisted of those associated with the GO terms of biological process (BP) and molecular function (MF) of redox process and oxidoreductase activity, respectively. The group is made up of several types of oxidoreductases where monooxygenases, reductases, dehydrogenases, a hydroxylase, a thioredoxin and a catalase are found. The latter, the catalase *Bccat*6 (Bcin05g04580), stood out for presenting an induction level of more than 5.4 times in the presence of external nitric oxide.

Genes categorized as related to nitrogen metabolism also represented a significant percentage. In this group, genes encoding a nitrite reductase (*BcniiA*), a nitrate reductase (*BcniaD*), the flavohemoglobin enzyme *Bcfhg*1, two nitrilases (Bcin12g06180 and Bcin13g05670), three *nmrA*-like domain-containing proteins, two amidases and a nitronate monooxygenase (Bcin04g06340, the gene adjacent to the flavohemoglobin coding gene) were found. One of the NmrA -like domain-containing proteins (Bcin11g06310) presented the highest induction level in this comparison, 9.9, while the induction level of another one was 4.9. On the other hand, the level of induction of the gene encoding flavohemoglobin was also 5.3, that of one of the nitrilases (Bcin12g06180) 4.3 and that of the *BcniiA* and *BcniaD* genes 4.0 and 3.3, respectively.

The next group of genes categorized was that related to general metabolism. In it, numerous hydrolases of different types were found: chitin deacetylase (*Bccda*1), nuclease, esterase, glycoside hydrolase, epoxide hydrolase, xyloglucan-specific endo-beta-1,4-glucanase and phosphoric diester hydrolase. Among them, an O-glycosyl hydrolase with an induction level of 4.4 and a nuclease and a carboxylesterase, both with an induction level of around 3, stood out. In addition, an acetyltransferase, a mevalonyl-CoA ligase and a methyltransferase also appeared differentially induced. The first one with a value of 4.3.

Several genes encoding proteins related to transmembrane transport were also induced. Among them, three major facilitator superfamily (MFS) transporters were found (a sugar transporter and a multidrug transporter with induction levels of 3.6 and 2.6, respectively, and the third with an induction level of 5.1), a Na^+/K^+ transporter and two oligopeptide transporters, one of them (Bcin08g03130) with an induction level of more than 7.4.

Finally, it is worth highlighting a cupin domain containing protein (Bcin14g05020), a protein related to the constitution of the ribosome and a protein with a DNA -binding TEA/ATTS domain that presented induction levels of 5.9, 3.9 and 2.0, respectively.

Among the 22 categorized downregulated genes, the group categorized as related to redox processes was mostly represented by different types of oxidoreductase enzymes (FAD flavoprotein,

dehydrogenase, peroxidase and monooxygenase). Two of them, an unidentified oxidoreductase and a monooxygenase, showed a repression value of -2.8 and -3.7, respectively.

The repressed genes identified for their participation in general metabolic processes were those that code for a glycosyl hydrolase, a hydroxymethylglutaryl-CoA synthase (-3.4), a hytanoyl-CoA dioxygenase (-3.5), a chaperone (-3.7) and an AMP-dependent synthetase/ligase (-3.9).

Several virulence-related proteins were also differentially repressed, showing values between -2 and -3. They were a cfem domain-containing protein (related to pathogenicity, sporulation and stress response), a necrosis inducing protein (*Bcnep*2), the GAS2 protein, regulated by *bmp*1 MAP kinase cascade, and a hydrolase of cutinase type.

A Glutamine amidotransferase (Bcin07g02370) that participates in nitrogen metabolism was the only observed representative of this category. One protein containing MFS domain and two containing Marvel domain (one of them with a repression value of -3.4) made up the group categorized as related to cell transport. It is worth mentioning the genes Bcin10g00010, Bcin08g02150 and Bcin11g05460 , all three related to the GO terms of membrane and integral component of membrane, whose repression values were the highest in the comparison (-4.0, -4.6 and -7.3).

The *Bccpd*3 gene (Bcin01g01590), a cyclophilin-dependent gene related to development and virulence, and the Bcin07g04050 gene, related to the constitution of the ribosome, presented repression values of -2.0 and -2.2, respectively.

The above results show the processes of normal cell dynamics that are affected by the nitric oxide released by the donor during the germination of the spores of the wild-type strain. They inform about the mechanisms that fungal cells activate in response to the conditions of nitrosative and oxidative stress created by the molecule. All of this activated in an intact biological system that represents the natural or reference situation in this analysis.

However, this unaltered system does not allow to know by itself the biological processes that are influenced by the detoxifying action of the flavohemoglobin enzyme in the biological context under study. Therefore, the inclusion of the *ΔBcfhg*1 strain in this transcriptomic analysis was essential. Its presence is undoubtedly necessary given that it represents a biological system lacking the gene encoding BCFHG1 and, therefore, its transcriptional profile should indicate the processes that are of our interest when compared with the profile of the system protected against NO, the strain B05.10.

Before analysing the effect that exogenous nitric oxide triggers on the unprotected system represented by the spores of the mutant strain against nitric oxide, it is necessary to pay attention to the potential effect that the mutation of the *Bcfhg*1 gene may have on the transcriptomic profile of the fungal spores. For this purpose, the comparison 2 versus 5 was the next to be analysed. In it, the transcriptomic profile of the spores of the wild-type strain B05.10 is compared with that of the spores of the mutant strain *ΔBcfhg*1, both cultured for 6 hours without exposure to NO. In this comparison, therefore, the modulating effect of the molecule is not taken into consideration, so that the DEGs detected in it can be

attributable to the only aspect that differentiates both strains, that is, the presence and absence of the gene encoding BCFHG1 in one and the other.

The analysis of this comparison allowed the detection of 4 DEGs using the same selection parameters as in the first comparative examined (adjusted P value of < 0.05 and log_2(fold change [FC]) of > 2 or < -2). Of these, two were upregulated genes and the other two were downregulated (the complete list of DEGs is presented in the Table 10, Appendix).

The two upregulated genes were Bcin04g06240 with a value of 3.7 and Bcin04g06250 with a value of 2.7. They code for a nitronate monooxygenase and an amylase-type hydrolase, respectively. Interestingly these two genes are closely linked to the flavohemoglobin coding gen *Bcfhg*1 (Bcin04g063239) which, as expected, appears as down regulated as it is not expressed the null mutant (it was generated by gene replacement of most of the ORF). The second down regulated gene just as a consequence of the mutation, is Bcin10g05210, a gene related to the GO term "integral component of membrane" and highly repressed (-9.2) in the mutant, respectively.

The third and last comparison analysed for this work was the one that compares the transcriptional profile of the spores of the strain *ΔBcfhg*1 cultivated for 4 hours in the absence of NO and then exposed to the donor for 2 hours, with that of the spores of the strain *ΔBcfhg*1 grown under the same conditions (comparison 5 versus 6). This comparison completes the analysis initially proposed to know the cellular processes influenced by the NO detoxifying action of the BCFHG1 enzyme. In it, 422 DEGs were detected for an adjusted P value of < 0.05 and log_2(fold change [FC]) of > 2 or < -2. Of the 422 DEGs, 265 were upregulated and 157 were downregulated genes (the complete list of DEGs is presented in the Table 11, Appendix). GO term enrichment analysis was performed with the DEGs of this comparative. GO enrichment analysis of the upregulated genes were indicated enrichment in terms such as oxidation-reduction process, cellulose metabolic process, beta-glucan catabolic process and polysaccharide metabolic process, from a total of 11 enriched GO terms (Table 3). The 23 enriched downregulated processes included terms related to glycogen metabolic process, cellular glucan metabolic process, cellular carbohydrate metabolic process, oxidation-reduction process, carbohydrate metabolic process, biotin metabolic process, polysaccharide metabolic process, glycerol metabolic process, phosphate ion transport and alditol metabolic process (Table 3).

Table 3. GO terms enriched among genes whose expression increases and decreases in response to NO in the *ΔBcfhg*1 strain (sample 5 vs sample 6).

Comparison 5 versus 6 (upregulated genes)				
GO.ID	Term	Annotated genes	Annotated DEGs	P value
GO:0055114	oxidation-reduction process	767	41	2,5E-09
GO:0000272	polysaccharide catabolic process	8	2	0,012
GO:0009251	glucan catabolic process	1	1	0,022

GO:0019058	viral life cycle	1	1	0,022
GO:0019079	viral genome replication	1	1	0,022
GO:0030243	cellulose metabolic process	1	1	0,022
GO:0030245	cellulose catabolic process	1	1	0,022
GO:0044247	cellular polysaccharide catabolic proces...	1	1	0,022
GO:0051275	beta-glucan catabolic process	1	1	0,022
GO:0016032	viral process	2	1	0,043
GO:0005976	polysaccharide metabolic process	16	2	0,047

Comparison 5 versus 6 (downregulated genes)

GO.ID	Term	Annotated genes	Annotated DEGs	P value
GO:0005977	glycogen metabolic process	3	2	0,0005
GO:0005978	glycogen biosynthetic process	3	2	0,0005
GO:0006112	energy reserve metabolic process	3	2	0,0005
GO:0009250	glucan biosynthetic process	5	2	0,0016
GO:0033692	cellular polysaccharide biosynthetic	5	2	0,0016
GO:0000271	polysaccharide biosynthetic process	6	2	0,0024
GO:0006073	cellular glucan metabolic process	6	2	0,0024
GO:0044042	glucan metabolic process	6	2	0,0024
GO:0044264	cellular polysaccharide metabolic	6	2	0,0024
GO:0044262	cellular carbohydrate metabolic process	23	3	0,0031
GO:0034637	cellular carbohydrate biosynthetic	9	2	0,0057
GO:0055114	oxidation-reduction process	767	18	0,0064
GO:0005975	carbohydrate metabolic process	270	9	0,0074
GO:0016051	carbohydrate biosynthetic process	13	2	0,0119
GO:0006768	biotin metabolic process	1	1	0,0131
GO:0009102	biotin biosynthetic process	1	1	0,0131
GO:0009081	branched-chain amino acid metabolic	14	2	0,0138
GO:0005976	polysaccharide metabolic process	16	2	0,0179
GO:0006071	glycerol metabolic process	2	1	0,026
GO:0015980	energy derivation by oxidation of organic compounds	20	2	0,0274
GO:0008152	metabolic process	2976	45	0,0308
GO:0006817	phosphate ion transport	3	1	0,0387
GO:0019400	alditol metabolic process	3	1	0,0387

Then, as in previous comparisons, a manual inspection of the genes was carried out. This inspection allowed the identification and/or categorization of a total of 224 DEGs (153 upregulated and 71 downregulated).

Of the 265 genes that presented an induction response in this comparison, 59 were common to the comparison 2 versus 3, while the rest, 206, were exclusive to the comparison 5 versus 6.

The group of genes encoding proteins related to the redox activity that appeared differentially induced in the two indicated comparisons was mainly composed of oxidoreductase enzymes. Among them, dehydrogenases are widely predominant (one of them with a value of 6.1), but there are also monooxygenases, the catalase *Bccat*6 (6.8), a thioredoxin, a hydroxylase and reductases (cytochrome P450 reductase, 3-oxoacyl-[acyl-carrier protein] reductase).

The same behaviour was observed in those genes belonging to this same group and that showed an induction response only in the comparison 5 versus 6. However, the heterogeneity was greater since monooxygenases (Bcin01g08630 with a 7.0, *BcboA*4 with a 6.1), dioxygenases, dehydrogenases (*Bcnde*4, *Bcnqo*1, *BcboA*17, Bcin15g05630 with a value of 4.7), a methyltransferase (4.1), a peroxidase (*Bcprx*2), a decarboxylase, a flavoprotein (*Bcalo*1) related to apoptosis-inducing factor 2, the laccase *Bclcc*7 (4.4), a sulfite oxidase (*Bcsox*1), the cytochrome c oxidase *Bccox*17, the glutathione S-transferases *Bcgst*1, *Bcgst*3 (4.0), *Bcgst*5 (4.0), *Bcgst*13 and *Bcgst*14, a glutamate-cysteine ligase related to the glutathione and various reductases (Peptide methionine sulphoxide reductase, Aldo/keto reductase, 2 -dehydropantoate 2- reductase) were detected.

This parallelism was also observed between the nitrogen metabolism genes simultaneously induced in the two comparisons and those induced, exclusively, in the comparison that analyses the effect of NO on the mutant strain. Thus, an amidase enzyme (Bcin03g08640) with a value of 2.5, a nitrilase enzyme (Bcin12g06180) with a value of 5.0 and three *nmrA*-like domain-containing proteins (Bcin03g00700 with a 4.0, Bcin08g04910 with a 6.9 and Bcin11g06310 with a 12.7) were induced both in the spores of the wild-type strain and in those of the mutant strain in the presence of NO. Meanwhile, in the group of genes induced only in the mutant spores in response to NO, a nitrilase enzyme (Bcin05g04960), an amidase (Bcin12g00040), a deaminated glutathione amidase (Bcin11g00510) and a greater number of *nmrA*-like domain-containing proteins than in the previous case (Bcin09g04560 (5.4), Bcin02g01880 (3.8), Bcin01g03270 (3.1), Bcin05g05290 (3.0), Bcin09g00910, Bcin02g05800 and Bcin12g00030) were found.

The genes categorized as related to the general metabolism that appeared induced in response to NO in the spores of the two strains considered encode for hydrolases of different types (phosphodiesterase, glucanase, chitin deacetylase Bccda1), a polyketide cyclase/dehydrase (5.7), an acetyltransferase (4.8) and a carboxylesterase (4.2). Again, among the genes induced only in the comparison 5 versus 6, belonging to this category, there was a greater variety. Different types of hydrolases were detected (acetylxylan esterase with a 3.1, gluconolactonase , glycoside hydrolases,

acetylhydrolase, acylphosphatase, nucleoside triphosphate hydrolase) and also transferases (acetyltransferase with a 3.3, coenzyme A transferase, N-acetyltransferase, glycosyltransferase, flavin prenyltransferase), but also several lyases, a dioxygenase possibly related to betalain biosynthesis, an isomerase, the polyketide synthase *Bcpks*15, a protein possibly related to wax synthesis and the cyclophilin-dependent gene 1 (*cpd*1), related to morphogenesis and virulence and whose value induction was 3.8.

In the case of genes belonging to the cell transport category, the number of them induced only in the mutant spores in response to the NO released by the donor was several times higher than the groupof genes common to the comparatives of wild and mutant spores. A Cu^{+} transporter (Bcin13g03870), witha 5.6, oligopeptide transporter (Bcin08g03130), a transporter with HPP domain (Bcin08g03130) and an MFS transporter (Bcin15g00040) with a value of 7.8 constituted this second group. Meanwhile , numerous MFS transporters (Bcin15g05620 with a 4.9, Bcin02g07500 with a 3.5, Bcin02g01270 with a 3.5), a hydrogen ion transmembrane transporter (3.6), the rhodopsin *Bcbop2*, a pantothenate transporter, the choline transporter *Bcpie*2, a sulphur transporter and a flotillin (3.2) were found in the comparison 5 versus 6 exclusively.

Only one gene classified in relation to virulence processes, Bcin10g03040, was found both in the comparison of the spores of the wild-type strain (2.1) and in that of the spores of the mutant strain (3.9). Apparently, the gene encodes a protein related to the transfer of nucleoside diphosphate sugars and the synthesis of capsular polysaccharide, considered virulence factors in some bacterial and yeast species. The number of genes of this category that were induced only in the mutant spores was greater: several hydrolases (endoglucanase with a 6.2, cellulose 1,4-beta-cellobiosidase, rhamnogalacturonan hydrolase), a pectate lyase, a cytochrome P450 monooxygenase (3.1) related to the biosynthesis of secondary metabolites and a protein, Bcin02g07490 (3.4), related to the biosynthesis of mycotoxins.

The genes classified in the development category were Bcin03g05500 (3.8), an oil body-associated protein-like related to seed germination, Bcin12g05260 (3.8), a membrane protein related to ubiquitination, Bcin05g04520 (2.4), involved in the maintenance of cellular morphology, Bcin12g06330 (2.2), a structural constituent of cell wall and Bcin14g05020 (6.8), a protein containing a conserved barrel Cupin 2 related to germins and plant storage proteins. This last gene showed an induction response in the comparisons of the two types of spores (5.9 in 2 versus 3), while the rest of the genes only appeared differentially induced in the comparison 5 versus 6.

In relation to the ribosome, a single gene could be identified (Bcin06g01560). This gene showed an induction response in the comparisons 2 versus 3 (3.9) and 5 versus 6 (3.5) at the same time and is linked to the structural constitution of the ribosome.

Genes classified in the categories of gene regulation and cell cycle regulation were only detectedas induced in the comparison of mutant spores, 5 versus 6.

Three genes containing a Zn(2)-C6 fungal-type DNA-binding domain (Bcin12g05920 with a 3.6), the Bcin14g00060 gene containing a Zinc finger C2H2 -type domain (6.7), a gene containing the two previous domains, the Bcin08g02710 gene containing a basic-leucine zipper domain (3.0), two genes described as fungal transcription factor (Bcin09g00740 with a 3.1) and Bcin01g10220, a serine threonine kinase (4.6) were the genes related to gene regulation.

Two genes, Bcin02g03440 (3.1) and Bcin02g04870 (2.2), were linked to the cell cycle because the first contains a chromo domain associated with the alteration of the structure of chromatin to the condensed morphology of heterochromatin and the second was identified as a histone involved in nucleosome assembly.

Finally, it is worth mentioning the behaviour of several genes that, although they could not be categorized, presented considerably high induction values in this comparison. Bcin02g06160 was induced in the two comparatives considered (2.9 in the case of spores from the wild-type strain and 5.3 in the case of mutants) and was associated with the description of Alpha/Beta hydrolase fold|Alpha. Bcin10g05210, a gene related to the GO term of "integral component of membrane", which showed a repression of -9.2 in the comparison 2 versus 5 was induced in the present comparison with a value of 7.4 and Bcin02g00550, an uncharacterized protein, induced only in the comparison 5 versus 6 (6.6).

Among the repressed genes, 36 were common to the two mentioned comparisons (2 versus 3 and 5 versus 6), while 121 were detected only in the comparison that contrasts the response of mutant spores grown in the absence and presence of exogenous NO.

A small group of genes encoding oxidoreductases enzymes were the only representatives of the category of oxidoreduction activity that showed a common repression response to the spores of both strains. Thus, the peroxidase *Bcprd*1, two dehydrogenases and two oxidoreductases of unknown type (one of them *Bcalf*1) presented repression values between -2.0 and -3.5. The number of differentially repressed oxidoreductases exclusively in the spores of the *ΔBcfhg*1 strain was higher and consisted of dehydrogenases (Bcin02g03670 with a -7.6), methyltransferases (Bcin06g04540 with a -6.3, Bcin14g05480 with a -6.2 and Bcin15g03170 with a -6.0), a dioxygenase, a tetrahydroxynaphthalene reductase (*Bcbrn*1) and a laccase (*Bclcc*6).

The same dynamics was observed in the case of genes belonging to the category of general metabolism. A hydroxymethylglutaryl-CoA synthase, a glycosyl hydrolase, a chaperone and a phytanoyl- CoA dioxygenase, all of them with repression values between -3.1 and -3.7, made up the group of genes repressed simultaneously in the two comparisons. On the other hand, several transferases (kinases, aminotransferase, methyltransferase, N-acyltransferase, 1,4-alpha-glucan branching enzyme, biotin synthase), lyases (glutamate decarboxylase, glycogen phosphorylase), hydrolases (ergosteryl-3beta-O-L-aspartate hydrolase with a -12.6, alpha-amylase, beta-glucosidase, glycoside hydrolase), oxidoreductases (D-xylose reductase, sorbose reductase), dehydratases (the L-galactonate dehydratase *Bclgd*1, dihydroxy- acid dehydratase), peptidases (tripeptidyl-peptidase I, Aspartic peptidase), a ferricrocin synthase

(*Bcnrps*2), an apolipoprotein, a pyrimidine precursor biosynthesis enzyme (*Bcnmt*1) and multifunctional enzymes (glycogen debranching enzyme, polyketide synthase, dethiobiotin synthetase / adenosylmethionine-8-amino-7-oxononanoate aminotransferase) suffered a repression of their expression by the effect of exogenous NO only in mutant spores.

The genes classified as related to cell transport consisted, for the most part, of MFS transporters (Bcin06g04140 and Bcin14g03450 related to sugar/inositol transport, Bcin02g04840 related to inorganic phosphate transport). But magnesium transport protein, a p-type atpase and two Marvel domain-containing proteins were also observed. Of all of them, both Marvel domain-containing proteins (Bcin16g04610 and Bcin04g00780) and an MFS transporter (Bcin10g00020) showed a simultaneous repression response in the spores of both strains, while the rest of the genes were differentially repressed only in the case of mutant spores. Regarding their FC values, they all ranged between -2.1 and -3.7, except in the case of the MFS transporter Bcin09g00960, which presented a value of -6.0.

Within the virulence category, two genes related to the *Egh*16-like virulence factor were found (Bcin06g05980 with a -6.1 and *gas*2), two lyases (the pectate lyase Bcin04g00470 with a -6.1 and the pectin lyase *Bcpga*2/*Bcpg*2), a cutinase and a cfem domain-containing protein, a domain related to proposed roles in fungal pathogenesis. The cutinase (Bcin13g05760) and *gas*2 (Bcin14g04260) presented a repression response both in the case of wild spores (-2.8 and -2.4, respectively) and in that of mutants (-2.3 and -2.9, respectively).

Two genes belonging to the developmental category (Bcin04g04700 and Bcin01g02140) were differentially repressed in the comparison of mutant spores exclusively. Bcin04g04700 (-5.6) is related to heterokaryon incompatibility proteins and Bcin01g02140 (-6.0) is *mat*1-1-5 of unknown function, one of the two genes that make up the *mat*1-1 *locus* that determines sexual compatibility in *B. cinerea*.

Bcin07g02370 was linked to nitrogen metabolism by encoding a glutamine amidotransferase . This gene was repressed, at the same time, in the comparison of wild spores (-2.2) and in the comparison of mutant spores (-2.5).

Finally, among the uncategorized genes that showed relevant FC values, the following were found:

Three genes (Bcin08g02150, Bcin09g05970 and Bcin10g00010) associated with the terms GO of membrane and integral component of membrane, and one gene (Bcin16g00990) with zinc ion binding and metal ion binding domains were repressed in the two comparatives under analysis, being their response more intense in the case of the comparison of the spores of the strain *ΔBcfhg*1. The respective FC values for the four genes, in the order of mention, were -4.6, -2.7, -4.0 and -2.0 in comparison 2 versus3 and -4.9, -5.6, -6.3 and -8.6 in comparison 5 versus 6.

The genes Bcin08g03340 (an uncharacterized protein), Bcin08g07090 (related to the description of hydrolytic enzyme), Bcin05g01900 (related to the GO term of integral component of membrane), Bcin15g01880 (with an ankyrin repeat-containing domain) and Bcin05g05550 (related to the description

of probable *brt*1, maybe a protein related to interaction with the environment) with respective FC values of -6.0, -6.1, -6.3, -6.3 and -6.8, were only found as differentially repressed in the comparison of mutant spores in response to NO.

3. Analysis of NO cell cycle targets

In the first part of this section, the results related to the analysis of the effect of NO on the development of *B. cinerea* using an approach based on microscopy techniques, NO modulating drugs, and histological staining were described. These results showed that the effect of the molecule on the germination of the fungus was a transient delay effect in the case of the wild-type strain B05.10 and a lasting blocking effect in the case of the mutant strain *ΔBcfhg*1. Estimations of the percentage of germination, of germ tube elongation rates and of nuclear division rates in both strains, all informed about this effect.

Taken together, these observations lead us to consider the possibility that there is a relationship between exogenous NO exposure and cell cycle regulation in our study system. This reflection is consistent with what was previously stated about the behaviour of the yeasts *S. cerevisiae* and *S. pombe* in response to nitrosative stress caused by NO (Horan *et al*., 2006; Majumdar *et al*., 2012) and is supported by previous studies carried out in our research group on this aspect.

The study of the tandem NO - *B. cinerea* has more than a decade of work by our group in order to find out the physiological functions in which the reactive molecule NO participates in the biology of this phytopathogenic fungus. In recent years, work has been done to study the ability of the pathogen to detoxify NO by means of the BCFHG1 flavohemoglobin, as a mechanism that contributes to its virulence. In this regard, with the intention of characterizing the physiological processes in which NO metabolism is relevant in the fungus, a first global expression analysis in response to NO was carried out by setting up a microarray gene expression profiling experiment of germinating spores of B05.10 and *ΔBcfhg*1 strains (Daniela Santander, Doctoral Thesis. University of Salamanca). That analysis, although carried out also during germination, involved specific experimental conditions which establish important differences: (1) spores were cultured in liquid minimal medium (Gamborg's B5 salts supplemented with 10 mM Sucrose and 10 mM KH_2PO_4 pH 6.5) in agitation, (2) DETA was added after 5 hours of incubation and (3) samples for expression analysis were collected one hour later. Considering these differences, that analysis and the results generated offered several interesting pieces of information that could be integrated in our current analysis. Thus, it allowed to identify functional categories of induced and repressed genes informative of the biological situation that was analysed. Specifically, in the case of the mutant strain, it was observed, among other aspects, that the functional categories "cell cycle", "DNA synthesis" and "nucleolus activity" were overrepresented among the genes repressed upon addition of NO.

A more detailed study of the list of genes whose expression was repressed identified groups of genes that in *S. cerevisiae* show coordinated expression in the cell cycle (Enserink and Kolodner, 2010).

The genes with a higher level of repression were the orthologs of the *mcm* (2-7) genes of *S. cerevisiae*, genes whose gene products make up a protein complex essential for the formation of the origins of replication and for the initiation of the synthesis of DNA (Lei and Tye, 2001) and that are expressed between the M phase and the G1 phase (Enserink and Kolodner, 2010). The expression of this group of genes is controlled by the transcription factor *mcm*1. A strong repression of genes that are specifically expressed in the G1 phase was also found. In this yeast, the expression of G1 -specific genes is controlled by the complexes MBF, a transcription factor made up of *mbp*1 and *swi*6, and SBF, a transcription factor made up of *swi*4 and *swi*6. Although there is a certain overlap between the classes of genes that are controlled by one and the other, MBF would preferentially control the expression of genes related to the replication itself and with DNA repair, while SBF regulates the expression of genes involved in the progress of the cell cycle, cell morphogenesis, and spindle polar body duplication (Enserink and Kolodner, 2010).

Another gene found in this same list was one described as "similar to M-phase inducer phosphatase", which a BLAST analysis identified as the ortholog of the gene encoding the CDC25 phosphatase enzyme from *S. pombe* (GRS (Genome Report System) of INRA). *Cdc*25 (*mih*1 in *S. cerevisiae*) participates in the activation of *cdk*1 (*cdc*2 in *S. pombe* and *cdc*28 in *S. cerevisiae*) by dephosphorylation. The latter is a key enzyme in the regulation of the cell cycle since it controls the entry of the cell to the mitosis phase from the G2 phase.

This simultaneous repression response of the genes that make up these clusters in the unprotected system against NO represented by the mutant spores, together with the way in which the molecule influences germination, elongation of the germ tube and nuclear division of the spores of the two strains considered allow proposing that exposure to NO can modulate the activity of proteins necessary for the transcription of these same clusters.

On the other hand, these results that show the influence that NO has on different regulating agents of the cell cycle were obtained from spore samples exposed to the NO DETA donor for 1 hour, after having allowed the activation of its transcriptomic germination program, during the previous five hours. The fact that the transcriptional response of these genes to the nitrosative stress situation created by the donor is detectable just 1 hour after exposure is indicative of a rapid signalling action by the molecule.

All these previous considerations determined us to hypothesize that, under the evaluated conditions, NO would be affecting the activity of these regulatory proteins through the covalent modification of cysteine (S-nitrosylation) and tyrosine (tyrosine nitration) residues, reactions lacking intermediates and, therefore, considered faster than other signalling routes also attributed to NO, such as the cGMP-dependent signalling pathway. Specifically, we proposed that the molecule would affect, through at least one of these two types of post-translational modifications, the proteins encoded by the genes *mbp*1, *swi*4, *swi*6, *cdc*2, *cdc*25 and *mcm*1.

This list of possible molecular targets for NO was completed with the inclusion of the enzyme nitrate reductase, encoded by gene *niaD*. This protein plays a relevant role in NO homeostasis since it

participates in the reductive synthesis of the molecule and in its regulation during fungal development (Cánovas *et al*., 2016). Furthermore, a possible S-nitrosylation to the Cys residues on the surface of this protein in plants has been described *in silico* (Fu *et al*., 2018).

The proteins selected as possible targets of NO were then subjected to an analysis that aimed to determine the possible alteration of their activity due to modifications of the S-nitrosylation and/or nitration type caused by the action of the molecule. The experimental approach initially designed to perform this analysis was based on the following points:

- Identification of genes homologous to those selected in *S. cerevisiae* and *S. pombe* in the genome of *B. cinerea*.
- The construction of translational fusions in which the GFP fused to the C-terminus of each of the candidate proteins.
- The assessment of the levels of S-nitrosylation and/or nitration of the different potential NO target proteins fused with the GFP protein.
- In those target proteins in which the presence of post-translational modifications caused by the molecule were detected, the determination of the alterations in their activity as a consequence of S-nitrosylation and/or nitration in relation to the control of the cell cycle.

3. 1 *In silico* analysis of the putative NO targets.

A bibliographic consultation (White, 2001) and the use of homology comparisons made with the different software and online databases described in section 22 of Materials and Methods allowed the identification and localization of the genes *mbp*1, *swi*6, *cdc*2, *cdc*25 and *mcm*1 and of the *niaD* gene in the annotated genome of *B. cinerea*. However, this same process did not yield any results regarding the presence of the homologous gene of *swi*4 in our study system. The results obtained are shown in Table 4.

Table 4. Common name, gene ID and length of the predicted protein of the genes selected as genes encoding putative NO targets.

S. pombe	*S. cerevisiae*	*B. cinerea*	
		Gene ID*	Predicted protein length
*res*2	*mbp*1	Bcin14g00280	684 residues
*cdc*10	*swi*6	Bcin12g00820	869 residues
*cdc*2	*cdc*28/*cdk*1	Bcin16g00490 (*Bccdk*1)	333 residues
*cdc*25	*mih*1	Bcin07g02410	556 residues
*map*1	*mcm*1	Bcin09g06140	227 residues
-	-	Bcin07g01270 (*niaD*)	907 residues

* Identification code for *loci* from the BcinB0510 reference genome annotations (van Kan *et al*., 2017).

Once the *loci* of the genes of interest had been identified in the genome of our study system, the next step was to detect the potential sites of post-translational modifications in the respective proteins. To this end, the amino acid sequences in FASTA format predicted for the candidate genes were submitted for predicting S-nitrosylation and tyrosine nitration sites under the medium threshold condition using the prediction tool of the GPS-SNO 1.0 (Xue *et al*., 2008) and GPS-YNO2 1.0 (Liu *et al*., 2011) software, respectively. Table 5 shows the results derived from this analysis, reporting the probability of amino acid sequences to undergo post-translational modifications due to the action of NO.

Table 5. Prediction results (position, peptide) of the potential S-nitrosylation and tyrosine nitration sites (in red) in the predicted amino acid sequences encoded by genes *mbp*1, *swi*6, *cdc*2, *cdc*25, *mcm*1 and *nia*D using GPS-SNO 1.0 and GPS-YNO2 1.0 software with a medium threshold condition.

Protein name	GPS-SNO 1.0 (Predicted S-nitrosylation sites)		GPS-YNO2 1.0 (Predicted tyrosine nitration sites)	
	Position	Peptide	Position	Peptide
CDC25	236	TSMSLGECFMESPPR	472	GRCFPQNYVEMDAKE
			545	MMSSPIFYDRGTPRR
	484	AKEHAYTCEREMGRL	556	TPRRQVSY*******
CDC2	No site was predicted		4	****MENYQKLEKIG
			15	EKIGEGTYGVVYKAK
MBP1	401	AKNKARKCVRALMGR	13	AKSGPGIYSATYSNV
			112	KLRAIFEYTPGEFSP
			370	LEKFIEIYHPDEVQR
			622	RKALVGEYIGALGVA
NiaD	170	TVPITLVCAGNRRKE	361	QTYRAKGYAYGGGGR
	881	GEQLVLICGPEALEK	400	DDYRDRAYENETLFG
SWI6	478	ETALMRACCVANNLD	216	AAQRKRLYNSGTENR
			530	RSPASKYYLESLLEF
MCM1	No site was predicted		200	EQQQAIAYQNYMAHQ

The GPS-SNO 1.0 software predicted two cysteine sites of CDC25 (Cys236 and Cys484) as potential S-nitrosylation sites while the GPS-YNO2 1.0 software predicted three nitration sites (Tyr472, Tyr545 and Tyr556) in this protein. In the case of CDC2, the GPS-SNO 1.0 algorithm did not predict any S- nitrosylation sites, but GPS-YNO2 1.0 did detect two tyrosines capable of being nitrated (Tyr4 and Tyr15). In the MBP1 protein sequence there was one S-nitrosylated cysteine (Cys401) and four nitrated tyrosines (Tyr13, Tyr112, Tyr370 and Tyr622) predicted by the applied algorithms. The protein encoded by the *niaD* gene presented two potential S-nitrosylation sites (Cys170 and Cys881) and two other potential nitration

sites (Tyr361 and Tyr400). In the SWI6 protein sequence, cysteine at position 478 was detected as a potential S-nitrosylation site and tyrosines at positions 216 and 530 as potential nitration sites. In the case of the MCM1 protein, the GPS-SNO 1.0 algorithm did not predict any S-nitrosylation sites, but nitration proved to be plausible at tyrosine at position 200 within the protein (Table 5).

3.2 Translational fusion of the GFP protein with the putative NO targets in B05.10 *B. cinerea* strain.

The plasmids pDONR^{TM}221 and pFPL-Gh (Gong *et al*., 2015) were used applying Gateway® technology (see sections 12 and 13.3 of Materials and Methods) to obtain the transformants of *B. cinerea* strain B05.10 carrying the translational fusions of the GFP protein with the different candidate proteins for molecular targets of NO. First, the ORF of each of the genes of interest was amplified by PCR, conserving its promoter region, but not its terminator region. For this, two primers were designed for each translational fusion that allowed us to amplify a fragment of variable length, depending on the gene, but that contained in all cases a stretch of around 600 nucleotides of the 5' region of the gene and that ended in the nucleotide immediately upstream of the stop codon. In this way, it was ensured that the fragment maintained the most important regulatory sequences of the 5' UTR region of the gene and, at the same time, lacked the stop codon. The oligonucleotides used (CDC25_attB_F1, CDC25_attB_R1, CDC2_attB_F1, CDC2_attB_R1, SWI6_attB_F1, SWI6_attB_R1, MBP1_attB_F1, MBP1_attB_R1, MCM1_attB_F1, MCM1_attB_R1, NR_attB_F1 and NR_attB_R1) included a stretch of 21 nucleotides of the specific sequence of the gene together with the corresponding *attB* adapter sequence (31 nucleotides in the case of the forward primer and 30 nucleotides in the case of the reverse primer) according to th e Gateway methodology. Sequences are presented in Table 8 (Appendix).

Once the fragment was amplified, it was purified and cloned into the donor vector pDONR ^{TM}221 by means of the BP recombination reaction (see section 13.3 of Materials and Methods). The recombination product, Entry clone, was used directly to transform competent cells of the DH5α line of *E. coli*. The colonies resulting from the transformation were subjected to a PCR screening that allowed the identification of those colonies carrying the plasmid of interest. In this analysis, the same oligos with the *attB* extensions used in the initial amplifications of the ORFs of each gene (gen_attB_F1/gen_attB_R1) were used (Figure 28A). Among the colonies that were carriers of the plasmid, one was chosen to extract the vector and check its correct size by digestion reactions with different enzymes (Figure 2 8B). In addition, the Entry clone was sequenced using the universal oligo M13R (Table 8. Appendix) to guarantee that its open reading frame had not been modified after its insertion into the donor vector and the absence of mutations in the cloned ORF (Figure 28C). The results of these analyses reported the correct cloning of all gene sequences in pDONR^{TM}221, except in the case of the *mcm*1 gene. In this case the analysis of the plasmid DNA obtained from the colonies transformed with the pENTRY-MCM1 vector were inconclusive and contradictory, leading to the definitive abandonment of the study of the gene. The other successfully recombined Entry plasmids were designated as pFAEN followed by the name of the ORF gene they carried and were stored in *E. coli* at -80 °C.

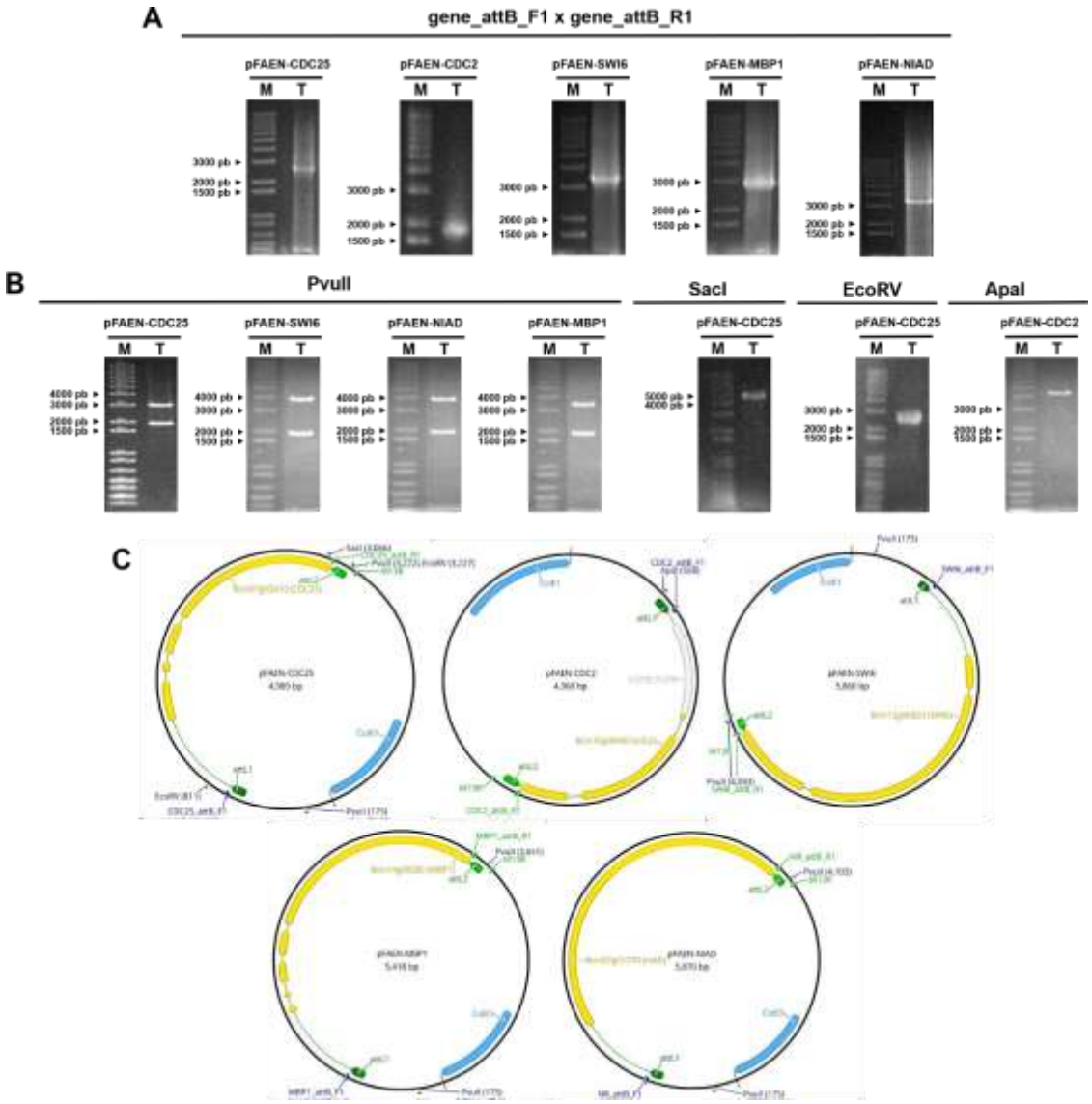

Figure 28. Identification by PCR and restriction analysis of positive *E. coli* clones carrying plasmids pFAEN-CDC25, pFAEN-CDC2, pFAEN-SWI6, pFAEN-MBP1 and pFAEN-NIAD and a schematic map of them. (A) PCR analysis carried out using plasmid DNA of the candidate clone as template and the corresponding pair of oligonucleotides with the *attB* extension (describe in Table 8. Appendix). Size of the amplified fragments were 2502 bp, 1881 bp, 3373 bp, 2931 bp and 3383 bp for the plasmids pFAEN-CDC25, pFAEN-CDC2, pFAEN-SWI6, pFAEN-MBP1 and pFAEN-NIAD, respectively. (B) Restriction enzyme analysis of the plasmid DNA from the candidate clones. The fragments released were 3047 bp and 1942 bp and 2416 bp and 2573 bp in the digestion of pFAEN-CDC25 with *Pvu*II and *EcoR*V, respectively, of 3918 bp and 1942 bp in the digestion of pFAEN-SWI6 with *Pvu*II, of 3928 bp and 1942 bp in the digestion of pFAEN-NIAD with *Pvu*II, of 3476 bp and 1942 pb in the digestion of pFAEN-MBP1 with *Pvu*II. In the rest of the cases, the digestion linearized the vector (M – Marker 1 Kb Plus DNA Ladder, Invitrogen. T – Candidate clone). (C) Scheme of the Entry vectors of the different genes of interest obtained after the BP recombination reactions with the Gateway® system. In them, the following components are shown: the cloned gene fragment flanked by the *attL* sequences, the ColE1 replication origin (ColE1), the annealing positions of the oligonucleotides with the *attB*sequences and of M13R and the cleavage sites of the restriction enzymes used in the mentioned analyses.

The plasmids pFAEN-CDC25, pFAEN-CDC2, pFAEN-SWI6, pFAEN-MBP1 and pFAEN-NIAD were used in the following recombination reaction of the Gateway® system together with the destination vector pFPL-Gh to obtain the corresponding expression clones. Since both plasmids contain the same selection marker (the kanamycin resistance cassette), those plasmid pFAEN molecules that did not

recombine with pFPL-Gh would remain in the ligation reaction and could transform *E. coli* cells during subsequent transformation. Furthermore, the transformation events with the plasmid pFAEN would be favoured to the detriment of those of pFPL -Gh since the former is an intact and supercoiled vector and, unlike the vector pFPL-Gh, does not require the cellular machinery of the bacteria to complete its assembly. To prevent this from happening, four of the five pFAEN plasmids were digested with the *Pvu*II enzyme prior to their addition to the LR recombination reaction since their dige stion allowed the release of the cloned fragment preserving the sites flanking *attL*. The exception was the vector pFAEN-CDC2 which was digested with the enzymes *Apa*I and *Pvu*I because *Pvu*II had a cleavage site within the *cdc*2 ORF. The five recombination reactions were used to transform competent *E. coli* cells. In a manner equivalent to the procedure with the pENTRY vectors, the colonies derived from the transformations were analysed by PCR to detect the carriers of the plasmids of interest. In these PCRs, up to three pairs of oligonucleotides were used (gen_attB_F1/gen_attB_R1, gen_attB_F1/GFP-2B and GFP+BamHIF/GFPuserR. See Table 8. Appendix). The plasmid DNA of one of the candidate colonies that turned out to be carriers of the vectorof interest for each Expression clone was examined by digestion with restriction enzymes that varied according to the vector analysed and sequenced with the oligos gen_attB_F1 and GFP -2B. In this way it was possible to confirm the correct transfer of the gene sequences of eac h of the five genes from pENTRY to pFPL-Gh (Figure 29). Following a nomenclature equivalent to that of the entry vectors, the five expression vectors obtained were named as pFAEX followed by the name of the ORF gene they carried and were stored in *E. coli* at -80 °C.

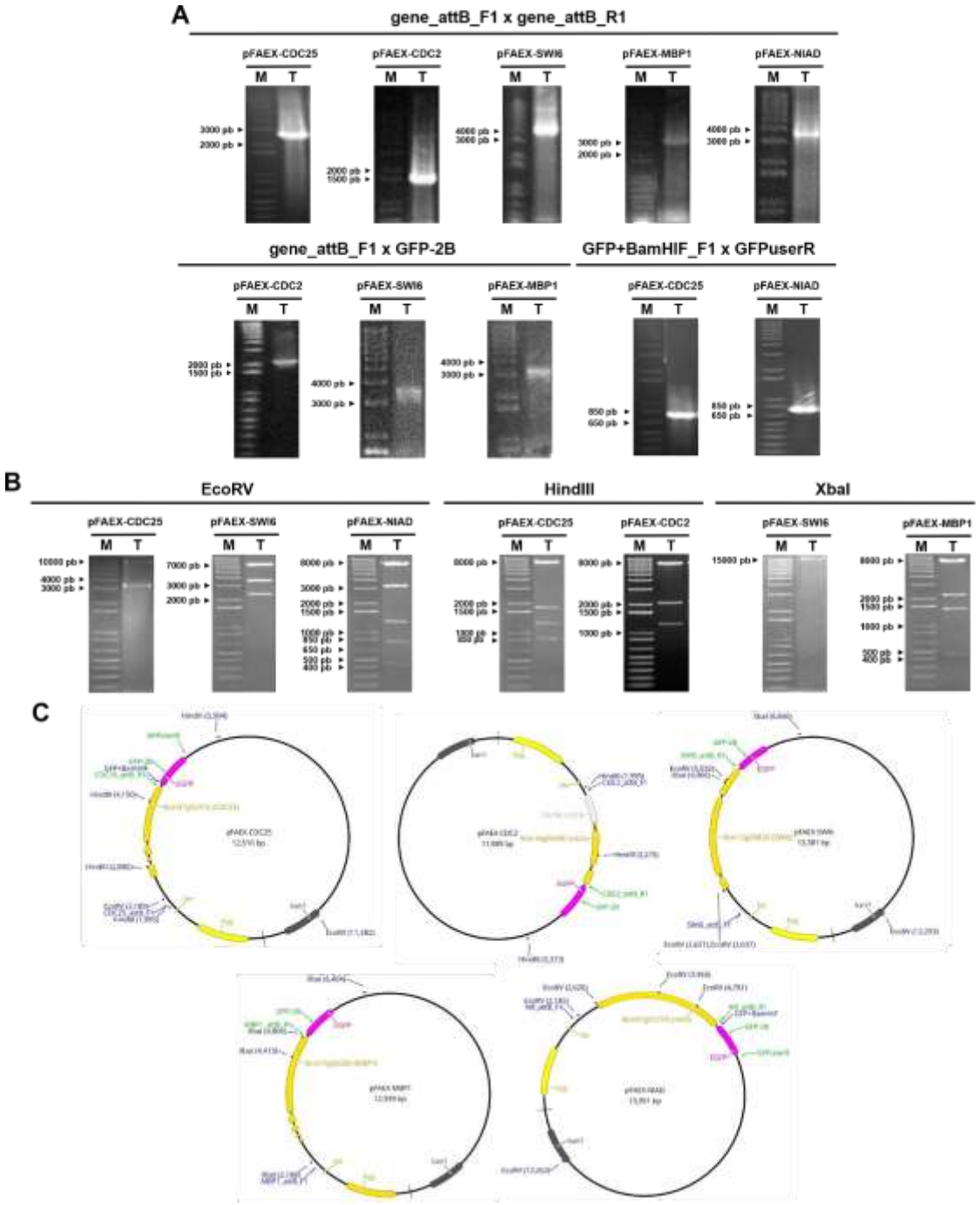

Figure 29. Identification by PCR and restriction analysis of positive *E. coli* clones carrying plasmids pFAEX-CDC25, pFAEX-CDC2, pFAEX-SWI6, pFAEX-MBP1 and pFAEX-NIAD and a schematic map of them. (A) PCR analysis carried out using plasmid DNA of the candidate clone as template and the pairs of oligonucleotides gen_attB_F1/ gen_attB_R1, gen_attB_F1/ GFP -2B and GFP+BamHIF/ GFPuserR amplifying fragments of the following sizes: 2146 pb, 3638 pb and 3196 pb with the pair gen_attB_F1/ GFP-2B for pFAEX-CDC2, pFAEX-SWI6 and pFAEX-MBP1, respectively and of 766 pb with the GFP+BamHIF/ GFPuserR pair for pFAEX-CDC25 and pFAEX-NIAD. The sizes of the fragments amplified with the gen_attB_F1/ gen_attB_R1 pair for the different plasmids were the same as indicated in Figure 28. (B) Restriction enzyme analysis of the plasmid DNA from the candidate clones. The fragments released were 9193 pb and 3317 pb and de 885 pb, 1270 pb, 1844 pb and 8511 pb in the digestion of pFAEX-CDC25 with *EcoR*V and *Hind*III, respectively; of 10 pb, 2395 pb, 3755 pb and 7221 pb and of 13381 pb in the digestion of pFAEX-SWI6 with *EcoR*V and *Xba*I, respectively; of 441 pb, 816 pb, 1339 pb, 3313 pb and 7482 pb in the digestion of pFAEX-NIAD with *EcoR*V; of 1280 pb, 2098 pb and 8511 pb in the digestion of pFAEX-CDC2 with *Hind*III and of 453 pb, 1538 pb, 2225 pb and 8723 pb in the digestion of pFAEX-MBP1 with *Xba*I (M – Marker 1 Kb Plus DNA Ladder, Invitrogen. T – Candidate clone). (C) Scheme of the Expression vectors of the different genes of interest obtained after the LR recombination reactions with the Gateway® system. In them, the following components are shown: the cloned gene fragment, the kanamycin-resistance cassette (kan1), the hygromycin-resistance cassette (hyg), the lac promoter (lac), the *gfp* ORF (EGFP) and the annealing positions of the oligonucleotides and the cleavage sites of the restriction enzymes used in the mentioned analyses.

These five Expression plasmids were used to transform protoplasts of the *B. cinerea* wild type strain B05.10 using the method described in section 16.2 of Materials and Methods. Those colonies that emerged with more vigorous growth on the plates were individually replicated on plates with selective medium and monosporic cultures were obtained from these primary transformants to guarantee their homokaryosis. These candidates were named with the name of the gene whose fusion they contained, followed by a number indicative of the primary transformant, and by the letter '*m*' with a second number indicative of the monosporic culture (for example CDC25_1_m1). Then, an analysis of these was carried out to verify the correct integration of the plasmid in the fungal genome. This analysis consisted of three steps and included at least two monosporic cultures from two different primary transformants.

For the first stage, the candidate transformants were inoculated in liquid medium and the mycelium obtained was used to extract genomic DNA as detailed in section 10.1 of Materials and Methods. This DNA served as a template for PCR reactions in which two fragments were amplified, which, taken together, spanned each complete translational fusion, from the genomic region immediately upstream of the fusion (M13R / GFP_fusión_R primers) to the region immediately downstream (gene_fusión_F / M13F primers) (Figure 30).

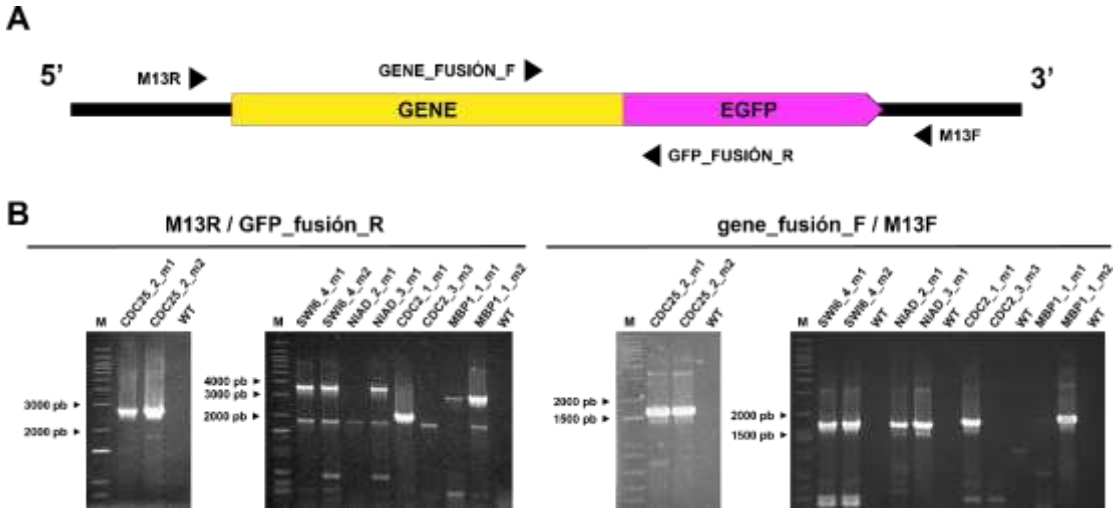

Figure 30. Identification by PCR of *B. cinerea* transformants with the plasmids pFAEX-CDC25, pFAEX-CDC2, pFAEX-SWI6, pFAEX-MBP1 and pFAEX-NIAD. (A). Generic schematic representation of the translational fusion of the GFP ORF (EGFP) with the ORF of CDC25, CDC2, SWI6, MBP1 and NIAD (GENE) (not drawn to scale). The annealing positions of the oligos used in the PCR analysis of the candidate transformants are indicated. (B) Products amplified in the diagnostic PCR reactions carried out using genomic DNA of the candidate transformants as template and the pairs of oligonucleotides M13R / GFP_fusión_R and gene_fusión_F / M13F amplifying fragments. Sizes are: 2653 pb, 3524 pb, 3534 pb, 2032 pb and 3082 pb with the pair M13R / GFP_fusión_R for pFAEX-CDC25, pFAEX-SWI6, pFAEX-NIAD, pFAEX-CDC2 and pFAEX-MBP1, respectively and of 1604 pb, 1600 pb, 1600 pb, 1720 pb and 1832 pb with the pair gene_fusión_F / M13F for pFAEX-CDC25, pFAEX-SWI6, pFAEX-NIAD, pFAEX-CDC2 and pFAEX-MBP1, respectively. M – Marker 1 Kb Plus DNA Ladder, Invitrogen. WT – PCR reaction used as negative control in which B05.10 strain genomic DNA was used as substrate, respectively. The names on each lane identify the different transformants analysed (see text).

The results obtained in the PCR reactions were heterogeneous, finding monosporic transformants in which only the amplification of one or another fragment was observed and monosporic transformants in which the entire translational fusion could be amplified. The monosporics transformants

analysed by PCR were also analysed by Southern blot hybridization. This second technique is more reliable and accurate and was used to try to corroborate the results of the previous stage. Following the procedure described in section 18.2 of Materials and Methods, the genomic DNA of the selected transformants together with the genomic DNA of the wild-type strain B05.10, included as a negative control, was digested with different restriction enzymes. Enzymes were used that cut only once in the Expression plasmid and that their restriction target was not found within the ORF of the gene of interest, the GFP ORF or the hygromycin resistance cassette. Furthermore, their cleavage frequencies in the genomic neighbourhood of the wild allele had to be high enough so that the fragments released from their digestions were of adequate sizes and easy to differentiate by electrophore sis (4-8 Kb). According to these requirements, the genomic DNA of the transformants carrying the CDC25 -GFP translational fusion was digested with *BamH*I, that of the carriers of the CDC2-GFP translational fusion with *Nco*I and that of the carriers of the rest of the fusions with *Sac*I. The digested genomic DNA samples were separated by agarose gel electrophoresis and transferred to a nylon filter. Hybridizations were carried out on this with a probe generated from the structural region of the hygromycin resistance cassette (Figure 31).

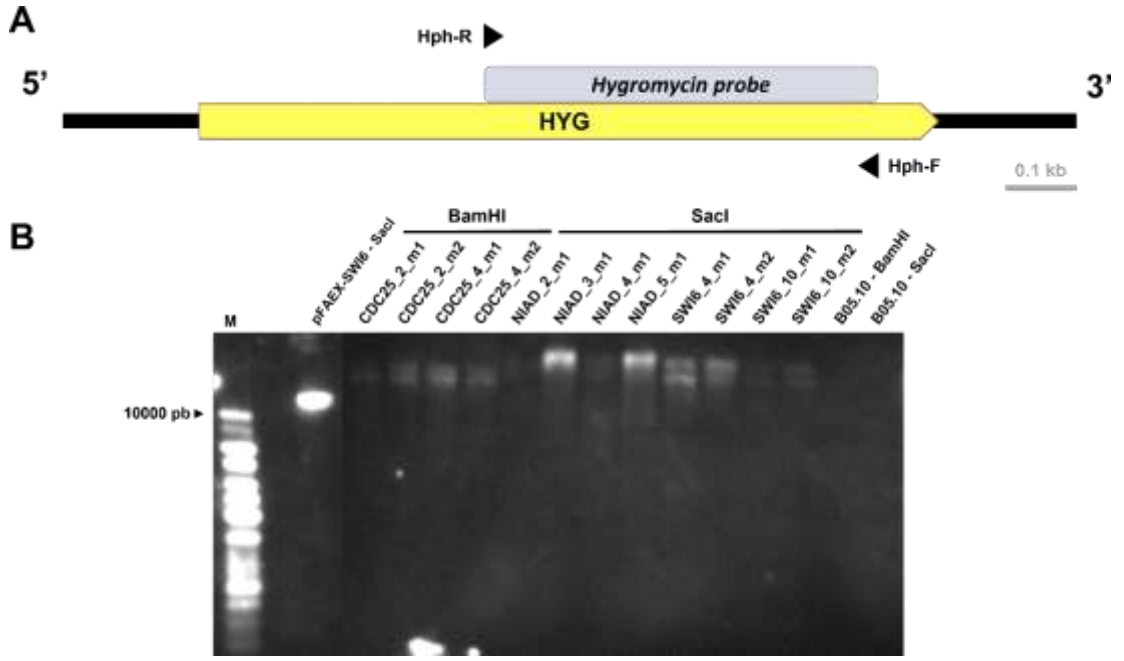

Figure 31. Analysis by Southern blot of *B. cinerea* transformants with the plasmids pFAEX-CDC25, pFAEX-SWI6 and pFAEX-NIAD. (A) Schematic representation of the structural region of the hygromycin resistance cassette from pFPL-Gh and the probe designed on it for Southern blot analysis. The annealing positions of the oligos used for the probe design (Hph-F / Hph-R) are indicated. (B) Hybridization of a membrane during verification by Southern blot analysis of the presence of *cdc*25::*gfp*, *swi*6::*gfp*, *niad*::*gfp*, *cdc*2::*gfp* and *mbp*1::*gfp* fusions in the genomic DNA of candidate transformants. Genomic DNA samples were digested with the indicated restriction enzymes, separated by agarose gel electrophoresis, and transferred to a nylon filter. Hybridization was carried out with the Hph-F / Hph-R probe indicated in A. Genomic DNA of the wild strain B05.10 and plasmid DNA of pFAEX-SWI6 were used as a negative control and positive control, respectively. The results are discussed in the text. The names on each lane identify the different analysed transformants (see text). M – Marker 1 kb DNA ladder, Biotools.

Figure 31 shows an image obtained during Southern blot analysis of the transformants carrying the translational fusions. The lanes belonging to the four transformers carrying the *cdc*25::*gfp* fusion

(CDC25_2_m1, CDC25_2_m2, CDC25_4_m1 and CDC25_4_m2) and the four carriers of the *swi*6::*gfp* fusion (SWI6_4_m1, SWI6_4_m2, SWI6_10_m1 and SWI6_m2) show two hybridization bands. The presence of these two bands, both greater than 10 kb (size of the largest band on the marker ladder), could fit two possible scenarios. In the first one, the genomic DNA of these transformants would have been partially digested so that the largest band would be undigested genomic DNA. The smallest band would correspond to at least one integration event of a copy of the vector. In the second scenario, the genomic DNA would have been completely digested and the two bands would correspond to plasmid integration events at different places in the genome. The uneven intensity of the bands, the intensity of the upper band being greater, in the case of the SWI6_4_m2 transformant, would support the occurrence of the first scenario in this transformant. On the other hand, in the case of the four transformants that carry the *niaD*::*gfp* fusion, there are lanes in which a single band is observed (NIAD_3_m1 and NIAD_5_m1) and lanes in which two are observed (NIAD_2_m1 and NIAD_4_m1). Be that as it may, this analysis confirms the presence of the hygromycin resistance cassette in the genome of the analysed transformants and additional hybridizations, using probes designed on the structural and flanking regionsof the genes of interest, would allow confirming or ruling out its location in the region of the homologous *locus*.

These results taken into consideration together with those obtained in the initial phase of PCR analysis point in the same direction, the correct integration into the fungal genome of at least one intact copy of the Expression plasmid for each translational fusion. However, they do not allow a clear answer regarding the characterization of the genotype of these transformants in relation to the number of integrated copies of each fusion. This aspect was assessed in the next stage of the analysis, in which the genomic DNA of the candidates was analysed by qPCR.

In the qPCR analysis, as described in section 17.3 of Materials and Methods, genomic DNA from the wild-type strain B05.10 was used as a template together with that of the candidate transformants carrying the different translational fusions. The DNA samples were obtained from mycelium grown under the usual conditions (see section 2.2 of Materials and Methods) using the extraction protocol described in section 10.1 of Materials and Methods. The reactions were carried out in triplicate, using, on the one hand, pairs of primers capable of amplifying a fragment of the coding region of each gene of interest (CDC25_silvestre_F/CDC25_silvestre_R, NR_silvestre_F/NR_silvestre_R, CC_SWI6_QR/CC_SWI6_QF, CC_CDC2_QF/CC_CDC2_QR y CC_MBP1_QF/CC_MBP1_QR) (Table 8. Appendix) and, on the other, a pair of primers of the coding region of the actin coding gene, *BcactA* (BactA-62F / BactA-131R) (Table 8. Appendix), used as an endogenous control (Figure 32).

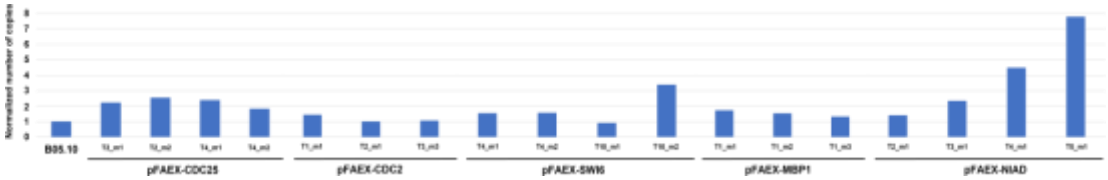

Figure 32. Copy number of the plasmids pFAEX-CDC25, pFAEX-CDC2, pFAEX-SWI6, pFAEX-MBP1 and pFAEX-NIAD in *B. cinerea* transformants analysed by qPCR. Histograms representing the number of copies of each fusion. Genomic DNA was extracted from 4 days-old mycelium of the different transformants incubated in liquid synthetic medium with shaking at 22°C, and qPCR was performed in triplicate. The bar of B05.10 represents the number of copies of *cdc25* gene in the wild type genome, a single copy gene. Fusion alleles copy number was determined using an adapted version of the method described in Hoebeeck *et al.* (2007), whereby the copy number of the fusion allele, previously referenced to that of the native allele, was normalized to the copy number of the single copy gene *Bcact*A, also previously referenced in a manner equivalent to that used with the fusion alleles (see epigraph 17.3 of the Materials and Methods section).

The integrated copy number of the corresponding translational fusion was not uniform among the evaluated transformants. Thus, the four transformants carrying the CDC25 -GFP fusion (CDC25_2_m1, CDC25_2_m2, CDC25_4_m1 and CDC25_4_m2) presented a normalized copy number value of 2.23, 2.54, 2.39 and 1.83, respectively. In the case of the monosporic transformants CDC2_1_m1, CDC2_2_m1 and CDC2_3_m3, the value obtained was lower and close to 1 (1.43, 1 and 1, respectively). A similar result was obtained in the case of the candidates carrying the MBP1-GFP fusion, where MBP1_1_m1, MBP1_1_m2 and MBP1_1_m3 presented values of 1.72, 1.53 and 1.31, respectively. Heterogeneity was greater in the case of the SWI6-GFP and NIAD-GFP fusions. The candidates SWI6_4_m1, SWI6_4_m2 and SWI6_10_m1 presented values of 1.53, 1.56 and 0.9, respectively, but the value of SWI6_10_m2 was 3.38. For their part, NIAD_2_m1, NIAD_3_m1, NIAD_4_m1 and NIAD_5_m1 showed values of 1.40, 2.33, 4.48 and 7.79, respectively.

With the method of Hoebeeck *et al.* (2007) (see section 17.3 of Materials and Methods) used to calculate the number of integrated copies of each fusion, a normalized copy number of 1 is expected for the strain B05.10 and a value of 2 for those candidate transformants containing, in addition to the native copy, a single copy of the corresponding fusion allele. The results obtained for some candidates, such as the transformants CDC25_4_m1 and NIAD_3_m1, fit this behaviour. However, some others present values greater than 2 (SWI6_10_m2 and NIAD_5_m1), indicative of multiple integration events, or less than 2 (CDC2_2_m1 and MBP1_1_m3), attributed to possible technical handling errors.

In any case, this three-phase analysis applied to the candidates bearing the different translationa l fusions has proven the presence of at least one complete copy of each expression vector in the corresponding transformants. This, together with the absence of obvious developmental alterations observed during their routine management (data not shown), allowed the selection of a group of candidates, all of them considered as true transformers and with a single copy of the corresponding fusion construction, for use in the next stage of their study as potential targets of NO.

3.3 Extraction and purification of fusion proteins

The strategy initially designed to assess the levels of S-nitrosylation and/or nitration of the different proteins under study by the action of NO, contemplated, in the first place, the collection of mycelia from the different transformants incubated during the germination window of the fungus in the presence or absence of the NO DETA donor. The use of this incubation time involved the cultivation of the fungus, in liquid medium and under the standard conditions (see section 2.2 of Materials and Methods), for 6 hours in the absence of the donor, in the case of the reference condition, or during 5 hours without NO plus one sixth hour of exposure to the donor, in the case of the experimental condition. These were the conditions in which changes in the expression of the cell cycle regulatory genes of interest had previously been detected (Daniela Santander, Doctoral Thesis. University of Salamanca). From these materials, the extraction of the protein fraction would be carried out and, by means of Western blot analysis with anti-GFP antibodies, the fusion protein produced in each transformant would be detected and quantified under the two established conditions. Finally, the level of S-nitrosylation and/or nitration of the fusion proteins would be evaluated. For the detection of the first type of post-translational modification, a system based on the biotin switch assay technique would be used, while for the determination of the occurrence or not of nitration of the proteins, Western Blot techniques would be used in hybridizations carried out with antibodies anti-nitrotyrosine.

To carry out this approach, mycelium samples were collected from the selected transformants after their incubation under the indicated conditions. The protein fractions were extracted from these samples according to the protocol described in sections 11.1 and 11.2 of Materials and Methods and were subjected to an analysis using the Bradford method (see section 11.3 of Materials and Methods) to quantify the amount of protein obtained. Once their concentrations were determined, a sample of the extract containing between 5 µg and 10 µg of protein was resolved in acrylamide gels by SDS-PAGE under denaturing conditions (see section 14.3 of Materials and Methods) and transferred to PVDF membranes by Western blot. The evolution of the process and the results obtained in the successive steps were satisfactory. However, it was not possible to identify any of the fusion proteins by their detection with anti-GFP antibodies (Figure 33A). Instead, the appearance of multiple bands of different sizes was observed, among which a ubiquitous band of between 50 and 75 kD was observed in all the samples analysed and whose nature could not be determined.

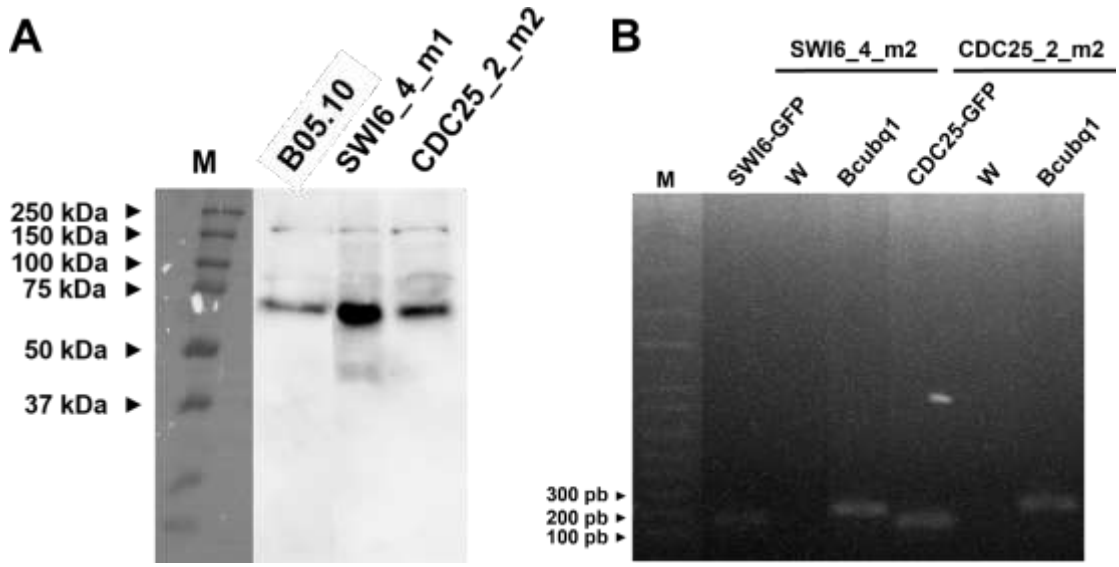

Figure 33. Protein detection by Western blot and level of transcriptional expression by semiquantitative PCR of *cdc*25::*gfp* and *swi*6::*gfp* in *B. cinerea* transformants carrying pFAEX-CDC25 or pFAEX-SWI6. (A) Mutant and wild strains of *B. cinerea* were cultivated in liquid synthetic medium with shaking for 6 hours at 22°C. Cultures were harvested and the total protein was extracted and analysed by Western blot using anti-GFP antibodies for detection of *cdc*25::*gfp* (88.888 kDa) and *swi*6::*gfp* (123.307 kDa). The protein extract of B05.10 was used as a negative control. The names on each lane identify the different strains analysed. M – Precision Plus Protein™ Dual Color Standards, Bio-Rad. (B) Mutant and wild type strains of *B. cinerea* were cultivated in liquid synthetic medium with shaking for 6 hours at 22°C. RNA was extracted from the harvested mycelium and used to synthesize cDNA. This was employed as a substrate in PCR reactions with the CDC25_fusión_F / GFP_fusión_R and SWI6_fusión_F / GFP_fusión_R oligonucleotide pairs to amplify a fragment from the fusion zone of *cdc*25::*gfp* and *swi*6::*gfp*, respectively, and the pair OBcubq1-F / OBcubq1-R to amplify a fragment of the structural region of the constitutive expression gene *Bcubq*1, used as a reference. The names on each lane identify the genetic origin of the amplified fragment. W – PCR reaction used as negative control in which Milli-Q water was used as substrate. M – Marker 1 Kb Plus DNA Ladder, Invitrogen.

The amounts of mycelium obtained from the cultures incubated for 6 hours (see section 11.1 of Materials and Methods) rarely exceeded the amount of 100 mg of sample, even gathering the mycelium from several flasks. Furthermore, the protein concentration determined by the Bradford technique was around 0.2 µg/µL for the extracts of all transformants. These data reporting relatively low yields led to the consideration that the accumulation of gene products was insufficient to allow detection of these on Western blot membranes. Therefore, samples of protein extracts from mycelium cultivated for 20 hours were used. The protein fraction derived from these older cultures should contain higher concentrations of the proteins of interest from larger amounts of mycelium (~ 200 mg).

At the same time, numerous attempts were made to purify the fusion proteins from the total protein extracts using GFP-Trap® technology (Chromotek) based on immunoprecipitation reactions (see section 11.2 of Materials and Methods). In this way, it was hoped to be able to isolate and concentrate the proteins of interest, obtaining a sample enriched in them that would make it possible to reach the concentration necessary for their detection during the development phase by immunodetection. However, neither the use of the samples from the 20 -hour incubation cultures nor the samples purified with the agarose beads facilitated the detection and visualization of the fusion proteins (not shown).

Another aspect that was taken into consideration was the expression profile of the genes under study. Specifically, the expression of the fusion proteins encoded by the *cdc*25 and *swi*6 genes with the

gfp gene was analysed, since the CDC25 and SWI6 proteins were among those that showed the most plausible S-nitrosylation and/or nitration modification sites *in silico* on their respective primary sequences (Table 3). This analysis was carried out by means of semi-quantitative conventional PCR using as substrate cDNA obtained from RNA samples from mycelium of the transformants CDC25_2_m2 and SWI6_4_m2 grown in liquid medium for 6 hours under the usual growth conditions (see sections 2.2, 10.3, 17.1 and 17.2 of Materials and Methods). In these PCR reactions, fragments comprising the region of the translational fusion of each transformant and a fragment of the structural region of a constitutive expression gene were amplified. Following the indications of section 17.1 of Materials and Methods, primers that attach in the flanking areas of one (CDC25_fusión_F / GFP_fusión_R) and another fusion (SWI6_fusión_F / GFP_fusión_R) and primers that attach in the ORF of the gene encoding ubiquitin (OBcubq1-F / OBcubq1-R) were used (Table 8. Appendix).

After comparing the intensity of the fluorescence emitted by the bands of the agarose gels corresponding to both fragments, it was determined that the expression level of the *cdc*25::*gfp* fusion was comparable to that of the *Bcubq*1 gene, while the expression level of *swi*6::*gfp* was found to be several times lower than that of the endogenous gene (Figure 33B). Consideration of these results does not justify the absence of the bands corresponding to the fusion proteins during the hybridization of the Western blot membranes, even in the case of the *swi*6::*gfp* fusion whose expression was low. Furthermore, it is known that, during the course of growth and development of the fungus, fungal cells are in a process of continuous and non-synchronous division, nuclei being found in all stages of the division cycle at any time of growth. Both considerations would support the presence of the fusion proteins in the protein extracts used at levels that would guarantee their susceptibility to be detected by the methods used in this work.

Discussion

1. Pharmacological analysis of strains B05.10 and *ΔBcfhg*1

The objective of this chapter of the work was to determine the effect of nitric oxide on germination and associated processes of *B. cinerea*. To do this, dormant and germinating spores of the wild-type strain B05.10 and of the mutant strain *ΔBcfhg*1 were incubated in the presence of different drugs that modulate NO levels and their effect on the germination rate, the elongation of the germ tube and the nuclear division was examined. The data obtained in these tests determined that the germination of the fungus in our experimental conditions is a non-synchronous process. In the absence of drugs, a small fraction of the conidia of both strains have already begun germination at 2 hpi. This fraction increases in a manner similar to sigmoidal growth over the next eight hours, with practically all the spores having germinated at 8 hpi. Germ tube elongation and nuclear division turned out to be, as might be expected, germination-dependent processes. In our trials, germination was accompanied by a conidia germ tube elongation rate that increased in a manner reminiscent of a linear increase and by an increase

similar to exponential in the number of nuclei. Leroch *et al*. (2013) obtained similar results of non-synchronous germination, germ tube elongation and nuclear division in conidia of *B. cinerea* incubated on different surfaces and growth media. However, for all the conditions they evaluated, the germination kinetics were always faster compared to our results. On the other hand, other authors have reported synchronous germination kinetics, such as Kokkelink *et al*. (2011), working with a strain of the fungus whose nuclei expressed GFP, or kinetics that were more delayed than ours, such as Robles-Kelly *et al*. (2017). Given that, in all the cases mentioned, the same strain as in this work was used, the wild-type strain B05.10, or derivatives, an explanation for this discrepancy between the observed kinetics could be related to the material of the different surfaces used and media supplements.

The germination dynamics of the fungus was altered by the variation of NO levels in a manner dependent on the flavohemoglobin enzyme BCFHG1. In the case of the wild-type strain, B05.10, an increase in the concentration of NO in the incubation medium caused a delay in its germination, while the effect was the opposite when the concentration of the gas decreased, either due to sequestration of the exogenous and/or endogenous NO or by inhibition of the internal production of the molecule. The delay effect proposition was made based on the observation that from 8 hpi in the presence of DETA, all the wild-type spores had germinated. In this series of experiments, the organic compound DETA was used as an exogenous NO donor, an amine selected because it releases NO at an almost constant level during the period of time considered in this work (Fitzhugh and Keefer, 2000; Juan Luis Turrión Gómez. Doctoral Thesis. University of Salamanca). Therefore, the germination results observed at 8-10 hpi prove that wild- type conidia germinate in the presence of the donor due to their ability to overcome the effects imposed by NO and not to a decrease in donor performance in NO release. The germination delay was accompanied by a parallel delay in the germ tube elongation and nuclear division processes. This parallelism observed in the effect of NO on these processes is expected. As germ tube elongation and nuclear division rates are not constant and increase with time, as demonstrated, if exposure to NO determines a delay in germination, also the length of the germ tubes and the number of nuclei will be, on average, smaller when the measurements and countings are made at a given time point. In principle, these effects were not dependent on the growth phase or morphotype in which the conidia were found during germination. The same delay effect on the three morphogenetic processes evaluated (germination, elongation of the germ tube and nuclear division) was observed when the donor was added to the spores both in dormant state and those in full germination. However, dormant spores required more time to respond to NO and return to normal development than germinating spores, in which the effects of the molecule were visible for less time.

The effect of NO on the mutant strain *ΔBcfhg*1 was more intense than in the wild-type strain, determining what we called a “freezing effect” of the germination process due to an increase in its environmental concentration. However, the decrease in the levels of NO of exogenous and/or endogenous origin restored or accelerated its germination capacity in a manner equivalent to what happened with the reference strain. In this case, the premise of a germination blocking effect was based

on the fact that practically all the spores remained ungerminated after 10 hours of incubation in the presence of the donor. This observation confirmed the constant kinetics of NO release by the donor and the inability of the mutant spores to deal with the effects derived from an increase in the concentration of the molecule. This long-lasting blocking effect also affected germ tube elongation and nuclear division to the same extent and was independent of the growth phase in which the spores were found when DETA was added to the culture medium.

This same regulatory effect of germination by nitric oxide had already been descr ibed previously in other organisms, such as in various plant species, with which a pharmacological approach was used, as in this study. Thus, in *Lilium longiflorum* and *Arabidopsis thaliana*, a NO donor negatively regulated the growth rate of the pollen tube, and this response was abrogated in the presence of the CPTIO (Prado *et al*., 2004; Prado *et al*., 2008). In *Camellia sinensis*, the NO donor DEA NONOate inhibited pollen germination and pollen tube growth in a dose-dependent manner, while cPTIO and L-NNA partially reversed these effects (Wang *et al*., 2012). Also, in fungal species such as *Colletotrichum coccodes* it has been described that the treatment of their spores with SNP (sodium nitroprusside), a NO donor, significantly inhibited their germination and development. This effect was counteracted by the NOS inhibitors L-NNA and L-NMMA that even accelerated germination and development compared to the control situation (Wang and Higgins, 2005). These authors performed preliminary trials to determine the appropriate donor working concentration. They looked for an adequate concentration that would delay the germination of *C. coccodes* rather than inhibit it completely. These tests suggested, similar to our results, that the effect of exogenous NO is concentration dependent, such that at concentrations of 1 mM or 500 µM no germination was observed, while at a concentration of 100 µM of SNP the germination of the fungus was merely delayed.

However, a different regulatory effect of the molecule and contrary to that shown in this work is also known on the early development of the pollen grain and spores. Wang *et al*. (2009b) revealed that an exogenous NO donor stimulated the growth of the *Pinus bungeana* pollen tube in a dose-dependent manner and Samalova *et al*. (2013) indicated that the NO scavenger PTIO caused a delay in the germination of the spores of the hemibiotrophic ascomycete *M. oryzae.* For their part, Yin *et al*. (2016) also determined a regulatory function of NO in the germination of urediniospores of *Puccinia striiformis* Westend f. sp. *tritici* and in the elongation of their germ tubes, where both the scavenger cPTIO and a precursor of the oxidative pathway of NO synthesis mediated by an NOS enzyme (the amino acid L- arginine) delayed germination and decreased the length of the germ tube of this type of spores. In addition, they deduced that NO should act together with ROS (reactive oxygen species) maintaining an optimal proportion with them in these development processes.

Our study, together with the previous ones, would confirm a general role of NO in regulating development processes related to germination in fungi. Similar responses are described in different fungal species but also different, even opposing, effects have been reported in related fungal species. These observations may seem contradictory, but they point to NO as a versatile regulator of germination and

early spore development. It is likely that this role is conserved given the importance that these physiological processes have in the life cycle of fungi (Baltussen *et al*., 2019). It is tempting to speculate that the components of the molecular systems mediating the regulatory function of NO in growth and development are conserved even in distantly related taxonomic groups, given the parallelism observed in the responses of some fungal and plant species.

During the analysis carried out to determine the sensitivity threshold to NO of the strains used in this work we found what can be considered a "biphasic response" to NO. This was characterized by a first response in which a strong repressive effect on germination and elongation of the germ tube is determined by very low DETA concentrations (7.5 µM), an effect markedly reduced at intermediate concentrations (between 15 – 62.5 µM). And then a second response which needs concentrations of NO donor around 125 µM to determine the same repression level observed during the first phase and that was dose-dependent up to the 500 µM concentration evaluated. This is a striking observation. It is known of the existence of biological processes in fungi related to the response to external stimuli such as light that are regulated by the intensity of the stimulus. This is the case of the phototropic response in *Phycomyces blakesleeanus*, from whose study, and taking into account the different responses to different light intensities, the proposition of the existence of two different photosystems was derived (Galland and Lipson, 1987). The idea of the germination process of the *B. cinerea* being regulated by processes dependent on the intensity of a stimulus would allow us to properly explain the biphasic response presented by wild-type conidia against the donor, considering that, in our case, the external stimulus is the NO released into the culture medium by DETA.

2. Evaluation of the regulatory effect of NO on the cell cycle in *B. cinerea* by post-translational modifications of regulatory proteins.

Another aspect that was of interest in our study was the speed with which the molecule exerted its effect on the development of the fungus. It had only been two hours since the addition of the donor when the effects of NO on the spores of both strains, in the two morphotypes evaluated, were visible. Such a rapid, immediate response must be mediated by a reduced number of elements or factors that participate in a reduced number of stages. It is even possible to propose the possible occurrence of a direct effect on the factors that control the germination process.

Being an easily diffused radical, NO has the ability to react with a variety of intracellular and extracellular targets and can act as an activator or inhibitor of enzymes, ion channels or transcription factors, thus regulating specific processes (Lindermayr *et al*., 2005). The reaction of NO with sulfhydryl groups and transition metals can cause the alteration of the activity of a protein (Stamler, 1994; Zhao *et al*., 2020). These processes are reversible and the resulting products in both cases, S-nitrosothiols and metallic nitrosyls, have intrinsic reactivities that allow their local action.

In *A. thaliana*, most of the modifications that NO makes on proteins appear to be regulated by S-nitrosylation of a single critical cysteine residue, which occurs by an oxygen-dependent chemical reaction or by transfer of NO from a nitrosothiol group to a sulfhydryl group on the protein (transnitrosylation).

Due to reactivity with intracellular reducing agents, for example, ascorbic acid or glutathione (GSH) and with reduced metal ions, such as Cu^{+}, nitrosothiols are exceptionally labile. This instability translates into half-lives ranging from seconds to a few minutes and therefore provides a very sensitive mechanism for the regulation of cellular processes (Lindermayr *et al.*, 2005).

Since the knowledge about the molecular processes in which NO participates in fungi is not yet sufficiently developed, it is risky to propose the adoption of NO signalling systems in plant developme nt for fungi. However, the NO regulatory activity in *A. thaliana* that we have just briefly described is highly conserved in living beings, so it can be considered that all this information referring to a model organism constitutes a useful basis for the study of the effect of NO in other organisms, in this specific case, in *B. cinerea*.

We can reason that, in the wild-type conidia of our system, once the donor has been added, the NO initiates the modification by S-nitrosylation of some important protein/s in the germination process, determining a loss of efficiency in its function, which can determine, in turn, the effect of delayed early development observed 2 hours later. S-nitrosylation, based on certainly labile bonds that depend on the redox state of the cellular environment, can be easily reversed spontaneously, at least partially, and in short periods of time, in particular in the presence of a very efficient NO elimination system, as is the case of flavohemoglobin BCFHG1, which maintains the redox state of the cell within limits compatible with proper cell function. This approach would allow to explain the recovery of the development parameters detected 8 hours and 4 hours after the addition of exogenous NO in the dormant and germinating spores of this strain, respectively.

This proposition also allows to satisfactorily explain the behaviour of the mutant strain *ΔBcfhg*1 for the same conditions. In this case, it is a mutant strain that is defective in the gene encoding the BCFHG1 enzyme, so it does not have that NO detoxification mechanism. When the spores of this strain come into contact with exogenous NO, whether or not the germination program has been triggered, the same situation described in the case of the reference strain is established: NO causes the modification of proteins involved in the germination process, which momentarily paralyzes this process. However, and unlike what happened with the B05.10 strain, now the levels of NO inside the cell are very high, since there is a constant supply of NO but there is no detoxification system for it. This determines a state of nitrosative stress within the cell that prevents the initially established S-nitrosylation modifications from being reversed. In addition, the constant supply of NO probably determine s that, if these were spontaneously reversed, they would re-establish immediately. The net effect would be a permanent modification of these proteins that lose their activity while NO levels remain high. In this way, the germination of the spores would enter a state of paralysis, being blocked.

The proposition to this mode of action of NO in the regulation of development based on post-translational modifications of proteins by S-nitrosylation is supported by the results derived from an analysis of a microarray experiment carried out in our research group in the past (Daniela Santander, Doctoral Thesis. University of Salamanca). The results of this analysis, made on gene expression profiling in response to NO in spores of B05.10 and *ΔBcfhg*1 strains and mentioned previously in this work, showed a potential action of NO on specific proteins of the cell cycle, among which are found some key regulators for the advancement of this process (the orthologs of the *mcm* (2-7) genes of *S. cerevisiae* and of *cdc*25 of *S. pombe*).

In order to validate our hypothesis about the mode of action of NO in the cell cycle, a series of transformants were obtained carrying fusion proteins between GFP and a group of proteins selected on the basis of their relevance in the regulation of the cell cycle and their potential susceptibility to being S-nitrosylated and/or nitrated. The protein extracts of these transformants were subjected to analysis using Western blot and immunodetection techniques, which unfortunately did not allow the dete ction of any of the fusion proteins of interest. Instead, the appearance of multiple bands was observed during the detection phase on the membranes. One of them, around 70 kDa, was present in all the samples analysed, which could suggest the presence in *B. cinerea* of a protein with an abundance in the cell equivalent to that of Rubisco in plants. The high concentration of this plant enzyme makes it difficult to detect low abundant proteins. Our fusion proteins could be found among the latter since their constructions conserve their respective endogenous promoter.

On the other hand, the presence of multiple bands of different sizes may be the result of fusion protein processing by the cellular machinery as a consequence of the presence of one or more extra copies of the genes of interest in the fungal genome. Gene silencing mechanisms capable of detecting homologous and repeated DNA sequences, which triggers their inactivation, have been described in fungi (Selker, 1990). An example of a cellular mechanism that could fit these characteristics would be the quelling phenomenon described in *N. crassa* (Romano and Macino, 1992; Cogoni and Macino, 1999). It isa transient mechanism that acts by generating small RNA molecules which target mRNAs to be silenced, causing the silencing of both transgenes and cognate endogenous mRNAs (Fulci and Macino, 2007). That said, the semiquantitative PCR analysis showed that the *cdc*25::*gfp* and *swi*6::*gfp* gene constructs were expressed at acceptable levels, therefore, if a gene silencing phenomenon took place, it would involve a mechanism that acts at the post-translational level, at least in the case of these two proteins. Whatever the reason for the inability to detect these proteins, further analysis would be necessary to find it out.

3. Differential gene expression analysis in response to NO exposure.

Our desire to learn more about the mechanisms by which NO negatively regulates the germination process in *B. cinerea* and how the presence or absence of the main NO detoxifying system of the fungus, the flavohemoglobin enzyme BCFHG1, influences the process, led us to the performance of a comparative transcriptomic study using RNAseq. This study allowed us to compare the spore gene expression profiles of the B05.10 and *ΔBcfhg*1 strains under conditions of exposure to NO once their

germination program had been triggered. Specifically, the conidia of both strains were kept in incubation for four hours and then exposed or not to the NO DETA donor for two more hours. During this two-hour period, the donor continuously releases nitric oxide into the culture medium. This is capable of crossing the cell wall of the spores by means of a passive capillary transport and accumulate in the intracellular space until reaching concentrations such that they impose an oxidative and nitrosative stress in the cellular environment (Schinko *et al.*, 2010).

3.1 Comparative 2 vs. 3 (germinating spores of B05.10 in NO exposed with non-exposed conditions).

In the case of wild-type conidia, the results of the transcriptomics study were a not so clear reflection of this situation. The induction of genes that are related to the generation of this type of stress was observed. This is the case of Bcin13g05380, Bcin07g02980 and Bcin07g00560, whose gene products carry the domain NADH:flavin oxidoreductase / NADH oxidase (PF00724), associated with the generationof ROS (Schumacher *et al*., 2014). But, at the same time, the downregulation of other genes of the same type was observed: Bcin01g00260 and Bcin18g00020, genes that code for proteins with an Aryl-alcohol oxidase vanillyl-alcohol oxidase domain (PF01565, PF02913) and a NADH:flavin oxidoreductase/NADH oxidase, N-terminal domain (PF00724), respectively.

However, at the same time, changes were also detected in the expression of numerous genes involved in the response to oxidative stress (Zhao *et al*., 2020). Thus, the genes Bcin07g02270, Bcin09g02130 and Bcin14g01380 were repressed. The first codes for a putative heat shock protein of the HSP70 family. HSPs are a family of intracellular proteins upregulated by a variety of different stressors playing a role against them (Jolly and Morimoto, 2000; Priya *et al*., 2013). The second encodes a dehydrin-like protein very similar to DPRB and DLPA from *A. nidulans*. The dehydrins are stress-protective proteins in *A. fumigatus* (Wartenberg *et al*., 2012). The third is the *BcAIF* gene, which codes for an AIF-like oxidoreductase 1, an enzyme associated with an alternative respiration pathway (retrograde response) (Schumacher *et al*., 2014). Several oxidoreductase enzymes, responsible for the detoxification of NO radicals or NO-derived reactive nitrogen species, were also differentially expressed: of the eight catalase enzymes annotated in the genome of the fungus, only *Bccat*6 (Bcin05g04580) appeared as DEG being strongly induced, but *Bccat*2 (Bcin11g06450), *Bccat*4 (Bcin05g00730) and *Bccat*8 (Bcin04g02010) showed the same response to a lesser extent. The remaining four, *BccatA* (Bcin06g01180), *Bccat*3 (Bcin06g04520), *Bccat*5 (Bcin03g01920) and *Bccat*7 (Bcin09g04400) decreased their expression. The nitrilase Bcin12g06180 was also significantly induced, while the other three, Bcin05g04960, Bcin02g03010 and Bcin14g00790, present in the genome, also increased its expression, especially Bcin05g04960. None of the 33 genes identified as encoding glutathione S-transferase enzymes and/or carriers of the Glutathione S-transferase domain (PR01266) were differentially expressed in wild-type spores according to our selection parameters. However, their behaviour was equally interesting. In fact, 17 of them increased their expression when these spores were exposed to exogenous NO, especially *Bcgst*1 (Bcin10g00740), *Bcgst*3 (Bcin11g00390), *Bcgst*5 (Bcin14g03160), *Bcgst*15 (Bcin14g03990) and Bcin15g00060. Meanwhile,

the expression of the rest decreased to one degree or another. The peroxidase *Bcprd*1 (Bcin13g05720) was also repressed and the genes Bcin08g04600, which encodes a protein with a DSBA -like thioredoxin domain (PF01323), Bcin04g06240, a monooxygenase nitronate that catalyses the oxidative denitrification of nitroalkanes (nitrated lipids) with the consequent generation of nitrate and nitrite (Marroquin -Guzman*et al*., 2017; Zhao *et al*., 2020) and the flavohemoglobin enzyme BCFHG1 (Bcin04g06230), were induced. The latter was one of the genes related to ROS and RNS detoxification with the highest induction value. This response is understandable given the important NO detoxifying role that the enzyme plays by transforming the molecule into NO_3^- through its dioxygenase function (Hausladen *et al*., 1998; Gardner *et al*., 1998).

It is presumable that the increase in intracellular nitrate concentration, as a result of the activity of this enzyme and other similar mechanisms such as nitronate monooxygenase, provoked the response of genes involved in the nitrate assimilation process, such as nitrate enzymes (*BcniaD*, Bcin07g01270) and nitrite (*BcniiA*, Bcin01g05790) reductases. These two enzymes showed a strong induction response. Two nitrate transporters, *BccrnA* (Bcin01g06290) and Bcin15g00040, the latter putative, showed a similar response. The first was not DEG, although its expression increased with exposure to NO, while the second had an induction response even greater than that presented by *BcniaD* or *BcniiA*. This behaviour is presented to us, in principle, as inexplicable, since the synthesis of nitrate in our system takes place at the intracellular level, mainly from NO as indicated, so it is not necessary to transport it from outside. However, the spontaneous oxidation of NO to NO_2^- has been described as a process that can take place both in the culture medium and inside the fungal cell (Yamasaki, 2000; Schinko *et al*., 2010). The occurrence of this phenomenon in the PDB ½ medium used to cultivate the fungus would allow to explain the induction or increase of the expression of these two transporters, but only if it is assumed that both are not specific nitrate transporters, but also show some susceptibility to nitrite transport, as occurs with transporters of this type in *A. nidulans* (Pfannmüller *et al*., 2017).

Putative regulatory proteins and proteins connected with lipid metabolism (lipases and esterases), all of them previously described as responding to NO_3^- in A. nidulans (Schinko *et al*., 2010), were also identified in our results. Specifically, we detected the induction of genes related to lipase activity (Bcin07g06590) and esterase (Bcin07g00040 and Bcin15g05700), but also the repression of two genes with the latter function (Bcin13g05760 and Bcin15g03320). Regarding regulatory proteins, three proteins with the *nmrA*-like domain (PF05368), Bcin03g00700, Bcin08g04910 and Bcin11g06310, were upregulated, with Bcin11g06310 being the gene with the highest induction value of the comparative sample 2 versus sample 3 (log_2(FC) = 9.9). *NmrA* (nitrogen metabolic regulation A) is a negative transcriptional regulator in various fungi, involved in regulating the activity of the GATA transcription factor *areA* during Nitrogen Catabolite Repression (NCR) (Han *et al*., 2016). NCR is a broad program of transcriptional regulation that allows fungi to use alternative or non-preferential nitrogen sources (nitrate, nitrite, purines, amides, most amino acids, and proteins) when preferential sources are not available or they are present in concentrations low enough to limit growth (ammonia, glutamine, and

glutamate) (Milhomem Cruz-Leite *et al*., 2020). The use of any of these secondary nitrogen sources is regulated at the transcriptional level and almost always requires the synthesis of a set of pathway-specific catabolic enzymes and permeases that are otherwise subject to NCR. Synthesis of the enzymes of a particular catabolic pathway typically requires two distinct positive signals: a global signal indicating nitrogen derepression and a pathway-specific signal indicating the presence of a substrate or an intermediate of that pathway. The first signal is mediated by global trans-acting GATA factors, while the second by pathway-specific regulatory proteins that frequently contain an N-terminal Cys_6/Zn_2 binuclear-cluster DNA binding domain (Marzluf, 1997). In *Aspergillus* spp., a genus where NCR has been well characterized, the nitrate assimilation pathway is composed of genes encoding nitrate reductase, nitrite reductase, a nitrate/nitrite transporter, and a specific nitrite transporter. These four genes are grouped in a cluster such that the sequences of the two reductase enzymes are diverge ntly oriented. A fifth gene, another nitrate/nitrite transporter, is found separated on the same chromosome (Marzluf, 1997; Pfannmüller *et al*., 2017). When the conditions are suitable, that is, low intracellular concentrations of the preferred nitrogen sources (nitrogen-starvation conditions) and the simultaneous presence of nitrate or nitrite as transcriptional inducers, the genes of this pathway are activated through the synergistic action of the general regulator of nitrogen metabolism AREA and the pathway specific regulator NIRA (Schinko *et al*., 2010; Marcos *et al*., 2016). AREA participates in the opening of the chromatin structure at the nitrate assimilation genes *loci*, binds to the bidirectional promoter region between nitrate and nitrite reductases and mediates the promoter binding of NIRA by direct protein–protein interaction (Pfannmüller *et al*., 2017).

In *B. cinerea*, *BcareA* (Bcin09g04960) and *Bcltf*9, *BcnirA* (Bcin08g05570) are the homologues of *areA* and *nirA*, respectively. In our study, these two genes did not appear as DEG in the comparison sample 2 versus sample 3, but their behaviour is interesting. The *areA* gene maintains stable expression levels between the 4-hour samples (Sample 1) and the 6-hour samples without a donor (Sample 2) that increase slightly when the spores were exposed to NO (Sample 3) (log_2(FC) = 0.256). The behaviour of *BcnirA* is different because, although between the 4-hour and 6-hour samples without a donor, its levels increase (log_2(FC) = 1.6), they decrease due to exposure to the molecule (log_2(FC) = -1.73). Taking all this information together, it appears that the spores of the wild-type strain are in a state of NCR after spending 2 hours in the presence of DETA.

The addition of the donor to the culture medium meant the presence of an alternative nitrogen source for the fungus, the nitrate produced from the oxidation of NO by the action of flavohemoglobin . Nitrate must have acted as a transcriptional inducer, favouring the activation of the genes of its assimilation pathway, that is, *BcniaD*, *BcniiA*, *BccrnA* and Bcin15g00040. Next, by the action of nitrate and nitrite reductases, the nitrate was reduced to ammonium, which was incorporated into the cellular amino acid pool via glutamate and glutamine biosynthesis (Schinko *et al*., 2010). Finally, the cell would have detected the repressing nitrogen source (ammonium / glutamine / glutamate) trigger ing the NCR. The first part of this proposition fits with the behaviour observed for nitrate assimilating genes and

flavogemoglobin gene, which were induced or increased their expression as a consequence of exposure to NO. It also fits with the behaviour of *BcnirA* for which the molecule appears to have had a repressive effect. However, the global regulator *areA* does not decrease its expression when *BcnirA* does. The opposite happens, its expression increases, although slightly, in the samples treated with DETA. Furthermore, according to the nitrogen regulation theory, the nitrate assimilation pathway genes should be repressed under NCR conditions. These discrepancies would not be such if one takes into account what happens in other fungal systems. The globally acting nitrogen regulatory protein not only controls nitrogen metabolism, but also exerts control over an important area of cellular metabolism, including many catabolic activities, some related to pathogenesis, as in *M. grisea* (Lau and Hamer, 1996; Marzluf, 1997). This makes it not surprising that *areA* expression levels in *Aspergillus* are fairly constant throughout the entire life cycle of the fungus (Marcos *et al*., 2016). Therefore, in our conditions, in wild-type conidia, it would be expected that *areA* would have been induced when the intracellular accumulation of nitrate reached the levels that triggered the de-repression response, a phenomenon that took place at some point during the two-hour incubation period in the presence of the donor. Later, at the time of harvesting of the samples, at the end of that two-hour period and with the NCR already activated, the expression levels of the global regulatory protein would have decreased to values closer to their baseline levels. The slight increase in its expression in the samples exposed to DETA could be associated with some other of the numerous metabolic processes that it controls and that could be being affected by NO.

On the other hand, in fungi such as *A. nidulans*, *N. crassa* or yeasts of the genus *Pichia*, the nitrate present in the growth medium induced the expression of nitrate assimilation genes (NIAD nitrate reductase, NIIA nitrite reductase and transporter of nitrate NRTA) by positive regulation by AREA and NIRA, while high concentrations of glutamine repressed them (Cove, 1979; Dunn-Coleman *et al*., 1981; Crawford and Arst, 1993; Marzluf, 1997; Siverio, 2002; Pfannmüller *et al*., 2017). The same was observed in *Fusarium fujikuroi*. However, Pfannmüller *et al*. (2017) also observed a partial and not a complete down- regulation of the expression of the *niaD* gene in a *ΔAREA* mutant of this same fungus, which led to the conclusion that while AREA is essential for activation for NIIA and NRTA, it is not for nitrate reductase. This aspect of AREA-independent regulation contrasted with that of *A. nidulans*, where the *areA* homolog was described as an obligate activator of all genes of the nitrate assimilation pathway. This difference in the pattern of nitrogen regulation between the two fungi was attributed to the different location of the genes of this pathway in their genomes. While in *A. nidulans*, four of the five proteins in the pathway (NIAD, NIIA, NRTA and NITA, the specific nitrite transporter) are clustered, in *F. fujikuroi* they are distributed over different chromosomes. This sparse distribution of genes could translate into a less synchronized form of transcriptional regulation compared to the more co-regulated form of *A. nidulans* where the cluster organization could make the rearrangements of histones in that region of the genome more accessible (Marzluf, 1997; Pfannmüller *et al*., 2017). This could be the case of *B. cinerea* where, as in *F. fujikuroi*, the *loci* of *BcniaD*, *BcniiA*, *BccrnA* and Bcin15g00040 are not grouped in a cluster.

Whatever the situation in our study system, it is important to take into account that the germination of the fungus was not synchronous in our experimental conditions. The time the donor exposure began was 4 hpi. At this time point, not all the spores had started the germination process and of those that had, not all were in the same state of development (Figure 21). This meant that each spore, in its particular stage of development and from that moment on, had to deal with a continuous flow of NO. Because the cellular machinery changes throughout the germination process, with different molecular mechanisms prevailing throughout each stage (Baltussen *et al.*, 2019), it is possible that this influenced the way each spore in particular (some still in a state of dormancy while others in full polarized growth) responded to the NO burst. It is conceivable that this lack of synchrony during germination development had a quantitative and not a qualitative effect on the response of the spores to the molecule. The conclusion derived from the analysis of the results of the 2 versus 3 comparison is that all the spores responded in the same way to process NO, using the same routes and not a different one depending on the stage of development in which they were found. However, it seems that the spores did not respond in unison: the cellular machinery of a fraction of them, possibly those in dormancy, responded in a delayed manner, while the machinery of another fraction, probably those already in full germination and with a metabolism fully active, responded more quickly. This assumption would explain the results of our transcriptomic analysis regarding nitrogen metabolism, where, as explained, differential changes in the expression of genes that are not completely compatible appear simultaneously.

Schinko *et al*. (2010) carried out a microarray experiment in *A. nidulans* with the intention of identifying genes that responded to the presence of nitrate in the culture medium (induced conditions), compared to the repression condition in which ammonia had been added to the cultures. The RNA samples used were obtained from cultures induced for only 30 minutes because a previous time series of nitrate induction analysis determined that the later time point samples could contain nitrate assimilation products, such as repressing nitrogen metabolites, which would negatively interfere with the genes of interest. In this previous analysis, they measured intracellular free amino acid levels together with the expression of several genes that report intracellular nitrogen status, among them *areA* and *niiA*, in induction cultures for 3 hours. They observed that the *areA* mRNA reached its peak within 30 minutes. After 40-50 minutes of induction, the highest levels were detected in the *niiA* mRNA, indicating maximum synergistic *nirA*–*areA* activity. This maximum coincided with a minimum in intracellular glutamine concentration. From 50 minutes on, the continuous assimilation of nitrate resulted in an increase in the concentration of glutamine. This increase caused the *areA* mRNA level to drop followed by the same effect on *niiA* mRNA.

Pfannmüller *et al*. (2017) studied the repressive effect of the nitrogen source on the synthesis of two secondary metabolites, gibberellin and bikaverin, in *F. fujikuroi*. They studied the expression of a gene involved in the synthesis of one or another metabolite in cultures of the wild-type strain and of the mutants *ΔNIAD*, *ΔNRTA*, *ΔNIRA*, and *ΔAREA*, all of them incapable of uptake or metabolization of nitrate or nitrite, incubated for 2 hours in the presence of 60 mM glutamine or 60 mM nitrate, after having been

cultured in a medium supplemented with 6 mM glutamine for three days. They observed a delay in the nitrogen-suppressing effect on the expression of the gibberellin synthesis gene in the cultures of the wild- type strain supplemented with nitrate compared to those supplemented with glutamine. This delay, which was at least ninety minutes, was explained as a consequence of the time-consuming conversion of nitrate to glutamine, the true effector of NCR, in cultures supplemented with nitrate. No significant repression of the gene in *ΔNIRA*, *ΔNIAD*, and *ΔNRTA* was observed in the presence of nitrate. The same effect, but to a lesser extent, was observed in the bikaverin synthesis gene. These authors used the same experimental design to analyse the transcriptional regulation of the *nirA*, *niaD* and *nrtA* genes. *nirA* experienced a delay effect in its repression similar to that described for the synthesis of gibberellins and bikaverin. *NirA* expression was not detected in the glutamine-treated samples, while its transcripts were detected at 30 minutes, but were absent at 120 minutes in the nitrate-treated samples. For its part, *nirA* expression was still detected 2 hours after nitrate addition in the *ΔNIAD* and *ΔAREA* mutants. The expression patterns of *niaD* and *nrtA* were very similar to those of the regulator *nirA*. Consistent with these results, the synthesis of *N. crassa* nitrate reductase mRNA is a rapid process, with the mRNA reaching its steady-state level within 15 min, upon induction and derepression (Marzluf, 1997).

Saving the distances between the fungi used in both studies (*Aspergillus*, *Fusarium*, *Neurospora*) and the particularities of the respective experimental designs, these results are applicable to our study system as indicative of the duration and rhythm of the catabolic processes of nitrate and of the different participating agents. All of them point in the same direction, the feasibility that nitrate triggers the changes in nitrogen metabolism already described (derepression, assimilation of nitrate and NCR) during the first 120 minutes of exposure of fungal cells to the induction medium. However, given that in our system we use NO and not nitrate as an inducer, one could speak of a delayed transcriptional state of the *B. cinerea* cells analysed in comparison with those of *A. nidulans* and *F. fujikuroi*. While, in these two fungi, the presence of nitrate directly triggered the activation of its assimilation pathway through *area* and *nirA*,in *B. cinerea*, a prior transformation of NO to nitrate by flavohemoglobin was necessary before that the latter produced the induction response. This NO oxidation process represents an additional stage in the metabolic changes detected in the other species that necessarily delayed the appearance of the succession of responses observed in *B. cinerea*.

The metabolic changes caused by the different nitrogen sources affect the conidiation process through NCR, but it seems that they are not relevant during germination, showing a greater influence on this process the state of cellular carbon (Qazi and Khachatourians, 2008; Steyaert *et al*., 2010; Daryaei *et al*., 2016). Therefore, it seems unlikely that the delayed effect on germination, germ tube elongation, and nuclear division observed in wild-type spores in response to NO could be attributed to them. On the contrary, numerous genes related to asexual development processes had their expression levels modified by the effect of the molecule, and the explanation for the behaviour of B05.10 can be found in them.

In our experimental conditions, approximately eighty percent of the wild-type spores have begun their germination after four hours of incubation in the absence of the donor, the vast majority being in

stage 1 of development (Figure 21). The remaining 20% have not yet germinated and are in the dormant or isotropic growth stage. Two-hour exposure to the donor supposes a delay in the germination of both fractions compared to the control situation. At 6 hpi, more than ninety percent of the conidia have germinated, but the presence of NO causes a good part of them to have been retarded in state 1 (about5 times more conidia in this state than in the situation of reference). In addition, the molecule also causes an increase in the percentage of non-germinated spores. Despite the increase, this percentage is still low, but it represents a doubling of the percentage of this type of spores compared to the non-induction situation. This time delay is manifested at the transcriptional level mainly through the alteration of the natural changes of metabolism and cell wall that occur during the germination process.

After its formation during conidiation, the mature conidium enters a dormant state from which it does not emerge until it is exposed to the appropriate environmental stimuli that promote its germination (Baltussen *et al*., 2021). In *A. fumigatus*, conidia at this stage predominantly present transcripts of genes involved in translation regulatory activity, RNA binding, and phosphorus and alcohol metabolism, being able to detect pyruvate decarboxylase and alcohol dehydrogenase (Lamarre *et al*., 2008; Teutschbein *et al*., 2010). In the case of *A. niger*, transcriptional activity of genes involved in gluconeogenesis, the glyoxylate cycle, GABA shunt and fermentation was found in dormant conidia (Novodvorska *et al*., 2013). Detection of these transcripts during this stage is indicative that fermentation plays a key role during dormancy. The break in dormancy during germination involves the transition from the resting cell to a vegetatively active cell. This process is characterized, among other things, by a change from a fermentative to a respiratory metabolism and by the immediate synthesis of proteins. In the two *Aspergillus* species mentioned, the genes belonging to the fermentative metabolism and oxidoreductase activity are repressed when dormancy is broken, while those related to RNA and phosphorus metabolism, the tricarboxylic acid (TCA) cycle, amino acid and protein synthesis, and protein complex assembly are induced (Lamarre *et al*., 2008; Novodvorska *et al*., 2013; Baltussen *et al*., 2019). In our comparison between the samples of the wild-type strain, we were able to detect several DEGs related to these cellular processes. Thus, Bcin01g11530, Bcin05g08390, Bcin10g01470 and Bcin14g01070 showed an induction response. All of them have an Alcohol dehydrogenase domain at one end of their predicted amino acid sequence (PF00107, PF08240). The same behaviour had Bcin07g00040 and Bcin06g01560. The first is a gene whose protein is very similar to that of AIM6 from *S. cerevisiae*. It is a protein of unknown function, required for respiratory growth and that presents a PLC-like phosphodiesterase domain (IPR017946). This structural domain is present in several phospholipase C (PLC) like phosphodiesterases (Hess *et al*., 2009; Giaever *et al*., 2002). The function of Bcin06g01560 is also not known, but its gene product appears to bea structural protein of the mitochondrial ribosome. For their part, Bcin05g04870, Bcin13g01020 and *Bcgad*1 (Bcin09g05020) showed a repression response. Bcin05g04870 codes for a succinate dehydrogenase/fumarate reductase flavoprotein that participates in the TCA cycle. In contrast, Bcin13g01020 codes for an uncharacterized protein, but highly similar to the mitochondrial carrier protein PET8. PET8 is an S-adenosylmethionine transporter of the mitochondrial inner membrane required for biotin biosynthesis and respiratory growth (el Moualij *et al*., 1997; Marobbio *et al*., 2003). *Bcgad*1 encodes

a glutamate decarboxylase that catalyzes the conversion of glutamate to GABA in the GABA shunt (Novodvorska *et al*., 2013).

The *Aspergillus cipC* gene encodes a conidium surface protein with unknown function. Its name derives from concanamycin-induced protein because its orthologue in *A. nidulans* was shown to be upregulated in response to the antibiotic concanamycin A, produced by *Streptomyces* species (Asif *et al*., 2006). In *A. carbonarius*, its expression was upregulated under the oxidative stress by the presence of hydrogen peroxide and was related not directly to mycotoxin ochratoxin A biosynthesis (Crespo-Sempere *et al*., 2013). Bcin02g00160 showed high similarity with this gene by BLA STP analysis and was downregulated as a consequence of exposure to DETA.

Interestingly, the *abaA* gene (Bcin05g04650), a transcription factor with the TEA/ATTS DNA-binding domain (PF01285), was induced. This protein controls the formation of conidiophore and conidium together with the central regulatory proteins *brlA* and *wetA* in *Aspergillus* and *Fusarium* (Hokyoung *et al*., 2013). Also, a putative calcineurin-dependent (CND) gene (*Bcgas*2/Bcin14g04260) and one cyclophilin-dependent (CPD) gene (*Bccpd*3/Bcin01g01590) were repressed, reporting a possible connection of NO with calcium regulation (Viaud *et al*., 2003).

The break in dormancy is followed by an increase in cell perimeter through isotropic growth. During this stage, the metabolic activities required for cellular growth, such as protein synthesis and carbohydrate metabolism, is maintained, but a predominant remodelling of the fungal cell wall takes place (Baltussen *et al*., 2019). In swelling conidia of *A. fumigatus*, the up-regulation of several cell wall-associated proteins was detected, in comparison with dormant conidia: ß-(1,3)-glucanosyltransferase BGT2 with ß-(1,6)-branching activity, the 1,3-ß-glucanosyltransferases GEL1 and GEL4 involved in the elongation of 1,3-ß-glucan chains, the GDP-mannose pyrophosphorylase SRB1 which catalyses the synthesis of GDP-mannose using mannose and GTP as substrates, and two GPI-anchored cell wall proteins (Suh *et al*., 2012; Baltussen *et al*., 2018). Similarly, in *A. niger*, genes encoding chitin synthases and GPI- anchored glucanosyltransferases increased their expression during isotropic growth (van Leeuwen *et al*., 2013). All these proteins are informative of a cell wall extension process, for which the addition of new material such as chitin is necessary. In our analysis on wild-type spores, we also detected changes in the expression of genes that participate in the swelling of the conidia. Among the DEGs that were induced were: Bcin05g04570, a choline dehydrogenase, whose protein bears a certain resemblance to CODA (putative choline oxidase) of *A. fumigatus* Af293, involved in the metabolism of glycine, serine and threonine and with a possible function in the stabilization of the membrane (Lamarre *et al*., 2008); *Bccda*1 (Bcin03g05710), a chitin deacetylase whose expression depends on the BMP1 MAP kinase cascade (Leroch *et al*., 2013) and several genes whose products are related to the GO terms of chitin binding (GO: 0008061) (Bcin03g05710 and Bcin16g00950) and hydrolase activity, hydrolyzing O-glycosyl compounds (GO: 0004553) (Bcin09g01150 and Bcin13g02320). Bcin02g02000, another gene associated with the term hydrolase activity, hydrolyzing O-glycosyl compounds, showed a repressive response to NO.

The behaviour of some of the previous genes, such as those related to chitin, could also be the manifestation of a part of the transcriptome of those spores that are already in the phase of polarized growth. At this stage, this polysaccharide is part, among others, of the set of compounds and agents that the cell sends to the polarization site to add new material (Baltussen *et al*., 2019). Another such compound is actin. A gene, the aforementioned Bcin07g02270, which codes for a chaperone of the HSP70 family with Actin-like ATPase domain (PS01132) and cell shape-determining protein MREB domain (PTHR42749) was repressed in response to exposure to DETA in wild-type conidia. MREB is a bacterial protein homologous to actin that is required in rod-shaped bacteria for maintenance of cell shape (Nurse and Marians, 2013).

Exposure to NO also influenced the secretome of the fungus where several lytic enzymes had their expression altered and in secondary metabolism, affecting three possible clusters.

Cutinase Bcin13g05760 and aspartic proteinase *Bcap*8 (Bcin12g02040) were repressed. At the same time, Bcin13g02320 was induced. The amino acid sequence encoded by this gene is highly similar to that encoded by the Afu1g04730 gene from *A. fumigatus* Af293. It is a putative endoglucanase that is part of the secretome of the fungus (Adav *et al*., 2013).

The sesquiterpen cyclase *Bcstc*5 (Bcin01g03520) is involved in a cluster of synthesis of unknown sesquiterpenes (Collado and Viaud, 2016) and was induced by NO. However, the genes Bcin10g00010, Bcin10g00020 and Bcin10g00030, constituents of a possible cluster together with Bcin10g00040 (Antoine Porquier, doctoral thesis. Université Paris Saclay (COmUE)), and the genes Bcin16g04610, Bcin16g04620 and Bcin16g04630, constituents of another possible cluster with Bcin16g04600, were repressed.

The changes observed in the expression of genes related to oxidative and fermentative metabolism seem to indicate a certain tendency of wild-type conidia towards the reestablishment of the latter as a consequence of exposure to DETA. At the same time, certain genes that inform germination progress, such as Bcin07g00040, Bcin06g01560 and *Bccda*1, are activated. This contradictory transcriptional behaviour is consistent with the morphological response obtained in pharmacological tests and allows more specific conclusions to be drawn about the effects of NO on the germination of this strain. The observed reactivation of the fermentative metabolism could indicate a temporary dormancy of the spores as a consequence of the NO burst. This dormant state would have been overcome after the cells had activated their response against oxidative and nitrosative stress, in which *Bcfhg*1 plays a key role, resuming germination processes again. Again, as was the case with the regulation of nitrogen metabolism,it is possible that the spores have responded with different speed depending on their stage of development. The percentage of wild-type spores in stage 0 of development at 6 hpi after two-hour exposure to DETA represents spores that were already in the same state at the time of donor addiction, at 4 hpi (Figure 21). They are spores that have maintained the fermentative metabolism characteristic ofthe dormant stage during the exposure time up to 6 hpi or that, at most, are found in the first moments after dormancy breakdown at this time point. Therefore, according to our assumption, their cellular machinery would be responding in a slower way to the stress imposed by NO compared to those that had already broken dormancy at 4 hpi. The fraction of spores that had broken dormancy at 4 hpi includes

conidia in stage 1 and 2 of development, but also those in stage 0 and which were in the isotropic growth phase. The reason is that the classification in stages of development of this work only took into consideration that the spore had not emitted the germinative primordium to include it in stage 0, regardless of whether or not it had broken dormancy. This set of spores, which was already in one of the active phases of the germination process at the moment in which the exposure to NO began, would already have a fully functioning cellular machinery, to a greater or lesser extent, which would have allowed to deal with the effects derived from NO more quickly and, ultimately, to restore germination during the time of exposure to the molecule.

In addition to inferring possible response dynamics by the fungus towards the stress created by the NO burst, our results also allow us to make assumptions about the mechanisms of action of the gas and the possible regulatory routes and signalling cascades involved.

In plants, regardless of the positive or negative regulatory nature of NO on pollen grain germination, it seems clear that the molecule stimulates the activity of the guanylate cyclase enzyme by increasing cGMP levels. In the case of *P. bungeana*, where NO showed a positive regulatory effect on the germination of its pollen grains, it was proposed that the molecule controls both the release of Ca^{2+} stored intracellularly and the flow of this cation from the extracellular space. The latter could be done through cyclic nucleotide-gated channels controlled by cGMP signalling pathway.

As a consequence, the cytoplasmic Ca^{2+} concentration increases, causing activation of vesicle trafficking and remodelling of actin cytoskeleton in the pollen tube, ultimately promoting tip growth (Wang *et al*., 2009; Prado *et al*., 2004; Prado *et al*., 2008). On the other hand, in pollen from *C. sinensis*, the repressive effect of NO on the pollen tube tip growth under cold stress was attributed to the accumulation of proline stimulated through cGMP signalling pathway (Wang *et al*., 2012).

In fungi, it is unlikely that the soluble guanylyl cyclase is a downstream target of NO since it seems that fungal genomes do not have sequences that code for this type of enzyme (Schaap, 2005; Samalova *et al*., 2013). Instead, it has been suggested that a tight balance between NO and ROS is essential for spore germination and germ tube growth in those few fungal species where the effect of the molecule on germination has been studied (Wang and Higgins, 2005; Samalova *et al*., 2013; Yin *et al*., 2016).

In our system, it seems that there are several routes that are affe cted in the wild-type strain by the effect of NO.

The repression of a putative calcineurin-dependent (CND) gene (*Bcgas*2/Bcin14g04260) and a cyclophilin-dependent (CPD) gene (*Bccpd*3/Bcin01g01590) could inform on the influence of NO on the calcineurin pathway. In *Aspergillus*, Calcineurin is a Ca^{2+} dependent phosphatase that in its inactive form constitutes a heterodimer composed of a catalytic subunit (CNA) and a regulatory subunit (CNB). The activation of the heterodimer is dependent on Ca^{2+}/calmodulin, so that when these bind to CNA, the enzyme is activated allowing its binding to the substrates it dephosphorylates (Stie and Fox , 2008). The transcription factor CRZA is an important downstream effector of calcineurin in *A. fumigatus* that when

dephosphorylated by the enzyme is translocated to the nucleus where it regulates genes of cell wall biosynthesis (Cramer *et al*., 2008; Juvvadi *et al*., 2014). Calcineurin can also interact directly with cell wall proteins to regulate germination, polarized growth, and cell wall structure (Lamoth *et al*., 2012, Baltussen *et al*., 2019). On the other hand, cyclophilins are a ubiquitous family of proteins with an intrinsic enzymatic activity of peptidyl-prolyl cis-trans isomerase that catalyses the rotation of X-Pro peptide bonds by accelerating the folding of certain proteins (Godoy *et al*., 2000). They have been implicated in a variety of cellular processes such as the response to environmental stresses, cell cycle control, regulation of calcium signalling, the control of transcription and fungal pathogenicity. One of the best studied is cyclophilin A because it is the primary cellular target of the immunosuppressive drug cyclosporin A. The resulting cyclophilin/cyclosporin complex is a strong inhibitor of calcineurin (Marks, 1996; Viaud *et al*., 2003). In our comparison of sample 2 vs. sample 3, none of the genes that code for these elements appear as DEG.

B. cinerea has about twenty putative cyclophilins in its genome. Of these, *Bcp*1 (Bcin05g06320), the already mentioned cyclophilin A, and *Bccyp*2 (Bcin05g03080) are the only two cyclophilins that have been shown to function as a receptor for cyclosporin A (Sun *et al*., 2021). Both decrease their expression in the presence of the donor (log_2(FC) = -1.20 and log_2(FC) = -0.22, respectively). Most of the rest of putative cyclophilins show the same behaviour, except for some exceptions in which their expression either remains constant or increases slightly due to exposure to NO. *Bcjar*1 (Bcin02g00190) encodes a histone 3 lysine 4 demethylase and has a regulatory function on *Bccyp*2 (Sun *et al*., 2021). This gene lowers its expression during exposure (log_2(FC) = -0.39). A similar behaviour has the *Bc4* gene (Bcin07g05520) that codes for the calmodulin protein (log_2(FC) = -0.51). The two subunits of calcineurin, the catalytic subunit *BccnA* (Bcin02g01540) and the regulatory subunit *Bccnb*1 (Bcin03g05990) do not seem to respond to the presence of the molecule (their expression levels decrease (log_2(FC) = -0.25) and increase (log_2(FC) = 0.036) very slightly, respectively). *Bcg*1 (Bcin05g06770) is the Gα subunit of a heterotrimeric G protein and *Bcrcn*1 (Bcin09g02820) is a calcipressin. In our system, the first is an upstream activator of calcineurin and the second a positive modulator of *BccnA* (Schumacher *et al*., 2008; Harren *et al*., 2012). None of them experienced a significant change in their expression by exposure to the molecule (log_2(FC) = 0.32 and log_2(FC) = -0.17, respectively). *Bccrz*1 (Bcin01g08230), the homologue of the *crzA* effector, also did not change its expression level due to exposure to DETA (log_2(FC) = -0.10). Therefore, no noticeable effect of nitric oxide or its derivatives is observed on the expression of the components of this pathway. However, there is a general repressive effect of most of them, especially of *Bcp*1. Impairment of calcineurin signalling in fungi resulted in pleiotropic phenotypes. In *A. fumigatus*, calcineurin mutants displayed severe defects in conidial germination, polarized hyphal growth, and conidium de velopment. Besides, they were incapable of causing disease in several experimental murine models of invasive pulmonary aspergillosis (Steinbach *et al*., 2006; da Silva Ferreira *et al*., 2007; Juvvadi *et al*., 2014). Conidia of the *ΔcrzA* strain of this same species displayed a significant delay and defect in germination and severe defect in polarized hyphal growth (Cramer *et al*., 2008). In *B. cinerea*, the *ΔbccnA* mutant showed a severe growth defect, did not produce conidia and was avirulent (Harren *et al*., 2012). The disruption of cyclophilin gene *Bccyp*2 did not impair the pathogen mycelial growth, osmotic and oxidative stress

adaptation as well as cell wall integrity, but delayed conidial germination and germling development, altered conidial and sclerotial morphology, reduced infection cushion formation, sclerotial production and virulence (Sun *et al*., 2021). However, vegetative growth on standard medium, conidial germination and conidiogenesis appeared unaltered in the *Δbcp*1 null mutant but was altered in symptom development on bean and tomato leaves (Viaud *et al*., 2003). *Bc*crz*1* deletion mutants were severely impaired in vegetative growth and differentiation, such as conidiation and sclerotium formation and cell wall and membrane integrity, as well as virulence (Schumacher *et al*., 2008). Several phenotypic traits were shared between *Ustilago hordei Δcna*1 and *Δcnb*1 and *B. cinerea ΔBccrz*1 mutants, one of them being cell-wall defects (Cervantes-Chávez *et al*., 2011).

Our situation is not comparable to that of these references because we are not dealing with mutants that lack some component or components of the pathway. However, the negative regulation that we observed on the cyclophilin A gene could be sufficient to derive similar results and be responsible for the wild-type germinative phenotype and its transcriptional profile. According to what has been described for this route in other filamentous fungi, the repression of cyclophilin A would prevent the inhibition of calcineurin. An inhibitory effect for which the absence of cyclosporin in our system does not necessarily represent a drawback that would have limited a possible repressive e ffect on calcineurin, since, in yeast and *B. cinerea*, there is some evidence that cyclophilin A and *Bccyp*2, respectively, interacts with calcineurin even in the absence of cyclosporine and it has been proposed that the activity of cyclosporine arises by taking advantage of a natural regulatory protein–protein interaction between cyclophilin A and calcineurin (Cardenas *et al*., 1994; Viaud *et al*., 2003; Sun *et al*., 2021). In any case, if the activity of calcineurin, necessary for correct germinative activity, is not being adversely affected by the action of cyclophilin, an alternative explanation of our results is necessary. The answer could be found in recent observations that suggest that cyclophilins could participate in an alternative form of regulation to that of calcineurin. At least, this is the case of *Bccyp*2, which functions in the upstream of cAMP-signalling regulating the infection-related development in this phytopathogenic fungi (Sun *et al*., 2021). The same or something similar could happen with *Bcp*1, so that the decrease in its number of transcripts would have affected the expression of *Bccpd*3, but it is also possible that of *Bcgas*2 (the CND gene), causing the repression of all of them.

Viaud *et al*. (2003) identified 18 CND genes (*Bccnd*1-18) and three CPD genes (*Bccpd*1-3) in nitrogen starvation condition, in *B. cinerea*. None of them, except for *Bccpd*3, was found among the DEG in the comparison of wild-type spores, presenting, with some exceptions, an expression pattern that decreased with exposure to the donor. *Bccpd*3 did not show significant homology to any other fungal protein by BLASTP. However, *Bcgas*2 has the Egh16-like virulence factor domain (PF11327). EGH16 is a protein from *Erysiphe graminis* f.sp. *hordei* that plays important roles during the early infection stage. *Bccnd*1 belongs to this same group of fungal proteins and also GAS1/2 from *M. oryzae*, which are appressoria-specific virulence factors required for appressorial penetration in host and lesion development (Justesen *et al*., 1996; Grell *et al*., 2003; Xue *et al*., 2002; Jin *et al*., 2013).

The expression of *Bcgas*2 is also regulated in a positive way by *bmp*1 MAP kinase cascade (Schamber *et al*., 2010). Cascades of this type use protein phosphorylation/dephosphorylation cycles to transduce information and in eukaryotes they are divided into modules made up of three interlinked protein kinases that are activated sequentially in the direction MAPKKK> MAPKK> MAPK. The latter is responsible for phosphorylating effector proteins that carry out output responses in the cytosol or in the nucleus (Schumacher, 2016). MAPK *bmp*1 (Bcin02g08170), together with MAPKKK *Bcste*11 (Bcin03g02630) and MAPKK *Bcste*7 (Bcin04g05630), forms its own module. *Bcste*50 (Bcin08g03660) and *Bcste*12 (Bcin10g05560) are also part of it. *Bcste*50 is an adapter protein that can bind to different components of the pathway performing a spatiotemporal control of the cascade response, while *Bcste*12 is one of the several effector proteins of this module (Schamber *et al*., 2010). This STE11-STE7-BMP1 cascade has been described as the signalling pathway involved in the control of germination induction of *B. cinerea* on hydrophobic surface, as is our case. However, in our transcriptional analysis on wild-type conidia, none of the components of this cascade had their expression affected in a significant way due to the action of NO (log2(FC) = -0.21, log_2(FC) = 0.20, log_2(FC) = -0.15, log_2(FC) = -0.13 and log_2(FC) = 0.37, respectively according to the order of mention). *Bcgas*2 was not the only gene regulated by this cascade that appeared differentially expressed in our analysis. *Bccda*1 (Bcin03g05710) is another gene regulated by *bmp*1 MAP kinase cascade whose expression level was induced in the samples of strain B05.10 treated with NO. Leroch *et al*. (2013) observed that the expression levels of *Bccda*1 in a *B. cinerea bmp*1 mutant were very low during the germination of its conidia compared to those of the conidia of the wild-type strain B05.10. The increased expression of *Bccda*1 observed in our analysis, together with the behaviour of the components of the *bmp*1 MAP kinase cascade, suggest that this regulatory pathway was not affected by the action of the molecule, so that the positive regulatory effect of NO on *Bccda*1 and the negative effect on *Bcgas*2 could be independent of this cascade.

Leroch *et al*. (2013) identified this gene as the most rapidly and strongly induced gene during germination on apple wax coated polystyrene containing 10 mM fructose, its maximum levels being after one hour and thereafter decreased to still high levels at two hours and half and four hours and to much lower levels at 15 hours. On the other hand, its induction was independent of the germination conditions and occurred in a similar manner on hard surfaces and in suspensions, in either minimal or full media, but its expression was strictly correlated with germination. In our culture conditions (conidia in suspension in PDB ½ medium on hydrophobic surfaces of polystyrene Petri dishes) this gene maintains the expression pattern described by these authors. Due to our experimental design, we only have the expression levels of the 4 hpi and 6 hpi, but it is enough to detect a decrease in its expression between both time points that would fit with the decrease in its expression observed from the first hour of germination in the workof Leroch *et al*. (2013). *Bccda*1 was identified as a member of a gene family encoding secreted proteins similar to chitin deacetylases and chitin binding proteins in other fungi. Chitin deacetylases enzymes carry out the deacetylation of chitin forming chitosan. This is a polymer of β1,4 linked glucosamine that plays multiple roles in the function of the fungal cell wall, including virulence and evasion of host immune responses. The role of chitosan in pathogenicity has been studied in the fungi *Puccinia graminis*,

Colletotrichum graminicola and *M. oryzae*, where it has been suggested that chitosan protects the appressorium from hydrolytic attack by chitinases present in the plant tissue and prevent the detection of chitin from plant pattern recognition receptors to evade plant immunity. In *S. cerevisiae*, chitosan appears to have a structural function and chitin deacetylases are specifically expressed during ascospore formation (Pammer *et al*., 1992; Christodoulidou *et al*., 1996; Geoghegan and Gurr, 2016; Mouyna *et al*., 2020). However, the seven putative chitin deacetylases of *A. fumigatus* did not play major roles in morphogenesis, cell wall integrity, adherence and virulence suggesting that chitosan is a minority component of the cell wall of this fungus (Mouyna *et al*., 2020). Therefore, these enzymes appear to be involved in different biological processes depending on the organism despite being widely distributed among fungi. Given the expression pattern of *Bccda*1 observed in our analysis and in that of Leroch *et al*. (2013), the chitin deacetylase activity attributed to its protein could be more related to the structural function described in *S. cerevisiae*. During germination, the isotropic growth phase and the polarized growth phase are associated, among other things, with the plasticization and molding of the conidium cell wall and the germ tube, respectively. The deacetylation of chitin alters its physical properties to enhance its solubility and flexibility, favouring the swelling of the conidium in one phase and the elongation of its germ tube in the other (Baltussen *et al*., 2019).

The genome of *B. cinerea* contains four other chitin deacetylases that could have the same or similar functions to that of *Bccda*1, although none of them was DEG in our analysis and their expression patterns differ. While *Bccda*3 (Bcin03g02970) and *Bccda*4 (Bcin09g00620) have an expression pattern similar to that of *Bccda*1, that is, their levels decrease during development (from 4 hpi to 6 hpi) and increase due to exposure to NO, *Bccda*2 (Bcin11g04800) and *Bccda*5 (Bcin01g08990) have a more constant pattern. Leroch *et al*. (2013) described the behaviours of *Bccda*3 and *Bccda*2 under their cultivation conditions and they resemble those observed in our work.

At the transcriptional level, the alteration of calcineurin signalling pathway also causes the alteration of the expression of genes linked to sexual and asexual development, highlighting its influence on the activator genes in the central development pathway. Thus, in *Beauveria bassiana*, the severe defects in aerial conidiation and conidial germination in *ΔcypB*, a mutant in the Cyclophilin B gene, were concurrent with drastically depressed expression of *brlA*, *abaA*, *wetA* and *vosA*, among others, in three- day-old cultures (Chu *et al*., 2017). *AbaA* and *brlA*, among others, were strongly negatively affected by deletion of calcineurin in *ΔMaCnA*, a *Metarhizium acridum* mutant in the *cnA* gene that showed deficiencies in filamentous growth, conidiation, and virulence (Cao *et al*., 2014). Chen *et al*. (2019) determined that CRZ1A in *Fusarium graminearum* was required for transcriptional induction of *abaA* and *wetA* as well as genes of the MAT *locus*, among others, since the expression of these genes decreased significantly in *ΔFgCrz1A* deletion strain. This mutant exhibited slower hyphal growth, and conidia formation and sexual reproduction were completely blocked.

According to Park *et al*. (2016) and Ni *et al*. (2010), in *Aspergillus*, conidiation is an event genetically programmed by *brlA*, *abaA* and *wetA* genes. From the induction by environmental and

developmental signals, a space-time gradient is established in the expression of these genes that, in collaboration with other genes, regulates the order of activation and the expression of conidiation-specific genes during conidiophore development and spore maturation.

The *brlA* gene is a key activator for developmental initiation and encodes two transcription units, brlAα and brlAß, that are specifically expressed during early phase of conidiation (as early as 10 hours after developmental induction, when vesicles start to form). Each subunit has different roles, and they are also regulated differently. BrlAα expression requires both *abaA* and *brlA*, while brlAß expression is independent of *brlA*. In turn, *brlA* is necessary for proper expression of conidiation-related genes such as *abaA*, *wetA*, *vosA*, and *rodA*.

The *abaA* gene encodes a developmental regulator for the differentiation of phialides, whose expression begins when these are formed 15 hours after induction, during the middle phase of asexual development and then disappears after formation of phialides. Its expression is dependent on *brlA*, but not *wetA*. It contains an ATTS/TEA DNA-binding domain and is required for expression of spore-specific genes, including *wetA*, *rodA*, *vosA*, and *velB*. In addition to this function, *abaA* also positively regulates autolysis and cell death.

The *wetA* gene is activated by *abaA* in the middle to late phases of conidiation. Similar to *brlA*, *wetA* also encodes two transcription units. The larger transcript begins to accumulate at 12 hours after induction, and both transcripts are present at very high levels at 24 hours after induction. Only the smaller transcript is found in mature conidia (48 hours after induction). This gene is essential for the completion of conidiation, but also functions in spore germination and early phase of fungal growth.

In addition to these three, another five genes perform relevant functions during conidiation: *stuA*, *medA*, *vosA*, *velB* and *rodA*.

StuA and *medA* are two developmental modifiers necessary for the precise spatial pattern in the multicellular conidiophore. *StuA* negatively regulates *brlA* and *abaA* in *A. nidulans*, although it activates the latter in yeast. *MedA*, for its part, negatively regulates the temporal expression of *brlA* while it is required for expression of *abaA* during development. VOSA and VELB are two regulatory proteins that belong to the Velvet family of proteins. Both function as repressors of conidiation. They also have an interdependent role in conidia maturation and viability. Their mRNA levels were high in conidia and regulated by *abaA* during middle phase of conidiation. Besides, the *vosA* or *velB* null mutant strains exhibita significant reduction in conidia viability, conidial trehalose amount, conidial tolerance against oxidative stress, and elevated conidial germination (Park *et al*., 2012; Park *et al*., 2016). The *rodA* gene encodes a hydrophobin and is essential for formation of the rodlet layer and hydrophobicity in conidia (Thau *et al*., 1994; Park *et al*., 2016).

The transcriptional response of these conidiation regulatory genes in the comparison of sample 2 versus sample 3 was uneven, with the *abaA* gene being the only resulting DEG. Of the three genes that make up the central development pathway, *brlA* is the only one for which an unambiguous ortholog has

not been found in the genome of *B. cinerea* (Amselem *et al*., 2011). However, the *Bcltf*2 gene (Bcin16g02090) has been proposed as a candidate (Schumacher, 2017). *Bcltf*2 kept its expression levels constant while the levels of *abaA* increased significantly and those of *wetA* (Bcin14g00990) decreased, but very slightly. The two developmental modifiers *stuA* (Bcin04g00280) and *medA* (*Bcltf*16, Bcin12g00460) kept their expression constant during exposure to DETA. The transcriptional levels of the Velvet *vosA* (*Bcvel*4, Bcin03g06410) and *velB* (*Bcvel*2, Bcin01g02730) genes remained constant and increased slightly, respectively. *RodA* also does not have its homologue in the *B. cinerera* genome. However, three genes encoding hydrophobins and six hydrophobin-like proteins have been identified in it (Mosbach *et al*., 2011). The hydrophobin class I *bhp*1 (Bcin02g07970) kept its expression constant while the two hydrophobin class II *Bhp*2 and *Bhp*3 (Bcin11g01450 and Bcin06g00510) were not expressed or did so at undetectable levels. Similar behaviours to these three genes were observed in the six hydrophobin- like proteins. Two other Velvet proteins, *Bcvel*1/*Bcvea* (Bcin15g03390) and *Bcvel*3 (Bcin07g05880), (homologous to *Aspergillus veA* and *velC*) and four of the components of the *Aspergillus fluG*-mediated pathway, *flbB* (Bcin15g00200), *flbC* (*Bcltf*15 Bcin06g05800), *flbD* (*Bcltf*12, Bcin10g04400) and *fluG* (Bcin06g01280), these upstream regulators of *brlA*, did not show any notable behaviour either.

The expression pattern of all these genes is, in principle, the expected one given that the biological samples used in this work did not consist of sporulating mycelium, but rather of germinating conidia. At most, one would have expected the detection of changes in the expression of genes characteristic of the last stage of conidiation, such as *wetA* or *vosA*, which are activated during conidia maturation and onwards (Ni *et al*., 2010). In contrast, the induction response detected in the *abaA* gene is intriguing for two reasons. On the one hand, neither its direct regulatory upstream *brlA* nor its downstream targets *wetA*, *vosA*, *velB* and *rodA* show increases in their transcriptional levels that could fit as a cause or consequence of the behaviour of this regulator, respectively. This could be consistent with previous observations made in *A. nidulans*, where it was determined that the expression pattern of *brlA* was not affected by a NO donor, neither in the control strain nor in *fhbAΔ fhbBΔ*, the double mutant for the two known flavohemoglobins in the fungus, after induction of conidiation, because an absence of correlation was found between the expression levels of *brlA* and the number of conidia (Marcos *et al*., 2016). However, Zhao *et al*. (2021) testified a maximum increase in transcription levels of *brlA*, *abaA*, and *wetA* of *Stemphylium eturmiunum* solid-medium cultures upon external NO application by SNP. At the same time, the application of cPTIO and sGC specific inhibitor NS-2080 all reduced expression levels down.

Our results could also be consistent with what was previously observed in *B. cinerea*, where the expression levels of *wetA* (and *abaA*) were not affected under conditions of induction of conidia by light or by the always conidia mutations (mutations of either component of the regulatory pathways of *Bcltf*2 that lead to an increase in its expression and causes light-independent conidiation) (Cohrs *et al*., 2016; Schumacher, 2017), and by observations that indicate that *Bcvel*4 (*vosA*) is not expressed in conditions of continuous light and light-dark for induction of conidiation or in continuous darkness for induction of sclerotia formation (Schumacher, 2017). Similar observations have also been made in the case of the

hydrophobins *bhp*1, *bhp*2 and *bhp*3, indicating that they are neither involved in conferring surface hydrophobicity to conidia and aerial hyphae nor are they required for virulence, but that they are required for normal sclerotium and apothecium development in the Leotiomycete (Mosbach *et al*., 2011; Terhem and van Kan, 2014). The second reason is the inconsistency in the *abaA* response between our results and those observed in *Beauveria*, *Metarhizium* and *Fusarium*. As has been commented, in these species, the interruption of the calcineurin pathway through the deletion of some of its components led to a downregulation in the expression of *abaA*. However, in our analysis the behaviour of this gene has been the opposite. The previously proposed downregulation of *Bcp*1 would have caused an induction and not a repression of *abaA*. All these observations taken together suggest, on the one hand, the existence in our system of a conidiation regulation pattern different from that proposed for *Aspergillus*, as was already the case with *F. graminearum*, where it was attributed to the morphological differences of the conidiophores of this species with those of *Aspergillus* (Son *et al*., 2013). On the other hand, the response of *abaA* to exposure to NO seems to be the result of an independent regulation of both the regulatory pathways in which it participates during conidiation in other filamentous fungi, as well as the calcineurin pathway.

Unlike *A. nidulans*, where the amount of *abaA* mRNA started to be reduced 24 hours after conidiation induction and mostly disappear in conidia (Ni and Yu, 2007; Ni *et al*., 2010), the *F. graminearum abaA* expression level was significantly upregulated at 6 hours after conidiation induction, which increased until 12 hours and was highly accumulated in conidium terminal cells indicating that additional functions of *abaA* exist in this fungus in addition to its participation in conidiation (Son *et al*., 2013). During conidia germination, there are also differ ences in the expression of *abaA* between species. In *F. graminearum*, the GFP signals of ABAA-GFP were highly fluorescent in the nuclei of terminal cells in mature conidia. However, the GFP signals became blurred after the conidia began to germinate and were undetectable 6 hours after germination which could suggest the repression of its expression (Son *et al*., 2013). In *A. fumigatus*, most transcripts present in dormant conidia persisted in the conidium after one year of storage at room temperature. Among them was *abaA* whose transcript remained present during storage at a high level. Its expression increased transiently in the initial 30 -min-time interval after germination, and then decreased for the remaining 60 min of the study (Lamarre *et al*., 2008). Similarly, in our study, *abaA* mRNA was present in wild-type conidia germinating at 4 hpi, but its levels were reduced by one third in samples from 6 hpi not exposed to the donor. On the other hand, the phenotype of the wild-type spores incubated together with NO resembles that observed in mutants of *F. graminearum* overexpressing *abaA*, which manifested pleiotropic defects such as impaired sexual and asexual development, retarded conidium germination, and reduced trichothecene production (Son *et al*., 2013). The authors observed a decrease in the germination rate of the mutants at 4 hours and 6 hours after incubation. However, there was no significant difference in the germination rates between wild-type and *abaA* overexpression mutant strains after incubation for 12 hours.

Taking all this information together indicates that *abaA* plays a role in biological pathways other than conidiation in some filamentous fungi. This together with reports that *abaA* is involved in the positive regulation of nuclear division in *A. nidulans* and *Penicillium marneffei* (Ye *et al*., 1999; Borneman *et al*., 2000) and in the control of maturation and dormancy in *F. graminearum* conidia through cell cycle regulation (Son *et al*., 2013) suggest a possible conserved function of this gene in *B. cinerea* and could explain the delay in germination of wild-type spores due to exposure to DETA. Given that this possible dormancy regulatory function by *abaA* seems independent of the central development pathway and the calcineurin pathway, it is possible to propose a potential regulatory effect of BMP1 MAP kinase cascade, as has been seen in *S. cerevisiae* between *tec*1 (*abaA* homolog) and *ste*12 and *fus*3 (*Bcste*12 and *Bcbmp*1 homologs, respectively) (Bardwell *et al*., 1998; Bardwell *et al*., 1998b; Bao *et al*., 2004; Matthew *et al*., 2018).

Another observation that would suggest the negative regulation of calcium signalling as a result of NO exposure is the repression detected in the *Bcgad*1 gene (Bcin09g05020). This gene is associated with the term glutamate decarboxylase (IPR010107). The enzyme glutamate decarboxylase participates in the synthesis of gamma-aminobutyric acid (GABA), a biomolecule of special interest among stress- responsive metabolites in plants and that is present in all prokaryotic and eukaryotic organisms. In the cytosol of plant cells, there is GABA shunt pathway, an alternative energy production pathway activated during cellular stress, when the function of TCA cycle is compromised (Salminen *et al*., 2016; Che-Othman*et al*., 2020). According to Ansari *et al*. (2021), GABA shunt pathway is a short metabolic pathway that involves three enzymes, glutamate decarboxylase, GABA transaminase, and succinic semialdehyde dehydrogenase. This pathway regulates GABA metabolism under stress conditions, participates in nitrogen assimilation in amino acids, achieves a balance of carbon/nitrogen metabolism, and influences other physiological processes, including plant growth and development. More specifically, oxidative stress conditions regulate the expression of the genes associated with GABA shunt, which causes an increase in the level of cytosolic GABA. This molecule binds to cell surface receptors, temporarily generating Ca^{2+}. Ca^{2+} activates GABA transporters, facilitating their transport into the cell. At the same time, glutamate decarboxylase is activated by Ca^{2+}/calmodulin. This enzyme converts glutamate to GABA, increasing the intracellular levels of the molecule that favour the expression of various signalling and metabolism- associated genes (elevates the photosynthetic activity and antioxidant enzyme activity and decreases ROS accumulation) and suppresses expression of genes associated with cell wall modifications. Furthermore, a possible positive regulation of glutamate decarboxylase by calcineurin signalling pathway has also been indicated in *Trichoderma atroviride* (Nižnanský *et al*., 2013) and a protective effect of GABA shunt and glutamate decarboxylase has been observed in yeast against oxidative stress (Coleman *et al*., 2001).

On the other hand, GABA shunt is active during fermentative metabolism in *A. nidulans*, so that the transcripts of the genes encoding the enzymes involved in this metabolic pathway presented relatively high levels in dormant conidia compared to germinating conidia (Novodvorska *et al*., 2013). Furthermore, the activity of the glutamate decarboxylase in *N. crassa* was manifested mainly in conidiating structures

and conidia and decreased during germination, suggesting that this pathway remains active during conidiation and/or dormancy (Christensen and Schmit, 1980; Novodvorska *et al*., 2013).

A BLASTP analysis of the *B. cinerea* genome yielded Bcin10g05230 and Bcin02g03910 as the homologues of the *A. nidulans* genes encoding a putative GABA transaminase and a putative succinic semialdehyde dehydrogenase, respectively. While the former decreased its expression levels, th e latter increased them in response to the molecule. In both cases the variation was very slight.

Consideration of this information as a whole suggests that, in our case, the downregulation of *Bcgad*1 in wild-type spores is due to an inactivity of the GABA shunt pathway. This could be attributed to the recovery of the cellular homeostatic state thanks to the intact defense machinery against oxidative stress that these conidia have and that allowed them to resume the germination process during the period of exposure to the source of stress.

A second MAP kinase cascade that could also have been influenced by exogenous NO, in addition to the BMP1 cascade, was the HOG-MAPK pathway. This cascade is known in fungi to play a key response against a wide range of stress conditions. In *A. fumigatus*, the pathway is composed of up to thirteen elements of which three dehydrin-like proteins, DPRA, DPRB, DPRC, are the downstream targets of the pathway effectors. In *A. nidulans*, *dlpA* is the ortholog of the dehydrins of *A. fumigatus*. In our biological system, this route seems to be simplified or to have elements different from those of *Aspergillus* since the analysis of the sequences of the *Aspergillus* components using BLASTP yielded redundant results in *B. cinerea* for some of the components. This is what happened with the aforementioned dehydrins, which were repeatedly associated with the genes Bcin09g02130 and *Bcpio*4 (Bcin03g04690). No information is available about them, except that *Bcpio*4 was significantly up-regulated during the outset of colonization in *A. thaliana* (Gioti *et al*., 2006). The transcriptional levels of both were reduced in response to NO, with Bcin09g02130 being the only DEG of the two. This behaviour is contrary to that expected for some proteins of this type under stress conditions similar to those suffered by our biological system due to the NO burst. Thus, in *A. fumigatus*, DPRA participates in the oxidative stress response, DPRB in the osmotic and pH stress responses and DPRC intervenes in tolerance against freezing. Meanwhile, DLPA from *A. nidulans* plays a role in the response to osmotic and thermal stresses. At the same time, these four genes have been associated with conidial dormancy because transcripts from all of them were detected in dormant conidia, but their transcriptional levels dropped significantly during germination in the absence of stress sources. More specifically, *dprA* was constitutively expressed in dormant conidia of *A. fumigatus*, at levels ~120 times more abundant than *DprB*. Both genes underwent a down-regulation with a 1000- and a 350-fold decrease in expression level in the first 30 minutes of germination, respectively. The expression of *DprA* was very weak from that first half hour and during the evaluated 24-hour period. In contrast, *DprB* increased its expression after 8 hours, doubling its levels at 24 hours. The expression pattern of *DprC* was equivalent to that of *DprA*, presenting a very intense decrease in its expression (2000- fold) in the first half hour of germination. In the case of *DlpA* in *A. nidulans*, its transcriptional levels remained low both during germination and during hyphal growth, during the 48-hour period analysed

(Wong Sak Hoi *et al*., 2011; Wong Sak Hoi *et al*., 2012; Hagiwara *et al*., 2014; Wartenberg *et al*., 2012). These observations suggest that the behaviour of the putative dehydrin Bcin09g02130 would be more similar to that of germinating conidia under standard growth conditions, that is, in the absence of a source of stress. Or, as is the case, in the presence of a source of stress that the spores are able to deal with. The response of the rest of the components of this route is also interesting. In *B. cinerea*, the homologues of the upstream components of the *Aspergillus* cascade (SSKB-PBS2-SAKA/MPKC) and *Saccharomyces* cascade (SSK2P/SSK22P-PBS2P-HOG1P) that regulate the expression of these proteins are known. They are MAPKKK *Bos*4 (Bcin11g03560), MAPKK *Bos*5 (Bcin09g06900) and MAPK *Bcsak*1 (Bcin15g03580) (Schumacher, 2016). None of them presented a significant change in their expression pattern due to exposure to the molecule, remaining practically constant in the case of *Bcsak*1 and rising and falling in the case of *Bos*4 (log_2(FC) = 0.73) and *Bos*5 (log_2(FC) = -0.30), respectively. A similar behaviour is found in the homologues, according to a BLASTP-type analysis, of the two-component signalling system that regulates this cascade upstream in the *Aspergillus* HOG-MAPK pathway: *tcsb* (*Bchhk*5/Bcin14g01870), *ypda* (*Bcypd*1/Bcin14g03630) and *sska* (*Brrg*1/Bcin08g01740); and in the transcription factor *atfA* (*Bcatf*1/Bcin09g00920) which is regulated by *sakA* and acts, in turn, on *dprA* in the Eurotiomycete (Baltussen *et al*., 2019). This situation is reminiscent of that observed in the BMP1 MAP kinase cascade or in the calcineurin pathway. In all of them, changes are detected in the expression of genes located at their end, while the upstream intermediaries did not experience significant changes in their transcriptional levels in response to the donor NO. This result could be explained if the possibility of a rapid regulatory response is contemplated, as already stated in the case of nitrogen metabolism. A regulation that against oxidative and nitrosative stress caused by the donor is capable of activating and deactivating the different gene programs in a fast and dynamic way to restore homeostasis in a short period of time. A predominant transcriptional regulation would fit this approach. Wong Sak Hoi *et al*. (2011) suggested this kind of regulation for the *dprA* and *dprB* genes in *A. fumigatus* by detecting a transient modulation of their gene expression within the previously described time frame in filamentous fungi for the regulation of various types of stress. Among them, oxidative stress for which the response time by fungal cells was establishedin 30-60 minutes (Li *et al*., 2008). However, this type of regulation would not be incompatible with post- translational regulation. Thus, Liu *et al*. (2008) detected a rapid and strong phosphorylation of *Bcsak*1 within 15 min and during at least 2 hours in cultures of *B. cinerea* treated with H_2O_2 during the analysis of the potential regulatory role of the *Bcbos*1 in *Bcsak*1 phosphorylation.

3.2 Comparative 2 vs. 5 (germinating spores of B05.10 with germinating spores of *ΔBcfhg*1, both in non-exposed conditions).

Once the possible cellular processes that are affected by NO burst in the protected system represented by wild-type spores have been described and discussed, the changes of the mutant transcriptome in relation to NO can be analysed and compared with the wild-type one to treat to define the protective role of flavohemoglobin BCFHG1 in the conditions studied. However, before that, it is necessary to look at the process of obtaining the *ΔBcfhg*1 mutant. The mutation was made using a gene replacement strategy. The ORF of the gene was replaced by the hygromycin resistance cassette (Turrion-

Gomez *et al*., 2010). This replacement led to the loss of a 1239 nucleotide fragment of the original genome sequence. An extension that makes it inevitable to think that the extraction of this fragment not only supposed the loss of the ORF of the gene of interest, but also supposed the elimination or truncation of the regulatory sequences of the neighbouring genes. This assumption is even more evident if one takes into account the proximity to which the genes of the genomic region of Bcin04g06230 are annotated and the divergent arrangement between some of them (Figure 34). For this reason, it was decided to analyse the results of the 2 vs 5 comparison (transcriptomic profile of the spores of the mutant strain *ΔBcfhg*1 compared with that of the spores of the wild-type strain B05.10, both cultured for 6 hours without exposure to NO). From it, 4 DEGs were derived: Bcin04g06240 and Bcin04g06250, which were upregulated and *Bcfhg*1 (Bcin04g06230) and Bcin10g05210, both downregulated.

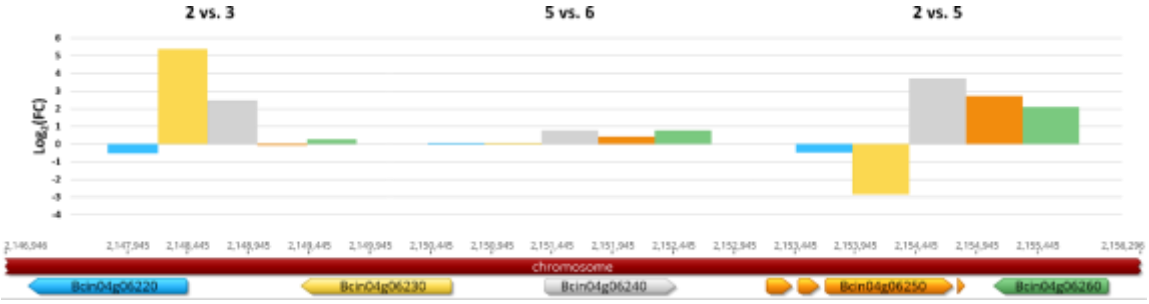

Figure 34. Histograms that represent the change in the expression levels of the genes Bcin04g06220, Bcin04g06230, Bcin04g06240, Bcin04g06250 and Bcin04g06260 in the comparatives 2 vs. 3, 5 vs. 6 and 2 vs. 5 and scheme of their genomic region (Geneious 10.2.6).

The behaviour of *Bcfhg*1 is as expected since the comparison supposes the confrontation of a strain that carries this gene with another where it is absent, but the same does not happen with the remaining three. Differential changes in the expression levels of Bcin04g06240, Bcin0 4g06250 and Bcin10g05210 must be attributed to the mutation. In the case of genes from the *Bcfhg*1 genomic neighbourhood, that is, Bcin04g06240 and Bcin04g06250, the reason is obvious. The Bcin04g06240 gene encodes for a putative nitronate monooxygenase, an enzyme that participates in the mitigation of the effects caused by nitrosative stress (Zhao *et al*., 2020). This gene was upregulated (log_2(FC) = 2.38) in the comparison of wild-type spores, but not in the comparison of mutant spores where its levels incr eased in a much less pronounced way (log_2(FC) = 0.80). Bcin04g06250 codes for a putative hydrolase amylase. In this case, no differential behaviour of the gene was observed in the two comparisons (log_2(FC) = -0.13 in sample 2 vs sample 3 and log_2(FC) = 0.44 in sample 5 vs sample 6). The Bcin04g06220 gene, located immediately upstream of *Bcfhg*1, carries an MFS domain (IPR011701) and, like Bcin04g06250, it was not differentially expressed either in the comparison of wild-type spores or in that of mutant spores. Not evenin the 2 vs 5 comparison, but a tendency change is detected. While in the comparisons 2 vs 3 and 2 vs 5 its expression decreased (log_2(FC) = -0.59 and log_2(FC) = -0.42, respectively), in the comparison 5 vs 6 it increased (log_2(FC) = 0.10). These results support our initial assumptions regarding the presence of

regulatory sequences of genes neighbouring *Bcfhg*1 in the 1239 base pair fragment deleted in the *ΔBcfhg*1 strain.

The explanation of the transcriptional profile of Bcin10g05210 is not as obvious as in the previous cases. This gene is not found in the genomic region of *Bcfhg*1, it is related to the GO term for integral component of membrane (GO:0016021) and could be exclusive to the *Botrytis* and *Sclerotinia* genera according to the results of BLASTN and BLASTP analyses performed. Their transcriptional levels were reduced by NO in wild-type spores (log_2(FC) = -0.64) but were strongly induced in mutant spores (log_2(FC) = 7.41). In the 2 vs 5 comparison, as mentioned, the gene was repressed (log_2(FC) = -9.28). These results suggest a possible positive regulation of the gene by flavohemoglobin. A regulation that, in the presence of oxidative stress, would exert the opposite effect, decreasing its expression. Baidya *et al*. (2011) raised the possibility that *A. nidulans* flavohemoglobin *fhbA* could influence other regulatory mechanisms in addition to those related to NO detoxification, such as the regulation of mycotoxin biosynthesis. In *Salmonella typhimurium*, a protective function of flavohemoglobin was detected against stress generated by nitric oxide, in an oxygen-independent way. As a possible explanation, it was suggested that the enzyme, by binding to NO in its heme group, could be able to transduce a NO signal through its redu ctase domain, leading to the positive regulation of protective genes (Crawford and Goldberg, 1998). Whichever mechanism is involved, it seems clear that flavohemoglobin has a certain regulatory role on this gene.

3.3 Comparative 5 vs. 6 (germinating spores of *ΔBcfhg*1 in NO exposed with non-exposed conditions).

In the results of the comparison of the mutant conidia, the oxidative stress situation created by the NO donor is more clearly reflected than in B05.10. The genes associated with the generation of ROS that were upregulated or downregulated in the wild-type spores present the same expression pattern in the mutant spores, but with higher fold change values in the case of the induced ones. To these we mustadd the genes *Bcsox*1 (Bcin07g04460) and Bcin02g01870. The former codes for sulfite oxidase 1 while the gene product of the latter has a domain NADH:flavin oxidoreductase / NADH oxidase (PF00724). These differences, although small, are the first indications of the vulnerability situation that mutant spores suffer from the deletion of the *Bcfhg*1 gene.

On the other side of the coin, among the genes involved in the response against oxidative stress,the putative heat shock protein Bcin07g02270 reappears as downregulated. However, Bcin15g02550, another heat shock protein, of the HSP20 family, is induced. The *Bcaif*1 gene encoding a putative AIF-like oxidoreductase 1 and related to retrograde response reappears as repressed, but two genes, *Bcnde*4 (Bcin03g08570) and *Bcalo*1 (Bcin05g02050), also related to this pathway are induced in mutant spores. The first encodes a putative external NADH dehydrogenase 4 and the second for a putative AMID-like oxidoreductase 1 (Schumacher *et al*., 2014).

The mitochondrial retrograde response is a retro-communicating system of the mitochondria with the nucleus as a consequence of adaptation to stress and that results in the promotion of cytoprotective mechanisms. In plants, where the chloroplast is also able to communicate with the nucleus

through this process, the mitochondrial retrograde response can be triggered by oxidative stress by affecting enzymes of the TCA cycle and the mitochondrial electron transport chain (ETC), among others. This mitochondrial dysfunction triggers a communication of the organelle with the nucleus through metabolic signalling pathways (Ca^{2+}/calmodulin, MAPKs) or general ROS signalling pathways (lipid peroxides, glutathione-ascorbate cycle, cytochrome respiratory pathway inhibitors). As a result, there is an altered nuclear gene expression mediated by transcription factors and leading to adapt the cell to the compromised homeostasis (Rhoads and Subbaiah, 2007). On the other hand, the key component of this pathway is the alternative oxidase (AOX), the last enzyme in the chain that transfers electrons to oxygen. This alternative respiratory pathway, together with the cytochrome respiratory pathway, constitute the mitochondrial ETC in fungi and other living beings. Both partially overlap, but while the alternative pathway has AOX as the terminal oxidase, the cytochrome respiratory pathway has the copper -containing cytochrome oxidase (COX) as the terminal oxidase (Rhoads and Subbaiah, 2007). An increase in the expression of *aox* was detected in response to oxidative stress in *Aspergillus*, *Magnaporthe* and *Paracoccidioides* (Yukioka *et al*., 1998; Magnani *et al*., 2007; Martins *et al*., 2011; Honda *et al*., 2012), while that oxidative stress reduced *Paaox* transcript levels in *Podospora anserina* (Corina *et al*., 2001). Furthermore, AOX activity contributes to oxidative stress resistance in *A. fumigatus* (Magnani *et al*., 2008).

In our study, the *Bcaox* gene (Bcin06g03440), encoding alternative oxidase, was not DEG in any comparison, but it considerably increased its expression levels in mutant spores (log_2(FC) = 1.32) while it decreased slightly in spores of the wild-type strain (log_2(FC) = -0.42). An increase in the expression levels of other components of the alternative pathway (*Bcnde*2-4, *Bcndi*1, *Bccyc*1, *Bcccp*2, *Bcucp*1, *Bcalo*1-4) was also detected in the two comparisons. On the other hand, the expression levels of a component of the non-alternative respiratory chain were affected. Thus, *Bccox*17 (Bcin02g03350), a COX copper chaperone involved in the delivery of copper for cytochrome c oxidase (COX) assembly (Attallah *et al*., 2007), was upregulated in mutant spores (log_2(FC) = 3.33), but not in the control spores where their expression levels also increased (log_2(FC) = 1.15). The response of other components of the chain was analysed, but a definite tendency of the effect of NO on them was not detected. This is striking in the case of complex IV components, since NO is known to inhibit the terminal acceptor of the chain cytochrome c oxidase (Black *et al*., 2021).

Taken together, this information suggests that, in our system, the increase in the expression in genes that encode enzymes of the alternative respiration pathway could indicate the reprogramming of the mitochondria by retrograde signalling probably because of their dysfunction caused by elevated ROS concentrations (Schumacher *et al*., 2014).

The explanation for the behaviour of *Bccox*17 could be in copper homeostasis. Schumacher *et al*. (2014) obtained a similar result for this gene in a microarray analysis in a mutant of *B. cinerea* lacking *Bcltf*1, a virulence-related gene encoding a GATA transcription factor. *ΔBctlf*1 was also affected by retrograde signalling in the same way as in our case, but more intensely. An altered copper homoeostasis

was the proposed explanation for the overexpression of *Bccox*17 and *Bcctr*3 (Bcin13g05210), a high-affinity copper transporter.

In our analysis, this nor the other two copper transporters (*Bcctr*1/Bcin01g07100 and *Bcctr*2/Bcin01g05510) annotated in the genome had a remarkable behaviour, their expression hardly changed by exposure to the molecule. However, several genes related to this element were differentially expressed: A putative tyrosinase (Bcin01g08630) was overexpressed in both comparisons ($\log_2$(FC) = 7.08 in the comparison of mutant spores and $\log_2$(FC) = 2.69 in the comparison of wild-type spores). A protein related to copper homeostasis, Bcin15g03090, decreased its expression in both comparisons, but only resulted as a DEG in the comparison of wild-type spores ($\log_2$(FC) = -1.67 in *ΔBcfhg*1 and $\log_2$(FC) = -2.86 in B05.10). Another putative copper chaperone, Bcin04g06310, was induced in the mutant spores ($\log_2$(FC) = 2.29 in *ΔBcfhg*1 and $\log_2$(FC) = 0.62 in B05.10). Laccase *Bclcc*6 (Bcin15g03330) was repressed in mutant spores ($\log_2$(FC) = -2.02 in *ΔBcfhg*1 and $\log_2$(FC) = -1.15 in B05.10), while laccase *Bclcc*7 (Bcin02g07640) was overexpressed in mutant spores ($\log_2$(FC) = 4.41 in *ΔBcfhg*1 and $\log_2$(FC) = 1.46 in B05.10). These results could report a deregulation of copper homoeostasis in mutant spores, as in the case of Schumacher *et al*. (2014).

Changes in the expression of the laccase *Bclcc*7 may be more related to its role in the cellular response to nitrosative stress. The same is true for various catalases. Among the eight catalases of the fungus genome, *Bccat*6, as happened in the reference strain, is DEG presenting a high induction value, even higher than the value it presented in B05.10. *Bccat*4 and *Bccat*2, which increased their expression in wild-type spores, maintain the same behaviour in *ΔBcfhg*1, the increase in expression being greater. In contrast, *Bccat*8 lowers its expression in mutant spores while it increased it in B05.10. BcCAT5, *catA*, *Bccat*3 and *Bccat*7 decreased their expression in wild-type spores. *Bccat*3 maintains this tendency, this negative response becoming more intense while the transcriptional levels of *Bccat*7 were practically undetectable in the mutant spores. For their part, *Bccat*5 and *catA* increase their expression levels. The nitralases Bcin05g04960 and Bcin12g06180 increased their induction response with respect to the values presented in B05.10, both being differentially upregulated by exposure of the mutant spores to DETA. However, Bcin02g03010 and Bcin14g00790 change the tendency that they showed in wild-type spores by lowering their expression levels in *ΔBcfhg*1 spores. In the comparison of sample 2 vs sample 3, no glutathione S-transferase protein and/or protein carrier of the Glutathione S-transferase domain was differentially expressed. In contrast, in the comparison of mutant spores, *Bcgst*1, *Bcgst*3, *Bcgst*5, *Bcgst*13 and *Bcgst*14 were upregulated, presenting a fold change value greater than 2. *Bcgst*9, *Bcgst*10, *Bcgst*11, *Bcgst*20, *Bcgst*21, Bcin14g02090, and Bcin15g00060 maintain their tendency of increasing expression, but *Bcgst*4, *Bcgst*15, *Bcgst*25, Bcin13g04210 and Bcin14g02970 change the tendency by decreasing their levels in response to NO in the mutant spores. *Bcgst*8, *Bcgst*12, *Bcgst*19, *Bcgst*24, *Bcgst*26, Bcin04g03580, Bcin09g00930, Bcin10g02820, Bcin11g04420, Bcin15g02740, *Bcgst*7, *Bcgst*6, *Bcgst*16, *Bcgst*17 and *Bcgst*22 decreased their expression in wild-type spores. Now, in the mutant spores, the first ten retain this behaviour, while the remaining five increase their expression in the *ΔBcfhg*1 spores exposed to the

donor. The transcriptional levels of *gst*II (Bcin01g04900) in the reference spores were undetectable, but in the mutant spores their expression increased during exposure to exogenous NO. *Bcprd*1 peroxidase maintained the repression response that it presented in wild-type spores, while Bcin08g04600 (encoding a protein with a DSBA-like thioredoxin domain) doubled its induction value in mutant spores with respect to the value it presented in the comparison 2 vs 3. Nitronate monooxygenase Bcin04g06240 increased its transcriptional levels in mutant spores exposed to nitrosative stress, but the increase was much lower compared to the value observed in the comparison of wild-type spores. This result, as already explained previously, was attributed to the deletion process of *Bcfhg*1 in the mutant strain. *Bcnqo*1, *Bcprx*2, and Bcin14g01940 had a very similar transcriptional pattern. All three were differentially induced in the 5 vs 6 comparison, while in the wild-type spores they showed only a slight increase in their expression when exposed to DETA. *Bcnqo*1 (NAD(P)H Quinone Dehydrogenase 1/Bcin06g06350) is a mitochondrial protein necessary for virulence in *B. cinerea* (An *et al*., 2016), but it also has a protective function against oxidative stress in other organisms (Ross and Siegel, 2021). *Bcprx*2 (Bcin12g00520) is a peroxyredoxin and Bcin14g01940 codes for the putative glutamate-cysteine ligase regulatory subunit. Glutamate-cysteine ligase catalyses the first step in the cellular GSH biosynthesis pathway.

These changes in the transcriptional profile of all these genes involved in the cellular response to oxidative stress between one comparative and another reveal, on the one hand, the greater susceptibility of *ΔBcfhg*1 cells to nitrosative stress imposed by exogenous NO and, on the other, the important protective role conferred by flavohemoglobin *Bcfhg*1 to alleviate the effects derived from exposure to the molecule.

The influence of this enzyme is also observed in the nitrate assimilation pathway. The gene encoding the enzyme nitrate reductase *BcniaD* and the gene encoding nitrite reductase *BcniiA* both showed an increase in their transcriptional levels in the mutant spores exposed to the donor ($\log_2$(FC) = 1.05 and $\log_2$(FC) = 1.40, respectively), but much lower than in wild-type spores ($\log_2$(FC) = 3.31 and $\log_2$(FC) = 4.08, respectively). The nitrate transporter *BccrnA* decreased its expression slightly while it increased it in wild-type spores for the same condition. The putative transporter Bcin15g00040 increases the induction response that it already exhibited in wild-type spores. In *A. nidulans*, a very similar behaviour of nitrate reductase activity was observed when *fhbAΔfhbBΔ* was exposed to the NO donor DetaNONOate and an important role of flavohemoglobins was proposed in protecting nitrate reductase activity from damage directly by the NO radicals or indirectly by NO-derived reactive nitrogen species at high concentrations of the molecule (Schinko *et al*., 2010). The enzyme has the same protective function on nitrite reductase (Schinko *et al*., 2010; Schinko *et al*., 2013; Marcos *et al*., 2016). Our results indicate the same protective effect of *Bcfhg*1 on *BcniaD* and *BcniiA*. However, despite this significant reduction in their induction, the transcriptional levels of both maintain a considerable increase. This is striking given that the enzyme flavohemoglobin, the main source of nitrate in our growing conditions and, therefore, the main inducer of *BcniaD* and, ultimately, *BcniiA*, is not present. Their induction could be due to trace amounts of nitrate that accumulate in this strain over time, as already observed in *A. nidulans*, where the

induction of genes of this pathway, such as NIIA and NRTA, was detected in an NIAD deletion mutant grown in a medium without the addition of nitrate (Pfannmüller *et al*., 2017). This phenomenon was called 'pseudo-constitutive' expression and was attributed to transporter-mediated NO_3^- accumulation, originating from traces of nitrate in the media (Schinko *et al*., 2013). It has already been mentioned that NO_2^- can be produced from the spontaneous oxidation of NO both outside and inside the cell (Yamasaki, 2000; Schinko *et al*., 2010). If this conversion takes place under our experimental conditions, it could explain the *BcniiA* response in mutant cells. Another possibility also described in *Aspergillus*, is the ability of the nitrate pathway to operate in the synthesis of NO. Specifically, Marcos *et al*. (2016) demonstrated that the nitrate reductase is partially responsible for the synthesis of NO employing nitrite as substrate. This nitrite could come from the spontaneous oxidation of NO and would explain the induction of *BcniaD*. However, given the intense conditions of nitrosative stress imposed by the NO burst, it is unlikely that cellular regulation promotes a greater internal accumulation of the molecule through nitrate reductase. Furthermore, the strong induction of the putative transporter Bcin15g00040, greater than in B05.10, would support the proposal of the entry of traces of nitrate present in the medium or that of the entry of nitrite derived from extracellular NO, as possible causes of the induction of *BcniaD* and *BcniiA*.

The response of the global regulator *areA* and the pathway specific regulator *Bcltf*9/*BcnirA* does not allow us to explain the induction of the nitrate assimilation pathway, since both show practically the same behaviour as in the comparison of wild-type spores: the transcriptional levels of *areA* increase very slightly while those of *BcnirA* decrease to the same extent as they did in B05.10. This result would suggest, as in the reference strain, the activation of the NCR. In the case of mutant spores, this repressive effect seems more intense because the number of induced genes whose product contains an *nmrA*-like domain is greater than in the wild-type strain. Thus, the three genes with these characteristics that were induced in B05.10 (Bcin03g00700, Bcin08g04910 and Bcin11g06310), do so again in *ΔBcfhg*1, but with a higher intensity (log_2(FC) = 4.08, log_2(FC) = 6.91 and log_2(FC) = 12.74, respectively) with Bcin11g06310 being the gene with the highest induction value in the comparison 5 vs 6. Seven more genes with the *nmrA*-like domain join the group showing fold change values greater than 2.

Taking these results together, they report that the transcriptional response to NO in relation to nitrogen metabolism in *B. cinerea* is dependent on flavohemoglobin *Bcfhg*1. This conclusion is contrary to that observed in *A. nidulans*, where treatment with a donor NO in both the wild-type strain and the *fhbAΔfhbBΔ* double mutant led to the same strong upregulation of the nitrate assimilation genes, attributing to nitrite formed by spontaneous NO oxidation more than to the formation of nitrate by flavohemoglobin the induction response due to the donor (Schinko *et al*., 2010). In our biological system, therefore, the importance of the enzyme as a protective system against the damage derived from the NO radical or the NO-derived reactive nitrogen species is once again evident.

Continuing with the analysis, as was observed for the B05.10 strain, numerous genes related to processes previously described for responding to NO_3^- in *A. nidulans* (Schinko *et al*., 2010) had their expression exclusively modified differentially in the comparison between mutant spores:

Five genes associated with signalling functions such as kinase activity were overexpressed while three others were repressed. A gene related to GTP-binding protein activity was upregulated. A gene associated with the terms isopropylmalate dehydratase (IPR015928), dihydroxy-acid dehydratase (K01687), both activities proposed to be involved in leucine biosynthesis, was downregulated. Five genes related to the term lipase varied their expression in one sense or another and the same happened with nine genes related to the term esterase (three of them already differentially expressed in B05.10 in response to NO), showing a possible affectation of the lipid metabolism.

Also, a helicase was repressed in the mutant strain and two genes related to the regulation of gene expression increased their expression. Of the latter two, one of them, Bcin02g04870, is similar to histone H1/5, which participates in the assembly of nucleosomes during the formation of chromatin fibres (IPR005818). In *ΔBcfhg*1, it intensified the induction response that it already presented in wild-type spores, exceeding the fold change value of 2 established as a threshold in the analysis. The other, Bcin02g03440, lowered its expression when B05.10 was exposed to the donor (log_2(FC) = -1.34), but it was overexpressed in *ΔBcfhg*1 for the same conditions (log_2(FC) = 3.14). Its product harbours a Chromo (CHRromatin Organization MOdifier) domain (PF00385), common in proteins related to the rearrangement and manipulation of chromatin to the condensed morphology of heterochromatin, where gene expression is repressed.

Given that intracellular nitrate levels in mutant spores are estimated to be not as high as in strain B05.10, the variation in the expression of these genes is probably a consequence of the general alteration that nitrogen metabolism undergoes rather than of induction derived specifically from an increase in the levels of this compound.

The change from a respiratory metabolism to a fermentative one observed to a certain degree in wild-type spores during exposure to DETA, is more evident in the mutant transcriptomic profile showing a possible dormancy of the cells as a consequence of exposure to the NO donor. Thus, the putative pyruvate decarboxylase Bcin02g06580 and eight genes related to alcohol de hydrogenase activity (IPR013149, IPR013154) were differentially induced in the mutant spores in response to NO (Bcin01g11530, Bcin05g08390, Bcin06g03810, Bcin06g05220, Bcin09g00850, Bcin10g01470, Bcin12g02050 and Bcin14g01070, four of them exclusively in *ΔBcfhg*1) (Lamarre *et al*., 2008; Teutschbein *et al*., 2010). Also, the upregulation of putative lactate dehydrogenase Bcin03g03280 and the downregulation of Bcin16g02700, Bcin05g04870, Bcin13g01020 and Bcin02g00470 point in the same direction. Bcin16g02700 and Bcin05g04870 are related to the terms Aconitase/3 -isopropylmalate dehydratase (IPR015928) and Succinate dehydrogenase/fumarate reductase flavoprotein (IPR027477), respectively. Both activities related to TCA cycle. Bcin13g01020 is an unknown protein associated with the term mitochondrial carrier *pet*8. Bcin02g00470 showed some homology with the *A. niger mtdA* gene andit is a predicted mannitol dehydrogenase that oxidizes mannitol to mannose. The mannitol serves as storage carbon sources and give conidia the ability to survive in stress conditions, it is known to be degraded during germination (Novodvorska *et al*., 2013).

However, the response detected in other genes suggests the presence of an active respiratory metabolism. Bcin06g01560, a protein of unknown function in the mitochondrial ribosome, and Bcin07g00040, required for respiratory growth, were already induced in B05.10 spores and maintain their level of induction in mutant spores. Two genes related to alcohol dehydrogenase activity (Bcin02g01730 and Bcin05g07670) were differentially downregulated only in *ΔBcfhg*1. The same happened with Bcin09g04240, a putative glycerol kinase. Genes related to glycerol metabolism showed high abundance in dormant conidia in *A. niger* and the levels decreased at the breaking of dormancy and did not show up-regulation at later stages of germination (Novodvorska *et al*., 2013). On the other hand, Bcin07g00400, whose product is related to citrate lyase activity (involved in TCA cycle), and Bcin07g05710, a putative ATPase involved in the mitochondrial respiratory chain, were overexpressed only in the mutant conidia.

The Bcin03g05500 gene is associated with the term oil body-associated protein-like (PF06884). In *A. thaliana*, OBAP1 protein is accumulated during seed maturation and disappears rapidly after germination (López-Ribera *et al*., 2014). In our analysis, its expression levels remained more or less constant between 4 hpi and 6 hpi when DETA was not present, in *ΔBcfhg*1. However, it was strongly induced when the donor was added to the culture medium (log_2(FC) = 3.89). Its expression profile was the same in the B05.10 spores, but its induction in the presence of NO was lower (log_2(FC) = 1.12).

The putative protein CIPC (a conidium surface protein that is induced under oxidative stress in *A. carbonarius* (Crespo-Sempere *et al*., 2013) maintained the repression response that it already exhibited in wild-type spores.

A disparate behaviour is also observed in some genes associated with the conidial swelling and polarized growth stages. Glycosylhydrolases degrade the polysaccharides of the cell wall, achieving their softening during isotropic growth (Lamarre *et al*., 2008). Six genes associated with the term hydrolase activity hydrolyzing O-glycosyl compounds (GO:0004553) were overexpressed while five were downregulated by exposure to nitric oxide. Two of the induced and one of the repressed already presented the same response in B05.10. Also, the Bcin03g05710 gene that codes for a protein with a chitin binding domain was induced in both comparisons.

During germ tube formation in conidia of *A. fumigatus*, *BtgE*, encoding ß-glucosidase was overexpressed compared to dormant conidia (Baltussen *et al*., 2019). In our system, Bcin01g11220 shows strong homology to *A. nidulans bgtB*/*bgl*2 and Bcin06g04840 is another putative beta-glucosidase. The first was overexpressed while the second was downregulated in the mutant spores. Both exhibited the same behaviour in wild-type spores, but with lower fold change values. Pectate lyases enzymes have also been detected in the *A. flavus* proteome during polarized growth (Baltussen *et al*., 2019). Bcin03g05820 encodes a putative pectate lyase that shows an induction response in the mutant spores (its expression was also increased in the reference spores, but very slightly). An expression profile very similar to this in both strains was shown by Bcin05g04520, associated with the term Pal1 cell morphology (PF08316). In fission yeast, PAL1 is a membrane associated protein that is involved in the maintenance of cylindrical cellular morphology, and it is involved in cellular morphogenesis and cell wall integrity (Ge *et al*., 2005).

The aforementioned Bcin07g02270, which codes for a putative chaperone of the HSP70 family and whose product contains the domains Actin-like ATPase domain (PS01132) and cell shape-determining protein MREB (PTHR42749), is repressed in *ΔBcfhg*1 to the same extent in the which it did in B05.10.

In a different train of thought, it seems that the absence of the flavohemoglobin enzyme in the mutant has caused a certain effect on the calcineurin pathway. *Bcgas*2, which was differentially repressed in B05.10, is also repressed in mutant spores and in a slightly more intense way (log_2(FC) = -2.91). Furthermore, a second gene whose product contains an Egh16 -like virulence factor domain is strongly repressed (log_2(FC) = -6.14) while in the reference spores it showed little repression. The rest of the CND genes (*Bccnd*1-18) show, in general terms, a behaviour similar to that of wild-type spores. Regarding the CPD genes, *Bccpd*3, which showed a differential repression response in B05.10, no longer does so in *ΔBcfhg*1, although it maintains the tendency (log_2(FC) = -0.38) and *Bccpd*2 is slightly induced (log_2(FC) = 0.31). However, the transcriptional levels of *Bccpd*1 are strongly increased in the mutant spores exposed to the donor, exceeding the established differential threshold (log_2(FC) = 3.38). If we look at the genes encoding the different components of the pathway (the cyclophilins *Bcp*1 and *Bccyp*2 and the other putative cyclophilins, the *Bccyp*2 regulator *Bcjar*1, calmodulin *Bc*4, the catalytic subunit of calcineurin *BccnA* and the regulatory subunit *Bccnb*1, the activator of calcineurin *Bcg*1, calcipressin *Bcrcn*1 and the effector *Bccrz*1), no remarkable change is observed in the expression levels of any of them, except in two. Cyclophilin A *Bcp*1 maintains the repression response that it already showed in the control spores, but in *ΔBcfhg*1 it is slightly more intense (log_2(FC) = -1.44). On the other hand, the expression levels of calcipressin *Bcrcn*1 (positive modulator of *BccnA*) changed their tendency in the mutant spores (log_2(FC) = 0.43) with respect to B05.10, where they decreased slightly.

In the case of the conidiation regulatory pathway, an attenuation of the effect that NO exertedon it in the control spores was detected. This proposition is made because the AbaA gene continues to be induced in the mutant spores, but less (log_2(FC) = 1.16) and the other components evaluated in B05.10 (*Bcltf*2, *wetA*, *stuA*, *medA*, VELVET proteins VOSA, VELB, BCVEA and BCVEL3, the hydrophobins *bhp*1, *bhp*2 and *bhp*3 and the regulators *fluG flbB*, *flbC*, *flbD* and *fluG*) maintain the pattern presented in B05.10. There is one exception which is *wetA*. This gene, whose expression is activated by *abaA* in *Aspergillus* (Park *et al*., 2016; Ni *et al*., 2010), was induced at levels similar to those of *abaA* (log_2(FC) = 1.12) while, let us remember, it lowers its expression slightly in the spores of B05.10.

Another pathway negatively influenced by the molecule in wild-type conidia was the GABA shunt pathway. The putative components of this pathway in our system (glutamate decarboxylase *Bcgad*1, GABA transaminase Bcin10g05230, and succinic semialdehyde dehydrogenase Bcin02g03910) showed the same response as in B05.10, highlighting *Bcgad*1, which decreased the intensity of its repression response observed in the control strain (log_2(FC) = -2.18) ceasing to be differentially expressed in the mutant conidia (log_2(FC) = -1.37). On the other hand, another glutamate decarboxylase (Bcin03g01040) appeared as a downregulated DEG in the comparison of mutant spores (log_2(FC) = -2.12) when it was also repressed in B05.10, but to a lesser extent (log_2(FC) = - 1.84). The response of these genes in B05.10 was

attributed to their intact oxidative stress response cellular machinery, which would have caused that the activation of this alternative energy production pathway was not necessary. The fact that these genes in the unprotected system show a pattern so similar to the one they presented in the control strain, makes it necessary to look for an alternative explanation. Their response is what one would expect to find in germinating conidia in the absence of stress (Novodvorska *et al*., 2013), but this approach is contrary to our situation. However, as was also mentioned in the analysis of B05.10, it is possible that the result observed in these genes is a consequence of the involvement, by NO and/or derived molecules, of regulatory components upstream of this pathway, such as, for example, components of the calcineurin pathway.

Of the two cascades of MAPKs that were described in the 2 vs 3 comparison due to a possible affectation by exogenous NO, it seems that the molecule exerts the same effect on the *bmp1* MAP kinase cascade in mutant spores. In contrast, the HOG-MAPK pathway does not seem to show the same influence as in B05.10.

The components of the first cascade, MAPKKK *Bcste*11, MAPKK *Bcste*7, *Bcste*50 and *Bcste*12 , practically did not vary their behaviour with respect to that shown in the control spores. MAPK *bmp1* either, but it is true that its downregulation is increased in *ΔBcfhg*1 (log_2(FC) = -0.82). On the other hand, the effect of NO on the targets downstream of this route is maintained as in the wild-type spores. The increase in the repression response of *Bcgas*2 has already been mentioned. In addition, chitin deacetylase *Bccda*1 (also positively regulated by the cascade) slightly increased the induction response in *ΔBcfhg*1 that it already presented in the first comparison (log_2(FC) = 2.12).

In this comparison between the mutant spores, another BMP1 -regulated gene appeared as DEG (Leroch *et al*., 2013). It is Bcin02g08710, related to negative acting transcription factor with a $Zn_{(2)}$-C_6 fungal-type DNA-binding domain, which was repressed (log_2(FC) = -4.88), presenting a lower repression in B05.10 spores (log_2(FC) = -1.45). According to Leroch *et al*. (2013), the expression of this gene is induced by germination in *B. cinerea*, reaching a maximum between 2.5 hours and 15 hours of incubation on apple wax-coated surfaces. Subsequently, targeted knockout mutagenesis did not reveal any obvious phenotype concerning germination, penetration, or infection.

The components of the HOG-MAPK pathway (MAPKKK *Bos*4, MAPKK *Bos*5, MAPK *Bcsak*1, *Bchhk*5, *Bcypd*1, *Brrg*1 and *Bcatf*1) also did not change their behaviour compared to that of wild spores, but the putative dehydrin Bcin09g02130 did. This gene drastically decreased its repression response in mutant spores to informative values of an absence of expression variation (log_2(FC) = -0.66). Their normalized count levels, therefore, did not decrease in the mutant spores to the extent that they did in B05.10 and remained in the order of 1000 units. Given that the homologues of this gene in *Aspergillus* are associated with the conidial dormancy process, these results would corroborate our hypothesis about NO burst as a trigger for a dormancy process in *B. cinerea* conidia. *Bcpio*4, another putative dehydrin, slightly increased in *ΔBcfhg*1 the repression response exhibited in B05.10 by NO.

On the other hand, three genes related to the terms ankyrin repeat, ankyrin repeat-containing domain, heterokaryon incompatibility or ankyrin and het domain-containing (IPR002110, IPR020683, IPR010730 and A0A0J5PTS0, respectively) varied their transcriptional levels differentially in the mutant spores. These are the genes Bcin12g05260, Bcin04g00740 and Bcin04g04700. The first was induced (log_2(FC) = 3.80) and it also did so to a lesser extent in B05.10. Meanwhile, the other two were repressed (log_2(FC) = -2.38 and log_2(FC) = -5.61, respectively) and they already did so, slightly, in the control spores. The het domain stands for heterokaryon incompatibility and refers to the response of autophagic - or apoptotic-type programmed cell death that can be triggered in filamentous fungi by fusion between two genetically incompatible individuals (Fedorova *et al*., 2005). The viability of these heterokaryons is genetically controlled by specific *loci* termed *het* or *vic* (for vegetative incompatibility) *loci*, at which heteroallelism cannot be tolerated in a heterokaryon. When two fungal individuals that differ genetically at a *het locus* fuse, the resulting heterokaryotic cells are rapidly destroyed or severely inhibited in their growth, depending on the *het locus* that is involved (Saupe, 2000). Calcium signalling pathways have been reported to play a role early in the execution of heterokaryon incompatibility and programmed cell death in *N. crassa* (Hutchison *et al*., 2009). This regulation would involve the hydrolysis of phosphatidylinositol 4,5-diphosphate by phospholipase C into 1,2-diacylglycerol and inositol 1,4,5-triphosphate, resulting in protein kinase C activation and Ca^{2+} release. A possible alteration of calcium signalling in the spores of the two studied strains of the fungus due to the effect of exposure to the molecule has already been mentioned in this work. Therefore, our results together with those of Hutchison *et al*. (2009) would allow to establish a possible regulatory effect of NO on the heterokaryon incompatibility response mediated by calcium signalling.

This vegetative recognition system was not the only one apparently affected by donor exposure. An alteration of the sexual recognition system, controlled by the mating type *loci* (Hutchison *et al*., 2009), was also observed. In *B. cinerea*, this genome region presents a single *locus*, *mat*1, with two idiomorphs, the mating type *mat*1 – 1 and the *mat*1 – 2, that encode transcription factors required for sexual development. Isolate B05.10 (mating type *mat*1-1) contains a *mat*1-1 idiomorph including a characteristic *mat*1-1-1 alpha-domain gene (Bcin01g02150) and an additional ORF (*mat*1-1-5/ Bcin01g02140) encoding a putative protein of unknown function (Amselem *et al*., 2011; De Miccolis Angelini *et al*., 2016). In our analysis, *mat*1-1-5 was the only differentially expressed ORF of the two at the *mat*1-1 *locus*. Specifically, it was downregulated (log_2(FC) = -6.00). This same response was shown in wild- type spores, but much less intense (log_2(FC) = -1.38). At the same time, the expression levels of *mat*1-1-1 decreased slightly and similarly in both strains when exposed to DETA (log_2(FC) = -0.46 in *ΔBcfhg*1 and log_2(FC) = -0.65 in B05.10). Chen *et al*. (2019) reported an essential role of calcium signalling in sexual reproduction in *F. graminearum* because a deletion mutant of the calcineurin-regulated effector *FgCrz*1A, showed a significant decrease in the expression levels of the *mat*1-1-1, *mat*1-1-2, *mat*1-1-3 and *mat*1-2- 1 genes, whereas the expression of all four genes was significantly increased in the wild-type strain after five days of sexual induction. Furthermore, *ΔFgCrz1A* was sterile in self-crosses and failed to produce

perithecia after 15 days of sexual induction, but the wild-type strain and the complementation strains produced mature perithecia under the same conditions.

On the other hand, a role of NO as a positive regulator of sexual development in *A. nidulans* has been observed. The addition of a NO-releasing compound drastically increased the formation of cleistothecia, sexual reproductive structures of the fungus, which was accompanied by a higher accumulation of *nsdD* and *steA* transcripts, two transcription factors necessary for sexual development. A similar effect had the deletion of flavohemoglobin *fhbA* because *ΔfhbA* and *ΔfhbA ΔfhbB* mutants presented an increase in Hülle cell (nursing cells for the formation of cleistothecia) production with respect to the control strain, but *ΔfhbB* did not show this effect. This phenotype of increased Hülle cell number was found independent of *nsdD* and *steA* expression in the *ΔfhbA* strain (Baidya *et al*., 2011).

In the same fungus, Marcos *et al*. (2016) observed an increase in the number of cleistothecia in *ΔfhbA ΔfhbB* compared to the wild-type strain, both grown under conditions that induce sexual development. As in the work of Baidya *et al*. (2011), the addition of a NO donor to the culture medium caused an intense increase in the number of cleistothecia in the control strain. However, the exogenous NO drastically reduced the number of cleistothecia in the mutant. They also measured the expression of *nsdD* in both strains in the absence of the donor and found that *nsdD* expression was higher in the flavohaemoglobin mutant than in the wild-type strain in all the time points tested suggesting that NO could play a role in the induction of the transcription of this gene. This effect of NO in the increased expression of the sexual developmental regulator *nsdD* in *ΔfhbA ΔfhbB* correlated with the amount of cleistothecia.

An effect of NO on the sexual development of *S. eturmiunum* similar to the previous ones has also been observed. Pseudothecia formation was increased in fungal cultures supplemented with the NO donor SNP, while the application of cPTIO or the sGC specific inhibitor NS-2080 inhibited it. The exposure to SNP also caused an increase in transcription levels of *mat*1 (up to 4.8 folds) and *mat*2 (up to 3.8 folds), the two genes involved in sexual reproduction in this species. However, the scavenger or the sGC inhibitor reduced the expression levels of these genes (Zhao *et al*., 2021).

The *Bcltf*1 gene, already mentioned previously in this work, is the homologue of *nsdD* in *B. cinerea* (Schumacher *et al*., 2014), while the homologue of STEA is the effector protein of the BMP1 MAP kinase cascade BCSTE12 (Schamber *et al*., 2010), also mentioned above. The response of the latter was already commented on when the behaviour of *Bcgas*2 was discussed. Its transcriptional levels were slightly increased in the comparisons of the two strains ($\log_2$(FC) = 0.13 in *ΔBcfhg*1 and $\log_2$(FC) = 0.37 in B05.10). The response of *Bcltf*1 was the same, but the increase was more intense than for *Bcste*12 ($\log_2$(FC) = 1.08 in *ΔBcfhg*1 and $\log_2$(FC) = 1.19 in B05.10).

All these results suggest that NO in the absence of *Bcfhg*1 might have a positive effect on the induction of sexual development in *B. cinerea*. However, as stated by Baidya *et al*. (2011) and Marcos *et*

al. (2016), it is possible that toxicity from the excessive amounts of NO in our experimental set up is only responsible for the effects seen on sexual development, especially in the mutant.

Baidya *et al*. (2011) also evaluated the effect of the molecule on secondary metabolism and determined that the deletion of the *A. nidulans fhbA*, and not of *fhbB*, induced a decrease of the toxic polyketide sterigmatocystin production. This phenotype was accompanied by a decrease in the expression of *aflR*, a transcription factor necessary for the activation of the sterigmatocystin gene cluster. Furthermore, supplementation with NO caused a recovery of the mycotoxin production near wild -type level and an increase of *aflR* expression levels in strains with a *fhbA* background.

In our analysis, the application of DETA caused the alteration of the expression of numerous genes related to secondary metabolism in the mutant strain. More specifically, the absence of flavohemoglobin had a potentiating effect on the response that these genes already showed, in the presence of exogenous NO, in the protected system of the control spores. Thus, the genes that lowered their expression levels in response to NO in the B05.10 spores, intensified this repression in the mutant spores. This is the case of polyketide synthase *Bcpks*7 (Bcin10g00040) involved in the synthesis of unknown amino-acid containing polyketides (log_2(FC) = -4.07 in *ΔBcfhg*1 and log_2(FC) = -1.95 in B05.10); the diterpene cyclase *Bcdtc*3 (Bcin08g03560) involved in the synthesis of diterpenes (-2.90 in *ΔBcfhg*1 and log_2(FC) = 1.67 in B05.10), the nonribosomal peptide synthetase *Bcnrps*5/*Bcnps*5 (Bcin04g01390) involved in the synthesis of unknown peptides (log_2(FC) = -2.68 in *ΔBcfhg*1 and log_2(FC) = -0.62 in B05.10), the thioesterase *Bcboa*10 (Bcin01g00100) involved in the synthesis of botcinic acid (log_2(FC) = -2.14 in *ΔBcfhg*1 and log_2(FC) = -1.42 in B05.10) and the putative ferrichrome synthase *Bcnrps*2/*Bcnps*2 (Bcin12g00690) participant in the synthesis of ferrichrome siderophores (log_2(FC) = -2.01 in *ΔBcfhg*1 and log_2(FC) = -1.36 in B05.10) (Collado and Viaud, 2016). For the latter, a possible function avoiding additional ROS formation via the Fenton reaction by means of iron chelation by the increased siderophore production has been suggested (Schumacher, 2017).

The equivalent effect was observed in those genes related to secondary metabolism that increased their expression in wild-type spores exposed to nitrosative stress. This is the case of the polyketide synthases *Bcpks*11 (Bcin14g01290) and *Bcpks*15 (Bcin05g06220) involved in the synthesis of unknown polyketides (log_2(FC) = 3.36 in *ΔBcfhg*1, log_2(FC) = 0.81 in B05.10 and log_2(FC) = 2.12 in *ΔBcfhg*1, log_2(FC) = 0.68 in B05.10, respectively), the sesquiterpen cyclase *Bcstc*5 (Bcin01g03520) involved in the synthesis of unknown sesquiterpenes (log_2(FC) = 3.08 in *ΔBcfhg*1 and log_2(FC) = 3.02 in B05.10), the P450 monooxygenase *Bcboa*4 (Bcin01g00040) involved in the synthesis of botcinic acid (log_2(FC) = 6.15 in *ΔBcfhg*1 and log_2(FC) = 2.67 in B05.10), the dehydrogenase *Bcboa*17 (Bcin01g00160) also involved in the synthesis of botcinic acid (log_2(FC) = 2.59 in *ΔBcfhg*1 and log_2(FC) = 1.85 in B05.10) and the opsin *Bcbop*2 (Bcin01g04540) (log_2(FC) = 2.69 in *ΔBcfhg*1 and log_2(FC) = 1.47 in B05.10).

This opsin is part of a gene cluster for the biosynthesis of retinal and carotenoids composed of three other genes: a phytoene dehydrogenase (*Bcphd*1/Bcin01g04550), a phytoene synthase (*Bcphs*1/Bcin01g04560) and a carotenoid oxygenase (*Bccao*1/Bcin01g04570). The first two participate in

the biosynthesis of carotenoid pigments (with protective function against oxidative stress), while *Bccao*1 is involved in the synthesis of retinal, the chromophore for opsin (Collado and Viaud, 2016). None of these three genes was DEG in any comparison, observing a slight increase in the expression in *Bcphd*1 and *Bccao*1, by exposure to the donor in both strains and a decrease in the expression of *Bcphs*1 for the same conditions. On the other hand, *B. cinerea* has another opsin, *Bcbop*1 (Bcin02g02670) (Schumacher, 2017), which increased its expression levels upon exposure to oxidative stress by H_2O_2 in a MAPK *Bcsak*1- dependent manner. However, its deletion did not affect stress responses of the fungus, which did happen in *S. sclerotiorum* (Heller *et al*., 2012; Lyu *et al*., 2016). In our analysis, it experienced a slight reduction in its transcriptional levels in both comparisons. The *Bcbop*2 homolog in *F. fujikuroi*, *carO*, mediates the retardation of conidial germination by green light (Garcia-Martinez *et al*., 2015), hinting at a possible regulatory role of *Bcbop*2 on asexual development.

The melanin biosynthesis cluster also responded to NO exposure. According to Schumacher, (2015), *B. cinerea* produces melanin of the 1,8-dihydroxynaphthalene (DHN) type thanks to two polyketide synthases, *Bcpks*12 and *Bcpks*13. The first is expressed during sclerotial development when the fungus is cultivated in constant darkness and provides 1,3,6,8 -tetrahydroxynaphthalene (T4HN), the precursor of the pathway for further conversion to DHN. *Bcpks*13 is expressed in conidiophores and conidia when the fungus is cultivated in the light and releases the hexaketide 2 -acetyl-1,3,6,8- tetrahydroxynaphthalene (AT4HN). This product could be incorporated in the conidial melanin polymer directly or can be converted by the hydrolase *Bcygh*1 to T4HN that enters the core pathway. T4HN is reduced to scytalone by the THN reductases *Bcbrn*2 (or *Bcbrn*1), with redundant function. Then a dehydration reaction carried out by the scytalone dehydratase *Bcscd*1 forming 1,3,8- trihydroxynaphthalene (T3HN). A second reduction reaction by *Bcbrn*1 (or *Bcbrn*2) produces vermelone from T3HN, which is converted by *Bcscd*1 into DHN. The DHN monomers would be finally polymerized by multicopper oxidases, but the enzymes involved in it are unidentified as no orthologues of known multicopper oxidases are present in *B. cinerea*. The transcription factor *Bcsmr*1 regulates positively sclerotial melanogenesis by physically linking with *Bcpks12*, while the transcription factors *Bcztf*1 and *Bcztf*2 contribute positively to regulation of conidial melanogenesis. Furthermore, two light-responsive transcription factors are predicted to be involved. One of them would activate *Bcpks*13-derived melanogenesis during conidial development and the other one would repress sclerotial development and its respective melanogenesis in the light. Laccase and tyrosinase-type enzymes have also been associated with the synthesis of this pigment in other fungi (Eisenman *et al*., 2012; Halaouli *et al*., 2006).

In our analysis, from the set of DHN melanogenic enzymes and regulatory proteins of *B. cinerea* , *Bcpks*12, *Bcpks*13, *Bcbrn*2, *Bcscd*1, *Bcscd*2, *Bcygh*1, *Bcsmr*1, *Bcztf*1 and *Bcztf*2 were not differentially expressed in the comparisons of either of the two strains. A very slight increase in the expression of *Bcpks*12, *Bcztf*1, *Bcztf*2 and *Bcsmr*1 was observed. In the latter, the increase in expression in the mutant spores was considerable ($\log_2$(FC) = 1.71 in *ΔBcfhg*1 and $\log_2$(FC) = 0.44 in B05.10). The others showed a low decrease in their expression, except for *Bcscd*1, whose levels fell more sharply ($\log_2$(FC) = -1.49 in

*ΔBcfhg*1 and log_2(FC) = -1.21 in B05.10). On the other hand, *Bcbrn*1, the laccases *Bclcc*6 and *Bclcc*7 and the putative tyrosinase Bcin01g08630 showed differential changes in their expression. As previously mentioned, the expression of *Bclcc*6 was repressed in both strains (log_2(FC) = -2.02 in *ΔBcfhg*1 and log_2(FC) = -1.15 in B05.10), while that of *Bclcc*7 was induced (log_2(FC) = 4.41 in *ΔBcfhg*1 and log_2(FC) = 1.46 in B05.10). The putative tyrosinase gene also increased its expression levels (log_2(FC) = 7.08 in *ΔBcfhg*1 and log_2(FC) = 2.69 in B05.10), but *Bcbrn*1 decreased them (log_2(FC) = -2.44 in *ΔBcfhg*1 and log_2(FC) = -1.90 in B05.10).

Melanin is associated with the cell wall contributing to fungal structures as conidia, sclerotia and appressoria, protecting them against UV radiation, oxidizing agents and desiccation and as virulence factor (Collado and Viaud, 2016). In *A. niger*, genes related to conidial melanin biosynthesis are expressed in dormant conidia, decreasing their expression during germination (Baltussen *et al*., 2019). On the other hand, the exposition to SNP stimulated the production of melanin in *S. eturmiunum* mycelium, while the application of cPTIO and sGC inhibitor NS2080 compromised the pigment biosynthesis (Zhao *et al*., 2021). Furthermore, SNP treatment of the Dothideomycete resulted in 9.4 folds increased transcription for *pks*1, 5.4 folds increased transcription for *pks*2 (two polyketide synthase genes involved in DHN-melanin synthesis), and 7.4 folds increased transcription for *tyr* (tyrosinase gene for DOPA-melanin biosynthesis). In contrast, 5-azacytidine (a DNA methylation inhibitor known to decrease melanin synthesis) treatment down-regulated in transcription for these three genes.

Our results suggest that NO would have a certain positive influence depende nt on *Bcfhg*1 on some of the regulatory genes of sclerotia melanogenesis, while a clear regulation is not observed for the equivalent regulatory elements in conidial melanogenesis. However, NO would have a negative regulatory effect dependent on *Bcfhg*1 on the different structural genes of the melanin biosynthetic pathway, which are common for the pigmentation of the two structures. On the other hand, the strong induction response of the putative tyrosinase gene, protein involved in the initial step of melanin synthesis (Halaouli *et al*., 2006) and of *Bclcc*7 would rule out, in principle, their possible participation in the biosynthetic pathway of this pigment.

The group of genes Bcin10g00010, Bcin10g00020 and Bcin10g00030 showed a differential repression response in the control spores exposed to the donor (log_2(FC) = -4.04, log_2(FC) = -2.02 and log_2(FC) = -3.87, respectively). This downregulation was increased in the case of mutant spores under the same conditions (log_2(FC) = -8.68, log_2(FC) = -3.70 and log_2(FC) = -4.64, respectively), to which it was joined Bcin10g00040 (log_2(FC) = -4.07 in *ΔBcfhg*1 and log_2(FC) = -1.95 in B05.10). A transcriptomic analysis determined that this group of genes forms a co-regulated cluster that is conserved in other ascomycete fungi, but not in the species close to *B. cinerea S. sclerotiorum*. Its expression is positively regulated by the VELVET BCVEL1 protein and since Bcin10g00040 codes for the polyketide synthase *Bcpks*7, it has been suggested that the cluster, in collaboration or not with genes from non-nearby *loci*, could participate in the production of a secondary metabolite (Antoine Porquier, doctoral thesis. Université Paris Saclay

(COmUE)). This information suggests a possible NO-mediated role of this cluster during conidiation and/or germination of the fungus and on which flavohemoglobin would have a protective role.

NO is involved in modulating secondary metabolism in many fungal species, having a versatile effect on the production of secondary metabolites (Zhao *et al*., 2020). Thus, it has a positive regulatory effect on the synthesis of some metabolites as in the aforeme ntioned case of Baidya *et al*. (2011) with the production of sterigmatocystin dependent on flavhemoglobin *fhbA* in *A. nidulans*. But a negative regulatory effect of NO burst on other different metabolic pathways has also been described. This is the case of the styrylpyrone biosynthesis in *Inonotus obliquus*, where the NO burst caused the S-nitrosylation of phenylalanine ammonia-lyase and 4-coumarate CoA ligase, two enzymes participating in the synthesisof this pigment (Zhao *et al*., 2016; Zhao *et al*., 2016b). Perhaps the best-known case of regulation of secondary metabolism by nitrogen is that of *F. fujikuroi*. In this fungus a regulation model has been described by which, in a simplified way, in nitrogen-limiting conditions, *areA*, which is highly expressed, activate, together with *areB* (a second GATA transcription factor), the synthesis of gibberellins and probably also that of fumonisin. *areA* also represses the transcription factor *meaB* which leads to the activation of the bikaverin gene cluster. a*reA* also induces the expression of its co-repressor *nmr*1, which negatively regulates *areA* by a feed-back loop. Under these conditions, the enzyme glutamine synthetase would also positively regulate the synthesis of gibberellins and bikaverin by sensing the low level of intracellular glutamine. In contrast, under nitrogen sufficient conditions, guanylate cyclase activity is repressed by high intracellular glutamine concentration, resulting in low *areA* mRNA levels. The repression of *areA* causes a reduction in the expression of the synthesis genes of gibberellins and fumonisin and the induction of *meaB*. The latter is involved in the repression of bikaverin synthesis. The remaining levels of *areB* activate the expression of the nitrogen-induced fusaric acid and apicidin F gene clusters. In this model, the TOR kinase plays an important role. In nitrogen-limiting conditions, the activity of TOR is low, but under nitrogen sufficient conditions, it is active repressing gibberellins and bikaverin clusters (Tudzynski, 2014).

In our analysis, the putative homologues of any of these genes were not DEG. *areA* (Bcin09g04960), *areB* (Bcin07g06570) and *meaB* (Bcin10g06020) slightly increased their transcriptional levels in both strains due to exposure to the donor. Instead, *tor* (Bcin01g11360) lowered them very slightly for the same conditions. The four genes associated with the term glutamine synthetase annotated in the genome of the fungus (Bcin06g01280/*BcfluG*, Bcin09g00040, Bcin09g00590 and Bcin14g03390) also did not show remarkable behaviours.

This result agrees with that established in *B. cinerera* for *Bctor*, which is known to play an important role in regulating the vegetative growth, but does not regulate germination (Xiong *et al*., 2019). Perhaps the exception is *nmr*1. It is necessary to keep in mind that the expression pattern of *nmr*1 in *F. fujikuroi* is opposite to that of the homolog *nmrA* in *A. nidulans*, the pattern considered in this work to discuss the results in relation to nitrogen metabolism. While the expression of *nmrA* is high under conditions of nitrogen-sufficiency, the expression of *nmr*1 is repressed under these conditions. Despite

these differences, both regulate *areA* activity (Tudzynski, 2014). In any case, Bcin15g02310 was the gene that showed the best homology results with NMRA in a BLASTP analysis, and this gene was not a DEG in our analysis, showing a slight increase in its expression in both comparisons. Despite this, it is possible that the high number of genes associated with the *nmrA*-like domain that were induced in the mutant spores exposed to DETA have influenced the alterations observed in some secondary metabolite pathways of the fungus. On the other hand, the apparent inactivity of the *F. fujikuroi* regulatory model in our system together with the intense situation of nitrosative stress that our results indicate that the burst of NO triggers in the spores of the *ΔBcfhg*1 strain, could suggest a different form of action for NO, mediated by post-translational modifications such as S-nitrosylation, in a situation more similar to that described for *I. obliquus* (Zhao *et al*., 2016; Zhao *et al*., 2016b).

An alteration of secretory activity during germination of the mutant spores in the presence of NO was also observed, highlighting the effect on the aspartic protease *Bcap*8 (Bcin12g02040). Espino *et al*. (2010) analysed the early secretome derived from *B. cinerea* conidia germinated for 16 hours in a minimal medium enriched with low-molecular weight host plant compounds. In this analysis, the *Bcap*8 protease constituted about one fourth of the protein mass secreted by the fungus. In contrast, in our analysis, its coding gene was repressed in wild-type spores (log_2(FC) = -3.89) and this effect was enhanced in the mutant spores (log_2(FC) = -4.23). The mutant affected in the *Bcap*8 gene showed a reduction in the protease activity detected in the extracellular medium, which was around 70% lower than in the wild type. However, no difference in virulence was observed for the mutant, as compared to the wild type. The great abundance of this type of protein in the fungal secretome (up to 34 proteases have been found experimentally) could explain the results of the intact virulence of the mutant due to overlapping enzymatic activities (ten Have *et al*., 2010; González *et al*., 2016).

CHAPTER II.

Characterization of the *Bcmed* gene.

Introduction

Conidiation is a common form of reproduction for phytopathogenic fungi and represents a critical event in those species not known to undergo sexual development (Chung *et al*., 2011). Furthermore, conidia are, in many cases, the first source of inoculum from which the disease spreads. Research on the mechanisms that regulate this asexual sporulation process is important because it can contribute to the search for targets that serve to reduce the initiating infection, avoiding its spread and thus controlling the disease. The genetic and molecular mechanisms that control conidiation have been exhaustively studied in model organisms such as *A. nidulans* or *N. crassa* (Ohara *et al*., 2004).

In the previous chapter it was already mentioned that, in the first of these fungi, this process is regulated via the key core regulatory proteins *brlA*, *abaA* and *wetA*, which regulates the order of expression of the genes that participate in conidiophore formation and spore maturation. *brlA* is expressed during early phase of conidiation and controls the beginning of conidiophore formation. *abaA* is the next key core component to be expressed and it does so in a BRLA-dependent manner. ABAA regulates the developmental process of phialides, and gene expression associated with late phase of conidiation. Among the genes in whose induction ABAA participates is *wetA*, which is necessary to complete the sporulative process and influences conidia viability and stress tolerance. These three transcription factors are controlled, in turn, by other regulatory pathways: the *fluG*-mediated pathway, the G protein-mediated pathway, the Velvet family proteins, the Ca^{2+}-Calcineurin pathway and the *ras* mediated signalling pathway. The first is located upstream of the key core and is composed of six genes, *fluG*, *flbA*, *flbB*, *flbC*, *flbD*, and *flbE*, which are necessary for an adequate activation of brlA expression. In the second, the hetero-trimeric G protein, composed of Gα (*gpaA* and *gpaB*), Gβ (*sfaD*) and Gγ (*gpgA*) subunits, control cAMP-PKA signalling pathway and repress conidiation. The Velvet protein family includes VEA, VELB, VELC, and VOSA. VEA, VELB and VOSA function as repressors of conidiation, but VOSA and VELB, in coordination with the central regulatory pathway, complete conidiogenesis (conidia maturation). The Ca^{2+}-Calcineurin pathway, described in detail in the first chapter of this work, is required for a correct conidiation. The heat-shock protein HSP90 interacts with calcineurin and has a positive regulatory effect on conidiation. The RAS protein family are monomeric GTPases in which RASA and RASB of *A. fumigatus* stand out for being required for proper production and formation of conidiophores and RHBA for being necessary for asexual development in a nitrogen source dependent manner.

This network of interconnected pathways includes other developmental factors and modifiers: *laeA*, *somA*, hydrophobins, trehalose, *stuA* and *medA*. *laeA* is a putative methyltransferase that interacts with some of the Velvet proteins for proper conidiation. SOMA is a transcription factor with a positive regulatory function upstream of conidiation-related genes. The hydrophobin RODA is essential for rodlet layer in conidia. The trehalose synthases TPSA and TPSB and the trehalose 6-phosphate phosphatase are necessary for conidiospore production due to trehalose protects against stress, particularly against thermal stress and dehydration, and is essential for long-term viability. STU and MEDA are two developmental modifiers necessary for the spatial pattern in the multicellular conidiophore (Park *et al*.,

2016; Ni *et al*., 2010; Baltussen *et al*., 2019). More specifically, *medA* was first described by Clutterbuck. (1969) in a mutational analysis of individual morphological mutants in *A. nidulans*. In this species, *ΔmedA* mutants show a delay in the production of phialides, a reduced number of conidia, the emergence of secondary conidiophores and overproduction of primary sterigmata (metulae) in a branching pattern that produces medusoid-like conidiophores. Furthermore, these mutants are cold sensitive. This incorrect morphology has been attributed, in part, to modified *brlA* and *abaA* expression since it has been established that *medA* modulates the core regulatory pathway at several levels. *medA* is expressed immediately after induction of conidiation and is present through all stages of conidiation. During the earliest stages of conidiophore development, MEDA represses *brlA* expression, which blocks the activation of *abaA* expression. In the transition from early to middle development, MEDA-mediate d repression must begin to be overridden. During middle development, MEDA could function as a coactivator with BRLA to provide maximum *abaA* expression and in later stages of conidiation, MEDA modulates negatively BRLA function and maintains its function as positive regulator of *abaA*. A regulatory role of the gene has also been suggested, together with *brlA* and *abaA*, of the expression of chitin synthase *chsC*, but not of *chsA* (Clutterbuck, 1969; Busby, *et al*., 1996; Ichinomiya *et al*., 2005; Etxebeste *et al*., 2010).

medA homologs are conserved among filamentous fungi: *medA* in *A. fumigatus*, *acr*1 gene in *M. grisea*, *med*1 in *Ustilago maydis*, *acon*-3 in *N. crassa* and *ren*1 in *F. oxysporum*. In *A. fumigatus*, the *medA* protein has a nuclear localization domain within the C-terminal region that is both necessary and sufficient to mediate the transcription factor function. The disruption of the gene markedly reduced conidiation. However, the conidiophore morphology was not that of the medusoid conidiophores of *A. nidulans*. Further, gene expression analysis suggested that MEDA governs conidiation in a manner independent of the core conidiation pathway genes. The mutant strain was impaired in biofilm production and adherence to plastic, as well as adherence to host *in vitro*, and exhibited reduced virulence in models of invasive aspergillosis (Gravelat *et al*., 2010; Al Abdallah *et al*., 2012). In *M. grisea*, the null mutation in the acropetal *acr*1 *locus* causes alteration in conidial pattern formation (hypermorphic conidiation phenotype). These conidia are nonpathogenic and fail to undergo infection-related morphogenesis (Lau and Hamer, 1998; Nishimura *et al*., 2000). *med*1 deletion mutants in *U. maydis* show both pre- and post-mating defects and are unresponsive to external pheromone. This is accompanied by a downregulation of *pfr*1, a regulatory transcription factor of the expression of a and b mating type genes, the a1 pheromone *mfa*1, and the pheromone receptor *pra*1. Additionally, the mutant showed a favoured production of glycolipids (Chacko and Gold, 2012). The *N. crassa* *acon*-3 is induced at late time points of conidiation and using its native promoter complemented the conidiation defects of the *A. nidulans ΔmedA* mutants (Chung *et al*., 2011). *ren*1 in *F. oxysporum* is a protein of nuclear localization and the corresponding mutant strains lacks normal conidiophores and phialides and form rod-shaped, conidium-like cells directly from hyphae by acropetal division. However, they exhibit normal vegetative growth and chlamydospore (a kind of ase xual spores) formation (Ohara *et al*., 2004).

In *B. cinerea*, the ortholog of *medA* is the light-responsive transcription factor 16 (*Bcltf*16/Bcin12g00460), whose expression is light-responsive and deregulated in always conidia mutants (mutants that present mutations in some protein of the light signalling system as protein Velvet complex or White collar complex) (Cohrs *et al*., 2016). Furthermore, it was upregulated in the transition from sclerotia to primordia during an RNAseq analysis on different stages of the sexual development of the fungus (Rodenburg *et al*., 2018).

In a previous study carried out in our research group with the intention of characterizing the processes that are modulated by exogenous or endogenous NO in our study system, specifically during analysis of data derived from a differential gene expression analysis comparing the expression pattern of germinating spores in the presence and absence of the NO scavenger c-PTIO, and with that of the developing mycelium, changes in the expression of a set of genes were detected. Among those genes responding to nitric oxide depletion, *Bcltf*16 gene stood out (Daniela Santander, Doctoral Thesis. University of Salamanca). Its transcriptional levels showed an 8.9 -fold higher expression level in the presence of the scavenger compared to the situation in the absence of c -PTIO (Figure 35). Based on these results, together with the antecedents mentioned in other fungal groups, we set out to determine the role of *B. cinerea medA* in development and virulence by deleting the gene and analysing various characteristics of the resulting phenotypes.

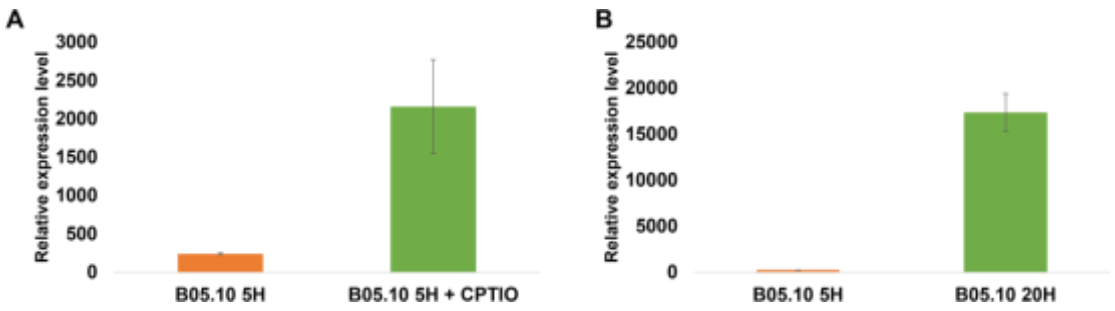

Figure 35. Relative expression of the *Bcmed* gene in the presence of c-PTIO (A) and in mycelium grown for 20 hours (B) in relation to its expression in the absence of c-PTIO in spores grown for 5 hours in minimal liquid medium (taken from Santander, D.; doctoral thesis).

Results

1. *In silico* analysis of *B. cinerea medA*.

According to the version of the *B. cinerea* genome consulted (B05.10 ASM14353v4), the *Bcmed* gene is annotated in GenBank with the code Bcin12g00460 (GeneID: 5834564) and is located in chromosome 12 between positions 157659 - 165282 in the forward strand. Two splice variants are annotated for this gene. Bcin12g00460.1 considers 5 exons between positions 159240 – 159644 the first one, positions 159772 – 160450 the second one, positions 160520 – 160694 the third one, positions

160774 - 162296 the fourth one and positions 162360 – 165282 the fifth one, separated by four introns of 127, 69, 79 and 63 nt, respectively. Translation or the predicted ORF from the start codon at position 160.655 within the third exon generates a 719 amino acids protein (XP_024551985.1). The second splice variant, Bcin12g00460.2, would be translated from the same start codon and, therefore, would also code for the same 719 amino acids protein. However, the 5' UTR of this variant is longer and more complex, deriving from alternative splicing of one additional intron within 5' UTR. In this variant a first exon would be considered, located between positions 157659 and 159235, and a second one between positions 159549 and 159644, both separated by an intron located between positions 159236 and 159548 (Figure 36).

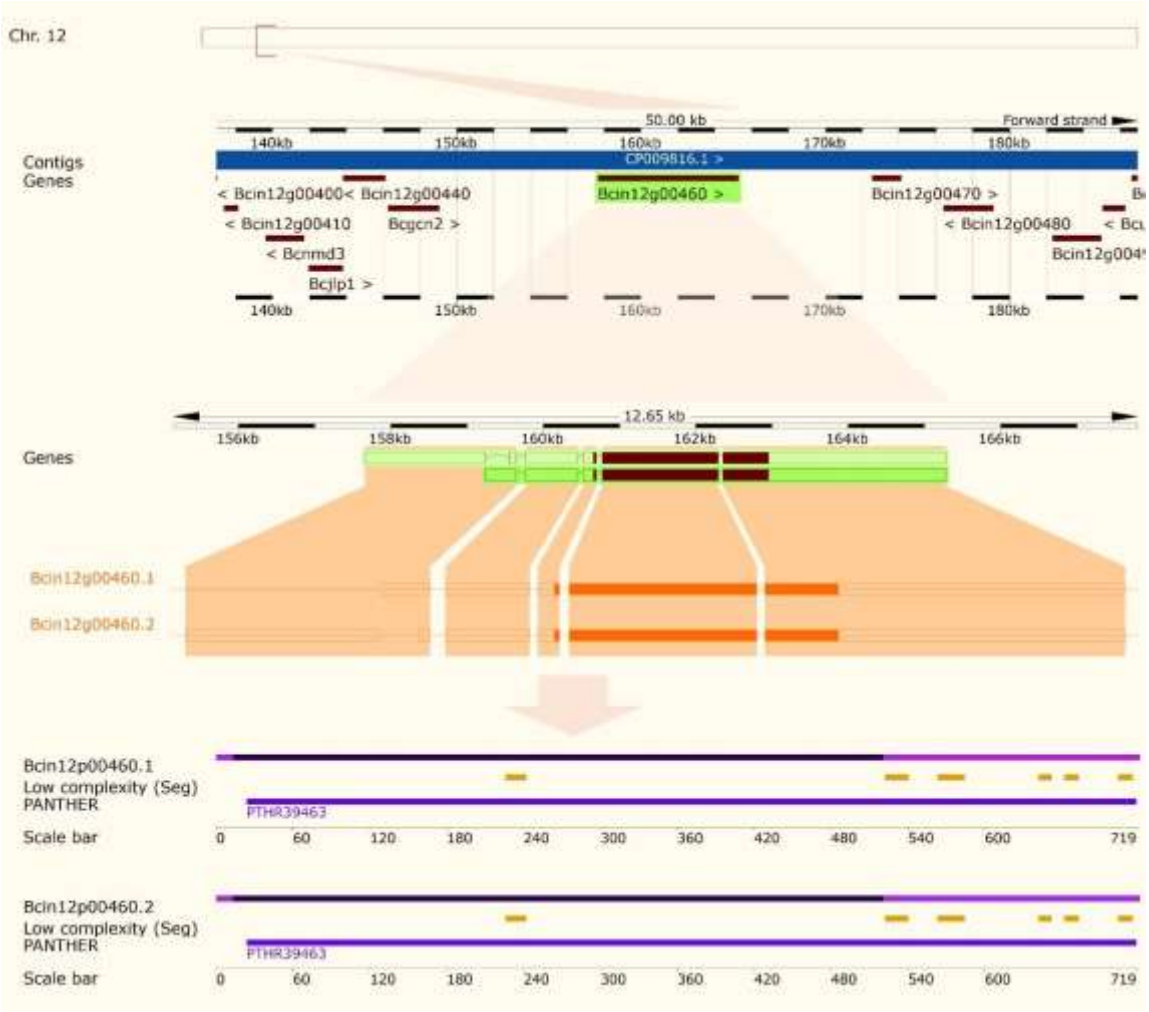

Figure 36. Schematic view of the position of *Bcmed* (Bcin12g00460) on chromosome 12 of the *B. cinerea* genome, of the structure of the transcripts Bcin12g00460.1 and Bcin12g00460.2 and of the location of some of the domains and features in their respective sequences (http: //fungi.ensembl.org).

Both transcripts have 13 domains and features (Table 6):

- According to PANTHER, it presents a domain belonging to an unnamed gene family (PTHR39463). This domain is associated with the GO terms of biological process "anatomical structure

morphogenesis, regulation of biological process and reproduction" and with the GO terms of cellular component "intracellular and nucleus".

- According to the predictor software MobiDB-lite presents six intrinsically disordered regions (IDRs).
- The SEG algorithm found six regions of low complexity.

Table 6. List of motifs and domains in *B. cinerea* MEDA protein. The domains were computationally predicted by InterProScan while intrinsically disordered regions were annotated with MobiDBLite predictor and low complexity regions were annotated with SEG program. The table shows the domains IDs in the original database and InterPro consortium, and the positions of the domains and features on the Ensembl peptide (http: //fungi.ensembl.org).

Domain source	Start	End
PANTHER (PTHR39463)	24	718
Feature type	Start	End
MobiDBLite	1	25
MobiDBLite	192	237
MobiDBLite	273	292
MobiDBLite	307	355
MobiDBLite	549	630
MobiDBLite	669	719
Seg	226	242
Seg	522	540
Seg	563	584
Seg	642	652
Seg	662	673
Seg	704	715

A phylogenetic analysis performed on the sequence of the predicted *Bcmed* protein and on homologous sequences obtained from a BLASTP analysis using the *B. cinerea* protein as input and a subsequent alignment of these sequences with that of *Bcmed*, determined that *medA* is found in representatives of the *Ascomycota*, *Basidiomycota* and *Mucoromycota* divisions. The amino acid sequence of *Bcmed* showed high homology along the entire sequence with those of the representatives of the indicated groups and the highest conservation was found around the region where *medA* minimal nuclear localization domain have been described in *A. fumigatus* (Abdallah *et al*., 2012) (Figure 37).

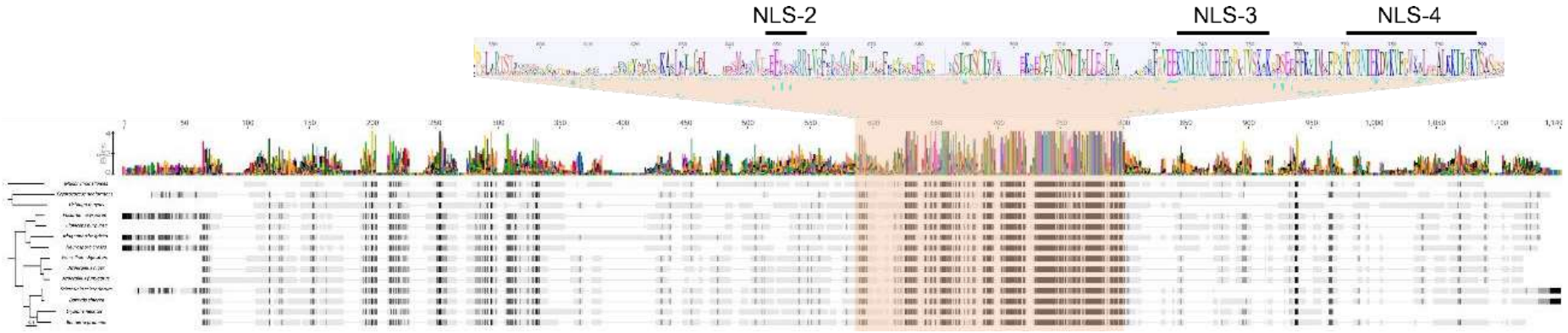

Figure 37. Phylogenetic tree and sequence alignment of the *Bcmed* (XP_024551985) predicted amino acid sequence with other *medA* orthologues from *Mucor circinelloides* (EPB82895), *Cryptococcus neoformans* (XP_568926), *U. maydis* (XP_011390017), *F. oxysporum* (BAC55015), *Claviceps purpurea* (CCE33149), *M. grisea* (BAC41196), *N. crassa* (XP_962851), *Penicilliumdigitatum* (XP_014535320), *A. niger* (XP_025460342), *A. fumigatus* (XP_755658), *S. sclerotiorum* (XP_001595576), *Erysiphe necator* (KHJ32623.1) and *Blumeria graminis* (EPQ64905.1). The orthologous sequences were obtained from NCBI (Genbank), and the phylogenetic tree was built up employing the Geneious Tree Builder using the Neighbor-Joining Tree Build Method with a Bootstrap resampling method with 1000 replicates. The alignment was performed with the CLustal Omega algorithm in Geneious software using the default settings. Three of the four putative nuclear localization sequences predicted in *A. fumigatus medA* are showed (NLS2-4).

2. *Bcmed* deletion in *B. cinerea*.

To obtain mutants of *B. cinerea* deficient in the wild-type allele of *Bcmed*, the plasmid pAAD4 (Alejandro Alonso Díaz, Master thesis. University of Salamanca) was used. This vector contains the hygromycin resistance expression cassette (promoter of *OliC* gene of *A. nidulans*, *hph* gene, and *TtrpC* terminator of *A. nidulans*) flanked by the 5' and 3' regions of the *Bcmed* gene, of 487 bp and 926 bp, respectively, which allows their integration into the homologous *locus* of the fungal genome through homologous recombination (Figure 38).

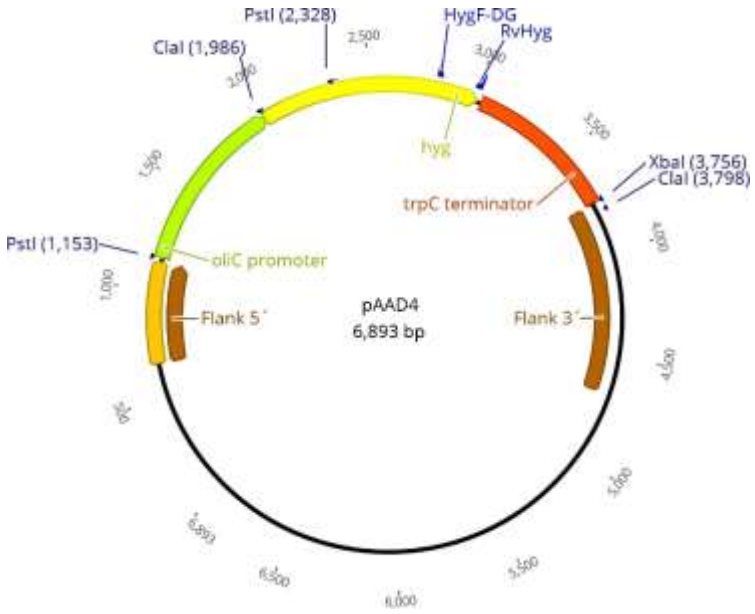

Figure 38. Scheme of plasmid pAAD4. The fragments of the 5' and 3' flanks of the *Bcmed* gene, the hygromycin resistance expression cassette composed of the promoter of the *OliC* gene of *A. nidulans*, the *hph* gene, and the *TtrpC* terminator of *A. nidulans*, the annealing positions of the HygF-DG and RvHyg oligonucleotides and the restriction targets of the enzyme *Pst*I and *Cla*I are represented.

This plasmid was used to transform protoplasts of the *B. cinerea* wild-type strain B05.10 using the method described in section 16.2 of Materials and Methods. Numerous fungal colonies, grown on the plates where the transformed protoplasts were seeded, were transferred to plates with medium supplemented with hygromycin. They were kept growing in this selective medium during several successive passages and then DNA was extracted and used to identify by PCR positive candidates (Alejandro Alonso. Master Thesis. University of Salamanca). Two gene replacement candidates, Bcmed34 and Bcmed84, and one transformant with the wild-type and the mutant alleles simultaneously, *Bcmed*16, were selected for further characterization by Southern analysis (Figure 39).

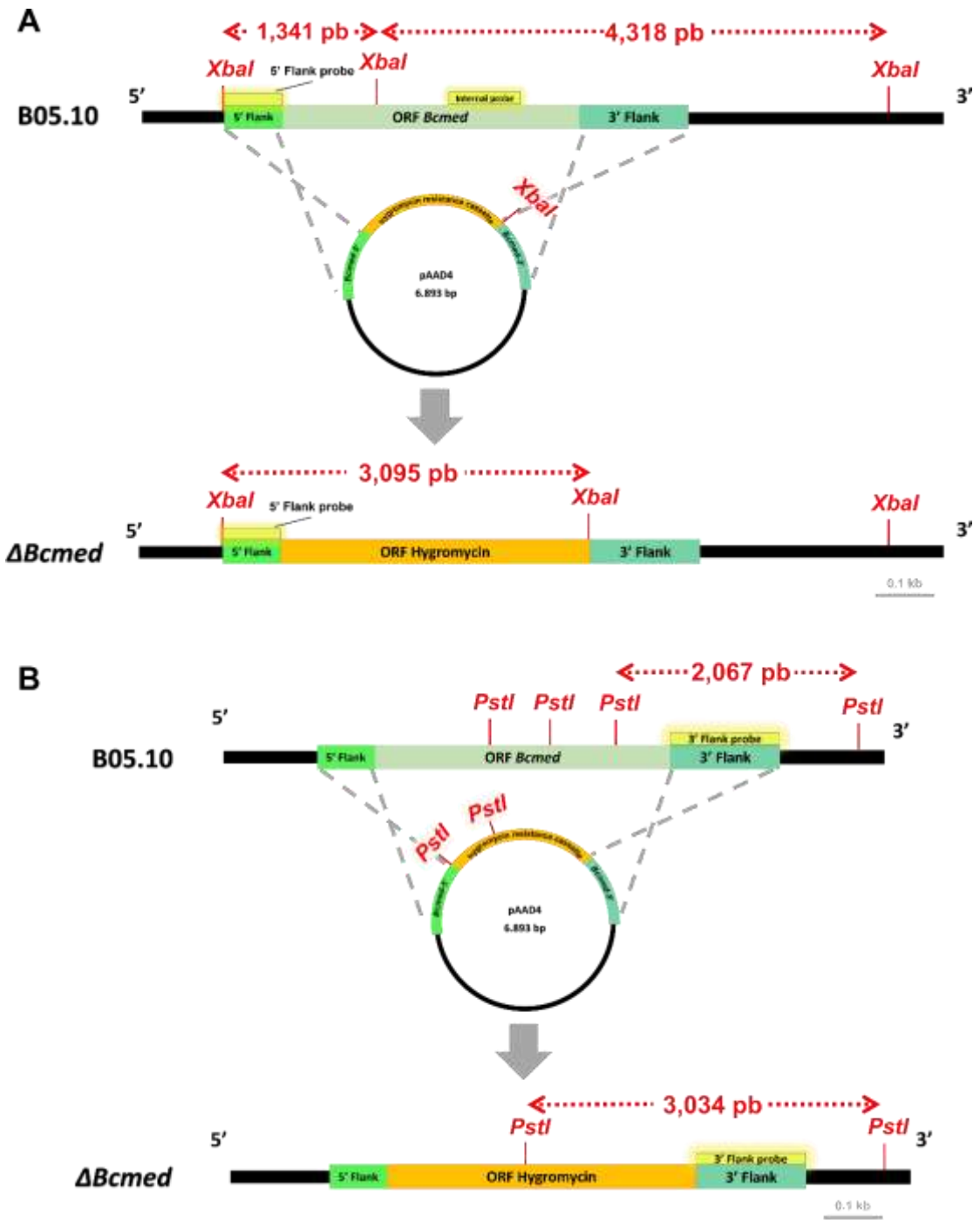

Figure 39. Simplified scheme of plasmid pAAD4 structure, of the genomic copy of the *Bcmed* gene (B05.10) and of the genomic copy of a transformant in which the wild-type allele of the *Bcmed* gene has been replaced by the mutant allele of the same gene cloned into plasmid pAAD4 (Δ*Bcmed*). The positions of the probes of the 5' flank and the internal region of *Bcmed* and of the restriction targets of the enzyme *Xba*I (A) and the positions of the probe of the 3' flank of *Bcmed* and of the restriction targets of *Pst*I (B), present in one or another copy and the sizes of the DNA fragments that are detected in hybridizations carried out with the different probes mentioned on the corresponding genomic DNA samples, are shown.

For this, following the indications of section 18.2 of Materials and Methods and as explained in chapter I, the genomic DNA of the selected transformants and of the wild-type strain B05.10 was digested with enzymes whose digestion released an informative band pattern and easily interpretable when the membrane was hybridized with the appropriate probe. Thus, the enzymes *Xba*I or *Pst*I were used

depending on the probe employed in the subsequent stage of hybridization of the membrane. The digested genomic DNA samples were transferred to a nylon membrane after being separated by agarose gel electrophoresis.

Subsequently, hybridizations were performed on the membrane with three different probes: A probe designed on the 3' flank of *Bcmed*, another designed within its structural region, and another designed on its 5' flank. *Xba*I-digested genomic DNA samples of the strains of interest were used for hybridizations with the probes of the 5' flank and the internal region of *Bcmed*. The genomic DNA samples transferred to the membranes that were to be hybridized with the *Bcmed* 3' flank probe were digested with the *Pst*I enzyme (Figures 39 and 40).

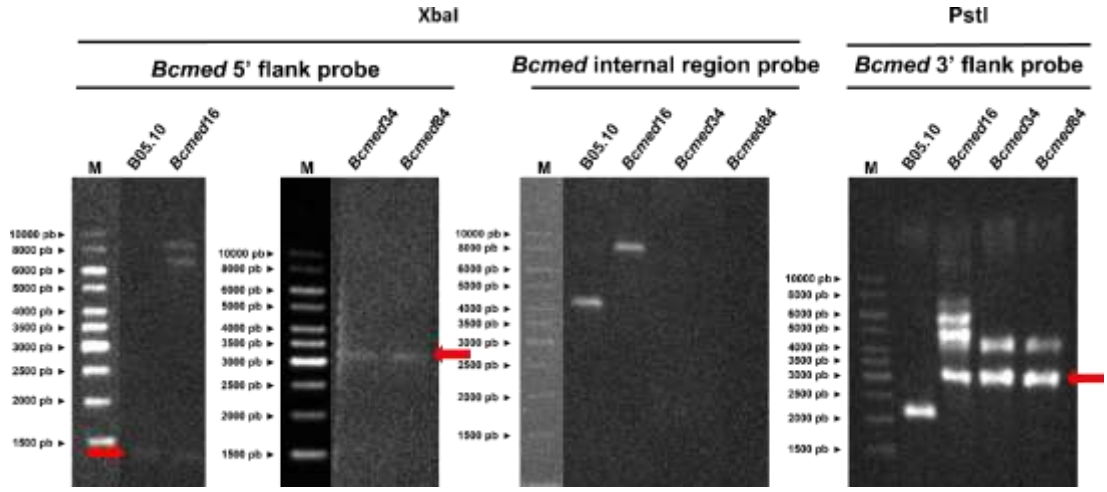

Figure 40. Analysis by Southern blot of *B. cinerea* transformants with the plasmid pAAD4. Genomic DNA samples from strains B05.10, *Bcmed*34, *Bcmed*84 and *Bcmed*16 were digested with the restriction enzyme *Xba*I when hybridization took place with the probe of the 5' flank or with the probe of the internal region of *Bcmed* and with the restriction enzyme *Pst*I when hybridization was carried out with the 3' flank probe of *Bcmed*. The digested samples were separated by agarose gel electrophoresis and transferred to a nylon membrane. From left to right: Hybridizations carried out with the probe derived from the 5' flank of *Bcmed*, with the probe from the internal region of *Bcmed* and with the probe derived from the 3' flank of *Bcmed*. The red arrows indicate the informative bands of the genotype indicated for each strain when greater explanatory clarity was considered necessary. B05.10 was used as a negative control. M - Marker 1 kb DNA ladder, Biotools.

As shown in Figure 40, the expected bands pattern was identified for the hybridizations of the B05.10 strain genomic DNA: bands of 1341 bp, 4318 bp and 2067 bp for the probe of the 5' flank, the probe of the inner region and the 3' flank probe, respectively (Figures 39 and 40). Furthermore, it was possible to determine that two candidates, number 34 and 84, were two true mutants for the *Bcmed* gene generated by gene replacement as a consequence of double homologous recombination event at the 5' and 3' flanking sequences of the *Bcmed* gene between the wild-type copy of this gene of the genome and the mutant copy of the pAAD4 vector. Thus, the hybridizations with the probes designed on the 5'and 3' flanks of the gene detected a single band for each transformant of 3095bp and 3034bp, respectively (the second band of around 4000bp that appears in the membrane hybridized with the probe on the 3' flank was attributed to partially digested genomic DNA). Hybridization with the probe of the internal region of the gene did not allow the detection of any band, which is consistent with the loss of the wild-type allele

in these strains. On the other hand, the genomic DNA of another candidate, number 16, presented a band in this last hybridization, but not the one corresponding to the wild-type allele, but around 8000bp. This and the band patterns of the other two hybridizations suggest a possible integration of the mutant allele into the homologous *locus* of the genome of this strain by a single recombination event on the 3' flank of *Bcmed*. Thus, candidate 16 is a transformant carrying the wild-type allele and the mutant allele simultaneously and was named *Bcmed*16. For their part, the two true mutants were named *ΔBcmed*34 and *ΔBcmed*84.

After obtaining the deficient strains in the *Bcmed* gene, a series of experiments was started that aimed to find out if the deletion of the gene caused a phenotype with relevant characteristics in *B. cinerea*in order to carry out its subsequent characterization. In these tests, different combinations of the strain s of interest were used, and their mycelial morphology, sporulation capacity and capacity to produce microconidia were evaluated.

3. Mycelial morphology of *ΔBcmed* strains

The first trait to be evaluated in the mutant strains was the morphology of their mycelium during saprophytic growth on a synthetic medium. According to section 2.2 on Materials and Methods, the strains B05.10, *ΔBcmed*34 and *ΔBcmed*84 were inoculated in the centre of MEA plates where they were kept in incubation for three days in the case of the wild-type strain and six days in the case of mutant strains, affected in their growth rate. After these times, a photographic record was made under the microscope, and it is represented in Figure 41.

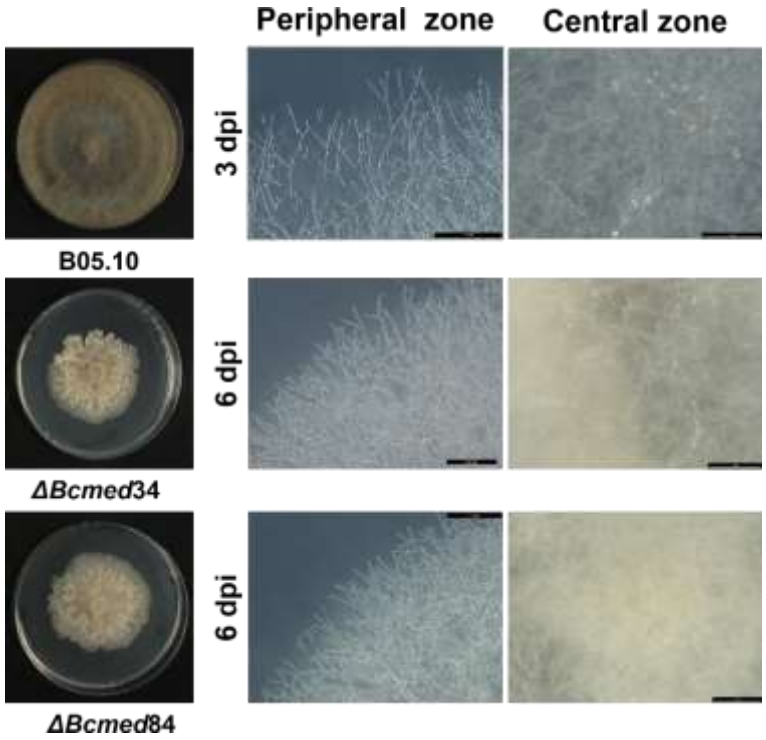

Figure 41. Photographs of colony morphology and optical microscopy images of the fungal growth of the central and peripheral zones of *B. cinerea* B05.10, *ΔBcmed*34 and *ΔBcmed*84 colonies after 3 or 6 days on solid medium MEA under incubation under standard conditions. dpi - days post inoculation. Scale bars, 1 mm.

The two strains deficient in the *Bcmed* gene are affected in their ability to grow saprophytically on synthetic media, with a considerable delay in their growth compared to B05.10 for a given time. With the naked eye, the colonies they form have a denser mycelium than that of the wild-type strain and are apparently sterile. These assumptions are confirmed by optical microscope images on the 6 -day-old plates. In the peripheral zone of the colonies, the denser appearance of the mycelium is due to a greater branching of the hyphae and a more compact growth than that of the wild-type strain. In the central zone of the plate, the more mature mycelium presents masses of cottony and whitish aerial hyphae, where the presence of conidiophores is not observed. On the other hand, the mycelium in the central zone of the plates inoculated with B05.10, for half the incubation time used in the mutant strains, shows a growth closer to the surface of the medium and less dense. Furthermore, conidiophores with macroconidia are already visible (Figure 41). On the other hand, the mutant mycelium has a perpetual beige colour that never becomes the characteristic dark brown of the strains, which would suggest a possible impairment of melanin synthesis.

4. Sporulation capacity of *ΔBcmed* strains.

The above results indicate the inability of the mutant strains to sporulate. However, the cultures used in the analysis were not incubated in optimal conditions for this. Therefore, to rule out that the absence of conidiophores in the mutant mycelium was not a consequence of unsuitable environmental conditions, an assay was carried out in which the reference strain and the two mutant strains were incubated under conditions conducive to sporulation (see section 5 of Materials and Methods). A part of the plates of each strain was exposed to ultraviolet light (at a wavelength that stimulates the sporulation of the fungus) and subsequently kept in darkness until the moment of taking images. A second part of the plates was also exposed to ultraviolet light but was then kept in the presence of white light. A third part, used as a control, was always kept in the dark without being exposed to ultraviolet light. This analysis was performed on two different media, MEA and Gamborg's B5, and the results obtained are shown in Figures 42 and 43.

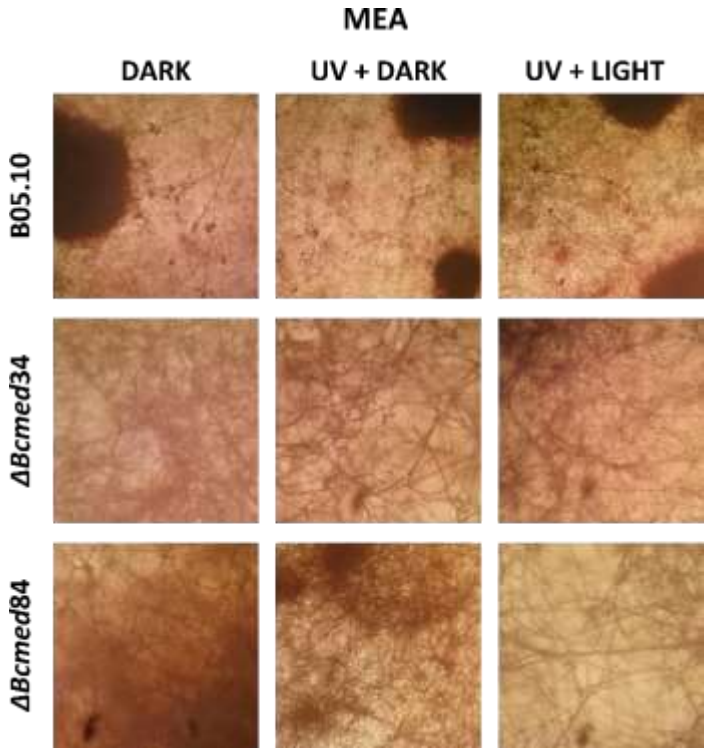

Figure 42. Microscopy analysis of macroconida production of *B. cinerea* B05.10, *ΔBcmed*34 and *ΔBcmed*84 strains on solid MEA medium. The strains were incubated under standard growth conditions until the colony reached the edge of the plate. Then, a fraction was exposed to UV light followed by incubation in the dark (UV + DARK). Another fraction was exposed to UV light followed by incubation in light (UV + LIGHT) and another fraction was incubated in the dark at all times without being exposed to UV light (DARK). The images were taken at different scales.

In the case of the test carried out using the MEA medium, B05.10 was able to sporulate under all the evaluated conditions. However, greater sporulation was observed when it was exposed to UV light compared to when it was not. The presence of sclerotia was also observed in the three types of culture. The *ΔBcmed* strains had a uniform behaviour among themselves, but different from that of the wild-type strain. Thus, neither *ΔBcmed*34 nor *ΔBcmed*84 showed sporulation under any of the incubation conditions, always showing their characteristic sterile beige mycelium (Figure 42). The presence of sclerotia was not observed either in the mutants cultures under the experimental conditions considered .

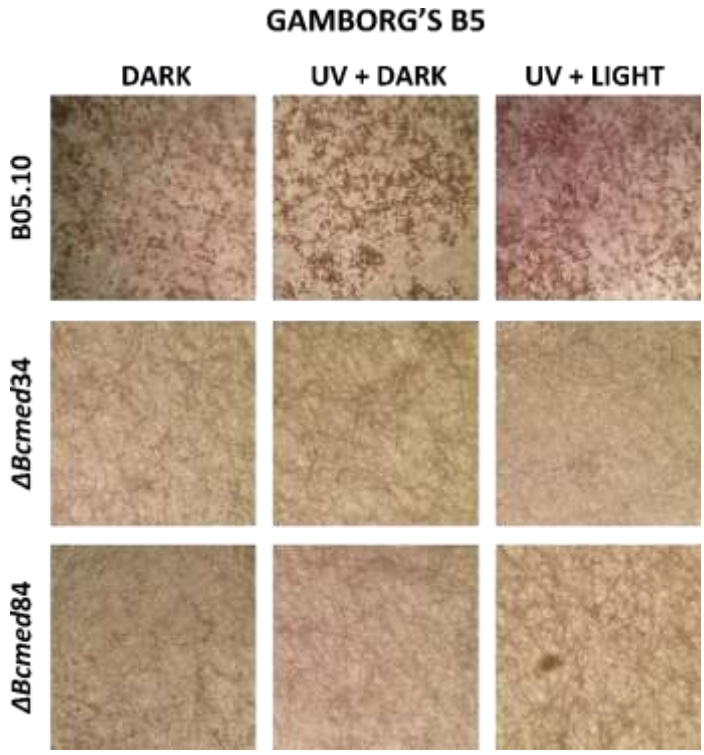

Figure 43. Microscopy analysis of macroconida production of *B. cinerea* B05.10, *ΔBcmed*34 and *ΔBcmed*84 strains on solid Gamborg's B5 medium. The strains were incubated under standard growth conditions until the colony reached the edge of the plate. Then, a fraction was exposed to UV light followed by incubation in the dark (UV + DARK). Another fraction was exposed to UV light followed by incubation in light (UV + LIGHT) and another fraction was incubated in the dark at all times without being exposed to UV light (DARK). The images were taken at different scales.

The results obtained using Gamborg's B5 as a culture medium are equivalent to those obtained on MEA medium. B05.10 presented sporulation in the three growth conditions, being more intense in those in which UV light was applied. At the same time, no conidiophores or spores were observed on the plates where the mutant strains were grown for any of the conditions. Furthermore, B05.10 produced sclerotia in the three types of culture, while the *ΔBcmed* strains did not form this type of non-sporic structures.

5. Microconidia production capacity of *ΔBcmed* strains.

The next aspect to be evaluated in the *ΔBcmed* mutants was their ability to produce microconidia. Thus, according to section 6 of Materials and Methods, the strains B05.10, *ΔBcmed*34 and *ΔBcmed*84 were inoculated on plates with two different media, MEA and PDA. The plates were subsequently incubated under stress conditions (exposure to cold and absence of light for prolonged periods of time) that favoured the production of the desired structures and images were taken of the biological material harvested from them without make numerical estimates (Figure 44).

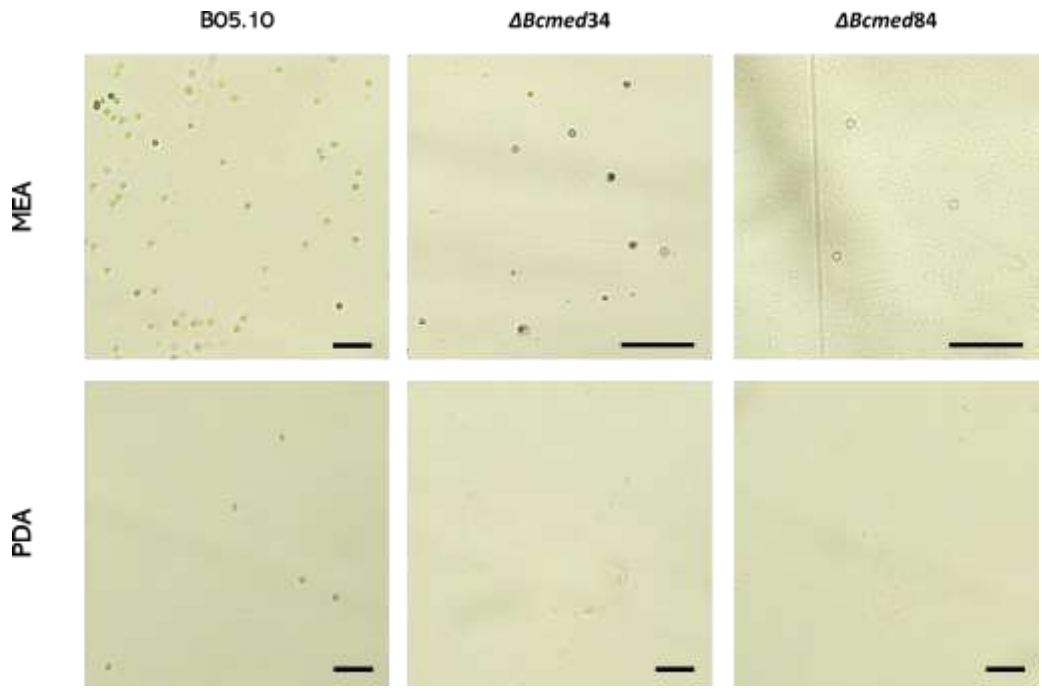

Figure 44. Optical microscopy images of the production of microconidia of *B. cinerea* B05.10, *ΔBcmed*34 and *ΔBcmed*84 strains on solid medium MEA and PDA after two months of incubation in the dark, the first month at 13°C - 14°C and the second at 0°C. Scale bars, 20 µm.

The same volume of microconidia suspensions of the different strains prepared in the same conditions were used to prepare slides for the qualitative evaluation under the microscope of their capacity to produce, or not, these structures. The B05.10 strain was able to produce microconidia in the two evaluated media, MEA and PDA, but the production was several times lower in the latter medium, under our experimental conditions. In the case of the two mutant strains, both behaved in a parallel manner, presenting microconidia when they were grown in the MEA medium, but not when they were grown in the PDA medium. The density of this type of spores produced by these strains in the MEA medium appeared to be considerably lower than that presented by the wild-type strain for the same conditions.

At this point, the manifestation by the *ΔBcmed* mutants of a phenotype very different from that of the reference strain was evident, showing alterations that affected both sexual and asexual development. Therefore, before continuing with the characterization of *Bcmed*, it was decided to generate a complemented transformant derived from one of the mutant strains by reintroducing the wild- type allele of *Bcmed* at an unknown, ectopic, position in the genome. In this way, it would be possible to verify that the mutant phenotype observed was specifically due to the deletion of the gene.

6. Construction of the *Bcmed*-complemented strain.

To carry out the complementation, the wild type allele has to be introduced in the mutant genetic background and a selection marker different from the one used to generate the mutant (resistance to hygromycin) is needed. To this end the plasmid pNR4 was used. As indicated in section 12.5 of Materials

and Methods, this plasmid contains the nourseothricin resistance cassette as a selectable marker for fungi. The *Bcmed* wild type allele would be cloned in it using the Gateway methodology.

First, the ORF of *Bcmed* gene was amplified by PCR. For this, it was necessary to design two primers made up of two parts. One part was a 21-22 nucleotide stretch of the promoter and terminator region sequence of the gene, respectively. The other part was a stretch of 29 nucleotides corresponding to the *attB* adapter sequences typical of the Gateway® system and that together with the *attP* sequences present in pNR4 allowed the cloning of the wild-type allele of *Bcmed* in this vector by recombination (see section 13.3 of Materials and Methods). The thus designed pair of primers (B3140F/B3140R, see Table 8, Appendix) amplified a 4034 bp fragment in length that included 780 bp from the promoter region and 809 bp from the terminator region.

The amplified fragment was purified and added to a BP recombination reaction together with pNR4 as a donor vector. The DH5α strain of *E. coli* was transformed with the recombination product using the heat shock method and six of the resulting colonies were screened by PCR, using primers B3140F/B3140R, to detect those carriers of the complementation plasmid. The six colonies analysed were positive, as they carried the complementation plasmid. Next, plasmid DNA from each colony was purified and analysed by digestion reactions with the restriction enzymes *EcoR*I and *Nar*I. This analysis made it possible to verify that the sizes of the fragments released in each digestion were those expected according to the predicted restriction map. Finally, samples undigested DNA of plasmid pNR4 and of the plasmid purified from colony T1 were resolved in the same electrophoresis to make a comparison of sizes between the empty vector and the vector with the cloned fragment (Figure 45). The T1 plasmid was selected as the complementation vector and was named pFAME. It was stored in *E. coli* at -80 °C.

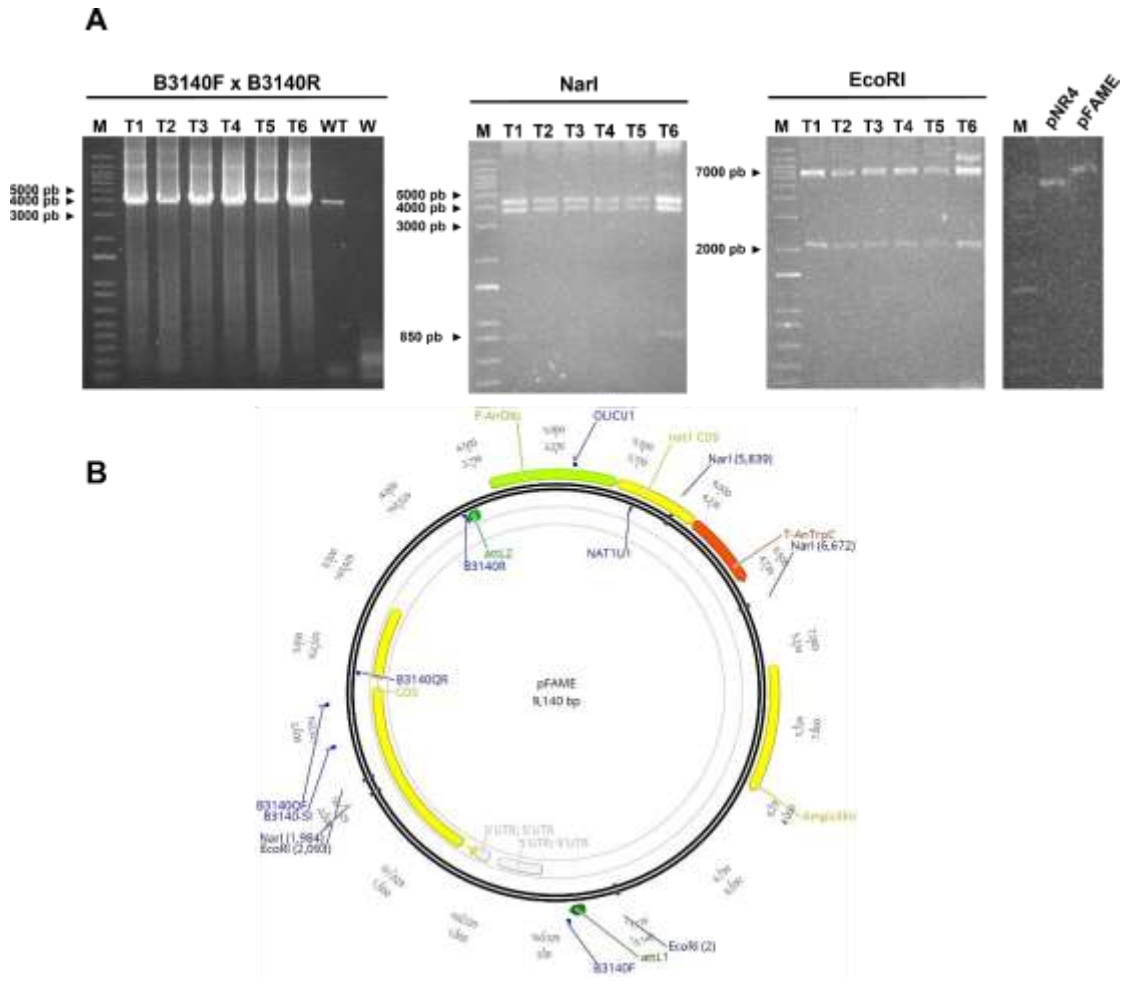

Figure 45. (A) Analysis by means of PCR reactions and enzymatic digestion of *E. coli* clones obtained upon transformation with the BP recombination reaction between pNR4 and *Bcmed* gene fragment. The PCR reactions were performed using plasmid DNA from the candidate clones (T1-T6) as template and the oligonucleotides pair B3140F/B3140R described in Table 8 of Appendix. The expected amplified fragment was 4034bp (first gel on the left). The digestion reactions were also carried out using plasmid DNA from the candidate clones and the fragments released were 833bp, 3855bp and 4452bp in the *Nar*I digestion, and 2091b and 7049bp in the *EcoR*I digestion (second and third panels from the left). Size comparison between undigested pNR4 and pFAME plasmid DNA is shown in the last panel. M – Marker 1 Kb Plus DNA Ladder, Invitrogen. T1-6 – Colonies of transforming *E. coli* and carriers of the analysed plasmid. WT/W – PCR reaction in which B05.10 strain genomic DNA, used as positive control, or Milli-Q water, used as negative control, was used as substrate, respectively. (B) Scheme of vector pFAME. It highlights the cloned genomic DNA fragment flanked by the sequences *attL*, the ampicillin-resistance cassette, the nourseothricin-resistance cassette, the annealing positions of the oligonucleotides B3140F, B3140R, B3140-SI, B3140QF, B3140QR, OLICU1 and NAT1U1 and the cleavage sites of the restriction enzymes *EcoR*I and *Nar*I, used in the aforementioned analyses.

Once obtained, protoplasts of the mutant strain *ΔBcmed*84 were transformed with plasmid pFAME, following the indications of section 16.2 of Materials and Methods. The plasmid sample used to transform was previously digested with the restriction enzyme *Sac*I, an enzyme that cuts only once in its backbone so that the plasmid was linearized without affecting any ORF of interest. This step of previous linearization of the plasmid by digestion was necessary to facilitate its penetration into the cells. The candidate colonies that grew in the plates where the protoplasts were seeded, were kept in selective medium during successive passages that promoted the homokaryosis process and then monosporic cultures were obtained. The genomic DNA of these was extracted, following the indications of section 10.1 of Materials and Methods, from mycelium samples grown in liquid medium to be used in a PCR

analysis that would allow to determine if the plasmid pFAME had been corre ctly integrated in their genomes.

Three pairs of oligonucleotides capable of amplifying a fragment of the internal region of *Bcmed* (B3140-SI / B3140QR), of the ORF of the hygromycin resistance cassette (HygF-DG/RvHyg) and of the ORF of the nourseothricin resistance cassette (OLICU1/NAT1U1), respectively (primers described in Figures 38 and 45 and Table 8, Appendix), were used. This analysis allowed the detection of a single complemented transforming strain that was named *ΔBcmed*-C (Figure 46).

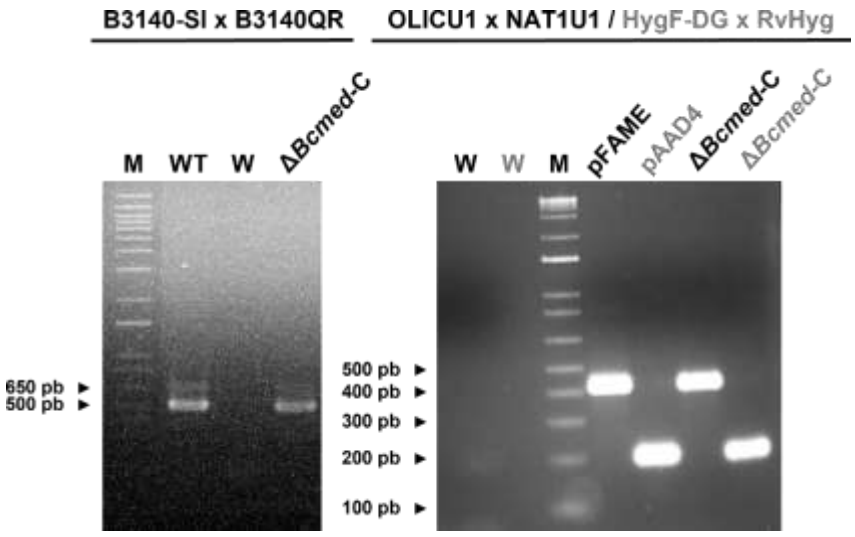

Figure 46. Analysis by PCR of the *B. cinerea* transformant obtained with plasmid pFAME. The PCR reactions were carried out using genomic DNA of the candidate as template and the pairs of oligonucleotides B3140-SI/B3140QR, HygF-DG/RvHyg and OLICU1/NAT1U1 amplifying fragments of 513pb, 199pb and 420pb, respectively. The annealing positions of the primers B3140-SI/B3140QR and OLICU1/NAT1U1 are indicated in Figure 45B and those of the primers HygF-DG/RvHyg are indicated in Figure 38. M – Marker 1 Kb Plus DNA Ladder, Invitrogen. WT / W – PCR in which B05.10 strain genomic DNA (used as positive control), or Milli-Q water (used as negative control), was used as substrate, respectively. pFAME / pAAD4 / *ΔBcmed*-C – PCR in which pFAME plasmid DNA (used as positive control), pAAD4 plasmid DNA (used as positive control), or complemented *ΔBcmed*84 strain genomic DNA, was used as substrate, respectively.

7. Saprophytic growth capacity of *ΔBcmed* strains.

Once the complemented strain was available, the characterization of the *ΔBcmed* mutant strains continued. The next aspect to be evaluated was its saprophytic growth capacity on synthetic media. This is a trait that had already been previously analysed in a first approximation, but then no quantitative analyses had been carried out to support the behaviour observed in the mutant strains. Now, the strains B05.10, *Bcmed*16, *ΔBcmed*34, *ΔBcmed*84 and *ΔBcmed*-C were cultured in plates with MEA medium (see section 2.2 of Materials and Methods) for six days, in which measurements of the perpendicular diameters of the colonies were taken every 24 hours. In addition, its growth rate was estimated between each 24 - hour period considered (Figure 47).

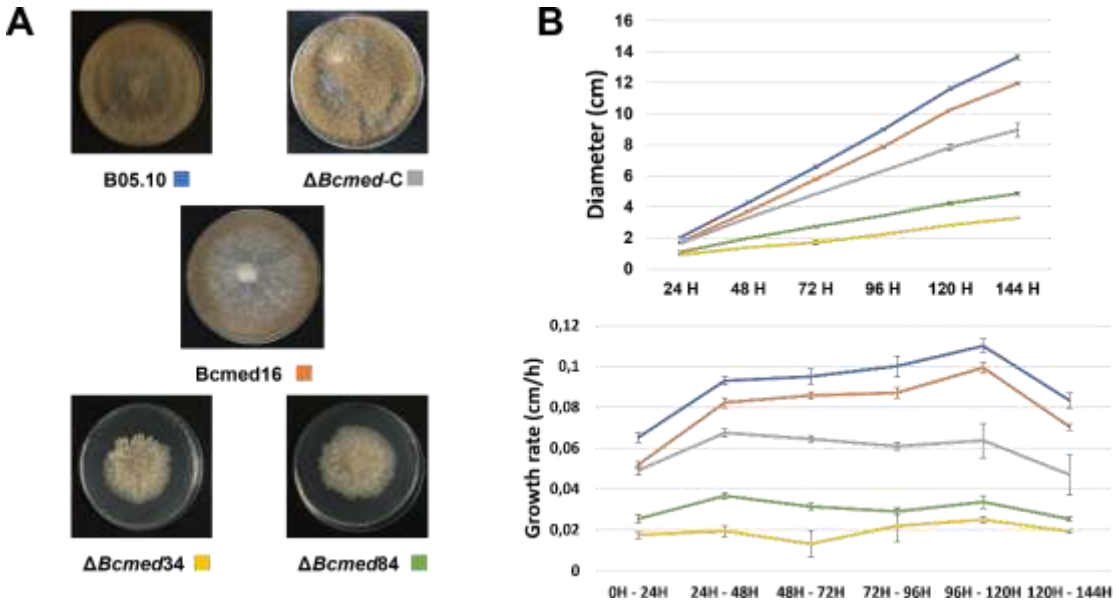

Figure 47. Analysis of the saprophytic growth capacity of *B. cinerea ΔBcmed* strains. (A) Comparison of the morphology of the colonies of *B. cinerea* B05.10, *Bcmed*16, *ΔBcmed*34, *ΔBcmed*84 and *ΔBcmed*-C strains after two weeks of incubation on solid medium MEA under standard conditions. (B) Colony diameter and colony growth rate of the strains in (A) grown in MEA medium under standard culture conditions. The growth data were taken at the different sampling times: 24h, 48h, 72h, 96h , 120h and 144h and the growth rate was calculated for the 24-hour intervals between the sampling times considered. Values are the means of three replicates ± SD.

Earlier in this chapter, the peculiar phenotype of Δ*Bcmed* strains regarding the appearance of their colonies to the naked eye in comparison with that of B05.10 had already been described. The inclusion of the *ΔBcmed*-C strain in this comparison allows us to deduce that the insertion of the *Bcmed* gene in the mutant background reversed the effects derived from the deletion of the gene, restoring the sporulation and growth capacity at levels similar to those of the wild-type strain (Figure 47A). However, this is not entirely true if the results related to the saprophytic growth capacity of one or the other strains are analysed. The B05.10 strain presented the greatest increase in its growth rate during the first 48 hours (0.065 cm/h between 0h-24h and 0.092 cm/h between 24h-48h), showing a mean colony diameter of 2.06 cm and of 4.29 cm at 24 hours and 48 hours, respectively. Thereafter , and until 120 hours, the diameter of the colony continued to increase, but at a less pronounced rate (6.57 cm at 72 hours, 8.98 cm at 96 hours, and 11.62 cm at 120 hours). This was the reflection of attenuated growth rate values (0.095 cm/h between 48h-72h, 0.100 cm/h between 72h-96h and 0.110 cm/h between 96h-120h). In the last 24-hour period considered, B05.10 presented a decrease in its growth rate (0.083 cm/h between 120h -144h), measuring the diameter of its colony 13.64 cm on average at 144 hours. For its part, *Bcmed*16 was the strain that showed the closest behaviour to that of B05.10 among the other strains evaluated. Its diameter and its growth rate were similar to those of the wild type but taking slightly lower values for all the times considered. Its growth rate increased from 0.051 cm/h between 0h-24h to 0.082 cm/h between 24h-48h. Its diameter was 3.72 cm at 48 hours and increased to 10.25 cm at 120 hours. During this course, their growth rate increased more slowly than in the first 48 hours. Between 120h-144h, this parameter decreased from 0.099 cm/h of the previous section to 0.070 cm/h and the diameter of its colony measured

11.96 cm on average at 144 hours. Meanwhile, the two mutant strains had a very similar behaviour between them. In both, their growth rate remained more or less constant during the time considered in the analysis, oscillating between 0.013 cm/h and 0.025 cm/h in *ΔBcmed*34 and between 0.025 cm/h and 0.036 cm/h in *ΔBcmed*84. In addition, *ΔBcmed*34 and *ΔBcmed*84 showed a decrease in their growth rate between 120 hours and 144 hours in a similar way to the reference strain, but in a softer way and their colonies were 3.29 cm and 4.85 cm in mean diameter at the 144 hours, respectively. The complemented strain showed an intermediate behaviour between B05.10 and the mutant strains. Its growth rate varied in parallel with that of B05.10 during the time of the assay. That is, this parameter showed a pronounced increase in the first 48-hour interval and decrease and last 24-hour interval of the test, respectively, very similar to those of the wild-type strain. Between one interval and another, its rate maintained a certain constancy. Despite this similarity, the growth rate always remained below the wild-type values, but above the values of the mutants. Thus, *ΔBcmed*-C had a growth rate of 0.049 cm/h between 0h-24h and 0.067 cm/h between 24h-48h. In the 48h-120h stretch, the data remained between 0.067 cm/h and 0.060 cm/h and in the last 24 hours, it was 0.063 cm/h between 96h-120h and 0.047 cm/h at 120h-144h. The mean diameter of its colony was also maintained between the reference values and the mutants, reaching the maximum value of 8.97 cm in the last sample point considered (Figure 47).

8. Virulence of *ΔBcmed* strains.

Since the mutation in *Bcmed* gene impaired the ability of the fungus to grow, it was considered that the ability of the pathogen to infect the host could also have been affected. To assess this aspect, bean plant leaves were infected with inocula of the strains B05.10, *Bcmed*16, *ΔBcmed*34, *ΔBcmed*84 and *ΔBcmed*-C following the indications of section 7.2 of Materials and Methods. After 72 hours of infection, the aggressiveness of the strains was evaluated by the mean of the measurements of the two perpendicular diameters of the lesions generated on the leaves (Figure 48).

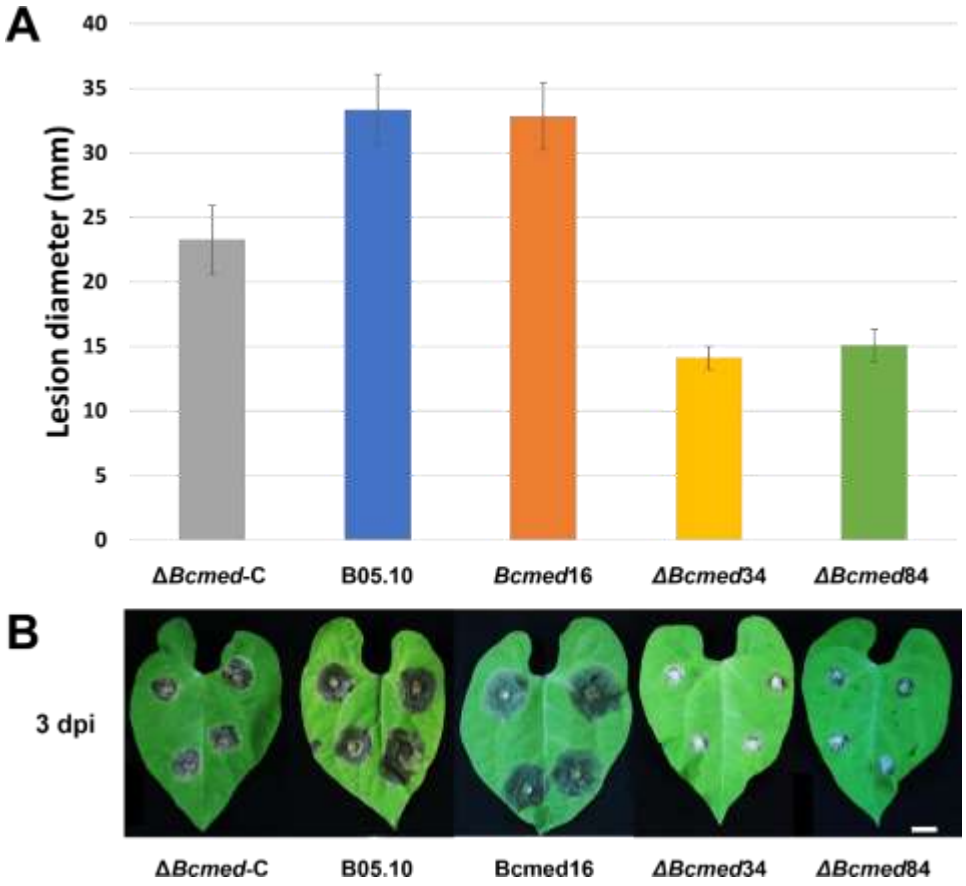

Figure 48. Evaluation of the aggressiveness in leaves of *P. vulgaris* of *B. cinerea ΔBcmed* strains. (A) Primary leaves of *P. vulgaris* plants were inoculated with plugs of 4-days-old vegetative mycelia of B05.10, *ΔBcmed*-C and *Bcmed*16 strains or with plugs of 7-days-old vegetative mycelia of *ΔBcmed* mutant strains. The inoculated leaves were incubated at 22°C with a photoperiod of 16 hours of light and 8 hours of darkness for 72 hours. Average lesion diameters and standard deviations were calculated from six lesions per strain with two measurements per lesion in assays performed in triplicate. (B) Representative images of the leaves inoculated with the indicated strains at 3 days post inoculation (3 dpi). Scale bars, 20 mm.

B05.10 and *Bcmed*16 showed very similar behaviour during the infection process, both showing a mean lesion diameter of 33 mm at 3 dpi. In contrast, the mycelium of *ΔBcmed*34 and *ΔBcmed*84 barely expanded from the inoculum in the same period of time, generating lesions of 14 and 15 mm in mean diameter at 3 dpi, respectively. *ΔBcmed*-C showed a level of aggressiveness intermediate between that of the reference strain and that of the mutant strains, the mean diameter of its lesions being 23 mm at 3 dpi (Figure 48).

9. Septation of *ΔBcmed* strains.

Another characteristic that was considered in the analysis of the *ΔBcmed* mutants was the septation of the mutant hyphae. Given the alteration in the growth pattern of the *ΔBcmed* strains observed previously in this chapter, it was thought that the septa localization and frequency in the mutant hyphae could be affected. Therefore, calcofluor white staining assays of mycelium samples from strains B05.10, *ΔBcmed*84 and *ΔBcmed*-C grown on solid medium were carried out. The different preparations were used to estimate the distance from the first septum of the hypha to its tip and to the second septum, respectively (Figure 49).

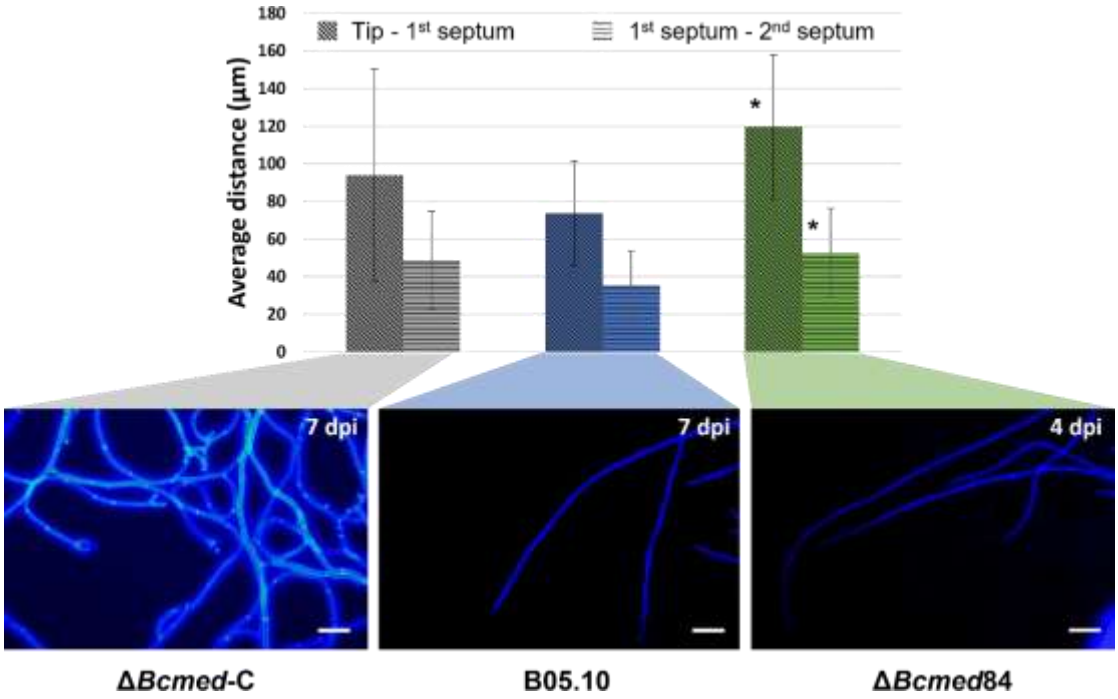

Figure 49. Distribution of septa in *B. cinerea ΔBcmed* strains hyphae. B05.10, *ΔBcmed*84 and *ΔBcmed*-C were grown on solid medium MEA covered with cellophane for 4 days (B05.10 and *ΔBcmed*-C) or 7 days (*ΔBcmed*84). Hyphae were stained with calcofluor white stain to visualize septa. The mean distance between the hyphal tip and the first septum and between t he fir st and second septa and standard deviations were calculated from 40 hyphae per strain in tests performed in triplicate (* indicates significant differences at P <0.05 - Student's t - between B05.10 and *ΔBcmed*84 strains). Representative images of mycelium samples stained from the indicated strains at 4 or 7 days post inoculation in plate (dpi) are shown below the histogram. Scale bars, 55 µm.

The mean distance from the tip to the first septum in the wild-type hyphae was 73.70 µm while the mean distance between the first and second septum was 35.15 µm. The septa frequency of the mutant strain *ΔBcmed*84 is lower with respect to that of the wild-type strain since the mean distance between the tip of the hypha and the first septum and between this and the se cond septum was greater than in B05.10 (119.59 µm and 52.49 µm, respectively). As already observed with its growth capacity on synthetic media and on the host, *ΔBcmed*-C presented intermediate septa frequency values between those of the wild type and of the mutant strain. Thus, 93.99 µm was the mean distance measured between the tips of its hyphae and the first septum and 48.61 µm was the mean distance from the first to the second septum (Figure 49).

The application of the statistical analysis of the Student t-test to the data of these strains, allowed to conclude that there are significant differences between the septa frequency (distance from the first septum of the hypha to its tip and to the second septum) of the strains B05.10 and ΔBcmed84. This indicates that the septa formation pattern of the fungus was influenced by the deletion of the *Bcmed* gene in the mutant strains.

10. *Bcmed* expression analysis.

With the intention of gaining an understanding of *Bcmed* in our study system, we analysed its expression levels in the B05.10 strain. For this, as described in sections 2.2 and 17.3 of Materials and Methods, an qPCR analysis was carried out using as the template cDNA samples generated from RNA extracted from samples of mycelium cultured in liquid medium in agitation and collected at different time points during early development of the fungus (from resting spores: -1 hours, to 20 hours developing mycelium). Three independent assays were carried out under these conditions with the harvest of two technical replicas of samples in each one of them and the PCR reactions were carried out in triplicate for each sample (used primers described in Table 8, Appendix). The expression pattern of *Bcmed* in the mentioned conditions is presented in Figure 50.

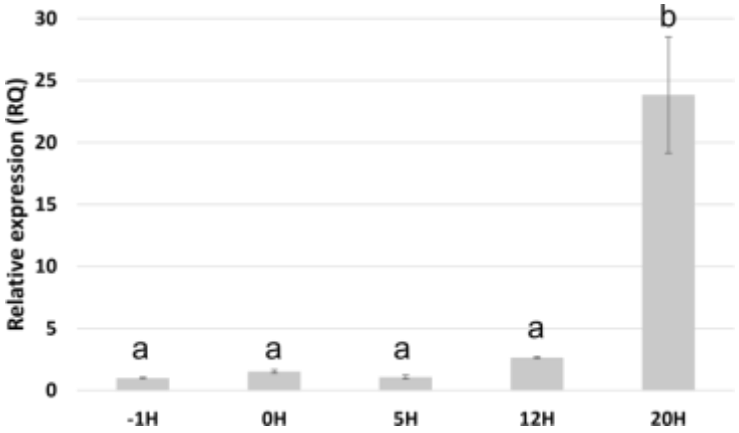

Figure 50. *Bcmed* expression analysis by qPCR in *B. cinerea* wild-type B05.10 strain during saprophytic growth in liquid minimal Gamborg's B5 medium culture in agitation. Samples were taken are the indicated time points. At each time point the expression values were normalized using the constitutively expressed ubiquitin *Bcubq*1 gene and referenced to the value obtained for the sample collected at -1h in which the spores were collected immediately after being inoculated into the corresponding flask (arbitrary value of 1.0). Bars show the means ± standard deviations of three independent biological experiments. The different letters represent significantly different groups (P < 0.05) as determined by one-way ANOVA followed by a Tukey's HSD test.

As shown, at the time points 0H and 5H, which delimitates the temporal window when germination occurs in the experimental conditions considered, the level of expression of *Bcmed* does not change significantly in relation to the level of expression in resting conidia (-1H). It increases at time point 12H (2.5 X), when the germ tubes elongate and reaches very high levels (24 X) when the mycelium grows and branches actively. Therefore, expression of *Bcmed* is developmentally regulated.

Discussion

In this chapter, the characterization of the *B. cinerea Bcmed* gene has been carried out using a strategy consisting of deleting the gene and analysing the resulting phenotypes. To complete our analysis of the evaluation of the function of *Bcmed* in the fungus, the complementation of one of the used mutant strains was carried out by reintroducing the wild-type allele in an unknown place in its genome. However,

the complemented strain failed to show a complete recovery of normal behaviour in terms of development, always presenting intermediate phenotypes between the mutant and the wild-type. This is an unexpected observation. Failure to fully restore the wild-type phenotype have been reported by other authors. A similar situation was reported by Rodenburg *et al*. (2018) when trying to complement mutants of *B. cinerea* for the four *mat* genes. For the *mat*1-1-5 gene, they obtained three independent transformants with an ectopic insertion of the intact gene (including flanking sequences, as in our case) in the mutant background. When these transformants were tested in crosses, all failed to show recovery of normal mating behaviour. As a possible cause that explained this result, they raised the possibility that the ectopic integration of the *mat*1-1-5 gene may have resulted in an inadequate level or temporal pattern of transcription, either because of the wrong chromatin context or because of the occurrence of meiotic silencing by unpaired DNA (MSUD) in an ectopic location. They were supported by equivalent results obtained in *N. crassa* crosses using a mutant strain that contained the *matA* gene in an ectopic location (Shiu *et al*., 2001).

Determining whether events of this type occur in our complemented strain would require further analysis, such as the study of gene expression levels compared to B05.10 or Δ*Bcmed* strains. In any case, using the Apollo platform, a collaborative, real-time, genome annotation web-based editor, we were able to determine the real extension of the promoter region of *Bcmed*, which appeared to be around 2.8 kb. In contrast, our complementation construct contained only 780 bp of the promoter region. It is possible, therefore, to raise the possibility that the lack of the complete promoter in the copy or copies present in the complemented strain is the true responsible for the behaviour observed in *ΔBcmed*-C, despite the fact that it is commonly accepted that the most important transcriptional regulatory elements of the promoter region of a gene (core promoter) are found around the first 800 bp upstream of the translation start codon. Despite this drawback, results have been obtained suggesting that the BCMED protein is necessary for virulence and asexual development processes in the fungus. Comparison of these results with those derived from similar analyses in other fungi reveals differences, but also similarities in the way in which this gene performs its function among these species.

The analysis of the expression pattern of *Bcmed* allowed us to propose that, during the first phases of the development of the fungus (the phase of activation of the spores, germination, and emission of the germ tube and during the elongation phase of the young mycelium), the gene is expressed in a stable, constitutive way, and its level increases enormously during the growth of the mature mycelium. These results represent a corroboration of the conclusions derived from the aforementioned analysis of global gene expression carried out in the past in our laboratory on a comparison between germinating spores with mature mycelium in development (Santander D.I., Doctoral Thesis. University of Salamanca, 2014). A developmentally regulated expression of the gene could therefore be proposed. This hyphal expression of *Bcmed* detected in both analyses is not exclusive to *B. cinerea*. It has also been detected in other fungi where gene expression has been studied. Thus, the expression of *medA* was analysed in mycelium of *A. fumigatus* grown in liquid medium. In this fungus, the gene was expressed, as in *B. cinerea* ,

constitutively. During the first 8 hours of incubation, its levels were relatively low and subsequently became three times higher at 12 hours. This higher level of expression remained constant for the remaining time that the assay lasted, five days (Gravelat *et al*., 2010). It must be considered that *B. cinerea* does not produce conidiophores when grown in liquid medium. Therefore, our analysis does n ot allow us to determine whether there is a possible induction of *Bcmed* during sporulation of the fungus, as has been observed in *F. oxysporum* and *A. nidulans*. In the first, *ren1* was expressed both during conidiation and during vegetative growth in liquid medium (Ohara *et al*., 2004). In *A. nidulans*, the expression of *medA* has been observed in germlings and vegetative hyphae, both in liquid medium and in solid medium. In the latter, in addition, in conidiophores (Ichinomiya *et al*., 2005; Chung *et al*., 2011). In contrast, *acr1* presented a spore-specific expression in *M. grisea* (Lau and Hamer, 1998). This certain homogeneity in gene expression is not maintained between species for other aspects studied.

The *ΔBcmed* strains saw their growth capacity on synthetic media very limited, showing a mycelium with a cottony appearance and lacking conidiophores with macroconidia. In *A. nidulans*, the *medA* mutation did not cause a defective mycelium in the growth of its hyphae nor did it lead to a sterile mycelium phenotype, lacking conidiophores, but it did affect their morphology, causing the appearance of aberrant-looking conidiophores with reiterated metulae-like cells and secondary conidiophores. Furthermore, a delay in conidial differentiation was observed (Clutterbuck, 1969; Busby *et al*., 1996; Ichinomiya *et al*., 2005; Etxebeste *et al*., 2010). In *A. fumigatus*, although the conidiophores were affected by the gene mutation while remaining poorly developed, they did not present the medusoid phen otype of *A. nidulans*. Conidiation was also greatly decreased, but mycelial growth rate was unaffected by deletion in solid or liquid medium (Gravelat *et al*., 2010; Al Abdallah *et al*., 2012). The normal conidiophores of the wild-type strain of *F. oxysporum* were replaced by rod-shaped cells in a single chain in the mutant in the *ren1* gene. However, the latter was not affected in its ability to grow on synthetic media nor did it present differences apparent to the naked eye in the morphology of its colony compared to the wild-type strain (Ohara *et al*., 2004). A very similar phenotype was detected in mutants of the *acr1* gene of *M. grisea* where hyphal growth was not affected by the mutation, but the formation of conidiophores was affected, which were replaced by an acropetal pattern of conidiation (development from the base towards the tip) (Lau and Hamer, 1998; Nishimura *et al*., 2000).

The deletion of the *Bcmed* gene in *B. cinerea* also apparently affected mycelial pigmentation since the mutant hyphae were lighter brown in colour than wild-type hyphae and never darkened. Given that melanin is the pigment that gives the pathogen its typical colour of grey mould (Doss *et al*., 2003), this phenotype could suggest that the synthesis of this pigment is affected by the mutation. Of all the *Bcmed* orthologs studied, only an effect on conidial pigmentation has been reported for *medA* in *A. fumigatus*. Among the developmental defects of the *ΔmedA* mutant conidia detected by Gravelat *et al*. (2010), a delay in their pigmentation was found. These remained bright green for a longer time and did not darken until after two weeks of growth. They examined the expression of a cluster of six genes which mediates conidial pigmentation and DHN melanin synthesis in the pathogen and observed that the transcriptional

levels of these genes were modestly reduced in 48 -hour-growing mycelium samples. Our data also suggest a negative regulation of the melanin synthesis homologous genes, but the repressive effect is probably more intense than in *A. fumigatus* since *ΔBcmed* mycelium does not recover the wild-type coloration at any time.

Our results also indicate that the mutation altered septation and the ability to produce microconidia in our study system. This last characteristic was also affected in the *F. oxysporum* strain *ΔREN*1, but in a different way. It was not eliminated, but was replaced, like its production of macroconidia, by the production of rod-shaped, conidium-like cells (Ohara *et al*., 2004). For its part, septation is also altered in those species where the *Bcmed* ortholog mutation modifies the pattern of conidia formation, these being formed by acropetal division. This results in chains of conidia linked together where the oldest conidia are at the base and the youngest are at the top. This is the case again of *F. oxysporum*, but also of *M. grisea*. In the first, wild-type macroconidia and microconidia are formed from phialides by basipetal division developmental mode from the apex toward the base without catenation of cells. The macroconidia are falcate and have three or four septa while microconidia are ellipsoidal and have no or one septum. The rod-shaped cells produced by the *ΔREN*1 strain, for their part, had no or one septum (Ohara *et al*., 2004). In *M. grisea*, conidiation takes place sympodially (development of conidia on a geniculate or zig-zag rachis). Spores generally have two septa and three spore compartments and easily detach from the conidiophore. Instead, the *acr*1 mutation causes the spores to be produced in a chain with one to more than ten septa. Furthermore, the boundaries between spor es are occasionally undefined and mutant spores do not readily detach (Lau and Hamer, 1998).

Virulence is significantly reduced in *Bcmed* ortholog mutants in *U. maydis*, *A. fumigatus*, and *M. grisea* (Chacko and Gold, 2012; Gravelat *et al*., 2010; Al Abdallah *et al*., 2012; Lau and Hamer, 1998; Nishimura *et al*., 2000). However, the *F. oxysporum ren1* mutant retains pathogenicity on susceptible melon plants (Ohara *et al*., 2004). In the case of *U. maydis*, a possible regulatory role of *med1* over the transcription factor *prf1 in planta* was suggested as a possible explanation for the virulence results obtained in maize plants (Chacko and Gold, 2012). Lau and Hamer (1998) suggested that the non- pathogenic phenotype of the *ΔACR*1 mutant could be due, in part, to its inability to produce a tip cell or spore tip mucilage (required for terminating conidiogenesis and arresting further spore growth) and/or its inability to attach to surfaces and form appressoria. A similar assumption was made by Gravelat *et al*. (2010) in the case of *A. fumigatus*, where the impaired virulence of the *ΔmedA* mutant was attributed to its decreased hyphal adherence. The exception posed by the behaviour of *F. oxysporum* in this series in terms of virulence, would be due to its lifestyle and infection mechanisms typical of a soil-borne pathogen. Unlike the airborne pathogens such as *M. grisea* that requires appressoria during infection, *F. oxysporum* directly penetrate root surface without formation of this structures, which indicates that *ren1* is probably not essential for the penetration and colonization of plant tissue (Ohara *et al*., 2004). In our case, the virulence defects observed in the *ΔBcmed* strains on bean leaves could be due, as also suggested by Gravelat *et al*. (2010) in *A. fumigatus*, to alterations in mycelial pigmentation. The *alb1* mutation, a

polyketide synthase belonging to the DHN-melanin pathway cluster, was associated with a significantly reduction of the virulence of *A. fumigatus* in mice (Langfelder *et al*., 1998; Tsai *et al*., 1998; Tsai *et al*., 1999). However, it is more likely that the reduction in the ability of the *ΔBcmed*34 and *ΔBcmed*84 strains to generate dispersive necrotic lesions is a consequence, at least in part, of alterations in their capacity for saprophytic growth and development.

From a macroscopic point of view, the appearance of the lesions produced by the strains evaluated in this regard in this work is similar. In all cases, the production of a necrotic lesion is observed from the agar disk with mycelium that constitutes the initial inoculum. The lesion acquires a brown colour that gradually darkens. This observation suggests that the ability of the mutant strains to penetrate host cells is unaffected, which would rule out some of the conclusions previously made about the *Bcmed* orthologs. However, the small measurements of the mean lesion diameter at 3 dpi indicate that the growth capacity of the mutants in infected tissue is more limited than that of B05.10, *Bcmed*16 or *ΔBcmed*-C. In any case, further analysis will be necessary to find out what are the mechanisms through which *Bcmed* regulates the virulence process of the pathogen. As was done previously with the other fungal pathogens mentioned, the analysis of the expression of genes that are regulated by the *Bcmed* orthologs would shed light on this aspect. Thus, the genes participating in the melanin synthesis pathway(*Bcpks12*, *Bcpks13*, *Bcbrn1*, *Bcbrn2*, *Bcscd1*, *Bcscd2*, *Bcygh1*, *Bcsmr1*, *Bcztf1* and *Bcztf2*), the ortholog of the transcription factor *prf1* of *U. maydis*, *Bcrox1*/Bcin09g02870 (an HMG box (high mobility group box) domain-containing protein) according to a BLASTP-type analysis, or putative adhesin genes would be good candidates.

The phenotypic differences between the *Bcmed* orthologous mutants discussed above, especially those related to the development of conidiophores and conidia, could be due to the different architecture of the conidiophore among species. In *A. nidulans*, the conidiophore is made up of thick-walled hyphal cells (foot cells). These are extended into the air to produce stalks, followed by the formation of a multinucleate vesicle. On top of the vesicle, the metulae and phialides, two layers of uninucleate reproductive cells, are formed by a budding-like process. The phialides undergo repeated asymmetric mitotic division to give rise to chains of conidia. The conidiophores of *A. fumigatus* are the same as those of *A. nidulans*, but lack metulae (Park *et al*., 2016; Ni *et al*., 2010). The conidiophore of *N. crassa* is more simplified and consists of the formation of proconidial chains by repeated apical budding. These chains subsequently undergo a septation process with subsequent separation into spores (Springer and Yanofsky, 1989). *F. oxysporum* produces three types of asexual spores, macroconidia, microconidia, and chlamydospores. Macroconidia are generally produced from the terminal phialides, on the conidiophore stalk, although they are also produced rarely from intercalary phialides, arising directly from the hyph ae. Microconidia are produced from intercalary phialides generally in false heads and chlamydospores are formed from hyphae (Ohara and Tsuge, 2004). In *M. grisea*, conidia are produced by an expansion and swelling of the apex of the conidiophore. Mitotic divisions of a single progenitor nucleus in the aerial conidiophore stalk gives rise to a three-celled teardrop-shaped conidium. After the formation of the first

conidia, the active apical tip moves to the side to produce the next spore. Multiple rounds of c onidiation result in a mature conidiophore bearing three to five spores grouped sympodially (Lau and Hamer, 1998).
B. cinerea form conidiophores with a globose basal cell. Near the top of the conidiophore are produced several short and septate sporogenous branches, each with a terminal ampulla on which conidia develop on short, fine denticles (Suzuki *et al*., 1977; Jarvis, 1977).

These differences at the morphological level extend to the molecular level, even within the same genus. The regulatory role of *medA* on the expression of the genes of the core developmental pathway, *brlA* and *abaA* in *A. nidulans*, has already been mentioned in this chapter. In contrast, in *A. fumigatus*, studies indicate that *medA* is not required for the expression of these regulatory genes (Gravelat *et al*., 2010). A similar behaviour has been described for the upstream activator of *brlA fluG* (Yu *et al*., 2006, Mah *et al*., 2006), which is necessary for conidiation and *brlA* expression in *A. nidulans*, but not in *A. fumigatus* where its deletion did not cause severe alterations in sporulation nor in *brlA* expression. In our study system, it is assumed that conidiation is regulated by a network of transcription factors in a similar way, but not identical to that of *A. nidulans*. Some components of the Eurotiomycete regulatory network are present in *B. cinerea* in addition to *medA*. Thus, the orthologues of *stuA* (Bcin04g00280) and of the Velvet complex *vosA* (*Bcvel4*), *velB* (*Bcvel2*), *veA* (*Bcvel1*/*Bcvea*), *velC* (*Bcvel3*) and the regulator *laeA* (*Bclae1*) are known. Also conserved are four of the components of the *fluG*-mediated regulatory pathway, *flbB* (Bcin15g00200), *flbC* (*Bcltf15*), *flbD* (*Bcltf12*) y *fluG* (Bcin06g01280). Of the three transcription factors of the core developmental pathway, *abaA* (Bcin05g04650) and *wetA* (Bcin14g00990) have their orthologs in
B. cinerea, but b*rlA* is absent, although *Bcltf2* could be its counterpart. This is a C_2H_2-type transcription factor, ortholog of *N. crassa sah-1* (short aerial hyphae) and *M. oryzae cos1* (conidiophore stalk-less) (Schumacher, 2017). *Bcltf1*, a GATA-type transcription factor orthologous to *N. crassa sub-1* and *A. nidulans nsdD* and *Bcwcl1* and *Bcwcl2*, two GATA-type transcription factors, which form the WCC complex and are also known in *N. crassa* and *A. nidulans*, mediate the transcription of genes in response to light (Canessa *et al*., 2013; Schumacher *et al*., 2014).

However, this pathogen also presents differences with respect to *A. nidulans*. The expression of *wetA* and *abaA* was not affected in conditions of induction of conidiation by light or by the always conidia mutations (mutations of either component of the regulatory pathways of *Bcltf2* that lead to an increase in its expression and causes light-independent conidiation). *Bcvel4* also showed an apparent insensitivity to light regulation (or lack thereof) (Cohrs *et al*., 2016; Schumacher, 2017). Furthermore, unlike *A. nidulans*, *B. cinerea* has the *VVD* (*Bcvvd1*) and *FRQ* (*Bcfrq1*) homologs of *N. crassa*, involved in photoadaptation and the circadian clock (Schumacher and Tudzynski, 2012; Chen *et al*., 2010). These observations could imply divergences in the regulation of light-controlled processes, such as conidiation, among these fungi. Specifically, it is known that in *B. cinerea* the expression of *Bcltf2* is mediated by white light, resulting in the activation of processes related to conidiation (conidiophore development, conidiogenesis and *Bcpks13*-derived melanogenesis) and, at the same time, the repression of sclerotial development (including *Bcpks12*-derived melanogenesis). The attenuation of *Bcltf2* expression is

mediated by blue light through the WCC complex, *Bcltf1* and the Velvet complex (Cohrs *et al*., 2016). The results presented in this chapter suggest a participation of *Bcmed* both in the development of conidiophores and in the development of sclerotia, so it is very likely that its expression is affected by the action of *Bcltf2*. Furthermore, given the regulatory behaviour that *medA* itself has on the core developmental pathway in *A. nidulans*, it is also likely that this supposed regulatory effect is mutual, affecting *Bcmed* on *Bcltf2* transcription.

In conclusion, the analysis in this chapter, taken together, provide evidence that the *Bcmed* geneis developmentally regulated and that, at the same time, its protein participates in asexual developmental and virulence processes, as do its known orthologs in other fungal species. However, given the morphological and molecular differences among these species, it is reasonable to expect that the activity of the *Bcmed* protein has specialized to some degree regulating the expression of different target genes than does its orthologs. In this sense, *Bcmed* could participate in regulate and fine-tune conidiation by affecting the expression levels of *Bcltf2*, or by acting in parallel with or downstream of *Bcltf2* in *B. cinerea*.

CHAPTER III.

Characterization of the *Bcorp*1 gene.

Introduction

Phytopathogenic fungi employ a wide variety of strategies to infect the host plant. These depend on the infection process of each particular fungus. Thus, in the case of *B. cinerea*, as a necrotrophic fungus, the secretion of a large set of proteins and secondary metabolites, together with the manipulation of the plant hyper-sensitive response, a form of programmed cell death, represent the central points of the infection strategy of the pathogen. The molecules (proteins, RNA, and low molecular weight compounds) that contribute to the progress of the infection cycle in any of its phases are considered virulence factors (González *et al*., 2016). The identification of these virulence factors is of interest not only because it increases general knowledge of the infection process, but also because any of these molecules is a potential target for disease control. Its recognition has traditionally been carried out by comparing strains of natural origin or mutants induced by ultraviolet or chemical mutagenesis that we re non-pathogenic with pathogenic ones, but these techniques were replaced by insertional mutagenesis techniques, including transposon tagging (Idnurm and Howlett, 2001; López-Berges *et al*., 2009). This technique is based on the use of transposons, which due to their ability to be excised from their initial location and integrated into another new region of the genome, allow the identification of genes of interest as insertion of a transposon both disrupts and tags a gene. Subsequently, the isolation of the inactivated gene is guaranteed by the use of the inserted transposon sequence as a tag to isolate the neighbouring host sequences (Becker *et al*., 2001; Dufresne and Daboussi, 2010). Villalba *et al*. (2001) used this technique, introducing impala, a Tc1 – mariner transposable element from *F. oxysporum*, in *M. grisea*. The transposition of the element was detected by excision of the *niaD* gene promoter and molecular analysis of the revertants using hybridization and sequencing. One non-pathogenic mutant (rev77) was obtained. The flanking areas of the impala insertion site in rev77 were analysed by inverse -PCR, cloning and sequencing and the mutant was successfully complemented with a 3 -kb genomic fragment from a wild-type *locus*. This gene, called 'orphan gene required for pathogenicity 1' (ORP1), was found to be essential for penetration of host tissue since rev77 differentiated melanized appressoria but was unable to penetrate into rice leaves and barley and did not cause lesions on them. At that time, this gene did not show homology with known genes in databases and has not yet been characterized.

On the other hand, in addition to our interest in the role of NO in *B. cinerea*, another of the strategies employed by our research group is the analysis of candidate genes for development or virulence factors or those already described as such in other phytopathogenic fungi. An alternative approach to those already mentioned to identify pathogenicity and/or development genes consists in detecting sequences whose expression levels are induced or repressed when the mycelium is grown *in vitro* in the presence of stressful conditions, such as alterations in the nitrogen or carbon source, alterations in the pH of the medium or photostimulation (Leal *et al*., 2010). This method is based on the hypothesis that these altered growth conditions are equivalent, to a certain degree, to the conditions encountered by the pathogen throughout the infective process or that the alteration of some component of the environment, such as essential amino acids, functions as a stimulus for the upregulation or downregulation of these

factors. Based on this hypothesis, candidate genes for pathogenicity factors have been identified in *Gibberella zeae*, *M. grisea* and *Fusarium graminearum* (Trail *et al*., 2003; Voigt *et al*., 2005; Donofrio *et al*., 2006; Leal *et al*., 2010). In this sense, the analysis of the microarray experiment of gene expression profiling in response to NO in spores of the fungus carried out by the group in the past can be seen as a tool that allows the identification of 'pathogenicity' and/or 'developmental' genes. As was the case with the *Bcmed* gene, during the analysis of the results of this experiment, the *orp*1 ortholog, *Bcorp*1, was found to be differentially expressed. *Bcorp*1 was found among the genes that were induced during the germination of wild-type spores of the fungus when they were exposed to the NO donor DETA (Daniela Santander, Doctoral Thesis. University of Salamanca). The fact that the gene is regulated by NO in *B. cinerea* and the relationship shown with pathogenicity, but also with development, of its ortholog in *M. grisea* make it an interesting candidate for its functional analysis. This chapter contains the first steps taken in the analysis of this gene, which is in a preliminary stage.

Results

The strategy used for the characterization of *Bcorp*1 is analogous to that followed with the description of the *Bcmed* gene. It begins with the description of the characteristics of the *locus* according to the information present in online databases. Then the process of obtaining mutant strains by means of a homologous recombination strategy is detailed and the results of preliminary analyses made with the intention of characterizing the phenotype resulting from the mutation are presented.

1. *In silico* analysis of *B. cinerea orp*1.

Homology comparisons made by BLASTP in Ensembl Fungi identified the *B. cinerea* Bcin09g01160 gene product as sharing significant homology with *M. grisea* ORP1. The Bcin09g01160 gene is found on chromosome 9 of the *B. cinerea* genome (B05.10 ASM14353v4), between positions 428,598-434,965. According to Ensembl Fungi, the gene gives rise to two transcripts, Bcin09g01160.1 and Bcin09g01160.2. The first one is 6088 nt in length and consists of five exons. Only the last two are coding exons. Translation initiates at position 432219 within the fourth exon giving rise to an 859 amino acids protein. The second transcript is 6022 nt in length and shares with the first one the first, second, fourth and fifth exon s, but an intron is recognized within the third exon and alternatively spliced giving rise to a transcript derived from six exons. It is also translated from the ATG codon at position 432219 and codes for the same 859 amino acids (Figure 51).

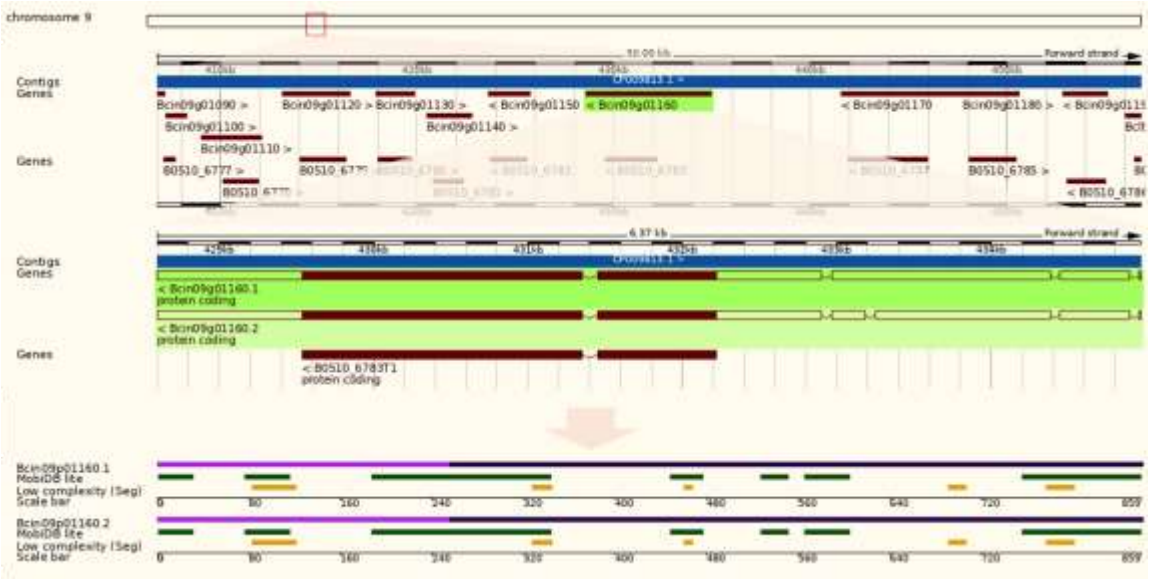

Figure 51. Schematic view of the position of *Bcorp*1 (Bcin09g01160) on chromosome 9 of *B. cinerea* genome, of the structure of the transcripts Bcin09g01160.1 and Bcin09g01160.2 and of the location of some of the domains and features in their re spective amino acids sequences (http: //fungi.ensembl.org).

The protein does not contain domains detectable by InterProScan but has 13 intrinsically disordered regions according to the MobiDB-lite predictor software and 5 low complexity regions according to the SEG algorithm (Figure 51, Table 7).

Table 7. List of motifs and domains in *B. cinerea orp1* protein. The intrinsically disordered regions were annotated with MobiDB-Lite predictor and low complexity regions were annotated with the SEG program. The table shows the positions of the features on the Ensembl peptide (http: //fungi.ensembl.org).

Feature type	Start	End
MobiDBLite	1	17
MobiDBLite	1	31
MobiDBLite	77	116
MobiDBLite	91	116
MobiDBLite	188	344
MobiDBLite	189	212
MobiDBLite	245	266
MobiDBLite	449	463
MobiDBLite	449	477
MobiDBLite	528	551
MobiDBLite	566	605
MobiDBLite	756	848
MobiDBLite	756	859
Seg	83	121
Seg	328	345
Seg	460	468
Seg	691	707
Seg	777	801

A phylogenetic analysis of the gene was also performed with orthologs present in several species representing only Pezizomycotina, since a BLASTP-type analysis reported its absence in other subdivisions. The *Bcorp*1 sequence presented a highly conserved region in the central region of its sequence of approximately 130 amino acids (Figure 52).

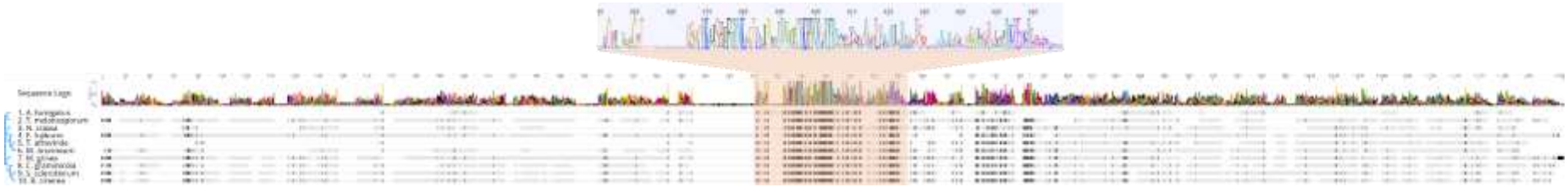

Figure 52. Phylogenetic tree and sequence alignment of the *Bcorp*1 predicted amino acid sequence (XP_024550701.1) with other *orp*1 orthologues from *A. fumigatus* (XP_749315.1), *Tuber melanosporum* (XP_002838149.1), *N. crassa* (XP_011394639.1), *F. fujikuroi* (XP_023430790.1), *Trichoderma atroviride* (XP_013942840.1), *Metarhiziumbrunneum* (XP_014545518.1), *M. grisea* (XP_030982001.1), *C. graminicola* (XP_008092229.1) and *S. sclerotiorum* (XP_001593520.1). The orthologous sequences were obtained from NCBI (Genbank) and the phylogenetic tree was built up using the Geneious Tree Builder usingthe Neighbor-Joining Tree Build Method with a Bootstrap resampling method with 100 replicates. The alignment was performed with the CLustal W algorithm in Geneious software using the default settings. The Sequence logo of the central zone of great homology with an extension of approximately 130 bp is shown enlarged.

2. *Bcorp*1 deletion in *B. cinerea*.

Mutants of *B. cinerea* lacking the *Bcorp*1 gene were obtained using the vector pAAD8 (Alejandro Alonso Díaz, Master Thesis. University of Salamanca). This plasmid harbours the 5' and 3' regions of the *Bcorp*1 gene, 696 bp and 929 bp, respectively, in a position such that they flank the hygromycin resistance expression cassette (promoter of the *OliC* gene of *A. nidulans*, *hph* gene, and *TtrpC* terminator from *A. nidulans*). Therefore, this construction thus designed allows the integration of the antibiotic resistance cassette in the *locus* of the Bcin09g01160 gene, producing a substitution between the two through homologous recombination between the corresponding sequences of the flanking regions of the mutant and the wild- type copies (Figure 53).

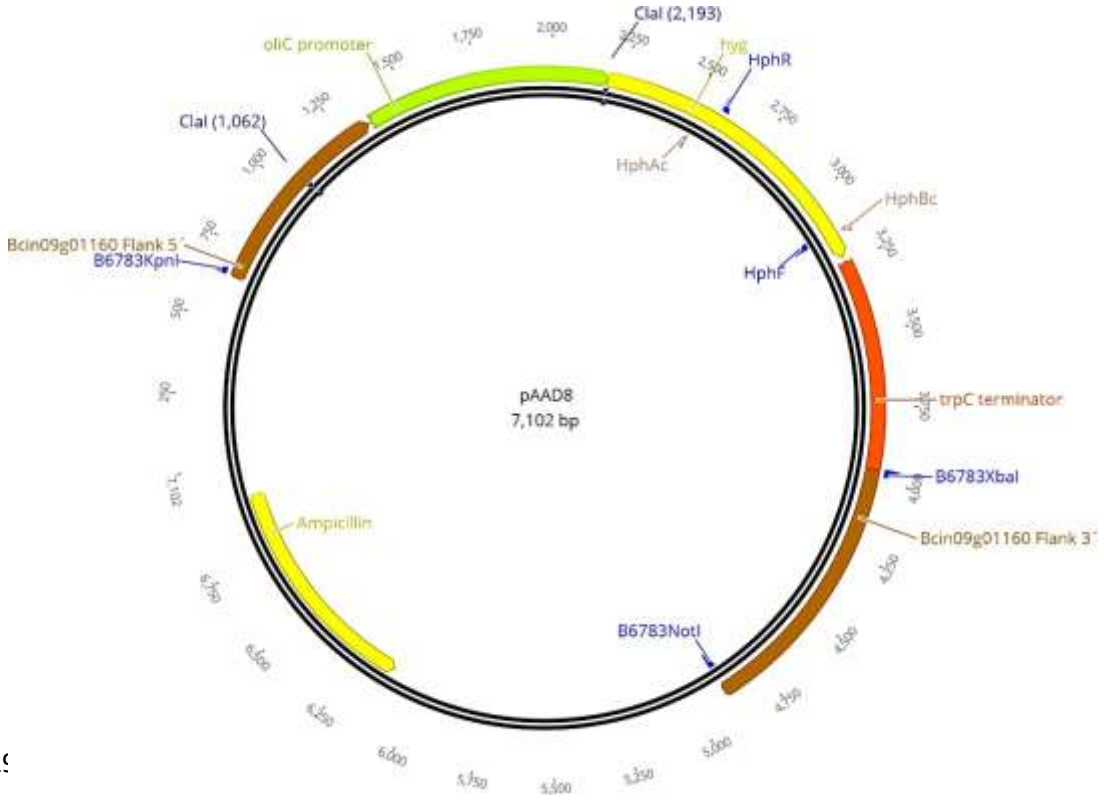

Figure 53. Scheme of plasmid pAAD8. The ampicillin antibiotic resistance gene, the 5' and 3' flanks of the *Bcorp*1 gene, the hygromycin resistance expression cassette composed of the promoter of the *OliC* gene of *A. nidulans*, the *hph* gene, and the *TtrpC* terminator of *A. nidulans*, the restriction targets of the enzyme *Cla*I and the annealing positions of the B6783FKpnI, B6783RNotI, B6783XbaI, HphAc, HphBc, HphF and HphR oligonucleotides are represented.

This plasmid was used as the template in a conventional PCR reaction with oligos B6783FKpnI and B6783RNotI (Table 8, Appendix) to amplify a 4236bp fragment containing the hygromycin resistance expression cassette and the two flanking regions of *Bcorp*1 already mentioned. Enough quantity of the fragment obtained in this way was purified and used to transform protoplasts of the *B. cinerea* wild-type strain B05.10 of the fungus using the method described in section 16.2 of Materials and Methods. It was decided to use a linear fragment as transforming DNA to favour its entry into the protoplasts and its homologous integration. Several dozens of primary transformants were analysed searching for true

mutants. For this, monosporic cultures were obtained from each of them after having favoured their homokaryosis for the mutant allele by growth in selective medium during several successive replications. A first PCR analysis with the appropriate oligos allowed to detect the presence or absence of the wild- type allele (oligos B6783FU/ORP1R2, see Table 8, Appendix) and of the mutant allele (oligos B6783FU/HphAc and B6783RD/HphBc, see Table 8, Appendix) in the genomic DNA of the mycelium of the candidates grown in liquid medium (see section 2.2 and 10.1 of Materials and Methods) (Figure 54).

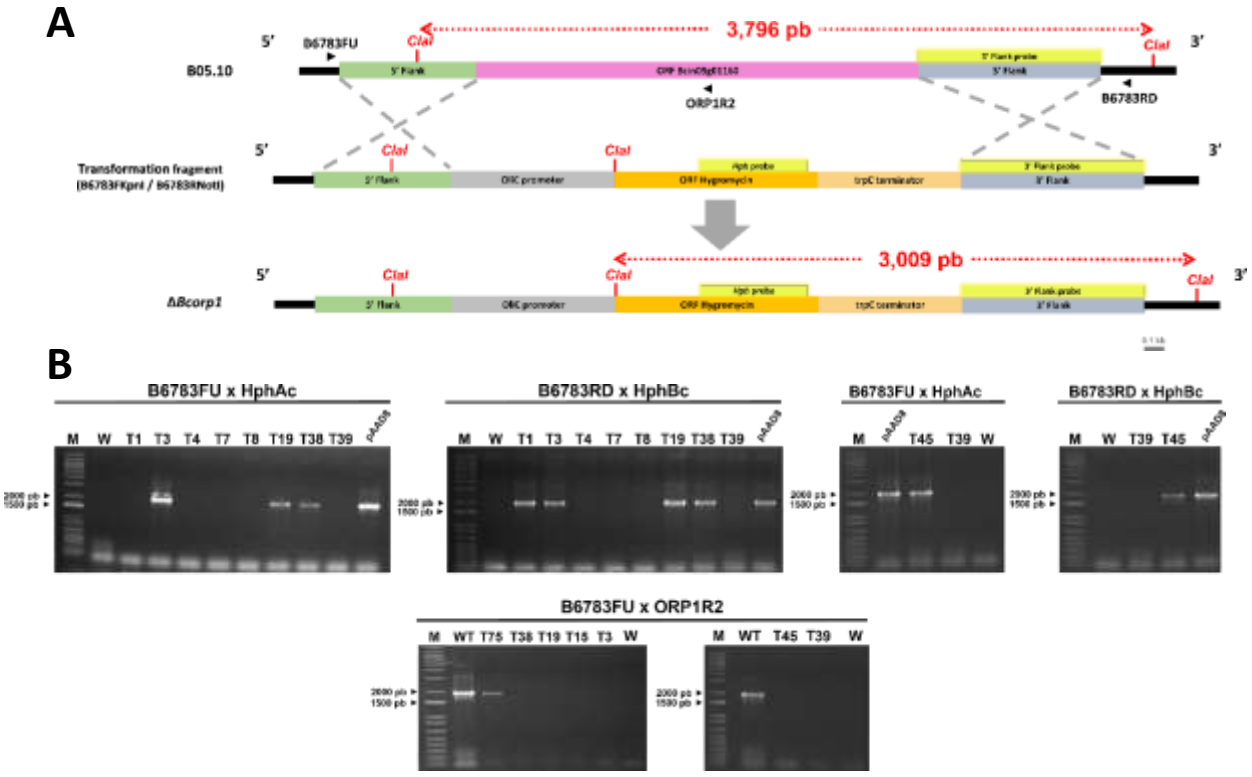

Figure 54. (A) Simplified scheme of B6783FKpnI / B6783RNotI fragment amplified from plasmid pAAD8 (Transformation fragment), of the genomic copy of the *Bcorp*1 gene (B05.10) and of the genomic copy of a transformant in which the wild-type allele of the *Bcorp*1 gene has been replaced by the mutant allele of the same gene (*ΔBcorp*1). The positions of the probes of the *Bcorp*1 3' flank and of the ORF hygromycin internal region, of the restriction targets of the enzyme *Cla*I and of the annealing positions of B6783FU, B6783RD and ORP1R2 primers, present in one or another copy and the sizes of the DNA fragments that are detected in hybridizations carried out with the different probes mentioned on the corresponding genomic DNA samples, are shown. (B) Analysis by PCR reactions of *B. cinerea* transformants with the B6783FKpnI / B6783RNotI fragment. The PCR reactions were carried out using genomic DNA of the candidate as template and the pairs of oligonucleotides B6783FU/HphAc, B6783RD/HphBc and B6783FU/ORP1R2 amplifying fragments of 1925 pb, 1901 pb and 1909 pb, respectively. The annealing positions of the HphAc and HphBc are indicated in Figure 53 and those of B6783FU, B6783RD and ORP1R2 are indicated in A. M – Marker 1 Kb Plus DNA Ladder, Invitrogen. WT / W – PCR reaction in which B05.10 strain genomic DNA (used as positive control), or Milli-Q water (used as negative control), was used as template, respectively. pAAD8 – PCR reaction in which pAAD8 plasmid DNA (used as positive control) was used as template. T – *B. cinerea* transformant candidate for *ΔBcorp*1.

Screening of candidate transformants by PCR analysis revealed the presence of transformants in which the replacement of the wild-type *Bcorp*1 allele with the mutant *hph* allele was successful. This is the case of transformants 3, 19 and 45. On the other hand, numerous candidates analysed presented an insertion of the plasmid pAAD8 by means of a single recombination event in one of the two flanks, such as transformant 1, or due to recombination events in unknown genome positions keeping the wild-type allele intact, such as transformant 75 (Figure 54).

Next, the genomic DNA of a small and selected group of candidates was subjected to a hybridization analysis by Southern blot. This group consisted of strain B05.10, as a negative control, transformant 1, whose PCR analysis determined that it could harbour the wild-type and mutant copies of *Bcorp*1 simultaneously, and a group of seven candidates, among which were some true mutants according to PCR analysis (transformants 3, 19 and 45) and other transformants for which this analysis did not provide conclusive results (15, 38, 39 and 75). Following the indications of section 18.2 of Materials and Methods and of chapter I, genomic DNA samples obtained from the mycelium of these strains were digested with the restriction enzyme *Cla*I. The digested genomic DNA samples were transferred to a nylon filter after their separation on an agarose gel by electrophoresis and hybridizations were performed on the membrane with two probes, one designed with the B6783RNotI/B6783FXbaI primers on the 3' flank of *Bcorp*1 (Table 8, Appendix) and another generated with the HphF/HphR primers from the structural region of the hygromycin resistance cassette (Table 8, Appendix) (Figure 55).

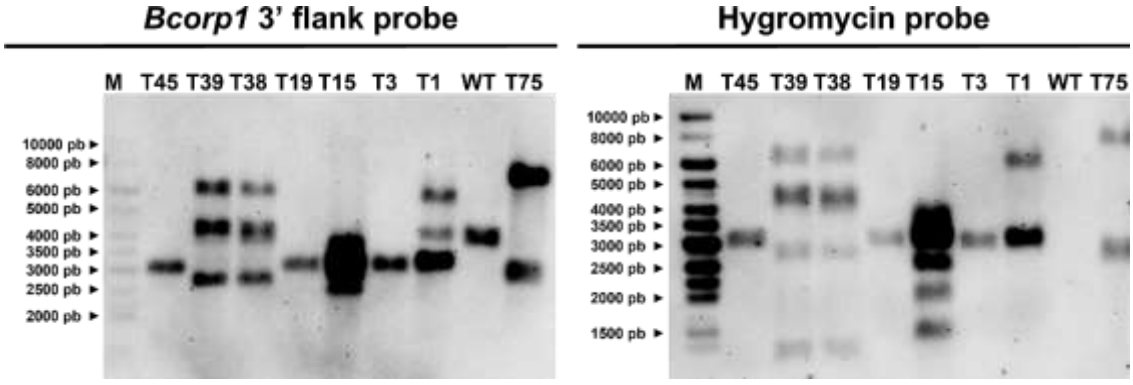

Figure 55. Analysis by Southern blot of *B. cinerea* transformants with the plasmid pAAD8. Genomic DNA samples from strain B05.10 and candidate transformants were digested with the restriction enzyme *Cla*I, separated by agarose gel electrophoresis, and transferred to a nylon filter. Hybridizations were carried out with a probe derived from the 3' flank of the *Bcorp*1 gene (B6783RNotI/B6783FXbaI annealing sites indicated in Figure 53) and with a probe designed from the ORF of the hygromycin resistance cassette (annealing sites of HphF/HphR indicated in Figure 53). Genomic DNA of B05.10 strain was used as a negative control. T – *B. cinerea* transformant candidate for *ΔBcorp*1. M – Marker 1 kb DNA ladder, Biotools.

The hybridizations with the probes used revealed the expected band pattern for the genomic DNA of the wild-type strain: a single band of 3796 bp for hybridization with the probe on the 3' flank of *Bcorp*1 and an absence of bands for hybridization with the *hph* structural region probe. On the other hand, the results obtained for candidates 3, 19 and 45 confirmed those already obtained by the previous PCR analysis, indicating that the three strains are true mutants for the *Bcorp*1 gene generated by gene replacement as a consequence of a double homologous recombination event at the 5' and 3' flanking sequences of the gene between its wild-type copy in the genome and the mutant copy of the pAAD8 vector. Thus, the same and unique 3009 bp band was detected by hybridizations of the genomic DNA of these three strains with one and the other probe. Candidate 1 together with candidates 15, 38, 39 and 75 presented hybridization patterns that do not fit the situation of transformants 3, 19 and 45. These strains show a hybridization pattern made up of two or more bands of different sizes. This result is due to one or

more ectopic integrations of the pAAD8 vector in their genomes (Figure 55). The three true mutant strains were named *ΔBcorp*1-3, *ΔBcorp*1-19 and *ΔBcorp*1-45.

The availability of the *ΔBcorp*1 mutants allowed the beginning of the analyses aimed at the functional characterization of *Bcorp*1. The first analysis carried out in this regard were pathogenicity tests that made it possible to determine if the mutant strains of *B. cinerea* had a non-pathogenic phenotype as did the mutants of *M. grisea* (Villalba *et al*., 2001).

3. Virulence of *ΔBcorp*1 strains.

The virulence tests were carried out on the two hosts used routinely in our laboratory, beans and grapevines. In order to carry out the virulence test on beans, inocula of the B05.10 strain, the *ΔBcorp*1-3, *ΔBcorp*1-19 and *ΔBcorp*1-45 strains and the ectopic strains 1, 15, 38, 39 and 75 cultivated as indicated in the section 2.2 of Materials and Methods were used. The bean plants with the inoculated cotyledon leaves were kept in incubation under the conditions established for this for 72 hours (sections 2 .3 and 7.2 of Materials and Methods). After this time, measurements of the two perpendicular diameters of the lesions present on the leaves were taken to make estimates of the aggressiveness of the different strains (Figure 56).

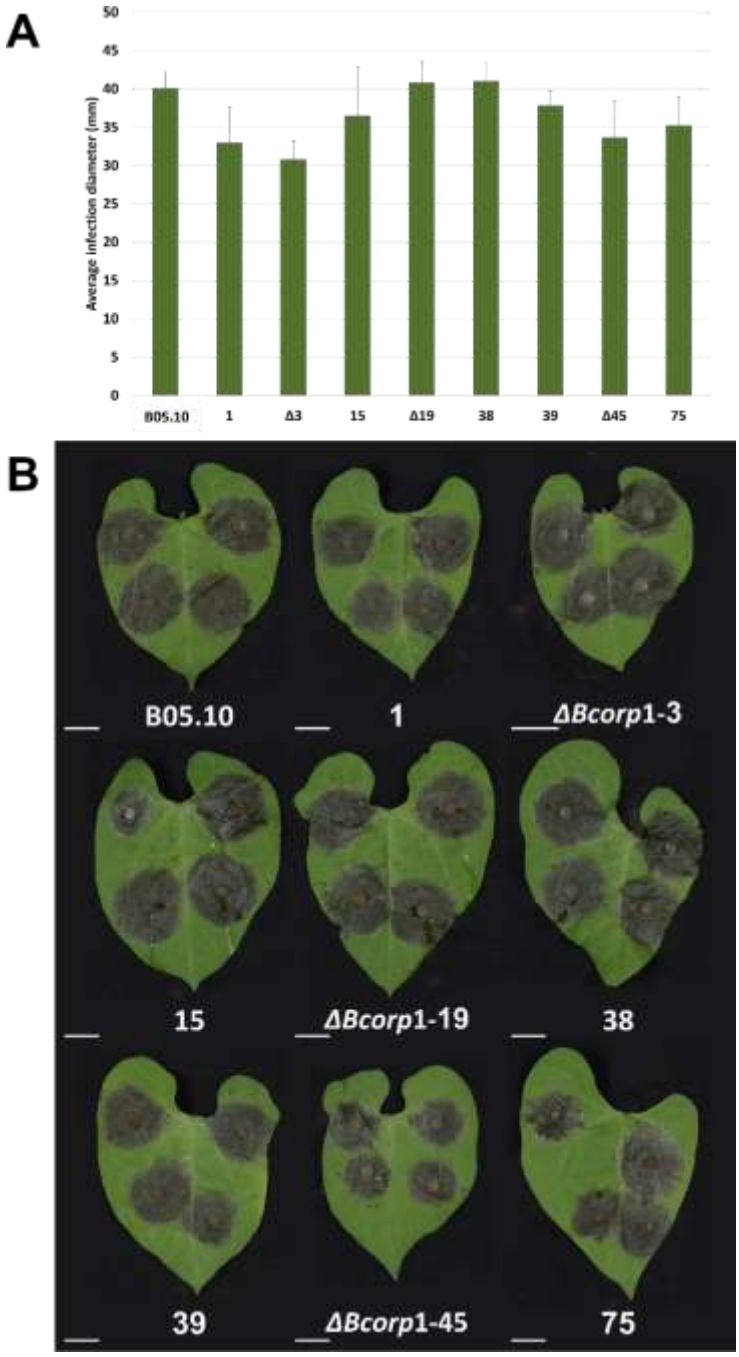

Figure 56. Evaluation of the aggressiveness in leaves of *P. vulgaris* of *B. cinerea ΔBcorp*1 strains. (A) Primary leaves of *P. vulgaris* plants were inoculated with plugs of 4-days-old vegetative mycelia of B05.10, *ΔBcorp*1-3, *ΔBcorp*1-19, *ΔBcorp*1-45, 1, 15, 38, 39 and 75 strains. The inoculated leaves were incubated at 22°C with a photoperiod of 16 hours of light and 8 hours of darkness for 72 hours. Average lesion diameters and standard deviations were calculated from eight lesions per strain with two measurements per lesion in assays performed in triplicate. (B) Representative images of the leaves inoculated with the strains indicated in A at 3 days post inoculation. Scale bars, 20 mm.

The *Bcorp1* gene mutation does not appear to have affected the ability of the fungus to infect bean plant leaves. All the strains evaluated, both the three mutant strains (*ΔBcorp*1-3, *ΔBcorp*1-19 and *ΔBcorp*1-45) and the ectopic strains (1, 15, 38, 39 and 75) formed necrotic lesions at 3 dpi on the leaves of the host similar in appearance and size to those formed by B05.10.

The virulence of the pathogen in vine was tested on leaves and fruits. Following the indications described in sections 7.1 and 7.3 of Materials and Methods, the detached vine leaves of the Juan García and Verdejo varieties and the table grapes were infected with the same type of inoculum as the bean leaves, plugs of 4-days-old vegetative mycelia cultivated under standard incubation conditions (section 2.2 of Materials and Methods). The strains used were B05.10, *ΔBcorp*1-3, *ΔBcorp*1-19 and *ΔBcorp*1-45. Images of the lesions produced by the fungus in both, leaves and fruits, after their incubation under the usual conditions for 120 hours were taken (section 2.3 of Materials and Methods). The incubation of the fruits lasted a further 72 hours to compare the behaviour of the strains in later stages of infection. In these tests, no estimate was made of the infective capacity of the pathogen due to the absence of necrotic lesions in the inoculations of some of the strains (Figure 57).

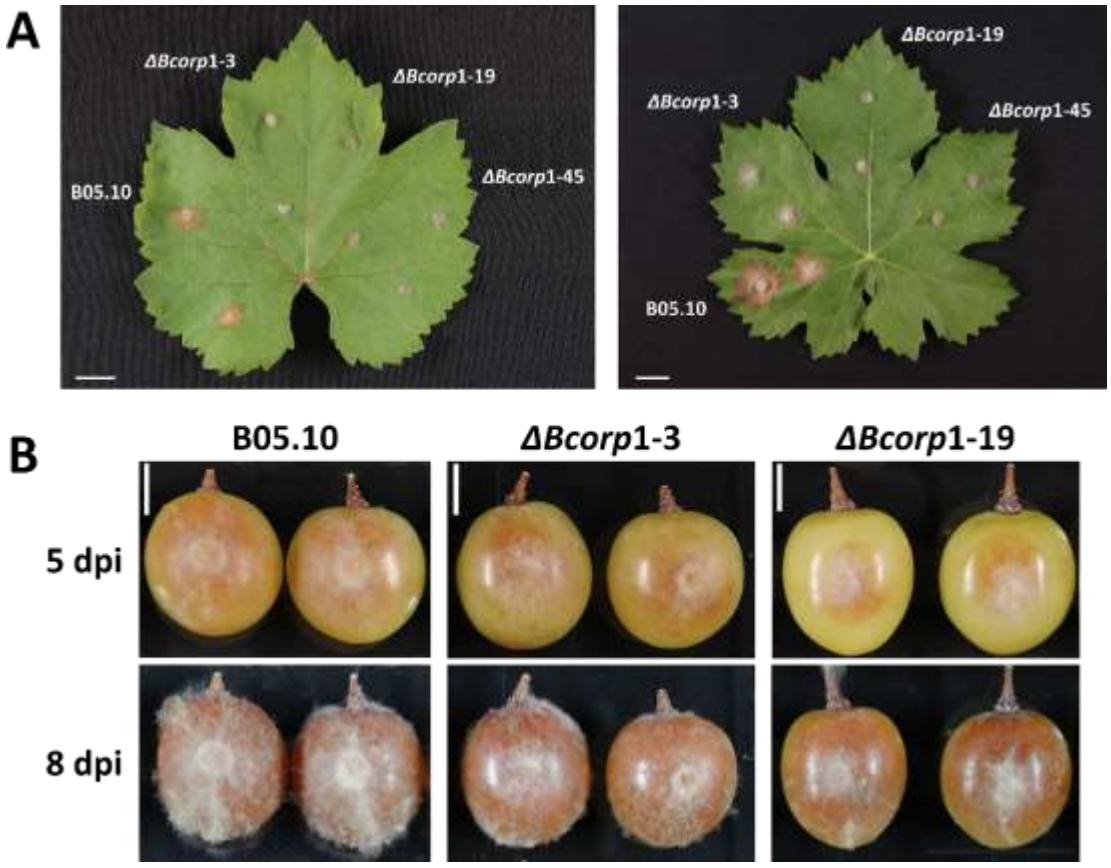

Figure 57. Evaluation of the aggressiveness in *V. vinifera* of *B. cinerea ΔBcorp*1 strains. (A) Representative images of detached *V. vinifera* leaves of Verdejo (left) and Juan García (right) varieties inoculated with plugs of 4-days-old vegetative mycelia of B05.10, *ΔBcorp*1-3, *ΔBcorp*1-19, and *ΔBcorp*1-45 strains. The inoculated leaves were incubated at 22°C with a photoperiod of 16 hours of light and 8 hours of darkness for 120 hours. Scale bars, 20 mm. (B) Representative images of *V. vinifera* table grapes inoculated with plugs of 4-days-old vegetative mycelia of B05.10, *ΔBcorp*1-3, and *ΔBcorp*1-19 strains. The fruits were incubated at 22°C with a photoperiod of 16 hours of light and 8 hours of darkness for 120 hours (5 dpi) and 192 hours (8 dpi). Scale bars, 10 mm.

Unlike what was observed in bean leaves, the deletion of the *Bcorp1* gene does seem to have affected the virulence of the pathogen in grapevines, as the mutant are unable to cause lesions in the leaves. In this host, differences are detected between the host varieties used in the inoculations with the B05.10 wild type strain. Thus, the leaves of the Verdejo variety seem to present a greater resistance to

the attack of the pathogen than the leaves of the Juan García variety since the lesions are always smaller in diameter. In any case, this strain has formed the usual necrotic lesions, of greater or less extent, at 120 hpi. In contrast, the lesions of the three mutant strains analysed are non-existent for the same sample time. The mycelium has barely expanded from the initial inoculum plug. This scarce growth, as happened with B05.10, has been more limited on Verdejo leaves than on Juan García's (Figure 57A).

The infective behaviour of the fungus on vine fruits has been different from that presented on leaves. When inoculated in fruits of the seedless Sweet Globe Green variety, the three strains evaluated, the wild type B05.10 strain and the two deletion mutants, *ΔBcorp*1-3 and *ΔBcorp*1-19, were able to colonize the fruits, but the timing appeared to be different, the mutants causing a delayed infection. At5 dpi, the decay of the fruits caused by the mutant strains was lower than that caused by the wild-type strain. At 8 dpi all the fruits were affected, but the grapes infected with the B05.10 strain presented a layer of aerial mycelium of more profuse growth and extension compared to the grapes infected with the mutant. Therefore, in this wound inoculation test differences between the wild type and the *ΔBcorp*1 mutants are observed, being the mutant strains less aggressive than the wild-type strain (Figure 57B).

4. The *ΔBcorp*1 strains do not show alterations in their capacity to acidify the medium.

As the *Bcorp*1 gene appears to be a pathogenicity factor, an in depth physiological and molecular characterization of the functions the gene may play during the establishment and progress of the interaction has to be addressed. Several aspects have been considered in a first instance. In a preliminar way, it has been analysed whether *Bcorp*1 has a role in the acidifying capacity of the fungus. For this, the strains B05.10, *ΔBcorp*1-3 and *ΔBcorp*1-19 were inoculated in Petri dishes with MEA medium. The pH of this culture medium had been adjusted to a value of 5.7 so that the fungus grew without difficulties. In addition, the Bromocresol Green Sultone Form indicator (0.045% (w/v)) was added, which changes from blue (pH ≥ 5.4) to green and yellow (pH ≤ 3.8) as the pH decreases. The growth of the fungus was followed under standard incubation conditions (section 2.2 of Materials and Methods) for 10 days. During this time period, the three strains grew in a similar way as the indicator turned from blue to yellowish green indicating that the acidifying capacity of the mutant strains has not been altered by the mutation, at least in a way that is noticeable to the naked eye (data not shown).

5. Subcellular localization of the *B. cinerea* ORP1 protein.

As no information about the function of the protein in any fungal system has been described, we considered that the determination of its subcellular localization could be informative. To this end it was decided to build up a gene fusion with the GFP protein and to generate transformants expre ssing which could be analysed by fluorescence and confocal microscopy. Chapter I described in detail the elaboration of transformants carrying the translational fusions of the gene encoding *gfp* with the genes encoding cell cycle regulatory proteins and potential nitric oxide targets. Simultaneously with the elaboration of these transformants and following the same design, transformation and analysis steps, the plasmids pFAEN-

ORP1 and pFAEX-ORP1 were obtained (Figure 58). With the latter, which harbours a translational fusion construct between the *gfp* gene and gene *Bcorp1*, protoplasts of the *B. cinerea* B05.10 were transformed. Several transformants carrying such a construct were obtained and analysed and are being analysed first by the fluorescence microscope. Preliminary experiments carried out with spores and with mycelium cultured in liquid B5 salts medium supplemented with saccharose and phosphate indicate that the level of expression of the fusion protein is low. Data are not presented at the moment, as further microscopy work is to be done.

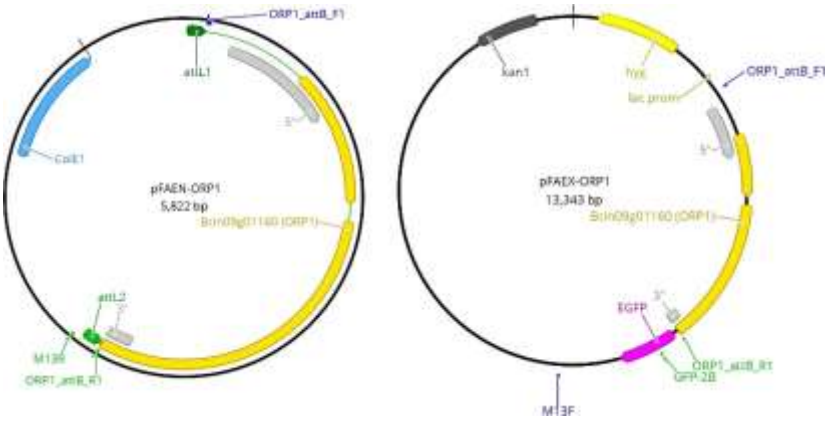

Figure 58. Schematic map of pFAEN-ORP1 and pFAEX-ORP1 plasmids. pFAEN-ORP1 (left side) is the Entry vector of the *Bcorp*1 gene obtained after the BP recombination reaction with the Gateway® system. In it, the following components are shown: the cloned gene fragment flanked by the *attL* sequences, the ColE1 replication origin (ColE1) and the annealing positions of the oligonucleotides ORP1_attB_F1, ORP1_attB_R1 and M13R (Table 8, Appendix). pFAEX-ORP1 (right side) is the Expression vectors of the *Bcorp*1 gene obtained after the LR recombination reaction with the Gateway® system. In it, the following components are shown: the cloned gene fragment, the kanamycin-resistance cassette (kan1), the hygromycin-resistance cassette (hyg), the lac promoter (lac), the GFP ORF (EGFP) and the annealing positions of the oligonucleotides ORP1_attB_F1, ORP1_attB_R1 and GFP-2B (Table 8, Appendix).

6. Differential gene expression analysis.

A powerful tool to investigate the functions a gene product participates in is the comparative transcriptomic analysis of a wild type individual with that of a mutant deficient in the gene of interest. Then, a comparative transcriptomic analysis using RNAseq between the B05.10 strain and one of the three deletion mutant strains obtained*, ΔBcorp*1-19, is currently being analysed. We decided first to determine possible differences in the global expression pattern due to the deletion of *Bcorp*1 during saprophytic growth. To obtain the biological material, 90 mm Petri dishes with MEA medium covered with a cellophane sheet were inoculated with plugs of vegetative mycelia from the edge of fungal colonies of the indicated strains actively growing under the same conditions. The inoculated plates were incubated in a germination chamber at 22°C with a photoperiod of 16 hours of light and 8 hours of darkness for 96 hours. After this time, the mycelium grown on the cellophane sheets of an area equivalent to the outer circu lar crown of the colony, about 10 mm thick, was collected. To do this, the surface of the plastic was scraped with the help of sterile tweezer, the mycelium obtained was immersed in 1.5 mL tubes containing 500 µL of RNAlater® Solution buffer (Invitrogen) and these were frozen in liquid nitrogen and stored at - 80°C.

Three independent biological tests were carried out, obtaining three repetitions for the samples of both strains. The subsequent steps of RNA extraction from the mycelium samples, the construction of the cDNA library, its sequencing and the quality and differential expression analyses were carried out in a manner equivalent to the transcriptional analysis performed on the strains B05.10 and *ΔBcfhg*1 in response to NO exposure (see section 20 of Materials and Methods and chapter I).

The study of the results is, at the moment, in an initial phase. However, the analysis of the comparison between the transcriptional profiles of the B05.10 and *ΔBcorp*1-19 samples resulted in obtaining 132 differentially expressed genes (adjusted P value of < 0.05 and $\log_2$(FC) of > 2 or < -2). Of these, 103 were downregulated and 29 upregulated genes (Table 12, Appendix).

Discussion

Interest in the study of the *Bcorp*1 gene arose, as mentioned above, from two previous observations. On the one hand, the analysis of the genes differentially expressed in a microarray experiment carried out during the culture of spores in germination of B05.10 in the presence of a NO donor determined a positive regulation of the transcriptional levels of the gene by the molecule (Daniela Santander, Doctoral Thesis. University of Salamanca). The differential expression analysis by RNAseq described in the first chapter of this work was perfor med under very similar conditions, but not identical to those of the microarray experiment. In both, spores of the same two strains of the fungus were used, the wild-type strain B05.10 and the mutant strain lacking the gene encoding flavohemoglobin *ΔBcfhg*1. The incubation of these was carried out in liquid medium and the NO donor, DETA in both cases, was added to the medium after an incubation time during which the spore germination program was triggered. Due to these similarities, it is inevitable to wonder what the expression pattern of *Bcorp*1 was like in this latest analysis. Their transcriptional levels increased slightly due to exposure to NO in the caseof wild-type spores ($\log_2$(FC) = 0.39), while they hardly varied in mutant spores for the same conditions ($\log_2$(FC) = -0.02). In the B05.10 spores, the same tendency is observed in the expression levels that the gene showed in the microarray experiment, an increase in expression, but the increase it now shows is several times less than that presented in the first analysis ($\log_2$(FC) = 2.18). The explanation for this change in behaviour could be found in the differences between the experimental designs of both experiments. As previously mentioned, for the microarray assay, the spores were incubated in Gamborg's B5 salts supplemented with 10 mM sucrose and 10 mM KH_2PO_4 pH 6.5 in agitation for 5 hours before adding the donor at a concentration of 125 µM. After one hour of exposure, the cultures were harvested. On the other hand, in the analysis by RNAseq, the spores were incubated in PDB ½ medium under static conditions for 4 hours. Then DETA, at a final concentration of 250 µM, was added to the cultures that were harvested two hours later. It is also possible that the technology used in one (microarray based on the detection of transcripts through hybridization with specific probes) and another analysis (RNAseq based on the sequencing of the whole transcriptome), has had an influence (Zhao *et al*., 2014; Rao *et al*.,

2019). In any case, as was the case with the cell cycle regulatory genes described in Chapter I, it seems that these differences have also affected the expression of *Bcorp*1 in an insurmountable way.

The second observation that motivated our interest in *Bcorp*1 was the succinct description that Villalba *et al*. (2001) made of its ortholog in *M. grisea*. In this short chapter, a first approach has been made to the characterization of the *Bcorp*1 gene through bioinformatic and phylogenetic analysis and virulence tests. Villalba *et al*. (2001) did not find sequences homologous to that of *M. grisea orp*1 among the sequences available in the databases at that time. Since then, the information uploaded and stored online has increased steadily, allowing us to detect the presence of the gene only among representatives of the Pezizomycotina subdivision. Furthermore, our results report a participation of the BCORP1 protein in the infection process of *B. cinerea*. This function agrees with that observed in *Magnaporthe* for *orp*1, where it was found to be essential for the penetration of the host leaves.

The information generated up to now suggests that *Bcorp*1, like its ortholog in *M. grisea*, is a pathogenicity factor, considering as such those genes necessary for disease development, but not essential for the pathogen to complete its lifecycle *in vitro* (Idnurm and Howlett, 2001). Besides the results obtained in the pathogenicity tests, this assumption would be supported by the fact that no obvious developmental alterations are observed in the *ΔBcorp*1 strains compared to B05.10. Mutant strains develop at the same rate as the control strain giving rise to the characteristic dark brown mycelium of this strain that contains spore-laden conidiophores that are capable of germination (data not shown). Furthermore, if we retrieve the results of the transcriptional analysis by RNAseq again, but now looking at the behaviour of the gene in the spores of the wild-type strain grown for 4 hours without exposure to NO (sample 1), an apparent constitutive expression of the gene is observed with little variation compared to the values of the samples of the 6 hours not exposed to DETA (sample 2) (log_2(FC) = -0.20) (data not shown). These observations would indicate an independence of the function of BCORP1 with respect to the processes of development of the pathogen.

A significant feature of the activity of the ORP1 protein is its apparent host dependence. Specifically, our results indicate that the protein participates in the infective process of grapevine, but not in that of bean. In the case of the leaves of the latter, the mutant strains formed necrotic lesions without apparent limitation and comparable to those formed by the reference strain. However, when the mutant strains were inoculated on grapevine leaves, they were not able to grow on the plant tissue and to propagate from the inoculum. The result was the absence of the necrotic lesions that B05.10 did form. These results are consistent with those reported by Reboledo *et al*. (2020). These authors performed genome wide transcriptional profiling of *B. cinerea* during different infection stages of the bryophyte *Physcomitrium patens*. They found that moss infection by the pathogen depended mainly on ROS generation and detoxification, transporter activities, plant cell wall degradation and modification, toxin production and probable plant defense evasion by effector proteins. Subsequently, they compared these results with available RNAseq data during angiosperm infection, including *A. thaliana*, *Solanum lycopersicum* and *Lactuca sativa*. They found similarities, but also differences (related to fungal CAZymes

(Carbohydrate-Active enZymes) genes and putative MFS transporter) between the infection and virulence functions that the pathogen employs in *P. patens* and angiosperms.

On the other hand, we also observed that the wild-type lesions were larger or smaller in diameter depending on the resistance of the grapevine variety used, but this aspect did not significantly influence the mutant behaviour, observing the same aphatogenicity phenotype in both the leaves of the Verdejo variety (more resistant) and those of the Juan García variety (more susceptible). In the case of table grapes used, the *ΔBcorp*1 strains were able to colonize the fruits, but certainly the mutant strains colonized the tissues more slowly than the wild type. Lovato *et al*. (2019) also detected common and specific grapevine responses by comparative transcriptomic analysis in Garganega, Müller-Thurgau and Sémillon (Blanco- Ulate *et al*., 2015) berries during noble rot infection by *B. cinerea*.

Together, these data suggest that *B. cinerea* has common molecular mechanisms involved in virulence and infection process used in all hosts it infects, while others are more specific to each particular host. At the same time, this different behaviour pattern of the fungus during infection would be influenced by the characteristics of the genetic backgrounds of the different cultivars and varieties of each host species.

Given the availability of published microarray or RNAseq data from our study system when interacting with different hosts, we looked through these to define the range of BCORP1 activity more precisely in relation to our results. The data examined were those resulting from infections of the fungus in *P. patens*, *A. thaliana*, *L. sativa*, *S. lycopersicum* and *V. vinifera* (Reboledo *et al*., 2020; De Cremer *et al*., 2013; Coolen *et al*., 2016; Srivastava *et al*., 2020; Haile *et al*., 2020; Kelloniemi *et al*., 2015). As already mentioned, Reboledo *et al*. (2020) performed a transcriptional analysis of *B. cinerea* during infection in *P. patens*. To do this, they sprayed 3-week-old moss colonies with a suspension of B05.10 strain spores ($2 \cdot 10^5$ spores/mL) and analysed three time points (4 hpi, 8 hpi and 24 hpi). The same procedure was used in the leaf infections of *A. thaliana*, *L. sativa*, *S. lycopersicum* using suspensions of $1 \cdot 10^5$ spores/mL, $5 \cdot 10^5$ spores/mL and $2 \cdot 10^5$ spores/mL of the wild-type strain, respectively. The available sample times were 12 and 24 hpi in *A. thaliana*, 16 and 23 hpi in *S. lycopersicum*, and 24 and 48 hpi in *L. sativa*. In the case of *V. vinifera*, flowers at full cap–fall stage from variety Pinot Noir were inoculated with a conidia suspension of the B05.10 strain ($2 \cdot 10^5$ spores/mL) and samples were collected at two time points, at 4 weeks post inoculation when the berries were still green and hard, and at 12 weeks post inoculation (ripe grapes). For the latter time point, two kinds of samples were collected: berries with visible egressed *Botrytis* (egressed-stage fungus) and berries without visible *Botrytis* sign from a *cluster* (pre- egressed-stage fungus). Kelloniemi *et al*., 2015 inoculated grape berries belonging to the cultivar Marselan in the equatorial area with three inoculum droplets spotted in a triangle, each of 10 µl with 5000 wild- type conidia, in PDB. The exocarp of the inoculated area was collected at 0, 16, 24, and 48 hpi to extract RNA. *Bcorp*1 was not found in the DEG lists of the sampling times of infections in *P. patens*, *A. thaliana*, *L. sativa* and *S. lycopersicum* (low expressed genes filtered for count values ≥ 3 in all samples and a false discovery rate ≤ 0.05 was used to determine significant DEGs by comparison with *B. cinerea* grown on

PDA as a control) or in the comparative analysis of the lists of the last three infections with that of moss (p-value adjusted threshold 0.05 and minimum $\log_2$ Fold Change 2) (Reboledo *et al*., 2020). The exception was the grapevine infection data. *Bcorp*1 was overexpressed ($\log_2$(FC) = 3.32) at 48 hpi on mature grape as compared to *in vitro* mycelium (corrected p-value < 0.05 and more than a twofold change in transcript level) (Kelloniemi *et al*., 2015). Besides, *Bcorp*1 was induced ($\log_2$(FC) = 1.14) during egression on ripe berry as compared to PDB grown fungus (p-value of < 0.01 and an absolute fold change of ≥ 2.0) (Haile *et al*., 2020). Therefore, these results support our preliminary observations by confirming that *Bcorp*1 is expressed in a host-dependent manner.

Finally, our results also allow us to venture the type of pathogenicity factor that *Bcorp*1 could be out of all the existing classes (Tudzynski and Sharon, 2003; Van de Wouw and Howlett, 2011). The absence of developmental defects in the mutant strains would, in principle, rule out its participation in the biosynthesis and the integrity of fungal cell walls. Furthermore, as these strains grew without apparent problems on the plant tissue of bean leaves, the possibility that *Bcorp*1 encodes a protein involved in the production of infection structures, in the penetration of the cuticle and cell wall, in fungal nutrition or in host colonization could also be ruled out. However, as the *ΔBcorp*1 strains were not able to grow on the grapevine plant tissue, it is possible that *Bcorp*1 is a gene involved in the recognition of the host and in signalling. It is true that the mutant strains were able to grow and colonize the table grapes, but it must be taken into account that an incision had been made in their surface prior to inoculation. Regardless of the role that BCORP1 plays during the infective process of *B. cinerea* in grapevine, further analyses are required to determine the characteristic factors of this host that cause the specific activation of the gene.

In summary, in this chapter, the first steps taken in the analysis for the characterization of the ortholog in *B. cinerea* of the *M. grisea orp*1 gene have been described. The results indicate that *Bcorp*1, like its ortholog in *Magnaporthe*, is involved in pathogenicity. Its action could be dependent on the host, the gene being specifically activated during grapevine infection. Likewise, the behaviour of the mutant strains suggests that *Bcorp*1 could encode a protein involved in the recognition of the host and in signalling.

Conclusions

Conclusions

- Nitric oxide modulates asexual development in *B. cinerea*, having an immediate and transitory negative regulatory effect on spore germination, germ tube elongation, and nuclear division rate.
- The flavohemoglobin enzyme BCFHG1 plays a key nitric oxide detoxifying function in protecting fungal cells from the damaging effects of nitrosative and oxidative stress caused by the molecule.
- *Bcmed* is a gene whose expression is developmentally regulated, and its gene product is necessary for the correct development of the mycelium, conidiation and the infective process in *B. cinerea*.
- *Bcorp*1 is a gene encoding a host specific pathogenicity factor essential for *B. cinerea* to infect *V. vinifera* leaves.

Conclusiones

- El óxido nítrico modula el desarrollo asexual en *B. cinerea* y tiene un efecto regulador negativo inmediato y transitorio sobre la germinación de las esporas, la elongación del tubo germinativo y la tasa de división nuclear.
- La enzima flavohemoglobina BCFHG1 desempeña una función detoxificadora clave del óxido nítrico en la protección de las células del hongo de los efectos dañinos del estrés nitrosativo y oxidativo causado por la molécula.
- *Bcmed* es un gen cuya expresión está regulada por el desarrollo y su producto génico es necesario para el correcto desarrollo del micelio, la conidiación y el proceso infeccioso en *B. cinerea*.
- *Bcorp*1 es un gen que codifica un factor de patogenicidad específico del hospedador esencial para que *B. cinerea* infecte las hojas de *V. vinífera*.

Appendix

Appendix

Table 8. List of primers used. (a) *Locus* in the genome of B05.10 *B. cinerea* strain; (b) plasmid.

Primer	*Locus*/Plasmid	Sequence (5' - 3')	Tm (°C)
CDC25_attB_F1	Bcin07g02410[a]	GGGGACAAGTTTGTACAAAAAAGCAGGCTTATCGTCTTCTTCAACTGGACGC	64
CDC25_attB_R1	Bcin07g02410[a]	GGGGACCACTTTGTACAAGAAAGCTGGGTAGTATGAGACTTGTCTTCGTGG	62
CDC2_attB_F1	Bcin16g00490[a]	GGGGACAAGTTTGTACAAAAAAGCAGGCTTACTAGTGCCGACAAGGATCATG	64
CDC2_attB_R1	Bcin16g00490[a]	GGGGACCACTTTGTACAAGAAAGCTGGGTAGTGGTATCCGTTTGTAGTTTTATACG	72
SWI6_attB_F1	Bcin12g00820[a]	GGGGACAAGTTTGTACAAAAAAGCAGGCTTAAAATGCAGGCATTGAGTCGCG	64
SWI6_attB_R1	Bcin12g00820[a]	GGGGACCACTTTGTACAAGAAAGCTGGGTAAACCCCCTCAACCCTTGTCAA	64
MBP1_attB_F1	Bcin14g00280[a]	GGGGACAAGTTTGTACAAAAAAGCAGGCTTAACCACATTCAAAGTCCATATC	58
MBP1_attB_R1	Bcin14g00280[a]	GGGGACCACTTTGTACAAGAAAGCTGGGTACAATTCATCCCCCATCTCTCT	62
MCM1_attB_F1	Bcin09g06140[a]	GGGGACAAGTTTGTACAAAAAAGCAGGCTTACCCTCTCCCACTTATTATTGC	62
MCM1_attB_R1	Bcin09g06140[a]	GGGGACCACTTTGTACAAGAAAGCTGGGTATGATTGATGTGTCTGCGGTTG	62
NIAD_attB_F1	Bcin07g01270[a]	GGGGACAAGTTTGTACAAAAAAGCAGGCTTAGATAAGAAAAAAAGGCACAAG	56
NIAD_attB_R1	Bcin07g01270[a]	GGGGACCACTTTGTACAAGAAAGCTGGGTAAAAGAAAAGTATATCTTGATC	52
GFP+BamHIF	pFPL-Gh[b]	ATGGTGAGCAAGGGCGAGGA	66.1
GFPuserR	pFPL-Gh[b]	CCAGATTCGTCAAGCTGT	59.3
GFP-2B	pFPL-Gh[b]	AAGTCGTGCTGCTTCATGTG	58
GFP_fusión_R	pFPL-Gh[b]	GAACAGCTCCTCGCCCTTGCT	59.5
M13F	pFPL-Gh[b]	GTAAAACGACGGCCAG	50.7
M13R	pFPL-Gh[b]	CAGGAAACAGCTATGAC	50
CDC25_fusión_F	Bcin07g02410[a]	CAGAAATGACGAGTTCCCCTATGATGA	60.4
CDC2_fusión_F	Bcin16g00490[a]	CGACATGAGCCAACCTCTTT	60
SWI6_fusión_F	Bcin12g00820[a]	GAGAGCGGTGGAGAGTGAGAGTGATG	61.4
MBP1_fusión_F	Bcin14g00280[a]	ATGGAGGAGGCCAGGTTAAT	60
NR_fusión_F	Bcin07g01270[a]	GGAAGCGTTGGAGAAGAGTGTGCA	61.4
CDC25_silvestre _F	Bcin07g02410[a]	ATTGCCAACTCCTCGTCGATCTCTC	60.7
CDC25_silvestre _R	Bcin07g02410[a]	CGTTCAATGGACCTGGTGAAGAGG	60.5
NR_silvestre_F	Bcin07g01270[a]	GAGGTAGGGAGGTTTGAGATGGATATGG	61.1
NR_silvestre_R	Bcin07g01270[a]	TGCACACTCTTCTCCAACGCTTCC	61.4
CC_SWI6_QF	Bcin12g00820[a]	TCGACTCAATTCATGCCAAA	56
CC_SWI6_QR	Bcin12g00820[a]	TTTGCGATTTTGAGATCACG	56
CC_CDC2_QF	Bcin16g00490[a]	CGACATGAGCCAACCTCTTT	51.7
CC_CDC2_QR	Bcin16g00490[a]	GTACATGCTTGCTTGGCAGA	51.3
CC_MBP1_QF	Bcin14g00280[a]	ATGGAGGAGGCCAGGTTAAT	51.7
CC_MBP1_QR	Bcin14g00280[a]	TCCCCTACCAAAGCCTTTCT	52.1
BactA-62F	Bcin16g02020[a]	TTGCACCATCGTCGATGAAG	60

BactA-131R	Bcin16g02020[a]	CCACCAATCCAGACGGAGTATT	66
B3140F	Bcin12g00460[a]	GGGGACAAGTTTGTACAAAAAAGCAGGCTGCGGGAACTTAAGATCGCTAG	64
B3140R	Bcin12g00460[a]	GGGGACCACTTTGTACAAGAAAGCTGGGTCTCGGGTGCAGTAGTGTCGTAG	70
B3140-SI	Bcin12g00460[a]	AGAATGGGAATCAAAGAGGCGGC	61.3
B3140QF	Bcin12g00460[a]	AAGGAAAGCCTGACAGCGAGGAA	60.2
B3140QR	Bcin12g00460[a]	AGCATGTGTGGGTGGAAGAGTCG	59.9
HygF-DG	pAAD4[b]	AGAGCTTGGTTGACGGCAATTTCG	62,2
RvHyg	pAAD4[b]	CTATTCCTTTGCCCTCGGACGAGTGCTG	67.8
OLICU1	pFAME[b]	GGAGGTTCGGCGTAGGGTTG	66
NAT1U1	pFAME[b]	CGCAGGGTGAAGCCGTCC	62
OBcubq1-F	Bcin02g04920[a]	ATTCAAGCCTCCCAAGGTCAG	64
OBcubq1-R	Bcin02g04920[a]	GATCGGTCGGTCTTGTAAACG	64
B6783FKpnI	Bcin09g01160[a]	TAGGTACCTCGAACGTGTCCG	66
B6783RNotI	Bcin09g01160[a]	GTGCGGCCGCTAGTCCCACCAC	76
B6783FU	Bcin09g01160[a]	CCGCAAATCAGTTCCATCAGG	64
B6783RD	Bcin09g01160[a]	CACTCACTCAATCAAGCAGCC	64
ORP1R2	Bcin09g01160[a]	CCAATCCTTGATAGTACCGG	60
HphAc	pAAD8[b]	CGGGCAGTTCGGTTTCAGGC	66
HphBc	pAAD8[b]	CGTCTGGACCGATGGCTGTG	66
HphF	pAAD8[b]	GCGCTTCTGCGGGCGATTTG	66
HphR	pAAD8[b]	CGGGTTCGGCCCATTCGGAC	68
B6783FXbaI	Bcin09g01160[a]	TCTCTAGACAGCAACGCTCCC	66

Table 9. List of DEGs from the transcriptional comparative 2 versus 3 (spores of B05.10 strain grown for 6 hours without exposure to NO versus spores of B05.10 strain grown for 4 hours and then exp osed to NO for 2 hours). Gene ID - Identification code for *loci* from the BcinB0510 reference genome annotations (van Kan *et al.*, 2017); Log_2(FC) – Logarithm base 2 of the fold change (in green > 2 or in pink < -2); padj – adjusted p value (< 0.05); KEGG Terms – codes of functional categories in KEGG database; KEGG definition – Descriptions of the KEGG terms.

Gene ID	Log_2(FC)	padj	KEGG Terms	KEGG definition
Bcin11g06310	9,903481318	1,76E-13		
Bcin06g06670	7,738643573	9,47E-07		
Bcin08g03130	7,461729259	4,15E-07		
Bcin14g05020	5,997944454	1,33E-86		
Bcin05g04580	5,44436606	4,77E-82	K03781	katE, CAT, catB, srpA; catalase [EC:1.11.1.6]
Bcin04g06230	5,309528903	2,29E-92	K05916	hmp, YHB1; nitric oxide dioxygenase [EC:1.14.12.17]
Bcin15g00040	5,159589825	1,55E-04		
Bcin08g04910	4,964457583	1,09E-38		
Bcin09g01150	4,492339569	8,28E-06		
Bcin13g05380	4,392313519	6,46E-09		
Bcin12g06180	4,34115604	6,62E-59	K10675	E4.2.1.66; cyanide hydratase [EC:4.2.1.66]
Bcin15g00050	4,327470796	7,93E-12	K22889	AYT1, TRI101; trichothecene 3-O-acetyltransferase [EC:2.3.1.-]
Bcin05g07510	4,256629521	1,43E-04		
Bcin10g01470	4,085528108	1,42E-36		
Bcin01g05790	4,081430716	1,08E-48	K17877	NIT-6; nitrite reductase (NAD(P)H) [EC:1.7.1.4]
Bcin06g01560	3,948057483	1,17E-24		
Bcin14g01090	3,657036554	0,003314059		
Bcin01g11530	3,333808115	8,71E-21		
Bcin05g08230	3,319096734	0,003768846	K19356	E1.14.99.54; lytic cellulose monooxygenase (C1-hydroxylating) [EC:1.14.99.54]
Bcin07g01270	3,317060931	2,02E-34	K10534	NR; nitrate reductase (NAD(P)H) [EC:1.7.1.1 1.7.1.2 1.7.1.3]
Bcin07g06590	3,267816372	7,30E-15		
Bcin05g04570	3,174771797	1,71E-32	K00108	betA, CHDH; choline dehydrogenase [EC:1.1.99.1]
Bcin13g00180	3,163681816	0,009426011	K07034	K07034; uncharacterized protein

Bcin15g05700	3,150609168	9,40E-24		
Bcin14g01490	3,107260185	4,84E-11		
Bcin07g00560	3,037492793	1,33E-10	K00354	E1.6.99.1; NADPH2 dehydrogenase [EC:1.6.99.1]
Bcin01g03520	3,028833929	0,037424337		
Bcin08g04620	3,024213724	0,024708106		
Bcin01g05190	2,99374613	8,79E-25		
Bcin03g08640	2,974738083	0,002913662	K01426	E3.5.1.4, amiE; amidase [EC:3.5.1.4]
Bcin02g06160	2,962557665	1,98E-07		
Bcin14g02060	2,932448596	0,002588199		
Bcin09g04670	2,841388921	0,004395512		
Bcin13g03590	2,816906949	8,15E-27		
Bcin12g05960	2,790103426	5,53E-04		
Bcin13g03870	2,780270008	3,59E-19	K17686	copA, ctpA, ATP7; P-type Cu+ transporter [EC:7.2.2.8]
Bcin05g08390	2,7140922	1,08E-20		
Bcin16g02770	2,71302546	0,002547119	K19305	NPII; deuterolysin [EC:3.4.24.39]
Bcin15g04320	2,687867723	1,77E-06	K22149	SIDI; mevalonyl-CoA ligase
Bcin08g04600	2,6795539	5,76E-15		
Bcin07g04940	2,644262351	0,002672596	K08157	TPO1; MFS transporter, DHA1 family, multidrug resistance protein
Bcin14g01070	2,639615294	9,64E-12	K00008	SORD, gutB; L-iditol 2-dehydrogenase [EC:1.1.1.14]
Bcin01g05050	2,627729721	5,85E-10		
Bcin07g00090	2,604180723	4,11E-08		
Bcin10g00430	2,574039945	1,43E-14		
Bcin11g04160	2,536530698	2,39E-05		
Bcin07g02980	2,504966929	6,37E-06	K00354	E1.6.99.1; NADPH2 dehydrogenase [EC:1.6.99.1]
Bcin02g04380	2,490976321	1,10E-10	K00480	E1.14.13.1; salicylate hydroxylase [EC:1.14.13.1]
Bcin16g00950	2,462025248	0,00109627		
Bcin13g02320	2,408738804	2,50E-05	K18576	XEG; xyloglucan-specific endo-beta-1,4-glucanase [EC:3.2.1.151]

Bcin07g04100	2,397361055	0,001638899		
Bcin04g06240	2,388268275	1,44E-19	K00459	ncd2, npd; nitronate monooxygenase [EC:1.13.12.16]
Bcin02g08100	2,374604541	0,016182588		
Bcin12g00760	2,3585065	4,08E-22	K06901	pbuG, azgA, ghxP, ghxQ, adeQ; adenine/guanine/hypoxanthine permease
Bcin01g11030	2,355555174	7,40E-06		
Bcin03g03040	2,315862247	0,019200044		
Bcin14g01350	2,308542578	0,019555676		
Bcin06g06700	2,307818965	6,11E-04	K16261	YAT; yeast amino acid transporter
Bcin06g00920	2,294927965	1,67E-24	K00589	MET1; uroporphyrin-III C-methyltransferase [EC:2.1.1.107]
Bcin04g00060	2,29252661	0,003846812		
Bcin13g05670	2,290354635	2,58E-10	K01501	E3.5.5.1; nitrilase [EC:3.5.5.1]
Bcin03g00700	2,27686385	1,09E-16		
Bcin08g04690	2,264672203	1,61E-04		
Bcin05g08340	2,254765566	3,06E-19		
Bcin12g01090	2,254644117	1,26E-05		
Bcin09g05270	2,228984493	8,80E-24		
Bcin06g06540	2,205009563	0,02156953		
Bcin06g00024	2,20342843	7,04E-12		
Bcin01g10850	2,202164952	1,67E-04		
Bcin10g03040	2,177532319	5,29E-08		
Bcin15g05670	2,158398126	0,004118558	K01536	ENA; P-type Na+/K+ transporter [EC:7.2.2.3 7.2.2.-]
Bcin15g05690	2,145070047	0,005428323		
Bcin01g09270	2,137720564	0,023487519		
Bcin08g00930	2,133663603	7,66E-04		
Bcin04g06610	2,128029579	1,44E-05		
Bcin07g00040	2,108197994	6,83E-11		
Bcin01g10270	2,103843956	1,10E-09		

Bcin05g05450	2,102825707	1,77E-11	K00059	fabG, OAR1; 3-oxoacyl-[acyl-carrier protein] reductase [EC:1.1.1.100]
Bcin01g11480	2,095282538	0,04297718	K14338	cypD_E, CYP102A, CYP505; cytochrome P450 / NADPH-cytochrome P450 reductase [EC:1.14.14.1 1.6.2.4]
Bcin03g05590	2,077949344	0,023843604		
Bcin03g08170	2,067084753	1,09E-09		
Bcin05g04650	2,062429281	1,31E-07	K09448	TEAD; transcriptional enhancer factor
Bcin13g03090	2,037228844	0,008939515		
Bcin08g00110	2,027244764	1,29E-04		
Bcin11g06380	2,018149037	2,16E-09		
Bcin09g04940	2,017602605	8,82E-09		
Bcin12g00060	2,009553598	0,046821787		
Bcin03g05710	2,000855295	4,99E-13		
Bcin16g04630	-2,007714167	1,02E-12		
Bcin14g01380	-2,008559467	2,01E-12		
Bcin16g02840	-2,013240814	0,015070056		
Bcin10g00020	-2,023400286	0,019211288		
Bcin03g01300	-2,032926136	3,68E-08		
Bcin02g07770	-2,043362504	0,00435213		
Bcin13g03240	-2,046981583	2,22E-04		
Bcin16g02590	-2,049647871	2,97E-07		
Bcin01g01590	-2,056047681	3,13E-08		
Bcin16g00990	-2,059421728	0,0035964		
Bcin12g05810	-2,070157421	1,79E-23		
Bcin05g00380	-2,07791327	2,36E-19		
Bcin06g03730	-2,083297255	9,29E-05		
Bcin03g05480	-2,087523627	0,000943873		
Bcin15g02280	-2,102392544	0,011982998		
Bcin06g00040	-2,116121772	0,009311472		

Bcin02g00160	-2,157759482	3,09E-45		
Bcin09g05960	-2,159655447	0,003446268		
Bcin09g05020	-2,189313417	1,75E-22	K01580	E4.1.1.15, gadB, gadA, GAD; glutamate decarboxylase [EC:4.1.1.15]
Bcin05g04870	-2,193435998	1,26E-12		
Bcin01g00260	-2,198861059	1,66E-06		
Bcin17g00040	-2,212824632	1,94E-05		
Bcin09g02130	-2,226695148	1,80E-27		
Bcin01g10740	-2,263750064	2,34E-05		
Bcin07g04050	-2,264244762	0,027846426		
Bcin07g02370	-2,281599788	6,12E-15		
Bcin12g03520	-2,319896874	4,19E-08		
Bcin16g04610	-2,354412313	2,53E-12		
Bcin02g02000	-2,41195895	9,02E-05		
Bcin16g04620	-2,419700848	6,62E-59		
Bcin13g05720	-2,420207475	2,82E-19		
Bcin15g03320	-2,436903273	0,013979077		
Bcin14g04260	-2,466382229	5,96E-27		
Bcin04g05020	-2,506733525	5,57E-11		
Bcin13g01020	-2,519361793	1,57E-10		
Bcin09g06560	-2,538666839	0,020181342		
Bcin02g06390	-2,557342696	2,55E-05		
Bcin09g05970	-2,70832869	0,03893185		
Bcin18g00020	-2,806676802	2,38E-22		
Bcin13g05760	-2,833437919	0,025538181	K08095	E3.1.1.74; cutinase [EC:3.1.1.74]
Bcin12g05820	-2,857231058	0,001749234		
Bcin15g03090	-2,869791132	0,00574885	K06201	cutC; copper homeostasis protein
Bcin07g04770	-3,202623372	6,86E-04		

Bcin04g00780	-3,40915356	1,83E-13		
Bcin04g04450	-3,421760506	1,84E-22	K01641	E2.3.3.10; hydroxymethylglutaryl-CoA synthase [EC:2.3.3.10]
Bcin05g06500	-3,526930642	1,54E-05		
Bcin07g02270	-3,736961486	9,70E-16		
Bcin05g05680	-3,763095885	6,03E-04		
Bcin10g00030	-3,871750873	5,89E-49		
Bcin12g02040	-3,890609563	3,54E-06	K01379	CTSD; cathepsin D [EC:3.4.23.5]
Bcin01g04420	-3,989049776	0,002231128		
Bcin10g00010	-4,046536389	2,07E-06		
Bcin08g02150	-4,641705185	2,54E-82		
Bcin11g05460	-7,301208698	1,71E-06		

Table 10. List of DEGs from the transcriptional comparative 2 versus 5 (spores of B05.10 strain grown for 6 hours without exposure to NO versus spores of *ΔBcfhg*1 strain grown for 6 hours without exposure to NO). Gene ID - Identification code for *loci* from the BcinB0510 reference genome annotations (van Kan *et al.*, 2017); Log_2(FC) – Logarithm base 2 of the fold change (in green > 2 or in pink < -2); padj – adjusted p value (< 0.05); KEGG Terms – codes of functional categories in KEGG database; KEGG definition – Descriptions of the KEGG terms.

Gene ID	Log_2(FC)	padj	KEGG Terms	KEGG definition
Bcin04g06240	3,753325559	4,63E-135	K00459	ncd2, npd; nitronate monooxygenase [EC:1.13.12.16]
Bcin04g06250	2,728713493	1,61E-15	K01176	AMY, amyA, malS; alpha-amylase [EC:3.2.1.1]
Bcin04g06230	-2,824904732	1,86E-34	K05916	hmp, YHB1; nitric oxide dioxygenase [EC:1.14.12.17]
Bcin10g05210	-9,289050536	6,61E-11		

Table 11. List of DEGs from the transcriptional comparative 5 versus 6 (spores of *ΔBcfhg*1 strain grown for 6 hours without exposure to NO versus spores of the mutant strain *ΔBcfhg*1 grown for 4 hours and then exposed to NO for 2 hours). Gene ID - Identification code for *loci* from the BcinB0510 reference genome annotations (van Kan *et al.*, 2017); Log_2(FC) – Logarithm base 2 of the fold change (in green > 2 or in pink < -2); padj – adjusted p value (< 0.05); KEGG Terms – codes of functional categories in KEGG database; KEGG definition – Descriptions of the KEGG terms.

Gene ID	Log_2(FC)	padj	KEGG Terms	KEGG definition
Bcin11g06310	12,74044352	1,98E-24		
Bcin15g00040	7,845197591	0,00013342		

Bcin10g05210	7,411173097	1,26E-05		
Bcin01g08630	7,085071863	0,00010774	K00505	TYR; tyrosinase [EC:1.14.18.1]
Bcin08g04910	6,914090625	2,58E-05		
Bcin05g04580	6,87476874	4,15E-91	K03781	katE, CAT, catB, srpA; catalase [EC:1.11.1.6]
Bcin14g05020	6,853352044	1,23E-233		
Bcin14g00060	6,766415328	0,00041946		
Bcin02g00550	6,667568624	0,03555755		
Bcin14g01690	6,242220712	0,00823187	K01179	E3.2.1.4; endoglucanase [EC:3.2.1.4]
Bcin01g00040	6,15225139	0,0039492		
Bcin10g01470	6,142884939	2,32E-11		
Bcin13g04050	5,98125961	0,01144882		
Bcin13g05170	5,98125961	0,01144882		
Bcin02g05830	5,959752614	0,01850506		
Bcin03g04050	5,83490259	0,01415497		
Bcin14g01350	5,796523146	5,57E-21		
Bcin13g03870	5,64627482	2,10E-164	K17686	copA, ctpA, ATP7; P-type Cu+ transporter [EC:7.2.2.8]
Bcin13g05380	5,536505723	2,73E-50		
Bcin09g04560	5,404620306	0,0011588		
Bcin02g06160	5,354006531	0,01057787		
Bcin12g06180	5,052180019	1,34E-53	K10675	E4.2.1.66; cyanide hydratase [EC:4.2.1.66]
Bcin05g08390	4,951177677	4,76E-59		
Bcin15g05620	4,910802046	1,18E-11		
Bcin13g03590	4,904352413	2,19E-113		
Bcin15g00050	4,86134828	4,26E-18	K22889	AYT1, TRI101; trichothecene 3-O-acetyltransferase [EC:2.3.1.-]
Bcin15g05690	4,776250732	0,0002127		
Bcin05g06390	4,771063013	0,00981921		
Bcin15g05630	4,769106323	0,00043237		

Bcin07g02980	4,748409998	9,91E-07	K00354	E1.6.99.1; NADPH2 dehydrogenase [EC:1.6.99.1]
Bcin01g10220	4,689552143	6,74E-23		
Bcin07g00560	4,646672545	1,85E-56	K00354	E1.6.99.1; NADPH2 dehydrogenase [EC:1.6.99.1]
Bcin10g00430	4,638334952	2,87E-187		
Bcin07g00090	4,600756001	2,39E-18		
Bcin03g08170	4,53450614	4,95E-63		
Bcin08g04600	4,532017312	4,88E-10		
Bcin01g05050	4,457883546	1,88E-30		
Bcin12g01090	4,450053561	3,22E-43		
Bcin02g07640	4,416492848	3,40E-20		
Bcin04g02550	4,334991608	0,00504726		
Bcin03g07680	4,322426438	9,26E-20		
Bcin04g03820	4,295335236	0,03382373		
Bcin15g05700	4,266207766	2,00E-06		
Bcin01g11530	4,254433301	1,04E-59		
Bcin05g02850	4,168818984	1,53E-08		
Bcin02g04380	4,161058994	3,03E-54	K00480	E1.14.13.1; salicylate hydroxylase [EC:1.14.13.1]
Bcin04g06610	4,159710896	4,73E-30		
Bcin01g11480	4,1556603	1,69E-06	K14338	cypD_E, CYP102A, CYP505; cytochrome P450 / NADPH-cytochrome P450 reductase [EC:1.14.14.1 1.6.2.4]
Bcin06g06670	4,151945841	0,00173559		
Bcin14g01490	4,106079785	2,96E-07		
Bcin14g03160	4,095466521	4,50E-14	K00799	GST, gst; glutathione S-transferase [EC:2.5.1.18]
Bcin03g00700	4,082031916	2,47E-32		
Bcin16g01680	4,079977911	7,33E-11	K03574	mutT, NUDT15, MTH2; 8-oxo-dGTP diphosphatase [EC:3.6.1.55]
Bcin14g01070	4,057682543	8,36E-20	K00008	SORD, gutB; L-iditol 2-dehydrogenase [EC:1.1.1.14]
Bcin01g09570	4,047832146	4,22E-72		
Bcin11g00390	4,009983062	9,66E-24	K00799	GST, gst; glutathione S-transferase [EC:2.5.1.18]

Bcin10g03040	3,984380675	4,51E-87		
Bcin08g03130	3,98094203	1,84E-07		
Bcin03g05500	3,896166567	4,62E-75		
Bcin02g01880	3,895769898	7,31E-28		
Bcin07g07020	3,88051995	1,78E-06		
Bcin07g03190	3,852010094	1,06E-77		
Bcin12g05930	3,830834271	1,89E-26		
Bcin05g07510	3,829548604	5,56E-20		
Bcin12g05260	3,8020079	0,00826764		
Bcin05g03600	3,79744212	0,00024499		
Bcin06g00024	3,770655961	1,72E-41		
Bcin07g07130	3,752315468	0,03999081		
Bcin12g01340	3,715310814	4,08E-24	K07393	ECM4, yqjG; glutathionyl-hydroquinone reductase [EC:1.8.5.7]
Bcin09g01150	3,706464547	5,72E-09		
Bcin10g00150	3,70479575	0,00037294		
Bcin11g06380	3,687363976	1,71E-53		
Bcin02g04490	3,65524364	3,78E-45		
Bcin08g00110	3,646413121	7,71E-13		
Bcin12g05920	3,637763463	1,07E-56		
Bcin02g07630	3,629908992	2,53E-37		
Bcin08g03460	3,624272017	4,00E-36		
Bcin07g04100	3,596516453	0,00036077		
Bcin01g03920	3,594948296	0,0005726		
Bcin06g01560	3,584584155	1,60E-16		
Bcin11g05080	3,576295191	1,03E-51	K05275	E1.1.1.65; pyridoxine 4-dehydrogenase [EC:1.1.1.65]
Bcin04g03000	3,572375228	2,92E-39	K18740	EXD1, EGL; exonuclease 3'-5' domain-containing protein 1
Bcin08g00930	3,571525343	3,95E-24		

Bcin02g07500	3,547055523	2,63E-24		
Bcin01g11030	3,546285803	1,50E-19		
Bcin02g05300	3,546259778	0,04317905		
Bcin02g01270	3,528182398	1,03E-18		
Bcin14g01310	3,504071618	0,00028921		
Bcin14g04680	3,48838047	0,01649359		
Bcin02g07490	3,443367483	4,52E-08		
Bcin12g00780	3,4255095	0,02087599		
Bcin04g00060	3,415554955	4,88E-08		
Bcin11g00780	3,385917767	2,48E-60		
Bcin12g05960	3,372392267	3,37E-79		
Bcin14g01290	3,360979846	0,00608995		
Bcin02g04860	3,342271752	1,99E-07		
Bcin02g03350	3,333746513	1,17E-16		
Bcin11g06390	3,330867171	4,52E-07		
Bcin09g00470	3,31632065	6,07E-07		
Bcin09g05490	3,310328901	5,76E-07		
Bcin13g05270	3,292710087	1,04E-15	K07192	FLOT; flotillin
Bcin06g03810	3,278284313	1,93E-06		
Bcin10g03710	3,259591878	1,75E-06		
Bcin06g00170	3,252699248	1,39E-06		
Bcin12g00040	3,238843122	0,00375635	K01426	E3.5.1.4, amiE; amidase [EC:3.5.1.4]
Bcin01g11520	3,221398739	1,06E-17		
Bcin13g02470	3,212089511	1,49E-21		
Bcin05g05450	3,196450481	1,33E-30	K00059	fabG, OAR1; 3-oxoacyl-[acyl-carrier protein] reductase [EC:1.1.1.100]
Bcin01g05190	3,172808514	7,24E-41		
Bcin09g00740	3,166427129	8,04E-20		

Bcin10g00740	3,164140677	7,01E-18	K00799	GST, gst; glutathione S-transferase [EC:2.5.1.18]
Bcin01g03270	3,159510211	0,00016212		
Bcin02g03440	3,146193005	0,01511867		
Bcin06g07010	3,124307802	0,00846196	K05972	AXE1; acetylxylan esterase [EC:3.1.1.72]
Bcin07g03430	3,123201583	1,46E-26	K00799	GST, gst; glutathione S-transferase [EC:2.5.1.18]
Bcin05g01320	3,122085557	0,00022632		
Bcin12g04940	3,11717462	2,61E-08	K21294	GLIC, ACLC, ROQR; gliotoxin/aspirochlorine/mycotoxins biosynthesis cytochrome P450 monooxygenase [EC:1.-.-.-]
Bcin01g03520	3,085638123	0,01187347		
Bcin06g07140	3,082577504	9,94E-06		
Bcin11g05000	3,057873328	0,00756075		
Bcin07g04460	3,045994146	1,86E-13	K00387	SUOX; sulfite oxidase [EC:1.8.3.1]
Bcin05g05290	3,044114142	8,90E-23		
Bcin12g00520	3,039765488	2,20E-05		
Bcin08g02710	3,011829719	3,41E-10		
Bcin07g04950	3,001201279	5,30E-16		
Bcin14g00580	2,997297076	0,00017764		
Bcin08g05730	2,990711281	2,39E-13		
Bcin15g05150	2,97656661	0,0003289	K20039	FDC1; phenacrylate decarboxylase [EC:4.1.1.102]
Bcin05g08230	2,964133058	0,02746334	K19356	E1.14.99.54; lytic cellulose monooxygenase (C1-hydroxylating) [EC:1.14.99.54]
Bcin02g06000	2,943930121	5,40E-17		
Bcin13g04040	2,905007333	2,31E-48	K07305	msrB; peptide-methionine (R)-S-oxide reductase [EC:1.8.4.12]
Bcin05g04810	2,881365599	3,48E-22		
Bcin02g01120	2,857902263	5,24E-08		
Bcin14g01660	2,844754378	1,44E-38		
Bcin16g02500	2,837047228	0,0002989		
Bcin05g02050	2,789624252	7,49E-27	K22745	AIFM2; apoptosis-inducing factor 2
Bcin01g04860	2,746366878	4,53E-07		

Bcin09g00910	2,738266444	6,08E-15		
Bcin02g06300	2,73414435	0,04360023		
Bcin10g04490	2,728317044	1,73E-06		
Bcin07g00400	2,717220853	1,99E-39		
Bcin02g01870	2,715538628	5,13E-21		
Bcin02g00840	2,707009682	3,00E-37		
Bcin01g04540	2,69044974	8,66E-08		
Bcin07g00040	2,689714538	1,77E-12		
Bcin02g09380	2,684148139	1,71E-11	K01053	gnl, RGN; gluconolactonase [EC:3.1.1.17]
Bcin09g06540	2,682188956	1,83E-07	K00457	HPD, hppD; 4-hydroxyphenylpyruvate dioxygenase [EC:1.13.11.27]
Bcin13g03090	2,681783121	0,00030825		
Bcin14g01700	2,681400218	0,00417009	K19668	CBH2, cbhA; cellulose 1,4-beta-cellobiosidase [EC:3.2.1.91]
Bcin14g02300	2,671656243	3,50E-14		
Bcin02g05800	2,660904532	7,15E-15		
Bcin05g07100	2,658640905	3,49E-13	K06911	PIR; quercetin 2,3-dioxygenase [EC:1.13.11.24]
Bcin11g00810	2,656510735	5,26E-46		
Bcin08g04770	2,650046282	1,35E-41	K02858	ribB, RIB3; 3,4-dihydroxy 2-butanone 4-phosphate synthase [EC:4.1.99.12]
Bcin01g07760	2,643990196	1,08E-12		
Bcin11g06150	2,640636435	0,03223168		
Bcin01g09270	2,638919942	1,75E-09		
Bcin12g01100	2,635611462	0,00392586	K18580	RHGA; rhamnogalacturonan hydrolase [EC:3.2.1.171]
Bcin03g08570	2,63100821	9,90E-07	K17871	ndh1; NADH:ubiquinone reductase (non-electrogenic) [EC:1.6.5.9]
Bcin12g03680	2,615479234	3,98E-13		
Bcin02g07910	2,611475453	3,55E-11		
Bcin05g01770	2,606773899	2,63E-06	K08254	E3.2.1.59; glucan endo-1,3-alpha-glucosidase [EC:3.2.1.59]
Bcin07g00570	2,596958359	7,22E-05		
Bcin06g06350	2,595946753	2,44E-11	K03809	wrbA; NAD(P)H dehydrogenase (quinone) [EC:1.6.5.2]

Bcin09g03770	2,593848369	1,71E-05		
Bcin01g00160	2,590455104	1,24E-20		
Bcin09g04940	2,586310688	2,10E-17		
Bcin13g03390	2,583320745	9,99E-10		
Bcin12g00030	2,581173258	1,46E-16		
Bcin12g04910	2,57484288	3,11E-20		
Bcin08g03740	2,574478059	2,66E-14		
Bcin02g06580	2,566768021	6,73E-20	K01568	PDC, pdc; pyruvate decarboxylase [EC:4.1.1.1]
Bcin03g08640	2,549476214	3,57E-10	K01426	E3.5.1.4, amiE; amidase [EC:3.5.1.4]
Bcin05g02400	2,54079412	1,14E-10		
Bcin05g02490	2,54014475	2,44E-53	K07304	msrA; peptide-methionine (S)-S-oxide reductase [EC:1.8.4.11]
Bcin12g02050	2,536887859	3,75E-12		
Bcin09g04450	2,532484299	1,30E-16		
Bcin05g04570	2,527587329	1,88E-13	K00108	betA, CHDH; choline dehydrogenase [EC:1.1.99.1]
Bcin09g00570	2,516804443	2,21E-07		
Bcin05g04520	2,495451474	6,74E-23		
Bcin14g03720	2,48790049	0,00922103		
Bcin12g01130	2,486422755	0,00102426		
Bcin14g04930	2,479663503	3,90E-07		
Bcin13g02320	2,476797446	5,98E-06	K18576	XEG; xyloglucan-specific endo-beta-1,4-glucanase [EC:3.2.1.151]
Bcin13g00670	2,474321789	2,69E-11		
Bcin08g00010	2,467028838	3,49E-24		
Bcin12g05590	2,457115028	0,01371601		
Bcin06g05110	2,45452067	1,79E-13	K06911	PIR; quercetin 2,3-dioxygenase [EC:1.13.11.24]
Bcin14g01430	2,444644598	1,81E-28		
Bcin03g00240	2,442154438	3,96E-27		
Bcin06g03050	2,437295567	1,14E-09		

Bcin11g04160	2,432146951	2,00E-06		
Bcin15g05270	2,421495022	6,35E-35		
Bcin16g02120	2,408123493	9,27E-16	K12608	CAF16; CCR4-NOT complex subunit CAF16
Bcin02g06200	2,402801706	0,01815889		
Bcin12g02840	2,396467032	2,58E-10	K01512	acyP; acylphosphatase [EC:3.6.1.7]
Bcin07g07120	2,392047614	0,00522558	K22889	AYT1, TRI101; trichothecene 3-O-acetyltransferase [EC:2.3.1.-]
Bcin03g01450	2,391917072	4,67E-12		
Bcin03g04480	2,331671839	0,00059699		
Bcin07g01490	2,321758276	0,00040763		
Bcin06g03820	2,319889035	2,78E-08		
Bcin05g05150	2,318061409	1,21E-12		
Bcin01g10850	2,314244998	8,50E-05		
Bcin07g01460	2,313469681	0,00041946		
Bcin09g00860	2,303870361	0,00456924		
Bcin03g00930	2,302705743	0,00027489		
Bcin04g06310	2,293780685	1,49E-19	K07213	ATOX1, ATX1, copZ, golB; copper chaperone
Bcin03g05820	2,29270181	0,00115862	K01728	pel; pectate lyase [EC:4.2.2.2]
Bcin16g00005	2,2816269	0,00470147		
Bcin02g02140	2,274798991	4,37E-05		
Bcin03g01460	2,271781144	4,26E-07		
Bcin16g01790	2,263034852	0,00505069		
Bcin07g05930	2,257921184	3,78E-07		
Bcin04g01080	2,254011624	3,72E-10	K00637	SOAT; sterol O-acyltransferase [EC:2.3.1.26]
Bcin14g01940	2,251361504	6,25E-20	K11205	GCLM; glutamate--cysteine ligase regulatory subunit
Bcin02g04870	2,248643549	6,01E-18	K11275	H1_5; histone H1/5
Bcin14g05510	2,247176541	5,15E-09		
Bcin10g01560	2,240804165	4,39E-06		

Bcin09g03940	2,234205391	1,48E-07	K09958	K09958; uncharacterized protein
Bcin10g05670	2,225200848	8,00E-19		
Bcin12g06330	2,223578006	1,04E-11		
Bcin09g00850	2,22274495	1,45E-10		
Bcin11g00510	2,221161374	2,02E-08	K11206	NIT1, ybeM; deaminated glutathione amidase [EC:3.5.1.128]
Bcin09g00460	2,220548422	5,24E-21		
Bcin11g03070	2,219412876	0,01102868		
Bcin03g06670	2,199819229	4,43E-05		
Bcin01g04340	2,196414649	2,95E-19	K00958	sat, met3; sulfate adenylyltransferase [EC:2.7.7.4]
Bcin14g03030	2,194132125	1,26E-11		
Bcin13g05160	2,193106915	8,14E-15		
Bcin02g04500	2,193034535	0,00016565		
Bcin03g08070	2,192421611	7,91E-14		
Bcin02g01350	2,165229281	1,25E-07		
Bcin04g04270	2,161928174	1,13E-17		
Bcin08g04920	2,154799501	0,00053178		
Bcin09g06320	2,151888539	0,00214123		
Bcin05g04960	2,149482564	0,03972587	K01501	E3.5.5.1; nitrilase [EC:3.5.5.1]
Bcin15g05160	2,144542946	0,00518494	K03186	ubiX, bsdB, PAD1; flavin prenyltransferase [EC:2.5.1.129]
Bcin03g05830	2,140688517	0,00195392	K16795	PAFAH1B2_3; platelet-activating factor acetylhydrolase IB subunit beta/gamma [EC:3.1.1.47]
Bcin13g02460	2,135799396	1,15E-06		
Bcin11g00870	2,134763636	4,60E-22		
Bcin05g06220	2,128955097	0,01118293		
Bcin03g05710	2,122268163	2,11E-10		
Bcin05g02100	2,108167792	4,88E-06		
Bcin06g05220	2,101044753	2,69E-12		
Bcin10g01840	2,099512159	5,98E-15	K08726	EPHX2; soluble epoxide hydrolase / lipid-phosphate phosphatase [EC:3.3.2.10 3.1.3.76]

Bcin02g03270	2,098151333	1,23E-25		
Bcin04g00990	2,095249142	0,00285316		
Bcin07g05710	2,094214884	7,12E-06	K08900	BCS1; mitochondrial chaperone BCS1
Bcin01g11220	2,084593673	9,07E-14	K01199	EGLC; glucan endo-1,3-beta-D-glucosidase [EC:3.2.1.39]
Bcin04g02680	2,084408718	2,76E-07		
Bcin15g00320	2,072238326	7,49E-11		
Bcin15g02550	2,060514577	1,30E-06	K13993	HSP20; HSP20 family protein
Bcin13g02110	2,060419154	8,37E-15		
Bcin04g02650	2,052845174	2,72E-12		
Bcin12g06010	2,050920669	5,17E-05		
Bcin04g04740	2,048962456	0,02682866		
Bcin16g00330	2,045964651	4,52E-11		
Bcin11g03340	2,042280995	0,00045737		
Bcin15g03840	2,036498801	5,64E-09		
Bcin01g11430	2,035902967	3,73E-15	K00077	panE, apbA; 2-dehydropantoate 2-reductase [EC:1.1.1.169]
Bcin06g06150	2,025256364	1,24E-14		
Bcin02g03110	2,017997207	1,15E-14		
Bcin13g05420	2,017736657	9,39E-31		
Bcin03g03280	2,012911479	1,16E-10		
Bcin02g06250	2,010716994	1,87E-12	K21766	TBCC; tubulin-specific chaperone C
Bcin03g03530	-2,005883277	0,04938142		
Bcin01g09450	-2,009888983	1,62E-14	K18102	GAAB, LGD1; L-galactonate dehydratase [EC:4.2.1.146]
Bcin05g08250	-2,010557172	0,01649359		
Bcin12g00690	-2,019216945	5,58E-07	K22148	SIDC; ferricrocin synthase
Bcin15g03330	-2,021009241	3,11E-12		
Bcin13g05720	-2,021972066	0,00100578		
Bcin12g05810	-2,033582438	2,08E-24		

Bcin15g03880	-2,038353251	0,03280541		
Bcin06g02530	-2,060963035	1,20E-11		
Bcin09g05960	-2,061163273	0,00049814		
Bcin10g00670	-2,061806605	1,17E-19		
Bcin06g02760	-2,066651948	9,03E-16		
Bcin06g05580	-2,084849799	7,14E-11		
Bcin06g00330	-2,109345782	1,38E-15	K01279	TPP1, CLN2; tripeptidyl-peptidase I [EC:3.4.14.9]
Bcin06g05790	-2,117337696	8,16E-08		
Bcin03g01040	-2,125720409	2,62E-15	K01580	E4.1.1.15, gadB, gadA, GAD; glutamate decarboxylase [EC:4.1.1.15]
Bcin01g10740	-2,130822473	0,00014521		
Bcin03g00540	-2,131727748	3,18E-14	K01176	AMY, amyA, malS; alpha-amylase [EC:3.2.1.1]
Bcin10g02370	-2,137533543	3,10E-10		
Bcin11g03150	-2,144248006	7,52E-06	K18703	SUGCT; succinate---hydroxymethylglutarate CoA-transferase [EC:2.8.3.13]
Bcin01g00100	-2,147323939	0,01911771		
Bcin06g04140	-2,152019108	0,00104215		
Bcin05g07670	-2,157565553	8,50E-09		
Bcin01g03070	-2,160168471	2,18E-08		
Bcin08g03150	-2,171063298	6,70E-08	K00863	DAK, TKFC; triose/dihydroxyacetone kinase / FAD-AMP lyase (cyclizing) [EC:2.7.1.28 2.7.1.29 4.6.1.15]
Bcin01g10630	-2,175529525	0,00133089		
Bcin05g01720	-2,176708154	0,01166578		
Bcin15g02090	-2,1793195	2,06E-24	K00700	GBE1, glgB; 1,4-alpha-glucan branching enzyme [EC:2.4.1.18]
Bcin02g02150	-2,185689929	1,55E-09		
Bcin09g02140	-2,189286746	0,00045356		
Bcin10g00720	-2,200941314	6,05E-06	K19200	IAL; isopenicillin-N N-acyltransferase like protein
Bcin16g04610	-2,203904213	2,93E-06		
Bcin16g04520	-2,218482307	3,15E-10		
Bcin08g06640	-2,218790054	0,00745006	K15271	HFM1, MER3; ATP-dependent DNA helicase HFM1/MER3 [EC:3.6.4.12]

Bcin06g05560	-2,244848653	1,07E-13		
Bcin01g10500	-2,245165856	7,31E-10		
Bcin08g02390	-2,250044092	1,57E-30		
Bcin07g03280	-2,252763735	6,32E-07		
Bcin14g01850	-2,257497423	9,39E-12		
Bcin14g03450	-2,262465106	0,00052298		
Bcin14g02440	-2,276401846	2,01E-10		
Bcin04g01410	-2,310127459	1,31E-36		
Bcin13g04290	-2,314374658	8,76E-06		
Bcin12g03480	-2,320182768	2,17E-72	K16369	CHO2; phosphatidylethanolamine N-methyltransferase [EC:2.1.1.17]
Bcin01g10310	-2,325913901	1,32E-18	K01196	AGL; glycogen debranching enzyme [EC:2.4.1.25 3.2.1.33]
Bcin17g00040	-2,328520738	2,54E-07		
Bcin05g01550	-2,331310996	8,65E-27	K17743	XR; D-xylose reductase [EC:1.1.1.307]
Bcin06g04840	-2,342202897	6,77E-08	K05349	bglX; beta-glucosidase [EC:3.2.1.21]
Bcin04g00880	-2,356652303	0,00062973		
Bcin08g01450	-2,365336837	1,71E-06		
Bcin01g08670	-2,366462475	2,24E-06		
Bcin12g02980	-2,368066586	3,15E-09		
Bcin13g05760	-2,369264357	0,00036148	K08095	E3.1.1.74; cutinase [EC:3.1.1.74]
Bcin04g05120	-2,375581819	3,11E-29		
Bcin04g00740	-2,38392744	4,09E-06		
Bcin03g01130	-2,385466246	2,58E-17	K00128	ALDH; aldehyde dehydrogenase (NAD+) [EC:1.2.1.3]
Bcin04g05020	-2,387391118	2,64E-05		
Bcin14g05550	-2,388414833	1,49E-07		
Bcin12g03250	-2,403252083	0,03017384		
Bcin13g01020	-2,408150788	5,16E-05		
Bcin03g09200	-2,409241759	0,00164058		

Bcin11g04710	-2,409941899	2,62E-28	K18097	GCY1; glycerol 2-dehydrogenase (NADP+) [EC:1.1.1.156]
Bcin12g02440	-2,439110319	1,04E-20	K00652	bioF; 8-amino-7-oxononanoate synthase [EC:2.3.1.47]
Bcin16g02700	-2,444104536	4,03E-28	K01687	ilvD; dihydroxy-acid dehydratase [EC:4.2.1.9]
Bcin04g04800	-2,446644801	5,05E-07	K17739	THNR; tetrahydroxynaphthalene reductase [EC:1.1.1.252]
Bcin12g02430	-2,44773243	2,24E-27	K19562	BIO3-BIO1; bifunctional dethiobiotin synthetase / adenosylmethionine --- 8-amino-7-oxononanoate aminotransferase [EC:6.3.3.3 2.6.1.62]
Bcin08g02080	-2,452647042	1,44E-70		
Bcin05g01780	-2,454755679	0,00484155		
Bcin02g06390	-2,462298685	7,01E-05		
Bcin16g04600	-2,476905286	0,00948545		
Bcin06g03330	-2,480831902	0,00066268		
Bcin10g04710	-2,486946741	2,35E-17		
Bcin13g03100	-2,488668552	0,00039639		
Bcin02g01730	-2,490221973	1,80E-05		
Bcin06g05780	-2,509694387	2,28E-21		
Bcin07g04770	-2,518173474	3,82E-05		
Bcin07g02260	-2,523774215	2,61E-08		
Bcin07g02370	-2,530003858	4,93E-08		
Bcin11g00140	-2,53386404	0,00015881		
Bcin08g05480	-2,561727828	4,52E-08		
Bcin04g04920	-2,580036813	7,06E-72	K18278	THI5; pyrimidine precursor biosynthesis enzyme
Bcin01g00260	-2,606367523	2,74E-05		
Bcin12g05820	-2,615109761	0,00103513		
Bcin11g04970	-2,624072904	0,02722777		
Bcin09g06660	-2,648927894	7,70E-06		
Bcin04g01430	-2,657156596	1,98E-51		
Bcin04g01390	-2,685620011	5,35E-09		
Bcin02g00470	-2,707939157	3,32E-19	K17742	SOU1; sorbose reductase [EC:1.1.1.289]

Bcin02g00160	-2,720553895	2,66E-77		
Bcin14g01380	-2,722439244	5,93E-10		
Bcin02g00280	-2,738968056	0,00219546		
Bcin11g04930	-2,742769902	1,34E-25		
Bcin11g05460	-2,763310437	0,00606165		
Bcin02g04840	-2,786801033	8,66E-08	K08176	PHO84; MFS transporter, PHS family, inorganic phosphate transporter
Bcin09g04240	-2,827773989	0,00191409	K00864	glpK, GK; glycerol kinase [EC:2.7.1.30]
Bcin15g03620	-2,853739417	5,25E-17	K00688	PYG, glgP; glycogen phosphorylase [EC:2.4.1.1]
Bcin06g02230	-2,865618143	2,86E-07		
Bcin09g03810	-2,871508864	4,13E-59		
Bcin08g03560	-2,902279941	0,04249817		
Bcin14g04260	-2,915100925	1,20E-09		
Bcin10g00380	-2,932855918	1,29E-08		
Bcin05g01260	-2,973706162	2,37E-07		
Bcin02g04660	-3,083355396	0,01212827		
Bcin15g03320	-3,093524431	5,06E-08		
Bcin04g02780	-3,106829743	0,04147542		
Bcin04g01140	-3,123733884	0,03284231		
Bcin04g04450	-3,141648181	5,61E-14	K01641	E2.3.3.10; hydroxymethylglutaryl-CoA synthase [EC:2.3.3.10]
Bcin18g00020	-3,15440091	3,26E-21		
Bcin13g05800	-3,165655457	0,00333849		
Bcin06g03730	-3,290704416	0,00285316		
Bcin04g01400	-3,291792536	3,84E-50		
Bcin12g03520	-3,298893379	8,81E-13		
Bcin06g05200	-3,319678265	2,35E-30		
Bcin02g02000	-3,327624188	1,39E-05		
Bcin12g02450	-3,336401311	3,91E-30	K01012	bioB; biotin synthase [EC:2.8.1.6]

Bcin14g00610	-3,395024081	0,01009027	K01184	E3.2.1.15; polygalacturonase [EC:3.2.1.15]
Bcin04g00480	-3,414314251	0,04724775		
Bcin05g04870	-3,521079065	7,15E-14		
Bcin09g07130	-3,57700318	0,00466786		
Bcin10g00020	-3,705259218	0,00051262		
Bcin01g08330	-3,709419064	6,58E-07	K00826	E2.6.1.42, ilvE; branched-chain amino acid aminotransferase [EC:2.6.1.42]
Bcin07g03730	-3,742027702	0,00706789		
Bcin04g00780	-3,762492119	2,56E-10		
Bcin07g02270	-3,778755151	3,90E-08		
Bcin05g06500	-3,784114617	0,00019557		
Bcin14g00260	-3,790469878	0,00067939		
Bcin16g02590	-3,911498296	1,43E-16		
Bcin10g00040	-4,078199328	3,01E-18		
Bcin12g02040	-4,233924869	1,00E-29	K01379	CTSD; cathepsin D [EC:3.4.23.5]
Bcin10g00030	-4,640808084	7,73E-39		
Bcin02g08710	-4,883243761	8,17E-06		
Bcin08g02150	-4,94851996	3,39E-51		
Bcin01g07900	-5,302964901	0,03241624		
Bcin02g08880	-5,430838605	0,02594341		
Bcin01g07390	-5,439933303	0,0200153		
Bcin02g00002	-5,616084194	0,01561972		
Bcin04g04700	-5,618913679	0,01508286		
Bcin09g05970	-5,673573618	0,0151542		
Bcin02g07840	-5,724061907	0,01515675		
Bcin11g01550	-5,791782319	0,00770946		
Bcin04g00050	-5,947268469	0,00534142		
Bcin01g02140	-6,000261755	0,04249817		

Bcin08g03340	-6,022927218	0,00417726			
Bcin09g00960	-6,031296177	0,00553815			
Bcin15g03170	-6,040580988	0,00733766			
Bcin04g00470	-6,111983776	0,0035882	K22539	PLY; pectate lyase [EC:4.2.2.2]	
Bcin06g05980	-6,148512825	0,00296644			
Bcin08g07090	-6,158353581	0,00322392			
Bcin14g05480	-6,235581689	0,00189196			
Bcin16g00990	-6,310523767	0,00151661			
Bcin05g01900	-6,315328166	0,00249097			
Bcin15g01880	-6,350411005	0,00164016			
Bcin06g04540	-6,376176197	0,0013734			
Bcin05g05550	-6,817140731	0,00038509			
Bcin02g03670	-7,640095938	1,32E-05			
Bcin10g00010	-8,68963571	3,13E-07			
Bcin08g05780	-12,61233067	0,01757496	K24279	ERDH; putative ergosteryl-3beta-O-L-aspartate hydrolase	

Table 12. List of DEGs from the transcriptional comparative between mycelium samples from B05.10 and *ΔBcorp*1-19 strains grown in solid medium. Gene ID - Identification code for *loci* from the BcinB0510 reference genome annotations (van Kan *et al.*, 2017); Log_2(FC) – Logarithm base 2 of the fold change (in green > 2 or in pink < -2); padj – adjusted p value (< 0.05).

Gene ID	Log_2(FC)	padj
Bcin05g05670	20,7693	0,000012829
Bcin08g06810	10,5364	0,000000061
Bcin14g01570	10,3517	0,002844483
Bcin04g02840	10,2756	0,000002623
Bcin07g04520	10,0955	0,000001459
Bcin10g00710	9,3555	0,029723519

Bcin13g03380	8,7363	0,018738422
Bcin06g04220	8,2945	0,028735054
Bcin14g02630	8,2552	0,033517644
Bcin15g04390	7,8525	0,027069724
Bcin10g00290	7,1746	0,000175120
Bcin04g06590	6,4098	0,013479564
Bcin02g01110	5,2174	0,026090273
Bcin13g03950	4,6415	0,000000130
Bcin12g06180	4,0996	0,003640570
Bcin15g04440	2,6588	0,002639354
Bcin02g03050	2,6205	0,016668096
Bcin01g10630	2,4413	0,002395353
Bcin08g00940	2,4321	0,003505611
Bcin16g00970	2,4146	0,000000000
Bcin07g01030	2,3037	0,014396545
Bcin02g07440	2,2073	0,000070297
Bcin06g05190	2,2070	0,000006305
Bcin11g04410	2,1717	0,003254757
Bcin08g02320	2,1568	0,000700032
Bcin03g00640	2,1466	0,036879031
Bcin16g02010	2,0981	0,012981509
Bcin13g00030	2,0899	0,000010235
Bcin04g01520	2,0684	0,000014554
Bcin10g01210	-2,0062	0,000062986
Bcin06g01430	-2,0091	0,000042057
Bcin09g01280	-2,0120	0,000101315

Bcin05g07120	-2,0129	0,000024461
Bcin14g03610	-2,0188	0,000024610
Bcin02g00740	-2,0196	0,003491236
Bcin11g00390	-2,0233	0,000000000
Bcin02g01440	-2,0243	0,000000141
Bcin08g01870	-2,0256	0,000010235
Bcin12g05030	-2,0358	0,000000000
Bcin11g05970	-2,0610	0,000004291
Bcin16g03040	-2,0731	0,000051145
Bcin09g02130	-2,0772	0,000000000
Bcin13g04860	-2,0900	0,000000002
Bcin04g02340	-2,0902	0,000003730
Bcin12g03680	-2,0915	0,000047464
Bcin02g02190	-2,1197	0,000236776
Bcin06g03010	-2,1344	0,000000000
Bcin08g06460	-2,1420	0,000003838
Bcin01g09640	-2,1502	0,019289352
Bcin13g03110	-2,1538	0,016290292
Bcin08g07080	-2,1641	0,000000000
Bcin08g06690	-2,1694	0,000002987
Bcin01g08380	-2,1896	0,000011782
Bcin13g03100	-2,1911	0,000076510
Bcin15g05180	-2,1972	0,000000000
Bcin01g04570	-2,2037	0,000012038
Bcin11g01700	-2,2058	0,000002203
Bcin11g05390	-2,2201	0,000000000

Bcin14g03810	-2,2326	0,000048634
Bcin04g02380	-2,2489	0,000008963
Bcin13g00370	-2,2624	0,000007439
Bcin06g04930	-2,2698	0,000005252
Bcin13g03270	-2,2858	0,040602731
Bcin11g01560	-2,2945	0,000002987
Bcin09g05020	-2,3165	0,000100964
Bcin14g03180	-2,3199	0,000000061
Bcin12g00900	-2,3229	0,000000228
Bcin09g02760	-2,3267	0,000000031
Bcin02g02720	-2,3302	0,000211518
Bcin14g00690	-2,3435	0,004668874
Bcin14g03590	-2,3607	0,000002779
Bcin07g02980	-2,3705	0,000099835
Bcin16g04430	-2,3764	0,000000010
Bcin01g10170	-2,4150	0,000003063
Bcin05g07190	-2,4327	0,010149342
Bcin09g05130	-2,4342	0,000000005
Bcin04g02370	-2,4489	0,000939157
Bcin03g02210	-2,4562	0,000000010
Bcin05g06000	-2,4994	0,000000009
Bcin11g04790	-2,5349	0,000000000
Bcin01g02940	-2,5424	0,000254180
Bcin12g00390	-2,5543	0,000000000
Bcin03g03280	-2,5808	0,000000000
Bcin09g01290	-2,5830	0,000005925

Bcin16g00060	-2,5970	0,000000000
Bcin13g00250	-2,6251	0,000000002
Bcin15g05120	-2,6758	0,000000906
Bcin16g04200	-2,6770	0,000013759
Bcin10g03770	-2,7053	0,000000000
Bcin12g06380	-2,7338	0,011465474
Bcin05g07680	-2,7473	0,000000008
Bcin16g02720	-2,7488	0,000000000
Bcin13g03460	-2,7714	0,000106138
Bcin08g01350	-2,7872	0,000000011
Bcin10g01980	-2,8001	0,000016415
Bcin09g00500	-2,8285	0,000000000
Bcin05g05240	-2,8643	0,000000002
Bcin03g02220	-2,8798	0,000000010
Bcin12g03980	-2,9026	0,000000006
Bcin03g01270	-2,9318	0,000000000
Bcin06g05410	-2,9523	0,000000192
Bcin01g04660	-2,9606	0,000001153
Bcin03g00540	-2,9727	0,000000018
Bcin03g05500	-2,9939	0,000000001
Bcin02g01950	-3,0198	0,000023159
Bcin01g11060	-3,0415	0,000000972
Bcin13g01790	-3,2348	0,000000061
Bcin06g03900	-3,2856	0,000000000
Bcin06g04920	-3,3158	0,000001306
Bcin09g04620	-3,3495	0,000016428

Bcin13g02920	-3,5495	0,000000000
Bcin05g03570	-3,9549	0,000000000
Bcin04g00160	-3,9984	0,000000000
Bcin16g00300	-4,2710	0,015183597
Bcin14g02430	-5,3019	0,001369946
Bcin13g05790	-6,6525	0,003069005
Bcin12g02480	-6,7474	0,007889291
Bcin08g01630	-8,1594	0,034160464
Bcin11g00880	-8,2869	0,025993312
Bcin03g01930	-8,3071	0,019351019
Bcin02g04950	-8,3494	0,015669603
Bcin12g00400	-8,4740	0,000000004
Bcin07g05900	-8,5014	0,008398401
Bcin07g00100	-8,6050	0,017506435
Bcin15g01590	-8,7820	0,003429112
Bcin04g06920	-8,8674	0,001923963
Bcin07g05020	-8,9845	0,001791058
Bcin01g06890	-9,0051	0,001111938
Bcin02g09100	-9,1063	0,000559305
Bcin11g05470	-9,1572	0,005972687
Bcin02g01880	-10,0544	0,003923887
Bcin06g01070	-12,4785	0,033277352

Bibliography

Adav, S. S., Ravindran, A., and Sze, S. K. (2013). Proteomic analysis of temperature dependent extracellular proteins from *Aspergillus fumigatus* grown under solid-state culture condition. *J Proteome Res*. 12(6), 2715-2731. doi: 10.1021/pr4000762.

Agrios, G. N. (2005). Plant Pathology. 5th Ed. Academic Press. San Diego. California, USA.

Al Abdallah, Q., Choe, S. I., Campoli, P., Baptista, S., Gravelat, F. N., Lee, M. J., and Sheppard, D. C. (2012). A conserved C-terminal domain of the *Aspergillus fumigatus* developmental regulator *MedA* is required for nuclear localization, adhesion and virulence. *PLoS One*, 7(11), e49959. doi: 10.1371/journal.pone.0049959.

Al-Bader, N., Vanier, G., Liu, H., Gravelat, F. N., Urb, M., Hoareau, C. Q., Campoli, P., Chabot, J., Filler, S. G., and Sheppard, D. C. (2010). Role of trehalose biosynthesis in *Aspergillus fumigatus* development, stress response, and virulence. *Infect Immun*. 78, 3007–3018. *https://doi.org/10.1128/IAI.00813-09*.

Alonso Díaz, Alejandro, 2015. Obtención de mutantes deficientes en el gen *Bcorp*1 y *Bcmed* en *Botrytis cinerea*. Master thesis. Salamanca: University of Salamanca.

Altschul, S. F., Gish, W., Miller, W., Myers, E. W. and Lipman, D. J. (1990). Basic local alignment search tool. *J. Mol. Biol*. 215, 403-410.

Amal, H., Gong, G., Gjoneska, E., Lewis, S. M., Wishnok, J. S., Tsai, L. H., and Tannenbaum, S. R. (2019). S -nitrosylation of E3 ubiquitin-protein ligase RNF213 alters non-canonical Wnt/Ca+2 signaling in the P301S mouse model of tauopathy. *Translational Psychiatry*, 9, 44. https ://doi.org/10.1038/s41398-019-0388-7

Amselem, J., Cuomo, C. A., van Kan, J. A., Viaud, M., Benito, E. P., Couloux, A., Coutinho, P. M., de Vries, R. P., Dyer, P. S., Fillinger, S., Fournier, E., Gout, L., Hahn, M., Kohn, L., Lapalu, N., Plummer, K. M., Pradier, J. M., Quévillon, E., Sharon, A., Simon, A., ten Have, A., Tudzynski, B., Tudzynski, P., Wincker, P., Andrew, M., Anthouard, V., Beever, R. E., Beffa, R., Benoit, I., Bouzid, O., Brault, B., Chen, Z., Choquer, M., Collémare, J., Cotton, P., Danchin, E. G., Da Silva, C. , Gautier, A., Giraud, C., Giraud, T., Gonzalez, C., Grossetete, S., Güldener, U ., Henrissat, B., Howlett, B. J., Kodira, C., Kretschmer, M., Lappartient, A., Leroch, M., Levis, C., Mauceli, E., Neuvéglise, C., Oeser, B., Pearson, M., Poulain, J., Poussereau, N., Quesneville, H., Rascle, C., Schumacher, J., Ségurens, B., Sexton, A., Silva, E., Sirven, C., Soanes, D. M., Talbot, N. J., Templeton, M., Yandava, C., Yarden, O., Zeng, Q., Rollins, J. A., Lebrun, M. H., and Dickman, M. (2011). Genomic analysis of the necrotrophic fungal pathogens *Sclerotinia sclerotiorum* and *Botrytis cinerea*. *PLoS Genet*. 7(8), e1002230. doi: 10.1371/journal.pgen.1002230.

An, B., Li, B., Li, H., Zhang, Z., Qin, G. and Tian, S. (2016). Aquaporin8 regulates cellular development and reactive oxygen species production, a critical component of virulence in *Botrytis cinerea*. *New Phytol*, 209: 1668- 1680. https://doi.org/10.1111/nph.13721

Andrews, S. A quality control tool for high throughput sequence data. FastQC http://www.bioinformatics.babraham.ac.uk/projects/fastqc/ (2014).

Ansari, M. I., Jalil, S. U., Ansari, S. A. *et al*. (2021). GABA shunt: a key-player in mitigation of ROS during stress. *Plant Growth Regul*. 94, 131–149. https://doi.org/10.1007/s10725-021-00710-y

Antoine Porquier. Etude des mécanismes de régulation du métabolisme secondaire chez *Botrytis cinerea*.. Biochimie, Biologie Moléculaire. Université Paris Saclay (COmUE), 2016. Français. ffNNT: 2016SACLS480ff. fftel -01756394v2f.

Arpin, N., Favre-Bonvin, J., and Thivend, S. (1977). Structure de la mycosporine 2, nouvelle molécule isolée de *Botrytis cinerea*. *Tetrahedron Lett*. 18, 819–820.

Ashburner, M., Ball, C. A., Blake, J. A., Botstein, D., Butler, H., Cherry, J. M., Davis, A. P., Dolinski, K., Dwight, S. S., Eppig, J. T., Harris, M. A., Hill, D. P., Issel-Tarver, L., Kasarskis, A., Lewis, S., Matese, J. C., Richardson, J. E., Ringwald, M., Rubin, G. M., and Sherlock, G. (2000). Gene ontology: tool for the unification of biology. The Gene Ontology Consortium. *Nat Genet*. 25(1), 25-9. doi: 10.1038/75556.

Asif, A. R., Oellerich, M., Amstrong, V. W., Riemenschneider, B., Monod, M., and Reichard, U. (2006). Proteome of conidial surface associated proteins of *Aspergillus fumigatus* reflecting potential vaccine candidates and allergens. *J Proteome Res*. 5(4), 954-962. doi: 10.1021/pr0504586.

Atay, O., and Skotheim, J. M. (2017). Spatial and temporal signal processing and decision making by MAPK pathways. *J Cell Biol*. 216, 317–330. https://doi.org/10.1083/jcb.201609124.

Attallah, C. V., Welchen, E. and Gonzalez, D. H. (2007). The promoters of *Arabidopsis thaliana* genes *AtCOX17-1* and -*2*, encoding a copper chaperone involved in cytochrome *c* oxidase biogenesis, are preferentially active in roots and anthers and induced by biotic and abiotic stress. *Physiologia Plantarum*, 129, 123- 134. *https://doi.org/10.1111/j.1399-3054.2006.00776.x*

Bibliography

Backhouse, D. and Willetts, H. J. (1984). A histochemical study of sclerotia of *Botrytis cinerea* and *Botrytis fabae*. *Can. J. Microbiol*. 30, 171-178.

Baidya, S., Cary, J. W., Grayburn, W. S., and Calvo, A. M. (2011). Role of nitric oxide and flavohemoglobin homolog genes in *Aspergillus nidulans* sexual development and mycotoxin production. *Appl Environ Microbiol*. 77(15), 5524-5528. *https://doi.org/10.1128/AEM.00638-11*

Baltussen, T. J. H., Coolen, J. P. M., Verweij, P. E., Dijksterhuis, J., and Melchers, W. J. G. (2021). Identifying Conserved Generic *Aspergillus* spp. Co-Expressed Gene Modules Associated with Germination Using Cross-Platform and Cross-Species Transcriptomics. *J Fungi (Basel)*. 7(4), 270. doi: 10.3390/jof7040270.

Baltussen, T. J. H., Coolen, J. P. M., Zoll, J., Verweij, P. E., and Melchers, W. (2018). Gene co-expression analysis identifies gene clusters associated with isotropic and polarized growth in *Aspergillus fumigatus* conidia. *Fungal Genet Biol*. 116, 62–72. *https://doi.org/10.1016/j.fgb.2018.04.013*.

Baltussen, T. J. H., Zoll, J., Verweij, P. E., and Melchers, W. J. G. (2019). Molecular Mechanisms of Conidial Germination in *Aspergillus* spp. *Microbiol Mol Biol Rev*. 84(1), e00049-19. doi: 10.1128/MMBR.00049-19.

Bao, M. Z., Schwartz, M. A., Cantin, G. T., Yates, J. R. 3rd, and Madhani, H. D. (2004). Pheromone-dependent destruction of the Tec1 transcription factor is required for MAP kinase signaling specificity in yeast. *Cell*. 119(7), 991-1000. doi: 10.1016/j.cell.2004.11.052.

Bardwell, L., Cook, J. G., Voora, D., Baggott, D. M., Martinez, A. R., and Thorner, J. (1998). Repression of yeast Ste12 transcription factor by direct binding of unphosphorylated Kss1 MAPK and its regulation by the Ste7 MEK. *Genes Dev*. 12(18), 2887-2898. doi: 10.1101/gad.12.18.2887.

Bardwell, L., Cook, J. G., Zhu-Shimoni, J. X., Voora, D., and Thorner, J. (1998b). Differential regulation of transcription: repression by unactivated mitogen-activated protein kinase Kss1 requires the Dig1 and Dig2 proteins. *Proc Natl Acad Sci U S A*. 95(26), 15400-15405. doi: 10.1073/pnas.95.26.15400.

Barry, S. M., Kers, J. A., Johnson, E. G., Song, L., Aston, P. R., Patel, B., Krasnoff, S. B., Crane, B. R., Gibson, D. M., Loria, R., and Challis, G. L. (2012). Cytochrome P450–catalyzed L-tryptophan nitration in thaxtomin phytotoxin biosynthesis. *Nat Chem Biol*. 8(10), 814-816. doi: 10.1038/nchembio.1048.

Bayry, J., Beaussart, A., Dufrene, Y. F., Sharma, M., Bansal, K., Kniemeyer, O., Aimanianda, V., Brakhage, A. A., Kaveri, S. V., Kwon-Chung, K. J., Latge, J. P., and Beauvais, A. (2014). Surface structure characterization of *Aspergillus fumigatus* conidia mutated in the melanin synthesis pathway and their human cellular immune response. *Infect Immun*. 82, 3141–3153. https://doi.org/10.1128/IAI.01726-14.

Becker, H. A., Saedler, H., and Lönnig, W. E. (2001). Transposable Elements in Plants. In: Brenner, S., Miller, J. H. (Eds.), *Encyclopedia of Genetics* (2020-2033). Academic Press. https://doi.org/10.1006/rwgn.2001.1639.

Beever, R. E., and Weeds, P. L. (2004). Taxonomy and genetic variation of *Botrytis* and *Botryotinia*. In: Elad Y., Williamson P., Tudzinski P., Delen N. (Eds.), *Botrytis: biology pathology and control* (29–52). Kluwer Academic, Dordrecht.

Benito, E. P., ten Have, A., van't Klooster, J. W., and van Kan, J. A. L. (1998). Fungal and plant gene expression during synchronized infection of tomato leaves by *Botrytis cinerea*. *Eur. J. Plant Pathol*. 104, 207-220.

Benito-Pescador, D., Santander, D., Arranz, M., Díaz-Mínguez, J. M., Eslava, A. P., van Kan, J. A., Benito, E. P. (2016). *Bcmimp*1, a *Botrytis cinerea* Gene Transiently Expressed *in planta*, Encodes a Mitochondrial Protein. *Front Microbiol*. 7, 213. doi: 10.3389/fmicb.2016.00213.

Biel, M., Seeliger, M., Pfeifer, A., Kohler, K., Gerstner, A., Ludwig, A., Jaissle, G., Fauser, S., Zrenner, E., and Hofmann, F. (1999). Selective loss of cone function in mice lacking the cyclic nucleotide-gated channel CNG3. *Proceedings of the National Academy of Sciences of the United States of America*, 96, 7553-7557. *doi:10.1073/pnas.96.13.7553*

Biel, M., Zong, X., Ludwig, A., Sautter, A. and Hofmann, F. (1999), Structure and function of cyclic nucleotide-gated channels. *Rev Physiol Biochem Pharmacol*, 135, 151–171.

Black, B., Lee, C., Horianopoulos, L. C., Jung, W. H., and Kronstad, J. W. (2021). Respiring to infect: Emerging links between mitochondria, the electron transport chain, and fungal pathogenesis. *PLoS Pathog*. 17(7), e1009661. *https://doi.org/10.1371/journal.ppat.1009661*

Blanco-Ulate, B., Amrine, K. C., Collins, T. S., Rivero, R. M., Vicente, A. R., Morales-Cruz, A., Doyle, C. L., Ye, Z., Allen, G., Heymann, H., Ebeler, S. E., and Cantu, D. (2015). Developmental and metabolic plasticity of white-skinned grape berries in response to *Botrytis cinerea* during noble rot. *Plant Physiol.* 169 (4), 2422-2443, 10.1104/pp.15.00852

Blum, M., Chang, H. Y., Chuguransky, S., Grego, T., Kandasaamy, S., Mitchell, A., Nuka, G., Paysan-Lafosse, T., Qureshi, M., Raj, S., Richardson, L., Salazar, G. A., Williams, L., Bork, P., Bridge, A., Gough, J., Haft, D. H., Letunic, I., Marchler-Bauer, A., Mi, H., Natale, D. A., Necci, M., Orengo, C. A., Pandurangan, A. P., Rivoire, C., Sigrist, C. J. A., Sillitoe, I., Thanki, N., Thomas, P. D., Tosatto, S. C. E., Wu, C. H., Bateman, A., and Finn, R. D. (2021). The InterPro protein families and domains database: 20 years on. *Nucleic Acids Res*. 49(D1), D344-D354. doi: 10.1093/nar/gkaa977.

Bokor, A. A. M., Van Kan, J. A. L., Poulter, R. T. M. (2010). Sexual mating of *Botrytis cinerea* illustrates PRP8 intein HEG activity. *Fungal Genet Biol*. 47, 392–398.

Bond, D. A., Jellis, G. J., Rowland, G. G., Le Guen, J., Robertson, L. D., Khalil, S. A., and Li-Juan, L. (1994). Present status and future strategy in breeding faba beans (*Vicia faba* L.) for resistance to biotic and abiotic stresses. In: Muehlbauer F. J., Kaiser W. J. (Eds.), *Expanding the Production and Use of Cool Season Food Legumes, vol 19. Current Plant Science and Biotechnology in Agriculture* (592-616). Springer Netherlands. 466 doi:10.1007/978-94-011-0798-3_36

Boolell, M., Allen, M. J., Ballard, S. A., Gepi-Attee, S., Muirhead, G. J., Naylor, A. M., Osterloh, I. H., and Gingell, C. (1996). Sildenafil: an orally active type 5 cyclic GMP-specific phosphodiesterase inhibitor for the treatment of penile erectile dysfunction. *Int J Impot Res*. 8(2), 47-52.

Boon, E. M., and Marletta, M. A. (2005). Ligand discrimination in soluble guanylate cyclase and the H -NOX family of heme sensor proteins. *Curr Opin Chem Biol*. 9(5), 441-6. doi: 10.1016/j.cbpa.2005.08.015.

Borghouts, C., Werner, A., Elthon, T., and Osiewacz, H. D. (2001). Copper-Modulated Gene Expression and Senescence in the Filamentous Fungus *Podospora anserina*. *Molecular and Cellular Biology*, 21, 390-399. *https://doi.org/10.1128/MCB.21.2.390-399.2001*

Borneman, A. R., Hynes, M. J., and Andrianopoulos, A. (2000). The *abaA* homologue of *Penicillium marneffei* participates in two developmental programmes: conidiation and dimorphic growth. *Molecular Microbiology,* 38, 1034-1047. *https://doi.org/10.1046/j.1365-2958.2000.02202.x*

Bradford, M. M. (1976). A rapid and sensitive method for the quantitation of microgram quantities of protein utilizing the principle of protein-dye binding. *Analytical Biochemistry*, 72, 248-254. DOI: 10.1006/abio.1976.9999.

Brown, B. C., and Borutaite, B. (2006). Interactions between nitric oxide, oxygen, reactive oxygen species and reactive nitrogen species. *Biochemical Society Transactions*, 34, 953–956. https ://doi.org/10.1042/BST03 40953

Bryan, N. S., Bian, K., and Murad, F. (2009). Discovery of the nitric oxide signaling pathway and targets for drug development. *Front Biosci*. 14, 1-18. doi: 10.2741/3228.

Busby, T. M., Miller, K. Y., and Miller, B. L. (1996). Suppression and enhancement of the *Aspergillus nidulans* medusa mutation by altered dosage of the bristle and stunted genes. Genetics, 143(1), 155-163. doi: 10.1093/genetics/143.1.155.

Bustin, S. A. (2000). Absolute quantification of mRNA using real-time reverse transcription polymerase chain reaction assays. *J. Mol. Endocrinol*. 25, 169–193.

Büttner, P., Koch, F., Voigt, K., Quidde, T., Risch, S., Blaich, R., Bruckner, B., and Tudzynski, P. (1994). Variations in ploidy among isolates of *Botrytis cinerea*: implications for genetic and molecular analyses. *Curr Genet*. 25(5), 445-50.

Cagas, S. E., Jain, M. R., Li, H., and Perlinm D. S. (2011). The proteomic signature of *Aspergillus fumigatus* during early development. *Mol Cell Proteomics*, 10, M111.010108. https://doi.org/10.1074/mcp.M111.010108.

Canessa, P., Schumacher, J., Hevia, M. A., Tudzynski, P., and Larrondo, L. F. (2013). Assessing the Effects of Light on Differentiation and Virulence of the Plant Pathogen *Botrytis cinerea:* Characterization of the *White Collar* Complex. *PLoS One*, 8(12), e84223. https://doi.org/10.1371/journal.pone.0084223

Chacko, N., and Gold, S. (2012). Deletion of the *Ustilago maydis* ortholog of the *Aspergillus* sporulation regulator *medA* affects mating and virulence through pheromone response. *Fungal Genet Biol*. 49(6), 426-432. doi: 10.1016/j.fgb.2012.04.002.

Canovas, D., Marcos, J. F., Marcos, A. T., and Strauss, J. (2016). Nitric oxide in fungi: is there NO light at the end of the tunnel? *Curr Genet*. 62(3), 513-518. doi: 10.1007/s00294-016-0574-6.

Bibliography

Cao, Y., Du, M., Luo, S., and Xia, Y. (2014). Calcineurin modulates growth, stress tolerance, and virulence in *Metarhizium acridum* and its regulatory network. *Appl Microbiol Biotechnol*. 98(19), 8253-8265. doi: 10.1007/s00253-014-5876-3.

Cardenas, M. E., Hemenway, C., Muir, R. S., Ye, R., Fiorentino, D., and Heitman, J. (1994). Immunophilins interact with calcineurin in the absence of exogenous immunosuppressive ligands. *EMBO J*. 13(24), 5944-5957.

Carlile, M. J., and Watkinson, S. C. (1994). *The fungi*. Academic Press, London, United Kingdom.

Cervantes-Chávez, J. A., Ali, S., and Bakkeren, G. (2011). Response to environmental stresses, cell-wall integrity, and virulence are orchestrated through the calcineurin pathway in *Ustilago hordei*. *Mol Plant Microbe Interact*. 24(2), 219-232. doi: 10.1094/MPMI-09-10-0202.

Chen, C. H., Dunlap, J. C., Loros, J. J. (2010). *Neurospora* illuminates fungal photoreception. *Fungal Genet Biol.* 47(11), 922–929. https://doi.org/10.1016/j.fgb.2010.07.005

Chen, L., Tong, Q., Zhang, C., and Ding, K. (2019). The transcription factor FgCrz1A is essential for fungal development, virulence, deoxynivalenol biosynthesis and stress responses in *Fusarium graminearum*. *Curr Genet*. 65(1), 153-166. doi: 10.1007/s00294-018-0853-5.

Che-Othman, M. H., Jacoby, R. P., Millar, A. H. and Taylor, N. L. (2020). Wheat mitochondrial respiration shifts from the tricarboxylic acid cycle to the GABA shunt under salt stress. *New Phytol*, 225, 1166- 1180. https://doi.org/10.1111/nph.15713

Christensen, R. L., and Schmit, J. C. (1980). Regulation and glutamic acid decarboxylase during *Neurospora crassa* conidial germination. *J Bacteriol*. 144, 983–990.

Christodoulidou, A., Bouriotis, V., and Thireos, G. (1996). Two sporulation-specific chitin deacetylase-encoding genes are required for the ascospore wall rigidity of *Saccharomyces cerevisiae*. *J. Biol. Chem.* 271, 31420–31425. 10.1074/jbc.271.49.31420

Chung, D. W., Greenwald, C., Upadhyay, S., Ding, S. L., Wilkinson, H. H., Ebbole, D. J., and Shaw, B. D. (2011). *Acon*-3, the *Neurospora crassa* ortholog of the developmental modifier, *medA*, complements the conidiation defect of the *Aspergillus nidulans* mutant. *Fungal Genetics and Biology*, 48(4), 370-376. https://doi.org/10.1016/j.fgb.2010.12.008

Chu, Z. J., Sun, H. H., Ying, S. H., and Feng, M. G. (2017). Vital role for cyclophilin B (CypB) in asexual development, dimorphic transition and virulence of *Beauveria bassiana*. *Fungal Genet Biol*. 105, 8-15. doi: 10.1016/j.fgb.2017.05.004.

Close, T. J. (1996). Dehydrins: emergence of a biochemical role of a family of plant dehydration proteins. *Physiol Plant*. 97, 795– 803. https://doi.org/10.1034/j.1399-3054.1996.970422.x.

Clutterbuck, A. J. (1969). A mutational analysis of conidial development in *Aspergillus nidulans*. *Genetics*, *63*(2), 317–327. https://doi.org/10.1093/genetics/63.2.317

Cogoni, C., and Macino, G. (1999). Gene silencing in *Neurospora crassa* requires a protein homologous to RNA-dependent RNA polymerase. *Nature*, 399(6732), 166-169. doi: 10.1038/20215.

Cohrs, K. C., Simon, A., Viaud, M., and Schumacher, J. (2016), Light governs asexual differentiation in the grey mould fungus *Botrytis cinerea* via the putative transcription factor BcLTF2. *Environ Microbiol*. 18(11), 4068- 4086. https://doi.org/10.1111/1462-2920.13431

Coleman, S. T., Fang, T.K., Rovinsky, S. A., Turano, F. J., and Moye-Rowley, W. S. (2001). Expression of a glutamate decarboxylase homologue is required for normal oxidative stress tolerance in *Saccharomyces cerevisiae*. *J. Biol. Chem*. 276, 244-250. 10.1074/jbc.M007103200

Collado, I. G., and Viaud, M. (2016). Secondary Metabolism in *Botrytis cinerea*: Combining Genomic and Metabolomic Approaches. In: Fillinger S., Elad Y. (Eds.) *Botrytis* – the Fungus, the Pathogen and its Management in Agricultural Systems (291-313). Springer, Cham. *https://doi.org/10.1007/978-3-319-23371-0_15*

Colmenares, A. J., Durán-Patrón, R. M., Hernández-Galán, R., Collado, I. G. (2002). Four new lactones from *Botrytis cinerea*. *J Nat Prod*. 65(11), 1724-1726. doi: 10.1021/np020107v.

Coolen, S., Proietti, S., Hickman, R., Davila Olivas, N. H., Huang, P. P., Van Verk, M. C., Van Pelt, J. A., Wittenberg, A. H., De Vos, M., Prins, M., Van Loon, J. J., Aarts, M. G., Dicke, M., Pieterse, C. M., and Van Wees, S. C. (2016). Transcriptome dynamics of *Arabidopsis* during sequential biotic and abiotic stresses. *Plant J*. 86(3), 249- 267. https://doi.org/10.1111/tpj.13167

Cooper, GM. (2000). The nucleus during mitosis. In: *The cell: a molecular approach* (2nd ed.). Sunderland, MA: Sinauer Associates.

Coulomb, C., Lizzi, Y., Roggero, P. J., Coulomb, P. O., and Agullon, O. (1998). Can copper be an elicitor? *Phytoma,* 512, 41–46.

Cove, D. J. (1979). Genetic studies of nitrate assimilation in *Aspergillus nidulans*. *Biol. Rev*. 54, 291–327.

Cramer, R. A. Jr., Perfect, B. Z., Pinchai, N., Park, S., Perlin, D. S., Asfaw, Y. G., Heitman, J., Perfect, J. R., and Steinbach, W. J. (2008). Calcineurin target CrzA regulates conidial germination, hyphal growth, and pathogenesis of *Aspergillus fumigatus*. *Eukaryot Cell*. 7(7), 1085-1097. doi: 10.1128/EC.00086-08.

Crawford, M. J., and Goldberg, D. E. (1998). Role for the *Salmonella* flavohemoglobin in protection from nitric oxide. *Journal of Biological Chemistry*, 273(20), 12543-12547. https://doi.org/10.1074/jbc.273.20.12543

Crawford, N. M., and Arst, H. N. (1993). The molecular genetics of nitrate assimilation in fungi and plants. *Annu. Rev. Genet*. 27, 115–146. doi: 10.1146/annurev.ge.27.120193.000555

Crespo-Sempere, A., *et al*. (2013). Characterization and disruption of the cipC gene in theochratoxigenic fungus *Aspergillus carbonarius*. *Food Res. Int*. 54(1), 697–705. https://doi.org/10.1016/j.foodres.2013.08.008

Cutler, H. G., Parker, S. R., Ross, S. A., Crumley, F. G., and Schreiner, P. R (1996). Homobotcinolide: a biologically active natural homolog of botcinolide from *Botrytis cinerea*. *Biosci Biotechnol Biochem*. 60(4), 656-658. doi: 10.1271/bbb.60.656.

Daryaei, A., Jones, E. E., Glare, R. T., and Falloon, E. R. (2016). Nutrient amendments affect *Trichoderma atroviride* conidium production, germination and bioactivity. *Biological Control*, 93, 8-14. https://doi.org/10.1016/j.biocontrol.2015.11.003.

da Silva, F. M. E., Heinekamp, T., Härtl, A., Brakhage, A. A., Semighini, C. P., Harris, S. D., Savoldi, M., de Gouvêa, P. F., de Souza, G. M. H., and Goldman, G. H. (2007). Functional characterization of the *Aspergillus fumigatus* calcineurin. *Fungal Genet Biol*. 44(3), 219-230. doi: 10.1016/j.fgb.2006.08.004.

Dean, R., Van Kan, J. A., Pretorius, Z. A., Hammond-Kosack, K. E., Di Pietro, A., Spanu, P. D., Rudd, J. J., Dickman, M., Kahmann, R., Ellis, J., and Foster, G. D. (2012). The Top 10 fungal pathogens in molecular plant pathology. *Mol Plant Pathol*. 13(4), 414-430.

De Cremer, K., Mathys, J., Vos, C., Froenicke, L., Michelmore, R. W., Cammue, B. P., and De Coninck, B. (2013). RNAseq-based transcriptome analysis of *Lactuca sativa* infected by the fungal necrotroph *Botrytis cinerea*. *Plant Cell Environ*. 36(11), 1992-2007. doi: 10.1111/pce.12106.

De Guido, M. A., Minafra, A., Santomauro, A., Pollastro, S., De Miccolis Angelini, R. M., and Faretra, F. (2005). Molecular characterization of mycoviruses from *Botryotinia fuckeliana*. *J Plant Pathol*. 87, 293.

Deighton, N., Muckenschnabel, I., Colmenares, A. J., Collado, I. G., and Williamson, B. (2001). Botrydial is produced in plant tissues infected by *Botrytis cinerea*. *Phytochemistry*, 57(5), 689-692. doi: 10.1016/s0031-9422(01)00088-7.

De Miccolis Angelini, R. M., Pollastro, S., and Faretra, F. (2016). Genetics of *Botrytis cinerea*. In: Fillinger S., Elad Y. (Eds.), *Botrytis* – the Fungus, the Pathogen and its Management in Agricultural Systems (35-53). Springer, Cham. https://doi.org/10.1007/978-3-319-23371-0_3

De Miccolis Angelini, R. M., Rotolo, C., Masiello, M., Pollastro, S., Ishii, H., and Faretra, F. (2012a). Genetic analysis and molecular characterisation of laboratory and field mutants of *Botryotinia fuckeliana* (*Botrytis cinerea*) resistant to QoI fungicides. *Pest Manag Sci*. 68(9), 1231-1240. doi: 10.1002/ps.3281.

d'Enfert, C. (1997). Fungal spore germination: insights from the molecular genetics of *Aspergillus nidulans* and *Neurospora crassa*. *Fungal Genet Biol*. 21, 163–172. *https://doi.org/10.1006/fgbi.1997.0975*.

Dik, A. J., and Wubben, J. P. (2004). Epidemiology of *Botrytis cinerea* diseases in greenhouses. In: Elad Y., Williamson B., Tudzynski P., Delen N. (Eds.), *Botrytis: biology, pathology and control* (319-333). Kluwer Academic Publishers, Dordrecht.

Dong, J., Zhang, M., Lu, L., Sun, L., and Xu, M. (2012). Nitric oxide fumigation stimulates flavonoid and phenolic accumulation and enhances antioxidant activity of mushroom. *Food Chemistry*, 135, 1220–1225. https ://doi.org/10.1016/j.foodc hem.2012.05.055

Donofrio, N. M., Lundy, R., Pan, H., Brown, D. E., Jeong, J. S., Coughlan, S., Mitchell. T. K., and Dean, R. A. (2006). Global gene expression during nitrogen starvation in the rice blast fungus, *Magnaporthe grisea*. *Fungal Genetics and Biology*, 43(9), 605-617. https://doi.org/10.1016/j.fgb.2006.03.005

Doss, R. P., Deisenhofer, J., Krug von Nidda, H. A., Soeldner, A. H., and McGuire, R. P. (2003). Melanin in the extracellular matrix of germlings of *Botrytis cinerea*. *Phytochemistry*, 63(6), 687-91. doi: 10.1016/s0031-9422(03)00323-6.

Dufresne, M., and Daboussi, MJ. (2010). Development of *Impala*-Based Transposon Systems for Gene Tagging in Filamentous Fungi. In: Sharon A. (Ed.), *Molecular and Cell Biology Methods for Fungi. Methods in Molecular Biology (Methods and Protocols)* (41-54). Humana Press. https://doi.org/10.1007/978-1-60761-611-5_4

Dunn-Coleman, N. S., Tomsett, A. B., and Garrett, R. H. (1981). The regulation of nitrate assimilation in *Neurospora crassa*: biochemical analysis of the nmr-1 mutants. *Mol. Gen. Genet*. 182, 234–239. doi: 10.1007/BF00269663

Durner, J., Gow, A. J., Stamler, J. S., and Glazebrook, J. (1999). Ancient origins of nitric oxide signaling in biological systems. *Proc. Natl. Acad. Sci. USA*, 96, 14206–14207.

Eisenman, H. C., and Casadevall, A. (2012). Synthesis and assembly of fungal melanin. *Appl Microbiol Biotechnol*. 93, 931–940. https://doi.org/10.1007/s00253-011-3777-2.

Elad, Y., Israeli, L., Fogel, M. *et al*. (2014b). Conditions influencing the development of sweet basil grey mould and cultural measures for disease management. *Crop Prot*. 64, 67–77.

Elad, Y., Pertot, I., Cotes, P. A. M., Stewart, A. (2015). Plant hosts of *Botrytis* spp. In: Fillinger S., Elad Y. (Eds.), Botrytis – The Fungus, The Pathogen and Its Management in Agricultural Systems ***(***413–486***),*** Cham: Springer International Publishing.

Elad, Y., Williamson, B., Tudzynski, P., and Delen, N. (2004). *Botrytis*: Biology, Pathology and Control. Dordrecht, The Netherlands. Kluwer Academic Press.

el Moualij, B., Duyckaerts, C., Lamotte-Brasseur, J., and Sluse, F. E. (1998). Phylogenetic classification of the mitochondrial carrier family of *Saccharomyces cerevisiae*. *Yeast*, 13(6), 573-581. doi: 10.1002/(SICI)1097-0061(199705)13:6<573::AID-YEA107>3.0.CO;2-I. Erratum in: Yeast 1998 Jan 15;14(1):101.

Engelhard, W. (1989). Soilborne plant pathogens: management of diseases with macro- and microelements. American Phytopathological Society Press, St. Paul.

Enserink, J. M., and Kolodner, R. D. (2010). An overview of Cdk1-controlled targets and processes. *Cell Div*. 5, 11. doi: 10.1186/1747-1028-5-11.

Eom, T. J., Moon, H., Yu, J. H., and Park, H. S. (2018). Characterization of the velvet regulators in *Aspergillus flavus*. *J Microbiol*. 56, 893–901. https://doi.org/10.1007/s12275-018-8417-4.

Epton, H. a. S., and Richmond, D. V. (1980). Formation, structure and germination of conidia. In: Coley-Smith J. R., Verhoeff K., and Jarvis W. R. (Eds.), *The Biology of Botrytis* (41-83), Academic Press, London.

Espino, J. J., Gutiérrez-Sánchez, G., Brito, N., Shah, P., Orlando, R., and González, C. (2010). The *Botrytis cinerea* early secretome. *Proteomics*. 10(16), 3020-3034. doi: 10.1002/pmic.201000037.

Etxebeste, O., Garzia, A., Espeso, E. A., and Ugalde, U. (2010). *Aspergillus nidulans* asexual development: making the most of cellular modules. *Trends Microbiol*. 18(12), 569-576. doi: 10.1016/j.tim.2010.09.007.

Faretra, F., and Antonacci, E. (1987). Production of apothecia of *Botryotinia fuckeliana* (de bary) Whetz. Under controlled environmental conditions. *Phytopathol Mediterr.* 26, 29–35.

Faretra, F., and Grindle, M. (1992). Genetic studies of *Botryotinia fuckeliana* (*Botrytis cinerea*). In: Verhoeff K., Malathrakis N. E., Williamson B. (Eds.), *Recent advances in Botrytis research* (7–17). PUDOC, Wageningen.

Faretra, F., and Pollastro, S. (1996). Genetic studies of the phytopathogenic fungus *Botryotinia fuckeliana* (*Botrytis cinerea*) by analysis of ordered tetrads. *Mycological Research*, 100, 620–624.

Faretra, F., Antonacci, E., and Pollastro, S. (1988). Sexual Behaviour and Mating System of *Botryotinia fuckeriana*, Teleomorph of *Botrytis cinerea*. *Journal of General Microbiology*, 134, 2543-2550.

Favre-Bonvin, J., Arpin, N., and Brevard, C. (1976). Structure de la mycosporine (P 310). *Can J Chem.* 54, 1105–1113.

Fedorova, N. D., Badger, J. H., Robson, G. D., Wortman, J. R., and Nierman, W. C. (2005). Comparative analysis of programmed cell death pathways in filamentous fungi. *BMC Genomics*. 6, 177. doi: 10.1186/1471-2164-6-177.

Fillinger, S., and Walker, A. S. (2016). Chemical Control and Resistance Management of *Botrytis* Diseases. In: Fillinger S., Elad Y. (Eds.), *Botrytis* – the Fungus, the Pathogen and its Management in Agricultural Systems. Springer, Cham. *https://doi.org/10.1007/978-3-319-23371-0_10*

Fillinger, S., Chaveroche, M. K., Shimizu, K., Keller, N., and d'Enfert, C. (2002). cAMP and ras signalling independently control spore germination in the filamentous fungus *Aspergillus nidulans*. *Mol Microbiol*. 44, 1001–1016. *https://doi.org/10.1046/j.1365-2958.2002.02933.x*.

Fillinger, S., Chaveroche, M. K., van Dijck, P., de Vries, R ., Ruijter, G., Thevelein, J., and d'Enfert, C. (2001). Trehalose is required for the acquisition of tolerance to a variety of stresses in the filamentous fungus *Aspergillus nidulans*. *Microbiology*, 147, 1851–1862. https://doi.org/10.1099/00221287-147-7-1851.

Finkers, R., van den Berg, P., van Berloo, R., ten Have, A., van Heusden, A. W., van Kan, J. A. L., and Lindhout, P. (2007). Three QTLs for *Botrytis cinerea* resistance in tomato. *Theoretical and Applied Genetics*, 114, 585–593.

Fitzhugh, A. L., and Keefer, L. K. (2000). Diazeniumdiolates: pro- and antioxidant applications of the "NONOates". *Free Radic Biol Med*. 28(10), 1463-1469. doi: 10.1016/s0891-5849(00)00251-3.

Fitzpatrick, J., and Kim, E. (2015). Synthetic modeling chemistry of iron-sulfur clusters in nitric oxide signaling. *Accounts of Chemical Research*, 48, 2453–2461. https ://doi.org/10.1021/acs.accou nts.5b00246

Fontaine, T., Beauvais, A., Loussert, C., Thevenard, B., Fulgsang, C. C., Ohno, N., Clavaud, C., Prevost, M. C., and Latge, J. P. (2010). Cell wall alpha1-3glucans induce the aggregation of germinating conidia of *Aspergillus fumigatus*. *Fungal Genet Biol*. 47, 707–712. *https://doi.org/10.1016/j.fgb.2010.04.006*.

Forrester, M. T., and Foster, M. W. (2012). Protection from nitrosative stress: a central role for microbial flavohemoglobin. *Free Radic Biol Med*. 52(9), 1620-1633. doi: 10.1016/j.freeradbiomed.2012.01.028.

Friebe, A., and Koesling, D. (2003). Regulation of nitric oxide-sensitive guanylyl cyclase. *Circulation Research*, 93, 96–105. https ://doi.org/10.1161/01.RES.00000 82524.34487.31

Fulci, V., and Macino, G. (2007). Quelling: post-transcriptional gene silencing guided by small RNAs in *Neurospora crassa*. *Curr Opin Microbiol*. 10(2), 199-203. doi: 10.1016/j.mib.2007.03.016.

Furukawa, K., Hoshi, Y., Maeda, T., Nakajima, T., and Abe, K. (2005). *Aspergillus nidulans* HOG pathway is activated only by two-component signalling pathway in response to osmotic stress. *Mol Microbiol*. 56, 1246 –1261. *https://doi.org/10.1111/j.1365-2958.2005.04605.x*.

Fu, Y. F., Zhang, Z. W., and Yuan, S. (2018). Putative Connections Between Nitrate Reductase *S*-Nitrosylation and NO Synthesis Under Pathogen Attacks and Abiotic Stresses. *Front Plant Sci*. 9, 474. doi: 10.3389/fpls.2018.00474.

Galagan, J. E., and Selker, E. U. (2004). RIP: the evolutionary cost of genome defense. *Trends Genet*. 20, 417–423.

Galland, P., and Lipson, E. D. (1987). Blue-light reception in *Phycomyces* phototropism: evidence for two photosystems operating in low-and high-intensity ranges. *Proceedings of the National Academy of Sciences*, 84(1), 104-108.
García-Martínez J., Brunk, M., Avalos, J., and Terpitz, U. (2015). The CarO rhodopsin of the fungus *Fusarium fujikuroi* is a light-driven proton pump that retards spore germination. *Sci Rep*. 5, 7798. doi: 10.1038/srep07798.
Gardner, P. R., Gardner, A. M., Brashear, W. T., Suzuki, T., Hvitved, A. N., Setchell, K. D., and Olson, J. S. (2006). Hemoglobins dioxygenate nitric oxide with high fidelity. Journal of Inorganic Biochemistry, 100, 542–550. https ://doi.org/10.1016/j.jinor gbio.2005.12.012

Gardner, P. R., Gardner, A. M., Martin, L. A., and Salzman, A. L. (1998). Nitric oxide dioxygenase: an enzymic function for flavohemoglobin. *Proc Natl Acad Sci U S A*, 95(18), 10378-83. doi: 10.1073/pnas.95.18.10378.

Geoghegan, I. A., and Gurr, S. J. (2016). Chitosan mediates germling adhesion in *Magnaporthe oryzae* and is required for surface sensing and germling morphogenesis. *PLoS Pathog.* 12, e1005703. 10.1371/journal.ppat.1005703

Ge, W., Chew, T. G., Wachtler, V., Naqvi, S. N., and Balasubramanian, M. K. (2005). The novel fission yeast protein Pal1p interacts with Hip1-related Sla2p/End4p and is involved in cellular morphogenesis. *Mol. Biol. Cell*. 16, 4124-4138.

Bibliography

Giaever, G., Chu, A. M., Ni, L., Connelly, C., Riles, L., Véronneau, S., Dow, S., Lucau-Danila, A., Anderson, K., André, B., Arkin, A. P., Astromoff, A., El-Bakkoury, M., Bangham, R., Benito, R., Brachat, S., Campanaro, S., Curtiss, M., Davis, K., Deutschbauer, A., Entian, K. D., Flaherty, P., Foury, F., Garfinkel, D. J., Gerstein, M., Gotte, D., Güldener, U., Hegemann, J. H., Hempel, S., Herman, Z., Jaramillo, D. F., Kelly, D. E., Kelly, S. L., Kötter, P., LaBonte, D., Lamb, D. C., Lan, N., Liang, H., Liao, H., Liu, L., Luo, C., Lussier, M., Mao, R., Menard, P., Ooi, S. L., Revuelta, J. L., Roberts, C. J., Rose, M., Ross - Macdonald, P., Scherens, B., Schimmack, G., Shafer, B., Shoemaker, D. D., Sookhai-Mahadeo, S., Storms, R. K., Strathern, J. N., Valle, G., Voet, M., Volckaert, G., Wang, C. Y., Ward, T. R., Wilhelmy, J., Winzeler, E. A., Yang, Y., Yen, G., Youngman, E., Yu, K., Bussey, H., Boeke, J. D., Snyder, M., Philippsen, P., Davis, R. W., and Johnston, M. (2002). Functional profiling of the *Saccharomyces cerevisiae* genome. *Nature*, 418(6896), 387-91. doi: 10.1038/nature00935.

Gioti, A., Simon, A., LePêcheur, P., Giraud, C., Pradier, J. M., Viaud, M., and Levis, C. (2006). Expression Profiling of *Botrytis cinerea* Genes Identifies Three Patterns of Up-regulation *in Planta* and an FKBP12 Protein Affecting Pathogenicity. *J. Mol. Biol*. 358, 372–386.

Giraud, T., Fortini, D., Levis, C., Lamarque, C., Leroux, P., Lobuglio, K., and Brygoo, Y. (1999). Two Sibling Species of the *Botrytis cinerea* Complex, transposa and vacuma, Are Found in Sympatry on Numerous Host Plants. *Phytopathology*, 89(10), 967-973. doi: 10.1094/PHYTO.1999.89.10.967.

Glass, N. L., Jacobson, D. J., Shiu, P. K. T. (2000). The genetics of fungal fusion and vegetative incompatibility in filamentous fungi. *Annu Rev Genet*. 34, 165–186.

Godoy, A. V., Lazzaro, A. S., Casalongué, C. A., and San Segundo, B. (2000). Expression of a *Solanum tuberosum* cyclophilin gene is regulated by fungal infection and abiotic stress conditions. *Plant Science*. 152, 123-134.

Gong, X., Fu, Y., Jiang, D., Li, G., Yi, X., and Peng, Y. (2007). L-arginine is essential for conidiation in the filamentous fungus *Coniothyrium minitans*. *Fungal Genet Biol*. 44(12), 1368-79.

Gong, X., Hurtado, O., Wang, B., Wu, C., Yi, M., Giraldo, M., Valent, B., Goodin, M., and Farman, M. (2015). pFPL Vectors for High-Throughput Protein Localization in Fungi: Detecting Cytoplasmic Accumulation of Putative Effector Proteins. *Mol Plant Microbe Interact*. 28(2), 107-121. doi: 10.1094/MPMI-05-14-0144-TA.

González, C., Brito, N., Sharon, A. (2016). Infection Process and Fungal Virulence Factors. In: Fillinger S., Elad Y. (Eds.), *Botrytis* – the Fungus, the Pathogen and its Management in Agricultural Systems (229-246). Springer, Cham. https://doi.org/10.1007/978-3-319-23371-0_12

Gourgues, M., Brunet-Simon, A., Lebrun, M. H., and Levis, C. (2004). The tetraspanin Bc-Pls1 is required for appressorium-mediated penetration of *Botrytis cinerea* into host plant leaves. *Molecular Microbiology*, 51, 619-629.

Götz, S., García-Gómez, J. M., Terol, J., Williams, T. D., Nagaraj, S. H., Nueda, M. J., Robles, M., Talón, M., Dopazo, J., and Conesa, A. (2008). High-throughput functional annotation and data mining with the Blast2GO suite. *Nucleic Acids Res*. 36(10), 3420-3435. doi: 10.1093/nar/gkn176.

Gravelat, F. N., Ejzykowicz, D. E., Chiang, L. Y., Chabot, J. C., Urb, M., Macdonald, K. D., al -Bader, N., Filler, S. G., and Sheppard, D. C. (2010). *Aspergillus fumigatus MedA* governs adherence, host cell interactions and virulence. *Cell Microbiol*. 12(4), 473-848. doi: 10.1111/j.1462-5822.2009.01408.x.

Grell, M. N., Mouritzen, P., and Giese, H. (2003). A *Blumeria graminis* gene family encoding proteins with a C-terminal variable region with homologues in pathogenic fungi. *Gene*, 311, 181-192.

Grindle, M. (1979). Phenotypic Differences Between Natural and Induced Variants of *Botrytis cinerea*. *Microbiology*, 111, 109–120.

Groves, J. W., and Loveland, C. A. (1953). The Connection between *Botryotinia fuckeliana* and *Botrytis cinerea*. *Mycologia*, 45(3), 415-425. DOI: *10.1080/00275514.1953.12024279*

Guimarães, R. L., Stotz, H., and Chetelat, R. T. (2004). Resistance to *Botrytis cinerea* in *Solanum lycopersicoides* is Dominant in Hybrids with Tomato, and Involves induced Hyphal Death. *Journal of Plant Pathology*, 110, 13-23.

Hagiwara, D., Suzuki, S., Kamei, K., Gonoi, T., and Kawamoto, S. (2014). The role of AtfA and HOG MAPK pathway in stress tolerance in conidia of *Aspergillus fumigatus*. *Fungal Genet Biol*. 73, 138–149. *https://doi.org/10.1016/j.fgb.2014.10.011*.

Hagiwara, D., Takahashi, H., Kusuya, Y., Kawamoto, S., Kamei, K., and Gonoi, T. (2016). Comparative transcriptome analysis revealing dormant conidia and germination associated genes in *Aspergillus* species: an essential role for AtfA in conidial dormancy. *BMC Genomics*, 17, 358. https://doi.org/10.1186/s12864-016-2689-z.

Haile, Z. M., Malacarne, G., Pilati, S., Sonego, P., Moretto, M., Masuero, D., Vrhovsek, U., Engelen, K., Baraldi, E., and Moser, C. (2020). Dual Transcriptome and Metabolic Analysis of *Vitis vinifera* cv. Pinot Noir Berry and *Botrytis cinerea* During Quiescence and Egressed Infection. *Front Plant Sci*. 10, 1704. doi: 10.3389/fpls.2019.01704.

Halaouli, S., Asther, M., Sigoillot, J. C., Hamdi, M., and Lomascolo, A. (2006). Fungal tyrosinases: new prospects in molecular characteristics, bioengineering and biotechnological applications. *J Appl Microbiol*. 100(2), 219-232. doi: 10.1111/j.1365-2672.2006.02866.x.

Hamada, W., Soulié, M. C., Malfatti, P., Bompeix, G., and Boccara, M. (1997). Stability and modulated expression of a hygromycin resistance gene integrated in *Botrytis cinerea* transformants. *FEMS Microbiology Letters*, 154, 187–193.

Hanahan, D., Jessee, J., and Bloom, F. R. (1995). Techniques for transformation of *E. coli*. In: DNA Cloning 3: A Practical Approach (1–36). IRL Press Ltd.

Han, X., Qiu, M., Wang, B., Yin, W. B., Nie, X., Qin, Q., Ren, S., Yang, K., Zhang, F., Zhuang, Z., and Wang, S. (2016). Functional Analysis of the Nitrogen Metabolite Repression Regulator Gene *nmrA* in *Aspergillus flavus*. *Front Microbiol*. 7, 1794. doi: 10.3389/fmicb.2016.01794.

Harren, K., Schumacher, J., and Tudzynski, B. (2012). The Ca2+ /Calcineurin-Dependent Signaling Pathway in the Gray Mold *Botrytis cinerea*: The Role of Calcipressin in Modulating Calcineurin Activity. *PLoS ONE*, 7(7), e41761. doi:10.1371/journal.pone.0041761

Harris, S. D., and Momany, M. (2004). Polarity in filamentous fungi: moving beyond the yeast paradigm. *Fungal Genet Biol*. 41(4), 391-400. doi: 10.1016/j.fgb.2003.11.007.

Harris, S. D. (2006). Cell polarity in filamentous fungi: shaping the mold. *Int Rev Cytol*. 251, 41–77. *https://doi.org/10.1016/S0074-7696(06)51002-2*.

Hartley, J. L., Temple, G. F., and Brasch, M. A. (2000). DNA Cloning Using *in vitro* Site-Specific Recombination. *Genome Research*, 10, 1788-1795.

Hausladen, A., Gow, A., and Stamler, J. S. (2001). Flavohemoglobin denitrosylase catalyzes the reaction of a nitroxyl equivalent with molecular oxygen. *Proc. Natl. Acad. Sci. USA*, 98, 10108–10112.

Hausladen, A., Gow, A. J., and Stamler, J. S. (1998). Nitrosative stress: Metabolic pathway involving the flavohemoglobin. *Proceedings of the National Academy of Sciences*, 95, 14100–14105. https ://doi.org/10.1073/pnas.95.24.14100

Heinrich, T. A., da Silva, R. S., Miranda, K. M., Switzer, C. H., Wink, D. A., anf Fukuto, J. M. (2013). Biological nitric oxide signaling: Chemistry and terminology. *British Journal of Pharmacology*, 169, 1417–1429.

Heller, J., Ruhnke, N., Espino, J. J., Massaroli, M., Collado, I. G., and Tudzynski, P. (2012). The Mitogen-Activated Protein Kinase BcSak1 of *Botrytis cinerea* Is Required for Pathogenic Development and Has Broad Regulatory Functions Beyond Stress Response. *Molecular Plant-Microbe Interactions®*, 25(6), 802-816. *https://doi.org/10.1094/MPMI-11-11-0299*

Hendriks, J., Oubrie, A., Castresana, J., Urbani, A., Gemeinhardt, S., and Saraste, M. (2000). Nitric oxide reductases in bacteria. *Biochimia Et Biophysica Acta*, 1459, 266–273. https ://doi.org/10.1016/S0005-2728(00)00161-4

Hennebert, G. L. (1973). *Botrytis* and *Botrytis*-like genera. *Persoonia*, 7, 183–204.

Hess, D. C., Myers, C. L., Huttenhower, C., Hibbs, M. A., Hayes, A. P., Paw, J., Clore, J. J., Mendoza, R. M., Luis, B. S., Nislow, C., Giaever, G., Costanzo, M., Troyanskaya, O. G., and Caudy, A. A. (2009). Computationally driven, quantitative experiments discover genes required for mitochondrial biogenesis. *PLoS Genet*. 5(3), e1000407. doi: 10.1371/journal.pgen.1000407.

Higgins, S. A., Schadt, C. W., Matheny, P. B., and Löffler, F.E. (2018). Phylogenomics reveal the dynamic evolution of fungal nitric oxide reductases and their relationship to secondary metabolism. *Genome Biology and Evolution*, 10, 2474–2489. https://doi.org/10.1093/gbe/evy187

Hiratsuka, K., Namba, S., Yamashita, S., *et al*. (1987). Linear plasmid-like DNA's in the fungus *Botrytis cinerea*. *Nippon Shokubutsu Byori Gakkaiho*, 53, 638–642.

Hoebeeck, J., Speleman, F., and Vandesompele, J. (2007). Real-Time Quantitative PCR as an Alternative to Southern Blot or Fluorescence In Situ Hybridization for Detection of Gene Copy Number Changes. In: Hilario E., Mackay J. (Eds.), *Methods in Molecular Biology vol. 353: Protocols for Nucleic Acid Analysis by Nonradioactive Probes* (205-226), *Humana Press Inc.*

Honda, Y., Hattori, T., and Kirimura, K. (2012). Visual expression analysis of the responses of the alternative oxidase gene (**aox1**) to heat shock, oxidative, and osmotic stresses in conidia of citric acid-producing *Aspergillus niger*. *J Biosci Bioeng*. 113, 338–342. https://doi.org/10.1016/j.jbiosc.2011.10.026

Horace, G. C., James, P. S., Richard, F. A., Byron, H. A., Patsy, D. C., and Rodney, G. R. (1988). Cinereain: A Novel Metabolite with Plant Growth Regulating Properties from *Botrytis cinerea*. *Agricultural and Biological Chemistry*, 52:7, 1725-1733. DOI: *10.1080/00021369.1988.10868905*

Horace, G. C., John, M. J., John, S. H., Deanne, D., Patsy, D. G., and Rodney. G. R. (1993). Botcinolide: A Biologically Active Natural Product from *Botrytis cinerea*. *Bioscience, Biotechnology, and Biochemistry*, 57(11), 1980– 1982, *https://doi.org/10.1271/bbb.57.1980*

Horan, S., Bourges, I., and Meunier, B. (2006). Transcriptional response to nitrosative stress in *Saccharomyces cerevisiae*. *Yeast,* 23(7), 519-535. doi: 10.1002/yea.1372.

Horchani, F., Prévot, M., Boscari, A., Evangelisti, E., Meilhoc, E., Bruand, C., Raymond, P., Boncompagni, E., Aschi - Smiti, S., Puppo, A., and Brouquisse, R. (2011). Both plant and bacterial nitrate reductases contribute to nitric oxide production in *Medicago truncatula* nitrogen-fixing nodules. *Plant Physiol*. 155(2), 1023-1036. doi: 10.1104/pp.110.166140.

Howitt, R. L. J., Beever, R. E., Pearson, M. N. *et al*. (1995). Presence of double-stranded RNA and virus-like particles in *Botrytis cinerea*. *Mycol Res*. 99, 1472–1478.

Hutchison, E., Brown, S., Tian, C., and Glass, N. L. (2009). Transcriptional profiling and functional analysis of heterokaryon incompatibility in *Neurospora crassa* reveals that reactive oxygen species, but not metacaspases, are associated with programmed cell death. *Microbiology (Reading, England)*, 155(Pt 12), 3957–3970. *https://doi.org/10.1099/mic.0.032284-0*

Hyde, K. D., Nilsson, R. H., Alias, S. A., Ariyawansa, H. A., Blair, J. E., Cai, L., de Cock, A. W. A. M., Dissanayake, A. J., Glockling, S. L., Goonasekara, I. D., *et al*. (2014). One stop shop: backbones trees for important phytopathogenic genera: I. *Fungal Divers*, 67, 21–125.

Ichinomiya, M., Ohta, A., and Horiuchi, H. (2005). Expression of asexual developmental regulator gene *abaA* is affected in the double mutants of classes I and II chitin synthase genes, *chsC* and *chsA*, of *Aspergillus nidulans*. *Curr Genet*. 48(3), 171-183. doi: 10.1007/s00294-005-0004-7.

Idnurm, A., and Howlett, BJ. (2001). Pathogenicity genes of phytopathogenic fungi. *Mol Plant Pathol*. 2(4), 241-255. doi: 10.1046/j.1464-6722.2001.00070.x.

Jacometti, M. A., Wratten, S. D., and Walter, M. (2007). Management of understorey to reduce the primary inoculum of *Botrytis cinerea*: Enhancing ecosystem services in vineyards. *Biological Control*, 40, 57–64.

Jaimes-Arroyo, R., Lara-Rojas, F., Bayram, O., Valerius, O., Braus, G. H., and Aguirre, J. (2015). The SrkA kinase is part of the SakA mitogen-activated protein kinase interactome and regulates stress responses and development in *Aspergillus nidulans*. *Eukaryot Cell*. 14, 495–510. *https://doi.org/10.1128/EC.00277-14*.

Jarvis, W. R. (1977). *Botryotinia* and *Botrytis* species: taxonomy, physiology, and pathogenicity; a guide to the literature. Agriculture Canada, Ottawa, Ontario. Hignell Printing Limited.

Jarvis, W. R. (1962). The infection of strawberry and raspberry fruits by *Botrytis cinerea* Fr. *Annals of Applied Biology*, 50, 569–575.

Jiang, H., Ouyang, H., Zhou, H., and Jin, C. (2008). GDP-mannose pyrophosphorylase is essential for cell wall integrity, morphogenesis and viability of *Aspergillus fumigatus*. *Microbiology*, 154, 2730–2739. https://doi.org/10.1099/mic.0.2008/019240-0.

Jin, Q., Li, C., Li, Y., Shang, J., Li, D., Chen, B., and Dong, H. (2013). Complexity of roles and regulation of the PMK1-MAPK pathway in mycelium development, conidiation and appressorium formation in *Magnaporthe oryzae*. *Gene Expr Patterns*, 13, 133-141.

Johanna, M. S., Richard, J. W., and Alison, S. (2010). Isolate-specific conidiation in *Trichoderma* in response to different nitrogen sources. *Fungal Biology*, 114(2–3), 179-188. https://doi.org/10.1016/j.funbio.2009.12.002.

Jolly, C., and Morimoto, R. I. (2000). Role of the heat shock response and molecular chaperones in oncogenesis and cell death. *J Natl Cancer Inst*. 92, 1564 –1572. *https://doi.org/10.1093/jnci/92.19.1564*.

Jones, P., Binns, D., Chang, H. Y., Fraser, M., Li, W., McAnulla, C., McWilliam, H., Maslen, J., Mitchell, A., Nuka, G., Pesseat, S., Quinn, A. F., Sangrador-Vegas, A., Scheremetjew, M., Yong, S. Y., Lopez, R., Hunter, S. (2014). InterProScan 5: genome-scale protein function classification. Bioinformatics, 30(9), 1236-40. doi: 10.1093/bioinformatics/btu031.

Justesen, A., Somerville, S., Christiansen, S., and Giese, H. (1996). Isolation and characterization of two novel genes expressed in germinating conidia of the obligate biotroph *Erysiphe graminis* f.sp. *hordei*. *Gene*, 170, 131-135.

Juvvadi, P. R., Lamoth, F., and Steinbach, W. J. (2014). Calcineurin-mediated regulation of hyphal growth, septation, and virulence in *Aspergillus fumigatus*. *Mycopathologia*, 178, 341–348. *https://doi.org/10.1007/s11046-014-9794-9*.

Kameda, K., Aoki, H., and Namiki, M. (1974). An alternative structure for botrallin a metabolite of *Botrytis allii*. *Tetrahedron Lett*. 1, 103–106.

Kanehisa, M. and Goto, S. (2000). KEGG: Kyoto Encyclopedia of Genes and Genomes. *Nucleic Acids Res.* 28, 27-30.

Kanehisa, M., Furumichi, M., Sato, Y., Ishiguro-Watanabe, M., and Tanabe, M. (2021). KEGG: integrating viruses and cellular organisms. *Nucleic Acids Res.* 49, D545-D551.

Kanehisa, M., Sato, Y., and Morishima, K. (2016). BlastKOALA and GhostKOALA: KEGG Tools for Functional Characterization of Genome and Metagenome Sequences. *J Mol Biol*. 428(4), 726-731. doi: 10.1016/j.jmb.2015.11.006.

Kanehisa, M. (2019). Toward understanding the origin and evolution of cellular organisms. *Protein Sci*. 28, 1947-1951.

Kawasaki, L., Sanchez, O., Shiozaki, K., and Aguirre, J. (2002). SakA MAP kinase is involved in stress signal transduction, sexual development and spore viability in *Aspergillus nidulans*. *Mol Microbiol*. 45, 1153–1163. *https://doi.org/10.1046/j.1365-2958.2002.03087.x*.

Kelloniemi, J., Trouvelot, S., Héloir, M. C., Simon, A., Dalmais, B., Frettinger, P., Cimerman, A., Fermaud, M., Roudet, J., Baulande, S., Bruel, C., Choquer, M., Couvelard, L., Duthieuw, M., Ferrarini, A., Flors, V., Le Pêcheur, P., Loisel, E., Morgant, G., Poussereau, N., Pradier, J. M., Rascle, C., Trdá, L., Poinssot, B., and Viaud, M.. (2015). Analysis of the Molecular Dialogue Between Gray Mold (*Botrytis cinerea*) and Grapevine (*Vitis vinifera*) Reveals a Clear Shift in Defense Mechanisms During Berry Ripening. *Mol Plant Microbe Interact*. 28(11), 1167-80. doi: 10.1094/MPMI-02-15-0039-R.

Khalil, Z. G., Kalansuriya, P., and Capon, R. J. (2014). Lipopolysaccharide (LPS) stimulation of fungal secondary metabolism. *Mycology*, 5, 168–178. https ://doi.org/10.1080/21501 203.2014.930530

Kim, D., Paggi, J. M., Park, C., Bennett, C., and Salzberg, S. L. (2019). Graph-based genome alignment and genotyping with HISAT2 and HISAT-genotype. *Nature Biotechnology*, 37(8), 907–915. https://doi.org/10.1038/s41587-019-0201-4

Kim, S. O., Orii, Y., Lloyd, D., Hughes, M. N., and Poole, R. K. (1999). Anoxic function for the *Escherichia coli* flavohaemoglobin (hmp): reversible binding of nitric oxide and reduction to nitrous oxide. *FEBS Lett*. 445, 389–394.

Kimura, Y., Fujioka, H., Hamasaki, T., Furihata, K., and Fujioka, S. (1995) Botryslactone, a new plant growth regulator produced by *Botrytis squamosa*. *Tetrahedron Lett*. 36, 7673–7676.

Kimura, Y., Fujioka, H., Nakajima, H., Hamasaki, T. and Nakashima, R. (1993). BSF-A, a New Plant Growth Regulator Produced by the Fungus, *Botrytis squamosa*. *Bioscience, Biotechnology, and Biochemistry*, 57(9), 1584- 1585, doi: *10.1271/bbb.57.1584*

Kizawa, H., Tomura, D., Oda, M., Fukamizu, A., Hoshino, T., Gotoh, O., Yasui, T., and Shoun, H. (1991). Nucleotide sequence of the unique nitrate/nitrite-inducible cytochrome P-450 cDNA from *Fusarium oxysporum*. *J Biol Chem*. 266(16), 10632-10637.

Kokkelink, L., Minz, A., Al-Masri, M., Giesbert, S., Barakat, R., Sharon, A., and Tudzynski, P. (2011). The small GTPase BcCdc42 affects nuclear division, germination and virulence of the gray mold fungus *Botrytis cinerea*. *Fungal Genet Biol*. 48(11), 1012-1019. doi: 10.1016/j.fgb.2011.07.007.

Konetschny-Rapp, S., Jung, G., and Huschka, H. G. *et al.* (1988). Isolation and identification of the principal siderophore of the plant pathogenic fungus *Botrytis cinerea*. *Biol Metals.* 1, 90–98. https://doi.org/10.1007/BF01138066

Kovacic, P., and Somanathan, R. (2014). Nitroaromatic compounds: Environmental toxicity, carcinogenicity, mutagenicity, therapy and mechanism. *J Appl Toxicol*. 34(8), 810-824. doi: 10.1002/jat.2980.

Kretschmer, M. (2009). Fungicide-Driven Evolution and Molecular Basis of Multidrug Resistance in Field Populations of the Grey Mould Fungus *Botrytis cinerea*. *PLOS Pathogens*, 5, e1000696.

Krijgsheld, P., Bleichrodt, R., van Veluw, G. J., Wang, F., Muller, W. H., Dijksterhuis, J., and Wosten, H. (2013). Development in *Aspergillus*. *Stud Mycol*. 74, 1–29. *https://doi.org/10.3114/sim0006*.

Lamarre, C., Sokol, S., Debeaupuis, J. P., Henry, C., Lacroix, C., Glaser, P., Coppée, J. Y., François, J. M., and Latgé, J. P. (2008). Transcriptomic analysis of the exit from dormancy of *Aspergillus fumigatus* conidia. *BMC Genomics*, 9, 417. doi: 10.1186/1471-2164-9-417.

Lamoth, F., Juvvadi, P. R., Fortwendel, J. R., and Steinbach, W. J. (2012). Heat shock protein 90 is required for conidiation and cell wall integrity in *Aspergillus fumigatus*. *Eukaryot Cell*. 11, 1324–1332. *https://doi.org/10.1128/EC.00032-12*.

Lamoth, F., Juvvadi, P. R., Gehrke, C., Asfaw, Y. G., and Steinbach, W. J. (2014). Transcriptional activation of heat shock protein 90 mediated via a proximal promoter region as trigger of caspofungin resistance in *Aspergillus fumigatus*. *J Infect Dis*. 209, 473– 481. *https://doi.org/10.1093/infdis/jit530*.

Landy, A. (1989). Dynamic, structural, and regulatory aspects of lambda site-specific recombination. *Annu Rev Biochem.* 58, 913-949. doi: 10.1146/annurev.bi.58.070189.004405.

Langfelder, K., Jahn, B., Gehringer, H., Schmidt, A., Wanner, G., and Brakhage, A. A. (1998). Identification of a polyketide synthase gene (*pksP*) of *Aspergillus fumigatus* involved in conidial pigment biosynthesis and virulence. *Med Microbiol Immunol*. 187(2), 79-89. doi: 10.1007/s004300050077.

Langfelder, K., Philippe, B., Jahn, B., Latge, J. P., and Brakhage, A. A. (2001). Differential expression of the *Aspergillus fumigatus* pksP gene detected *in vitro* and *in vivo* with green fluorescent protein. *Infect Immun*. 69, 6411–6418. *https://doi.org/10.1128/IAI.69.10.6411-6418.2001*.

Lara-Rojas, F., Sanchez, O., Kawasaki, L., and Aguirre, J. (2011). *Aspergillus nidulans* transcription factor AtfA interacts with the MAPK SakA to regulate general stress responses, development and spore functions. *Mol Microbiol*. 80, 436–454. https://doi.org/10.1111/j.1365-2958.2011.07581.x.

Lau, G., and J. E. Hamer. (1996). Regulatory genes controlling MPG1 expression and pathogenicity in the rice blast fungus *Magnaporthe grisea*. *Plant Cell*, 8, 771–781.

Lau, G. W., and Hamer, J. E. (1998). Acropetal: a genetic *locus* required for conidiophore architecture and pathogenicity in the rice blast fungus. *Fungal Genet Biol*. 24(1-2), 228-39. doi: 10.1006/fgbi.1998.1053.

Leal, G. A., Gomes, L. H., Albuquerque, P. S., Tavares, F. C., and Figueira, A. (2010). Searching for *Moniliophthora perniciosa* pathogenicity genes. *Fungal Biol*. 114(10), 842-854. doi: 10.1016/j.funbio.2010.07.009.

Lei, M. and Tye, B. K. (2001). Initiating DNA synthesis: from recruiting to activating the MCM complex. *J Cell Sci*. 114(Pt 8), 1447-54.

Leroch, M., Kleber, A., Silva, E., Coenen, T., Koppenhofer, D., Shmaryahu, A., Valenzuela, P. D. T., and Hahn, M. (2013). Transcriptome profiling of *Botrytis cinerea* conidial germination reveals upregulation of infectionrelated genes during the prepenetration stage. *Eukaryot Cell*, 12(4), 614-626.

Li, B., Fu, Y., Jiang, D., Xie, J., Cheng, J., Li, G., Hamid, M. I., and Yi, X. (2010) Cyclic GMP as a second messenger in the nitric oxide-mediated conidiation of the mycoparasite *Coniothyrium minitans*. *Appl Environ Microbiol*. 76(9), 2830-2836. doi: 10.1128/AEM.02214-09.

Li, C., Cao, S., Wang, K., Lei, C., Ji, N., Xu, F., Jiang, Y., Qiu, L., Zheng, Y. (2021). Heat Shock Protein HSP24 Is Involved in the BABA-Induced Resistance to Fungal Pathogen in Postharvest Grapes Underlying an NPR1-Dependent Manner. *Front Plant Sci*. 12, 646147. doi: 10.3389/fpls.2021.646147.

Li, F., Long, T., Lu, Y., Ouyang, Q., and Tang, C. (2004). The yeast cell-cycle network is robustly designed. *Proc Natl Acad Sci U S A*, 101(14), 4781-4786. doi: 10.1073/pnas.0305937101.

Limon, M. C., Rodriguez-Ortiz, R., and Avalos, J. (2010). Bikaverin production and applications. *App Microb Biotechnol*. 87, 21–29.

Lindermayr, C., Saalbach, G., and Durner, J. (2005). Proteomic Identification of *S*-Nitrosylated Proteins in *Arabidopsis*. *Plant Physiol*. 137(3), 921–930.

Lin, X., Alspaugh, J. A., Liu, H., and Harris, S. (2014). Fungal morphogenesis. *Cold Spring Harb Perspect Med*. 5, a019679. *https://doi.org/10.1101/cshperspect.a019679*.

Li, Q., McNeil, B., and Harvey, L. M. (2008). Adaptive response to oxidative stress in the filamentous fungus *Aspergillus niger* B1-D. *Free Radic Biol Med*. 44, 394–402.

Liu, W., Leroux, P., and Fillinger, S. (2008). The HOG1-like MAP kinase Sak1 of *Botrytis cinerea* is negatively regulated by the upstream histidine kinase Bos1 and is not involved in dicarboximide- and phenylpyrrole-resistance. *Fungal Genet Biol*. 45, 1062–1074.

Liu, Z., Cao, J., Ma, Q., Gao, X., Ren, J., Xue, Y. (2011). GPS-YNO2: computational prediction of tyrosine nitration sites in proteins. *Mol Biosyst*. 7(4), 1197-204. doi: 10.1039/c0mb00279h.

López-Berges, M. S., DI Pietro, A., Daboussi, M. J., Wahab, H. A., Vasnier, C., Roncero, M. I., Dufresne, M., and Hera, C. (2009). Identification of virulence genes in *Fusarium oxysporum* f. sp. *lycopersici* by large-scale transposon tagging. *Molecular plant pathology*, *10*(1), 95–107. https://doi.org/10.1111/j.1364-3703.2008.00512.x

López-Ribera, I., La Paz, J. L., Repiso, C., García, N., Miquel, M., Hernández, M. L., Martínez-Rivas, J. M., and Vicient, C. M. (2014). The evolutionary conserved oil body associated protein OBAP1 participates in the regulation of oil body size. *Plant Physiol*. 164(3), 1237-1249. doi: 10.1104/pp.113.233221.

Lorenz, D. H., and Eichhorn, K. W. (1983). Untersuchungen an *Botryotinia fuckeliana* Whetz., dem Perfektstadium von *Botrytis cinerea* Pers. *ZPflanzenkranh Pflanzenschutz*, 90, 1–11.

Lovato, A., Zenoni, S., Tornielli, G. B., Colombo, T., Vandelle, E., and Polverari, A. (2019). Specific molecular interactions between *Vitis vinifera* and *Botrytis cinerea* are required for noble rot development in grape berries. *Postharvest Biol. Technol*. 25, 110924–110938. doi: 10.1016/j.postharvbio.2019.05.025

Love, M. I., Huber, W., and Anders, S. (2014). Moderated estimation of fold change and dispersion for RNA-seq data with DESeq2. *Genome Biology*, 15(12), 550. https://doi.org/10.1186/s13059-014-0550-8

Lucas, K. A., Pitari, G. M., Kazerounian, S., Ruiz-Stewart, I., Park, J., Schulz, S., Chepenik, K. P., and Waldman, S. A. (2000). Guanylyl cyclases and signaling by cyclic GMP. *Pharmacol Rev*. 52(3), 375-414.

Lyu, X., Shen, C., Fu, Y., Xie, J., Jiang, D., Li, G., and Cheng, J. (2016). The Microbial Opsin Homolog Sop1 is involved in *Sclerotinia sclerotiorum* Development and Environmental Stress Response. *Front Microbiol*. 6, 1504. doi: 10.3389/fmicb.2015.01504.

Magnani, T., Soriani, F. M., Martins, V. de P., Policarpo, A. C., Sorgi, C. A., Faccioli, L. H., Curti, C., and Uyemura, S. A . (2008). Silencing of mitochondrial alternative oxidase gene of *Aspergillus fumigatus* enhances reactive oxygen species production and killing of the fungus by macrophages. *J Bioenerg Biomembr*. 40(6), 631-636. doi: 10.1007/s10863-008-9191-5.

Magnani, T., Soriani, F. M., Martins, V. P., Nascimento, A. M., Tudella, V. G, Curti, C., and Uyemura, S. A. (2007). Cloning and functional expression of the mitochondrial alternative oxidase of *Aspergillus fumigatus* and its induction by oxidative stress. *FEMSMicrobiol Lett*. 271(2), 230-238. doi: 10.1111/j.1574-6968.2007.00716.x.

Mah, J. H., and Yu, J. H. (2006). Upstream and downstream regulation of asexual development in *Aspergillus fumigatus*. *Eukaryotic cell*. *5*(10), 1585–1595. https://doi.org/10.1128/EC.00192-06

Maier, J., Hecker, R., Rockel, P., and Ninnemann, H. (2001). Role of nitric oxide synthase in the light-induced development of sporangiophores in *Phycomyces blakesleeanus*. *Plant Physiol*. 126(3), 1323-1330.

Majumdar, U., Biswas, P., Subhra, S. T., Maiti, D., and Ghosh, S. (2012). Regulation of cell cycle and stress responses under nitrosative stress in *Schizosaccharomyces pombe*. *Free Radic Biol Med*. 52(11-12), 2186-2200. doi: 10.1016/j.freeradbiomed.2012.03.026.

Marcos, A. T., Ramos, M. S., Marcos, J. F., Carmona, L., Strauss, J., and Cánovas, D. (2016). Nitric oxide synthesis by nitrate reductase is regulated during development in *Aspergillus*. *Molecular Microbiology*, 99(1), 15–33. https://doi.org/10.1111/mmi.13211

Marks, A. R. (1996). Cellular functions of immunophilins. *Physiol Rev*. 76(3), 631-649. doi: 10.1152/physrev.1996.76.3.631.

Marobbio, C. M., Agrimi, G., Lasorsa, F. M., and Palmieri, F. (2003). Identification and functional reconstitution of yeast mitochondrial carrier for S-adenosylmethionine. *EMBO J*. 22(22), 5975-5982. doi: 10.1093/emboj/cdg574.

Marroquin-Guzman, M., Hartiline, D., Wright, J. D., Elowsky, C., Bourret, T. J., and Wilson, R. A. (2017). The Magnaphorthe oryzae nitrooxidative stress response suppresses rice innate immunity during blast disease. *Nature Microbiology*, 2, 17054.

Bibliography

Martinez, F., Corio-Costet, M. F., Levis, C. *et al*. (2008). New PCR primers applied to characterize distribution of *Botrytis cinerea* populations in French vineyards. *Vitis*, 47, 217–226.

Martinez, F., Dubos, B., and Fermaud, M. (2005). The role of saprotrophy and virulence in the population dynamics of *Botrytis cinerea* in vineyards. *Phytopathology*, 95, 692–700.

Martins, V. P., Dinamarco, T. M., Soriani, F. M., Tudella, V. G., Oliveira, S. C., Goldman, G. H., Curti, C., and Uyemura, S. A. (2011). Involvement of an alternative oxidase in oxidative stress and mycelium-to-yeast differentiation in *Paracoccidioides brasiliensis*. *Eukaryot Cell*. 10(2), 237-248. doi: 10.1128/EC.00194-10.

Marzluf, G. A. (1997). Genetic regulation of nitrogen metabolism in the fungi. *Microbiol Mol Biol Rev*. 61(1), 17-32. doi: 10.1128/mmbr.61.1.17-32.1997.

Miceli, A., Ippolito, A., Linsalata, V., and Nigro, F. (1999). Effect of preharvest calcium treatments on decay and biochemical changes in table grape during storage. *Phytopathol Mediterr*. 38, 47–53.

Milhomem, C.-L. V. R., Salem-Izacc, S. M., Novaes, E., Neves, B. J., de Almeida, B. W., O'Hara, S. S. L., Paccez, J. D., Parente-Rocha, J. A., Pereira, M., Maria de Almeida, S. C., and Borges, C. L. (2020). Nitrogen Catabolite Repression in members of *Paracoccidioides* complex. *Microb Pathog*. 149, 104281. doi: 10.1016/j.micpath.2020.104281.

Mistry, J., Chuguransky, S., Williams, L., Qureshi, M., Salazar, G. A., Sonnhammer, E. L. L., Tosatto, S. C. E., Paladin, L., Raj, S., Richardson, L. J., Finn, R. D., and Bateman, A. (2021). Pfam: The protein families database in 2021. *Nucleic Acids Res.* 49(D1), D412-D419. doi: 10.1093/nar/gkaa913.

Momany, M. (2002). Polarity in filamentous fungi: establishment, maintenance and new axes. *Curr Opin Microbiol.* 5, 580–585. https://doi.org/10.1016/S1369-5274(02)00368-5.

Mosbach, A., Leroch, M., Mendgen, K. W., and Hahn, M. (2011). Lack of evidence for a role of hydrophobins in conferring surface hydrophobicity to conidia and hyphae of *Botrytis cinerea*. *BMC Microbiol*. 11, 10. doi: 10.1186/1471-2180-11-10.

Mouyna, I., Dellière, S., Beauvais, A., Gravelat, F., Snarr, B., Lehoux, M., Zacharias, C., Sun, Y., de Jesus, C. S., Pearlman, E., Sheppard, D. C., and Latgé, J. P. (2020). What Are the Functions of Chitin Deacetylases in *Aspergillus fumigatus*? *Front Cell Infect Microbiol*. 10, 28. doi: 10.3389/fcimb.2020.00028.

Mundy, D. (2008). A review of the direct and indirect effects of nitrogen on botrytis bunch rot in wine grapes. *New Zealand Plant Protection*, 61, 306-310.

Nicot, P. C., Bardin, M., Alabouvette, C. *et al*. (2011). Potential of biological control based on published research. 1. Protection against plant pathogens of selected crops. In: Nicot P. C. (Ed.), *Classical and augmentative biological control against diseases and pests: critical status analysis and review of factors influencing their success* (1-11). IOBC/WPRS, Zurich.

Ni, M., and Yu, J. H. (2007). A novel regulator couples sporogenesis and trehalose biogenesis in *Aspergillus nidulans*. *PLoS One*, 2, e970. https://doi.org/10.1371/journal.pone.0000970.

Ni, M., Gao, N., Kwon, N. J., Shin, K. S. and Yu, J. H. (2010). Regulation of *Aspergillus* Conidiation. In: Borkovich K. A., Ebbole D. j. (Eds.), *Cellular and Molecular Biology of Filamentous Fungi* (557-576), ASM Press https://doi.org/10.1128/9781555816636.ch35

Ninnemann, H., and Maier, J. (1996). Indications for the occurrence of nitric oxide synthases in fungi and plants and the involvement in photoconidiation of *Neurospora crassa*. *Photochem Photobiol*. 64(2), 393-398.

Nishimura, M., Hayashi, N., Jwa, N. S., Lau, G. W., Hamer, J. E., and Hasebe, A. (2000). Insertion of the LINE retrotransposon MGL causes a conidiophore pattern mutation in *Magnaporthe grisea*. *Mol Plant Microbe Interact*. 13(8), 892-894. doi: 10.1094/MPMI.2000.13.8.892.

Nižňanský L, Kryštofová S, Vargovič P, Kaliňák M, Simkovič M, and Varečka L. (2013). Glutamic acid decarboxylase gene disruption reveals signalling pathway(s) governing complex morphogenic and metabolic events in *Trichoderma atroviride*. *Antonie Van Leeuwenhoek*. 104(5), 793-807. doi: 10.1007/s10482-013-9989-y.

Novodvorska, M., Hayer, K., Pullan, S. T., Wilson, R., Blythe, M. J., Stam, H., Stratford, M., and Archer, D. B. (2013). Trancriptional landscape of *Aspergillus niger* at breaking of conidial dormancy revealed by RNA-sequencing. BMC Genomics, 14, 246. *https://doi.org/10.1186/1471-2164-14-246*.

Nurse, P., and Marians, K. J. (2013). Purification and characterization of *Escherichia coli* MreB protein. *J Biol Chem*. 288(5), 3469-3475. doi: 10.1074/jbc.M112.413708.

Nurse, P. (1985). Cell cycle control genes in yeast, *Trends in Genetics*, 1, 51-55, *https://doi.org/10.1016/0168-9525(85)90023-X*.

Ohara, T., Inoue, I., Namiki, F., Kunoh, H., and Tsuge, T. (2004). *REN1* Is Required for Development of Microconidia and Macroconidia, but Not of Chlamydospores, in the Plant Pathogenic Fungus *Fusarium oxysporum*. *Genetics*, 166 (1), 113–124, https://doi.org/10.1534/genetics.166.1.113

Ohara, T., and Tsuge, T. (2004). FoSTUA, encoding a basic helix-loop-helix protein, differentially regulates development of three kinds of asexual spores, macroconidia, microconidia, and chlamydospores, in the fungal plant pathogen *Fusarium oxysporum*. *Eukaryotic cell*. *3*(6), 1412–1422. https://doi.org/10.1128/EC.3.6.1412-1422.2004

Ongena, M., Henry, G., and Thonart, P. (2010). The role of cyclic lipopetides in the biocontrol activity of *Bacillus subtilis*. In: Gisi U., Chet I., Gullino M. L. (Eds.), *Recent developments in the management of plant diseases* . Plant Pathology in the 21st Century. 1, 59–69.

Osherov, N., and May, G. S. (2001). The molecular mechanisms of conidial germination. *FEMS Microbiol Lett*. 199, 153–160. *https://doi.org/10.1111/j.1574-6968.2001.tb10667.x*.

Overeem, J. C., and Van Dijkman, A. (1968). Botrallin, a novel quinone produced by *Botrytis allii*. *Rec Trav Chim NL*. 87, 940–944.

Pammer, M., Briza, P., Ellinger, A., Schuster, T., Stucka, R., Feldmann, H., and Breitenbach, M. (1992). DIT101 (CSD2, CAL1), a cell cycle-regulated yeast gene required for synthesis of chitin in cell walls and chitosan in spore walls. *Yeast*. 8(12), 1089-1099. doi: 10.1002/yea.320081211.

Park, H. S. and Yu, J. H. (2016). Developmental regulators in *Aspergillus fumigatus*. J Microbiol. 54(3), 223–231. https://doi.org/10.1007/s12275-016-5619-5

Park, H. S., Bayram, O., Braus, G. H., Kim, S. C., and Yu, J. H. (2012). Characterization of the velvet regulators in *Aspergillus fumigatus*. *Mol Microbiol*. 86, 937–953. *https://doi.org/10.1111/mmi.12032*.

Park, H. S., Ni, M., Jeong, K. C., Kim, Y. H., and Yu, J. H. (2012b). The role, interaction and regulation of the Velvet regulator VelB in *Aspergillus nidulans*. *PLoS One*, 7, e45935. *https://doi.org/10.1371/journal.pone.0045935*.

Parry, R., Nishino, S., and Spain, J. (2011). Naturally-occurring nitro compounds. *Nat Prod Rep*. 28(1), 152-167. doi: 10.1039/c0np00024h.

Pearson, M. N., and Bailey, A. M. (2013). Viruses of *Botrytis*. *Adv Virus Res*. 86, 249–272.

Pertea, M., Pertea, G. M., Antonescu, C. M., Chang, T. C., Mendell, J. T., and Salzberg, S. L. (2015). StringTie enables improved reconstruction of a transcriptome from RNA-seq reads. *Nature Biotechnology*, 33(3), 290–295. https://doi.org/10.1038/nbt.3122

Pfaffl, M. W. (2001). A new mathematical model for relative quantification in real-time RT-PCR. *Nucleic Acids Res.* 29, e45.

Pfannmüller, A., Boysen, J. M., and Tudzynski, B. (2017). Nitrate Assimilation in *Fusarium fujikuroi* Is Controlled by Multiple Levels of Regulation. *Front Microbiol*. 8, 381. doi: 10.3389/fmicb.2017.00381.

Pihet, M., Vandeputte, P., Tronchin, G., Renier, G., Saulnier, P., Georgeault, S., Mallet, R., Chabasse, D., Symoens, F., and Bouchara, J. P. (2009). Melanin is an essential component for the integrity of the cell wall of *Aspergillus fumigatus* conidia. *BMC Microbiol*. 9, 177. https://doi.org/10.1186/1471-2180-9-177.

Pollastro, S., De Miccolis Angelini, R. M., Rotolo, C., *et al.* (2007). Characterisation of vacuma and transposa biotypes of *Botryotinia fuckeliana*. In: Abstracts of the XIV international *Botrytis* symposium, Cape Town, 21–26 October 2005.

Pollastro, S., Faretra, F., Santomauro, A. *et al.* (1996). Studies on pleiotropic effects of mating type, benzimidazole-resistance and dicarboximide-resistance genes in near-isogenic strains of *Botryotinia fuckeliana* (*Botrytis cinerea*). *Phytopathol Mediterr*. 35, 48–57.

Potgieter, C. A., Castillo, A., Castro, M., Cottet, L., and Morales, A. (2013). A wild-type *Botrytis cinerea* strain co-infected by double-stranded RNA mycoviruses presents hypovirulence-associated traits. *Virol J*. 10, 220. doi: 10.1186/1743-422X-10-220.

Prado, A. M., Colaco, R., Moreno, N., Silva, A. C., and Feijo, J. A. (2008). Targeting of pollen tubes to ovules is dependent on nitric oxide (NO) signaling. *Mol Plant*. 1, 703–714.

Bibliography

Prado, A. M., Porterfield, D. M., and Feijo, J. A. (2004). Nitric oxide is involved in growth regulation and re-orientation of pollen tubes. *Development*, 131, 2707–2714.

Prats, E., Carver, T. L., and Mur, L. A. (2008). Pathogen-derived nitric oxide influences formation of the appressorium infection structure in the phytopathogenic fungus *Blumeria graminis*. *Res Microbiol*. 159(6), 476-80.

Priya, S., Sharma, S. K., and Goloubinoff, P. (2013). Molecular chaperones as enzymes that catalytically unfold misfolded polypeptides. *FEBS Lett*. 587, 1981–1987. *https://doi.org/10.1016/j.febslet.2013.05.014*.

Qazi, S. S., and Khachatourians, G. G. (2008). Addition of exogenous carbon and nitrogen sources to aphid exuviae modulates synthesis of proteases and chitinase by germinating conidia of *Beauveria bassiana*. *Arch Microbiol*. 189, 589–596. https://doi.org/10.1007/s00203-008-0355-9

Quidde, T., Büttner, P., and Tudzynski, P. (1999). Evidence for Three Different Specific Saponin-detoxifying Activitiesin *Botrytis cinerea* and Cloning and Functional Analysis of a Gene Coding for a Putative Avenacinase. *European Journalof Plant Pathology*, 105, 273–283.

Rao, S., Van Vleet, T. R., Ciurlionis, R., Buck, W. R., Mittelstadt, S. W., Blomme, E. A. G., and Liguori, M. J. (2019). Comparison of RNA-Seq and Microarray Gene Expression Platforms for the Toxicogenomic Evaluation of Liver From Short-Term Rat Toxicity Studies. *Frontiers in Genetics*, 9, 636. DOI=10.3389/fgene.2018.00636.

Reboledo, G., Agorio, A., Vignale, L., Batista-García, R. A., and Ponce De León, I. (2020). *Botrytis cinerea* Transcriptome during the Infection Process of the Bryophyte *Physcomitrium patens* and Angiosperms. *J Fungi*, 7(1), 11. doi: 10.3390/jof7010011

Reece, J. B., Urry, L. A., Cain, M. L., Wasserman, S. A., Minorsky, P. V. and Jackson, R. B. (2011). The cell cycle. In: *Campbell biology* (10th ed.). San Francisco, CA. Pearson.

Reglinski, T., Poole, R. P., Whitaker, G., and Hoyte, S. M. (1997). Induced resistance against *Sclerotinia sclerotiorum* in kiwifruit leaves. *Plant Pathology*, 46, 716-721.

Reuveni, R., Raviv, M., and Bar, R. (1989). Sporulation of *Botrytis cinerea* as affected by photoselective sheets and filters. *Ann Appl Biol*. 115, 417–424.

Rhoads, D. M., and Subbaiah, C. C. (2007). Mitochondrial retrograde regulation in plants. *Mitochondrion*, 7, 177-194. https://doi.org/10.1016/j.mito.2007.01.002

Riquelme, M., Aguirre, J., Bartnicki-Garcia, S., Braus, G. H., Feldbrugge, M., Fleig, U., Hansberg, W., Herrera-Estrella, A., Kamper, J., Kuck, U., Mourino-Perez, R. R., Takeshita, N., and Fischer, R. (2018). Fungal morphogenesis, from the polarized growth of hyphae to complex reproduction and infection structures. *Microbiol Mol Biol Rev*. 82, e00068-17. https://doi.org/10.1128/MMBR.00068-17.

Riquelme, M. (2013). Tip growth in filamentous fungi: a road trip to the apex. *Annu Rev Microbiol*. 67, 587–609. https://doi.org/10.1146/annurev-micro-092412-155652.

Robles-Kelly, C., Rubio, J., Thomas, M., Sedán, C., Martinez, R., Olea, A. F., Carrasco, H., Taborga, L., and Silva-Moreno, E. (2017). Effect of drimenol and synthetic derivatives on growth and germination of *Botrytis cinerea*: Evaluation of possible mechanism of action. *Pestic Biochem Physiol*. 141, 50-56. doi: 10.1016/j.pestbp.2016.11.006.

Rodenburg, S. Y. A., Terhem, R. B., Veloso, J., Stassen, J. H. M., and van Kan, J. A. L. (2018). Functional Analysis of Mating Type Genes and Transcriptome Analysis during Fruiting Body Development of *Botrytis cinerea*. *mBio*. 9(1), e01939-01917. doi: 10.1128/mBio.01939-17.

Romano, N., and Macino, G. (1992). Quelling: transient inactivation of gene expression in *Neurospora crassa* by transformation with homologous sequences. *Mol Microbiol*. 6(22), 3343-3353. doi: 10.1111/j.1365-2958.1992.tb02202.x.

Ross, D., and Siegel, D. (2021). The diverse functionality of NQO1 and its roles in redox control. *Redox Biol*. 41, 101950, https://doi.org/10.1016/j.redox.2021.101950.

Salminen, A., Jouhten, P., Sarajärvi, T., Haapasalo, A., and Hiltunen, M. (2016). Hypoxia and GABA shunt activation in the pathogenesis of Alzheimer's disease. *Neurochem Int*. 92, 13-24. doi: 10.1016/j.neuint.2015.11.005.

Samalova, M., Johnson, J., Illes, M., Kelly, S., Fricker, M., and Gurr, S. (2013). Nitric oxide generated by the rice blast fungus *Magnaporthe oryzae* drives plant infection. *New Phytologist*, 197, 207–222.

Sambrook, J., Fritsch, E. F., and Maniatis, T. (1989). Molecular cloning: a laboratory manual. *Cold Spring Habor Laboratory Press*.

Samuel, S., Veloukas, T., Papavasileiou, A., Karaoglanidis, G. S. (2012). Differences in Frequency of Transposable Elements Presence in *Botrytis cinerea* Populations from Several Hosts in Greece. *Plant Dis*. 96(9), 1286-1290. doi: 10.1094/PDIS-01-12-0103-RE.

Sanger, F., Nicklen, S., and Coulson, A. R. (1977). DNA sequencing with chain-terminating inhibitors. *Proc. Natl. Acad. Sci.* 74, 5463–5467.

Santander Gordón, Daniela Isabel, 2014. *Estudio del metabolismo del óxido nítrico (NO) en Botrytis cinerea: mecanismos de producción y efectos fisiológicos*. Doctoral thesis. Salamanca: University of Salamanca.

Sarikaya, B. O., Bayram, O., Valerius, O., Park, H. S., Irniger, S., Gerke, J., Ni, M., Han, K. H., Yu, J. H., and Braus, G. H. (2010). LaeA control of velvet family regulatory proteins for light-dependent development and fungal celltype specificity. *PLoS Genet*. 6, e1001226. https://doi.org/10.1371/journal.pgen.1001226.

Saupe, S. J. (2000). Molecular genetics of heterokaryon incompatibility in filamentous ascomycetes. *Microbiology and molecular biology reviews: MMBR*, *64*(3), 489–502. *https://doi.org/10.1128/MMBR.64.3.489-502.2000*

Schaap, P. (2005). Guanylyl cyclases across the tree of life. *Front Biosci*. 10, 1485-1498. doi: 10.2741/1633.

Schamber, A., Leroch, M., Diwo, J., Mendgen, K., and Hahn, M. (2010). The role of mitogen-activated protein (MAP) kinase signalling components and the Ste12 transcription factor in germination and pathogenicity of *Botrytis cinerea*. *Molecular plant pathology*, 11(1), 105–119. https://doi.org/10.1111/j.1364-3703.2009.00579.x

Scharf, D. H., Heinekamp, T., and Brakhage, A. A. (2014). Human and plant fungal pathogens: the role of secondary metabolites. *PLoS Pathog*. 10, e1003859.

Schindelin, J., Arganda-Carreras, I., Frise, E., Kaynig, V., Longair, M., Pietzsch, T., Preibisch, S., Rueden, C., Saalfeld, S., Schmid, B., Tinevez, J. Y., White, D. J., Hartenstein, V., Eliceiri, K., Tomancak, P., and Cardona, A. (2012). Fiji: an open-source platform for biological-image analysis. *Nat Methods*, 9(7), 676-82. doi: 10.1038/nmeth.2019.

Schinko, T., Berger, H., Lee, W., Gallmetzer, A., Pirker, K., Pachlinger, R., Buchner, I., Reichenauer, T., Güldener, U., and Strauss, J. (2010). Transcriptome analysis of nitrate assimilation in *Aspergillus nidulans* reveals connections to nitric oxide metabolism. *Mol Microbiol*. 78(3), 720-738. doi: 10.1111/j.1365-2958.2010.07363.x.

Schinko, T., Gallmetzer, A., Amillis, S., and Strauss, J. (2013). Pseudo-constitutivity of nitrate-responsive genes in nitrate reductase mutants. *Fungal Genet Biol*. 54, 34–41.

Schmitt, A., Ibarra, F., and Francke, W. (2005). Resistance inducing constituents in extracts of *Reynoutria sachalinensis*. In: Dehne H. W., Gisi U., Kuck K. H., Russell P. E., Lyr H. (Eds.) Modern fungicides and antifung al compounds IV: proceedings of the 14th international Reinhardsbrunn symposium, April 25–29 2004, Friedrichroda, Germany. British Crop Production Council, Alton

Schmitt, A., Strathmann, S., Emslie, K. A. *et al*. (1996). Use of *Regalia sachalinensis* extracts for induced resistance in integrated disease control: effects on *Botrytis cinerea*. XIth international Botrytis symp 23–27 June, Wageningen, 69.

Schumacher, J., and Tudzynski, P. (2012). Morphogenesis and Infection in *Botrytis cinerea*. In: Pérez-Martín J., Di Pietro A. (Eds.), *Morphogenesis and Pathogenicity in Fungi. Topics in Current Genetics* , 22. Springer. https://doi.org/10.1007/978-3-642-22916-9_11

Schumacher, J. (2017). How light affects the life of *Botrytis*. *Fungal Gen. Biol.* 106, 26-41. https://doi.org/10.1016/j.fgb.2017.06.002

Schumacher, J. (2016). Signal Transduction Cascades Regulating Differentiation and Virulence in *Botrytis cinerea*. In: Fillinger S., Elad Y. (Eds.), *Botrytis* – the Fungus, the Pathogen and its Management in Agricultural Systems (247-267). Springer, Cham. https://doi.org/10.1007/978-3-319-23371-0_13

Schumacher, J., Simon, A., Cohrs, K. C., Viaud, M., and Tudzynski, P. (2014). The Transcription Factor BcLTF1 Regulates Virulence and Light Responses in the Necrotrophic Plant Pathogen *Botrytis cinerea*. *PLOS Genetics*, 10(1), e1004040. https://doi.org/10.1371/journal.pgen.1004040

Schumacher, J., Viaud, M., Simon, A., and Tudzynski, B. (2008). The Galpha subunit BCG1, the phospholipase C (BcPLC1) and the calcineurin phosphatase co-ordinately regulate gene expression in the grey mould fungus *Botrytis cinerea*. *Mol Microbiol*. 67(5), 1027-1050. doi: 10.1111/j.1365-2958.2008.06105.x.

Selker, E. U. (1990). Premeiotic instability of repeated sequences in *Neurospora crassa*. *Annu Rev Genet*. 24, 579-613. doi: 10.1146/annurev.ge.24.120190.003051.

Shirane, N., Masuko, M., and Hayashi, Y. (1989). Light microscopic observation of nuclei and mitotic chromosomes of *Botrytis* species. *Phytopathology*, 79, 728–730.

Shirane, N., Masuko, M., and Hayashi, Y. (1988). Nuclear behavior and division in germinating conidia of *Botrytis cinerea*. *Phytopathology*, 78, 1627–1630.

Shiu, P. K., Raju, N. B., Zickler, D., Metzenberg, R. L. (2001). Meiotic silencing by unpaired DNA. *Cell*, 107(7), 905-916. doi: 10.1016/s0092-8674(01)00609-2.

Shpialter, L., David, D. R., Dori, I., Yermiahu, U., Pivonia, S., Levite, R., Elad Y. (2009). Cultural methods and environmental conditions affecting gray mold and its management in *lisianthus*. *Phytopathology*, 99(5), 557-570. doi: 10.1094/PHYTO-99-5-0557.

Shwab, E. K., Juvvadi, P. R., Waitt, G., Soderblom, E. J., Moseley, M. A., Nicely, N. I., and Steinbach, W. J. (2017). Phosphorylation of *Aspergillus fumigatus* PkaR impacts growth and cell wall integrity through novel mechanisms. *FEBS Lett*. 591, 3730–3744. *https://doi.org/10.1002/1873-3468.12886*.

Siverio, J. M. (2002). Assimilation of nitrate by yeasts. *FEMS Microbiol. Rev*. 26, 277–284. doi: 10.1111/j.1574-6976.2002.tb00615.x

Smith, R. E. (1900). *Botrytis* and *Sclerotinia*: Their Relation to Certain Plant Diseases and to Each Other. *Botanical Gazette*, 29(6), 369-407

Som, T., and Kolaparthi, V. S. (1994). Developmental decisions in *Aspergillus nidulans* are modulated by Ras activity. *Mol Cell Biol*. 14, 5333–5348. *https://doi.org/10.1128/mcb.14.8.5333*.

Son, H., Kim, M. G., Min, K., Seo, Y. S., Lim, J. Y., Choi, G. J., Kim, J. C., Chae, S. K., and Lee, Y. W. (2013). AbaA regul ates conidiogenesis in the ascomycete fungus *Fusarium graminearum*. *PLoS One*. 8(9), e72915. doi: 10.1371/journal.pone.0072915.

Springer, M. L., and Yanofsky, C. (1989). A morphological and genetic analysis of conidiophore development in *Neurospora crassa*. *Genes Dev*. 3(4), 559-571. doi: 10.1101/gad.3.4.559.

Srivastava, D. A., Arya, G. C., Pandaranayaka, E. P., Manasherova, E., Prusky, D. B., Elad, Y., Frenkel, O., and Harel, A. (2020). Transcriptome Profiling Data of *Botrytis cinerea* Infection on Whole Plant *Solanum lycopersicum*. *Mol Plant Microbe Interact*. 33(9), 1103-1107. doi: 10.1094/MPMI-05-20-0109-A.

Staats, M., and Van Kan, J. A. L. (2012). Genome update of *Botrytis cinerea* strains B05.10 and T4. *Eukaryot Cell.* 11, 1413–1414.

Staats, M., van Baarlen, P., and van Kan, J. A. L. (2005). Molecular phylogeny of the plant pathogenic genus *Botrytis* and the evolution of host specificity. *Molecular Biology and Evolution*, 22, 333–346.

Stamler, J. S. (1994). Redox signaling: nitrosylation and related target interactions of nitric oxide. *Cell*. 78(6), 931-6.

Steinbach, W. J., Cramer, R. A. Jr., Perfect, B. Z., Asfaw, Y. G., Sauer, T. C., Najvar, L. K., Kirkpatrick, W. R., Patterson, T. F., Benjamin, D. K. Jr., Heitman, J., and Perfect, J. R. (2006). Calcineurin controls growth, morphology, and pathogenicity in *Aspergillus fumigatus*. *Eukaryot Cell*. 5(7), 1091-1103. doi: 10.1128/EC.00139-06.

Stie, J., and Fox, D. (2008). Calcineurin regulation in fungi and beyond. *Eukaryot Cell*. 7(2), 177-186. doi: 10.1128/EC.00326-07.

Stierle, D. B., Stierle, A. A., and Kunz, A. (1998). Dihydroramulosin from *Botrytis* sp. *J Nat Prod*. 61, 1277–1278.

Suh, M.-J., Fedorova, N. D., Cagas, S. E., Hastings, S., Fleischmann, R. D., Peterson, S. N., Perlin, D. S., Nierman, W. C., Pieper, R., and Momany, M. (2012). Development stage-specific proteomic profiling uncovers small, lineage specific proteins most abundant in the *Aspergillus fumigatus* conidial proteome. *Proteome Sci*. 10, 30. *https://doi.org/10.1186/1477-5956-10-30*.

Sun, J., Sun, C. H., Chang, H. W., Yang, S., Liu, Y., Zhang, M. Z., Hou, J., Zhang, H., Li, G. H., and Qin, Q. M. (2021). Cyclophilin BcCyp2 Regulates Infection-Related Development to Facilitate Virulence of the Gray Mold Fungus *Botrytis cinerea*. *Int J Mol Sci.* 22(4), 1694. doi: 10.3390/ijms22041694.

Supek, F., Bošnjak, M., Škunca, N., and Šmuc, T. (2011). REVIGO summarizes and visualizes long lists of gene ontology terms. *PLoS One*, 6(7), e21800. doi: 10.1371/journal.pone.0021800.

Suzuki, Y., Kumagai, T., and Oda, Y. (1977). *Locus* of blue and near ultraviolet reversible photoreaction in the stages of conidial development in *Botrytis cinerea*. *J Gen Microbiol*. 98(1), 199-204. doi: 10.1099/00221287-98-1-199.

Tabei, Y., Kitade, S., Nishizawa, Y., Kikuchi, N., Kayano, T., Hibi, T., and Akutsu, K. (1998). Transgenic cucumber plants harboring a rice chitinase gene exhibit enhanced resistance to gray mold (*Botrytis cinerea*). *Plant Cell Rep*. 17(3), 159-164. doi: 10.1007/s002990050371.

Tani, H., Koshino, H., Sakuno, E., and Nakajima, H. (2005). Botcinins A, B, C, and D, metabolites produced by *Botrytis cinerea*, and their antifungal activity against *Magnaporthe grisea*, a pathogen of rice blast disease. *J Nat Prod*. 68(12), 1768-1772. doi: 10.1021/np0503855.

Tani, H., Koshino, H., Sakuno, E., Cutler, H. G., and Nakajima, H. (2006). Botcinins E and F and Botcinolide from *Botrytis cinerea* and structural revision of botcinolides. *J Nat Prod*. 69(4), 722-725. doi: 10.1021/np060071x.

Tao, L., and Yu, J. H. (2011). AbaA and WetA govern distinct stages of *Aspergillus fumigatus* development. *Microbiology*, 157, 313–326. *https://doi.org/10.1099/mic.0.044271-0*.

ten Have, A., Espino, J. J., Dekkers, E., Van Sluyter, S. C., Brito, N., Kay, J., González, C., and van Kan, J. A. (2010). The *Botrytis cinerea* aspartic proteinase family. *Fungal Genet Biol*. 47(1), 53-65. doi: 10.1016/j.fgb.2009.10.008.

ten Have, A., van Berloo, R., Lindhout, P., and van Kan, J. A. L. (2007). Partial stem and leaf resistance against the fungal pathogen *Botrytis cinerea* in wild relatives of tomato. *European Journal of Plant Pathology*, 117, 153–166.

Terhem, R. B., and van Kan, J. A. (2014). Functional analysis of hydrophobin genes in sexual development of *Botrytis cinerea*. *Fungal Genet Biol*. 71, 42-51. doi: 10.1016/j.fgb.2014.08.002.

Teutschbein, J., Albrecht, D., Pötsch, M., Guthke, R., Aimanianda, V., Clavaud, C., Latgé, J. P., Brakhage, A. A., and Kniemeyer, O. (2010). Proteome profiling and functional classification of intracellular proteins from conidia of the human-pathogenic mold *Aspergillus fumigatus*. *J Proteome Res*. 9(7), 3427-3442. doi: 10.1021/pr9010684.

Thakur, R., and Shankar, J. (2017). Proteome profile of *Aspergillus terreus* conidia at germinating stage: identification of probable virulent factors and enzymes from mycotoxin pathways. *Mycopathologia*, 182, 771–784. *https://doi.org/10.1007/s11046-017-0161-5*.

Thau, N., Monod, M., Crestani, B., Rolland, C., Tronchin, G., Latge, J. P., and Paris, S. (1994). rodletless mutants of *Aspergillus fumigatus*. *Infect. Immun*. 62, 4380–4388.

The Gene Ontology resource: enriching a GOld mine (2021). *Nucleic Acids Res.* 49(D1), D325-D334.

The UniProt Consortium (2021). UniProt: the universal protein knowledgebase in 2021, **Nucleic Acids Research**, 49(D1), D480–D489, https://doi.org/10.1093/nar/gkaa1100

Trail, F., Xu, J. R., Miguel, P. S., Halgren, R. G., and Kistler, H. C. (2003). Analysis of expressed sequence tags from *Gibberella zeae* (anamorph *Fusarium graminearum*). *Fungal Genetics and Biology*, 38(2), 187-197. https://doi.org/10.1016/S1087-1845(02)00529-7

Tsai, H. F., Chang, Y. C., Washburn, R. G., Wheeler, M. H., and Kwon-Chung, K. J. (1998). The developmentally regulated *alb1* gene of *Aspergillus fumigatus*: its role in modulation of conidial morphology and virulence. *J Bacteriol*. 180(12), 3031-3038. doi: 10.1128/JB.180.12.3031-3038.1998.

Tsai, H. F., Wheeler, M. H., Chang, Y. C., and Kwon-Chung, K. J. (1999). A developmentally regulated gene cluster involved in conidial pigment biosynthesis in *Aspergillus fumigatus*. *Journal of bacteriology*, *181*(20), 6469–6477. https://doi.org/10.1128/JB.181.20.6469-6477.1999

Tudzynski, B. (2014). Nitrogen regulation of fungal secondary metabolism in fungi. *Front. Microbiol*. 5, 656. *https://doi.org/10.3389/fmicb.2014.00656*

Tudzynski, P., and Kokkelink, L. (2009). *Botrytis cinerea*: Molecular Aspects of a Necrotrophic Life Style. In: P.D.H.B. Deising (Ed.), *Plant Relationships* (29-50), *Springer Berlin Heidelberg*.

Tudzynski, P., and Sharon, A. (2003). Fungal Pathogenicity Genes. In: Arora, D. K., Khachatourians, G. G. (Eds.). *Applied Mycology and Biotechnology* (187-212), Elsevier. https://doi.org/10.1016/S1874-5334(03)80012-6.

Turrion-Gomez, J. L. and Benito, E. P. (2011). Flux of nitric oxide between the necrotrophic pathogen *Botrytis cinerea* and the host plant. *Mol Plant Pathol*. 12(6), 606-16.

Turrion-Gomez, J. L., Eslava, A. P., and Benito, E. P. (2010). The flavohemoglobin BCFHG1 is the main NO detoxification system and confers protection against nitrosative conditions but is not a virulence factor in the fungal necrotroph *Botrytis cinerea*. *Fungal Genet Biol*. 47(5), 484-96.

Vallejo, I., Carbú, M., Muñoz. F. *et al*. (2002). Inheritance of chromosome-length polymorphisms in the phytopathogenic ascomycete *Botryotinia fuckeliana* (anam. *Botrytis cinerea*). *Mycol Res*. 106, 1075–1085.

Vallejo, I., Santos, M., Cantoral, J. M. *et al*. (1996). Chromosomal polymorphism in *Botrytis cinerea* strains. *Hereditas*, 124, 31–38.

Valsecchi, I., Dupres, V., Stephen-Victor, E., Guijarro, J., Gibbons, J., Beau, R., Bayry, J., Coppee, J. Y., Lafont, F., Latge, J. P., and Beauvais, A. (2017). Role of hydrophobins in *Aspergillus fumigatus*. *J Fungi*. 4, E2. https://doi.org/10.3390/jof4010002.

Valsecchi, I., Sarikaya-Bayram, O., Wong, S. H. J, Muszkieta, L., Gibbons, J., Prevost, M. C., Mallet, A., Krijnse-Locker, J., Ibrahim-Granet, O., Mouyna, I., Carr, P., Bromley, M., Aimanianda, V., Yu, J. H., Rokas, A., Braus, G. H., Saveanu, C., Bayram, O., and Latge, J. P. (2017). MybA, a transcription factor involved in conidiation and conidial viability of the human pathogen *Aspergillus fumigatus*. *Mol Microbiol*. 105, 880–900. *https://doi.org/10.1111/mmi.13744*.

Van Der Vlugt-Bergmans, C. J. B., Brandwagt, B. F., Vant't Klooster, J. W., Wagemakers, C. A. M., and van Kan, J. A. L. (1993). Genetic variation and segregation of DNA polymorphisms in *Botrytis cinerea*. *Mycological Research*, 97(10), 1193–1200.

van de Veerdonk, F. L., Gresnigt, M. S., Romani, L., Netea, M. G., and Latge, J. P. (2017). *Aspergillus fumigatus* morphology and dynamic host interactions. *Nat Rev Microbiol*. 15, 661– 674. *https://doi.org/10.1038/nrmicro.2017.90*.

Van de Wouw, A. P., and Howlett, B. J. (2011). Fungal pathogenicity genes in the age of 'omics'. *Molecular plant pathology*, *12*(5), 507–514. https://doi.org/10.1111/j.1364-3703.2010.00680.x

Van Kan, J. A., Goverse, A., Van der Vlugt-Bergmans, C. J. B. (1993). Electrophoretic karyotype analysis of *Botrytis cinerea*. *Neth J Plant Pathol*. 99, 119–128.

van Kan, J. A. (2006). Licensed to kill: the lifestyle of a necrotrophic plant pathogen. *Trends Plant Sci*. 11(5), 247-253. doi: 10.1016/j.tplants.2006.03.005.

Van Kan, J. A. L., Stassen, J. H., Mosbach, A., Van Der Lee, T. A., Faino, L., Farmer, A. D., Papasotiriou, D. G., Zhou, S., Seidl, M. F., Cottam, E., Edel, D., Hahn, M., Schwartz, D. C., Dietrich, R. A., Widdison, S., Scalliet, G. (2017). A g apless genome sequence of the fungus *Botrytis cinerea*. *Mol Plant Pathol*. 18(1), 75-89. doi: 10.1111/mpp.12384.

van Leeuwen, M. R., Krijgsheld, P., Wyatt, T. T., Golovina, E. A., Menke, H., Dekker, A., Stark, J., Stam, H., Bleichrodt, R., Wosten, H. A. B., and Dijksterhuis, J. (2013). The effect of natamycin on the transcriptome of conidia of *Aspergillus niger*. *Stud Mycol*. 74, 71– 85. *https://doi.org/10.3114/sim0013*.

Viaud, M., Brunet-Simon, A., Brygoo, Y., Pradier, J. M., and Levis, C. (2003). Cyclophilin A and calcineurin functions investigated by gene inactivation, cyclosporin A inhibition and cDNA arrays approaches in the phytopathogenic fungus *Botrytis cinerea*. *Mol Microbiol*. 50(5), 1451-1465. doi: 10.1046/j.1365-2958.2003.03798.x.

Villalba, F., Lebrun, M. H., Hua-Van, A., Daboussi, M. J., and Grosjean-Cournoyer, M. C. (2001). Transposon impala, a novel tool for gene tagging in the rice blast fungus *Magnaporthe grisea*. *Mol Plant Microbe* Interact. 14(3), 308-15. doi: 10.1094/MPMI.2001.14.3.308.

Voigt, C. A., Schäfer, W., and Salomon, S. (2005). A secreted lipase of *Fusarium graminearum* is a virulence factor required for infection of cereals. *The Plant Journal*, 42(3), 364-375. https://doi.org/10.1111/j.1365-313X.2005.02377.x

Wang, J., and Higgins, V. J. (2005). Nitric oxide has a regulatory effect in the germination of conidia of *Colletotrichum coccodes*. *Fungal Genet Biol*. 42(4), 284-92.

Wang, Q., Liang, X., Dong, Y., Xu, L., Zhang, X., Hou, J., and Fan, Z. (2012). Effects of exogenous nitric oxide on cadmium toxicity, element contents and antioxidative system in perennial ryegrass. *Plant Growth Regul*. 69, 11–20.

Wang, Y., Chen, T., Zhang, C., Hao, H., Liu, P., Zheng, M., Baluška, F., Šamaj, J., and Lin, J. (2009). Nitric oxide modulates the influx of extracellular Ca2+ and actin filament organization during cell wall construction in *Pinus bungeana* pollen tubes. *New* Phytol. 182(4), 851-862. doi: 10.1111/j.1469-8137.2009.02820.x.

Wang, Z., Gerstein, M., and Snyder, M. (2009). RNA-Seq: a revolutionary tool for transcriptomics. *Nat. Rev. Genet.* 10, 57–63.

Wartenberg, D., Vodisch, M., Kniemeyer, O., Albrecht-Eckardt, D., Scherlach, K., Winkler, R., Weide, M., and Brakhage, A. A. (2012). Proteome analysis of the farnesol-induced stress response in *Aspergillus nidulans* -- the role of a putative dehydrin. *J Proteomics*, 75, 4038–4049. https://doi.org/10.1016/j.jprot.2012.05.023.

White, R. J. (2001). Gene transcription: mechanisms and control. Blackwell Science.

Wiemann, P., and Keller, N. P. (2014). Strategies for mining fungal natural products. *J Ind Microbiol Biotechnol*. 41, 301–313.

Williamson, B., Tudzynski, B., Tudzynski, P., van Kan, J. A. (2007). *Botrytis cinerea*: the cause of grey mould disease. *Mol Plant Pathol*. 8(5), 561-580. doi: 10.1111/j.1364-3703.2007.00417.x.

Winters, M. J., and Pryciak, P. M. (2018). Analysis of the thresholds for transcriptional activation by the yeast MAP kinases Fus3 and Kss1. *Molecular Biology of the Cell*, 29(5), 669-682. https://doi.org/10.1091/mbc.E17-10-0578

Wong, S. H. J., Beau, R., and Latge, J. P. (2012). A novel dehydrin-like protein from *Aspergillus fumigatus* regulates freezing tolerance. *Fungal Genet Biol*. 49, 210–216. *https://doi.org/10.1016/j.fgb.2012.01.005*.

Wong, S. H. J, Lamarre, C., Beau, R., Meneau, I., Berepiki, A., Barre, A., Mellado, E., Read, N. D., and Latge, J. P. (2011). A novel family of dehydrin-like proteins is involved in stress response in the human fungal pathogen *Aspergillus fumigatus*. *Mol Biol Cell*. 22, 1896 –1906. https://doi.org/10.1091/mbc.E10-11-0914.

Wu, M. D., Zhang, L., Li, G. Q., Jiang, D. H., Hou, M. S., and Huang, H. C. (2007). Hypovirulence and doublestranded RNA in *Botrytis cinerea*. *Phytopathology*, 97, 1590–1599.

Wu, M., Zhang, L., Li, G., Jiang, D., and Ghabrial, S. A. (2010). Genome characterization of a debilitation-associated mitovirus infecting the phytopathogenic fungus *Botrytis cinerea*. *Virology*, 406(1), 117-26. doi: 10.1016/j.virol.2010.07.010.

Wyatt, T. T., van Leeuwen, M. R., Wosten, H. A. B., and Dijksterhuis, J. (2014). Mannitol is essential for the development of stress-resistant ascospores in *Neosartorya fischeri* (*Aspergillus fischeri*). *Fungal Genet Biol*. 64, 11–24. *https://doi.org/10.1016/j.fgb.2013.12.010*.

Wyatt, T. T., Wosten, H. A. B., and Dijksterhuis, J. (2013). Fungal spores for dispersion in space and time. *Adv Appl Microbiol*. 85, 43–91. https://doi.org/10.1016/B978-0-12-407672-3.00002-2.

Xiong, F., Liu, M., Zhuo, F., Yin, H., Deng, K., Feng, S., Liu, Y., Luo, X., Feng, L., Zhang, S., Li, Z., and Ren, M. (2019). Host-induced gene silencing of BcTOR in *Botrytis cinerea* enhances plant resistance to grey mould. *Molecular plant pathology*, 20(12), 1722–1739. *https://doi.org/10.1111/mpp.12873*

Xue, C., Park, G., Choi, W., Zheng, L., Dean, R. A., and Xu, J. R. (2002). Two novel fungal virulence genes specifically expressed in appressoria of the rice blast fungus. *Plant Cell*. 14, 2107-2119.

Xue, Y., Ren, J., Gao, X., Jin, C., Wen, L., and Yao, X. (2008). GPS 2.0, a tool to predict kinase-specific phosphorylation sites in hierarchy. *Mol Cell Proteomics*, 7(9), 1598-608. doi: 10.1074/mcp.M700574-MCP200.

Yamasaki, H. (2000). Nitrite-dependent nitric oxide production pathway: implications for involvement of active nitrogen species in photoinhibition *in vivo*. *Philos Trans R Soc Lond B Biol Sci*. 355, 1477–1488.

Ye, X. S., Lee, S.-L., Wolkow, T. D., McGuire, S.-L., Hamer, J. E., Wood, G. and Osmani, S. A. (1999). Interaction between developmental and cell cycle regulators is required for morphogenesis in *Aspergillus nidulans*. *The EMBO Journal*, 18, 6994-7001. *https://doi.org/10.1093/emboj/18.24.6994*

Yin, S., Gao, Z., Wang, C., Huang, L., Kang, Z., and Zhang, H. (2016). Nitric oxide and reactive oxygen species coordinately regulate the germination of *Puccinia striiformis* f. sp. *tritici* Urediniospores. Frontiers in Microbiology, 7, 178. https ://doi.org/10.3389/fmicb.2016.00178

Yin, Y. N., Kim, Y. K., and Xiao, C. L. (2012). Molecular characterization of pyraclostrobin resistance and structural diversity of the cytochrome b gene in *Botrytis cinerea* from apple. *Phytopathology*, 102, 315–322.

Yu, J. H., Mah, J. H., and Seo, J. A. (2006). Growth and developmental control in the model and pathogenic *aspergilli*. *Eukaryot Cell*, 5(10), 1577-1584. doi: 10.1128/EC.00193-06.

Yukioka, H., Inagaki, S., Tanaka, R., Katoh, K., Miki, N., Mizutani, A., and Masuko, M. (1998). Transcriptional activation of the alternative oxidase gene of the fungus *Magnaporthe grisea* by a respiratory-inhibiting fungicide and hydrogen peroxide. *Biochim Biophys Acta*. 1442(2-3), 161-169. doi: 10.1016/s0167-4781(98)00159-6.

Zhang, L., Wu, M. D., Li, G. Q. *et al*. (2010). Effect of Mitovirus infection on formation of infection cushions and virulence of *Botrytis cinerea*. *Physiol Mol Plant Pathol*. 75, 71–80.

Zhang, Y., Shi, H., Liang, S., Ning, G., Xu, N., Lu, J., Liu, X., and Lin, F. (2015). MoARG1, MoARG5,6 and MoARG7 involved in arginine biosynthesis are essential for growth, conidiogenesis, sexual reproduction, and pathogenicity in *Magnaporthe oryzae*. *Microbiol Res*. 180, 11-22. doi: 10.1016/j.micres.2015.07.002.

Zhao, S., Fung-Leung, W. P., Bittner, A., Ngo, K., and Liu, X. (2014). Comparison of RNA-Seq and Microarray in Transcriptome Profiling of Activated T Cells. *PLoS One*, 9(1), e78644. https://doi.org/10.1371/journal.pone.0078644

Zhao, Y., He, M., Ding, J., Xi, Q., Loake, G. J., and Zheng, W. (2016a). Regulation of anticancer styrylpyrone biosynthesis in the medicinal mushroom Inonotus obliquus requires thioredoxin mediated transnitrosylation of S-nitrosoglutathione reductase. *Scientific Reports*, 6, 37601. https ://doi.org/10.1038/srep37601

Zhao, Y., He, M., Xi, Q., Ding, J., Hao, B., Keller, N. P., and Zheng, W. (2016b). Reversible S -nitrosylation limits over synthesis of fungal styrylpyrone upon nitric oxide burst. *Applied Microbiology and Biotechnology*, 100, 4123–4134. https ://doi.org/10.1007/s00253-016-7442-7

Zhao, Y., Lim, J., Xu, J., Yu, J. H., and Zheng, W. (2020). Nitric oxide as a developmental and metabolic si gnal in filamentous fungi. *Mol Microbiol*. 113(5), 872-882. doi: 10.1111/mmi.14465.

Zhao, Y., Xi, Q., Xu, Q., He, M., Ding, J., Dai, Y., Keller, N. P., and Zheng, W. (2015). Correlation of nitric oxide produced by an inducible nitric oxide synthase-like protein with enhanced expression of the phenylpropanoid pathway in *Inonotus obliquus* cocultured with *Phellinus morii*. *Appl Microbiol Biotechnol*. 99(10), 4361-4372. doi: 10.1007/s00253-014-6367-2.

Zhao, Y., Yuan, W., Sun, M., Zhang, X., and Zheng, W. (2021). Regulatory effects of nitric oxide on reproduction and melanin biosynthesis in onion pathogenic fungus *Stemphylium eturmiunum*. *Fungal Biol*. 125, 519– 531.

Zheng, W., Liu, Y., Pan, S., Yuan, W., Dai, Y., and Wei, J. (2011). Involvements of S-nitrosylation and denitrosylation in the production of polyphenols by Inonotus obliquus. *Applied Microbiology Biotechnology*, 90, 1763–1772. https ://doi.org/10.1007/s00253-011-3241-3

Zhou, S., Narukami, T., Masuo, S., Shimizu, M., Fujita, T., Doi, Y., Kamimura, Y., and Takaya, N. (2013). NO -inducible nitrosothionein mediates NO removal in tandem with thioredoxin. *Nat Chem Biol*. 9(10), 657-63. doi: 10.1038/nchembio.1316.